RPP-7464
Revision 0

Simulations for the Hanford Immobilized Low-Activity Tank Waste Performance Assessment: 2001 Version

Prepared for the U.S. Department of Energy
Assistant Secretary for Environmental Management

Office of River Protection

P.O. Box 450
Richland, Washington 99352

Approved for public release; further dissemination unlimited

RPP-7464
Revision 0

Simulations for the Hanford Immobilized Low-Activity Tank Waste Performance Assessment: 2001 Version

R. J. Puigh
Fluor Federal Services

F. M. Mann
CH2M Hill

Date Published
February 2001

Prepared for the U.S. Department of Energy
Assistant Secretary for Environmental Management

Office of River Protection

P.O. Box 450
Richland, Washington 99352

Approved for public release; further dissemination unlimited

TRADEMARK DISCLAIMER

Reference herein to any specific commercial product, process, or service by trade name, trademark, manufacturer, or otherwise, does not necessarily constitute or imply its endorsement, recommendation, or favoring by the United States Government or any agency thereof or its contractors or subcontractors.

This report has been reproduced from the best available copy.

Printed in the United States of America

Simulations For The Hanford Immobilized Low-Activity Tank Waste Performance Assessment: 2001 Version

R.J. Puigh and F.M. Mann

February 2001

This page intentionally left blank.

CONTENTS

1.0 INTRODUCTION 1
1.1 Purpose 1
1.2 Background 1
1.3 Contents of this Report 2
2.0 SIMULATION APPROACH 2
2.1 System Model 3
2.2 Separation of Calculations 6
2.3 Near Field Flow Calculations 6
2.4 Waste Form Calculations 7
2.5 Far Field Calculations 7
2.6 Groundwater Calculations 7
2.7 Integration Calculations 8
3.0 ILAW CASES 10
3.1 Near-Field Moisture Flow 10
3.2 Waste Form 11
3.3 Far Field Moisture Flow and Contaminant Transport 13
3.4 Groundwater 17
4.0 Summary of estimated impacts 20
5.0 REFERENCES 29
APPENDIX A - Near Field, Far Field, and Estimated Impact Calculations for the Hanford Immobilized, Low-Activity Tank Waste Performance Assessment: 2001 Version A-1
APPENDIX B - Waste Form Release Calculations for the 2001 Immobilized Low-Activity Waste Performance Assessment B-1
APPENDIX C - Groundwater Flow and Transport Calculations Supporting the Immobilized Low-Activity Waste Disposal Facility Performance Assessment C-1
APPENDIX D - Compact Disk Format D-1

LIST OF TABLES

Table 3-1. Near Field Cases. 10

Table 3-2. Summary of Waste Form Sensitivity Calculations. 11

Table 3-3. Far Field Flow Cases. 13

Table 3-4. Far Field Transport Cases. 14

Table 3-5. Groundwater Cases 17

Table 4-1. Summary of Estimated Impacts for 2001 ILAW PA 21

LIST OF FIGURES

Figure 2-1. Eight Sequential Steps for the Groundwater Pathway. 4

Figure 2-2. Modeling Strategy for Assessing ILAW Disposal System. 5

Acronyms

BBI	best basis inventory
CA	Composite Analysis
CERCLA	Comprehensive Environmental Response, Compensation, and Liability Act of 1980
CFEST	Coupled Fluid, Energy, and Solute Transport (computer code)
CFR	Code of Federal Regulations
DNFSB	Defense Nuclear Facilities Safety Board
DOE	Department of Energy
ILAW	Immobilized Low-Activity Waste
ILAW PA	Immobilized Low-Activity Waste Performance Assessment
LFRG	Low-Level Waste Disposal Facility Federal Review Group
NRC	Nuclear Regulatory Commission
PA	Performance Assessment
RCRA	Resource Conservation and Recovery Act
RH	remotely handled (refers to trench disposal facility design)
STORM	Subsurface Transport Over Reactive Multiphases (computer code)
TWRS EIS	Tank Waste Remediation System Environmental Impact Statement
TWRSO&UP	Tank Waste Remediation System Operation and Utilization Plan (Kirkbride 1999)
WAC	Washington Administrative Code

This page intentionally left blank.

1.0 INTRODUCTION

1.1 Purpose

This document provides a compilation of the simulations conducted in support of the Hanford Immobilized Low-Activity Tank Waste Performance Assessment (ILAW PA) to be issued in 2001. This document provides a description of the simulation approach and a description of the simulations for the near field, waste form, far field, groundwater, and integration calculations. The detailed results from these simulations are documented in the three appendices that are the primary references for these calculations.

1.2 Background

The Hanford Site, in south-central Washington State, has been used extensively for producing defense materials by the Department of Energy (DOE) and its predecessors, the U.S. Atomic Energy Commission and the U.S. Energy Research and Development Administration. Starting in the 1940's, Hanford Site operations were dedicated primarily to producing nuclear weapons materials. In the 1960's, operations were expanded to producing electricity from a dual-purpose reactor, conducting diverse research projects, and managing waste. In the late 1980's, the Site's original mission ended. This mission left a large inventory of radioactive and mixed waste stored in buried single- and double-shell tanks in the Hanford Site 200 Areas.

Today, the Site's missions are environmental restoration, energy-related research, and technology development. As part of its environmental restoration mission, DOE is proceeding with plans to permanently dispose of the waste stored on site. These plans are based on the Hanford Federal Facility Agreement and Consent Order (Tri-Party Agreement) (Ecology 1998-1) and the Record of Decision for the Tank Waste Remediation Systems Environmental Impact Statement (DOE 1997a). These documents call for the waste to be retrieved from the Hanford Site's single- and double-shell tanks, then treated to separate the low-level fraction (now called the low-activity fraction) from the high-level and transuranic fractions. Both fractions will then be immobilized.

The two products (the small volume of high-level immobilized waste and the much larger volume of low-activity waste) will be disposed of in different locations. The high-level waste will be stored on the Hanford Site until sent to a federal geologic repository. The low-activity immobilized waste will be placed in a near-surface disposal system in the 200 East Area of the Hanford Site. On the order of 160,000 m^3 (5,6000,000 ft^3) of low-activity immobilized waste will be disposed of under this plan. This is among the largest amounts of waste in the DOE Complex (DOE 1997b) and has one of the largest inventories of long-lived radionuclides at a low-level waste disposal facility.

The Hanford Immobilized Low-Activity Tank Waste Performance Assessment provides an analysis of the long-term environmental and health impacts of the onsite disposal of Hanford

immobilized low-activity tank waste packages. The purpose of the 1998 version was to provide an assessment that would bound the impacts given the limited site-specific and waste-specific data available. The assessment was based on the requirements of DOE Order 5820.2a with the acknowledgment that the order was undergoing revision. This document was conditionally accepted by the Department of Energy and formed part of the basis for the issuance of a Disposal Authorization Statement for the Hanford Site, including the disposal of ILAW (DOE 1999).

Since the release of the 1998 version of the Hanford Immobilized Low-Activity Tank Waste Performance Assessment, a significant data collection activity has been undertaken to support the next performance assessment analysis scheduled to be released in 2001. Specific new data since the last performance assessment include: new glass corrosion data on more relevant glass compositions, site-specific hydrology and geochemical data, and a revised model for the groundwater flow underneath the Hanford Site. The data have been compiled into a single document, *Data Packages for the Hanford Immobilized Low-Activity Tank Waste Performance Assessment: 2001 Version* (Mann/Puigh 2000).

The next version (known as the 2001 ILAW PA) has used the site-specific and waste form-specific data that have been collected in the past few years. The emphasis of the 2001 ILAW PA has been on how these new data affect the conclusions of the 1998 ILAW PA. These new data and analyses will fulfill the conditions of the DOE headquarters acceptance. The 2001 ILAW PA also follows the guidance of the new DOE order on radioactive waste management (DOE O 435.1), particularly in the areas of document content and format. This document together with the data report (Mann/Puigh 2000) form the technical underpinning for the 2001 ILAW PA.

1.3 Contents of this Report

This report contains the results from the simulations that have been conducted in support for the 2001 ILAW performance assessment. Section 2 describes the simulation approach that was used to estimate the impacts associated with groundwater protection scenarios defined in Mann (1999). Section 3 provides a summary of simulation cases run for the 2001 ILAW PA. Section 4 provides a summary of the estimated impacts for the exposure scenarios investigated in the 2001 ILAW PA. Appendices A, B, and C contain the detailed, separately published reports associated with the 2001 ILAW calculations (Bacon 2001, Bergeron 2000, and Finfrock 2000). Appendix D contains a description of the file structure for a compact disk (CD) containing the input and selected output files from the calculations. Not covered in this report are the results for the inadvertent intruder or the air release exposure scenarios. These calculations are summarized in the 2001 ILAW PA.

2.0 SIMULATION APPROACH

This section describes the approach used for performing the moisture flow and contaminant transport calculations for the 2001 ILAW PA. The approach is based on the

groundwater pathway being the most important pathway for estimated impacts to the environment. The approach is also based on using the strengths of the various available computer codes to represent the system.

2.1 System Model

Previous long-term environmental assessments at the Hanford Site have consistently shown that the groundwater pathway is the most important. This pathway also requires the most calculations. The conceptual model used for this and earlier Hanford Site performance assessments take the following eight steps:

1. The water leaves the very-near-surface soil region at the infiltration rate.

2. The water moves toward the waste form, but most of it is diverted by any intact capillary barrier.

3. The water that is not diverted is chemically modified by the local environment, interacts with the waste form, accumulates contaminants, and again is chemically modified by the local environment.

4. The water (possibly a reduced amount) leaves the disposal facility carrying contaminants with it. Some contaminants may interact with the material in the disposal facility, slowing the release of the contaminants to the surrounding natural environment.

5. The water moves through the undisturbed, unsaturated zone (vadose zone) below the disposal facility down to the unconfined aquifer. The contaminants also are transported through the vadose zone, again possibly undergoing some geochemical sorption.

6. The water and contaminants move and mix with the water in the unconfined aquifer until they are extracted from the aquifer and brought to the surface or until they reach the Columbia River.

7. Contaminants are normally extracted by being carried to the surface with groundwater being pumped through a well.

8. The radionuclide contaminants then result in human exposure through a variety of pathways (ingestion, inhalation, and external radiation).

Figure 2-1 shows these eight steps as a flow chart.

Figure 2-1. Eight Sequential Steps for the Groundwater Pathway.

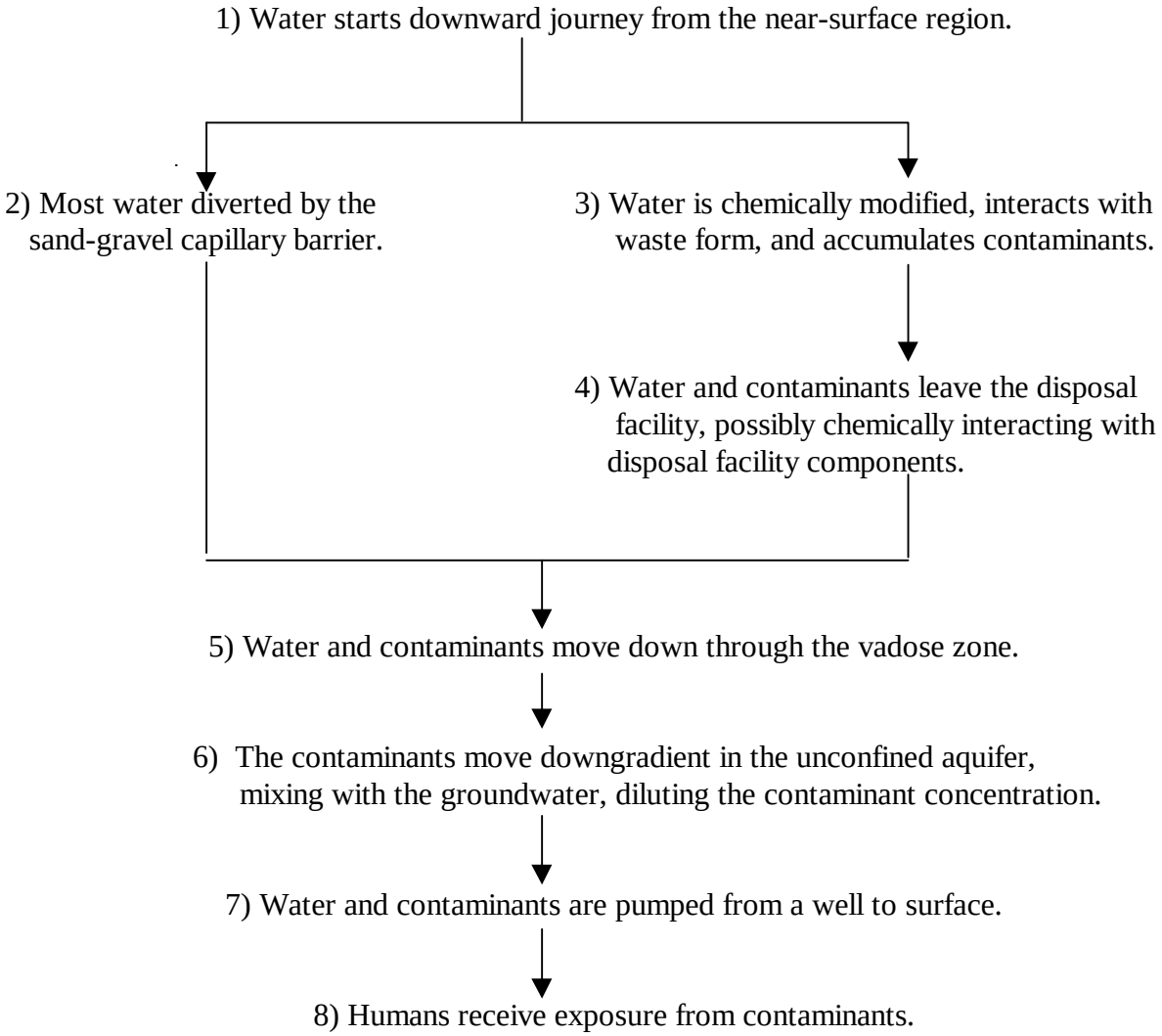

The results for each step are computed separately and used in the next step so that computations can be made more easily. Such an approach is taken to maximize computational efficiency. Some of the computer simulations take 100 hours of computer time; some take a few minutes. Each is a highly specialized calculation. However, the overall model is always considered at each step and consistent data are used throughout.

The strategy for the current computations is to define a base analysis case, then develop sensitivity cases derived from that base analysis case. In some instances the sensitivity cases are built on an alternative case, such as the one describing the concrete vault concept.

Computer codes have been used for four purposes:

- to calculate contaminant release rates from the waste packages and from the disposal facility,

- to calculate moisture flow and contaminant transport in the vadose zone (including moisture flow into the disposal facility),
- to calculate moisture flow and contaminant transport in groundwater, and
- to merge the results of the preceding codes.

Figure 2-2 illustrates also the overall computational strategy for the ILAW PA.

Figure 2-2. Modeling Strategy for Assessing ILAW Disposal System.

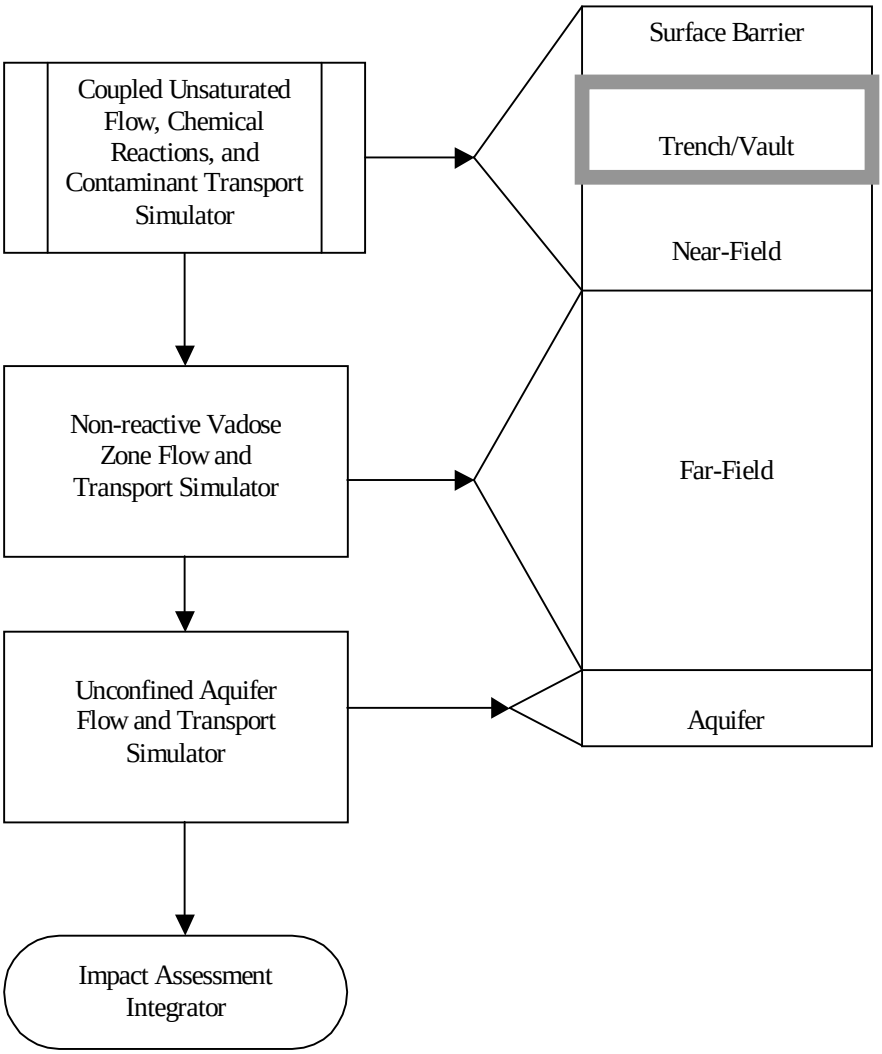

2.2 Separation of Calculations

The near-field environment is defined as the domain through the trench or vault to some distance below the floor of the disposal facility. A coupled unsaturated flow, chemical reactions, and contaminant transport simulator (STORM) was used within the near-field (Bacon 2000) to estimate the contaminant release and transport. The moisture flow into the near field was calculated using the computer code VAM3DF (Huyakorn 1999). The plume exiting the region near the vault is expected to be of high ionic strength and pH, and will migrate down into the near-field vadose zone for some distance. However, at some distance from the disposal vaults, geochemical conditions will approach those more typical of the Hanford vadose zone and for which simplifying assumptions (such as linear sorption, negligible precipitation/dissolution, no changes in hydraulic properties, and no fluid density gradient effects) can be used. This region is defined as the far-field environment and can be simulated using standard, non-reactive (chemical reactions not specifically included in calculations) flow and transport codes. For the ILAW PA, computations in the far-field domain were done using VAM3DF, a variably saturated flow and transport code.

The primary reason for switching from the near-field simulator to VAM3DF is to apply a less complicated code for the far field, and therefore a faster turnaround for the numerical simulations. The radionuclide flux exiting the far-field domain to the unconfined aquifer is provided by VAM3DF.

Calculations in the groundwater aquifer are performed using the Hanford Site model and associated code, CFEST-96 (Gupta 1987). The Hanford Site Groundwater Program has recommended this code for performing saturated flow and transport simulations for the Hanford Site. The site-wide model and local scale models are used to estimate the dilution (well intercept factor) associated with the concentration of contaminants in a given downgradient groundwater well.

Finally, the results of each of the sequential calculations are combined to estimate the impacts from the disposal system using the INTEG program (Mann 1996). This program combines the results from the far field calculations, the groundwater calculations, and the dosimetry data to estimate impacts related to the performance objectives.

2.3 Near Field Flow Calculations

Near field flow calculations were performed using the VAM3DF code to determine the moisture flow into the disposal facility and around the waste form. The near-field region (primarily the engineered facility) significantly alters the flow field from what would be present in an undisturbed environment. It is necessary, therefore, to predict these flow fields so that the fluid flux into the far field can be characterized and the appropriate waste form release simulations are used. The flow fields in the near field are primarily driven by the surface recharge rates and the facility design. The material properties of the backfill and surrounding soils also affect the results, but to a lesser degree. These 2-D calculations are reported in Finfrock (2000) (see also Appendix A).

2.4 Waste Form Calculations

The *Subsurface Transport Over Reactive Multiphases* (STORM) code (Bacon 2000) is the source-term code used for estimating the time-dependent flux of radionuclides released from the waste form and the subsequent transport of contaminants in the disposal facility. STORM contains two important factors that allow the code to simulate the processes in the disposal facility. First, the code is based on basic principles of physics, chemistry, and thermodynamics that provide the best estimate of contaminant release over the spatial and long time periods of interest. Second, the model for the disposal facility can be coupled with a model for radionuclide release, thus providing the ability to couple the effects of facility design with waste form performance.

Using chemical reaction rates (including the glass corrosion rates) and moisture values in the trench (or vault) fromVAM3DF, STORM provides the source term for the vadose zone calculations. STORM calculates the following:

- The flow of moisture in the disposal facility
- The degradation of the waste form with corresponding release of radionuclides
- The chemical reactions that depend on time and space (including the formation of secondary mineral phases and the consumption of water)
- The transport of the water and contaminants through the disposal facility.

These 1-D calculations are reported in Bacon (2001) (see also Appendix B).

2.5 Far Field Calculations

The far field calculations were performed using the computer code VAM3DF to calculate the moisture flow and the contaminant transport. The far field is the region of the model domain that extends from the base of the engineered facility down to the top of the water table. Two primary model geometries are simulated, representing the remote handled trench and the alternate (vault) facility design. The far-field modeling process consists of two stages, first the steady state flow fields are calculated, and then the contaminant transport is calculated. These two steps use the same basic model but with different boundary conditions and material property data. These 2-D calculations are reported in Finfrock (2000) (see also Appendix A).

2.6 Groundwater Calculations

The Richland Field Manager (Wagoner 1996) directed the Hanford Groundwater Program to establish a single groundwater model for the Hanford Site. The Hanford Groundwater Program selected the conceptual and numerical model described in Wurstner et al. (1995) and Cole et al. (1997) as the consolidated site-wide ground-water model. The Coupled, Fluid,

Energy, and Solute Transport (CFEST) code, the ground-water flow and transport code used in numerical implement of the selected model, was selected as the interim code. Documentation of code formulation, user's guides, and verification are given in Gupta (1987). Documentation of the development of the selected site-wide model and its specific implementation and recent applications with the CFEST code at Hanford is provided in Wurstner (1997), Cole (1997), and Kincaid (1998). Documentation of the review and selection of the site-wide ground-water model selection process is summarized in DOE/RL (2000). A local model was developed for the ILAW disposal site and calculations were performed for post-Hanford conditions. These calculations are reported in Bergeron 2000 (see also Appendix C).

2.7 Integration Calculations

INTEG (Mann 1996b) calculates a specific impact (whether dose rate or concentration level) based on the inventory, vadose zone transport, aquifer transport, and dosimetry factors. The dose rate calculated depends on the type of dosimetry factor (i.e., all-pathways, drinking water). The program solves the following equation for each year under consideration.

$$\textit{Response} = \sum_i I_i(t)\, \Gamma_i(t)\, w_i\, D_i \,/\, (r\, A) \qquad (3.9)$$

where

I_i = the amount (or inventory) of radionuclide (Ci) or hazardous chemical (kg) i. The time-dependent value is calculated by INTEG based on the initial inventory and on decay and the ingrowth from other radionuclides.

Γ_i = the flux of contaminants at the bottom of the vadose zone normalized to an unit source inventory for radionuclide ([Ci/y]/Ci) or hazardous chemical ([kg/y]/kg) i. The time-dependent value is calculated by VAM3DF.

w_i = the ratio of the concentration of radionuclide i at the well location relative to the contaminant concentration at the bottom of the vadose zone directly beneath the disposal facility (dimensionless). This quantity was called the well intercept factor in earlier Hanford performance assessments. The peak value as calculated by CFEST is used.

D_i = the dose rate factor (mrem/y per Ci/m^3). The values are taken from Rittmann (1999). D_i is unity when the response that is calculated is a concentration.

r = the recharge rate (m/y). The value at 10,000 years is used at all analysis times.

A = the area over which the contaminant flux enters the aquifer (m^2). The value used is the area of the disposal facility being modeled.

The program is modeled after GRTPA (Rittmann 1993), which served a similar function in earlier work (Rawlins 1994 and Mann 1995b). INTEG allows greater freedom in specifying data

used in the integration. The code has been benchmarked against the results of GRTPA (Mann 1996). An auxiliary code was written to translate the output of VAM3DF into a readable format for INTEG. These calculations are reported in Finfrock (2000) (see also Appendix A).

3.0 ILAW CASES

This section summarizes the different simulation cases calculated in support of the 2001 ILAW PA. For a more detailed description of these cases see Bacon (2001) for the waste form simulations, Finfrock (2000) for the near field and far field simulations, and estimated dose calculations, and Bergeron (2000) for the groundwater simulations.

3.1 Near-Field Moisture Flow

The near-field cases represent changes to the surface recharge or the near field geometry or material properties. The individual cases are described in Table 3-1.

Table 3-1. Near Field Cases.

Case Name	Case ID	Case Description
Base Case	nf42	This case used the basic trench design with the capillary break in place but consisting entirely of sand (and therefore non-functional). The recharge over the cap region was 4.2 mm/y. The side slope and undisturbed region beyond the cap were treated as having a recharge of 50 mm/y.
Low Recharge	nf01	Identical to the base case except that the recharge over the cap is 0.1 mm/y.
Rupert Sand	nf09	Identical to the base case except that the recharge over the cap is 0.9 mm/y, corresponding to Rupert sand.
High Recharge	nf50	Identical to the base case except that the recharge over the cap is 50 mm/y.
No Side Slope	nf42-all	Identical to the base case except that the recharge in the side slope and undisturbed area is 4.2 mm/y instead of 50 mm/y.
Sand Backfill	nf42-sand	Hanford sand is used as the backfill material in the facility.
Best Estimate Case (Capillary Break)	nf42-break	Identical to base case except that the capillary break is functional.
Short Capillary Break	nf42-shortbreak	Identical to the best estimate case except that the capillary break only extends 44 m (instead of 49 m) from the trench centerline.
Vertical Capillary	nf42-vert	Identical to the best estimate case except that a second,

Case Name	Case ID	Case Description
Break		vertical, capillary break has been added under the edge of the horizontal capillary break.
Failed Capillary Break (Subsidence)	nf42-subsidence	Identical to the best estimate case except that a region of the capillary break has subsided. A region of the capillary barrier 1 m long (starting at 10 m from the centerline) is displaced downward 0.3 m (the void at the top is filled with sand and the underlying backfill is displaced by gravel).
Capillary Break With High Recharge	nf50-break	Identical to the best estimate case except that the entire surface recharge is at 50 mm/y.
Alternate Facility Design (Vault)	nf42-vault	This case is similar to the base case (using the same recharges and material properties) but has the alternate (vault) facility design.

3.2 Waste Form

The waste form cases represent different assumptions on the release mechanisms and different environmental effects (primarily recharge, and facility cases). Table 3-2 summarizes the waste form calculations.

Table 3-2. Summary of Waste Form Sensitivity Calculations.

Case Name	Case ID	Description
Base Case	WFA	Trench model, 4.2 mm/y infiltration
Forward Rate	WFB	Trench model, forward rate, 4.2 mm/y infiltration
Concrete Vault - Base	WFC	Trench model, 4.2 mm/y infiltration
Low Recharge	WFD	Trench model, 0.1 mm/yr infiltration
No Ion Exchange	WF1	Trench model, Assume no Ion Exchange
No Secondary Phase	WF2	Trench model, Assume no Secondary Phase Formation during waste form corrosion

Case Name	Case ID	Description
Rupert Sand	WF4	Trench model, 0.9 mm/y infiltration rate
High Recharge	WF6	Trench model, 50 mm/y infiltration rate
Recharge = 0.5 mm/y	WF7	Trench model, 0.5 mm/y infiltration rate
Recharge = 10 mm/y	WF8	Trench model, 10 mm/y infiltration rate
STORM - Far Field	WF9	Trench model, Extend WFA to groundwater
Top Conditioning Layer	WF10	Trench model, Add conditioning layer at top
Sand Backfill	WF11	Trench model, Change filler material in trench to sand
10X Waste Form Aqueous Diffusion	WF14	Trench model, Increase diffusion for all aqueous species by a factor of 10
Concrete Vault - backfill	WF16	Vault model, Replace concrete everywhere with backfill material
Concrete v - Rupert Sand	WF19	Vault model, 0.9 mm/y infiltration rate
Concrete Vault - Low Recharge	WF21	Vault model, 0.1 mm/y infiltration
Steel	WF25	Trench model, Include steel in waste packages
Uranium Release	WF26	Trench model, Replace Tc w/U
2-D Trench - Base	WF27	Trench model, Full 2-D simulation
Alternate Glass	WF28/WFx	Trench model, Increase Waste Loading / Alternate Glass Formulation (HLP-31)
5X Ion Exchange - Forward	WF30	Trench model, increase ion exchange rate by 5X, forward rate, 4.2 mm/y infiltration

3.3 Far Field Moisture Flow and Contaminant Transport

The far field flow cases represent changes to the fluid influx to the far field (i.e., a near-field case), far field geometry, or material properties. The individual cases are described in Table 3-3.

Table 3-3. Far Field Flow Cases.

Case Name	Case ID	Case Description
Base Case	42base-f	Base case geometry. Top boundary fluid flux derived from near-field base case [nf42].
Low Recharge	01-f	Top boundary fluid flux derived from near-field low recharge case [nf01].
Rupert Sand	09-f	Top boundary fluid flux derived from near-field Rupert sand case [nf09].
High Recharge	50-f	Top boundary fluid flux derived from near-field high recharge case [nf50].
No Side Slope	42all-f	Top boundary fluid flux derived from near-field no side slope case [nf42-all].
Capillary Break	42break-f	Top boundary fluid flux derived from near-field capillary break case [nf42-break].
Deep Vadose Zone	42deep-f	The gravel layer is extended down an additional 3 m (to a depth of 106 m). Top boundary fluid flux derived from near-field base case [nf42].
Clastic Dike	42dike-f	A clastic dike is inserted under the middle of the facility region. The clastic dike is 0.5 m wide and extends through the entire far-field. Top boundary fluid flux derived from near-field base case [nf42].
No Sand Layer	42grav-f	Sand layer is replaced with gravel. Top boundary fluid flux derived from near-field base case [nf42].
Isotropic	42iso-f	Sand and Gravel layers have isotropic conductivity properties. Top boundary fluid flux derived from near-field base case [nf42].
No Gravel Layer	42sand-f	Gravel layer is replaced with Hanford sand. Top boundary

Case Name	Case ID	Case Description
		fluid flux derived from near-field base case [nf42].
Sand Backfill	42sandfill-f	Top boundary fluid flux derived from near-field sand backfill case [nf42-sand].
Short Capillary Break	42short-f	Top boundary fluid flux derived from near-field short capillary break case [nf42-shortbreak].
Failed Capillary Break (subsidence)	42sub-f	Top boundary fluid flux derived from near-field subsidence case [nf42-subsidence].
Vertical Capillary Break	42vert-f	Top boundary fluid flux derived from near-field vertical capillary break case [nf42-vert].
Capillary Break with High Recharge	50break-f	Top boundary fluid flux derived from near-field capillary break with high recharge case [nf50-break].
Vault	42vault-f	Vault geometry model (similar to base case except that it is only 35 m wide instead of 60 m). Top boundary fluid flux derived from near-field vault case [nf42-vault].

The flow calculations are then used to calculate the contaminant transport through the vadose zone. The individual cases are described in Table 3-4.

Table 3-4. Far Field Transport Cases.

Case Name	Case ID	Case Description
Base Case	42base-t	Base case geometry. Fluid velocity fields taken from fluid flow base case. Top boundary contaminant flux derived from waste form base case.
Low Recharge	01-t	Fluid velocity fields taken from fluid flow low recharge case. Top boundary contaminant flux derived from waste form low recharge case.
Rupert Sand	09-t	Fluid velocity fields taken from fluid flow Rupert sand case. Top boundary contaminant flux derived from waste form Rupert sand case.

Case Name	Case ID	Case Description
High Recharge	50-t	Fluid velocity fields taken from fluid flow high recharge case. Top boundary contaminant flux derived from waste form high recharge case.
No Side Slope	42all-t	Fluid velocity fields taken from fluid flow no side slope case. Top boundary contaminant flux derived from waste form base case.
Alternate Glass	42altglass-t	Fluid velocity fields taken from fluid flow base case. Top boundary contaminant flux derived from waste form alternate glass case.
Capillary Break	42break-t	Fluid velocity fields taken from fluid flow capillary break case. Top boundary contaminant flux derived from waste form low recharge case (conservative assumption).
Concrete Layer	42conc-t	A 1-m layer at the top of the model is given alternate K_d values for I and U nuclides. Fluid velocity fields taken from fluid flow base case. Top boundary contaminant flux derived from waste form base case.
Conditioning Layer	42cond-t	Fluid velocity fields taken from fluid flow base case. Top boundary contaminant flux derived from waste form conditioning layer case.
Deep Vadose Zone	42deep-t	The gravel layer is extended down an additional 3 m (to a depth of 106 m). Fluid velocity fields taken from fluid flow deep vadose zone case. Top boundary contaminant flux derived from waste form base case.
High Diffusion	42diff-t	The diffusion coefficients for the sand and gravel are multiplied by a factor of 10. Fluid velocity fields taken from fluid flow base case. Top boundary contaminant flux derived from waste form base case.
Clastic Dike	42dike-t	A clastic dike is inserted under the middle of the facility region. Fluid velocity fields taken from fluid flow clastic dike case. Top boundary contaminant flux derived from waste form base case.
High Dispersion	42disp-t	The dispersion coefficients for the sand and gravel are multiplied by a factor of 2. Fluid velocity fields taken from fluid flow base case. Top boundary contaminant flux derived from waste form base case.
Forward Rate	42for-t	Fluid velocity fields taken from flow base case. Top boundary contaminant flux derived from waste form forward rate case.

Case Name	Case ID	Case Description
No Sand Layer	42grav-t	Sand layer is replaced with gravel. Fluid velocity fields taken from fluid flow no sand case. Top boundary contaminant flux derived from waste form base case.
Isotropic	42iso-t	Fluid velocity fields taken from fluid flow isotropic case. Top boundary contaminant flux derived from waste form base case.
No Gravel Layer	42sand-t	Gravel layer is replaced with Hanford sand. Fluid velocity fields taken from fluid flow no gravel case. Top boundary contaminant flux derived from waste form base case.
No Ion Exchange	42noion-t	Fluid velocity fields taken from fluid flow base case. Top boundary contaminant flux derived from waste form no ion exchange case.
No Secondary Reactions	42nosecond-t	Fluid velocity fields taken from fluid flow base case. Top boundary contaminant flux derived from waste form no secondary reactions case.
Sand Backfill	42sandfill-t	Fluid velocity fields taken from fluid flow base case. Top boundary contaminant flux derived from waste form sand backfill case.
High Diffusion in Glass	42sdiff-t	Fluid velocity fields taken from fluid flow base case. Top boundary contaminant flux derived from waste form high diffusion case.
Short Capillary Break	42short-t	Fluid velocity fields taken from fluid flow short capillary break case. Top boundary contaminant flux derived from waste form low recharge case.
Failed Capillary Break (subsidence)	42sub-t	Fluid velocity fields taken from fluid flow failed capillary break case. Top boundary contaminant flux derived from a composite of waste form cases base, low recharge, Rupert sand, and high recharge.
Steel Casing	42steel-t	Fluid velocity fields taken from fluid flow base case. Top boundary contaminant flux derived from waste form steel casing case.
Vertical Capillary Break	42vert-t	Fluid velocity fields taken from fluid flow vertical capillary case. Top boundary contaminant flux derived from waste form low recharge case.
Capillary Break with	50break-t	Fluid velocity fields taken from fluid flow capillary break with high recharge case. Top boundary contaminant flux derived from waste

Case Name	Case ID	Case Description
High Recharge		form low recharge case.
Pulse	pulse-t	Fluid velocity fields taken from fluid flow base case. Top boundary contaminant flux is a 1 Ci pulse distributed over 1 y.
Vault	42vault-t	Vault geometry model (similar to base case except that it is only 35 m wide instead of 60 m). Fluid velocity fields taken from fluid flow vault case. Top boundary contaminant flux derived from waste form vault case.

3.4 Groundwater

The groundwater cases represent changes to the facility layout and boundary conditions associated with selected groundwater sensitivity cases. The individual cases are described in Table 3-5.

Table 3-5. Groundwater Cases

Case Name	Regional Model Case ID	Local Model Case ID	Case Description
Base Analysis Case	GWRSBCa	GWLSBCa	RH trenches in northeast corner of disposal site. Concentration of source entering the aquifer was assumed to be 1 Ci/m^3. Rate of mass flux associated with this concentration is a function of the infiltration rate of 4.2 mm/y assumed for the disposal facility. Resulting solute flux entering the aquifer through the trench area for this infiltration rate is 4.2 x 10^{-3} Ci/y/m^2.
South Location	GWRSBCa	GWLSSC1	RH trenches in south end of disposal site, 4.2 mm/y local infiltration rate. Contaminant loading same as the base analysis case.
90° Rotation	GWRSBCa	GWLSSC2	RH trench orientation rotated 90°, trenches at south end of disposal site. Contaminant loading rate same as the base analysis case.

Smaller Layout	GWRSBCb	GWLSBCa	Decrease "footprint" of disposal facility to 36,750 m^2 (concrete vault concept). Contaminant loading rate same as the base analysis case.
Larger Layout	GWRSBCa	GWLSSC5	Increase "footprint" of disposal facility to include area between trenches. Contaminant loading rate same as the base analysis case.
Existing Vault Site	GWRSBCc	GWLSBCc	Use existing vault layout and site-specific hydraulic properties. Contaminant loading rate same as the base analysis case.
Well Pumping Rate = 30 L/day	GWRSBCa	GWLSSC3a	Increase in well pumping rate from 10 L/day to 30 L/day at 100-m well location. Contaminant loading rate same as the base analysis case.
Well Pumping Rate = 100 L/day	GWRSBCa	GWLSSC3b	Increase in well pumping rate from 10 L/day to 100 L/day at 100-m well location. Contaminant loading rate same as the base analysis case.
Well Pumping Rate = 300 L/day	GWRSBCa	GWLSSC3c	Increase in well pumping rate from 10 L/day to 300 L/day at 100-m well location. Contaminant loading rate same as the base analysis case.
Well Pumping Speed Rate = 1000 L/day	GWRSBCa	GWLSSC3d	Increase in well pumping rate from 10 L/day to 1000 L/day at 100-m well location. Contaminant loading rate same as the base analysis case.
Reduce Hydraulic Conductivity of Hanford Formation	GWRSBCa	GWLSSC4	Reduce the hydraulic properties for the Hanford formation to the values for the underlying Ringold Formation. Contaminant loading rate same as the base analysis case.
Increase Regional Recharge (3X)	GWRSSC7	GWLSSC7	Increase the regional recharge by a factor of 3, resulting in water table elevation of 3 m. Contaminant loading rate same as the base analysis case.

Decrease Regional Recharge (3X)	GWRSSC8	GWLSSC8	Decrease the regional recharge by a factor of 3, resulting in water table lowering of 1.2 m. Contaminant loading rate same as the base analysis case.
Decrease Regional Upgradient Boundaries (2X)	GWRSSC9	GWLSSC9	Reduce the simulated boundary fluxes associated with Cold Creek, Dry Creek, and springs emanating from Rattlesnake Ridge by a factor of 2. Contaminant loading rate same as the base analysis case.

4.0 SUMMARY OF ESTIMATED IMPACTS

This section summarizes the detailed results from the waste form, vadose zone, groundwater, and INTEG calculations to estimate the impacts for the different sensitivity cases investigated in this performance assessment. The details for the waste form calculations are provided in Bacon (2001). The details for the near field, far field, and INTEG results can be found in Finfrock (2000). The details for the groundwater results can be found in Bergeron (2000). Appendix D includes a description of the input and selected output files that are included with this performance assessment on a compact disc (CD) that is available on request.

Table 4-1 summarizes the results for the estimated impacts to the beta-photon drinking water dose, the alpha concentration, and the all-pathway dose for the all-pathway farmer scenario except where noted. The estimated impacts are associated with a downgradient well located 100 m below the ILAW site except where noted. The estimated impacts are provided for 1,000 and 10,000 years after facility closure. The maximum estimated impacts also are provided. In general the maximum estimated impacts for the alpha concentration and all-pathway dose occurs for the maximum time calculated (typically 20,000 years after facility closure [except for the base analysis case where it is 100,000 years after facility closure]). Also included in Table 4-1 are the file names for the INTEG calculations.

Table 4-1. Summary of Estimated Impacts for 2001 ILAW PA

INTEG Filename	Case Designation	Estimated Impact at 1,000 y after Facility Closure (1)			Estimated Impact at 10,000 y after Facility Closure (1)			Maximum Estimated Impact (1) [peak time or max time for calculation]		
		beta/ photon dose (mrem/y)	alpha concen. (pCi/L)	all-pathways dose (mrem/y)	beta-photon dose (mrem/y)	alpha concen. (pCi/L)	all-pathways dose (mrem/y)	beta-photon dose (mrem/y)	alpha concen. (pCi/L)	all-pathways dose (mrem/y)
42base	Base analysis case	2.13E-05	1.02E-16	7.78E-05	1.02E-02	3.39E-02	7.00E-02	1.25E-02 [76,500 y]	5.42E-01 [100,000 y]	5.88E-01 [100,000 y]
42break	Best estimate case	4.67E-11	2.25E-22	1.71E-10	3.46E-07	5.01E-08	1.31E-06	1.85E-06 [20,000 y]	9.29E-07 [20,000 y]	7.63E-06 [20,000 y]
Facility Cases										
42break	Full barrier	4.67E-11	2.25E-22	1.71E-10	3.46E-07	5.01E-08	1.31E-06	1.85E-06 [20,000 y]	9.29E-07 [20,000 y]	7.63E-06 [20,000 y]
50break	Full barrier - 50 mm/y	2.09E-09	9.64E-21	7.33E-09	7.92E-07	8.94E-07	3.76E-06	3.03E-06 [20,000 y]	5.43E-06 [20,000 y]	1.63E-05 [20,000 y]
42vert	Vertical barrier	0.00E+00	0.00E+00	0.00E+00	2.03E-07	8.97E-09	7.51E-07	1.2E-06 [20,000 y]	3.14E-07 [20,000 y]	4.68E-06 [20,000 y]
42short	Shorter capillary break	8.53E-10	4.10E-21	3.12E-09	1.05E-06	6.03E-07	4.41E-06	3.94E-06 [20,000 y]	5.24E-06 [20,000 y]	1.94E-05 [20,000 y]
42vault	Concrete vault - base	6.05E-03	9.19E-10	2.21E-02	1.81E-02	6.94E-01	7.38E-01	1.85E-02 [20,000 y]	7.41E-01 [20,000 y]	7.90E-01 [20,000 y]
42all	No sideslope	1.10E-06	5.28E-18	4.01E-06	9.98E-03	8.61E-03	4.48E-02	1.21E-02 [17,400 y]	2.76E-01 [20,000 y]	3.13E-01 [20,000 y]
Waste Form Release										

Table 4-1. Summary of Estimated Impacts for 2001 ILAW PA

INTEG Filename	Case Designation	Estimated Impact at 1,000 y after Facility Closure (1)			Estimated Impact at 10,000 y after Facility Closure (1)			Maximum Estimated Impact (1) [peak time or max time for calculation]		
		beta/ photon dose (mrem/y)	alpha concen. (pCi/L)	all-pathways dose (mrem/y)	beta-photon dose (mrem/y)	alpha concen. (pCi/L)	all-pathways dose (mrem/y)	beta-photon dose (mrem/y)	alpha concen. (pCi/L)	all-pathways dose (mrem/y)
42for	Forward rate	2.08E-04	9.98E-16	7.59E-04	9.08E-02	3.32E-01	6.54E-01	9.89E-02 [20,000 y]	3.13E+00 [20,000 y]	3.41E+00 [20,000 y]
42noion	No ion exchange	1.68E-05	8.06E-17	6.13E-05	8.41E-03	2.72E-02	5.71E-02	1.04E-02 [20,000 y]	2.91E-01 [20,000 y]	3.21E-01 [20,000 y]
42highion	Forward rate + 5X ion exchange	2.18E-04	1.05E-15	7.97E-04	1.00E-01	3.92E-01	7.46E-01	1.09E-01 [18,700 y]	3.45E+00 [20,000 y]	3.77E+00 [20,000 y]
42nosec	No secondary phase	1.06E-05	5.08E-17	3.86E-05	5.39E-03	1.75E-02	3.67E-02	6.60E-03 [20,000 y]	1.86E-01 [20,000 y]	2.05E-01 [20,000 y]
01	Recharge = 0.1 mm/y	6.95E-12	3.34E-23	2.54E-11	7.16E-07	1.84E-08	2.64E-06	3.23E-06 [20,000 y]	6.30E-07 [20,000 y]	1.24E-05 [20,000 y]
09	Recharge = 0.9 mm/y	3.76E-09	1.81E-20	1.38E-08	1.41E-04	5.18E-06	5.22E-04	1.81E-04 [20,000 y]	2.57E-04 [20,000 y]	9.10E-04 [20,000 y]
50	Recharge = 50 mm/y	4.00E-2	2.63E-01	3.99E-01	3.76E-02	1.52E+00	1.61E+00	7.62E-02 [300 y]	1.56E+00 [3,400 y]	1.65e+00 [3,400 y]
42sandfill	Sand backfill	4.48E-04	2.15E-15	1.64E-03	1.77E-02	1.76E-01	2.35E-01	1.80E-02 [4,700 y]	6.65E-01 [20,000 y]	7.11E-01 [20,000 y]

Table 4-1. Summary of Estimated Impacts for 2001 ILAW PA

INTEG Filename	Case Designation	Estimated Impact at 1,000 y after Facility Closure (1)			Estimated Impact at 10,000 y after Facility Closure (1)			Maximum Estimated Impact (1) [peak time or max time for calculation]		
		beta/ photon dose (mrem/y)	alpha concen. (pCi/L)	all-pathways dose (mrem/y)	beta-photon dose (mrem/y)	alpha concen. (pCi/L)	all-pathways dose (mrem/y)	beta-photon dose (mrem/y)	alpha concen. (pCi/L)	all-pathways dose (mrem/y)
42sdiff	10X WF aqueous diffusion	4.03E-06	1.94E-17	1.47E-05	1.20E-04	1.21E-03	1.61E-03	1.31E-04 [20,000 y]	4.52E-03 [20,000 y]	4.89E-03 [20,000 y]
42steel	Steel included	2.18E-05	1.05E-16	7.96E-05	1.01E-02	3.39E-02	6.98E-02	1.49E-02 [20,000 y]	3.57E-01 [20,000 y]	4.02E-01 [20,000 y]
42condlayr	Top conditioning Layer	2.11E-05	1.02E-16	7.72E-05	9.44E-03	3.31E-02	6.66E-02	1.10E-02 [20,000 y]	3.26E-01 [20,000 y]	3.58E-01 [20,000 y]
42altglass	HLP-31 glass	2.57E-03	1.24E-14	9.41E-03	6.77E-01	3.87E+00	6.23E+00	6.78E-01 [9,200 y]	2.40E+01 [20,000 y]	2.56E+01 [20,000 y]
Vadose Zone Cases										
42iso	Isotropic field flow	1.32E-05	6.35E-17	4.83E-05	1.02E-02	1.26E-02	4.96E-02	1.22E-02 [20,000 y]	3.02E-01 [20,000 y]	3.39E-01 [20,000 y]
42sand	All sand	5.37E-06	2.58E-17	1.96E-05	1.00E-02	2.54E-03	3.91E-02	1.24E-02 [52,500 y]	5.36E-01 [100,000 y]	5.85E-01 [100,000 y]
42grav	All gravel	1.04E-04	1.84E-09	3.80E-04	1.05E-02	3.60E-01	3.87E-01	1.24E-02 [52,000 y]	5.43E-01 [100,000 y]	5.92E-01 [100,000 y]
42deep	VZ - 3 m thicker	1.78E-05	8.56E-17	6.51E-05	1.02E-02	3.24E-02	6.86E-02	1.24E-02 [52,000 y]	5.37E-01 [100,000 y]	5.86E-01 [100,000 y]
42dike	Clastic dike	1.91E-05	9.16E-17	6.96E-05	1.01E-02	2.81E-02	6.42E-02	1.22E-02 [20,000 y]	3.32E-01 [20,000 y]	3.68E-01 [20,000 y]

Table 4-1. Summary of Estimated Impacts for 2001 ILAW PA

INTEG Filename	Case Designation	Estimated Impact at 1,000 y after Facility Closure [1]			Estimated Impact at 10,000 y after Facility Closure [1]			Maximum Estimated Impact [1] [peak time or max time for calculation]		
		beta/ photon dose (mrem/y)	alpha concen. (pCi/L)	all-pathways dose (mrem/y)	beta-photon dose (mrem/y)	alpha concen. (pCi/L)	all-pathways dose (mrem/y)	beta-photon dose (mrem/y)	alpha concen. (pCi/L)	all-pathways dose (mrem/y)
42ukd0	U $K_d = 0$	2.13E-05	6.12E-04	2.09E-04	1.02E-02	3.07E-01	1.29E-01	1.24E-02 [52,500 y]	5.41E-01 [100,000 y]	5.87E-01 [100,000 y]
42kd0	$K_d = 0$ for all radionuclides [2]	3.11E-05	1.6E-02 (3.78E-06)	3.68E-02	1.49E-02	4.34e+00 (5.95E-03)	8.69E+00	1.82E-02 [54,500 y]	4.70E+00 [15,000 y] (5.15E-02 [100,000 y])	9.05E+00 [13,000 y]
42diff	10X increase in Difusion	3.17E-05	1.52E-16	1.16E-04	1.02E-02	4.46E-02	8.05E-02	1.22E-02 [20,000 y]	3.57E-01 [20,000 y]	3.93E-01 [20,000 y]
42disp	2X increase in dispersion	3.76E-05	1.81E-16	1.37E-04	1.02E-02	5.17E-02	8.73E-02	1.22E-02 [20,000 y]	3.50E-01 [20,000 y]	3.86E-01 [20,000 y]
Groundwater Cases										
42base[4]	Well intercept. = 1000m	1.58E-05	7.58E-17	5.78E-05	7.58E-03	2.52E-02	5.20E-02	9.29E-03 [76,500 y]	4.03E-01 [100,000 y]	4.37E-01 [100,000 y]
42base[4]	Well intercept. = CR	1.99E-06	9.52E-18	7.26E-06	9.52E-04	3.16E-03	6.53E-03	1.17E-03 [76,500 y]	5.06E-02 [100,000 y]	5.49E-02 [100,000 y]
42base[4]	Trench at south end	3.20E-05	1.53E-16	1.17E-04	1.53E-02	5.09E-02	1.05E-01	1.88E-02 [76,500 y]	8.13E-01 [100,000 y]	8.82E-01 [100,000 y]

Table 4-1. Summary of Estimated Impacts for 2001 ILAW PA

INTEG Filename	Case Designation	Estimated Impact at 1,000 y after Facility Closure (1)			Estimated Impact at 10,000 y after Facility Closure (1)			Maximum Estimated Impact (1) [peak time or max time for calculation]		
		beta/ photon dose (mrem/y)	alpha concen. (pCi/L)	all-pathways dose (mrem/y)	beta-photon dose (mrem/y)	alpha concen. (pCi/L)	all-pathways dose (mrem/y)	beta-photon dose (mrem/y)	alpha concen. (pCi/L)	all-pathways dose (mrem/y)
42base(4)	90° rotation	4.07E-05	1.95E-16	1.49E-04	1.95E-02	6.47E-02	1.34E-01	2.39E-02 [76,500 y]	1.04E+00 [100,000 y]	1.12E+00 [100,000 y]
42base(4)	Smaller layout	5.75E-06	2.75E-17	2.10E-05	2.75E-03	9.15E-03	1.89E-02	3.38E-03 [76,500 y]	1.46E-01 [100,000 y]	1.59E-01 [100,000 y]
42base(4)	Larger layout	2.56E-05	1.22E-16	9.34E-05	1.22E-02	4.07E-02	8.40E-02	1.50E-02 [76,500 y]	6.50E-01 [100,000 y]	7.06E-01 [100,000 y]
42vault(5)	Existing vault site	2.60E-03	3.95E-10	9.50E-03	7.78E-03	2.98E-01	3.17E-01	7.74E-03 [20,000 y]	3.19E-01 [100,000 y]	3.40E-01 [100,000 y]
42base(4)	30 L/d pumping	2.13E-05	1.02E-16	7.78E-05	1.02E-02	3.39E-02	7.00E-02	1.25E-02 [76,500 y]	5.42E-01 [100,000 y]	5.88E-01 [100,000 y]
42base(4)	100 L/d pumping	2.13E-05	1.02E-16	7.78E-05	1.02E-02	3.39E-02	7.00E-02	1.25E-02 [76,500 y]	5.42E-01 [100,000 y]	5.88E-01 [100,000 y]
42base(4)	300 L/d pumping	2.13E-05	1.02E-16	7.78E-05	1.02E-02	3.39E-02	7.00E-02	1.25E-02 [76,500 y]	5.42E-01 [100,000 y]	5.88E-01 [100,000 y]
42base(4)	1000 L/d pumping	2.13E-05	1.02E-16	7.78E-05	1.02E-02	3.39E-02	7.00E-02	1.25E-02 [76,500 y]	5.42E-01 [100,000 y]	5.88E-01 [100,000 y]
42base(4)	Reduced hyd. Cond (3X)	2.55E-04	1.22E-15	9.32E-04	1.22E-01	4.06E-01	8.39E-01	1.50E-01 [76,500 y]	6.49E+00 [100,000 y]	7.04E+00 [100,000 y]
42base(4)	Regional recharge increase (3X)	1.96E-05	9.38E-17	7.16E-05	9.38E-03	3.12E-02	6.44E-02	1.15E-02 [76,500 y]	4.99E-01 [100,000 y]	5.41E-01 [100,000 y]

Table 4-1. Summary of Estimated Impacts for 2001 ILAW PA

INTEG Filename	Case Designation	Estimated Impact at 1,000 y after Facility Closure (1)			Estimated Impact at 10,000 y after Facility Closure (1)			Maximum Estimated Impact (1) [peak time or max time for calculation]		
		beta/ photon dose (mrem/y)	alpha concen. (pCi/L)	all-pathways dose (mrem/y)	beta-photon dose (mrem/y)	alpha concen. (pCi/L)	all-pathways dose (mrem/y)	beta-photon dose (mrem/y)	alpha concen. (pCi/L)	all-pathways dose (mrem/y)
42base(4)	Regional recharge decrease (3X)	1.45E-05	6.94E-17	5.29E-05	6.94E-03	2.31E-02	4.76E-02	8.50E-03 [76,500 y]	3.69E-01 [100,000 y]	4.00E-01 [100,000 y]
42base(4)	Decrease regional upgradient boundaries (2X)	1.79E-05	8.57E-17	6.54E-05	8.57E-03	2.85E-02	5.88E-02	1.05E-02 [76,500 y]	4.55E-01 [100,000 y]	4.94E-01 [100,000 y]
Inventory Cases										
42maxTc	Increase Tc inventory 5X	7.03E-05	1.02E-16	2.98E-04	3.35E-02	3.39E-02	1.75E-01	3.99E-02 [20,000 y]	5.37E-01 [100,000 y]	6.95E-01 [100,000 y]
42noTc	Reduce Tc to 0	9.00E-06	1.02E-16	2.26E-05	4.33E-03	3.39E-02	4.38E-02	6.05E-03 [100,000 y]	5.37E-01 [100,000 y]	5.59E-01 [100,000 y]
42-2i	Double I inventory	3.01E-05	1.02E-16	1.00E-04	1.45E-02	3.39E-02	8.10E-02	1.82E-02 [80,000 y]	5.37E-01 [100,000 y]	6.01E-01 [100,000 y]
42-2u	Double U inventory	2.13E-05	1.02E-16	7.78E-05	1.02E-02	5.82E-02	7.55E-02	1.24E-02 [52,000 y]	8.72E-01 [96,000 y]	6.77E-01 [100,000 y]
42ub	All inventory at bounding	5.52E-05	4.83E-16	1.73E-04	2.66E-02	1.86E-01	3.11E-01	3.47E-02 [100,000 y]	2.76E+00 [100,000 y]	2.95E+00 [32,000 y]

Table 4-1. Summary of Estimated Impacts for 2001 ILAW PA

INTEG Filename	Case Designation	Estimated Impact at 1,000 y after Facility Closure (1)			Estimated Impact at 10,000 y after Facility Closure (1)			Maximum Estimated Impact (1) [peak time or max time for calculation]		
		beta/ photon dose (mrem/y)	alpha concen. (pCi/L)	all-pathways dose (mrem/y)	beta-photon dose (mrem/y)	alpha concen. (pCi/L)	all-pathways dose (mrem/y)	beta-photon dose (mrem/y)	alpha concen. (pCi/L)	all-pathways dose (mrem/y)
42ubmaxTc	Bounding value + max Tc	1.02E-04	4.83E-16	3.85E-04	4.90E-02	1.86E-01	4.12E-01	5.96E-02 [50,500 y]	2.76E+00 [100,000 y]	3.07E+00 [32,000 y]
Dosimetry Cases										
ind-100m	Industrial	9.86E-06	1.02E-16	9.86E-06	4.71E-03	3.39E-02	1.69E-02	5.71E-03 [53,000 y]	5.37E-01 [100,000 y]	2.08E-01 [100,000 y]
res-100m	Residential	2.88E-05	1.02E-16	3.44E-05	1.38E-02	3.39E-02	5.68E-02	1.68E-02 [53,000 y]	5.37E-01 [100,000 y]	6.89E-01 [100,000 y]
agr-100m	Agricultural	2.88E-05	1.02E-16	1.26E-04	1.38E-02	3.39E-02	1.01E-01	1.68E-02 [53,000 y]	5.37E-01 [100,000 y]	7.48E-01 [100,000 y]
nat-CR	Native American (3)	4.52E-06	1.07E-17	2.77E-05	2.16E-03	3.55E-03	2.22E-02	2.63E-03 [52,500 y]	5.62E-02 [100,000 y]	1.64E-01 [100,000 y]
CRPop-CR	CR population (3)	1.12E-02	1.07E-17	3.42E-02	5.33E+00	3.55E-03	3.28E+02	6.49E+0 [53,000 y]	5.62E-02 [100,000y]	2.91E+02 [100,000 y]
DOE-100m	DOE dose parameters	2.00E-05	1.02E-16	7.15E-05	9.59E-03	3.39E-02	6.35E-02	1.17E-02 [57,000 y]	5.37E-01 [100,000 y]	5.26E-01 [100,000 y]
Other Sensitivity Cases										

Table 4-1. Summary of Estimated Impacts for 2001 ILAW PA

INTEG Filename	Case Designation	Estimated Impact at 1,000 y after Facility Closure (1)			Estimated Impact at 10,000 y after Facility Closure (1)			Maximum Estimated Impact (1) [peak time or max time for calculation]		
		beta/ photon dose (mrem/y)	alpha concen. (pCi/L)	all-pathways dose (mrem/y)	beta-photon dose (mrem/y)	alpha concen. (pCi/L)	all-pathways dose (mrem/y)	beta-photon dose (mrem/y)	alpha concen. (pCi/L)	all-pathways dose (mrem/y)
42sub	Cap break subsidence	5.33E-09	2.56E-20	1.95E-08	3.97E-03	2.35E-05	1.45E-02	5.22E-03 [19,000 y]	1.28E-02 [20,000 y]	3.15E-02 [20,000 y]
Pulse42	Pulse	7.41E+00	3.56E-11	2.71E+01	5.18E-12	6.50E+01	6.29E+01	1.69E+01 [1,380 y]	6.93E+01 [11,100 y]	6.72E+01 [11,200 y]
42instant (2)	Instantaneous VZ transport	2.87E-03	1.48E+0 (3.49E-04)	3.39E+00	1.61E-02	4.68E+00 (6.4E-03)	9.36E+00	7.96E-01 [33 y]	4.83E+00 [13,100 y] (5.16E-02 [100,000 y])	9.43E+00 [11,100 y]
42conc	Concrete K_ds	1.37E-05	1.02E-16	5.87E-05	9.98E-03	5.56E-04	3.73E-02	1.24E-02 [53,000 y]	4.74E-01 [100,000 y]	5.22E-01 [100,000 y]

(1) The estimated impacts are associated with a well located 100 meters downgradient form the ILAW site.

(2) The numbers in parentheses are the estimated radium concentrations.

(3) The estimated impacts are calculated for a well just before the aquifer flows into the Columbia River. The appropriate WIF is provided in Bergeron 2000.

(4) The estimated impacts use the ratio of the WIFs provided in Bergeron (2000) times the Base Analysis Case estimated impacts.

(5) The estimated impact use the existing vault WIF provided in Bergeron (2000) with the vault calculation.

5.0 REFERENCES

Bacon 2000, D.H. Bacon, M.D. White, and B.P. McGrail, *Subsurface Transport Over Reactive Multiphases (STORM): A General, Coupled Nonisothermal Multiphase Flow, Reactive Transport, and Porous Medium Alteration Simulator, Version2, User's Guide*, PNNL-13108, Pacific Northwest National Laboratory, Richland, Washington, February 2000.

Bacon 2001, D. H. Bacon and B. P. McGrail, *Waste Form Release Calculations for the 2001 Immobilized Low-Activity Waste Performance Assessment*, PNNL-13369, Pacific Northwest National Laboratory, Richland, Washington, February 2001. This document is included in Appendix B of this report.

Bergeron 2000, M. P. Bergeron and S. K. Wurstner, *Groundwater Transport Calculations Supporting the Immobilized Low-Activity Waste Disposal Facility Performance Assessment*, PNNL-13400, Pacific Northwest National Laboratory, Richland, Washington, December 2000. This document is included in Appendix C of this report.

Cole 1997, C. R. Cole, S. K. Wurstner, M. P. Bergeron, M. D. Williams, P. D. Thorne, *Three-dimensional Analysis of Future Groundwater Flow Conditions and Contaminant Plume Transport in the Hanford Site Unconfined Aquifer System: FY 1997 Status Report*, PNNL-11801, Pacific Northwest Laboratory, Richland, Washington, December 1997.

DOE 1997a, "Record of Decision for the Tank Waste Remediation System, Hanford Site, Richland, Washington," Federal Register, Volume 62, page 8693, February 26, 1997.

DOE 1997b, *Waste Management Programmatic Environmental Impact Statement For Managing Treatment, Storage, and Disposal of Radioactive and Hazardous Waste*, DOE/EIS-0200-F, U.S. Department of Energy, Washington, D.C., May 1997.

[Pages 50 to 59 of the summary provide information of the low-level waste in the DOE complex, while pages 70 through 77 discusses high-level waste. Note that this EIS does not separate the Hanford Site tank waste into low- and high-level components.]

DOE 1999, Conditional Acceptance of the Immobilized Low-Activity Tank Waste Disposal Facility Performance Assessment and the Hanford Site 200 Plateau Composite Analysis, Memorandum from James J. Fiore and Mark W. Frei to Richard French and Keith A. Klein, U.S. Department of Energy, Washington, D.C., October 20, 1999.

DOE/RL 2000, *Selection and Review of a Site-Wide Groundwater Model at the Hanford Site*, DOE/RL-2000-11, U.S. Department of Energy, Richland Operations Office, Richland, Washington, May 2000.

Ecology 1998, Washington State Department of Ecology, U. S. Environmental Protection Agency, U. S. Department of Energy, Hanford Facility Agreement and Consent Order, as amended through December 31, 1998, 89-10, Rev. 6. This document is available from any of the parties.

[1. Appendix D lists the activities and associated milestones. Activities 45 (closure of single-shell tanks), 50 (pretreatment processing), 60 (vitrification of Hanford low-level waste), and 90 (disposal of the immobilized low-activity waste) cover areas of concern for this performance assessment.]

Gupta 1987, S. K. Gupta, C. R. Cole, C. T. Kincaid, and A. M. Monti, *Coupled Fluid, Energy, and Solute Transport (CFEST) Model: Formulation and User's Manual*, BMI/ONWI-660, Battelle Memorial Institute, Columbus, Ohio, October 1987.

Finfrock 2000, S. H. Finfrock, E. J. Freeman, R. Khaleel, and R. J. Puigh, *Near Field, Far Field, and Estimated Impact Calculations for the Hanford Immobilized Low-Activity Tank Waste Performance Assessment: 2001 Version*, RPP-7463, Fluor Federal Services, Richland, Washington, December 2000. This document is included in Appendix A of this report.

Huyakon and Panday 1999, P.S. Huyakon and S Panday, *VAM3DF - Variably Saturated Analysis Model in Three Dimensions for the Data Fusion System: Documentation and User's Guide*, Version 2.0, HydroGeologic, Inc., Herndon, Virginia, 1999.

Kincaid 1998, C. T. Kincaid, M. P. Bergeron, C. R. Cole, M. D. Freshley, N. L. Hassig, V. G. Johnson, D. I. Kaplan, R. J. Serne, G. P. Streile, D. L. Strenge, P. D. Thorne, L. W. Vail, G. A. Whyatt, S. K. Wurstner, *Composite Analysis for Low-Level Waste Disposal in the 200-Area Plateau of the Hanford Site*, PNNL-11800, Pacific Northwest National Laboratory, Richland, Washington, March 1998.

Mann 1996, F. M. Mann, *INTEG: A Program to Calculate Groundwater Contamination and Human Doses*, WHC-SD-WM-RPT-219, Westinghouse Hanford Company, Richland, Washington, June 1996.

Mann 1999, F. M. Mann, *Scenarios for the Hanford Immobilized Low-Activity Waste (ILAW) Performance Assessment*, HNF-EP-0828, Rev. 3, Lockheed Martin Hanford Company, Richland, Washington, August 1999. Also Appendix B of Mann/Puigh 2000.

Mann/Puigh 2000, F. M. Mann and R. J. Puigh II, *Data Packages for the Hanford Immobilized Low-Activity Tank Waste Performance Assessment: 2001 Version*, HNF-5636, Rev. 0A, Fluor Federal Services, Richland, Washington, February 2000.

Rawlins 1994, J. A. Rawlins, R. A. Karnesky, R. Khaleel, A. H. Lu, F. M. Mann, B. P. McGrail, W. J. McMahon, M. G. Piepho, P. D. Rittmann, and F. A. Schmittroth, Impacts of *Disposal System Design Options on Low-Level Glass Waste Disposal System Performance*, WHC-EP-0810, Revision 0, Richland, Washington, September 1994.

Rittmann 1993, P. D. Rittmann, *GRTPA - A Program to Calculate Human Dose from PORFLOW Output*, WHC-SD-WM-UM-018, Westinghouse Hanford Company, Richland, Washington, November 1993.

Wagoner 1996, J. D. Wagoner (Manager, Richland Operations), letter to contractors, Richland, Washington, re: "Single 'Groundwater Project' for the Hanford Site', Department of Energy, Richland, Washington, September 5, 1996.

Wurstner 1997, S. K. Wurstner, Thorne, M. A. Chamness, M. D. Freshley, and M. D. Williams, *Development of a Three-dimensional Groundwater Model of the Hanford Site Unconfined Aquifer System: FY 1995 Status Report*, PNL-10886, Pacific Northwest Laboratory, Richland, Washington, December 1997.

This page intentionally left blank.

APPENDIX A

APPENDIX A

Near Field, Far Field, and Estimated Impact Calculations for the Hanford Immobilized, Low-Activity Tank Waste Performance Assessment: 2001 Version

Prepared by:

SH Finfrock, EJ Freeman, R Khaleel, and RJ Puigh
Fluor Federal Services

Date Published
December 2000

Prepared for the Department of Energy

CH2M Hill Hanford Group, Inc.
Richland, Washington

Hanford Management and Integration Contractor for the
U.S. Department of Energy under Contract DE-AC06-99RL14047

This page intentionally left blank

1.0 INTRODUCTION A-7
2.0 METHODS A-8
2.1 VAM3DF A-8
2.2 INTEG A-8
2.3 UTILITY CODES A-9
2.3.1 Bcflow A-10
2.3.2 Storm2vam A-10
2.3.3 Botflux A-11
3.0 MODELS AND ASSUMPTIONS A-13
3.1 NEAR FIELD MODELS A-13
3.1.1 Model Description A-13
3.1.2 Boundary and Initial Conditions A-15
3.1.3 Grid Spacing A-16
3.1.4 Code Inputs and Outputs A-16
3.2 FAR FIELD MODELS A-16
3.2.1 Model Descriptions A-17
3.2.2 Boundary and Initial Conditions A-18
3.2.3 Grid Spacing A-20
3.2.4 Time Steps A-20
3.2.5 Code Inputs and Outputs A-20
3.3 INTEGRATION CALCULATIONS A-21
4.0 CASE DESCRIPTIONS A-22
4.1 NEAR FIELD CASES A-22
4.2 FAR FIELD FLOW CASES A-22
4.3 FAR FIELD TRANSPORT CASES A-22
4.4 INTEGRATION CASES A-22
4.5 SPECIAL CASES A-29
4.5.1 Bathtub Effect A-29
4.5.2 Instantaneous Vadose Zone Transport A-29
4.5.3 Instantaneous Waste Form Release A-29
5.0 SIMULATION RESULTS A-30
5.1 NEAR FIELD A-30

5.2 FAR FIELD FLOW CASES A-31
5.3 FAR FIELD TRANSPORT CASES A-33
5.4 INTEGRATION CASES A-37
5.5 SPECIAL CASES A-45
5.5.1 Bathtub Case A-45
5.5.2 Instantaneous Vadose Zone Transport A-52
5.5.3 Instantaneous Waste Form Release A-52
6.0 REFERENCES A-54
APPENDIX A. DATA FILE ARCHIVE A-56
APPENDIX B. INTEG LIBRARY FILES A-63
APPENDIX C. BCFLOW A-72
APPENDIX D. STORM2VAM A-80
APPENDIX E. BOTFLUX A-91
APPENDIX F. PEER REVIEW A-108

List of Tables

Table 3-1. Hydraulic Properties for Near Field Materials A-15
Table 3-2. Hydraulic Heads for Various Recharge Estimates for Hanford Sand Unit A-15
Table 3-3. Hydraulic Properties for Far Field Materials A-17
Table 3-4. Transport Properties for Far Field Materials A-18
Table 3-5. Hydraulic Heads for Various Recharge Estimates for Hanford Gravel Unit A-18
Table 3-6. Trench Facility INTEG Parameters A-21
Table 4-1. Near Field Cases A-23
Table 4-2. Far Field Flow Cases A-24
Table 4-3. Far Field Transport Cases A-25
Table 4-4. Integration Cases A-27
Table 5-1. Waste Region Darcy Velocities for the Various Near Field Cases A-30
Table 5-2. Normalized Contaminant Release Rates at the Water Table A-37
Table 5-3. Integration Results A-38
Table 5-4. Fractional Radionuclide Concentration for Bathtub Effect A-46
Table 5-5. Estimated Impacts for Bathtub Release after 100 and 1,000 Years A-48
Table 5-6. Instantaneous Waste Form Release Peak Times A-52

List of Figures

Figure 3-1. Trench Facility Model Cross Section....A-13
Figure 3-2. Vault Facility Model Cross Section....A-14
Figure 3-3. Simplified Conceptual Model of the Translation of 1D Waste Form Packages to a 2D Model for the ILAW Remote Handled Trench....A-19
Figure 5-1. Darcy Velocity at the Top of the Far Field for Different Trench Scenarios....A-31
Figure 5-2. Volumetric Water Content in the Far Field for the Base Analysis Case....A-32
Figure 5-3. Volumetric Water Content In the Far Field for the Best Estimate Case....A-33
Figure 5-4. Source Concentration at Top of the Far Field at 1000 Years for K_d=0 mL/g....A-35
Figure 5-5. Source Concentration at Bottom of Far Field at 1,000 Years for K_d=0 mL/g....A-35
Figure 5-6. Normalized Contaminant Flux into Aquifer at Four Recharge Rates....A-36
Figure 5-7. Normalized Contaminant Flux into the Aquifer at 4.2 mm/y for Four Geochemical Retardation Factors....A-36
Figure 5-8. Tc-99 Released from the STORM model as a Function of Time to Bathtub Failure....A-47
Figure 5-9. Estimated All-Pathway Dose at Well 100 m Downgradient Assuming All Radionuclides are Not Retarded....A-51
Figure 5-10. Estimated All-Pathway Dose at Well 100 m Downgradient Assuming Only Radionuclides with K_d = 0 or 0.6 mL/g are Not Retarded....A-52
Figure 5-11. Instantaneous Waste Form Release Case – Release Rates to Aquifer....A-53

This page intentionally left blank.

1.0 INTRODUCTION

Prediction of the expected dose, to a downstream receptor, resulting from the release of contaminants from the Immobilized Low-Activity Waste (ILAW) disposal site is a multi-step process that includes several different modeling operations. The process can be roughly divided into five modeling phases: migration of moisture into the disposal facility, release of contaminants from the waste form, transport of the contaminants through the vadose zone, dilution of the contaminant in the groundwater, and doses due to predicted exposures.

This report documents the models and calculations used to predict the near field moisture flow, the far field moisture flow, the contaminant transport in the vadose zone, and the estimated impacts associated with various exposure scenarios (doses based on established exposure scenarios [Mann 1999]). Appendix A describes the data file archive for the calculations described in this report.

Transport of contaminants through the vadose zone is driven by water infiltration into the disposal site and regulated by the physical and chemical nature of the sediments surrounding and beneath the waste packages. These factors, combined with the contaminant release rate from the waste form (Bacon 2000a), determine the rate of contaminant flux into the groundwater. This process consists of three major steps: near field fluid flow modeling, far field fluid flow modeling, and far field contaminant transport modeling. The near field designation applies to the region above and surrounding the waste packages, down to a depth of approximately 5 m below the bottom of the engineered facility. The far field is the region beneath the near field, down to the water table.

The near field and far field model parameters are based on hydraulic and physical properties taken from data packages specific to the ILAW site (compiled in Mann/Puigh 2000a). The stratigraphic profile is derived from borehole lithologic logs, drilled at and near the ILAW site, compiled by Reidel and Horton (1999). Recharge through the surface cover is reported in the data package by Fayer et al. (1999). Hydraulic properties for materials in the near field are reported in Fayer (1992) and Meyer (1999). Hydraulic properties of the porous media in the far field are tabulated in Khaleel (1999). The chemical properties of the near field materials (except waste form) and the far field materials are presented in Kaplan (1999).

The predicted doses are determined by taking the normalized release rate of contaminants into the groundwater, multiplying by the facility inventory of the various radionuclides, applying decay and dilution factors, and multiplying the expected nuclide exposures by the corresponding dose factors (Rittmann 1999).

2.0 METHODS

The primary calculations discussed in this report are performed with two independent computer codes: VAM3DF and INTEG. In addition three utility codes (Bcflow, Storm2vam, and Botflux) are used to process required data into the necessary formats required for VAM3DF and INTEG. These codes are discussed in this section.

2.1 VAM3DF

VAM3DF (typically called VAM) is a proprietary vadose zone/groundwater modeling code. The code and supporting documentation are provided by HydroGeoLogic (HGL) (Huyakorn and Panday 1999). Earlier versions of VAM have been in use at the Hanford Site since the 1980's.

VAM3DF is a three-dimensional saturated-unsaturated groundwater flow and solute transport code, designed for a wide range of physical scenarios including variable water table position and highly non-linear soil moisture conditions. The code employs Galerkin and upstream weighted residual procedures for solving the flow and transport equations.

VAM3DF has been verified and validated (Finfrock 1999). Earlier versions of VAM (e.g., VAM3DCG) have been verified and validated for use at Hanford (Lu and Langford 1995, and Puigh 1998).

For the calculations discussed in this report, VAM3DF is used in two different modes: flow and transport. The flow calculations are used to predict the steady state fluid flow fields in the regions of interest. The transport calculations predict the rate of transport of contaminants in the steady-state fluid flow fields predicted by the flow calculation.

In the context of this study, the flow calculations require only a standard VAM3DF input file (which specifies geometry, materials, boundary conditions, and similar parameters) to run. The flow calculation calculates head, saturation, and three-dimensional fluid flow velocities throughout the model. The output includes a standard (summary) output file, a velocity field file (used by the transport calculations), a data file for plotting, and a flux file indicating flow rates across the boundaries (used by the Bcflow, Botflux, and Storm2vam utility codes).

The transport calculations require the standard input file and the velocity file from the corresponding flow run. The transport run calculates the contaminant concentration throughout the model at each time step. The output includes a standard (summary) output file, and a data file for plotting (this file is also used by the Botflux utility code).

2.2 INTEG

INTEG (Mann 1996) is a computer code developed to take a time variant, normalized contaminant release rate from a waste facility to the groundwater, and determine the resulting expected dose rate.

The code first determines the concentration of each nuclide at the point of interest by solving the equation:

$$C_i(t) = I_i(t)*G_i(t)*R/[r*A]$$

where:

$C_i(t)$ = Concentration at the point of interest for contaminant i at time t.
$I_i(t)$ = Inventory of contaminant i at time t.
$G_i(t)$ = The normalized contaminant flux rate into the groundwater at time t for contaminant i.
R = The well intercept factor (dilution factor from the release point to the exposure point).
r = Surface recharge rate
A = Surface area of facility

Subsequently, INTEG calculates the expected dose at the point of interest by solving the equation:

$$D(t) = \Sigma_i \; Df_i * C_i(t)$$

where i varies over all of the nuclides of interest and Df_i is the dose factor for nuclide i for a given exposure scenario.

The dose factors, inventory, recharge rate, and surface area are all defined by the problem specification. The normalized contaminant flux rate is a result of the VAM3DF transport calculations where the appropriate flux rate is chosen based on the isothermal sorption coefficient (K_d) of the given nuclide (which is part of the problem specification). Finally, the time dependent contaminant inventory is the initial inventory (part of the problem specification) reduced by INTEG according to the given contaminant's decay rate (other nuclides may build up due to the decay of parent nuclides).

The recharge rate, facility area, and well intercept factors are all specified with a script file that controls the execution of the code. This file also specifies the names of files that contain the remainder of the input data. The initial inventory, nuclide decay factors and K_d's, and dose factors are all specified with library files that are reproduced in Appendix B. The primary results of the INTEG calculations are time dependent doses (drinking water and all-pathway) for a given exposure scenario and alpha emitter concentration. These data are written to an output file (the name is specified in the script file). Similar data are written to another file for each nuclide in the database.

2.3 UTILITY CODES

Three utility codes were developed to process the data results of one step in the modeling effort into a form usable as input in another step. These codes primarily just read and write data

and perform simple mathematical operations on the data (e.g., converting units, interpolating between grid positions, etc.).

2.3.1 Bcflow

The Bcflow code takes the volumetric fluid flow rates across the bottom boundary of a near field flow calculation and calculates the effective recharge rate across the top boundary of a far field flow calculation.

The flow rates for each boundary node are read in from the boundary flux (fpl) file from the near field flow calculation. The code assumes that the flow calculation specified the bottom boundary nodes as nodes to be tracked, and that they are the first nodes so specified, and that they are specified in order from left to right within the model. There is also an implicit assumption that the flow run has reached steady-state by the last time step printed to the fpl file.

The code also reads in node coordinate data from an input file named grids.txt. This file must contain the following information:

- The number of node columns in the near field model.
- The x coordinate value for each column (in 8f10.3 format) – from the VAM3DF output.
- The number of columns and the number of rows in the far field model.
- The x coordinate value for each column (in 8f10.3 format) – from the VAM3DF output.

The results of the Bcflow calculation is a file (named bcflow.out), which contains the effective recharge rate for each node in the top boundary of the far field model. The data are in the format required for the VAM3DF input and can be inserted directly into the VAM3DF standard input file.

The source code for Bcflow, along with an example input and output file, are presented in Appendix C.

2.3.2 Storm2vam

The Storm2vam code is used to take one-dimensional contaminant release data from the STORM code (Bacon 2000b) output and produce two-dimensional data that serves as a boundary condition input for the far field transport calculations. The STORM data are in different units than what is needed for VAM3DF and it uses much finer timestepping than is allowed for VAM3DF input. In addition, the STORM calculation is one-dimensional and assumes a certain height (typically the maximum height) for the waste in the facility. In the case of the trench facility, however, the actual height varies so the facility must be broken into regions of different height and the release rate multiplied by the fraction of full height. The code takes the STORM data, converts it to the needed units (Ci/y), factors in the waste height and element width, and prints out a subset of the data in the format required for use in the VAM3DF input file.

Storm2vam requires as input the Bcflow output file from the corresponding near field flow calculation, a Storm2vam input file, and the STORM data file (named 'fluxes'). The STORM data are assumed to be in units of micro-mols/m^2/s. The input file contains the following information:

- Atomic weight of nuclide to be modeled (99.0 for Tc99).
- Ratio of activity to mass (Ci/g) for nuclide (.017 for Tc99).
- Minimum skip factor, maximum skip factor, skip factor multiplier, and maximum number of steps to print.
- Number of waste zones in facility.
- Maximum x coordinate position of first zone and the fraction of full waste height in this zone. This line is repeated for each zone.
- The number of columns and rows in the far field model.
- The x coordinate value for each column (in 8f10.3 format).

The skip factor is the number of time steps in the STORM data to skip over when creating the VAM3DF input. This starts small and is increased at each step by the multiplier until the maximum is reached.

The code produces two output files: storm2vam.out and storm2vam.g17. The '.out' file is a short summary of the results of the conversion and the '.g17' file contains the full data in a format that can be inserted directly into the VAM3DF input file. The code also prints out the equivalent length of the facility if all zones were full height waste. This number is needed for calculating the effective inventory of the model (based on the STORM data), which is used as an input for the Botflux code.

The source code for Storm2vam, along with an example input and output files, are shown in Appendix D.

2.3.3 Botflux

The Botflux code takes the contaminant concentration at the bottom boundary nodes from one or more far field transport calculation and multiplies them by the volumetric fluid flow across the boundary (from the far field flow calculation) to determine the total contaminant transport rate across the boundary. The data are printed out in a format usable by the INTEG code. Typically, transport calculations with different K_d values are combined into a single output file using this code.

The code requires a nodal data (ppl) file from each far field transport calculation to be included, and a boundary flux (fpl) file from the corresponding far field flow calculation. In addition a number of direct inputs are required (these are typically redirected from a file). The required inputs are described below:

- Name of the flow calculation fpl file.

- Number of columns and rows in the far field model.
- Effective nuclide inventory in the model.
- Normalization flag (1 -> the flux will be normalized such that the integral will equal 1.0).
- Time offset (a number of years to add to the time step, equal to the time between the effective date of the INTEG inventory data and the start of the VAM3DF transport
- calculations).
- Number of transport calculations to include (up to a maximum of 8).
- Name of transport calculation nodal data file. This is repeated for each transport
- calculation to be included.

The effective inventory should be calculated from the following equation:

$$I = H * r1 * r2 * Pg * r3 * L$$

where:

H = Height of waste assumed in STORM calculation (typically 5.6 m for the trench and 8.4 m for the vault).
r1 = Fraction of full density of glass (typically 0.98).
r2 = Fraction of height (H) that is glass (typically 0.85).
Pg = Density of glass in mol/m^3 (typically 38776.1450).
r3 = Ratio of nuclide to glass in micromols/mol (typically 0.659).
L = Equivalent length of waste region if all waste were full height (from Storm2vam output).

The output of the code is time dependent, normalized contaminant flux across the bottom boundary of the model. The data are written to a file named botflux.out, where each transport case corresponds to a column in the file. The output file can be used as input for an INTEG calculation after replacing the header lines with the required INTEG header lines.

The source code for Botflux, along with an example input and output files, are shown in Appendix E.

3.0 MODELS AND ASSUMPTIONS

3.1 NEAR FIELD MODELS

The near field region (primarily the engineered facility) significantly alters the flow field from what would be present in an undisturbed environment. It is necessary, therefore, to predict these flow fields so that the fluid flux into the far field can be characterized and the appropriate waste form release simulations used. The flow fields in the near field are primarily driven by the surface recharge rates and the facility design. The material properties of the backfill and surrounding soils will also affect the results, but to a lesser degree.

3.1.1 Model Description

Figure 3-1 is a sketch of the remote handled trench disposal facility. The near field region is modeled as a two dimensional, half cell which is symmetrical about the centerline. The top of the near field model corresponds to the bottom of the RCRA subtitle C surface cap (not modeled), and is bounded below by an arbitrary contact immediately below the engineered facility which is located at 15 meters below the pre-disposal site surface grade. The upper-most region of the near field model represents a capillary barrier with a 1 m thick sand layer over a 1 m thick gravel layer. The capillary barrier peaks at the center of the facility at 2.98 m above surface grade, and slopes down at a 2% grade to where the cap ends (at 49 m from the centerline, where the barrier is 2 m above surface grade). Beyond the end of the barrier, the model represents a 'side slope', consisting of backfill material, out to the right hand side of the model.

Figure 3-1. Trench Facility Model Cross Section

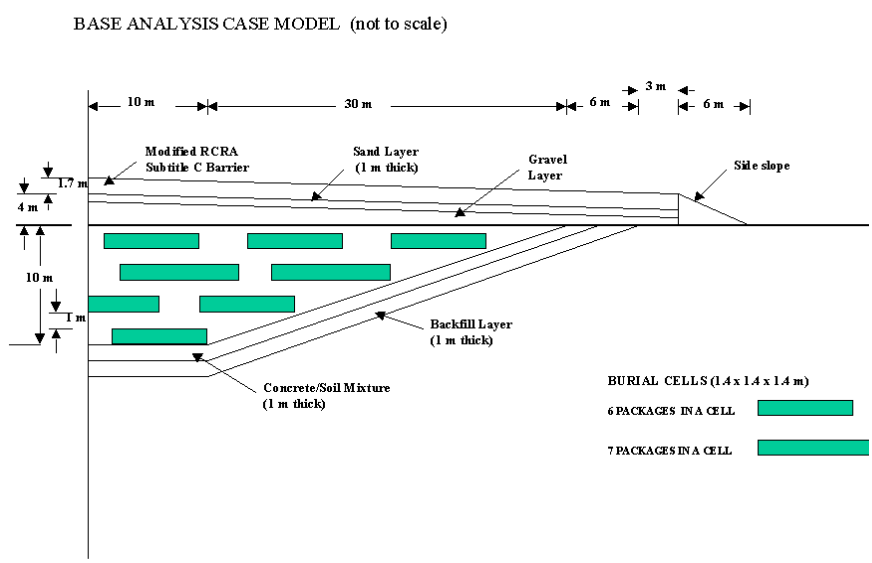

The trench extends from the pre-facility surface grade down to –10 m depth. The floor of the trench extends horizontally from 0 to 10 m, then slopes upward at a 3:1 incline for 30 m. All material inside of the trench is treated as backfill (in the base case), while the sediments outside of the trench are Hanford sands.

The alternate facility (concrete vault concept, see Figure 3-2) top is set 1 m above the pre-facility surface grade and extends down 8 m. The vault forms a box structure that extends 11.5 m out from the centerline. The vault is set in a trench that extends out 17.5 m from the centerline and then slopes up at a 1:1.5 incline for 13.5 m. Again, the material inside the vault, and the material surrounding the vault in the trench, is backfill and the material outside of the trench is Hanford sands. The vault walls are 1 m thick and are modeled as backfill to represent fully degraded concrete. The capillary barrier over the vault peaks at 4.0 m above the pre-facility surface grade (at the centerline) and extends out 17.5 m to the end of the cap. Beyond this point, the downward slope continues with backfill material out to the right hand edge of the model (37 m).

Figure 3-2. Vault Facility Model Cross Section

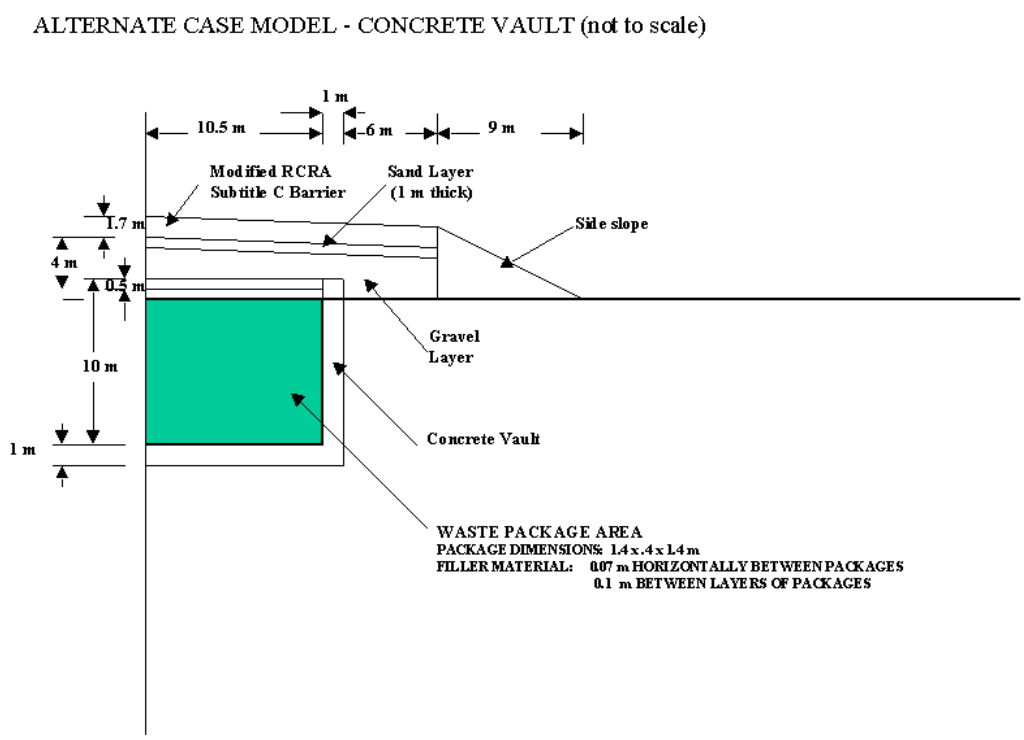

The hydraulic properties used for the various materials in the models are shown in Table 3-1.

Table 3-1. Hydraulic Properties for Near Field Materials

Material	Hydraulic Conductivity K_s (m/y)	Specific Storage S_s (m^{-1})	Saturated Water Content θ_s	Residual Water Saturation θ_r	α (m^{-1})	n*
Backfill	6.03E+2	1.0E-4	0.316	0.1550	3.5	1.72
Sand (barrier)	1.10E+5	1.0E-4	0.419	0.0119	493.0	2.19
Gravel (barrier)	3.45E+4	1.0E-4	0.445	0.0225	7.26	2.80
Hanford Sand	9.09E+2	1.0E-4	0.375	0.1090	5.7	1.77

* This parameter is referred to as β in VAM3DF nomenclature.

3.1.2 Boundary and Initial Conditions

Boundary conditions include flux in at the top of the model and a corresponding constant hydraulic head condition (see Table 3-2) at the bottom of the model. The side boundaries are given the default reflective boundary condition.

Flux applied to the top of the model ranged from 1.0E-4 m/y to 5.0E-2 m/y, depending upon assumed surface recharge conditions. The base case recharge is assumed to be 4.2E-3 m/y over the region where the barrier is present and 5.0E-2 m/y beyond the barrier. This case assumed that the barrier is no longer functional and recharge to the waste packages is at a steady-rate of 4.2E-3 m/y from above. The near field calculations are only performed for fluid flow so there is no contaminant flux included in the models.

The initial condition for the calculations is a constant pressure head corresponding to the predominant recharge rate in the model (see Table 3-2).

Table 3-2. Hydraulic Heads for Various Recharge Estimates for Hanford Sand Unit

Recharge (mm/y)	Pressure Head (m)	Hydraulic Head at Bottom of Near Field
0.1	-7.	-22.0
0.9	-4.	-19.0
4.2	-2.5	-17.5
50.	-1.4	-16.4

3.1.3 Grid Spacing

The near field model is simulated as a two dimensional, vertical slice through the ILAW facility. Lateral gridding is represented by the X coordinate and vertical gridding is represented by the Y coordinate. The grid spacing strategy was developed through an interactive approach that provided the best convergence behavior within a practical model size. The elements in the model are predominantly rectangular, however the elements at the top of the model, representing the capillary break region, are non-rectangular. These elements slope down from left to right, providing interfaces that are at a 2% grade relative to the pre-facility surface grade. This gradient serves to drive the capillary break function.

The near field trench model consists of 137 x 58 quadrilateral grid blocks in the X and Y directions, respectively, for a total of 7946 nodes in an X-Y plane. A third dimension (Z) is required for definition of the model elements. The Z coordinates are 0 and 1, representative of unit depth. A minimum of two Z-planes are required to define the model elements. Therefore, the total number of nodes for the model is 15892, which encompass 7752 elements. Grid spacing in the X direction is 0.5 m through most of the model but drops to 0.25 m near the end of the capillary break (where high run-off conditions are expected). Grid spacing in the Y direction ranges from 0.5 m down to 0.01 meters where material interfaces exist.

The near field vault model consists of 75 x 76 quadrilateral grid blocks in the X and Y directions, respectively, for a total of 5700 nodes in an X-Y plane. There are 11,400 total nodes for both required planes, which represent 5550 model elements. The gridding variations are similar to those in the trench model.

3.1.4 Code Inputs and Outputs

The near field flow calculations use a standard VAM3DF input. The desired output is the boundary flux (fpl) file, which contains the fluid flux at the bottom boundary nodes for a subset of the time steps. The fpl file is used in creating the boundary condition input for the far field calculations (both flow and transport). The input to the far field flow case is created using the Bcflow utility code. The results are produced in a file named bcflow.out. This file, after the header lines are removed, can be inserted directly into a VAM3DF input file. The input to the far field transport case is created using the Storm2vam utility code (which is also used to process the waste form release data). One of the output files from this code, storm2vam.g17, can be imported directly into a VAM3DF input file.

3.2 FAR FIELD MODELS

The far field is the region of the model domain that extends from the base of the engineered facility down to the top of the water table. Two primary model geometries are simulated, representing the remote handled trench and the alternate (vault) facility design. The far field modeling process consists of two stages, first the steady state flow fields are calculated, and then the contaminant transport is calculated. These two steps use the same basic model but with different boundary conditions and material property data, reflective of the flow versus transport problem.

3.2.1 Model Descriptions

The model extends 60 m in the X direction, for the remote handled trench, and 35 m for the vault model. This is the only direct difference between the two geometries (boundary conditions will differ on a case by case basis).

The vertical (Y) dimension for the models extends from below the bottom of the waste disposal facilities down to the ground water. The material beneath the waste facilities is Hanford sand, which is assumed to extend to a depth of 65 m below surface level, at the left hand side of the model, and slopes down to 66 m at the right hand side. Beneath the Hanford sand is the Hanford gravel that extends to the projected post-Hanford water table at 103 m below surface grade. Each material is represented as a homogeneous medium for the respective sediment types. Material hydraulic and physical properties are defined in Khaleel (1999) and are listed in Tables 3-3 and 3-4. The selection of locations for material boundaries are based on well log data reported by Reidel and Horton (1999).

The sediments are assumed to be anisotropic, which means there is spatial distortion caused by lateral pressure gradients and/or sediment layering in the system. Anisotropy of the hydraulic conductivity vectors is assigned to the X and Y directions based on the curves generated by Khaleel (1999). The anisotropy ratio is estimated as 15 for the Hanford sand and 2 for the Hanford gravel (Khaleel 1999). The horizontal hydraulic conductivity (K_h) is then set equal to the reported hydraulic conductivity, while the vertical hydraulic conductivity (K_v) is calculated by dividing K_h by the anisotropy ratio.

For all far field cases, two different transport cases are run to address differences in nuclide isothermal sorption coefficients (K_d). One with a K_d of 0.0 mL/g and another with a K_d of 0.6 mL/g. These K_d's apply to Hanford sands, the K_d in the gravel layer is taken to be one tenth of the value in the sand layer. For the base case, K_d's of 4.0 mL/g and 10.0 mL/g were also used. A variation of the base case was also run using K_d's of 2 and 100 mL/g for the upper one meter in the far field in order to simulate the chemical retardation effect of a concrete layer immediately below the facility.

Table 3-3. Hydraulic Properties for Far Field Materials

Material	Hydraulic Conductivity (Horizontal) K_s (m/y)	Specific Storage S_s	Saturated Water Content θ_s	Residual Water Saturation θ_r	α (m^{-1})	n*
Hanford Sand	9.09E+2	1.0E-4	0.375	0.1090	5.7	1.768
Hanford Gravel	1.77E+2	1.0E-4	0.138	0.07250	2.1	1.374

* This parameter is referred to as β in VAM3DF nomenclature.

Table 3-4. Transport Properties for Far Field Materials

Material	Longitudal Dispersivity (m)	Transverse Dispersivity (m)	Apparent Molecular Diffusion Coefficient (m^2/y)	Effective Porosity	Bulk Density (g/cm^3)
Hanford Sand	2.0	0.2	0.0213	0.375	1.71
Hanford Gravel	0.3	0.03	0.00563	0.138	2.19

3.2.2 Boundary and Initial Conditions

Boundary flow conditions for the model are defined by a constant flux rate at the upper model boundary and a constant hydraulic head at the model base. Fluid fluxes at the surface are derived from the outflow of the near field cases and remain constant over time. Hydraulic heads at the model base corresponds to the pressure head in the Hanford gravel given the steady-state surface flux (see Table 3-5). Side boundaries are implicitly defined as no flow by the numerical code used.

The initial condition for the far field flow calculations is a constant pressure head corresponding to the predominant recharge rate at the surface (see Table 3-5).

Table 3-5. Hydraulic Heads for Various Recharge Estimates for Hanford Gravel Unit

Recharge (mm/y)	Pressure Head (m)	Hydraulic Head at Bottom of Far Field
0.1	-30.	-133.
0.9	-14.	-117.
4.2	-7.	-110.
50.	-3.	-106.

For the contaminant transport calculations, the boundary conditions are time variant mass flux rates (Ci/y at each node) for the top layer of nodes. The contaminant fluxes are derived from the facility release rates as calculated with the STORM code (Bacon 2000b). In addition, the fluid fluxes into the far field are required inputs just as they are for the far field flow calculation. Finally, the steady state flow fields predicted by the far field flow calculations are required inputs.

The facility release rates are calculated in a one-dimensional domain, and must therefore be converted to a two-dimensional domain for use in the far field calculations. This is done by multiplying the facility release rate ($Ci/m^2/y$) by the surface area corresponding to each node. In addition, the one-dimensional model is based on a stack of four waste packages. However, in the

trench, the number of packages stacked varies with distance from the centerline. The facility release rate, therefore, must be reduced by a factor corresponding to the number of waste packages above any given node. Based on the placement of waste packages from the trench design specifications, four packages may be expected to extend out about 8.5 meters. Beyond 8.5 meters there are only three packages that contribute contamination for an additional 6.5 meters. The concentration from these packages is assumed to be 0.75 times the release from four packages. Two packages account for a nine-meter interval with a release rate 0.5 times the original source strength. Waste release equal to one package extends an additional eight meters. Contaminant flux beyond the last waste package is explicitly assigned a value of zero. See Figure 3-3 for a graphical representation of this pattern. The boundaries between these regions do not correspond exactly to the gridding pattern used in constructing the model so the regions will be slightly different sizes than stated here. This does not have a significant impact on the results, however, because the results are normalized to the implied inventory before use. The conversion of the STORM data to the required VAM3DF input is done with the Storm2vam utility code.

Figure 3-3. Simplified Conceptual Model of the Translation of 1D Waste Form Packages to a 2D Model for the ILAW Remote Handled Trench.

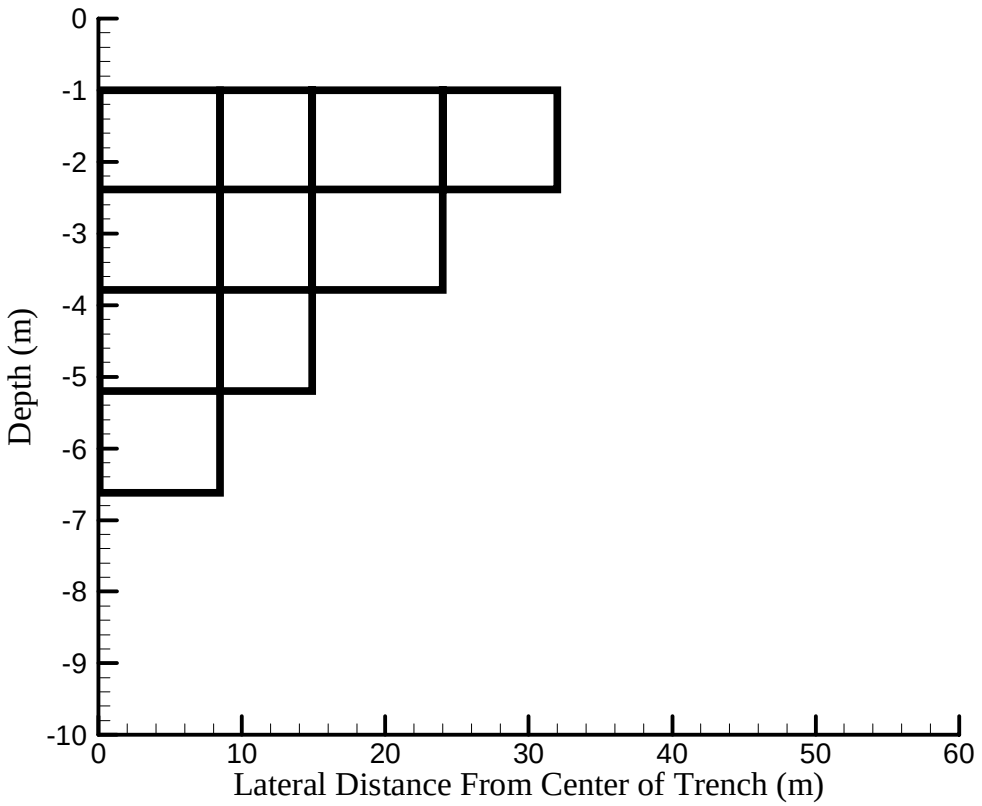

3.2.3 Grid Spacing

The far field model is simulated as a two dimensional, vertical slice through the ILAW site. Lateral gridding is represented by the X coordinate and vertical gridding is represented by the Y coordinate. The gridding in the far field model is similar to that found in the near field model, except that the only non-rectangular elements are in the vicinity of the sand/gravel interface.

The far field trench model consists of 137 x 75 quadrilateral grid blocks in the X and Y directions, respectively, for a total of 10275 nodes in an X-Y plane. A third dimension is required for definition of the model elements. The Z coordinates are 0 and 1, representative of unit depth. A minimum of two Z-planes are required to define the model elements. Therefore, the total number of nodes for the model is 20,550, which encompass 10,064 elements. Grid spacing in the X direction is 0.5 m through most of the model but drops to 0.25 m near the end of the capillary break (where high run-off conditions are expected). Grid spacing in the Y direction ranges from 2.0 m down to 0.25 meters where material interfaces exist.

The far field vault model consists of 71 x 85 quadrilateral grid blocks in the X and Y directions, respectively, for a total of 6,035 nodes in an X-Y plane. There are 12,070 total nodes for both required planes, which represent 5,880 model elements. The gridding variations are similar to those in the trench model.

3.2.4 Time Steps

The initial time step size for fluid flow simulations is small (typically 1.0E-04 y), which is incrementally multiplied by 1.05 until a maximum allowable step size of 10 y is reached. The time step may be reduced automatically in the calculation if convergence problems are encountered but will otherwise remain at the maximum. The calculation then proceeds until the maximum time (typically 2,000 y) is reached.

For the transport simulations, different time stepping patterns are used depending on the times of interest. A typical pattern is 1 y steps out to 100 y, then 10 y steps out to 10,000 y, followed by 20 y steps out to the maximum time (typically 20,000 y).

3.2.5 Code Inputs and Outputs

The far field flow calculations use a standard VAM3DF input file. The top boundary conditions input are derived from the fpl file (via the Bcflux utility code) from the corresponding near field case. The desired output from these calculations is the velocity (vel) file, which contains the Darcy velocity and saturation data for each element. This file is used directly by the VAM3DF transport calculation.

The far field transport calculations use a standard VAM3DF input file and a VAM3DF vel file as inputs. The top boundary conditions input are derived from the waste form release data and the fpl file from the corresponding near field flow calculation. These data are processed by the Storm2vam utility code to produce a file named storm2vam.g17, which can be imported

directly into the VAM3DF input file. The vel file is produced by the corresponding far field flow calculation. The desired output is the nodal data (ppl) file, which contains contaminant concentrations at all nodes for a subset of the time steps. This file is processed by the Botflux utility code to produce a file named botflux.out, which contains normalized data for the contaminant flux rate into the groundwater.

3.3 INTEGRATION CALCULATIONS

The integration calculations take the contaminant release rates from the far field transport calculations and apply decay factors, well intercept factors, and dose factors to determine the expected dose rates over time to down stream receptors. This is done with the INTEG code.

The INTEG cases require several different input files. These include half-life and decay path information for the nuclides considered by the code, K_d's for the important elements, dose factors, and the calculated release rate to the groundwater. All of these files, except for the release rate file, are library files that change for only a few specific cases. The release rate file is created from the botflux.out file from the corresponding far field transport case. A few key parameters such as the recharge rate, facility footprint area, and well intercept factor are input through the script file (run.bat) used to execute the code. The primary output of the code is in a file named casename.out, which contains total dose and nuclide concentration information. Another file, casename.dat, contains similar information broken down by nuclide.

The facility parameters are shown in Tables 3-6 and -7. The base case input files are included in the data file archive, which is described in Appendix A.

Table 3-6. Trench Facility INTEG Parameters

Infiltration rate (mm/y)	0.1	0.9	4.2	50.
Facility Footprint (m^2)	124800.			
Well Intercept Factor* (at 100 m)	2.51E-05	2.26E-04	1.05E-03	1.26E-02

* Well Intercept Factor from Bergeron 2000

Table 3-7. Vault Facility INTEG Parameters

Infiltration rate (mm/y)	0.1	0.9	4.2	50.
Facility Footprint (m^2)	33327.			
Well Intercept Factor (at 100 m)	6.7E-06	6.1E-05	2.8E-04	3.4E-03

* Well Intercept Factor from Bergeron 2000

4.0 CASE DESCRIPTIONS

A number of different cases were evaluated to determine the effect of varying different parameters and assumptions. Some of these cases required a new calculation at every step (near field, far field flow, waste form, far field transport, and integration), some required only a new integration case, and others required a subset of the other steps, in addition to a new integration case. This section describes the different cases calculated at each step. The linkage between these cases is shown in Table A-1. Model details of the different cases can be found in the data file archive, which is described in Appendix A.

4.1 NEAR FIELD CASES

The near field cases represent changes to the surface recharge or the near field geometry or material properties. The individual cases are described in Table 4-1.

4.2 FAR FIELD FLOW CASES

The far field flow cases represent changes to the fluid influx to the far field (i.e., a near field case), far field geometry, or material properties. The individual cases are described in Table 4-2.

4.3 FAR FIELD TRANSPORT CASES

The far field transport cases represent changes to the fluid influx to the far field (i.e., a near field case), the waste form, far field geometry, or material properties. The individual cases are described in Table 4-3.

4.4 INTEGRATION CASES

The integration cases represent any changes to the near field, far field, waste form, or exposure factors. The individual cases are described in Table 4-4.

Table 4-1. Near Field Cases

Case Name	Case ID	Case Description
Base Case	nf42	This case used the basic trench design with the capillary break in place but consisting entirely of sand (and therefore non-functional). The recharge over the cap region was 4.2 mm/y. The side slope and undisturbed region beyond the cap were treated as having a recharge of 50 mm/y.
Low Recharge	nf01	Identical to the base case except that the recharge over the cap is 0.1 mm/y.
Rupert Sand	nf09	Identical to the base case except that the recharge over the cap is 0.9 mm/y, corresponding to Rupert sand.
High Recharge	nf50	Identical to the base case except that the recharge over the cap is 50 mm/y.
No Side Slope	nf42-all	Identical to the base case except that the recharge in the side slope and undisturbed area is 4.2 mm/y instead of 50 mm/y.
Sand Backfill	nf42-sand	Hanford sand is used as the backfill material in the facility.
Best Estimate Case (Capillary Break)	nf42-break	Identical to base case except that the capillary break is functional.
Short Capillary Break	nf42-shortbreak	Identical to the best estimate case except that the capillary break only extends 44 m (instead of 49 m) from the centerline.
Vertical Capillary Break	nf42-vert	Identical to the best estimate case except that a second, vertical, capillary break has been added under the tip of the horizontal capillary break.
Failed Capillary Break (Subsidence)	nf42-subsidence	Identical to the best estimate case except that a region of the capillary break has subsided. A region of the capillary barrier 1 m long (starting at 10 m from the centerline) is displaced downward 0.3 m (the void at the top is filled with sand and the underlying backfill is displaced by gravel).
Capillary Break With High Recharge	nf50-break	Identical to the best estimate case except that the entire surface recharge is at 50 mm/y.
Alternate Facility Design (Vault)	nf42-vault	This case is similar to the base case (using the same recharges and material properties) but has the alternate (vault) facility design.

Table 4-2. Far Field Flow Cases

Case Name	Case ID	Case Description
Base Case (42base)	42base-f	Base case geometry. Top boundary fluid flux derived from near field base case.
Low Recharge	01-f	Top boundary fluid flux derived from near field low recharge case.
Rupert Sand	09-f	Top boundary fluid flux derived from near field Rupert sand case.
High Recharge	50-f	Top boundary fluid flux derived from near field high recharge case.
No Side Slope	42all-f	Top boundary fluid flux derived from near field no side slope case.
Capillary Break	42break-f	Top boundary fluid flux derived from near field capillary break case.
Deep Vadose Zone	42deep-f	The gravel layer is extended down an additional 3 m (to a depth of 106 m). Top boundary fluid flux derived from near field base case.
Clastic Dike	42dike-f	A clastic dike is inserted under the middle of the facility region. The vertical clastic, 0.5 m wide, is located 16 m from the trench center line and extends through the entire far field. Top boundary fluid flux derived from near field base case.
No Sand Layer	42grav-f	Sand layer is replaced with gravel. Top boundary fluid flux derived from near field base case.
Isotropic	42iso-f	Sand and Gravel layers have isotropic conductivity properties. Top boundary fluid flux derived from near field base case.
No Gravel Layer	42sand-f	Gravel layer is replaced with Hanford sand. Top boundary fluid flux derived from near field base case.
Sand Backfill	42sandfill-f	Top boundary fluid flux derived from near field sand backfill case.
Short Capillary Break	42short-f	Top boundary fluid flux derived from near field short capillary break case.
Failed Capillary Break (subsidence)	42sub-f	Top boundary fluid flux derived from near field subsidence case.
Vertical Capillary Break	42vert-f	Top boundary fluid flux derived from near field vertical capillary break case.
Capillary Break with High Recharge	50break-f	Top boundary fluid flux derived from near field capillary break with high recharge case.
Vault	42vault-f	Vault geometry model (similar to base case except that it is only 35 m wide instead of 60 m). Top boundary fluid flux derived from near field vault case.

Table 4-3. Far Field Transport Cases

Case Name	Case ID	Case Description
Base Case (42base)	42base-t	Base case geometry. Fluid velocity fields taken from fluid flow base case. Top boundary contaminant flux derived from waste form base case.
Low Recharge	01-t	Fluid velocity fields taken from fluid flow low recharge case. Top boundary contaminant flux derived from waste form low recharge case.
Rupert Sand	09-t	Fluid velocity fields taken from fluid flow Rupert sand case. Top boundary contaminant flux derived from waste form Rupert sand case.
High Recharge	50-t	Fluid velocity fields taken from fluid flow high recharge case. Top boundary contaminant flux derived from waste form high recharge case.
No Side Slope	42all-t	Fluid velocity fields taken from fluid flow no side slope case. Top boundary contaminant flux derived from waste form base case.
Alternate Glass	42altglass-t	Fluid velocity fields taken from fluid flow base case. Top boundary contaminant flux derived from waste form alternate glass case.
Capillary Break	42break-t	Fluid velocity fields taken from fluid flow capillary break case. Top boundary contaminant flux derived from waste form low recharge case (conservative assumption).
Concrete Layer	42conc-t	A 1 m layer at the top of the model is given alternate K_d values for I and U nuclides. Fluid velocity fields taken from fluid flow base case. Top boundary contaminant flux derived from waste form base case.
Conditioning Layer	42cond-t	Fluid velocity fields taken from fluid flow base case. Top boundary contaminant flux derived from waste form conditioning layer case.
Deep Vadose Zone	42deep-t	The gravel layer is extended down an additional 3 m (to a depth of 106 m). Fluid velocity fields taken from fluid flow deep vadose zone case. Top boundary contaminant flux derived from waste form base case.
High Diffusion	42diff-t	The diffusion coefficients for the sand and gravel are multiplied by a factor of 10. Fluid velocity fields taken from fluid flow base case. Top boundary contaminant flux derived from waste form base case.
Clastic Dike	42dike-t	A clastic dike is inserted under the middle of the facility region. Fluid velocity fields taken from fluid flow clastic dike case. Top boundary contaminant flux derived from waste form base case.
High Dispersion	42disp-t	The dispersion coefficients for the sand and gravel are multiplied by a factor of 2. Fluid velocity fields taken from fluid flow base case. Top boundary contaminant flux derived from waste form base case.

Forward Rate	42for-t	Fluid velocity fields taken from flow base case. Top boundary contaminant flux derived from waste form forward rate case.
No Sand Layer	42grav-t	Sand layer is replaced with gravel. Fluid velocity fields taken from fluid flow no sand case. Top boundary contaminant flux derived from waste form base case.
Isotropic	42iso-t	Fluid velocity fields taken from fluid flow isotropic case. Top boundary contaminant flux derived from waste form base case.
No Gravel Layer	42sand-t	Gravel layer is replaced with Hanford sand. Fluid velocity fields taken from fluid flow no gravel case. Top boundary contaminant flux derived from waste form base case.
No Ion Exchange	42noion-t	Fluid velocity fields taken from fluid flow base case. Top boundary contaminant flux derived from waste form no ion exchange case.
No Secondary Reactions	42nosecond-t	Fluid velocity fields taken from fluid flow base case. Top boundary contaminant flux derived from waste form no secondary reactions case.
Sand Backfill	42sandfill-t	Fluid velocity fields taken from fluid flow base case. Top boundary contaminant flux derived from waste form sand backfill case.
High Diffusion in Glass	42sdiff-t	Fluid velocity fields taken from fluid flow base case. Top boundary contaminant flux derived from waste form high diffusion case.
Short Capillary Break	42short-t	Fluid velocity fields taken from fluid flow short capillary break case. Top boundary contaminant flux derived from waste form low recharge case.
Failed Capillary Break (subsidence)	42sub-t	Fluid velocity fields taken from fluid flow failed capillary break case. Top boundary contaminant flux derived from a composite of waste form cases base, low recharge, Rupert sand, and high recharge.
Steel Casing	42steel-t	Fluid velocity fields taken from fluid flow base case. Top boundary contaminant flux derived from waste form steel casing case.
Vertical Capillary Break	42vert-t	Fluid velocity fields taken from fluid flow vertical capillary case. Top boundary contaminant flux derived from waste form low recharge case.
Capillary Break with High Rchrg.	50break-t	Fluid velocity fields taken from fluid flow capillary break with high recharge case. Top boundary contaminant flux derived from waste form low recharge case.
Pulse	pulse-t	Fluid velocity fields taken from fluid flow base case. Top boundary contaminant flux is a 1 Ci pulse distributed over 1 y.
Vault	42vault-t	Vault geometry model (similar to base case except that it is only 35 m wide instead of 60 m). Fluid velocity fields taken from fluid flow vault case. Top boundary contaminant flux derived from waste form vault case.

Table 4-4. Integration Cases

Case Name	Case ID	Case Description
Base Case	42base	This case uses the default library files and parameters. The contaminant release rate is taken from the far field transport base case.
Low Recharge	01	Recharge of 0.1 mm/y and associated WIF. The contaminant release rate is taken from the far field transport low recharge case.
Rupert Sand	09	Recharge of 0.9 mm/y and associated WIF. The contaminant release rate is taken from the far field transport Rupert sand case.
High Recharge	50	Recharge of 50 mm/y and associated WIF. The contaminant release rate is taken from the far field transport high recharge case.
Double Iodine Inventory	42-2i	Uses inventory file inv3-2i.bac. The contaminant release rate is taken from the far field transport base case.
Double Uranium Inventory	42-2u	Uses inventory file inv3-2u.bac. The contaminant release rate is taken from the far field transport base case.
No Side Slope	42all	The contaminant release rate is taken from the far field transport no side slope case.
Alternate Glass	42altglass	The contaminant release rate is taken from the far field transport alternate glass case.
Capillary Break	42break	The contaminant release rate is taken from the far field transport capillary break case.
Concrete Layer	42conc	The contaminant release rate is taken from the far field transport base case and the concrete layer case.
Conditioning Layer	42condlayr	The contaminant release rate is taken from the far field transport conditioning layer case.
Deep Vadose Zone	42deep	The contaminant release rate is taken from the far field transport deep vadose zone case.
High Diffusion	42diff	The contaminant release rate is taken from the far field transport high diffusion case.
Clastic Dike	42dike	The contaminant release rate is taken from the far field transport clastic dike case.
High Dispersion	42disp	The contaminant release rate is taken from the far field transport high dispersion case.
Forward Rate	42for	The contaminant release rate is taken from the far field transport forward rate case.
No Sand Layer	42grav	The contaminant release rate is taken from the far field transport no sand case.
Instant Transport	42instant	This case is not based on a far field calculation. Instead the waste form release rate from the base analysis case is used as the release rate into the groundwater.
Isotropic	42iso	The contaminant release rate is taken from the far field transport isotropic case.

All Nuclide K_d's = 0.0	42kd0	Uses K_d file kd-0.bac. The contaminant release rate is taken from the far field transport base case.
All Tank Tc in ILAW.	42maxtc	Uses inventory file inv3-maxtc.bac. The contaminant release rate is taken from the far field transport base case.
No Gravel Layer	42sand	The contaminant release rate is taken from the far field transport no gravel layer case.
No Ion Exchange	42noion	The contaminant release rate is taken from the far field transport no ion exchange case.
No Secondary Reactions	42nosec	The contaminant release rate is taken from the far field transport no secondary reaction case.
No Tc in ILAW	42notc	Uses inventory file inv3-notc.bac. The contaminant release rate is taken from the far field transport base case.
Sand Backfill	42sandfill	The contaminant release rate is taken from the far field transport sandfill case.
High Diffusion in Glass	42sdiff	The contaminant release rate is taken from the far field transport high diffusion in glass case.
Short Capillary Break	42short	The contaminant release rate is taken from the far field transport short capillary break case.
Failed Capillary Break (subsidence)	42sub	The contaminant release rate is taken from the far field transport subsidence case.
Steel Casing	42steel	The contaminant release rate is taken from the far field transport steel casing case.
Upper Bound Inventory	42ub	Uses inventory file inv-ub3.bac. The contaminant release rate is taken from the far field transport base case.
Upper Bound Inventory and All Tank Tc in ILAW	42ubmaxtc	Uses inventory file inv-ub3maxtc.bac. The contaminant release rate is taken from the far field transport base case.
Uranium K_d=0	42ukd0	Uses K_d file kd-u0.bac. The contaminant release rate is taken from the far field transport base case.
Vertical Capillary Break	42vert	The contaminant release rate is taken from the far field transport vertical capillary break case.
Capillary Break with High Recharge	50break	A recharge rate of 50 mm/y is used. The contaminant release rate is taken from the far field transport high recharge capillary break case.
Pulse	pulse42	The contaminant release rate is taken from the far field transport pulse case.
Vault	42vault	Uses alternate facility footprint area. The contaminant release rate is taken from the far field transport vault case.

4.5 SPECIAL CASES

4.5.1 Bathtub Effect

A simplified model was used to estimate the effect of trapping water for a period of time in the disposal facility (sometimes referred to as the “bathtub effect”). This model assumed the trench was saturated with moisture at time, t = 0, and the glass released its contaminants into the free water. After a period of time, the trench was assumed to release all the trapped water in the trench uniformly through its bottom. Piston flow of this water was assumed to instantaneously transport the contaminant concentration to the aquifer. The estimated impacts at a well 100 meters downgradient from the disposal facility were then estimated.

The amount of contaminant released from the LAWBP1 glass was calculated using STORM (Bacon 2000b). The calculation assumed a saturated condition within the model initially and calculated the amount of TcO_4 released from LAWABP1 glass as a function of time. To estimate the total radionuclide released, the amount of TcO_4 released in the STORM model as a function of residence time is first divided by the amount of Tc initially in the glass associated with the model and then multiplied by the total radionuclide inventory reported in Wootan (1999). This approach assumes that the radionuclide release scales as the release of TcO_4 calculated by STORM. The total water for the disposal facility's six trenches is estimated assuming the free pore volume associated with the backfill material (porosity = 0.316 [Meyer 1999])and the glass (porosity = 0.02) is filled with water. For one trench the maximum number of waste packages is 14,064 (Puigh 1999) and the total volume within one trench is 118,000 m^3. Therefore, the total water in the disposal facility is estimated to be 27,580 m^3. The total amount of radionuclideTcO_4 released divided by the total water in the disposal facility gives the average Tc concentration as a function of time before failure of the bathtub bottom. The results presented in Section 5 assume all trenches fail at the same time as a conservative calculation.

4.5.2 Instantaneous Vadose Zone Transport

The instantaneous release case was designed to evaluate the impact of the vadose zone on the release rate. In order to determine this, a calculation was performed where the contaminant flux into the groundwater was assumed to equal the facility release rate. This was done by taking the base case facility release rate, normalizing it, converting it to Ci/y, and entering it into an INTEG calculation. No near field or far field calculations were required for this case.

4.5.3 Instantaneous Waste Form Release

The instantaneous waste form release case was performed to determine the travel time and degree of spreading of a unit release into the vadose zone. In order to determine this, a base case calculation was performed where the facility release rate was replaced with a constant 1 Ci/y release for 1 y.

5.0 SIMULATION RESULTS

5.1 NEAR FIELD

This section describes the results (primarily the vertical Darcy velocity through the disposal facility) for the near field cases.

In general, the vertical Darcy velocity through a region will correspond to the recharge at the surface. The high recharge region outside of the facility (for most cases) results in a high flow plume that spreads out under the capillary barrier resulting in fluid velocities through the facility that are higher than the recharge rate above the facility. The capillary break (in the cases where it is functioning) greatly reduce the velocities through the waste region. The interface between the trench backfill and the surrounding Hanford sand behaves somewhat like a capillary barrier and results in a funneling effect that increases the fluid velocities in the facility. This effect, however, occurs mostly outside the waste containing region.

The Darcy velocities in the immediate vicinity of the waste are of the most interest, because that drives the release rate. To provide a comparison between the different cases, the minimum and maximum Darcy velocities in the waste region are documented in Table 5-1.

Figure 5-1 shows the fluid flux distribution out the bottom of the near field (and consequently into the top of the far field) for four scenarios. The first case assumes a uniform flux of 4.2E-3 m/y in the region of the capillary barrier. This case assumes that the barrier has failed and the flow into the facility is the same as that through an overlying sand layer. This case shows the greatest flux rate through the waste packages. The barrier case assumes the capillary barrier is functional and restricts vertical migration. This case shows the lowest flow rates through the waste packages. The short barrier case represents a capillary barrier shortened by 5 m. Flow through the waste region is higher than that from the full barrier due to the closer proximity of the waste to the high flow region. The final case assumes that the capillary barrier fails at about 10 m from the trench center line. This case shows that locally, where the barrier is breached, flow approaches that of the non-barrier case. However, flow adjacent to the breach drops off on both sides and ultimately achieves a comparable flow rate to that of the barrier case.

Table 5-1. Waste Region Darcy Velocities for the Various Near Field Cases

Case Name	Minimum Darcy Velocity (mm/y)	Maximum Darcy Velocity (mm/y)
Base Case	4.1	4.3
Low Recharge	0.098	0.11
Rupert Sand	0.87	0.95
High Recharge	49.	51.
No Side Slope	4.2	4.2
Sand Backfill	4.1	4.2
Best Estimate Case (Capillary Break)	1.2×10^{-4}	8.5×10^{-3}
Short Capillary Break	1.2×10^{-4}	1.5×10^{-2}

Case Name	Minimum Darcy Velocity (mm/y)	Maximum Darcy Velocity (mm/y)
Vertical Capillary Break	1.2×10^{-4}	8.3×10^{-3}
Failed Capillary Break (Subsidence)	0.0094	11.1
Capillary Break With High Recharge	1.0×10^{-3}	1.0×10^{-1}
Alternate Facility Design (Vault)	4.1	4.8

Figure 5-1. Darcy Velocity at the Top of the Far Field for Different Trench Scenarios

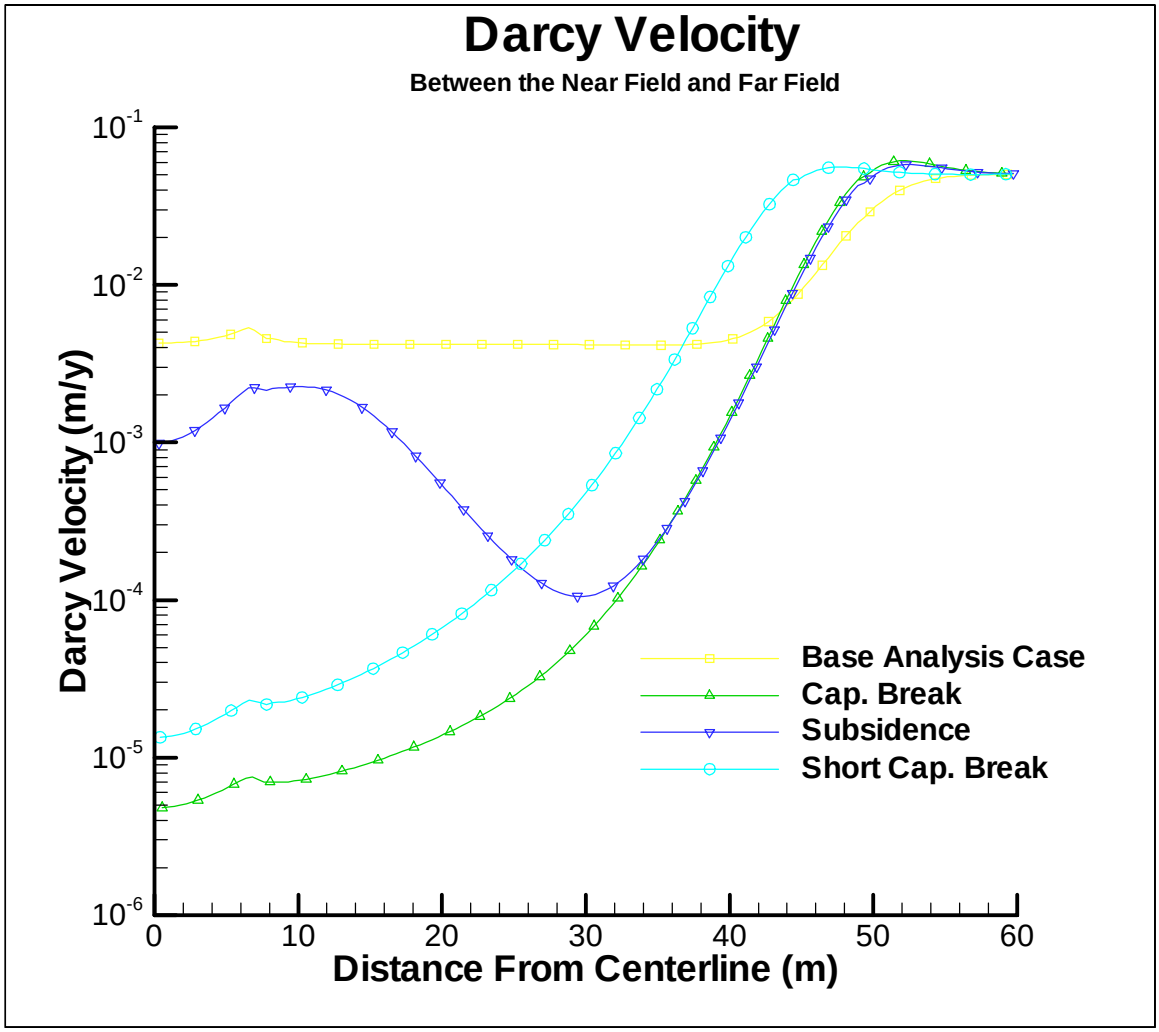

5.2 FAR FIELD FLOW CASES

Outputs from the far field flow calculations consist of two-dimensional velocity fields that are used in the far field transport calculations.

The velocity fields in the far field region are driven by the fluid influx at the top of the region (from the corresponding near field calculation, see Figure 5-1). The velocities also respond to differences in the hydraulic properties of the far field materials.

Volumetric Water content at steady-state for the base case (4.2E-3 m/y over nonfunctional capillary barrier) and the full barrier case are shown in Figures 5-2 and 5-3, respectively. The most noticeable difference between the two cases is that the barrier case is much drier than the base case beneath the barrier region. There is also more lateral variability for the barrier case, reflecting the extreme difference between the left and right boundaries. The high recharge region at the upper right corner is broader for the full barrier case. This is a result of the run-off from the top of the barrier. The water distribution differences appear to be more pronounced in the Hanford sands directly beneath the capillary barrier than in the lower Hanford gravels.

Figure 5-2. Volumetric Water Content in the Far Field for the Base Analysis Case

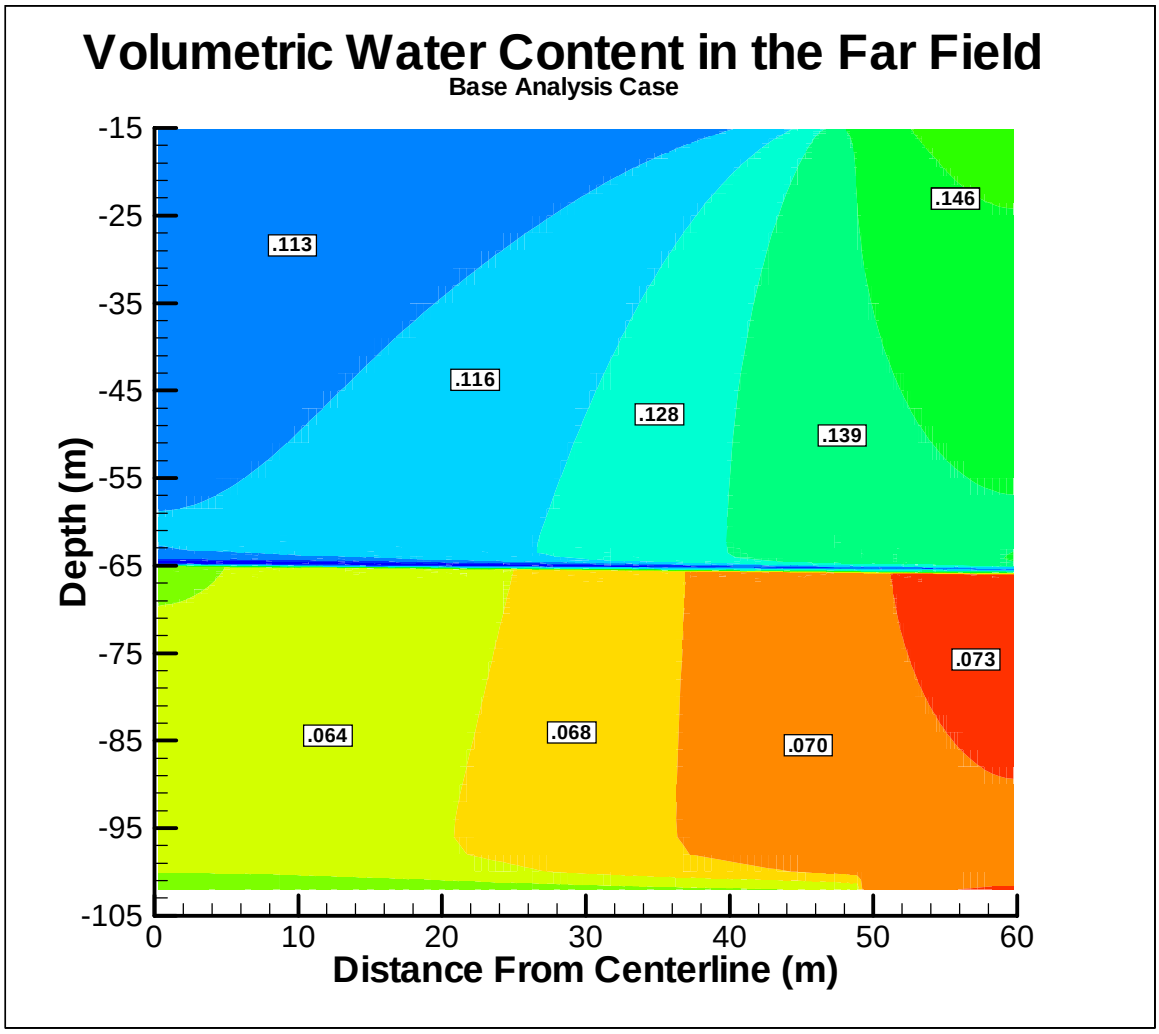

Figure 5-3. Volumetric Water Content In the Far Field for the Best Estimate Case

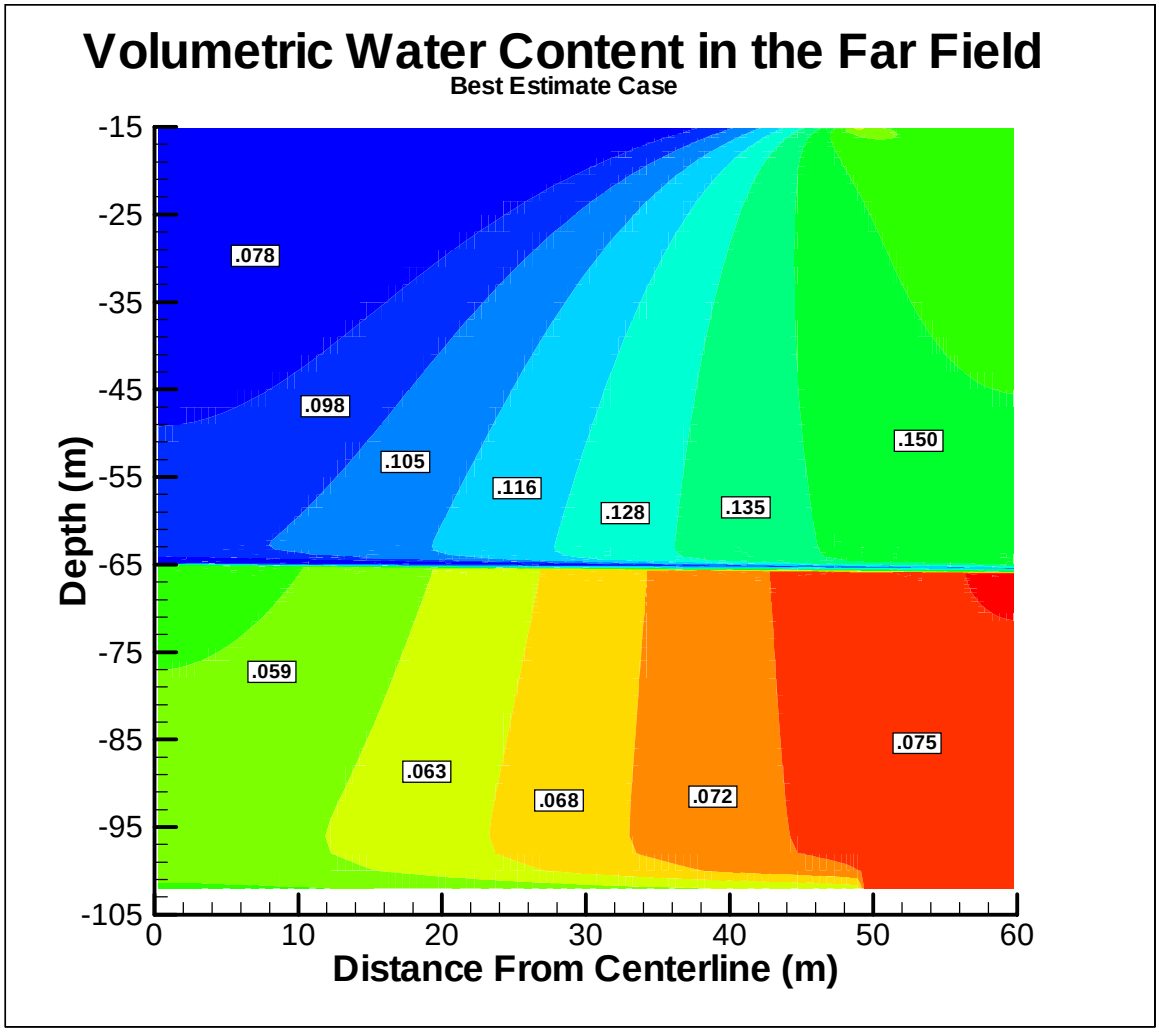

5.3 FAR FIELD TRANSPORT CASES

Output from the far field transport calculations is used to predict contaminant release rates to the water table. Fluid flux into the far field from the near field, and the resultant far field velocity field, drives contaminant migration to the water table.

Figure 5-4 shows contaminant concentration (Ci/m^3) at the top surface of the far field region at 1,000 y. Three cases are evaluated for concentration for an assumed K_d condition of 0 mL/g, the base case, the best estimate case, and the subsidence case. As expected from the fluid flow results, the concentration for the non-barrier case shows the greatest concentration values initially. The subsidence case concentrations, however, exceed the base case in the vicinity of the failure. This is because the velocities directly under the failure exceed those of the base case,

resulting in a higher release rate. By the time the plume reaches the bottom of the facility it has spread out and the velocities dropped, as can be seen in Figure 5.1-1. The capillary break case (without subsidence) shows a concentration curve similar to that for the base case but about two orders of magnitude lower. Also note that at the upper surface, the step function used to represent the waste package distribution can be clearly seen in both the base and best estimate cases.

Figure 5-5 shows the concentration profile at the bottom of the far field at 1000 y. The three cases that are evaluated represent scenarios that could result in perturbation of concentration distribution at ground water. The no-barrier case shows the highest concentration, which gradually declines over the range of the waste packages, then declines at a steeper rate beyond the last package. The full barrier case shows the lowest concentration levels, with a peak at about 20 m from the trench center and declining to either side of the peak (this behavior is caused by the outer edge of the plume reaching groundwater sooner than the center). The capillary break case concentration approaches the no barrier concentration at the center but falls off faster. The greatest difference in release rate to ground water is between the non-barrier and full barrier cases.

Figures 5-6 and 5-7 show the fractional release rates at the bottom of the far field for the cases where the surface recharge rates are incrementally increased and for the cases where the K_d is incrementally increased, respectively. In Figure 5-7, the K_d=0.0 and 0.6 mL/g cases refer to the K_d of the sand layer in the vadose zone (the gravel layer K_d is a factor of 10 lower than the sand for all cases). This figure also shows the facility release rate for reference. As may be expected, higher contaminant fluxes are associated with higher flow rates and lower K_d.

For all cases, the general shape of the release curve is similar. The peak time and value, however, vary significantly between the cases. Table 5-2 provides a comparison between the cases by showing the normalized contaminant transport rates into the aquifer (for K_d=0 mL/g) at times of 1,000 y and 10,000 y.

Figure 5-4. Source Concentration at Top of the Far Field at 1,000 Years for K_d=0 mL/g

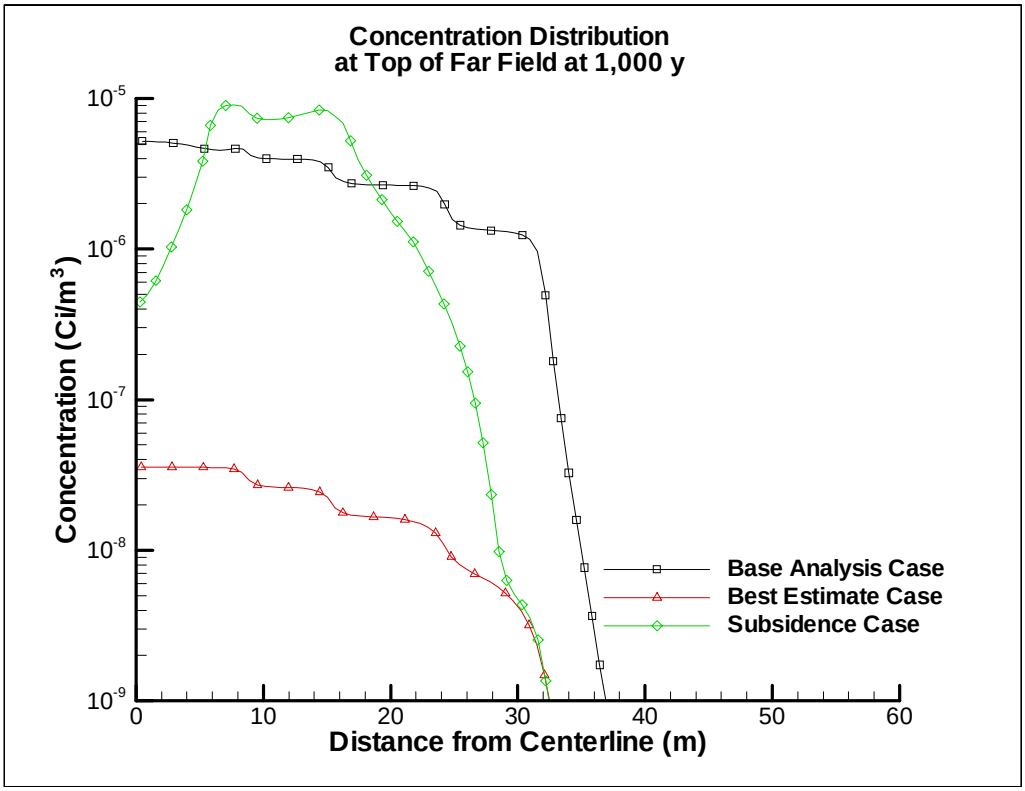

Figure 5-5. Source Concentration at Bottom of Far Field at 1,000 Years for K_d=0 mL/g

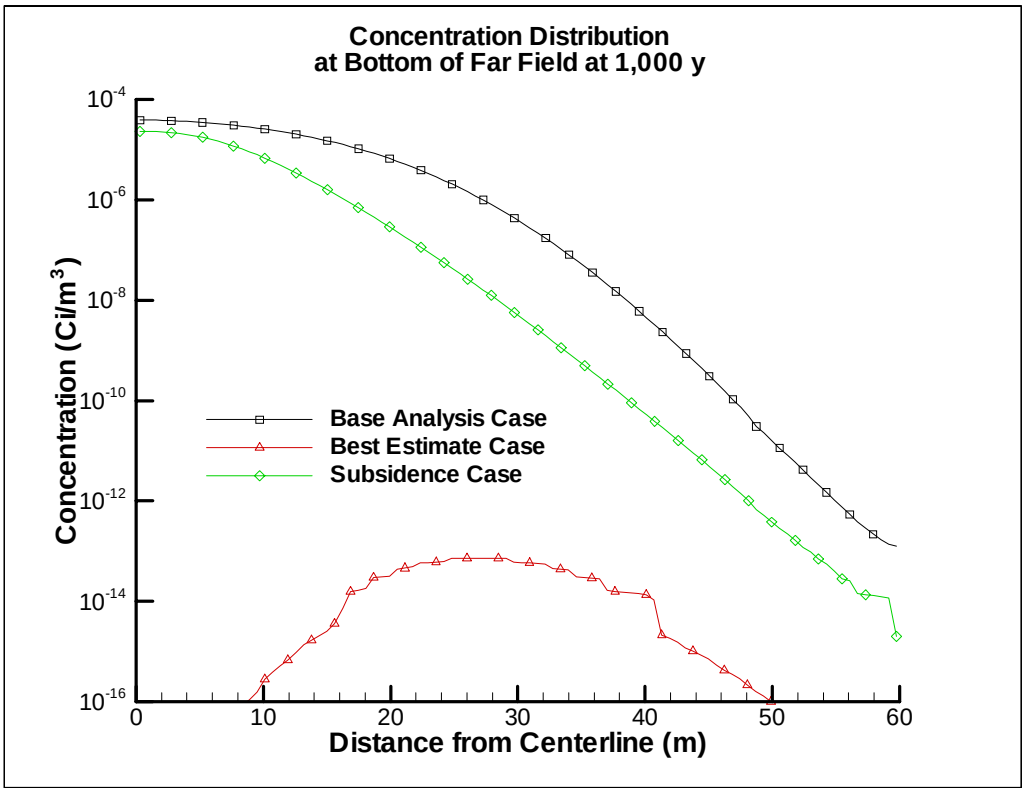

Figure 5-6. Normalized Contaminant Flux into Aquifer at Four Recharge Rates

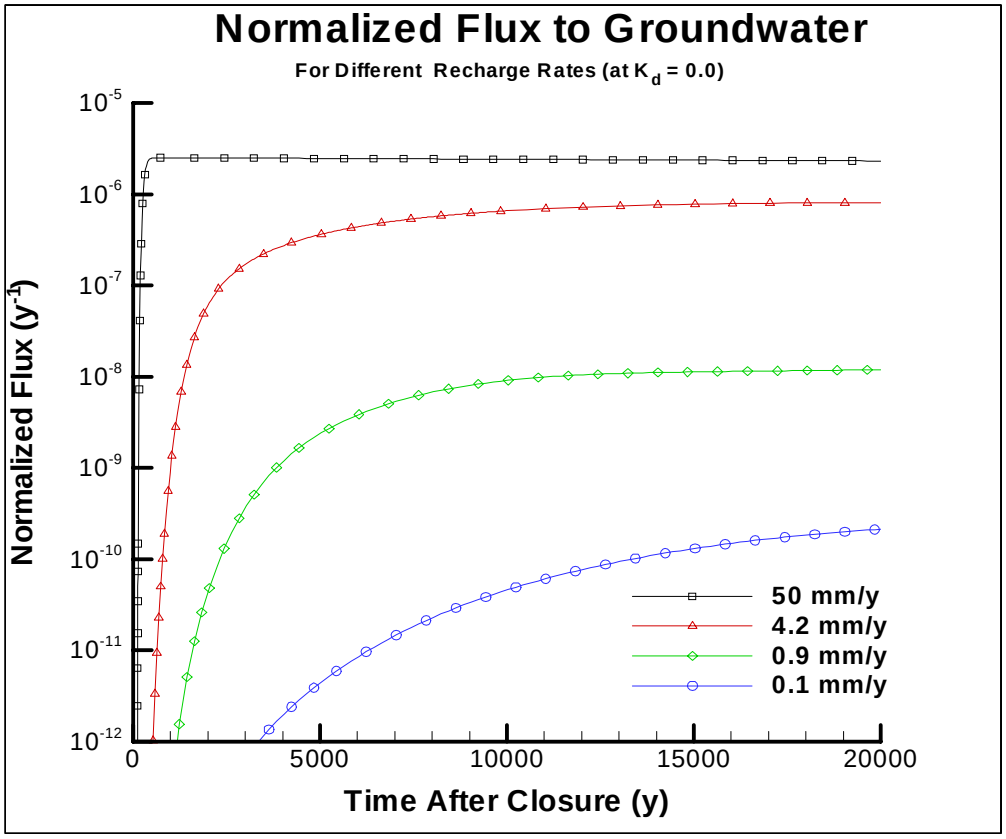

Figure 5-7. Normalized Contaminant Flux into the Aquifer at 4.2 mm/y for Four Geochemical Retardation Factors

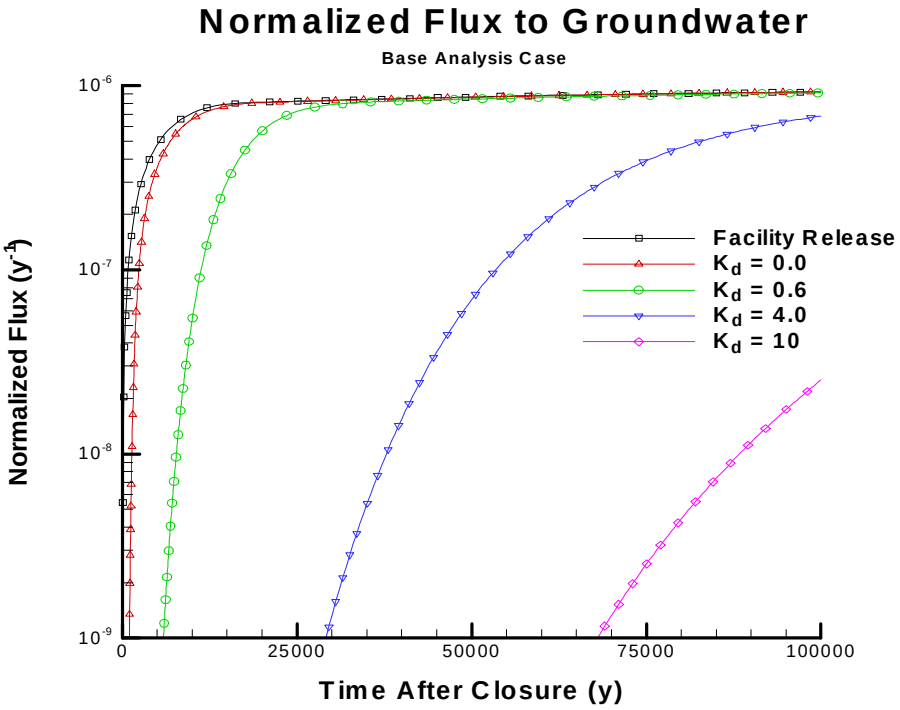

Table 5-2. Normalized Contaminant Release Rates at the Water Table

Case Name	Release Rate at 1,000 y (Ci/y)	Release Rate at 10,000 y (Ci/y)
Base Case	1.35E-09	6.60E-07
Low Recharge	4.38E-16	4.63E-11
Rupert Sand	2.37E-13	9.13E-09
High Recharge	2.51E-06	2.42E-06
No Side Slope	6.95E-11	6.47E-07
Alternate Glass	1.63E-07	4.39E-05
Capillary Break	2.96E-15	2.25E-11
Concrete Layer	1.35E-09	6.60E-07
Conditioning Layer	1.34E-09	6.13E-07
Deep Vadose Zone	1.13E-09	6.59E-07
High Diffusion	2.01E-09	6.61E-07
Clastic Dike	1.21E-09	6.55E-07
High Dispersion	2.38E-09	6.60E-07
Forward Rate	1.31E-08	5.89E-06
No Sand Layer	6.58E-09	6.78E-07
Isotropic	8.36E-10	6.64E-07
No Gravel Layer	3.40E-10	6.50E-07
No Ion Exchange	1.06E-09	5.46E-07
No Secondary Reactions	6.69E-10	3.50E-07
Sand Backfill	2.84E-08	1.15E-06
High Diffusion in Glass	2.56E-10	7.79E-09
Short Capillary Break	5.40E-14	6.79E-11
Failed Capillary Break (subsidence)	3.38E-13	2.58E-07
Steel Casing	1.38E-09	6.56E-07
Vertical Capillary Break	0.0000E+00	1.32E-11
Capillary Break with High Recharge	1.26E-13	5.10E-11
Pulse	4.69E-04	3.36E-16
Vault	3.81E-07	1.17E-06

5.4 INTEGRATION CASES

Output from the integration calculations gives the predicted dose versus time results that form the basis for comparing the ILAW facility to the performance limits.

Table 5-3 summarizes the results for each of the integration cases.

Table 5-3. Integration Results

INTEG Filename	Case Designation	Estimated Impact at 1,000 y after Facility Closure (1)			Estimated Impact at10,000 y after Facility Closure (1)			Maximum Estimated Impact (1) [peak time or max time for calculation]		
		beta/ photon dose (mrem/y)	alpha concen. (pCi/L)	all-pathways dose (mrem/y)	beta-photon dose (mrem/y)	alpha concen. (pCi/L)	all-pathways dose (mrem/y)	beta-photon dose (mrem/y)	alpha concen. (pCi/L)	all-pathways dose (mrem/y)
42base	Base analysis case	2.13E-05	1.02E-16	7.78E-05	1.02E-02	3.39E-02	7.00E-02	1.25E-02 [76,500 y]	5.42E-01 [100,000 y]	5.88E-01 [100,000 y]
42break	Best estimate case	4.67E-11	2.25E-22	1.71E-10	3.46E-07	5.01E-08	1.31E-06	1.85E-06 [20,000 y]	9.29E-07 [20,000 y]	7.63E-06 [20,000 y]
Facility Cases										
42break	Full barrier	4.67E-11	2.25E-22	1.71E-10	3.46E-07	5.01E-08	1.31E-06	1.85E-06 [20,000 y]	9.29E-07 [20,000 y]	7.63E-06 [20,000 y]
50break	Full barrier - 50 mm/y	2.09E-09	9.64E-21	7.33E-09	7.92E-07	8.94E-07	3.76E-06	3.03E-06 [20,000 y]	5.43E-06 [20,000 y]	1.63E-05 [20,000 y]
42vert	Vertical barrier	0.00E+00	0.00E+00	0.00E+00	2.03E-07	8.97E-09	7.51E-07	1.2E-06 [20,000 y]	3.14E-07 [20,000 y]	4.68E-06 [20,000 y]
42short	Shorter capillary break	8.53E-10	4.10E-21	3.12E-09	1.05E-06	6.03E-07	4.41E-06	3.94E-06 [20,000 y]	5.24E-06 [20,000 y]	1.94E-05 [20,000 y]
42vault	Concrete vault - base	6.05E-03	9.19E-10	2.21E-02	1.81E-02	6.94E-01	7.38E-01	1.85E-02 [20,000 y]	7.41E-01 [20,000 y]	7.90E-01 [20,000 y]
42all	No side slope	1.10E-06	5.28E-18	4.01E-06	9.98E-03	8.61E-03	4.48E-02	1.21E-02 [17,400 y]	2.76E-01 [20,000 y]	3.13E-01 [20,000 y]
Waste Form Release										
42for	Forward rate	2.08E-04	9.98E-16	7.59E-04	9.08E-02	3.32E-01	6.54E-01	9.89E-02 [20,000 y]	3.13E+00 [20,000 y]	3.41E+00 [20,000 y]

Table 5-3. Integration Results

INTEG Filename	Case Designation	Estimated Impact at 1,000 y after Facility Closure (1)			Estimated Impact at10,000 y after Facility Closure (1)			Maximum Estimated Impact (1) [peak time or max time for calculation]		
		beta/ photon dose (mrem/y)	alpha concen. (pCi/L)	all-pathways dose (mrem/y)	beta-photon dose (mrem/y)	alpha concen. (pCi/L)	all-pathways dose (mrem/y)	beta-photon dose (mrem/y)	alpha concen. (pCi/L)	all-pathways dose (mrem/y)
42noion	No ion exchange	1.68E-05	8.06E-17	6.13E-05	8.41E-03	2.72E-02	5.71E-02	1.04E-02 [20,000 y]	2.91E-01 [20,000 y]	3.21E-01 [20,000 y]
42highion	Forward rate + 5X ion exchange	2.18E-04	1.05E-15	7.97E-04	1.00E-01	3.92E-01	7.46E-01	1.09E-01 [18,700 y]	3.45E+00 [20,000 y]	3.77E+00 [20,000 y]
42nosec	No secondary phase	1.06E-05	5.08E-17	3.86E-05	5.39E-03	1.75E-02	3.67E-02	6.60E-03 [20,000 y]	1.86E-01 [20,000 y]	2.05E-01 [20,000 y]
01	Recharge = 0.1 mm/y	6.95E-12	3.34E-23	2.54E-11	7.16E-07	1.84E-08	2.64E-06	3.23E-06 [20,000 y]	6.30E-07 [20,000 y]	1.24E-05 [20,000 y]
09	Recharge = 0.9 mm/y	3.76E-09	1.81E-20	1.38E-08	1.41E-04	5.18E-06	5.22E-04	1.81E-04 [20,000 y]	2.57E-04 [20,000 y]	9.10E-04 [20,000 y]
50	Recharge = 50 mm/y	4.00E-2	2.63E-01	3.99E-01	3.76E-02	1.52E+00	1.61E+00	7.62E-02 [300 y]	1.56E+00 [3,400 y]	1.65e+00 [3,400 y]
42sandfill	Sand backfill	4.48E-04	2.15E-15	1.64E-03	1.77E-02	1.76E-01	2.35E-01	1.80E-02 [4,700 y]	6.65E-01 [20,000 y]	7.11E-01 [20,000 y]
42sdiff	10X WF aqueous diffusion	4.03E-06	1.94E-17	1.47E-05	1.20E-04	1.21E-03	1.61E-03	1.31E-04 [20,000 y]	4.52E-03 [20,000 y]	4.89E-03 [20,000 y]
42steel	Steel included	2.18E-05	1.05E-16	7.96E-05	1.01E-02	3.39E-02	6.98E-02	1.49E-02 [20,000 y]	3.57E-01 [20,000 y]	4.02E-01 [20,000 y]
42condlayr	Top conditioning Layer	2.11E-05	1.02E-16	7.72E-05	9.44E-03	3.31E-02	6.66E-02	1.10E-02 [20,000 y]	3.26E-01 [20,000 y]	3.58E-01 [20,000 y]
42altglass	HLP-31 glass	2.57E-03	1.24E-14	9.41E-03	6.77E-01	3.87E+00	6.23E+00	6.78E-01 [9,200 y]	2.40E+01 [20,000 y]	2.56E+01 [20,000 y]

Table 5-3. Integration Results

INTEG Filename	Case Designation	Estimated Impact at 1,000 y after Facility Closure (1)			Estimated Impact at10,000 y after Facility Closure (1)			Maximum Estimated Impact (1) [peak time or max time for calculation]		
		beta/ photon dose (mrem/y)	alpha concen. (pCi/L)	all-pathways dose (mrem/y)	beta-photon dose (mrem/y)	alpha concen. (pCi/L)	all-pathways dose (mrem/y)	beta-photon dose (mrem/y)	alpha concen. (pCi/L)	all-pathways dose (mrem/y)
Vadose Zone Cases										
42iso	Isotropic field flow	1.32E-05	6.35E-17	4.83E-05	1.02E-02	1.26E-02	4.96E-02	1.22E-02 [20,000 y]	3.02E-01 [20,000 y]	3.39E-01 [20,000 y]
42sand	All sand	5.37E-06	2.58E-17	1.96E-05	1.00E-02	2.54E-03	3.91E-02	1.24E-02 [52,500 y]	5.36E-01 [100,000 y]	5.85E-01 [100,000 y]
42grav	All gravel	1.04E-04	1.84E-09	3.80E-04	1.05E-02	3.60E-01	3.87E-01	1.24E-02 [52,000 y]	5.43E-01 [100,000 y]	5.92E-01 [100,000 y]
42deep	VZ - 3 m thicker	1.78E-05	8.56E-17	6.51E-05	1.02E-02	3.24E-02	6.86E-02	1.24E-02 [52,000 y]	5.37E-01 [100,000 y]	5.86E-01 [100,000 y]
42dike	Clastic dike	1.91E-05	9.16E-17	6.96E-05	1.01E-02	2.81E-02	6.42E-02	1.22E-02 [20,000 y]	3.32E-01 [20,000 y]	3.68E-01 [20,000 y]
42ukd0	U $K_d = 0$	2.13E-05	6.12E-04	2.09E-04	1.02E-02	3.07E-01	1.29E-01	1.24E-02 [52,500 y]	5.41E-01 [100,000 y]	5.87E-01 [100,000 y]
42kd0	$K_d = 0$ for all radionuclides (2)	3.11E-05	1.6E-02 (3.78E-06)	3.68E-02	1.49E-02	4.34e+00 (5.95E-03)	8.69E+00	1.82E-02 [54,500 y]	4.70E+00 [15,000 y] (5.15E-02 [100,000 y])	9.05E+00 [13,000 y]
42diff	10X increase in Diffusion	3.17E-05	1.52E-16	1.16E-04	1.02E-02	4.46E-02	8.05E-02	1.22E-02 [20,000 y]	3.57E-01 [20,000 y]	3.93E-01 [20,000 y]
42disp	2X increase in dispersion	3.76E-05	1.81E-16	1.37E-04	1.02E-02	5.17E-02	8.73E-02	1.22E-02 [20,000 y]	3.50E-01 [20,000 y]	3.86E-01 [20,000 y]
Groundwater Cases										

Table 5-3. Integration Results

INTEG Filename	Case Designation	Estimated Impact at 1,000 y after Facility Closure (1)			Estimated Impact at10,000 y after Facility Closure (1)			Maximum Estimated Impact (1) [peak time or max time for calculation]		
		beta/ photon dose (mrem/y)	alpha concen. (pCi/L)	all-pathways dose (mrem/y)	beta-photon dose (mrem/y)	alpha concen. (pCi/L)	all-pathways dose (mrem/y)	beta-photon dose (mrem/y)	alpha concen. (pCi/L)	all-pathways dose (mrem/y)
42base(4)	Well intercept. = 1000m	1.58E-05	7.58E-17	5.78E-05	7.58E-03	2.52E-02	5.20E-02	9.29E-03 [76,500 y]	4.03E-01 [100,000 y]	4.37E-01 [100,000 y]
42base(4)	Well intercept. = CR	1.99E-06	9.52E-18	7.26E-06	9.52E-04	3.16E-03	6.53E-03	1.17E-03 [76,500 y]	5.06E-02 [100,000 y]	5.49E-02 [100,000 y]
42base(4)	Trench at south end	3.20E-05	1.53E-16	1.17E-04	1.53E-02	5.09E-02	1.05E-01	1.88E-02 [76,500 y]	8.13E-01 [100,000 y]	8.82E-01 [100,000 y]
42base(4)	90° rotation	4.07E-05	1.95E-16	1.49E-04	1.95E-02	6.47E-02	1.34E-01	2.39E-02 [76,500 y]	1.04E+00 [100,000 y]	1.12E+00 [100,000 y]
42base(4)	Smaller layout	5.75E-06	2.75E-17	2.10E-05	2.75E-03	9.15E-03	1.89E-02	3.38E-03 [76,500 y]	1.46E-01 [100,000 y]	1.59E-01 [100,000 y]
42base(4)	Larger layout	2.56E-05	1.22E-16	9.34E-05	1.22E-02	4.07E-02	8.40E-02	1.50E-02 [76,500 y]	6.50E-01 [100,000 y]	7.06E-01 [100,000 y]
42vault(5)	Existing vault site	2.60E-03	3.95E-10	9.50E-03	7.78E-03	2.98E-01	3.17E-01	7.74E-03 [20,000 y]	3.19E-01 [100,000 y]	3.40E-01 [100,000 y]
42base(4)	30 L/d pumping	2.13E-05	1.02E-16	7.78E-05	1.02E-02	3.39E-02	7.00E-02	1.25E-02 [76,500 y]	5.42E-01 [100,000 y]	5.88E-01 [100,000 y]
42base(4)	100 L/d pumping	2.13E-05	1.02E-16	7.78E-05	1.02E-02	3.39E-02	7.00E-02	1.25E-02 [76,500 y]	5.42E-01 [100,000 y]	5.88E-01 [100,000 y]
42base(4)	300 L/d pumping	2.13E-05	1.02E-16	7.78E-05	1.02E-02	3.39E-02	7.00E-02	1.25E-02 [76,500 y]	5.42E-01 [100,000 y]	5.88E-01 [100,000 y]
42base(4)	1000 L/d pumping	2.13E-05	1.02E-16	7.78E-05	1.02E-02	3.39E-02	7.00E-02	1.25E-02 [76,500 y]	5.42E-01 [100,000 y]	5.88E-01 [100,000 y]

Table 5-3. Integration Results

INTEG Filename	Case Designation	Estimated Impact at 1,000 y after Facility Closure (1)			Estimated Impact at10,000 y after Facility Closure (1)			Maximum Estimated Impact (1) [peak time or max time for calculation]		
		beta/ photon dose (mrem/y)	alpha concen. (pCi/L)	all-pathways dose (mrem/y)	beta-photon dose (mrem/y)	alpha concen. (pCi/L)	all-pathways dose (mrem/y)	beta-photon dose (mrem/y)	alpha concen. (pCi/L)	all-pathways dose (mrem/y)
42base(4)	Reduced hyd. Cond (3X)	2.55E-04	1.22E-15	9.32E-04	1.22E-01	4.06E-01	8.39E-01	1.50E-01 [76,500 y]	6.49E+00 [100,000 y]	7.04E+00 [100,000 y]
42base(4)	Regional recharge increase (3X)	1.96E-05	9.38E-17	7.16E-05	9.38E-03	3.12E-02	6.44E-02	1.15E-02 [76,500 y]	4.99E-01 [100,000 y]	5.41E-01 [100,000 y]
42base(4)	Regional recharge decrease (3X)	1.45E-05	6.94E-17	5.29E-05	6.94E-03	2.31E-02	4.76E-02	8.50E-03 [76,500 y]	3.69E-01 [100,000 y]	4.00E-01 [100,000 y]
42base(4)	Decrease regional upgradient boundaries (2X)	1.79E-05	8.57E-17	6.54E-05	8.57E-03	2.85E-02	5.88E-02	1.05E-02 [76,500 y]	4.55E-01 [100,000 y]	4.94E-01 [100,000 y]
Inventory Cases										
42maxTc	Increase Tc inventory 5X	7.03E-05	1.02E-16	2.98E-04	3.35E-02	3.39E-02	1.75E-01	3.99E-02 [20,000 y]	5.37E-01 [100,000 y]	6.95E-01 [100,000 y]
42noTc	Reduce Tc to 0	9.00E-06	1.02E-16	2.26E-05	4.33E-03	3.39E-02	4.38E-02	6.05E-03 [100,000 y]	5.37E-01 [100,000 y]	5.59E-01 [100,000 y]
42-2i	Double I inventory	3.01E-05	1.02E-16	1.00E-04	1.45E-02	3.39E-02	8.10E-02	1.82E-02 [80,000 y]	5.37E-01 [100,000 y]	6.01E-01 [100,000 y]
42-2u	Double U inventory	2.13E-05	1.02E-16	7.78E-05	1.02E-02	5.82E-02	7.55E-02	1.24E-02 [52,000 y]	8.72E-01 [96,000 y]	6.77E-01 [100,000 y]
42ub	All inventory at bounding	5.52E-05	4.83E-16	1.73E-04	2.66E-02	1.86E-01	3.11E-01	3.47E-02 [100,000 y]	2.76E+00 [100,000 y]	2.95E+00 [32,000 y]
42ubmaxTc	Bounding value + max Tc	1.02E-04	4.83E-16	3.85E-04	4.90E-02	1.86E-01	4.12E-01	5.96E-02 [50,500 y]	2.76E+00 [100,000 y]	3.07E+00 [32,000 y]

Table 5-3. Integration Results

INTEG Filename	Case Designation	Estimated Impact at 1,000 y after Facility Closure [1]			Estimated Impact at10,000 y after Facility Closure [1]			Maximum Estimated Impact [1] [peak time or max time for calculation]		
		beta/ photon dose (mrem/y)	alpha concen. (pCi/L)	all-pathways dose (mrem/y)	beta-photon dose (mrem/y)	alpha concen. (pCi/L)	all-pathways dose (mrem/y)	beta-photon dose (mrem/y)	alpha concen. (pCi/L)	all-pathways dose (mrem/y)
Dosimetry Cases										
ind-100m	Industrial	9.86E-06	1.02E-16	9.86E-06	4.71E-03	3.39E-02	1.69E-02	5.71E-03 [53,000 y]	5.37E-01 [100,000 y]	2.08E-01 [100,000 y]
res-100m	Residential	2.88E-05	1.02E-16	3.44E-05	1.38E-02	3.39E-02	5.68E-02	1.68E-02 [53,000 y]	5.37E-01 [100,000 y]	6.89E-01 [100,000 y]
agr-100m	Agricultural	2.88E-05	1.02E-16	1.26E-04	1.38E-02	3.39E-02	1.01E-01	1.68E-02 [53,000 y]	5.37E-01 [100,000 y]	7.48E-01 [100,000 y]
nat-CR	Native American [3]	4.52E-06	1.07E-17	2.77E-05	2.16E-03	3.55E-03	2.22E-02	2.63E-03 [52,500 y]	5.62E-02 [100,000 y]	1.64E-01 [100,000 y]
CRPop-CR	CR population [3]	1.12E-02	1.07E-17	3.42E-02	5.33E+00	3.55E-03	3.28E+02	6.49E+0 [53,000 y]	5.62E-02 [100,000y]	2.91E+02 [100,000 y]
DOE-100m	DOE dose parameters	2.00E-05	1.02E-16	7.15E-05	9.59E-03	3.39E-02	6.35E-02	1.17E-02 [57,000 y]	5.37E-01 [100,000 y]	5.26E-01 [100,000 y]
Other Sensitivity Cases										
42sub	Cap break subsidence	5.33E-09	2.56E-20	1.95E-08	3.97E-03	2.35E-05	1.45E-02	5.22E-03 [19,000 y]	1.28E-02 [20,000 y]	3.15E-02 [20,000 y]
Pulse42	Pulse	7.41E+00	3.56E-11	2.71E+01	5.18E-12	6.50E+01	6.29E+01	1.69E+01 [1,380 y]	6.93E+01 [11,100 y]	6.72E+01 [11,200 y]
42instant [2]	Instantaneous VZ transport	2.87E-03	1.48E+0 (3.49E-04)	3.39E+00	1.61E-02	4.68E+00 (6.4E-03)	9.36E+00	7.96E-01 [33 y]	4.83E+00 [13,100 y] (5.16E-02 [100,000 y])	9.43E+00 [11,100 y]

Table 5-3. Integration Results

INTEG Filename	Case Designation	Estimated Impact at 1,000 y after Facility Closure (1)			Estimated Impact at10,000 y after Facility Closure (1)			Maximum Estimated Impact (1) [peak time or max time for calculation]		
		beta/ photon dose (mrem/y)	alpha concen. (pCi/L)	all-pathways dose (mrem/y)	beta-photon dose (mrem/y)	alpha concen. (pCi/L)	all-pathways dose (mrem/y)	beta-photon dose (mrem/y)	alpha concen. (pCi/L)	all-pathways dose (mrem/y)
42conc	Concrete K_ds	1.37E-05	1.02E-16	5.87E-05	9.98E-03	5.56E-04	3.73E-02	1.24E-02 [53,000 y]	4.74E-01 [100,000 y]	5.22E-01 [100,000 y]

(1) The estimated impacts are associated with a well located 100 meters downgradient form the ILAW site.
(2) The numbers in parentheses are the estimated radium concentrations.
(3) The estimated impacts are calculated for a well just before the aquifer flows into the Columbia River. The appropriate WIF is provided in Bergeron 2000.
(4) The estimated impacts use the ratio of the WIFs provided in Bergeron 2000 times the Base Analysis Case estimated impacts.
(5) The estimated impact use the existing vault WIF provided in Bergeron 2000 with the vault calculation.

5.5 SPECIAL CASES

5.5.1 Bathtub Case

Table 5-4 summarizes the released TcO_4 concentration as a function of time from the STORM calculations. Figure 5-8 shows the buildup of the Tc concentration in the free water inside the trench as a function of time within the STORM model (Bacon 2000b). Over the first two years the Tc concentration within the model increases rapidly. Over the next thousand years the Tc concentration increases at an approximately linear rate with time. At 100 years the Tc concentration in the trench model is 4.08×10^{-4} micromoles/L and at 1,000 years the Tc concentration in the trench model is 5.56×10^{-3} micromoles/L.

To estimate the impacts for this scenario, the trench was assumed to provide an impermeable barrier for moisture flow out of the trench for a period of time, T. After this period of time, the bottom of the trench was assumed to be completely permeable and piston flow of the trench water into the aquifer was assumed. Therefore, the contaminant concentration in the trench is assumed to be equal to the contaminant concentration entering the aquifer. The transport times through the vadose zone and the aquifer are ignored.

The estimated impacts are calculated using the following equation,

$$\textit{Response} = \Sigma_i \; I_i(t)\, \Gamma_i(t)\, w_i\, D_i$$

where:

I_i= the amount (or inventory) of radionuclide i (Ci) from Wootan 1999. The time-dependent value is calculated based on the initial inventory and on decay. The ingrowth from other radionuclides is included for these short times.

Γ_i= the fractional concentration at the bottom of the vadose zone. This concentration is assumed equal to the average trench concentration normalized for the fracional release of each radionuclide at time t.

w_i = the ratio of the concentration of radionuclide i at the well location relative to the contaminant concentration at the bottom of the vadose zone (dimensionless). This quantity is called the well intercept factor in earlier Hanford performance assessments. The WIF for the Base Analysis Case is used (WIF = 1.05×10^{-3}).

D_i = the dose rate factor (mrem/y per pCi/L). The values are taken for the all pathway farmer scenario in Rittmann (1999) for estimated dose impacts. D_i is unity when the response that is calculated is a concentration.

Table 5-4. Fractional Radionuclide Concentration for Bathtub Effect

Time Since Facility Closure (y)	STORM Model – Released Tc		Fractional Concentration[2] (10^{-12}/L)
	(micromoles)	Fraction Released[1] (ppm)	
3.169E-08	3.367E-07	2.825E-06	1.707E-08
1.901E-06	4.636E-07	3.889E-06	2.350E-08
1.141E-04	8.051E-06	6.754E-05	4.082E-07
2.738E-03	1.809E-04	1.517E-03	9.170E-06
1.916E-02	1.338E-03	1.123E-02	6.785E-05
9.582E-02	8.354E-03	7.008E-02	4.235E-04
1.000E+00	9.754E-02	8.183E-01	4.945E-03
2.000E+00	1.466E-01	1.230E+00	7.434E-03
5.000E+00	2.063E-01	1.730E+00	1.046E-02
1.000E+01	2.619E-01	2.197E+00	1.328E-02
2.000E+01	3.721E-01	3.122E+00	1.886E-02
5.000E+01	7.222E-01	6.059E+00	3.661E-02
1.000E+02	1.364E+00	1.145E+01	6.917E-02
2.000E+02	2.835E+00	2.379E+01	1.437E-01
5.000E+02	8.231E+00	6.905E+01	4.173E-01
1.000E+03	1.862E+01	1.562E+02	9.441E-01
2.000E+03	4.001E+01	3.357E+02	2.028E+00
5.000E+03	9.222E+01	7.737E+02	4.675E+00
7.500E+03	1.205E+02	1.011E+03	6.108E+00
1.000E+04	1.387E+02	1.164E+03	7.034E+00
1.250E+04	1.505E+02	1.262E+03	7.629E+00
1.500E+04	1.574E+02	1.320E+03	7.979E+00
1.750E+04	1.611E+02	1.351E+03	8.165E+00
2.000E+04	1.628E+02	1.366E+03	8.254E+00
3.000E+04	1.690E+02	1.417E+03	8.566E+00

(1) Fraction released = Tc released / Tc in model (0.1192 moles)
(2) Fractional Concentration = fraction released / water content in six trenches

Figure 5-8. Tc-99 Released from the STORM model as a Function of Time to Bathtub Failure

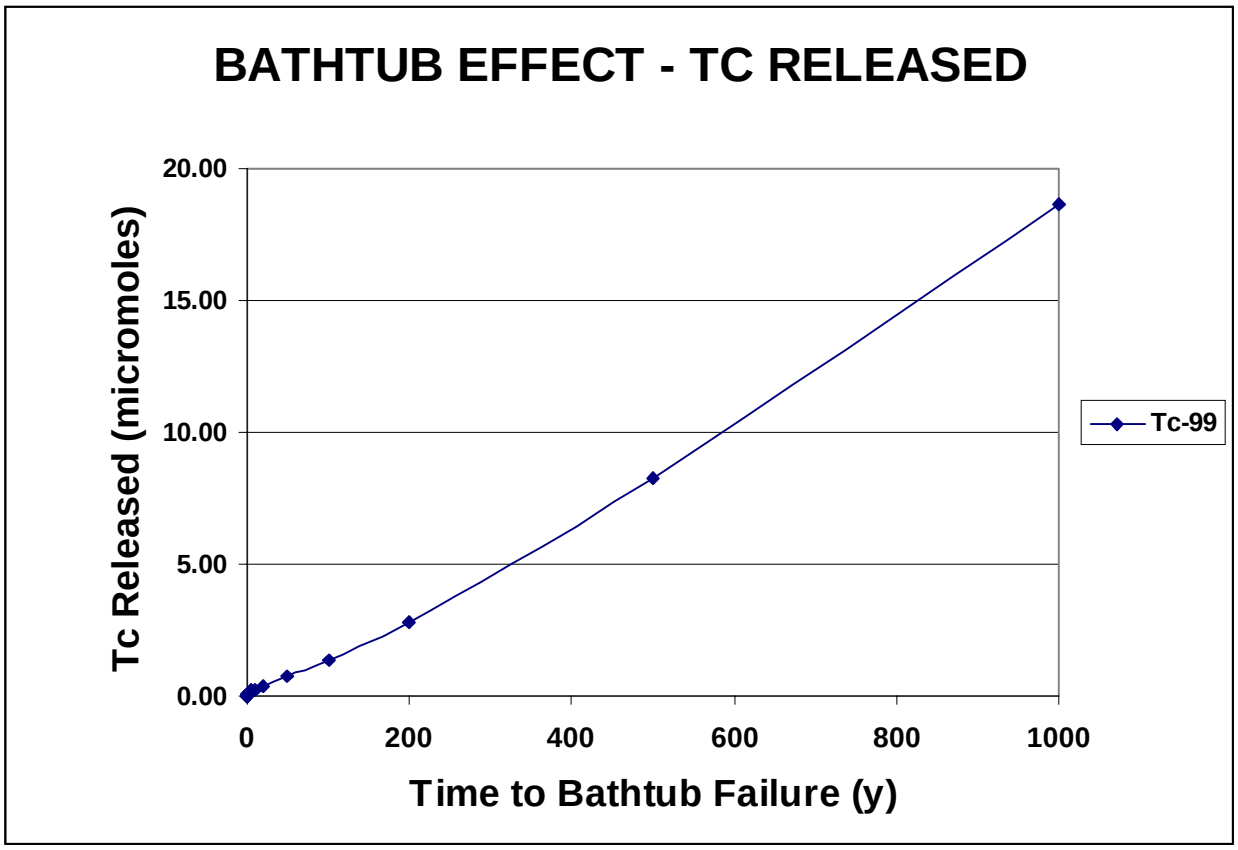

Table 5-5 provides the estimated impacts for each radionuclide for the beta-photon drinking water dose, the all-pathway dose, and the alpha concentration in the aquifer associated with a well located 100 m downgradient from the disposal facility for trench bottom failures at 100 and 1,000 years after facility closure. The recharge rate at the ILAW disposal site is assumed to be 4.2 mm/y. These estimated impacts are associated with the all-pathways farmer scenario with the dose factors taken from Rittmann (1999).

Table 5-5. Estimated Impacts for Bathtub Release after 100 and 1,000 Years

Material	K_d Value (1) (mL/g)	ILAW Inventory (2) (Ci)	Bathtub effect ends after 100 Years			Bathtub effect ends after 1,000 Years		
			Beta-Photon Drinking Water Dose (mrem/y)	All-Pathways Dose (mrem/y)	Alpha Concentration (pCi/L)	Beta-Photon Drinking Water Dose (mrem/y)	All-Pathways Dose (mrem/y)	Alpha Concentration (pCi/L)
3-H	0	0	0.00E+00	0.00E+00	0.00E+00	0.00E+00	0.00E+00	0.00E+00
14-C	4	0	0.00E+00	0.00E+00	0.00E+00	0.00E+00	0.00E+00	0.00E+00
60-Co	150	4180	7.53E-11	2.37E-10	0.00E+00	4.13E-61	1.30E-60	0.00E+00
59-Ni	80	167	1.37E-06	2.07E-06	0.00E+00	1.85E-05	2.80E-05	0.00E+00
63-Ni	80	16200	1.43E-04	2.16E-04	0.00E+00	3.84E-06	5.80E-06	0.00E+00
79-Se	4	48	1.64E-05	4.01E-05	0.00E+00	2.23E-04	5.47E-04	0.00E+00
90-Sr (a)	10	4500000	9.48E-01	1.37E+00	0.00E+00	3.07E-09	4.42E-09	0.00E+00
93-Zr	150	1250	8.13E-05	1.18E-04	0.00E+00	1.11E-03	1.61E-03	0.00E+00
93m-Nb	80	836	2.56E-05	2.73E-04	0.00E+00	3.49E-04	3.73E-03	0.00E+00
99-Tc	0	5790	3.31E-04	1.49E-03	0.00E+00	4.51E-03	2.02E-02	0.00E+00
106-Ru	0.6	894	5.51E-44	7.37E-44	0.00E+00	0.00E+00	0.00E+00	0.00E+00
113m-Cd	**	7970	6.28E-05	8.67E-05	0.00E+00	5.23E-23	7.22E-23	0.00E+00
126-Sn	80	169	1.40E-04	6.91E-04	0.00E+00	1.90E-03	9.40E-03	0.00E+00
125-Sb	**	52000	5.78E-18	1.77E-17	0.00E+00	4.50E-116	1.38E-115	0.00E+00
129-I	0	22	2.38E-04	6.02E-04	0.00E+00	3.25E-03	8.22E-03	0.00E+00
134-Cs	80	376	1.51E-23	4.19E-23	0.00E+00	8.26E-154	2.29E-153	0.00E+00
137-Cs (b)	80	911000	7.71E-02	2.15E-01	0.00E+00	9.80E-10	2.73E-09	0.00E+00
151-Sm	**	780000	4.17E-03	5.76E-03	0.00E+00	5.56E-05	7.68E-05	0.00E+00
152-Eu	150	307	6.62E-08	2.35E-07	0.00E+00	4.28E-27	1.52E-26	0.00E+00
154-Eu	150	37700	2.43E-07	7.20E-07	0.00E+00	9.71E-38	2.88E-37	0.00E+00
155-Eu	150	31500	3.38E-12	5.52E-12	0.00E+00	5.93E-69	9.70E-69	0.00E+00
210-Pb(c)	**	0	0.00E+00	2.05E-05	3.97E-06	0.00E+00	5.82E-04	1.13E-04
226-Ra(c)	10	0.057	0.00E+00	3.73E-06	1.61E-05	0.00E+00	1.08E-04	4.67E-04

Table 5-5. Estimated Impacts for Bathtub Release after 100 and 1,000 Years

Material	K_d Value [1] (mL/g)	ILAW Inventory [2] (Ci)	Bathtub effect ends after 100 Years			Bathtub effect ends after 1,000 Years		
			Beta-Photon Drinking Water Dose (mrem/y)	All-Pathways Dose (mrem/y)	Alpha Concentration (pCi/L)	Beta-Photon Drinking Water Dose (mrem/y)	All-Pathways Dose (mrem/y)	Alpha Concentration (pCi/L)
228-Ra(c)	10	33	7.23E-05	9.27E-05	0.00E+00	9.87E-04	1.27E-03	0.00E+00
227-Ac(c)	150	0.0606	0.00E+00	2.57E-04	1.25E-04	0.00E+00	3.82E-03	1.86E-03
228-Th(c)	150	0	0.00E+00	4.34E-04	3.81E-03	0.00E+00	7.23E-04	6.35E-03
229-Th(c)	150	0.34	0.00E+00	4.13E-04	7.29E-04	0.00E+00	3.51E-02	6.20E-02
230-Th(c)	150	0	0.00E+00	1.55E-06	4.00E-06	0.00E+00	1.61E-04	4.14E-04
232-Th	150	1.28	0.00E+00	1.80E-04	9.30E-05	0.00E+00	2.46E-03	1.27E-03
231-Pa(c)	0.6	0.344	0.00E+00	1.79E-04	2.53E-05	0.00E+00	2.63E-03	3.72E-04
232-U	0.6	34.6	0.00E+00	6.51E-04	6.51E-04	0.00E+00	1.17E-06	1.17E-06
233-U	0.6	131	0.00E+00	2.08E-03	9.51E-03	0.00E+00	2.84E-02	1.30E-01
234-U	0.6	44.1	0.00E+00	6.85E-04	3.20E-03	0.00E+00	9.36E-03	4.37E-02
235-U	0.6	1.79	0.00E+00	2.64E-05	1.30E-04	0.00E+00	3.60E-04	1.77E-03
236-U	0.6	1.43	0.00E+00	2.12E-05	1.04E-04	0.00E+00	2.89E-04	1.42E-03
238-U	0.6	48.3	0.00E+00	7.12E-04	3.51E-03	0.00E+00	9.72E-03	4.79E-02
237-Np	0.6	81	0.00E+00	1.76E-02	5.91E-03	0.00E+00	2.44E-01	8.21E-02
238-Pu	150	106	0.00E+00	5.74E-03	2.68E-03	0.00E+00	1.09E-04	5.11E-05
239-Pu	150	3050	0.00E+00	5.21E-01	2.21E-01	0.00E+00	6.93E+00	2.93E+00
240-Pu	150	525	0.00E+00	8.87E-02	3.76E-02	0.00E+00	1.10E+00	4.67E-01
241-Pu	150	7170	2.70E-05	3.34E-05	0.00E+00	4.86E-23	6.01E-23	0.00E+00
242-Pu	150	0.0449	0.00E+00	7.31E-06	3.26E-06	0.00E+00	9.98E-05	4.45E-05
241-Am	150	10800	0.00E+00	1.57E+00	6.45E-01	0.00E+00	5.06E+00	2.08E+00
242m-Am	150	1.72	1.22E-04	1.50E-04	0.00E+00	1.99E-05	2.46E-05	0.00E+00
243-Am	150	0.689	0.00E+00	1.20E-04	4.94E-05	0.00E+00	1.50E-03	6.20E-04
242-Cm	150	57.6	0.00E+00	4.01E-06	5.29E-05	0.00E+00	6.55E-07	8.65E-06

Table 5-5. Estimated Impacts for Bathtub Release after 100 and 1,000 Years

Material	K_d Value (1) (mL/g)	ILAW Inventory (2) (Ci)	Bathtub effect ends after 100 Years			Bathtub effect ends after 1,000 Years		
			Beta-Photon Drinking Water Dose (mrem/y)	All-Pathways Dose (mrem/y)	Alpha Concentration (pCi/L)	Beta-Photon Drinking Water Dose (mrem/y)	All-Pathways Dose (mrem/y)	Alpha Concentration (pCi/L)
243-Cm	150	6.73	0.00E+00	3.01E-05	1.79E-05	0.00E+00	1.28E-13	7.61E-14
244-Cm	150	101	0.00E+00	5.42E-05	4.01E-05	0.00E+00	7.95E-19	5.89E-19
Subtotal (mobile)(3)			5.69E-04	2.40E-02	2.30E-02	7.76E-03	3.23E-01	3.07E-01
Total (all)			1.03E+00	3.80E+00	9.34E-01	1.24E-02	1.35E+01	5.86E+00

(1) K_d values taken from Mann/Puigh 2000b
(2) Inventory taken from Wootan 1999
(3) Subtotal of mobile radionuclide estimated impacts includes all radionuclides with K_d = 0 or 0.6 mL/g

If none of the contaminants are chemically retarded in their transport through the vadose zone, then the maximum estimated all-pathways dose as a function of the trench bathtub effect time is shown in Figure 5-9. The major contributors to the all pathway dose assuming the bottom fails after 100 years are ^{90}Sr, ^{241}Am, ^{239}Pu, and ^{137}Cs. The major contributors to the all-pathway dose assuming the trench bottom fails after 1,000 years are ^{239}Pu, ^{241}Am, ^{240}Pu, and ^{237}Np.

Hanford tank leak analyses and laboratory measurements (Myers et. al. 1998) have shown that even in leak situations selected radionuclides are chemically retarded as they migrate through the vadose zone. Therefore, for the postulated bathtub effect, only the more mobile radionuclides are anticipated to migrate unretarded through the vadose zone. If only the radionuclides with K_d = 0 mL/g and K_d = 0.6 mL/g are assumed to be transported unhindered through the vadose zone then the maximum, estimated impacts doses for different trench bottom failure times are given as the mobile subtotal in Table 5-5. Shown in Figure 5-10 is the estimated all-pathway doses assuming only the radionuclides with K_d = 0 and 0.6 mL/g are transported unretarded through the vadose zone. The major contributors to the all pathway dose assuming the bottom fails after 100 years are ^{99}Tc, ^{129}I, ^{233}U, ^{234}U, ^{238}U, and ^{237}Np. The major contributors to the all-pathway dose assuming the trench bottom fails after 1,000 years are the same radionuclides that contribute if the bottom were to fail after 100 years.

Figure 5-9. Estimated All-Pathway Dose at Well 100 m Downgradient Assuming All Radionuclides are Not Retarded

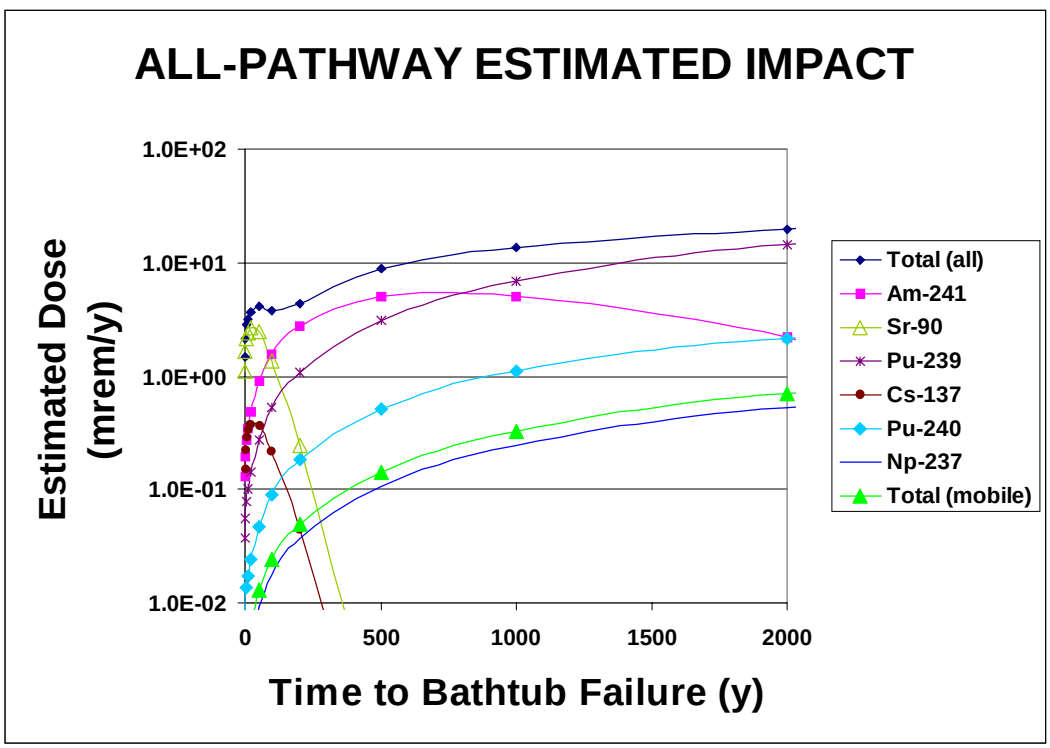

Figure 5-10. Estimated All-Pathway Dose at Well 100 m Downgradient Assuming Only Radionuclides with K_d = 0 or 0.6 mL/g are Not Retarded

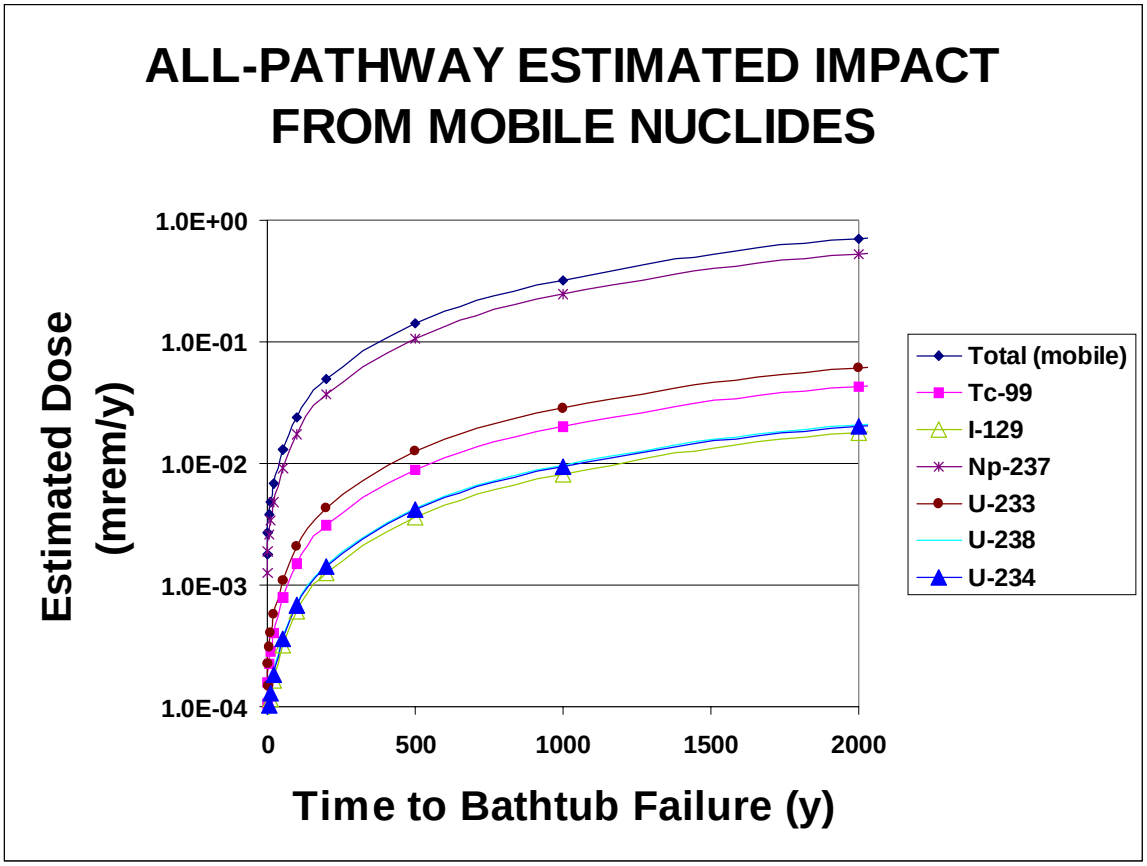

5.5.2 Instantaneous Vadose Zone Transport

The instantaneous vadose zone transport case results are reported in section 5.4.

5.5.3 Instantaneous Waste Form Release

The primary results of interest from the instantaneous waste form release case are the time of peak release rate to the groundwater, and the spread of the peak (full width, half maximum). These values are reported in Table 5-6. Figure 5-11 shows the results graphically.

Table 5-6. Instantaneous Waste Form Release Peak Times

	K_d=0 mL/g	K_d=0.6 mL/g
Peak Time (y)	1,420	11,200
Spread (y)	850	8,150

Figure 5-11. Instantaneous Waste Form Release Case – Release Rates to Aquifer

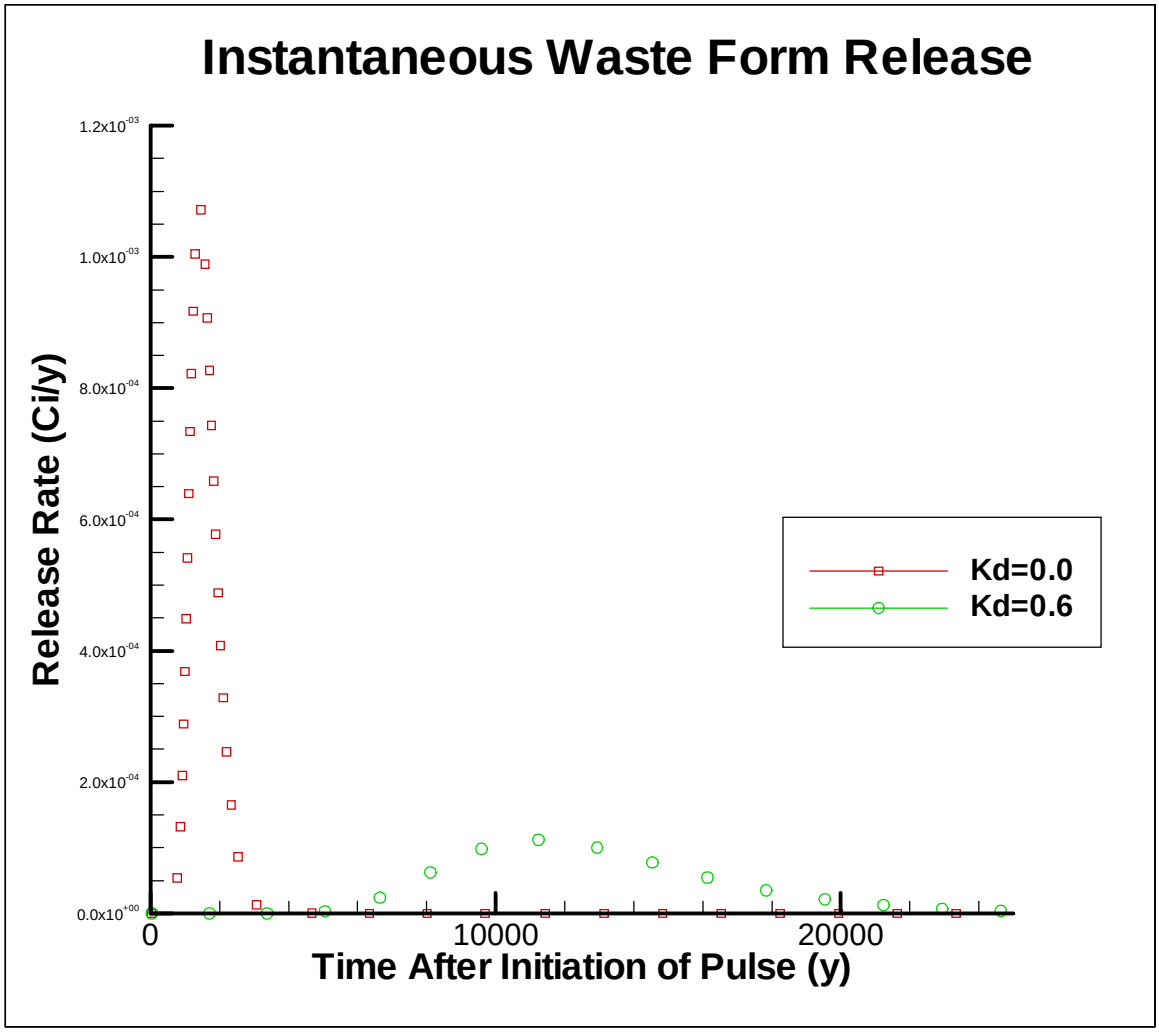

6.0 REFERENCES

Bacon 2000a, Bacon, D. H., and B. P. McGrail, 2000, *Waste Form Release Calculations for the 2001 Immobilized Low-Activity Waste Performance Assessment*, PNNL-13369, Pacific Northwest National Laboratory, Richland, Washington. This document forms part of Puigh 2000b.

Bacon 2000b, D. H. Bacon, M. D. White, and B. P. McGrail, *Subsurface Transport Over Reactive Multiphases (STORM): A General, Coupled, Nonisothermal Multiphase Flow, Reactive, Transport, and Porous Medium Alteration Simulator, Version 2; User's Guide*, PNNL-13108, Pacific Northwest National Laboratory, Richland, Washington, February 2000. Also Appendix D of Mann/Puigh 2000a.

Bergeron 2000, M. P. Bergeron and S. K. Wurstner, *Groundwater Transport Calculations Supporting the Immobilized Low-Activity Waste Disposal Facility Performance Assessment*, PNNL-13400. Pacific Northwest National Laboratory, Richland, Washington, December 2000.

Fayer M.J., M.L. Rockhold, M.D. Campbell, 1992, *Hydrologic Modeling of Protective Barriers: Comparison of Field Data and Simulation Results*, Soil Sci. Soc. of Am. J., 56:690-700.

Fayer M.J., E.M. Murphy, J.L. Downs, F.O. Khan, C.W. Lindenmeier, B.N. Bjornstad, 1999, *Recharge Data Package for the Immobilized Low-Activity Waste 2001 Performance Assessment*, PNNL-13033, Pacific Northwest National Laboratory, Richland, Washington, December 1999. Also Appendix J of Mann/Puigh 2000a.

Finfrock 2000a, S. H. Finfrock, *Verification and Validation for VAM3DF, Version 1.00 (FFS Version 1.00)*, HNF-5636, Fluor Federal Services, Richland, Washington, January 2000.

Huyakorn P.S., and S. Panday, 1999, *VAM3DF : Variably Saturated Analysis Model in Three-Dimensions for the Data Fusion System, Version 2.0*, HydroGeoLogic Inc., Herndon, Virginia.

Kaplan 1999, D. L. Kaplan And R. J. Serne, *Geochemical Data Package For The Immobilized Low-Activity Waste Performance Assessment*, PNNL - 13037, Pacific Northwest National Laboratory, Richland, Washington, December 1999.

Khaleel R., 1999, *Far Field Hydrology Data Package for Immobilized Low-Activity Tank Waste Performance Assessment*, HNF-4769 Rev. 1. Fluor Federal Services, Richland, Washington, December 1999.

Lu, A. H. and D. W. Langford, 1995, *Verification and Benchmark Testing of Version 3.1 of the VAM3DCG Flow and Transport Computer Code for Use in Performance Assessment at Hanford*, WHC-SD-ER-CSWD-007, Westinghouse Hanford Company, Richland, Washington.

Mann F.M., 1996, *INTEG: A Program to Calculate Groundwater Contamination and Human Dose, WHC-SD-WM-RPT-219*, Westinghouse Hanford Company, Richland, Washington.

Mann, F. M. 1999, *Scenarios for the Hanford Immobilized Low-Activity Waste (ILAW) Performance Assessment*, HNF-EP-0828, Rev. 3, Lockheed Martin Hanford Company, Richland, Washington, August 1999. Also Appendix B of Mann/Puigh 2000a.

Mann/Puigh 2000a, F. M. Mann and R. J. Puigh II, *Data Packages for the Hanford Immobilized Low-Activity Tank Waste Performance Assessment: 2001 Version*, HNF-5636, prepared by Fluor Federal Services for Fluor Daniel Hanford Company, Richland, Washington, February 2000.

Mann/Puigh 2000b, F. M. Mann, S. H. Finfrock, E. J. Freeman, R. J. Puigh II, D. H. Bacon, M. P. Bergeron, B. P. McGrail, and S. K. Wurstner, *White Paper Updating the Conclusions of 1998 ILAW Performance Assessment*, DOE/ORP-2000-07, U.S. Department of Energy, Office of River Protection, Richland, Washington, April 2000.

Meyer P.D., and R.J. Serne, 1999, *Near Field Hydrology Data Package for the Immobilized Low-Activity Waste 2001 Performance Assessment*, PNNL-13035, Pacific Northwest National Laboratory, Richland, Washington.

Myers D.A., D.L. Parker, G. Gee, V.G. Johnson, G.V. Last, R.J. Serne, and D.J. Moak 1998, *Findings of the Extension of Borehole 41-09-39, 241-SX Tank Farm*, HNF-2855, Lockheed Martin Hanford Corporation, Richland, Washington..

Puigh R.J., 1998, *Results of Benchmarking Unix and PC Versions of VAM3D-CG Computer Code*, FDNW-RJP-48-016, Fluor Daniel Northwest, Inc., Richland, Washington.

Reidel S.P., and D.G. Horton, 1999, *Geologic Data Package for the 2001 Immobilized Low-Activity Waste Performance Assessment*, PNNL-12257 Rev. 12, Pacific Northwest National Laboratory, Richland, Washington.

Rittmann 1999, P. D. Rittmann, *Exposure Scenarios And Unit Dose Factors For The Hanford Immobilized Low-Activity Tank Waste Performance Assessment*, HNF-SD-WM-TI-707, Rev. 1, prepared by Fluor Federal Services for Fluor Daniel Hanford Company, Richland, Washington, December 1999. Also Appendix O of Mann/Puigh 2000a.

Wootan 1999, D. W. Wootan, *Immobilized Low Activity Tank Waste Inventory Data Package*, HNF-4921, Rev. 0, prepared by Fluor Daniel Northwest, Inc., for Fluor Daniel Hanford Company, September 1999. Also Appendix H of Mann/Puigh 2000a.

APPENDIX A. DATA FILE ARCHIVE

The input and output files associated with the VAM3DF and INTEG calculations have been archived on a CD.

This appendix describes the directory structure of the archive.

The output files for each sensitivity case have been copied onto a compact disk (CD) that is available on request. Table A-1 provides a cross-reference between the sensitivity case descriptions and the summary output files for the waste form, vadose zone, and dose estimate (INTEG) results.

All files on the CD are stored under a directory structure that defines the type of files and case names. The top directory is named 'ILAW;' beneath it are four directories named 'Near Field', 'Far Field', 'Waste Form' and 'Integration.' The 'Near Field' directory contains subdirectories corresponding to different near field VAM3DF calculations, which in turn contain the input and output files associated with that case. The 'Far field' directory contains similar information for the VAM3DF far field calculations. The 'Waste Form' directory contains subdirectories corresponding to different waste form cases, which in turn contain the data files used in the calculations. The 'Integration' directory contains subdirectories corresponding to the INTEG cases, which in turn contain the input and output files for each INTEG calculation.

The near field case subdirectory names correspond to the near field cases identified in Table A-1. Each subdirectory contains four files: 'casename.inp', 'casename.out', 'casename.fpl', (where 'casename' is replaced with the case name), and 'bcflow.out'. The '.inp' file is the standard VAM3DF input file that specifies the calculation parameters. The 'casename.out' file is the VAM3DF standard output file, and the '.fpl' file contains the fluid flux data that is used by the Bcflow code to create the boundary condition inputs for the far field calculations. The 'bcflow.out' file is the result of the Bcflow calculation.

The far field case subdirectory names correspond to the far field cases identified in Table A-1. The cases are divided into two categories: flow (indicated by a '-f' suffix) and transport (indicated by a '-t-#' suffix, where the '#' indicates the K_d value used in that case). Each flow case subdirectory contains four files: 'casename.inp', 'casename.out', 'casename.fpl', and 'casename.vel' (where 'casename' is replaced with the case name). The '.inp' file is the standard VAM3DF input file that specifies the calculation parameters. The '.out' file is the VAM3DF standard output file, and the '.fpl' file contains the fluid flux data that is used by the Botflux code to calculate the flux across the bottom boundary. The '.vel' file contains the velocity field used in the transport calculation. Each transport case subdirectory contains five files: 'casename.inp', 'casename.out', 'casename.ppl' (where 'casename' is replaced with the case name), 'bf.inp', and 'botflux.out'. The '.inp' file is the standard VAM3DF input file that specifies the calculation parameters. The '.out' file is the VAM3DF standard output file, and the '.ppl' file (which is 'zipped') contains the contaminant concentration data that is used by the Botflux code to calculate the flux across the bottom boundary. The 'bf.inp' file contains the input parameters for

Botflux, and the 'botflux.out' file contains the results of the Botflux calculation (which are used as input to the INTEG calculations).
The waste form case subdirectory names begin with the name of the STORM case (e.g., case WFA is in directory WFA-base-42) identified in Table A-1. Each subdirectory contains two files: 'storm2vam.out' and 'storm2vam.g17.' Some subdirectories may contain multiple versions of each file, with a suffix indicating which near field flow calculation they are associated with. The '.out' files contain excerpted data from the STORM output data. These data are in three columns, corresponding to time (year), release rate (micromols/m^2/secomd), and release rate (Ci/m^2/year). The '.g17' files contain the release rate data (converted to Ci/year for each node) in the format required for input to the far field transport calculations.

The integration subdirectory names correspond to the INTEG cases identified in Table A-1. Each subdirectory contains four files named: 'run.bat,' 'vad casename.bac,' 'casename.out,' and 'casename.dat' (where 'casename' is replaced with the case name). The 'run.bat' file contains some of the input parameters required for the INTEG run, including the well intercept factor (WIF), recharge rate, and the names of the data files used in the INTEG calculation (all the data files are in the 'lib' subdirectory under the integration directory). The 'vad-casename.bac' file contains the data from the corresponding far field transport calculations. These data are the release rate (in Ci/year) from the vadose zone into the groundwater with the first column being time (in years) and the subsequent columns each corresponding to a different K_d (typically only the first two K_d columns are used, with the remainder being filled with 0s). The 'casename.out' file contains the general results of the INTEG calculation and the 'casename.dat' file contains the detailed results for each nuclide.

Table A-1. ILAW Cases

Case	Description	Waste Form Case	Near Field Case	Far Field Flow Case	Far Field Transport Case	INTEG Case
1	Base Case:					
1-1	Base Analysis Case	wfa	nf42	42base-f	42base-t	42base
2	Scenario Cases:					
2-1	Well at 1000m	Hand calculated by multiplying base case by ratio of WIF's.				
2-2	Well at Col. River	Hand calculated by multiplying base case by ratio of WIF's.				
2-3	30 L/d pumping	Hand calculated by multiplying base case by ratio of WIF's.				
2-4	100 L/d pumping	Hand calculated by multiplying base case by ratio of WIF's.				
2-5	300 L/d pumping	Hand calculated by multiplying base case by ratio of WIF's.				
2-6	1000 L/d pumping	Hand calculated by multiplying base case by ratio of WIF's.				
2-7	Reduced Hydraulic Conductivity (3X) in Groundwater	Hand calculated by multiplying base case by ratio of WIF's.				
2-8	Regional Recharge Increase (3x)	Hand calculated by multiplying base case by ratio of WIF's.				
2-9	Regional Recharge Decrease (3x)	Hand calculated by multiplying base case by ratio of WIF's.				
	Decrease Regional Upgradient Boundaries (2x)	Hand calculated by multiplying base case by ratio of WIF's.				
2-10	Industrial	wfa	nf42	42base-f	42base-t	ind-100m
2-11	Residential	wfa	nf42	42base-f	42base-t	res-100m
2-12	Agricultural	wfa	nf42	42base-f	42base-t	agr-100m
2-13	Native American	wfa	nf42	42base-f	42base-t	nat-cr

Case	Description	Waste Form Case	Near Field Case	Far Field Flow Case	Far Field Transport Case	INTEG Case
2-14	Columbia River Population	wfa	nf42	42base-f	42base-t	crpop-cr
2-15	DOE Dose Factors	wfa	nf42	42base-f	42base-t	doe-100m
3	Inventory Cases:					
3-1	Upper Bound Inventory.	wfa	nf42	42base-f	42base-t	42ub
3-2	Maximum Tc99.	wfa	nf42	42base-f	42base-t	42maxtc
3-3	No Tc	wfa	nf42	42base-f	42base-t	42notc
3-4	Double I	wfa	nf42	42base-f	42base-t	42-2I
3-5	Double U	wfa	nf42	42base-f	42base-t	42-2u
3-6	Upper bound + max Tc	wfa	nf42	42base-f	42base-t	42ubmaxtc
4	Recharge Cases:					
4-1	Rupert Sand.	wf4	nf09	09-f	09-t	09
4-2	High Recharge.	wf6	nf50	50-f	50-t	50
4-3	Low Recharge.	wfd	nf01	01-f	01-t	01
5	Geology Cases:					
5-1	Hanford Formation Sandy.	wfa	nf42	42sand-f	42sand-t	42sand
5-2	Hanford Formation Gravelly.	wfa	nf42	42grav-f	42grav-t	42grav
5-3	Clastic Dikes.	wfa	nf42	42dike-f	42dike-t	42dike
5-4	Deep Water Table.	wfa	nf42	42deep-f	42deep-t	42deep
6	Facility Cases:					
6-1	Capillary Break (Best Estimate Case).	wfd	nf42-break	42break-f	42break-t	42break
6-2	No Side Slope	wfa	nf42-all	42all-f	42all-t	42all
6-3	Vertical	wfd	nf42-vert	42vert-f	42vert-t	42vert

Case	Description	Waste Form Case	Near Field Case	Far Field Flow Case	Far Field Transport Case	INTEG Case
	Capillary Break.					
6-4	Short Break.	wfd	nf42-shortbreak	42short-f	42short-t	42short
6-5	Capillary Break with High Recharge	wfd	nf50-break	50break-f	50break-t	50break
6-6	Sand Backfill.	wf11	nf42-sand	42sandfill-f	42sandfill-t	42sandfil l
6-7	Alternate Facility Design (Vault).	wf16	nf42-vault	42vault-f	42vault-t	42vault
6-8	Trench Located at South End of Site	Hand calculated by multiplying base case by ratio of WIF's.(1)				
6-9	Trench Rotated 90°	Hand calculated by multiplying base case by ratio of WIF's.(1)				
6-10	Smaller Layout	Hand calculated by multiplying base case by ratio of WIF's.(1)				
6-11	Larger Layout	Hand calculated by multiplying base case by ratio of WIF's.(1)				
6-12	Existing Vault Site	Hand calculated by multiplying new vault case by ratio of WIF's.(1)				
7	Degradation Cases:					
7-1	Surface Barrier.	no barrier = base case; barrier ~ cap break				
7-2	Degraded Capillary Break (Subsidence).	wfa	nf42-subsidence	42sub-f	42sub-t	42sub
7-3	Bath Tub Effect.	See Section 5.5.1				
8	Hydrologic Parameter Cases:					
8-1	Isotropic Conductivity.	wfa	nf42	42iso-f	42iso-t	42iso
8-2	Sand Backfill.	Same as 6-5				

Case	Description	Waste Form Case	Near Field Case	Far Field Flow Case	Far Field Transport Case	INTEG Case
8-3	Hanford Formation Sandy	Same as 5-1				
8-4	Hanford Formation Gravelly	Same as 5-2				
8-5	Instantaneous Transport	wfa	N/A	N/A	N/A	42instant
8-6	High Diffusion	wfa	nf42	42base-f	42diff-t	42diff
8-7	High Dispersion	wfa	nf42	42base-f	42disp-t	42disp
9	Waste Form Cases:					
9-1	Forward Rate.	wfb	nf42	42base-f	42for-t	42for
9-2	Simplified Full Reaction Network (no ion exchange).	wf1	nf42	42base-f	42noion-t	42noion
9-3	Infiltration Rate. Same as recharge cases above.	Same as 4-1 – 4-3				
9-4	Sand Backfill.	Same as 6-5				
9-5	Steel Containers.	wf25	nf42	42base-f	42steel-t	42steel
9-6	Chemical Conditioning Layer.	wf10	nf42	42base-f	42cond-t	42condlayr
9-7	Alternate Facility (Vault)	Same as 6-6				
9-8	Alternate Glass.	wf28	nf42	42base-f	42altglass-t	42altglass
9-9	Diffusion Parameter.	wf14	nf42	42base-f	42diff-t	42diff
9-10	No secondary reactions.	wf2	nf42	42base-f	42nosec-t	42nosec
9-11	High Ion Exchange.	wf30	nf42	42base-f	42highion-t	42highion
9-12	Pulse.	N/A	nf42	42base-f	pulse-t	pulse42
10	Geochemical Cases:					

Case	Description	Waste Form Case	Near Field Case	Far Field Flow Case	Far Field Transport Case	INTEG Case
10-1	Uranium Trapping.	wfa	nf42	42base-f	42base-t, 42conc-t	42conc
10-2	Uranium K_d = 0.0 mL/g.	wfa	nf42	42base-f	42base-t	42ukd0
10-3	All K_d = 0.0 mL/g.	wfa	nf42	42base-f	42base-t	42kd0

(1) WIF's for these cases are provided in Bergeron 2000.

APPENDIX B. INTEG LIBRARY FILES

This appendix lists the library files used as inputs to the INTEG code. There are five files included, each representing a different data set: inventory, half-lives, K_d's, drinking water dose factors, and all-pathways dose factors. The inventory data is taken from Wootan (1999), half-life data and the dose factors data are taken from Rittmann (1999), and the K_d data are taken from Mann/Puigh (2000b).

ILAW Nuclide Inventory Data File ‘inv3.bac’

inv	ILAW inventory (ci), cm242 neglected
h 3	0.00E+00
c 14	0.00E+00
ni 59	1.67E+02
co 60	4.18E+03
ni 63	1.62E+04
se 79	4.80E+01
sr 90	4.50E+06
zr 93	1.25E+03
nb 93m	8.36E+02
tc 99	5.79E+03
ru106	8.94E+02
cd113m	7.97E+03
sb125	5.20E+04
sn126	1.69E+02
i 129	2.20E+01
cs134	3.76E+02
cs137	9.11E+05
sm151	7.80E+05
eu152	3.07E+02
eu154	3.77E+04
eu155	3.15E+04
ra226	5.70E-02
ac227	6.06E-02
ra228	3.30E+01
th229	3.40E-01
pa231	3.44E-01
th232	1.28E+00
u 232	3.46E+01
u 233	1.31E+02
u 234	4.41E+01
u 235	1.79E+00
u 236	1.43E+00
np237	8.10E+01
pu238	1.06E+02
u 238	4.83E+01
pu239	3.05E+03
pu240	5.25E+02
am241	1.08E+04
pu241	7.17E+03
pu242	4.49E-02
am243	6.89E-01
cm243	6.73E+00
cm244	1.01E+02
chem-1	1.00E+00

ILAW Nuclide Half Life Data File ‘t123.bac’

t12	y	From Table 5 from HNF-SD-WM-TI-707, Rev. 1, fix u-236,				
h 3	12.33	1.0	0.0	1.0	0.0	1.0
be 10	1.60E+06	1.0	0.0	1.0	0.0	1.0
c 14	5730.	1.0	0.0	1.0	0.0	1.0
na 22	2.6019	1.0	0.0	1.0	0.0	1.0
cl 36	300992.	1.0	0.0	1.0	0.0	1.0
k 40	1.277E+09	1.0	0.0	1.0	0.0	1.0
mn 54	0.85454	1.0	0.0	1.0	0.0	1.0
fe 55	2.7299	1.0	0.0	1.0	0.0	1.0
co 60	5.2713	1.0	0.0	1.0	0.0	1.0
ni 59	74999.	1.0	0.0	1.0	0.0	1.0
ni 63	100.1	1.0	0.0	1.0	0.0	1.0
se 79	805000.	1.0	0.0	1.0	0.0	1.0
rb 87	4.80E+10	1.0	0.0	1.0	0.0	1.0
sr 90	28.149	1.0	0.0	1.0	0.0	1.0
zr 93	1.53E+06nb 93m	1.0	0.0	1.0	0.0	1.0
nb 93m	16.13	1.0	0.0	1.0	0.0	1.0
nb 94	20300.	1.0	0.0	1.0	0.0	1.0
mo 93	3500.nb 93m	1.0	0.0	1.0	0.0	1.0
tc 99	211097.	1.0	0.0	1.0	0.0	1.0
ru106	1.01736	1.0	0.0	1.0	0.0	1.0
pd107	6.50E+06	1.0	0.0	1.0	0.0	1.0
ag108m	127.	1.0	0.0	1.0	0.0	1.0
cd109	1.26653	1.0	0.0	1.0	0.0	1.0
cd113m	14.1	1.0	0.0	1.0	0.0	1.0
in115	4.41E+14	1.0	0.0	1.0	0.0	1.0
sn121m	54.998	1.0	0.0	1.0	0.0	1.0
sn126	246000.	1.0	0.0	1.0	0.0	1.0
sb125	2.7299te125	1.0	0.0	1.0	0.0	1.0
i 129	1.57E+07	1.0	0.0	1.0	0.0	1.0
cs134	2.0619	1.0	0.0	1.0	0.0	1.0
cs135	2.30E+06	1.0	0.0	1.0	0.0	1.0
cs137	29.999	1.0	0.0	1.0	0.0	1.0
ba133	10.52	1.0	0.0	1.0	0.0	1.0
pm147	2.6233sm147	0.0	1.0	0.0	1.0	1.0
sm147	1.06E+11	1.0	0.0	1.0	0.0	1.0
sm151	89.997	1.0	0.0	1.0	0.0	1.0
eu150	35.798	1.0	0.0	1.0	0.0	1.0
eu152	13.33gd152	1.0	0.0	1.0	0.0	1.0
eu154	8.5919	1.0	0.0	1.0	0.0	1.0
eu155	4.68	1.0	0.0	1.0	0.0	1.0
gd152	1.08E+14	0.0	1.0	0.0	1.0	1.0
ho166m	1200.	1.0	0.0	1.0	0.0	1.0
re187	5.0E+10	1.0	0.0	1.0	0.0	1.0
tl204	3.7801	1.0	0.0	1.0	0.0	1.0
pb210	22.30	0.0	1.0	0.0	1.0	1.0
bi207	32.198	0.0	1.0	1.0	0.0	1.0
po209	102.0	0.0	1.0	0.0	1.0	1.0
ra226	1600.pb210	0.0	1.0	2.0	4.0	1.0
ra228	5.7498th228	0.0	1.0	1.0	0.0	1.0
ac227	21.769bi207	0.0	1.0	4.0	5.0	1.0
th228	1.9129pb208	0.0	1.0	2.0	5.0	1.0
th229	7340.po209	0.0	1.0	4.0	5.0	1.0
th230	75380.ra226	0.0	1.0	0.0	1.0	1.0
th232	1.405E+10ra228	0.0	1.0	0.0	1.0	1.0
pa231	32759.ac227	0.0	1.0	0.0	1.0	1.0
u 232	69.799th228	0.0	1.0	0.0	1.0	1.0
u 233	159198.th229	0.0	1.0	0.0	1.0	1.0
u 234	245694.th230	0.0	1.0	0.0	1.0	1.0
u 235	7.037E+08pa231	0.0	1.0	1.0	1.0	1.0

u 236	2.342E+07th232	0.0	1.0	2.0	1.0	1.0
u 238	4.468E+09u 234	0.0	1.0	2.0	1.0	1.0
np237	2.14E+06u 233	0.0	1.0	1.0	1.0	1.0
pu236	2.8999u 232	0.0	1.0	0.0	1.0	1.0
pu238	87.697u 234	0.0	1.0	0.0	1.0	1.0
pu239	24110.u 235	0.0	1.0	0.0	1.0	1.0
pu240	6563.u 236	0.0	1.0	0.0	1.0	1.0
pu241	14.35am241	0.0	1.0	1.0	0.0	1.0
pu242	373507.u 238	0.0	1.0	0.0	1.0	1.0
pu244	8.00E+07pu240	0.0	1.0	2.0	1.0	1.0
am241	432.7np237	0.0	1.0	0.0	1.0	1.0
am242m	141.pu238	0.0	1.0	1.0	1.0	0.82782
am243	7370.pu239	0.0	1.0	1.0	1.0	1.0
cm243	28.499pu239	0.0	1.0	0.0	1.0	1.0
cm244	18.10pu240	0.0	1.0	0.0	1.0	1.0
cm245	8500.pu241	0.0	1.0	0.0	1.0	1.0
cm246	4730.pu242	0.0	1.0	0.0	1.0	1.0
cm247	1.60E+07am243	0.0	1.0	1.0	1.0	1.0
cm248	339981.pu244	0.0	1.0	1.0	1.0	0.9174
chem-1	0.	0.0	0.0	0.0	0.0	1.0
chem-2	0.	0.0	0.0	0.0	0.0	1.0
chem-3	0.	0.0	0.0	0.0	0.0	1.0
chem-4	0.	0.0	0.0	0.0	0.0	1.0

ILAW Nuclide K_d Data File ‘kd1.bac’

```
vadlab   ILAW PA
h   3     Kd=0.0
c  14     Kd=4.0
ni 59     Kd=80.0
co 60     Kd=150.0
ni 63     Kd=80.0
se 79     Kd=4.0
sr 90     Kd=10.0
zr 93     Kd=150.0
nb 93m    Kd=80.0
tc 99     Kd=0.0
ru106     Kd=0.6
cd113m    Kd=0.0
sb125     Kd=0.0
sn126     Kd=80.0
i 129     Kd=0.0
cs134     Kd=80.0
cs137     Kd=80.0
sm151     Kd=0.0
eu152     Kd=150.0
eu154     Kd=150.0
eu155     Kd=150.0
ra226     Kd=10.0
ac227     Kd=150.0
ra228     Kd=10.0
th229     Kd=150.0
pa231     Kd=0.6
th232     Kd=150.0
u 232     Kd=0.6
u 233     Kd=0.6
u 234     Kd=0.6
u 235     Kd=0.6
u 236     Kd=0.6
np237     Kd=0.6
pu238     Kd=150.0
u 238     Kd=0.6
pu239     Kd=150.0
pu240     Kd=150.0
am241     Kd=150.0
pu241     Kd=150.0
pu242     Kd=150.0
am243     Kd=150.0
cm243     Kd=150.0
cm244     Kd=150.0
gd152     Kd=0.0
pb210     Kd=80.0
bi207     Kd=0.0
po209     Kd=150.0
th228     Kd=150.0
th230     Kd=150.0
chem-1    Kd=0.0
```

ILAW Drinking Water Dose Factors Data File ‘dw2.bac’

dw	mrem/y/pCi/l	ingestion; from table 38, HNF-SD-WM-TI-707 rev 1,
h 3	3.46e-05	
be 10	2.52e-03	
c 14	1.13e-03	
na 22	6.21e-03	
cl 36	1.64e-03	
k 40	1.00e-02	
mn 54	1.50e-03	
fe 55	3.28e-04	
co 60	1.45e-02	
ni 59	1.13e-04	
ni 63	3.12e-04	
se 79	4.70e-03	
rb 87	2.66e-03	
sr 90	8.26e-02	
zr 93	8.96e-04	
nb 93m	2.82e-04	
nb 94	3.86e-03	
mo 93	7.29e-04	
tc 99	7.88e-04	
ru106	1.48e-02	
pd107	8.05e-05	
ag108m	4.11e-03	
cd109	7.07e-03	
cd113m	8.69e-02	
in115	8.53e-02	
sn121m	1.22e-03	
sn126	1.14e-02	
sb125	2.00e-03	
i 129	1.49e-01	
cs134	3.96e-02	
cs135	3.82e-03	
cs137	2.70e-02	
ba133	1.84e-03	
pm147	5.67e-04	
sm147	9.99e-02	
sm151	2.10e-04	
eu150	3.43e-03	
eu152	3.50e-03	
eu154	5.16e-03	
eu155	8.26e-04	
gd152	8.69e-02	
ho166m	4.36e-03	
re187	5.14e-06	
tl204	1.81e-03	
pb210	3.95e+00	
bi207	2.96e-03	
po209	1.29e+00	
ra226	7.18e-01	
ra228	7.78e-01	
ac227	7.99e+00	
th228	4.38e-01	
th229	2.18e+00	
th230	2.96e-01	
th232	1.47e+00	
pa231	5.72e+00	
u 232	7.07e-01	
u 233	1.56e-01	
u 234	1.53e-01	
u 235	1.44e-01	

u 236	1.45e-01
u 238	1.45e-01
np237	2.40e+00
pu236	6.32e-01
pu238	1.73e+00
pu239	1.91e+00
pu240	1.91e+00
pu241	3.70e-02
pu242	1.81e+00
pu244	1.79e+00
am241	1.97e+00
am242m	1.96e+00
am243	1.96e+00
cm243	1.36e+00
cm244	1.09e+00
cm245	2.02e+00
cm246	2.00e+00
cm247	1.85e+00
cm248	7.34e+00
chem-1	0.0
chem-2	0.0
chem-3	0.0
chem-4	0.0

ILAW All Pathways Dose Factors Data File ‘dw2.bac’

allpath	mrem/y/pCi/l	allpath total; from table 38 HNF-SD-WM-TI-707 rev 1
h 3	4.58E-05	
be 10	3.19E-03	
c 14	4.67E-03	
na 22	5.21E-02	
cl 36	4.81E-02	
k 40	2.83E-02	
mn 54	6.19E-03	
fe 55	6.05E-04	
co 60	4.57E-02	
ni 59	1.71E-04	
ni 63	4.71E-04	
se 79	1.15E-02	
rb 87	7.50E-03	
sr 90	1.19E-01	
zr 93	1.30E-03	
nb 93m	3.01E-03	
nb 94	5.26E-02	
mo 93	1.19E-03	
tc 99	3.54E-03	
ru106	1.98E-02	
pd107	1.93E-04	
ag108m	2.51E-02	
cd109	9.60E-03	
cd113m	1.20E-01	
in115	1.27E-01	
sn121m	4.54E-03	
sn126	5.63E-02	
sb125	5.34E-03	
i 129	3.77E-01	
cs134	1.10E-01	
cs135	1.01E-02	
cs137	7.53E-02	
ba133	4.68E-03	
pm147	7.70E-04	
sm147	1.43E-01	
sm151	2.90E-04	
eu150	1.47E-02	
eu152	1.24E-02	
eu154	1.53E-02	
eu155	1.35E-03	
gd152	1.36E-01	
ho166m	1.78E-02	
re187	8.74E-06	
tl204	4.66E-03	
pb210	5.17E+00	
bi207	1.42E-02	
po209	1.83E+00	
ra226	9.29E-01	
ra228	9.97E-01	
ac227	1.03E+01	
th228	5.69E-01	
th229	2.83E+00	
th230	3.88E-01	
th232	1.94E+00	
pa231	7.08E+00	
u 232	1.00E+00	
u 233	2.19E-01	
u 234	2.14E-01	
u 235	2.03E-01	

u 236	2.04E-01
u 238	2.03E-01
np237	2.97E+00
pu236	7.79E-01
pu238	2.14E+00
pu239	2.36E+00
pu240	2.36E+00
pu241	4.57E-02
pu242	2.24E+00
pu244	2.22E+00
am241	2.43E+00
am242m	2.43E+00
am243	2.42E+00
cm243	1.68E+00
cm244	1.35E+00
cm245	2.50E+00
cm246	2.47E+00
cm247	2.29E+00
cm248	9.09E+00
chem-1	0.0
chem-2	0.0
chem-3	0.0
chem-4	0.0

APPENDIX C. BCFLOW

This appendix documents the Bcflow utility code. It includes an input and output description, example input and output files, and a source code listing.

The Bcflow code takes the volumetric fluid flow rates across the bottom boundary of a near field flow calculation and calculates the effective recharge rate across the top boundary of a far field flow calculation.

The flow rates for each boundary node are read in from the boundary flux (fpl) file from the near field flow calculation. The code assumes that the flow calculation specified the bottom boundary nodes as nodes to be tracked, and that they are the first nodes so specified, and that they are specified in order from left to right. There is also an implicit assumption that the flow run has reached steady-state by the last time step printed to the fpl file.

The code also reads in node coordinate data from an input file named grids.txt. This file must contain the following information:

- The number of node columns in the near field model.
- The x coordinate value for each column (in 8f10.3 format).
- The number of columns and the number of rows in the far field model.
- The x coordinate value for each column (in 8f10.3 format).

The results of the Bcflow calculation is a file (named bcflow.out), which contains the effective recharge rate for each node in the top boundary of the far field model. The data are in the format required for the VAM3DF input and can be inserted directly into the VAM3DF standard input file.

Example Bcflow input file ‘grids.txt’ (base case):

```
137
     0.000     0.500     1.000     1.500     2.000     2.500     3.000     3.500
     4.000     4.500     5.000     5.500     6.000     6.500     7.000     7.500
     8.000     8.500     9.000     9.500    10.000    10.500    11.000    11.500
    12.000    12.500    13.000    13.500    14.000    14.500    15.000    15.500
    16.000    16.500    17.000    17.500    18.000    18.500    19.000    19.500
    20.000    20.500    21.000    21.500    22.000    22.500    23.000    23.500
    24.000    24.500    25.000    25.500    26.000    26.500    27.000    27.500
    28.000    28.500    29.000    29.500    30.000    30.500    31.000    31.500
    32.000    32.500    33.000    33.500    34.000    34.500    35.000    35.500
    36.000    36.500    37.000    37.500    38.000    38.500    39.000    39.500
    40.000    40.500    41.000    41.500    42.000    42.500    43.000    43.500
    44.000    44.500    45.000    45.500    46.000    46.500    47.000    47.500
    48.000    48.250    48.500    48.750    49.000    49.250    49.500    49.750
    50.000    50.250    50.500    50.750    51.000    51.250    51.500    51.750
    52.000    52.250    52.500    52.750    53.000    53.250    53.500    53.750
    54.000    54.250    54.500    54.750    55.000    55.250    55.500    55.750
    56.000    56.500    57.000    57.500    58.000    58.500    59.000    59.500
    60.000
137 75
     0.000     0.500     1.000     1.500     2.000     2.500     3.000     3.500
     4.000     4.500     5.000     5.500     6.000     6.500     7.000     7.500
     8.000     8.500     9.000     9.500    10.000    10.500    11.000    11.500
    12.000    12.500    13.000    13.500    14.000    14.500    15.000    15.500
    16.000    16.500    17.000    17.500    18.000    18.500    19.000    19.500
    20.000    20.500    21.000    21.500    22.000    22.500    23.000    23.500
    24.000    24.500    25.000    25.500    26.000    26.500    27.000    27.500
    28.000    28.500    29.000    29.500    30.000    30.500    31.000    31.500
    32.000    32.500    33.000    33.500    34.000    34.500    35.000    35.500
    36.000    36.500    37.000    37.500    38.000    38.500    39.000    39.500
    40.000    40.500    41.000    41.500    42.000    42.500    43.000    43.500
    44.000    44.500    45.000    45.500    46.000    46.500    47.000    47.500
    48.000    48.250    48.500    48.750    49.000    49.250    49.500    49.750
    50.000    50.250    50.500    50.750    51.000    51.250    51.500    51.750
    52.000    52.250    52.500    52.750    53.000    53.250    53.500    53.750
    54.000    54.250    54.500    54.750    55.000    55.250    55.500    55.750
    56.000    56.500    57.000    57.500    58.000    58.500    59.000    59.500
    60.000
```

Example Bcflow input file ‘fpl’ (base case):

(Intermediate time step data has been deleted from this file listing.)

```
VAM3DF VERSION 1.0
base case; 4.2mm/yr & 50mm/yr; no cap barrier (all sand)
     1   274
 1    2    3    4    5    6    7    8    9   10   11   12   13   14   15   16   17
18   19   20   21   22   23   24   25   26   27   28   29   30   31   32   33   34
35   36   37   38   39   40   41   42   43   44   45   46   47   48   49   50   51
52   53   54   55   56   57   58   59   60   61   62   63   64   65   66   67   68
69   70   71   72   73   74   75   76   77   78   79   80   81   82   83   84   85
86   87   88   89   90   91   92   93   94   95   96   97   98   99   100  101  102
103  104  105  106  107  108  109  110  111  112  113  114  115  116  117  118  119
120  121  122  123  124  125  126  127  128  129  130  131  132  133  134  135  136
137 7810 7811 7812 7813 7814 7815 7816 7817 7818 7819 7820 7821 7822 7823 7824 7825
7826 7827 7828 7829 7830 7831 7832 7833 7834 7835 7836 7837 7838 7839 7840 7841 7842
7843 7844 7845 7846 7847 7848 7849 7850 7851 7852 7853 7854 7855 7856 7857 7858 7859
7860 7861 7862 7863 7864 7865 7866 7867 7868 7869 7870 7871 7872 7873 7874 7875 7876
7877 7878 7879 7880 7881 7882 7883 7884 7885 7886 7887 7888 7889 7890 7891 7892 7893
7894 7895 7896 7897 7898 7899 7900 7901 7902 7903 7904 7905 7906 7907 7908 7909 7910
7911 7912 7913 7914 7915 7916 7917 7918 7919 7920 7921 7922 7923 7924 7925 7926 7927
7928 7929 7930 7931 7932 7933 7934 7935 7936 7937 7938 7939 7940 7941 7942 7943 7944
7945 7946
STEP =   600TIME =  0.431E+04 *** NODAL FLUID FLUX VALUES ***
-1.068E-03-2.139E-03-2.144E-03-2.152E-03-2.165E-03-2.183E-03-2.207E-03-2.238E-03
-2.279E-03-2.330E-03-2.392E-03-2.461E-03-2.527E-03-2.564E-03-2.527E-03-2.398E-03
-2.318E-03-2.267E-03-2.213E-03-2.180E-03-2.160E-03-2.142E-03-2.129E-03-2.122E-03
-2.116E-03-2.111E-03-2.108E-03-2.106E-03-2.104E-03-2.103E-03-2.102E-03-2.102E-03
-2.101E-03-2.101E-03-2.101E-03-2.100E-03-2.100E-03-2.100E-03-2.100E-03-2.100E-03
-2.099E-03-2.099E-03-2.099E-03-2.099E-03-2.099E-03-2.098E-03-2.098E-03-2.098E-03
-2.097E-03-2.097E-03-2.096E-03-2.096E-03-2.095E-03-2.095E-03-2.094E-03-2.093E-03
-2.092E-03-2.091E-03-2.090E-03-2.089E-03-2.088E-03-2.086E-03-2.085E-03-2.083E-03
-2.081E-03-2.080E-03-2.078E-03-2.077E-03-2.075E-03-2.075E-03-2.075E-03-2.076E-03
-2.078E-03-2.083E-03-2.090E-03-2.101E-03-2.117E-03-2.140E-03-2.170E-03-2.212E-03
-2.267E-03-2.339E-03-2.432E-03-2.551E-03-2.702E-03-2.892E-03-3.127E-03-3.417E-03
-3.772E-03-4.201E-03-4.715E-03-5.325E-03-6.042E-03-6.877E-03-7.845E-03-8.973E-03
-7.757E-03-5.611E-03-6.169E-03-6.958E-03-3.736E-02 2.434E-02-5.955E-03-6.733E-03
-7.314E-03-7.786E-03-8.196E-03-8.567E-03-8.909E-03-9.230E-03-9.531E-03-9.815E-03
-1.008E-02-1.033E-02-1.056E-02-1.078E-02-1.098E-02-1.116E-02-1.133E-02-1.148E-02
-1.162E-02-1.174E-02-1.185E-02-1.195E-02-1.203E-02-1.211E-02-1.218E-02-1.223E-02
-1.843E-02-2.474E-02-2.486E-02-2.495E-02-2.502E-02-2.506E-02-2.509E-02-2.511E-02
-1.256E-02 1.050E-03 2.100E-03 2.100E-03 2.100E-03 2.100E-03 2.100E-03 2.100E-03
 2.100E-03 2.100E-03 2.100E-03 2.100E-03 2.100E-03 2.100E-03 2.100E-03 2.100E-03
 2.100E-03 2.100E-03 2.100E-03 2.100E-03 2.100E-03 2.100E-03 2.100E-03 2.100E-03
 2.100E-03 2.100E-03 2.100E-03 2.100E-03 2.100E-03 2.100E-03 2.100E-03 2.100E-03
 2.100E-03 2.100E-03 2.100E-03 2.100E-03 2.100E-03 2.100E-03 2.100E-03 2.100E-03
 2.100E-03 2.100E-03 2.100E-03 2.100E-03 2.100E-03 2.100E-03 2.100E-03 2.100E-03
 2.100E-03 2.100E-03 2.100E-03 2.100E-03 2.100E-03 2.100E-03 2.100E-03 2.100E-03
 2.100E-03 2.100E-03 2.100E-03 2.100E-03 2.100E-03 2.100E-03 2.100E-03 2.100E-03
 2.100E-03 2.100E-03 2.100E-03 2.100E-03 2.100E-03 2.100E-03 2.100E-03 2.100E-03
 2.100E-03 2.100E-03 2.100E-03 2.100E-03 2.100E-03 2.100E-03 2.100E-03 2.100E-03
 2.100E-03 2.100E-03 2.100E-03 2.100E-03 2.100E-03 2.100E-03 2.100E-03 2.100E-03
 2.100E-03 2.100E-03 2.100E-03 2.100E-03 2.100E-03 2.100E-03 2.100E-03 2.100E-03
 2.100E-03 1.575E-03 1.050E-03 1.050E-03 1.050E-03 1.050E-03 1.250E-02 1.250E-02
 1.250E-02 1.250E-02 1.250E-02 1.250E-02 1.250E-02 1.250E-02 1.250E-02 1.250E-02
 1.250E-02 1.250E-02 1.250E-02 1.250E-02 1.250E-02 1.250E-02 1.250E-02 1.250E-02
 1.250E-02 1.250E-02 1.250E-02 1.250E-02 1.250E-02 1.250E-02 1.250E-02 1.250E-02
 1.250E-02 1.875E-02 2.500E-02 2.500E-02 2.500E-02 2.500E-02 2.500E-02 2.500E-02
 2.500E-02 1.250E-02
```

Example Bcflow output file ‘bcflow.out’ (base case):

```
Bcflow 1.0: fluid flux from flow run converted to input for transport run

 Flow Run:
base case; 4.2mm/yr & 50mm/yr; no cap barrier (all sand)
         137

10139    1 1.068E-03
10140    1 2.139E-03
10141    1 2.144E-03
10142    1 2.152E-03
10143    1 2.165E-03
10144    1 2.183E-03
10145    1 2.207E-03
10146    1 2.238E-03
10147    1 2.279E-03
10148    1 2.330E-03
10149    1 2.392E-03
10150    1 2.461E-03
10151    1 2.527E-03
10152    1 2.564E-03
10153    1 2.527E-03
10154    1 2.398E-03
10155    1 2.318E-03
10156    1 2.267E-03
10157    1 2.213E-03
10158    1 2.180E-03
10159    1 2.160E-03
10160    1 2.142E-03
10161    1 2.129E-03
10162    1 2.122E-03
10163    1 2.116E-03
10164    1 2.111E-03
10165    1 2.108E-03
10166    1 2.106E-03
10167    1 2.104E-03
10168    1 2.103E-03
10169    1 2.102E-03
10170    1 2.102E-03
10171    1 2.101E-03
10172    1 2.101E-03
10173    1 2.101E-03
10174    1 2.100E-03
10175    1 2.100E-03
10176    1 2.100E-03
10177    1 2.100E-03
10178    1 2.100E-03
10179    1 2.099E-03
10180    1 2.099E-03
10181    1 2.099E-03
10182    1 2.099E-03
10183    1 2.099E-03
10184    1 2.098E-03
10185    1 2.098E-03
10186    1 2.098E-03
10187    1 2.097E-03
10188    1 2.097E-03
10189    1 2.096E-03
10190    1 2.096E-03
10191    1 2.095E-03
10192    1 2.095E-03
```

10193	1	2.094E-03
10194	1	2.093E-03
10195	1	2.092E-03
10196	1	2.091E-03
10197	1	2.090E-03
10198	1	2.089E-03
10199	1	2.088E-03
10200	1	2.086E-03
10201	1	2.085E-03
10202	1	2.083E-03
10203	1	2.081E-03
10204	1	2.080E-03
10205	1	2.078E-03
10206	1	2.077E-03
10207	1	2.075E-03
10208	1	2.075E-03
10209	1	2.075E-03
10210	1	2.076E-03
10211	1	2.078E-03
10212	1	2.083E-03
10213	1	2.090E-03
10214	1	2.101E-03
10215	1	2.117E-03
10216	1	2.140E-03
10217	1	2.170E-03
10218	1	2.212E-03
10219	1	2.267E-03
10220	1	2.339E-03
10221	1	2.432E-03
10222	1	2.551E-03
10223	1	2.702E-03
10224	1	2.892E-03
10225	1	3.127E-03
10226	1	3.417E-03
10227	1	3.772E-03
10228	1	4.201E-03
10229	1	4.715E-03
10230	1	5.325E-03
10231	1	6.042E-03
10232	1	6.877E-03
10233	1	7.845E-03
10234	1	8.973E-03
10235	1	7.757E-03
10236	1	5.611E-03
10237	1	6.169E-03
10238	1	6.958E-03
10239	1	3.736E-02
10240	1	0.000E+00
10241	1	5.955E-03
10242	1	6.733E-03
10243	1	7.314E-03
10244	1	7.786E-03
10245	1	8.196E-03
10246	1	8.567E-03
10247	1	8.909E-03
10248	1	9.230E-03
10249	1	9.531E-03
10250	1	9.815E-03
10251	1	1.008E-02
10252	1	1.033E-02
10253	1	1.056E-02
10254	1	1.078E-02
10255	1	1.098E-02

```
10256    1 1.116E-02
10257    1 1.133E-02
10258    1 1.148E-02
10259    1 1.162E-02
10260    1 1.174E-02
10261    1 1.185E-02
10262    1 1.195E-02
10263    1 1.203E-02
10264    1 1.211E-02
10265    1 1.218E-02
10266    1 1.223E-02
10267    1 1.843E-02
10268    1 2.474E-02
10269    1 2.486E-02
10270    1 2.495E-02
10271    1 2.502E-02
10272    1 2.506E-02
10273    1 2.509E-02
10274    1 2.511E-02
10275    1 1.256E-02
```

Bcflow source code listing:

```
      program bcflow

      real xcd(200),xcd1(200),flow(500),flux(200),recharge(200)
       character filename*80,line*80,line2*80,line3*80,message*80

      message="Bcflow 1.0: fluid flux from flow run converted "//
     &  "to input for transport run"

       open(20,file="bcflow.out")

      write(*,*)
       write(*,*)'Enter Fluid Flux Filename: '
       read(*,*)filename
       open(12,file=filename,status="old",readonly)

      read(12,*)
       read(12,'(a80)',iostat=ioresult)line

       write(*,*)
       write(*,'(a80)')message
       write(*,*)
      write(*,*)'Flow Run: '
       write(*,'(a80)')line

       write(20,*)
       write(20,'(a80)')message
       write(20,*)
      write(20,*)'Flow Run: '
       write(20,'(a80)')line


c     get fluid flux data from flow run

       read(12,*,iostat=ioresult)n,nbnd
      nline=ceiling(float(nbnd)/20.0)

       do i=1,nline
         read(12,*)
       enddo

      nline=ceiling(float(nbnd)/8.0)

c     assume that bottom boundary nodes are listed first
       do while (ioresult.eq.0)
         read(12,'(a80)',iostat=ioresult)line
         if(ioresult.eq.0)then
           line3=line
           do i=1,nline
             iptr=(i-1)*8+1
             iptr2=min(iptr+7,nbnd)
             read(12,'(a80)')line2
             read(line2,'(8e10.3)')(flow(j),j=iptr,iptr2)
           enddo
         endif
      enddo

       close(12)

      write(*,'(a80)')line3

      write(*,*)
```

```
      write(*,*)'Enter Grid Coordinate Filename: '
      read(*,*)filename
      open(14,file=filename,status="old",readonly)
      read(14,*)nx1
      read(14,*)(xcd1(i),i=1,nx1)
      read(14,*)nx,ny
      read(14,*)(xcd(i),i=1,nx)


      do i=1,nx1
         flux(i)=-flow(i)
         if(flux(i).lt.0)then
           flux(i)=0.
         endif
      enddo

c     following section is for cases where the gridding does not match

      goto 100

c     calc recharge at each node in output model
      do i=2,nx1-1
         recharge(i)=flux(i)/(.5*(xcd1(i+1)-xcd1(i-1)))
      enddo
      recharge(1)=flux(1)/(.5*(xcd1(2)-xcd1(1)))
      recharge(nx1)=flux(nx1)/(.5*(xcd1(nx1)-xcd1(nx1-1)))
      do i=1,nx1
         if(recharge(i).lt.0)then
           recharge(i)=0.
         endif
      enddo

c     interpolate fluid flux to match new case's gridding
      do i=1,nx
         i1=1
         do while (xcd1(i1+1).le.xcd(i) .and. i1.lt.nx1-1)
           i1=i1+1
        enddo
         if(i.eq.1)then
           delx=.5*(xcd(2)-xcd(1))
         else if(i.eq.nx)then
           delx=.5*(xcd(nx)-xcd(nx-1))
         else
           delx=.5*(xcd(i+1)-xcd(i-1))
         endif
        flux(i)= delx*(((xcd(i)-xcd1(i1))/(xcd1(i1+1)-xcd1(i1)))*
     &    (recharge(i1+1)-recharge(i1))+recharge(i1))
      enddo

100   continue

      write(20,*)nx
      write(20,*)
      do i=1,nx
         node=(ny-1)*nx
         write(20,'(2i5,1p,e10.3)')node+i,1,flux(i)
      enddo

      end
```

APPENDIX D. STORM2VAM

This appendix documents the Storm2vam utility code. It includes an input and output description, example input and output files, and a source code listing.

The Storm2vam code is used to take one-dimensional contaminant release data from the STORM code (Bacon 2000b) output and produce two-dimensional data that serves as a boundary condition input for the far field transport calculations. The STORM data are in different units than what is needed for VAM3DF and it uses much finer timestepping than is allowed for VAM3DF input. In addition, the STORM calculation is one-dimensional and assumes a certain height (typically the maximum height) for the waste in the facility. In the case of the trench facility, however, the actual height varies so the facility must be broken into regions of different height and the release rate multiplied by the fraction of full height. The code takes the STORM data, converts it to the needed units (Ci/y), factors in the waste height and element width, and prints out a subset of the data in the format required for use in the VAM3DF input file.

Storm2vam requires as input the Bcflow output file from the corresponding near field flow calculation, a Storm2vam input file, and the STORM data file (named 'fluxes'). The STORM data are assumed to be in units of micro-mols/m^2/s. The input file contains the following information:

- Atomic weight of nuclide to be modeled (99.0 for Tc99).
- Ratio of activity to mass (in Ci/g) for nuclide (.017 for Tc99).
- Minimum skip factor, maximum skip factor, skip factor multiplier, and maximum
- number of steps to print.
- Number of waste zones in facility.
- Maximum x coordinate position of first zone and the fraction of full waste height in this zone. This line is repeated for each zone.
- The number of columns and rows in the far field model.
- The x coordinate value for each column (in 8f10.3 format).

The skip factor is the number of time steps in the STORM data to skip over when creating the VAM3DF input. This starts small and is increased at each step by the multiplier until the maximum is reached.

The code produces two output files: storm2vam.out and storm2vam.g17. The '.out' file is a short summary of the results of the conversion and the '.g17' file contains the full data in a format that can be inserted directly into the VAM3DF input file. The code also prints out the equivalent length of the facility if all zones were full height waste. This number is needed for calculating the effective inventory of the model (based on the STORM data), which is used as an input for the Botflux code.

Example Storm2vam input file ‘storm2vam.in’ (base case):

```
99.                 mol wgt. for tc99
0.017               Ci/g for tc99
10 250 2. 150       time step skip controls (min, max, factor, maxn)
4                   waste zones
 8.5 1.00
15.0 0.75
24.0 0.50
32.0 0.25
137 75
     0.000     0.500     1.000     1.500     2.000     2.500     3.000     3.500
     4.000     4.500     5.000     5.500     6.000     6.500     7.000     7.500
     8.000     8.500     9.000     9.500    10.000    10.500    11.000    11.500
    12.000    12.500    13.000    13.500    14.000    14.500    15.000    15.500
    16.000    16.500    17.000    17.500    18.000    18.500    19.000    19.500
    20.000    20.500    21.000    21.500    22.000    22.500    23.000    23.500
    24.000    24.500    25.000    25.500    26.000    26.500    27.000    27.500
    28.000    28.500    29.000    29.500    30.000    30.500    31.000    31.500
    32.000    32.500    33.000    33.500    34.000    34.500    35.000    35.500
    36.000    36.500    37.000    37.500    38.000    38.500    39.000    39.500
    40.000    40.500    41.000    41.500    42.000    42.500    43.000    43.500
    44.000    44.500    45.000    45.500    46.000    46.500    47.000    47.500
    48.000    48.250    48.500    48.750    49.000    49.250    49.500    49.750
    50.000    50.250    50.500    50.750    51.000    51.250    51.500    51.750
    52.000    52.250    52.500    52.750    53.000    53.250    53.500    53.750
    54.000    54.250    54.500    54.750    55.000    55.250    55.500    55.750
    56.000    56.500    57.000    57.500    58.000    58.500    59.000    59.500
    60.000
```

Example Storm2vam input file ‘fluxes’ (base case, excerpt only):

```
Time Step,Node,Time (yr    ),Horizontal Distance (m     ),TcO4-             Diffusive
Flux (moles/m2/s) ,TcO4-             Advective Flux (moles/m2/s) ,
    1,    1, 3.168809E-08, 5.000000E-01, 2.998914E-24,-1.329853E-17,
    2,    1, 6.654498E-08, 5.000000E-01, 2.998915E-24,-1.329854E-17,
    3,    1, 1.048876E-07, 5.000000E-01, 2.998915E-24,-1.329853E-17,
    4,    1, 1.470644E-07, 5.000000E-01, 2.998915E-24,-1.329854E-17,
    5,    1, 1.934589E-07, 5.000000E-01, 2.998916E-24,-1.329854E-17,
    6,    1, 2.444929E-07, 5.000000E-01, 2.998917E-24,-1.329854E-17,
    7,    1, 3.006303E-07, 5.000000E-01, 2.998917E-24,-1.329854E-17,
    8,    1, 3.623814E-07, 5.000000E-01, 2.998917E-24,-1.329855E-17,
    9,    1, 4.303077E-07, 5.000000E-01, 2.998917E-24,-1.329854E-17,
   10,    1, 5.050265E-07, 5.000000E-01, 2.998917E-24,-1.329854E-17,
   11,    1, 5.872172E-07, 5.000000E-01, 2.998917E-24,-1.329854E-17,
   12,    1, 6.776271E-07, 5.000000E-01, 2.998917E-24,-1.329854E-17,
   13,    1, 7.770779E-07, 5.000000E-01, 2.998917E-24,-1.329854E-17,
   14,    1, 8.864737E-07, 5.000000E-01, 2.998917E-24,-1.329854E-17,
   15,    1, 1.006809E-06, 5.000000E-01, 2.998917E-24,-1.329854E-17,
   16,    1, 1.139178E-06, 5.000000E-01, 2.998917E-24,-1.329855E-17,
   17,    1, 1.284784E-06, 5.000000E-01, 2.998916E-24,-1.329854E-17,
   18,    1, 1.444951E-06, 5.000000E-01, 2.998917E-24,-1.329854E-17,
   19,    1, 1.621134E-06, 5.000000E-01, 2.998918E-24,-1.329855E-17,
   20,    1, 1.814935E-06, 5.000000E-01, 2.998918E-24,-1.329855E-17,
   21,    1, 1.901285E-06, 5.000000E-01, 2.998918E-24,-1.329855E-17,
   22,    1, 1.996270E-06, 5.000000E-01, 2.998918E-24,-1.329855E-17,
   23,    1, 2.100754E-06, 5.000000E-01, 2.998918E-24,-1.329855E-17,
   24,    1, 2.215686E-06, 5.000000E-01, 2.998918E-24,-1.329855E-17,
   25,    1, 2.342111E-06, 5.000000E-01, 2.998917E-24,-1.329854E-17,
   26,    1, 2.481179E-06, 5.000000E-01, 2.998917E-24,-1.329854E-17,
   27,    1, 2.634153E-06, 5.000000E-01, 2.998917E-24,-1.329854E-17,
   28,    1, 2.802425E-06, 5.000000E-01, 2.998917E-24,-1.329855E-17,
```

Example Storm2vam output file ‘storm2vam.out’ (base case):

```
 fluxes from Storm
 time    umol/s/m2       Ci/yr/m2
  3.1688089E-08 -1.3298526E-17  7.0630393E-16
  5.8721719E-07 -1.3298536E-17  7.0630446E-16
  3.4151030E-06 -1.3298546E-17  7.0630499E-16
  1.1245520E-04 -1.3298536E-17  7.0630446E-16
  1.5639920E-02 -1.3298536E-17  7.0630446E-16
   5.458254     -5.8145598E-16  3.0881964E-14
   24.03677     -1.9572646E-12  1.0395315E-10
   69.04455     -2.0560954E-11  1.0920220E-09
   184.2423     -7.6988929E-11  4.0889931E-09
   323.2148     -1.4409297E-10  7.6529858E-09
   468.9361     -2.1330177E-10  1.1328765E-08
   620.3211     -2.8384464E-10  1.5075399E-08
   777.4906     -3.5547162E-10  1.8879611E-08
   941.6262     -4.2847531E-10  2.2756941E-08
   1112.927     -5.0272381E-10  2.6700388E-08
   1288.445     -5.7689237E-10  3.0639587E-08
   1467.832     -6.5086131E-10  3.4568185E-08
   1651.954     -7.2496431E-10  3.8503902E-08
   1841.192     -7.9937523E-10  4.2455973E-08
   2035.793     -8.7413859E-10  4.6426763E-08
   2238.349     -9.5004704E-10  5.0458372E-08
   2447.845     -1.0265497E-09  5.4521539E-08
   2665.395     -1.1038668E-09  5.8627958E-08
   2891.504     -1.1819897E-09  6.2777175E-08
   3127.600     -1.2611636E-09  6.6982224E-08
   3373.836     -1.3412097E-09  7.1233586E-08
   3631.313     -1.4222427E-09  7.5537358E-08
   3901.526     -1.5044047E-09  7.9901106E-08
   4185.269     -1.5875766E-09  8.4318486E-08
   4484.671     -1.6719687E-09  8.8800668E-08
   4800.631     -1.7573506E-09  9.3335430E-08
   5136.482     -1.8440336E-09  9.7939285E-08
   5494.248     -1.9318747E-09  1.0260465E-07
   5877.033     -2.0207847E-09  1.0732679E-07
   6290.286     -2.1110085E-09  1.1211871E-07
   6738.681     -2.2023416E-09  1.1696954E-07
   7229.167     -2.2946847E-09  1.2187401E-07
   7770.821     -2.3878755E-09  1.2682351E-07
   8381.787     -2.4824034E-09  1.3184403E-07
   9149.827     -2.5860074E-09  1.3734659E-07
   10139.69     -2.6973253E-09  1.4325884E-07
   11139.69     -2.7891713E-09  1.4813692E-07
   12139.69     -2.8630203E-09  1.5205914E-07
   13134.37     -2.9212472E-09  1.5515165E-07
   14134.37     -2.9669713E-09  1.5758013E-07
   15133.19     -3.0016123E-09  1.5941995E-07
   16133.19     -3.0273193E-09  1.6078529E-07
   17133.19     -3.0452154E-09  1.6173578E-07
   18132.87     -3.0551612E-09  1.6226402E-07
   19132.87     -3.0635303E-09  1.6270852E-07
   20120.38     -3.0718152E-09  1.6314854E-07
   21120.38     -3.0800302E-09  1.6358484E-07
   22120.38     -3.0881673E-09  1.6401702E-07
   23120.38     -3.0962244E-09  1.6444494E-07
   24120.38     -3.1042022E-09  1.6486867E-07
   25120.38     -3.1121012E-09  1.6528818E-07
   26120.38     -3.1199214E-09  1.6570353E-07
   27120.38     -3.1276632E-09  1.6611470E-07
   28120.38     -3.1353264E-09  1.6652172E-07
```

29120.38	-3.1429113E-09	1.6692455E-07
30119.17	-3.1504173E-09	1.6732321E-07
31119.17	-3.1578464E-09	1.6771779E-07
32119.17	-3.1651974E-09	1.6810820E-07
33119.17	-3.1724703E-09	1.6849448E-07
34119.17	-3.1796663E-09	1.6887667E-07
35119.17	-3.1867864E-09	1.6925482E-07
36119.17	-3.1938283E-09	1.6962883E-07
37119.17	-3.2007954E-09	1.6999886E-07
38119.17	-3.2076852E-09	1.7036479E-07
39119.17	-3.2144993E-09	1.7072669E-07
40118.91	-3.2212384E-09	1.7108462E-07
41118.91	-3.2279024E-09	1.7143856E-07
42118.91	-3.2344902E-09	1.7178844E-07
43118.91	-3.2410052E-09	1.7213446E-07
44118.91	-3.2474454E-09	1.7247650E-07
45118.91	-3.2538114E-09	1.7281462E-07
46118.91	-3.2601033E-09	1.7314879E-07
47118.91	-3.2663234E-09	1.7347915E-07
48118.91	-3.2724694E-09	1.7380557E-07
49118.91	-3.2785423E-09	1.7412812E-07
50103.00	-3.2845224E-09	1.7444573E-07
51103.00	-3.2904512E-09	1.7476061E-07
52103.00	-3.2963103E-09	1.7507179E-07
53103.00	-3.3020973E-09	1.7537914E-07
54103.00	-3.3078134E-09	1.7568274E-07
55103.00	-3.3134584E-09	1.7598255E-07
56103.00	-3.3190333E-09	1.7627865E-07
57103.00	-3.3245384E-09	1.7657104E-07
58103.00	-3.3299743E-09	1.7685974E-07
59103.00	-3.3353402E-09	1.7714473E-07
60056.57	-3.3404934E-09	1.7741843E-07
61056.57	-3.3457233E-09	1.7769619E-07
62056.57	-3.3508853E-09	1.7797035E-07
63056.57	-3.3559793E-09	1.7824090E-07
64056.57	-3.3610064E-09	1.7850789E-07
65054.29	-3.3659644E-09	1.7877122E-07
66054.29	-3.3708574E-09	1.7903109E-07
67054.29	-3.3756824E-09	1.7928735E-07
68054.29	-3.3804413E-09	1.7954011E-07
69054.29	-3.3851344E-09	1.7978937E-07
70053.60	-3.3897603E-09	1.8003506E-07
71053.60	-3.3943224E-09	1.8027735E-07
72053.60	-3.3988183E-09	1.8051614E-07
73053.60	-3.4032492E-09	1.8075147E-07
74053.60	-3.4076164E-09	1.8098342E-07
75053.60	-3.4119183E-09	1.8121190E-07
76053.60	-3.4161574E-09	1.8143704E-07
77053.60	-3.4203322E-09	1.8165878E-07
78053.60	-3.4244434E-09	1.8187713E-07
79053.60	-3.4284924E-09	1.8209218E-07
80050.02	-3.4324774E-09	1.8230382E-07
81050.02	-3.4364014E-09	1.8251224E-07
82050.02	-3.4402623E-09	1.8271729E-07
83050.02	-3.4440624E-09	1.8291912E-07
84050.02	-3.4478000E-09	1.8311765E-07
85050.02	-3.4514771E-09	1.8331293E-07
86050.02	-3.4550942E-09	1.8350505E-07
87050.02	-3.4586500E-09	1.8369390E-07
88050.02	-3.4621450E-09	1.8387952E-07
89050.02	-3.4655812E-09	1.8406202E-07
90050.00	-3.4689571E-09	1.8424133E-07
91050.00	-3.4722731E-09	1.8441744E-07

```
  92050.00     -3.4755312E-09  1.8459049E-07
  93050.00     -3.4787302E-09  1.8476038E-07
  94050.00     -3.4818701E-09  1.8492716E-07
  95050.00     -3.4849532E-09  1.8509090E-07
  96050.00     -3.4879770E-09  1.8525149E-07
  97050.00     -3.4909442E-09  1.8540909E-07
  98050.00     -3.4938541E-09  1.8556364E-07
  99050.00     -3.4967071E-09  1.8571517E-07
  100000.0     -3.4993650E-09  1.8585634E-07

node multipliers
 0.2500000
 0.5000000
 0.5000000
 0.5000000
 0.5000000
 0.5000000
 0.5000000
 0.5000000
 0.5000000
 0.5000000
 0.5000000
 0.5000000
 0.5000000
 0.5000000
 0.5000000
 0.5000000
 0.5000000
 0.5000000
 0.5000000
 0.3750000
 0.3750000
 0.3750000
 0.3750000
 0.3750000
 0.3750000
 0.3750000
 0.3750000
 0.3750000
 0.3750000
 0.3750000
 0.3750000
 0.3750000
 0.2500000
 0.2500000
 0.2500000
 0.2500000
 0.2500000
 0.2500000
 0.2500000
 0.2500000
 0.2500000
 0.2500000
 0.2500000
 0.2500000
 0.2500000
 0.2500000
 0.2500000
 0.2500000
 0.2500000
 0.2500000
 0.1250000
 0.1250000
 0.1250000
```

```
0.1250000
0.1250000
0.1250000
0.1250000
0.1250000
0.1250000
0.1250000
0.1250000
0.1250000
0.1250000
0.1250000
0.1250000
6.2500000E-02
```

Example Storm2vam output file ‘storm2vam.g17’ (base case, excerpt only):

```
0   72    0   65    0    0                                grp15
10204    1 0.000E+00 2.080E-03
10205    1 0.000E+00 2.078E-03
10206    1 0.000E+00 2.077E-03
10207    1 0.000E+00 2.075E-03
10208    1 0.000E+00 2.075E-03
10209    1 0.000E+00 2.075E-03
10210    1 0.000E+00 2.076E-03
10211    1 0.000E+00 2.078E-03
10212    1 0.000E+00 2.083E-03
10213    1 0.000E+00 2.090E-03
10214    1 0.000E+00 2.101E-03
10215    1 0.000E+00 2.117E-03
10216    1 0.000E+00 2.140E-03
10217    1 0.000E+00 2.170E-03
10218    1 0.000E+00 2.212E-03
10219    1 0.000E+00 2.267E-03
10220    1 0.000E+00 2.339E-03
10221    1 0.000E+00 2.432E-03
10222    1 0.000E+00 2.551E-03
10223    1 0.000E+00 2.702E-03
10224    1 0.000E+00 2.892E-03
10225    1 0.000E+00 3.127E-03
10226    1 0.000E+00 3.417E-03
10227    1 0.000E+00 3.772E-03
10228    1 0.000E+00 4.201E-03
10229    1 0.000E+00 4.715E-03
10230    1 0.000E+00 5.325E-03
10231    1 0.000E+00 6.042E-03
10232    1 0.000E+00 6.877E-03
10233    1 0.000E+00 7.845E-03
10234    1 0.000E+00 8.973E-03
10235    1 0.000E+00 7.757E-03
10236    1 0.000E+00 5.611E-03
10237    1 0.000E+00 6.169E-03
10238    1 0.000E+00 6.958E-03
10239    1 0.000E+00 3.736E-02
10240    1 0.000E+00 0.000E+00
10241    1 0.000E+00 5.955E-03
10242    1 0.000E+00 6.733E-03
10243    1 0.000E+00 7.314E-03
10244    1 0.000E+00 7.786E-03
10245    1 0.000E+00 8.196E-03
10246    1 0.000E+00 8.567E-03
10247    1 0.000E+00 8.909E-03
10248    1 0.000E+00 9.230E-03
10249    1 0.000E+00 9.531E-03
10250    1 0.000E+00 9.815E-03
10251    1 0.000E+00 1.008E-02
10252    1 0.000E+00 1.033E-02
10253    1 0.000E+00 1.056E-02
10254    1 0.000E+00 1.078E-02
10255    1 0.000E+00 1.098E-02
10256    1 0.000E+00 1.116E-02
10257    1 0.000E+00 1.133E-02
10258    1 0.000E+00 1.148E-02
10259    1 0.000E+00 1.162E-02
10260    1 0.000E+00 1.174E-02
10261    1 0.000E+00 1.185E-02
10262    1 0.000E+00 1.195E-02
10263    1 0.000E+00 1.203E-02
```

```
10264    1 0.000E+00 1.211E-02
10265    1 0.000E+00 1.218E-02
10266    1 0.000E+00 1.223E-02
10267    1 0.000E+00 1.843E-02
10268    1 0.000E+00 2.474E-02
10269    1 0.000E+00 2.486E-02
10270    1 0.000E+00 2.495E-02
10271    1 0.000E+00 2.502E-02
10272    1 0.000E+00 2.506E-02
10273    1 0.000E+00 2.509E-02
10274    1 0.000E+00 2.511E-02
10275    1 0.000E+00 1.256E-02
10139    1  131    0
3.1688E-085.8722E-073.4151E-061.1246E-041.5640E-025.4583E+002.4037E+016.9045E+01
1.8424E+023.2321E+024.6894E+026.2032E+027.7749E+029.4163E+021.1129E+031.2884E+03
1.4678E+031.6520E+031.8412E+032.0358E+032.2383E+032.4478E+032.6654E+032.8915E+03
3.1276E+033.3738E+033.6313E+033.9015E+034.1853E+034.4847E+034.8006E+035.1365E+03
5.4942E+035.8770E+036.2903E+036.7387E+037.2292E+037.7708E+038.3818E+039.1498E+03
1.0140E+041.1140E+041.2140E+041.3134E+041.4134E+041.5133E+041.6133E+041.7133E+04
1.8133E+041.9133E+042.0120E+042.1120E+042.2120E+042.3120E+042.4120E+042.5120E+04
2.6120E+042.7120E+042.8120E+042.9120E+043.0119E+043.1119E+043.2119E+043.3119E+04
3.4119E+043.5119E+043.6119E+043.7119E+043.8119E+043.9119E+044.0119E+044.1119E+04
4.2119E+044.3119E+044.4119E+044.5119E+044.6119E+044.7119E+044.8119E+044.9119E+04
5.0103E+045.1103E+045.2103E+045.3103E+045.4103E+045.5103E+045.6103E+045.7103E+04
5.8103E+045.9103E+046.0057E+046.1057E+046.2057E+046.3057E+046.4057E+046.5054E+04
6.6054E+046.7054E+046.8054E+046.9054E+047.0054E+047.1054E+047.2054E+047.3054E+04
7.4054E+047.5054E+047.6054E+047.7054E+047.8054E+047.9054E+048.0050E+048.1050E+04
8.2050E+048.3050E+048.4050E+048.5050E+048.6050E+048.7050E+048.8050E+048.9050E+04
9.0050E+049.1050E+049.2050E+049.3050E+049.4050E+049.5050E+049.6050E+049.7050E+04
9.8050E+049.9050E+041.0000E+05
1.7658E-161.7658E-161.7658E-161.7658E-161.7658E-167.7205E-152.5988E-112.7301E-10
1.0222E-091.9132E-092.8322E-093.7688E-094.7199E-095.6892E-096.6751E-097.6599E-09
8.6420E-099.6260E-091.0614E-081.1607E-081.2615E-081.3630E-081.4657E-081.5694E-08
1.6746E-081.7808E-081.8884E-081.9975E-082.1080E-082.2200E-082.3334E-082.4485E-08
2.5651E-082.6832E-082.8030E-082.9242E-083.0469E-083.1706E-083.2961E-083.4337E-08
3.5815E-083.7034E-083.8015E-083.8788E-083.9395E-083.9855E-084.0196E-084.0434E-08
4.0566E-084.0677E-084.0787E-084.0896E-084.1004E-084.1111E-084.1217E-084.1322E-08
4.1426E-084.1529E-084.1630E-084.1731E-084.1831E-084.1929E-084.2027E-084.2124E-08
4.2219E-084.2314E-084.2407E-084.2500E-084.2591E-084.2682E-084.2771E-084.2860E-08
4.2947E-084.3034E-084.3119E-084.3204E-084.3287E-084.3370E-084.3451E-084.3532E-08
4.3611E-084.3690E-084.3768E-084.3845E-084.3921E-084.3996E-084.4070E-084.4143E-08
4.4215E-084.4286E-084.4355E-084.4424E-084.4493E-084.4560E-084.4627E-084.4693E-08
4.4758E-084.4822E-084.4885E-084.4947E-084.5009E-084.5069E-084.5129E-084.5188E-08
4.5246E-084.5303E-084.5359E-084.5415E-084.5469E-084.5523E-084.5576E-084.5628E-08
4.5679E-084.5730E-084.5779E-084.5828E-084.5876E-084.5923E-084.5970E-084.6016E-08
4.6060E-084.6104E-084.6148E-084.6190E-084.6232E-084.6273E-084.6313E-084.6352E-08
4.6391E-084.6429E-084.6464E-08
1.0680E-031.0680E-031.0680E-031.0680E-031.0680E-031.0680E-031.0680E-031.0680E-03
1.0680E-031.0680E-031.0680E-031.0680E-031.0680E-031.0680E-031.0680E-031.0680E-03
1.0680E-031.0680E-031.0680E-031.0680E-031.0680E-031.0680E-031.0680E-031.0680E-03
1.0680E-031.0680E-031.0680E-031.0680E-031.0680E-031.0680E-031.0680E-031.0680E-03
1.0680E-031.0680E-031.0680E-031.0680E-031.0680E-031.0680E-031.0680E-031.0680E-03
1.0680E-031.0680E-031.0680E-031.0680E-031.0680E-031.0680E-031.0680E-031.0680E-03
1.0680E-031.0680E-031.0680E-031.0680E-031.0680E-031.0680E-031.0680E-031.0680E-03
1.0680E-031.0680E-031.0680E-031.0680E-031.0680E-031.0680E-031.0680E-031.0680E-03
1.0680E-031.0680E-031.0680E-031.0680E-031.0680E-031.0680E-031.0680E-031.0680E-03
1.0680E-031.0680E-031.0680E-031.0680E-031.0680E-031.0680E-031.0680E-031.0680E-03
1.0680E-031.0680E-031.0680E-031.0680E-031.0680E-031.0680E-031.0680E-031.0680E-03
1.0680E-031.0680E-031.0680E-031.0680E-031.0680E-031.0680E-031.0680E-031.0680E-03
1.0680E-031.0680E-031.0680E-031.0680E-031.0680E-031.0680E-031.0680E-031.0680E-03
1.0680E-031.0680E-031.0680E-031.0680E-031.0680E-031.0680E-031.0680E-031.0680E-03
1.0680E-031.0680E-031.0680E-031.0680E-031.0680E-031.0680E-031.0680E-031.0680E-03
1.0680E-031.0680E-031.0680E-031.0680E-031.0680E-031.0680E-031.0680E-031.0680E-03
```

Storm2vam source code listing:

```
      program storm2vam

c      convert umol/sq. m/s (STORM) to Ci/sq. m/yr (VAM)

      parameter sec_year=3.15576e+7
      parameter maxstep=200000
       parameter maxvstep=1000
       parameter maxnode=1000
       parameter maxzone=10

       real advflux(maxstep),difflux(maxstep),stime(maxstep)
       real xcd(maxnode),flow(maxnode),rnode(maxnode)
      real flux(maxvstep),tflux(maxvstep),vtime(maxvstep)
       real weight,rcig,xmax(maxzone),yfrac(maxzone)
      character filename*80,dum*5,line*80

       open(10,file='fluxes.',status='old', readonly)
      open(20, file='storm2vam.out', status='unknown')
      open(22, file='storm2vam.g17', status='unknown')

      write(*,*)'Enter Name of Input File: '
       read(*,*)filename
      open(15, file=filename, status='old', readonly)

      write(*,*)'Enter Name of BCFLOW Output File: '
       read(*,*)filename
      open(17, file=filename, status='old', readonly)

c     ******************** Read Input File (Constants and Node Coordinates)

c     Atomic Weight of Nuclide (e.g., 99.0 for Tc99)
       read(15,*)weight

c     Ratio of Ci to g for Nuclide (e.g., 0.017 for Tc99)
      read(15,*)rcig

c     Number of Time Steps to Skip (i.e., 1000 -> use every 1000th step)
       read(15,*)minskip,maxskip,iskipfactor,maxvsteps

c     Number of waste zones (with different stacking height)
      read(15,*)nzone
      if(nzone.gt.maxzone-1)then
         write(*,*)'Too many waste zones - aborting!'
         stop
       endif

c     Max x for zone and fraction of base height
      do i=1,nzone
         read(15,*)xmax(i),yfrac(i)
       enddo
       yfrac(nzone+1)=0.

c     Number of nodes in x and y directions
      read(15,*)nx,ny
      if(nx.gt.maxnode)then
         write(*,*)'Too many nodes - aborting!'
         stop
       endif
       read(15,*)(xcd(i),i=1,nx)
       nnodes=nx*ny
```

```
c     ************ Read in Fluid Fluxes from Output of BCFLOW Code

      do i=1,4
         read(17,*)
       enddo
       read(17,'(a80)')line
       write(*,*)'Flow Run: '
       write(*,*)line
       read(17,*)nfnodes
       read(17,*)
      do i=1,nfnodes
         read(17,'(2i5,e10.3)')i1,i2,flow(i)
       enddo
       if(nfnodes.ne.nx)then
         write(*,*)'Input File and Flow File Nodes Do Not Match - ',
     &    'Aborting!'
         stop
       endif

c     ************ read in STORM advective and diffusive fluxes ***********

      i=0
      read(10,*,iostat=iocheck)
       do while(iocheck.eq.0 .and. i.lt.maxstep)
         i=i+1
        read(10,'(a5,1x,i5,1x,4(e13.3,1x))',iostat=iocheck)dum(1:5),
     &    inode,stime(i),dx,difflux(i),advflux(i)
       enddo
      nstep=i-1

c     ************* write out converted data
      i=1
      i1=1
       istep=minskip
      do while(i.le.nstep .and. i1.le.maxvsteps)
         vtime(i1)=stime(i)
         tflux(i1)=difflux(i)+advflux(i)
c       convert from micro-mol/s/m2 to Ci/yr/m2
         flux(i1)=-1.*tflux(i1)*sec_year*weight*rcig*1.0E-06
         flux(i1)=max(flux(i1),0.)
         ilast=i
         i1last=i1
         i=i+istep
         istep=iskipfactor*istep
         if(istep.gt.maxskip)then
           istep=maxskip
         endif
         i1=i1+1
      enddo

      if(ilast.lt.nstep .and. i1last.lt.maxvsteps)then
         i=nstep
         i1=i1last+1
         i1last=i1
         vtime(i1)=stime(i)
         tflux(i1)=difflux(i)+advflux(i)
         flux(i1)=-1.*tflux(i1)*sec_year*weight*rcig*1.0E-06
         flux(i1)=max(flux(i1),0.)
       endif
      nstep1=i1last

       write(20,*)'fluxes from Storm'
```

```
      write(20,*)'time    umol/s/m2       Ci/yr/m2'
      do i=1,nstep1
        write(20,*)vtime(i),tflux(i),flux(i)
      enddo

c     ************** generate multipliers for each node
      i=0
      do while(i.lt.nx .and. xcd(i+1).le.xmax(nzone))
        i=i+1
         j=1
         do while(j.lt.nzone .and. xcd(i).gt.xmax(j))
           j=j+1
         enddo
         if(i.eq.1)then
           deltax=.5*(xcd(2)-xcd(1))
         else if(i.eq.nx)then
           deltax=.5*(xcd(nx)-xcd(nx-1))
         else if(xcd(i+1).gt.xmax(nzone))then
           deltax=.5*(xcd(i)-xcd(i-1))+(xmax(nzone)-xcd(i))
         else
           deltax=.5*(xcd(i+1)-xcd(i-1))
         endif
         rnode(i)=yfrac(j)*deltax
      enddo
      ng17=i

      write(20,*)
      write(20,*)'node multipliers'
      totmult=0
      do i=1,ng17
         totmult=totmult+rnode(i)
         write(20,*)rnode(i)
      enddo

      write(*,*)'Effective Waste Footprint (m2): ',totmult

c     ************** write out g15/g17 data
      if(ng17.gt.nx)then
         ng17=nx
      endif
      ng15=nx-ng17

      write(22,'(6i5,30x,"grp15")')0,ng15,0,ng17,0,0
      ntmp=(ny-1)*nx
      do i=ng17+1,nx
         write(22,'(2i5,1p,2e10.3)')ntmp+i,1,0.,flow(i)
      enddo
      do i=1,ng17
         write(22,'(4i5)')ntmp+i,1,nstep1,0
         write(22,'(1p,8e10.4)')(vtime(j),j=1,nstep1)
         write(22,'(1p,8e10.4)')(rnode(i)*flux(j),j=1,nstep1)
         write(22,'(1p,8e10.4)')(flow(i),j=1,nstep1)
      enddo

      end
c234567890123456789012345678901234567890123456789012345678901234567890
```

APPENDIX E. BOTFLUX

This appendix documents the Botflux utility code. It includes an input and output description, example input and output files, and a source code listing.

The Botflux code takes the contaminant concentration at the bottom boundary nodes from one or more far field transport calculation and multiplies them by the volumetric fluid flow across the boundary (from the far field flow calculation) to determine the total contaminant transport rate across the boundary. The data are printed out in a format usable by the INTEG code. Typically, transport calculations with different K_d values are combined into a single output file using this code.

The code requires a nodal data (ppl) file from each far field transport calculation to be included, and a boundary flux (fpl) file from the corresponding far field flow calculation. In addition a number of direct inputs are required (these are typically redirected from a file). The required inputs are described below:

- Name of the flow calculation fpl file.
- Number of columns and rows in the far field model.
- Effective nuclide inventory in the model.
- Normalization flag (a value of 2 implies that the flux will be normalized such that the integral will equal 1.0).
- Time offset (a number of years to add to the time step, equal to the time between the effective date of the INTEG inventory data and the start of the VAM3DF transport
- calculations).
- Number of transport calculations to include (up to a maximum of 8).
- Name of transport calculation nodal data file. This is repeated for each transport
- calculation to be included.

The effective inventory should be calculated from the following equation:

$$I = H * r1 * r2 * Pg * r3 * L$$

where,

H = Height of waste assumed in STORM calculation (typically 5.6 m for the trench and 8.4 m for the vault).
r1 = Fraction of full density of glass (typically 0.98).
r2 = Fraction of height (H) that is glass (typically 0.85).
Pg = Density of glass in mol/m3 (typically 38776.1450).
r3 = Ratio of nuclide to glass in micromols/mol (typically 0.659).
L = Equivalent length of waste region if all waste were full height (from Storm2vam output).

The output of the code is time dependent, normalized contaminant flux across the bottom boundary of the model. The data are written to a file named botflux.out, where each transport

case corresponds to a column in the file. The output file can be used as input for an INTEG calculation after replacing the header lines with the required INTEG header lines.

```
Example Botflux input parameters (base case):

..\42base-f\42base-f.fpl
137 75
4.025
0
36.
6
42base-t-0.ppl
..\42base-t-06\42base-t-06.ppl
..\42base-t-4\42base-t-4.ppl
..\42base-t-10\42base-t-10.ppl
..\42base-t-80\42base-t-80.ppl
..\42base-t-150\42base-t-150.ppl
```

Example Botflux input file ‘fpl’ (base case, excerpts only):

```
VAM3DF VERSION 1.0
base case; 4.2mm/yr; 50mm/yr sideslope
     1   274
1    2    3    4    5    6    7    8    9   10   11   12   13   14   15   16   17   18
19   20   21   22   23   24   25   26   27   28   29   30   31   32   33   34   35
36   37   38   39   40   41   42   43   44   45   46   47   48   49   50   51   52
53   54   55   56   57   58   59   60   61   62   63   64   65   66   67   68   69
70   71   72   73   74   75   76   77   78   79   80   81   82   83   84   85   86
87   88   89   90   91   92   93   94   95   96   97   98   99  100  101  102  103
104  105  106  107  108  109  110  111  112  113  114  115  116  117  118  119  120
121  122  123  124  125  126  127  128  129  130  131  132  133  134  135  136
137101391014010141101421014310144101451014610147101481014910150101511015210153101541 01
551015610157101581015910160101611016210163101641016510166101671016810169101701017110 17
210173101741017510176101771017810179101801018110182101831018410185101861018710188101 89
101901019110192101931019410195101961019710198101991020010201102021020310204102051020 61
020710208102091021010211102121021310214102151021610217102181021910220102211022210223 10
224102251022610227102281022910230102311023210233102341023510236102371023810239102401 02
411024210243102441024510246102471024810249102501025110252102531025410255102561025710 25
810259102601026110262102631026410265102661026710268102691027010271102721027310274102 75
STEP =   704TIME =  0.200E+04 *** NODAL FLUID FLUX VALUES ***
-1.635E-03-3.271E-03-3.273E-03-3.277E-03-3.282E-03-3.288E-03-3.295E-03-3.304E-03
-3.315E-03-3.326E-03-3.339E-03-3.354E-03-3.370E-03-3.387E-03-3.406E-03-3.426E-03
-3.448E-03-3.471E-03-3.495E-03-3.521E-03-3.548E-03-3.577E-03-3.607E-03-3.639E-03
-3.672E-03-3.707E-03-3.743E-03-3.781E-03-3.820E-03-3.861E-03-3.904E-03-3.948E-03
-3.993E-03-4.040E-03-4.089E-03-4.139E-03-4.191E-03-4.245E-03-4.300E-03-4.356E-03
-4.415E-03-4.475E-03-4.536E-03-4.600E-03-4.665E-03-4.731E-03-4.799E-03-4.869E-03
-4.941E-03-5.014E-03-5.088E-03-5.165E-03-5.243E-03-5.322E-03-5.403E-03-5.486E-03
-5.570E-03-5.656E-03-5.743E-03-5.831E-03-5.921E-03-6.013E-03-6.106E-03-6.200E-03
-6.295E-03-6.392E-03-6.490E-03-6.589E-03-6.690E-03-6.791E-03-6.893E-03-6.997E-03
-7.101E-03-7.207E-03-7.313E-03-7.420E-03-7.528E-03-7.638E-03-7.748E-03-7.859E-03
-7.971E-03-8.085E-03-8.200E-03-8.318E-03-8.438E-03-8.562E-03-8.690E-03-8.824E-03
-8.966E-03-9.119E-03-9.285E-03-9.469E-03-9.679E-03-9.921E-03-1.021E-02-1.055E-02
-8.236E-03-5.618E-03-5.763E-03-5.926E-03-4.684E-01 4.584E-01-3.992E-03-4.109E-03
-4.215E-03-4.311E-03-4.398E-03-4.478E-03-4.550E-03-4.617E-03-4.678E-03-4.734E-03
-4.785E-03-4.832E-03-4.876E-03-4.916E-03-4.953E-03-4.988E-03-5.019E-03-5.049E-03
-5.076E-03-5.101E-03-5.125E-03-5.147E-03-5.167E-03-5.186E-03-5.203E-03-5.219E-03
-7.851E-03-1.052E-02-1.056E-02-1.060E-02-1.063E-02-1.065E-02-1.067E-02-1.068E-02
-5.340E-03 1.068E-03 2.139E-03 2.144E-03 2.152E-03 2.165E-03 2.183E-03 2.207E-03
 2.238E-03 2.279E-03 2.330E-03 2.392E-03 2.461E-03 2.527E-03 2.564E-03 2.527E-03
 2.398E-03 2.318E-03 2.267E-03 2.213E-03 2.180E-03 2.160E-03 2.142E-03 2.129E-03
 2.122E-03 2.116E-03 2.111E-03 2.108E-03 2.106E-03 2.104E-03 2.103E-03 2.102E-03
 2.102E-03 2.101E-03 2.101E-03 2.101E-03 2.100E-03 2.100E-03 2.100E-03 2.100E-03
 2.100E-03 2.099E-03 2.099E-03 2.099E-03 2.099E-03 2.099E-03 2.098E-03 2.098E-03
 2.098E-03 2.097E-03 2.097E-03 2.096E-03 2.096E-03 2.095E-03 2.095E-03 2.094E-03
 2.093E-03 2.092E-03 2.091E-03 2.090E-03 2.089E-03 2.088E-03 2.086E-03 2.085E-03
 2.083E-03 2.081E-03 2.080E-03 2.078E-03 2.077E-03 2.075E-03 2.075E-03 2.075E-03
 2.076E-03 2.078E-03 2.083E-03 2.090E-03 2.101E-03 2.117E-03 2.140E-03 2.170E-03
 2.212E-03 2.267E-03 2.339E-03 2.432E-03 2.551E-03 2.702E-03 2.892E-03 3.127E-03
 3.417E-03 3.772E-03 4.201E-03 4.715E-03 5.325E-03 6.042E-03 6.877E-03 7.845E-03
 8.973E-03 7.757E-03 5.611E-03 6.169E-03 6.958E-03 3.736E-02-2.212E-16 5.955E-03
 6.733E-03 7.314E-03 7.786E-03 8.196E-03 8.567E-03 8.909E-03 9.230E-03 9.531E-03
 9.815E-03 1.008E-02 1.033E-02 1.056E-02 1.078E-02 1.098E-02 1.116E-02 1.133E-02
 1.148E-02 1.162E-02 1.174E-02 1.185E-02 1.195E-02 1.203E-02 1.211E-02 1.218E-02
 1.223E-02 1.843E-02 2.474E-02 2.486E-02 2.495E-02 2.502E-02 2.506E-02 2.509E-02
 2.511E-02 1.256E-02
```

Example Botflux input file ‘ppl’ (base case, excerpts only):

```
TITLE,IMODL,NP,NE
VAM3DF VERSION 1.0
base case; 4.2 mm/yr; Kd=0.
     0 10275 10064
    **** X,Y,Z and INITIAL CONCENTRATIONS ****


STEP =  1990 TIME =  0.100E+06 *** X,Y,Z and NODAL CONCENTRATION VALUES ***
   0.0000000      -103.00000       0.0000000      0.38784252E-04
  0.50000000      -103.00000       0.0000000      0.38742433E-04
   1.0000000      -103.00000       0.0000000      0.38617987E-04
   1.5000000      -103.00000       0.0000000      0.38412963E-04
   2.0000000      -103.00000       0.0000000      0.38130014E-04
   2.5000000      -103.00000       0.0000000      0.37772205E-04
   3.0000000      -103.00000       0.0000000      0.37342881E-04
   3.5000000      -103.00000       0.0000000      0.36845557E-04
   4.0000000      -103.00000       0.0000000      0.36283833E-04
   4.5000000      -103.00000       0.0000000      0.35661334E-04
   5.0000000      -103.00000       0.0000000      0.34981669E-04
   5.5000000      -103.00000       0.0000000      0.34248413E-04
   6.0000000      -103.00000       0.0000000      0.33465106E-04
   6.5000000      -103.00000       0.0000000      0.32635266E-04
   7.0000000      -103.00000       0.0000000      0.31762416E-04
   7.5000000      -103.00000       0.0000000      0.30850106E-04
   8.0000000      -103.00000       0.0000000      0.29901943E-04
   8.5000000      -103.00000       0.0000000      0.28921612E-04
   9.0000000      -103.00000       0.0000000      0.27912898E-04
   9.5000000      -103.00000       0.0000000      0.26879688E-04
   10.000000      -103.00000       0.0000000      0.25825969E-04
   10.500000      -103.00000       0.0000000      0.24755826E-04
   11.000000      -103.00000       0.0000000      0.23673412E-04
   11.500000      -103.00000       0.0000000      0.22582932E-04
   12.000000      -103.00000       0.0000000      0.21488612E-04
   12.500000      -103.00000       0.0000000      0.20394664E-04
   13.000000      -103.00000       0.0000000      0.19305258E-04
   13.500000      -103.00000       0.0000000      0.18224492E-04
   14.000000      -103.00000       0.0000000      0.17156356E-04
   14.500000      -103.00000       0.0000000      0.16104708E-04
   15.000000      -103.00000       0.0000000      0.15073243E-04
   15.500000      -103.00000       0.0000000      0.14065468E-04
   16.000000      -103.00000       0.0000000      0.13084674E-04
   16.500000      -103.00000       0.0000000      0.12133906E-04
   17.000000      -103.00000       0.0000000      0.11215943E-04
   17.500000      -103.00000       0.0000000      0.10333267E-04
   18.000000      -103.00000       0.0000000      0.94880394E-05
   18.500000      -103.00000       0.0000000      0.86820836E-05
   19.000000      -103.00000       0.0000000      0.79168633E-05
   19.500000      -103.00000       0.0000000      0.71934726E-05
   20.000000      -103.00000       0.0000000      0.65126302E-05
   20.500000      -103.00000       0.0000000      0.58746804E-05
   21.000000      -103.00000       0.0000000      0.52796010E-05
   21.500000      -103.00000       0.0000000      0.47270196E-05
   22.000000      -103.00000       0.0000000      0.42162343E-05
   22.500000      -103.00000       0.0000000      0.37462418E-05
   23.000000      -103.00000       0.0000000      0.33157690E-05
   23.500000      -103.00000       0.0000000      0.29233084E-05
   24.000000      -103.00000       0.0000000      0.25671553E-05
   24.500000      -103.00000       0.0000000      0.22454467E-05
   25.000000      -103.00000       0.0000000      0.19561990E-05
   25.500000      -103.00000       0.0000000      0.16973455E-05
   26.000000      -103.00000       0.0000000      0.14667711E-05
```

26.500000	-103.00000	0.0000000	0.12623451E-05
27.000000	-103.00000	0.0000000	0.10819499E-05
27.500000	-103.00000	0.0000000	0.92350733E-06
28.000000	-103.00000	0.0000000	0.78500007E-06
28.500000	-103.00000	0.0000000	0.66449040E-06
29.000000	-103.00000	0.0000000	0.56013485E-06
29.500000	-103.00000	0.0000000	0.47019549E-06
30.000000	-103.00000	0.0000000	0.39304793E-06
30.500000	-103.00000	0.0000000	0.32718640E-06
31.000000	-103.00000	0.0000000	0.27122618E-06
31.500000	-103.00000	0.0000000	0.22390364E-06
32.000000	-103.00000	0.0000000	0.18407430E-06
32.500000	-103.00000	0.0000000	0.15070911E-06
33.000000	-103.00000	0.0000000	0.12288957E-06
33.500000	-103.00000	0.0000000	0.99801525E-07
34.000000	-103.00000	0.0000000	0.80728356E-07
34.500000	-103.00000	0.0000000	0.65043594E-07
35.000000	-103.00000	0.0000000	0.52203262E-07
35.500000	-103.00000	0.0000000	0.41738147E-07
36.000000	-103.00000	0.0000000	0.33246110E-07
36.500000	-103.00000	0.0000000	0.26384740E-07
37.000000	-103.00000	0.0000000	0.20864235E-07
37.500000	-103.00000	0.0000000	0.16440893E-07
38.000000	-103.00000	0.0000000	0.12910931E-07
38.500000	-103.00000	0.0000000	0.10105012E-07
39.000000	-103.00000	0.0000000	0.78831732E-08
39.500000	-103.00000	0.0000000	0.61303780E-08
40.000000	-103.00000	0.0000000	0.47526072E-08
40.500000	-103.00000	0.0000000	0.36734349E-08
41.000000	-103.00000	0.0000000	0.28310154E-08
41.500000	-103.00000	0.0000000	0.21755682E-08
42.000000	-103.00000	0.0000000	0.16672033E-08
42.500000	-103.00000	0.0000000	0.12741168E-08
43.000000	-103.00000	0.0000000	0.97107034E-09
43.500000	-103.00000	0.0000000	0.73811179E-09
44.000000	-103.00000	0.0000000	0.55949556E-09
44.500000	-103.00000	0.0000000	0.42292925E-09
45.000000	-103.00000	0.0000000	0.31874947E-09
45.500000	-103.00000	0.0000000	0.23948132E-09
46.000000	-103.00000	0.0000000	0.17928414E-09
46.500000	-103.00000	0.0000000	0.13368151E-09
47.000000	-103.00000	0.0000000	0.99220188E-10
47.500000	-103.00000	0.0000000	0.73200113E-10
48.000000	-103.00000	0.0000000	0.53503868E-10
48.250000	-103.00000	0.0000000	0.44579451E-10
48.500000	-103.00000	0.0000000	0.36806114E-10
48.750000	-103.00000	0.0000000	0.29899638E-10
49.000000	-103.00000	0.0000000	0.23604230E-10
49.250000	-103.00000	0.0000000	0.23533175E-10
49.500000	-103.00000	0.0000000	0.20236257E-10
49.750000	-103.00000	0.0000000	0.17578827E-10
50.000000	-103.00000	0.0000000	0.15333512E-10
50.250000	-103.00000	0.0000000	0.13415047E-10
50.500000	-103.00000	0.0000000	0.11738166E-10
50.750000	-103.00000	0.0000000	0.10274448E-10
51.000000	-103.00000	0.0000000	0.89812602E-11
51.250000	-103.00000	0.0000000	0.78443918E-11
51.500000	-103.00000	0.0000000	0.68496320E-11
51.750000	-103.00000	0.0000000	0.59827698E-11
52.000000	-103.00000	0.0000000	0.52153837E-11
52.250000	-103.00000	0.0000000	0.45474735E-11
52.500000	-103.00000	0.0000000	0.39506176E-11
52.750000	-103.00000	0.0000000	0.34390268E-11

53.000000	-103.00000	0.0000000	0.29984903E-11
53.250000	-103.00000	0.0000000	0.26005864E-11
53.500000	-103.00000	0.0000000	0.22737368E-11
53.750000	-103.00000	0.0000000	0.19753088E-11
54.000000	-103.00000	0.0000000	0.17195134E-11
54.250000	-103.00000	0.0000000	0.14921397E-11
54.500000	-103.00000	0.0000000	0.12931878E-11
54.750000	-103.00000	0.0000000	0.11226575E-11
55.000000	-103.00000	0.0000000	0.98054898E-12
55.250000	-103.00000	0.0000000	0.85265128E-12
55.500000	-103.00000	0.0000000	0.73896445E-12
55.750000	-103.00000	0.0000000	0.63948846E-12
56.000000	-103.00000	0.0000000	0.56843419E-12
56.500000	-103.00000	0.0000000	0.42632564E-12
57.000000	-103.00000	0.0000000	0.34106051E-12
57.500000	-103.00000	0.0000000	0.25579538E-12
58.000000	-103.00000	0.0000000	0.21316282E-12
58.500000	-103.00000	0.0000000	0.17053026E-12
59.000000	-103.00000	0.0000000	0.14210855E-12
59.500000	-103.00000	0.0000000	0.12789769E-12
60.000000	-103.00000	0.0000000	0.12789769E-12

Example Botflux output file ‘botflux.out’ (base case):

```
Botflux 1.0: flux out the bottom of a VAM transport run

 Flow Run:
base case; 4.2mm/yr; 50mm/yr sideslope

 nodes:          137          75       10275
 Inventory:    4.025000
 Normalization Flag:            0
 Delay Time (yrs):    36.00000
 Number of Transport Cases:            6


 Transport Run:
base case; 4.2 mm/yr; Kd=0.


 Transport Run:
base case; 4.2 mm/yr; Kd=0.6


 Transport Run:
base case; 4.2 mm/yr; Kd=4


 Transport Run:
base case; 4.2 mm/yr; Kd=10


 Transport Run:
base case; 4.2 mm/yr; Kd=80.0


 Transport Run:
base case; 4.2 mm/yr; Kd=150

3.6000E+01  0.0000E+00  0.0000E+00  0.0000E+00  0.0000E+00  0.0000E+00  0.0000E+00  0.0000E+00  0.0000E+00
4.1000E+01  0.0000E+00  0.0000E+00  0.0000E+00  0.0000E+00  0.0000E+00  0.0000E+00  0.0000E+00  0.0000E+00
4.6000E+01  0.0000E+00  0.0000E+00  0.0000E+00  0.0000E+00  0.0000E+00  0.0000E+00  0.0000E+00  0.0000E+00
5.1000E+01  0.0000E+00  0.0000E+00  0.0000E+00  0.0000E+00  0.0000E+00  0.0000E+00  0.0000E+00  0.0000E+00
5.6000E+01  0.0000E+00  0.0000E+00  0.0000E+00  0.0000E+00  0.0000E+00  0.0000E+00  0.0000E+00  0.0000E+00
6.1000E+01  0.0000E+00  0.0000E+00  0.0000E+00  0.0000E+00  0.0000E+00  0.0000E+00  0.0000E+00  0.0000E+00
6.6000E+01  0.0000E+00  0.0000E+00  0.0000E+00  0.0000E+00  0.0000E+00  0.0000E+00  0.0000E+00  0.0000E+00
7.1000E+01  0.0000E+00  0.0000E+00  0.0000E+00  0.0000E+00  0.0000E+00  0.0000E+00  0.0000E+00  0.0000E+00
7.6000E+01  0.0000E+00  0.0000E+00  0.0000E+00  0.0000E+00  0.0000E+00  0.0000E+00  0.0000E+00  0.0000E+00
8.1000E+01  0.0000E+00  0.0000E+00  0.0000E+00  0.0000E+00  0.0000E+00  0.0000E+00  0.0000E+00  0.0000E+00
8.6000E+01  0.0000E+00  0.0000E+00  0.0000E+00  0.0000E+00  0.0000E+00  0.0000E+00  0.0000E+00  0.0000E+00
9.1000E+01  0.0000E+00  0.0000E+00  0.0000E+00  0.0000E+00  0.0000E+00  0.0000E+00  0.0000E+00  0.0000E+00
9.6000E+01  0.0000E+00  0.0000E+00  0.0000E+00  0.0000E+00  0.0000E+00  0.0000E+00  0.0000E+00  0.0000E+00
1.0100E+02  0.0000E+00  0.0000E+00  0.0000E+00  0.0000E+00  0.0000E+00  0.0000E+00  0.0000E+00  0.0000E+00
1.0600E+02  0.0000E+00  0.0000E+00  0.0000E+00  0.0000E+00  0.0000E+00  0.0000E+00  0.0000E+00  0.0000E+00
1.1100E+02  0.0000E+00  0.0000E+00  0.0000E+00  0.0000E+00  0.0000E+00  0.0000E+00  0.0000E+00  0.0000E+00
1.1600E+02  0.0000E+00  0.0000E+00  0.0000E+00  0.0000E+00  0.0000E+00  0.0000E+00  0.0000E+00  0.0000E+00
1.2100E+02  0.0000E+00  0.0000E+00  0.0000E+00  0.0000E+00  0.0000E+00  0.0000E+00  0.0000E+00  0.0000E+00
1.2600E+02  0.0000E+00  0.0000E+00  0.0000E+00  0.0000E+00  0.0000E+00  0.0000E+00  0.0000E+00  0.0000E+00
1.3100E+02  0.0000E+00  0.0000E+00  0.0000E+00  0.0000E+00  0.0000E+00  0.0000E+00  0.0000E+00  0.0000E+00
1.3600E+02  0.0000E+00  0.0000E+00  0.0000E+00  0.0000E+00  0.0000E+00  0.0000E+00  0.0000E+00  0.0000E+00
1.8600E+02  0.0000E+00  0.0000E+00  0.0000E+00  0.0000E+00  0.0000E+00  0.0000E+00  0.0000E+00  0.0000E+00
2.3600E+02  0.0000E+00  0.0000E+00  0.0000E+00  0.0000E+00  0.0000E+00  0.0000E+00  0.0000E+00  0.0000E+00
2.8600E+02  0.0000E+00  0.0000E+00  0.0000E+00  0.0000E+00  0.0000E+00  0.0000E+00  0.0000E+00  0.0000E+00
3.3600E+02  3.5642E-16  0.0000E+00  0.0000E+00  0.0000E+00  0.0000E+00  0.0000E+00  0.0000E+00  0.0000E+00
3.8600E+02  6.4414E-15  0.0000E+00  0.0000E+00  0.0000E+00  0.0000E+00  0.0000E+00  0.0000E+00  0.0000E+00
4.3600E+02  4.8830E-14  0.0000E+00  0.0000E+00  0.0000E+00  0.0000E+00  0.0000E+00  0.0000E+00  0.0000E+00
4.8600E+02  2.5593E-13  0.0000E+00  0.0000E+00  0.0000E+00  0.0000E+00  0.0000E+00  0.0000E+00  0.0000E+00
5.3600E+02  1.0246E-12  0.0000E+00  0.0000E+00  0.0000E+00  0.0000E+00  0.0000E+00  0.0000E+00  0.0000E+00
5.8600E+02  3.3427E-12  0.0000E+00  0.0000E+00  0.0000E+00  0.0000E+00  0.0000E+00  0.0000E+00  0.0000E+00
6.3600E+02  9.2836E-12  0.0000E+00  0.0000E+00  0.0000E+00  0.0000E+00  0.0000E+00  0.0000E+00  0.0000E+00
6.8600E+02  2.2669E-11  0.0000E+00  0.0000E+00  0.0000E+00  0.0000E+00  0.0000E+00  0.0000E+00  0.0000E+00
```

7.3600E+02	4.9850E-11	0.0000E+00	0.0000E+00	0.0000E+00	0.0000E+00	0.0000E+00	0.0000E+00	0.0000E+00
7.8600E+02	1.0053E-10	0.0000E+00	0.0000E+00	0.0000E+00	0.0000E+00	0.0000E+00	0.0000E+00	0.0000E+00
8.3600E+02	1.8851E-10	0.0000E+00	0.0000E+00	0.0000E+00	0.0000E+00	0.0000E+00	0.0000E+00	0.0000E+00
8.8600E+02	3.3214E-10	0.0000E+00	0.0000E+00	0.0000E+00	0.0000E+00	0.0000E+00	0.0000E+00	0.0000E+00
9.3600E+02	5.5449E-10	0.0000E+00	0.0000E+00	0.0000E+00	0.0000E+00	0.0000E+00	0.0000E+00	0.0000E+00
9.8600E+02	8.8287E-10	0.0000E+00	0.0000E+00	0.0000E+00	0.0000E+00	0.0000E+00	0.0000E+00	0.0000E+00
1.0360E+03	1.3479E-09	0.0000E+00	0.0000E+00	0.0000E+00	0.0000E+00	0.0000E+00	0.0000E+00	0.0000E+00
1.0860E+03	1.9822E-09	0.0000E+00	0.0000E+00	0.0000E+00	0.0000E+00	0.0000E+00	0.0000E+00	0.0000E+00
1.1360E+03	2.8186E-09	0.0000E+00	0.0000E+00	0.0000E+00	0.0000E+00	0.0000E+00	0.0000E+00	0.0000E+00
1.1860E+03	3.8881E-09	0.0000E+00	0.0000E+00	0.0000E+00	0.0000E+00	0.0000E+00	0.0000E+00	0.0000E+00
1.2360E+03	5.2187E-09	0.0000E+00	0.0000E+00	0.0000E+00	0.0000E+00	0.0000E+00	0.0000E+00	0.0000E+00
1.2860E+03	6.8335E-09	0.0000E+00	0.0000E+00	0.0000E+00	0.0000E+00	0.0000E+00	0.0000E+00	0.0000E+00
1.3360E+03	8.7497E-09	0.0000E+00	0.0000E+00	0.0000E+00	0.0000E+00	0.0000E+00	0.0000E+00	0.0000E+00
1.3860E+03	1.0978E-08	0.0000E+00	0.0000E+00	0.0000E+00	0.0000E+00	0.0000E+00	0.0000E+00	0.0000E+00
1.4360E+03	1.3524E-08	0.0000E+00	0.0000E+00	0.0000E+00	0.0000E+00	0.0000E+00	0.0000E+00	0.0000E+00
1.4860E+03	1.6385E-08	0.0000E+00	0.0000E+00	0.0000E+00	0.0000E+00	0.0000E+00	0.0000E+00	0.0000E+00
1.5360E+03	1.9555E-08	0.0000E+00	0.0000E+00	0.0000E+00	0.0000E+00	0.0000E+00	0.0000E+00	0.0000E+00
1.5860E+03	2.3020E-08	0.0000E+00	0.0000E+00	0.0000E+00	0.0000E+00	0.0000E+00	0.0000E+00	0.0000E+00
1.6360E+03	2.6766E-08	0.0000E+00	0.0000E+00	0.0000E+00	0.0000E+00	0.0000E+00	0.0000E+00	0.0000E+00
1.6860E+03	3.0773E-08	0.0000E+00	0.0000E+00	0.0000E+00	0.0000E+00	0.0000E+00	0.0000E+00	0.0000E+00
1.7360E+03	3.5020E-08	0.0000E+00	0.0000E+00	0.0000E+00	0.0000E+00	0.0000E+00	0.0000E+00	0.0000E+00
1.7860E+03	3.9486E-08	0.0000E+00	0.0000E+00	0.0000E+00	0.0000E+00	0.0000E+00	0.0000E+00	0.0000E+00
1.8360E+03	4.4147E-08	0.0000E+00	0.0000E+00	0.0000E+00	0.0000E+00	0.0000E+00	0.0000E+00	0.0000E+00
1.8860E+03	4.8982E-08	0.0000E+00	0.0000E+00	0.0000E+00	0.0000E+00	0.0000E+00	0.0000E+00	0.0000E+00
1.9360E+03	5.3969E-08	0.0000E+00	0.0000E+00	0.0000E+00	0.0000E+00	0.0000E+00	0.0000E+00	0.0000E+00
1.9860E+03	5.9086E-08	0.0000E+00	0.0000E+00	0.0000E+00	0.0000E+00	0.0000E+00	0.0000E+00	0.0000E+00
2.0360E+03	6.4315E-08	0.0000E+00	0.0000E+00	0.0000E+00	0.0000E+00	0.0000E+00	0.0000E+00	0.0000E+00
2.0860E+03	6.9637E-08	0.0000E+00	0.0000E+00	0.0000E+00	0.0000E+00	0.0000E+00	0.0000E+00	0.0000E+00
2.1360E+03	7.5036E-08	2.1087E-16	0.0000E+00	0.0000E+00	0.0000E+00	0.0000E+00	0.0000E+00	0.0000E+00
2.1860E+03	8.0496E-08	6.1128E-16	0.0000E+00	0.0000E+00	0.0000E+00	0.0000E+00	0.0000E+00	0.0000E+00
2.2360E+03	8.6005E-08	1.2365E-15	0.0000E+00	0.0000E+00	0.0000E+00	0.0000E+00	0.0000E+00	0.0000E+00
2.2860E+03	9.1549E-08	2.2353E-15	0.0000E+00	0.0000E+00	0.0000E+00	0.0000E+00	0.0000E+00	0.0000E+00
2.3360E+03	9.7120E-08	3.6271E-15	0.0000E+00	0.0000E+00	0.0000E+00	0.0000E+00	0.0000E+00	0.0000E+00
2.3860E+03	1.0271E-07	5.8121E-15	0.0000E+00	0.0000E+00	0.0000E+00	0.0000E+00	0.0000E+00	0.0000E+00
2.4360E+03	1.0830E-07	8.5255E-15	0.0000E+00	0.0000E+00	0.0000E+00	0.0000E+00	0.0000E+00	0.0000E+00
2.4860E+03	1.1390E-07	1.2502E-14	0.0000E+00	0.0000E+00	0.0000E+00	0.0000E+00	0.0000E+00	0.0000E+00
2.5360E+03	1.1949E-07	1.7989E-14	0.0000E+00	0.0000E+00	0.0000E+00	0.0000E+00	0.0000E+00	0.0000E+00
2.5860E+03	1.2507E-07	2.5305E-14	0.0000E+00	0.0000E+00	0.0000E+00	0.0000E+00	0.0000E+00	0.0000E+00
2.6360E+03	1.3064E-07	3.5597E-14	0.0000E+00	0.0000E+00	0.0000E+00	0.0000E+00	0.0000E+00	0.0000E+00
2.6860E+03	1.3619E-07	4.9123E-14	0.0000E+00	0.0000E+00	0.0000E+00	0.0000E+00	0.0000E+00	0.0000E+00
2.7360E+03	1.4172E-07	6.7204E-14	0.0000E+00	0.0000E+00	0.0000E+00	0.0000E+00	0.0000E+00	0.0000E+00
2.7860E+03	1.4723E-07	9.0802E-14	0.0000E+00	0.0000E+00	0.0000E+00	0.0000E+00	0.0000E+00	0.0000E+00
2.8360E+03	1.5272E-07	1.2173E-13	0.0000E+00	0.0000E+00	0.0000E+00	0.0000E+00	0.0000E+00	0.0000E+00
2.8860E+03	1.5817E-07	1.6182E-13	0.0000E+00	0.0000E+00	0.0000E+00	0.0000E+00	0.0000E+00	0.0000E+00
2.9360E+03	1.6360E-07	2.1304E-13	0.0000E+00	0.0000E+00	0.0000E+00	0.0000E+00	0.0000E+00	0.0000E+00
2.9860E+03	1.6900E-07	2.7817E-13	0.0000E+00	0.0000E+00	0.0000E+00	0.0000E+00	0.0000E+00	0.0000E+00
3.0360E+03	1.7438E-07	3.6036E-13	0.0000E+00	0.0000E+00	0.0000E+00	0.0000E+00	0.0000E+00	0.0000E+00
3.0860E+03	1.7972E-07	4.6341E-13	0.0000E+00	0.0000E+00	0.0000E+00	0.0000E+00	0.0000E+00	0.0000E+00
3.1360E+03	1.8503E-07	5.9145E-13	0.0000E+00	0.0000E+00	0.0000E+00	0.0000E+00	0.0000E+00	0.0000E+00
3.1860E+03	1.9031E-07	7.4966E-13	0.0000E+00	0.0000E+00	0.0000E+00	0.0000E+00	0.0000E+00	0.0000E+00
3.2360E+03	1.9556E-07	9.4388E-13	0.0000E+00	0.0000E+00	0.0000E+00	0.0000E+00	0.0000E+00	0.0000E+00
3.2860E+03	2.0078E-07	1.1807E-12	0.0000E+00	0.0000E+00	0.0000E+00	0.0000E+00	0.0000E+00	0.0000E+00
3.3360E+03	2.0597E-07	1.4679E-12	0.0000E+00	0.0000E+00	0.0000E+00	0.0000E+00	0.0000E+00	0.0000E+00
3.3860E+03	2.1112E-07	1.8142E-12	0.0000E+00	0.0000E+00	0.0000E+00	0.0000E+00	0.0000E+00	0.0000E+00
3.4360E+03	2.1625E-07	2.2296E-12	0.0000E+00	0.0000E+00	0.0000E+00	0.0000E+00	0.0000E+00	0.0000E+00
3.4860E+03	2.2134E-07	2.7256E-12	0.0000E+00	0.0000E+00	0.0000E+00	0.0000E+00	0.0000E+00	0.0000E+00
3.5360E+03	2.2640E-07	3.3146E-12	0.0000E+00	0.0000E+00	0.0000E+00	0.0000E+00	0.0000E+00	0.0000E+00
3.5860E+03	2.3143E-07	4.0110E-12	0.0000E+00	0.0000E+00	0.0000E+00	0.0000E+00	0.0000E+00	0.0000E+00
3.6360E+03	2.3643E-07	4.8306E-12	0.0000E+00	0.0000E+00	0.0000E+00	0.0000E+00	0.0000E+00	0.0000E+00
3.6860E+03	2.4140E-07	5.7909E-12	0.0000E+00	0.0000E+00	0.0000E+00	0.0000E+00	0.0000E+00	0.0000E+00
3.7360E+03	2.4634E-07	6.9119E-12	0.0000E+00	0.0000E+00	0.0000E+00	0.0000E+00	0.0000E+00	0.0000E+00
3.7860E+03	2.5125E-07	8.2151E-12	0.0000E+00	0.0000E+00	0.0000E+00	0.0000E+00	0.0000E+00	0.0000E+00
3.8360E+03	2.5612E-07	9.7240E-12	0.0000E+00	0.0000E+00	0.0000E+00	0.0000E+00	0.0000E+00	0.0000E+00
3.8860E+03	2.6097E-07	1.1465E-11	0.0000E+00	0.0000E+00	0.0000E+00	0.0000E+00	0.0000E+00	0.0000E+00
3.9360E+03	2.6578E-07	1.3467E-11	0.0000E+00	0.0000E+00	0.0000E+00	0.0000E+00	0.0000E+00	0.0000E+00
3.9860E+03	2.7057E-07	1.5760E-11	0.0000E+00	0.0000E+00	0.0000E+00	0.0000E+00	0.0000E+00	0.0000E+00
4.0360E+03	2.7532E-07	1.8380E-11	0.0000E+00	0.0000E+00	0.0000E+00	0.0000E+00	0.0000E+00	0.0000E+00
4.0860E+03	2.8004E-07	2.1363E-11	0.0000E+00	0.0000E+00	0.0000E+00	0.0000E+00	0.0000E+00	0.0000E+00
4.1360E+03	2.8474E-07	2.4749E-11	0.0000E+00	0.0000E+00	0.0000E+00	0.0000E+00	0.0000E+00	0.0000E+00
4.1860E+03	2.8940E-07	2.8581E-11	0.0000E+00	0.0000E+00	0.0000E+00	0.0000E+00	0.0000E+00	0.0000E+00
4.2360E+03	2.9404E-07	3.2907E-11	0.0000E+00	0.0000E+00	0.0000E+00	0.0000E+00	0.0000E+00	0.0000E+00
4.2860E+03	2.9864E-07	3.7776E-11	0.0000E+00	0.0000E+00	0.0000E+00	0.0000E+00	0.0000E+00	0.0000E+00
4.3360E+03	3.0322E-07	4.3244E-11	0.0000E+00	0.0000E+00	0.0000E+00	0.0000E+00	0.0000E+00	0.0000E+00
4.3860E+03	3.0777E-07	4.9367E-11	0.0000E+00	0.0000E+00	0.0000E+00	0.0000E+00	0.0000E+00	0.0000E+00
4.4360E+03	3.1229E-07	5.6208E-11	0.0000E+00	0.0000E+00	0.0000E+00	0.0000E+00	0.0000E+00	0.0000E+00
4.4860E+03	3.1678E-07	6.3834E-11	0.0000E+00	0.0000E+00	0.0000E+00	0.0000E+00	0.0000E+00	0.0000E+00
4.5360E+03	3.2124E-07	7.2314E-11	0.0000E+00	0.0000E+00	0.0000E+00	0.0000E+00	0.0000E+00	0.0000E+00
4.5860E+03	3.2567E-07	8.1725E-11	0.0000E+00	0.0000E+00	0.0000E+00	0.0000E+00	0.0000E+00	0.0000E+00
4.6360E+03	3.3007E-07	9.2147E-11	0.0000E+00	0.0000E+00	0.0000E+00	0.0000E+00	0.0000E+00	0.0000E+00
4.6860E+03	3.3445E-07	1.0366E-10	0.0000E+00	0.0000E+00	0.0000E+00	0.0000E+00	0.0000E+00	0.0000E+00
4.7360E+03	3.3880E-07	1.1637E-10	0.0000E+00	0.0000E+00	0.0000E+00	0.0000E+00	0.0000E+00	0.0000E+00

4.7860E+03	3.4312E-07	1.3035E-10	0.0000E+00	0.0000E+00	0.0000E+00	0.0000E+00	0.0000E+00	0.0000E+00
4.8360E+03	3.4741E-07	1.4572E-10	0.0000E+00	0.0000E+00	0.0000E+00	0.0000E+00	0.0000E+00	0.0000E+00
4.8860E+03	3.5167E-07	1.6257E-10	0.0000E+00	0.0000E+00	0.0000E+00	0.0000E+00	0.0000E+00	0.0000E+00
4.9360E+03	3.5591E-07	1.8103E-10	0.0000E+00	0.0000E+00	0.0000E+00	0.0000E+00	0.0000E+00	0.0000E+00
4.9860E+03	3.6012E-07	2.0120E-10	0.0000E+00	0.0000E+00	0.0000E+00	0.0000E+00	0.0000E+00	0.0000E+00
5.0360E+03	3.6430E-07	2.2321E-10	0.0000E+00	0.0000E+00	0.0000E+00	0.0000E+00	0.0000E+00	0.0000E+00
5.0860E+03	3.6845E-07	2.4719E-10	0.0000E+00	0.0000E+00	0.0000E+00	0.0000E+00	0.0000E+00	0.0000E+00
5.1360E+03	3.7258E-07	2.7328E-10	0.0000E+00	0.0000E+00	0.0000E+00	0.0000E+00	0.0000E+00	0.0000E+00
5.1860E+03	3.7668E-07	3.0162E-10	0.0000E+00	0.0000E+00	0.0000E+00	0.0000E+00	0.0000E+00	0.0000E+00
5.2360E+03	3.8075E-07	3.3235E-10	0.0000E+00	0.0000E+00	0.0000E+00	0.0000E+00	0.0000E+00	0.0000E+00
5.2860E+03	3.8480E-07	3.6564E-10	0.0000E+00	0.0000E+00	0.0000E+00	0.0000E+00	0.0000E+00	0.0000E+00
5.3360E+03	3.8882E-07	4.0164E-10	0.0000E+00	0.0000E+00	0.0000E+00	0.0000E+00	0.0000E+00	0.0000E+00
5.3860E+03	3.9282E-07	4.4052E-10	0.0000E+00	0.0000E+00	0.0000E+00	0.0000E+00	0.0000E+00	0.0000E+00
5.4360E+03	3.9678E-07	4.8246E-10	0.0000E+00	0.0000E+00	0.0000E+00	0.0000E+00	0.0000E+00	0.0000E+00
5.4860E+03	4.0072E-07	5.2763E-10	0.0000E+00	0.0000E+00	0.0000E+00	0.0000E+00	0.0000E+00	0.0000E+00
5.5360E+03	4.0464E-07	5.7624E-10	0.0000E+00	0.0000E+00	0.0000E+00	0.0000E+00	0.0000E+00	0.0000E+00
5.5860E+03	4.0853E-07	6.2846E-10	0.0000E+00	0.0000E+00	0.0000E+00	0.0000E+00	0.0000E+00	0.0000E+00
5.6360E+03	4.1239E-07	6.8451E-10	0.0000E+00	0.0000E+00	0.0000E+00	0.0000E+00	0.0000E+00	0.0000E+00
5.6860E+03	4.1623E-07	7.4460E-10	0.0000E+00	0.0000E+00	0.0000E+00	0.0000E+00	0.0000E+00	0.0000E+00
5.7360E+03	4.2004E-07	8.0893E-10	0.0000E+00	0.0000E+00	0.0000E+00	0.0000E+00	0.0000E+00	0.0000E+00
5.7860E+03	4.2383E-07	8.7774E-10	0.0000E+00	0.0000E+00	0.0000E+00	0.0000E+00	0.0000E+00	0.0000E+00
5.8360E+03	4.2759E-07	9.5125E-10	0.0000E+00	0.0000E+00	0.0000E+00	0.0000E+00	0.0000E+00	0.0000E+00
5.8860E+03	4.3133E-07	1.0297E-09	0.0000E+00	0.0000E+00	0.0000E+00	0.0000E+00	0.0000E+00	0.0000E+00
5.9360E+03	4.3504E-07	1.1133E-09	0.0000E+00	0.0000E+00	0.0000E+00	0.0000E+00	0.0000E+00	0.0000E+00
5.9860E+03	4.3872E-07	1.2024E-09	0.0000E+00	0.0000E+00	0.0000E+00	0.0000E+00	0.0000E+00	0.0000E+00
6.0360E+03	4.4238E-07	1.2971E-09	0.0000E+00	0.0000E+00	0.0000E+00	0.0000E+00	0.0000E+00	0.0000E+00
6.0860E+03	4.4601E-07	1.3978E-09	0.0000E+00	0.0000E+00	0.0000E+00	0.0000E+00	0.0000E+00	0.0000E+00
6.1360E+03	4.4962E-07	1.5047E-09	0.0000E+00	0.0000E+00	0.0000E+00	0.0000E+00	0.0000E+00	0.0000E+00
6.1860E+03	4.5321E-07	1.6182E-09	0.0000E+00	0.0000E+00	0.0000E+00	0.0000E+00	0.0000E+00	0.0000E+00
6.2360E+03	4.5677E-07	1.7383E-09	0.0000E+00	0.0000E+00	0.0000E+00	0.0000E+00	0.0000E+00	0.0000E+00
6.2860E+03	4.6030E-07	1.8656E-09	0.0000E+00	0.0000E+00	0.0000E+00	0.0000E+00	0.0000E+00	0.0000E+00
6.3360E+03	4.6382E-07	2.0002E-09	0.0000E+00	0.0000E+00	0.0000E+00	0.0000E+00	0.0000E+00	0.0000E+00
6.3860E+03	4.6730E-07	2.1424E-09	0.0000E+00	0.0000E+00	0.0000E+00	0.0000E+00	0.0000E+00	0.0000E+00
6.4360E+03	4.7076E-07	2.2926E-09	0.0000E+00	0.0000E+00	0.0000E+00	0.0000E+00	0.0000E+00	0.0000E+00
6.4860E+03	4.7420E-07	2.4511E-09	0.0000E+00	0.0000E+00	0.0000E+00	0.0000E+00	0.0000E+00	0.0000E+00
6.5360E+03	4.7761E-07	2.6182E-09	0.0000E+00	0.0000E+00	0.0000E+00	0.0000E+00	0.0000E+00	0.0000E+00
6.5860E+03	4.8100E-07	2.7941E-09	0.0000E+00	0.0000E+00	0.0000E+00	0.0000E+00	0.0000E+00	0.0000E+00
6.6360E+03	4.8436E-07	2.9793E-09	0.0000E+00	0.0000E+00	0.0000E+00	0.0000E+00	0.0000E+00	0.0000E+00
6.6860E+03	4.8770E-07	3.1740E-09	0.0000E+00	0.0000E+00	0.0000E+00	0.0000E+00	0.0000E+00	0.0000E+00
6.7360E+03	4.9102E-07	3.3786E-09	0.0000E+00	0.0000E+00	0.0000E+00	0.0000E+00	0.0000E+00	0.0000E+00
6.7860E+03	4.9431E-07	3.5933E-09	0.0000E+00	0.0000E+00	0.0000E+00	0.0000E+00	0.0000E+00	0.0000E+00
6.8360E+03	4.9758E-07	3.8187E-09	0.0000E+00	0.0000E+00	0.0000E+00	0.0000E+00	0.0000E+00	0.0000E+00
6.8860E+03	5.0082E-07	4.0549E-09	0.0000E+00	0.0000E+00	0.0000E+00	0.0000E+00	0.0000E+00	0.0000E+00
6.9360E+03	5.0404E-07	4.3023E-09	0.0000E+00	0.0000E+00	0.0000E+00	0.0000E+00	0.0000E+00	0.0000E+00
6.9860E+03	5.0724E-07	4.5613E-09	0.0000E+00	0.0000E+00	0.0000E+00	0.0000E+00	0.0000E+00	0.0000E+00
7.0360E+03	5.1041E-07	4.8322E-09	0.0000E+00	0.0000E+00	0.0000E+00	0.0000E+00	0.0000E+00	0.0000E+00
7.0860E+03	5.1356E-07	5.1154E-09	0.0000E+00	0.0000E+00	0.0000E+00	0.0000E+00	0.0000E+00	0.0000E+00
7.1360E+03	5.1668E-07	5.4112E-09	0.0000E+00	0.0000E+00	0.0000E+00	0.0000E+00	0.0000E+00	0.0000E+00
7.1860E+03	5.1978E-07	5.7200E-09	0.0000E+00	0.0000E+00	0.0000E+00	0.0000E+00	0.0000E+00	0.0000E+00
7.2360E+03	5.2286E-07	6.0421E-09	0.0000E+00	0.0000E+00	0.0000E+00	0.0000E+00	0.0000E+00	0.0000E+00
7.2860E+03	5.2591E-07	6.3778E-09	0.0000E+00	0.0000E+00	0.0000E+00	0.0000E+00	0.0000E+00	0.0000E+00
7.3360E+03	5.2895E-07	6.7276E-09	0.0000E+00	0.0000E+00	0.0000E+00	0.0000E+00	0.0000E+00	0.0000E+00
7.3860E+03	5.3195E-07	7.0918E-09	0.0000E+00	0.0000E+00	0.0000E+00	0.0000E+00	0.0000E+00	0.0000E+00
7.4360E+03	5.3494E-07	7.4706E-09	0.0000E+00	0.0000E+00	0.0000E+00	0.0000E+00	0.0000E+00	0.0000E+00
7.4860E+03	5.3790E-07	7.8646E-09	0.0000E+00	0.0000E+00	0.0000E+00	0.0000E+00	0.0000E+00	0.0000E+00
7.5360E+03	5.4084E-07	8.2740E-09	0.0000E+00	0.0000E+00	0.0000E+00	0.0000E+00	0.0000E+00	0.0000E+00
7.5860E+03	5.4375E-07	8.6991E-09	0.0000E+00	0.0000E+00	0.0000E+00	0.0000E+00	0.0000E+00	0.0000E+00
7.6360E+03	5.4664E-07	9.1403E-09	0.0000E+00	0.0000E+00	0.0000E+00	0.0000E+00	0.0000E+00	0.0000E+00
7.6860E+03	5.4951E-07	9.5981E-09	0.0000E+00	0.0000E+00	0.0000E+00	0.0000E+00	0.0000E+00	0.0000E+00
7.7360E+03	5.5236E-07	1.0073E-08	0.0000E+00	0.0000E+00	0.0000E+00	0.0000E+00	0.0000E+00	0.0000E+00
7.7860E+03	5.5518E-07	1.0564E-08	0.0000E+00	0.0000E+00	0.0000E+00	0.0000E+00	0.0000E+00	0.0000E+00
7.8360E+03	5.5799E-07	1.1073E-08	0.0000E+00	0.0000E+00	0.0000E+00	0.0000E+00	0.0000E+00	0.0000E+00
7.8860E+03	5.6077E-07	1.1600E-08	0.0000E+00	0.0000E+00	0.0000E+00	0.0000E+00	0.0000E+00	0.0000E+00
7.9360E+03	5.6352E-07	1.2145E-08	0.0000E+00	0.0000E+00	0.0000E+00	0.0000E+00	0.0000E+00	0.0000E+00
7.9860E+03	5.6626E-07	1.2709E-08	0.0000E+00	0.0000E+00	0.0000E+00	0.0000E+00	0.0000E+00	0.0000E+00
8.0360E+03	5.6897E-07	1.3291E-08	0.0000E+00	0.0000E+00	0.0000E+00	0.0000E+00	0.0000E+00	0.0000E+00
8.0860E+03	5.7166E-07	1.3892E-08	0.0000E+00	0.0000E+00	0.0000E+00	0.0000E+00	0.0000E+00	0.0000E+00
8.1360E+03	5.7433E-07	1.4513E-08	0.0000E+00	0.0000E+00	0.0000E+00	0.0000E+00	0.0000E+00	0.0000E+00
8.1860E+03	5.7697E-07	1.5153E-08	0.0000E+00	0.0000E+00	0.0000E+00	0.0000E+00	0.0000E+00	0.0000E+00
8.2360E+03	5.7960E-07	1.5814E-08	0.0000E+00	0.0000E+00	0.0000E+00	0.0000E+00	0.0000E+00	0.0000E+00
8.2860E+03	5.8220E-07	1.6494E-08	0.0000E+00	0.0000E+00	0.0000E+00	0.0000E+00	0.0000E+00	0.0000E+00
8.3360E+03	5.8478E-07	1.7195E-08	0.0000E+00	0.0000E+00	0.0000E+00	0.0000E+00	0.0000E+00	0.0000E+00
8.3860E+03	5.8734E-07	1.7917E-08	0.0000E+00	0.0000E+00	0.0000E+00	0.0000E+00	0.0000E+00	0.0000E+00
8.4360E+03	5.8988E-07	1.8661E-08	0.0000E+00	0.0000E+00	0.0000E+00	0.0000E+00	0.0000E+00	0.0000E+00
8.4860E+03	5.9239E-07	1.9425E-08	0.0000E+00	0.0000E+00	0.0000E+00	0.0000E+00	0.0000E+00	0.0000E+00
8.5360E+03	5.9489E-07	2.0211E-08	0.0000E+00	0.0000E+00	0.0000E+00	0.0000E+00	0.0000E+00	0.0000E+00
8.5860E+03	5.9736E-07	2.1019E-08	0.0000E+00	0.0000E+00	0.0000E+00	0.0000E+00	0.0000E+00	0.0000E+00
8.6360E+03	5.9981E-07	2.1849E-08	0.0000E+00	0.0000E+00	0.0000E+00	0.0000E+00	0.0000E+00	0.0000E+00
8.6860E+03	6.0224E-07	2.2701E-08	0.0000E+00	0.0000E+00	0.0000E+00	0.0000E+00	0.0000E+00	0.0000E+00
8.7360E+03	6.0465E-07	2.3576E-08	0.0000E+00	0.0000E+00	0.0000E+00	0.0000E+00	0.0000E+00	0.0000E+00
8.7860E+03	6.0704E-07	2.4474E-08	0.0000E+00	0.0000E+00	0.0000E+00	0.0000E+00	0.0000E+00	0.0000E+00

8.8360E+03	6.0941E-07	2.5395E-08	0.0000E+00	0.0000E+00	0.0000E+00	0.0000E+00	0.0000E+00	0.0000E+00
8.8860E+03	6.1176E-07	2.6339E-08	0.0000E+00	0.0000E+00	0.0000E+00	0.0000E+00	0.0000E+00	0.0000E+00
8.9360E+03	6.1409E-07	2.7306E-08	0.0000E+00	0.0000E+00	0.0000E+00	0.0000E+00	0.0000E+00	0.0000E+00
8.9860E+03	6.1639E-07	2.8297E-08	0.0000E+00	0.0000E+00	0.0000E+00	0.0000E+00	0.0000E+00	0.0000E+00
9.0360E+03	6.1868E-07	2.9312E-08	0.0000E+00	0.0000E+00	0.0000E+00	0.0000E+00	0.0000E+00	0.0000E+00
9.0860E+03	6.2094E-07	3.0350E-08	0.0000E+00	0.0000E+00	0.0000E+00	0.0000E+00	0.0000E+00	0.0000E+00
9.1360E+03	6.2319E-07	3.1413E-08	0.0000E+00	0.0000E+00	0.0000E+00	0.0000E+00	0.0000E+00	0.0000E+00
9.1860E+03	6.2541E-07	3.2500E-08	0.0000E+00	0.0000E+00	0.0000E+00	0.0000E+00	0.0000E+00	0.0000E+00
9.2360E+03	6.2761E-07	3.3611E-08	0.0000E+00	0.0000E+00	0.0000E+00	0.0000E+00	0.0000E+00	0.0000E+00
9.2860E+03	6.2980E-07	3.4747E-08	0.0000E+00	0.0000E+00	0.0000E+00	0.0000E+00	0.0000E+00	0.0000E+00
9.3360E+03	6.3196E-07	3.5907E-08	0.0000E+00	0.0000E+00	0.0000E+00	0.0000E+00	0.0000E+00	0.0000E+00
9.3860E+03	6.3410E-07	3.7092E-08	0.0000E+00	0.0000E+00	0.0000E+00	0.0000E+00	0.0000E+00	0.0000E+00
9.4360E+03	6.3623E-07	3.8302E-08	0.0000E+00	0.0000E+00	0.0000E+00	0.0000E+00	0.0000E+00	0.0000E+00
9.4860E+03	6.3833E-07	3.9536E-08	0.0000E+00	0.0000E+00	0.0000E+00	0.0000E+00	0.0000E+00	0.0000E+00
9.5360E+03	6.4041E-07	4.0796E-08	0.0000E+00	0.0000E+00	0.0000E+00	0.0000E+00	0.0000E+00	0.0000E+00
9.5860E+03	6.4248E-07	4.2081E-08	0.0000E+00	0.0000E+00	0.0000E+00	0.0000E+00	0.0000E+00	0.0000E+00
9.6360E+03	6.4452E-07	4.3391E-08	0.0000E+00	0.0000E+00	0.0000E+00	0.0000E+00	0.0000E+00	0.0000E+00
9.6860E+03	6.4654E-07	4.4726E-08	0.0000E+00	0.0000E+00	0.0000E+00	0.0000E+00	0.0000E+00	0.0000E+00
9.7360E+03	6.4854E-07	4.6086E-08	0.0000E+00	0.0000E+00	0.0000E+00	0.0000E+00	0.0000E+00	0.0000E+00
9.7860E+03	6.5052E-07	4.7472E-08	0.0000E+00	0.0000E+00	0.0000E+00	0.0000E+00	0.0000E+00	0.0000E+00
9.8360E+03	6.5248E-07	4.8883E-08	0.0000E+00	0.0000E+00	0.0000E+00	0.0000E+00	0.0000E+00	0.0000E+00
9.8860E+03	6.5442E-07	5.0319E-08	0.0000E+00	0.0000E+00	0.0000E+00	0.0000E+00	0.0000E+00	0.0000E+00
9.9360E+03	6.5635E-07	5.1781E-08	0.0000E+00	0.0000E+00	0.0000E+00	0.0000E+00	0.0000E+00	0.0000E+00
9.9860E+03	6.5825E-07	5.3267E-08	0.0000E+00	0.0000E+00	0.0000E+00	0.0000E+00	0.0000E+00	0.0000E+00
1.0036E+04	6.6014E-07	5.4780E-08	0.0000E+00	0.0000E+00	0.0000E+00	0.0000E+00	0.0000E+00	0.0000E+00
1.0536E+04	6.7785E-07	7.1510E-08	0.0000E+00	0.0000E+00	0.0000E+00	0.0000E+00	0.0000E+00	0.0000E+00
1.1036E+04	6.9385E-07	9.0670E-08	1.4867E-16	0.0000E+00	0.0000E+00	0.0000E+00	0.0000E+00	0.0000E+00
1.1536E+04	7.0839E-07	1.1209E-07	7.6294E-16	0.0000E+00	0.0000E+00	0.0000E+00	0.0000E+00	0.0000E+00
1.2036E+04	7.2160E-07	1.3556E-07	2.3997E-15	0.0000E+00	0.0000E+00	0.0000E+00	0.0000E+00	0.0000E+00
1.2536E+04	7.3353E-07	1.6080E-07	5.8459E-15	0.0000E+00	0.0000E+00	0.0000E+00	0.0000E+00	0.0000E+00
1.3036E+04	7.4426E-07	1.8752E-07	1.2927E-14	0.0000E+00	0.0000E+00	0.0000E+00	0.0000E+00	0.0000E+00
1.3536E+04	7.5386E-07	2.1542E-07	2.6886E-14	0.0000E+00	0.0000E+00	0.0000E+00	0.0000E+00	0.0000E+00
1.4036E+04	7.6243E-07	2.4419E-07	5.3328E-14	0.0000E+00	0.0000E+00	0.0000E+00	0.0000E+00	0.0000E+00
1.4536E+04	7.7004E-07	2.7353E-07	1.0063E-13	0.0000E+00	0.0000E+00	0.0000E+00	0.0000E+00	0.0000E+00
1.5036E+04	7.7677E-07	3.0315E-07	1.8214E-13	0.0000E+00	0.0000E+00	0.0000E+00	0.0000E+00	0.0000E+00
1.5536E+04	7.8269E-07	3.3278E-07	3.1745E-13	0.0000E+00	0.0000E+00	0.0000E+00	0.0000E+00	0.0000E+00
1.6036E+04	7.8786E-07	3.6219E-07	5.3541E-13	0.0000E+00	0.0000E+00	0.0000E+00	0.0000E+00	0.0000E+00
1.6536E+04	7.9235E-07	3.9115E-07	8.7559E-13	0.0000E+00	0.0000E+00	0.0000E+00	0.0000E+00	0.0000E+00
1.7036E+04	7.9622E-07	4.1948E-07	1.3900E-12	0.0000E+00	0.0000E+00	0.0000E+00	0.0000E+00	0.0000E+00
1.7536E+04	7.9953E-07	4.4702E-07	2.1502E-12	0.0000E+00	0.0000E+00	0.0000E+00	0.0000E+00	0.0000E+00
1.8036E+04	8.0230E-07	4.7365E-07	3.2500E-12	0.0000E+00	0.0000E+00	0.0000E+00	0.0000E+00	0.0000E+00
1.8536E+04	8.0454E-07	4.9924E-07	4.8091E-12	0.0000E+00	0.0000E+00	0.0000E+00	0.0000E+00	0.0000E+00
1.9036E+04	8.0630E-07	5.2373E-07	6.9801E-12	0.0000E+00	0.0000E+00	0.0000E+00	0.0000E+00	0.0000E+00
1.9536E+04	8.0772E-07	5.4706E-07	9.9562E-12	0.0000E+00	0.0000E+00	0.0000E+00	0.0000E+00	0.0000E+00
2.0036E+04	8.0895E-07	5.6917E-07	1.3969E-11	0.0000E+00	0.0000E+00	0.0000E+00	0.0000E+00	0.0000E+00
2.0536E+04	8.1010E-07	5.9006E-07	1.9309E-11	0.0000E+00	0.0000E+00	0.0000E+00	0.0000E+00	0.0000E+00
2.1036E+04	8.1122E-07	6.0971E-07	2.6317E-11	0.0000E+00	0.0000E+00	0.0000E+00	0.0000E+00	0.0000E+00
2.1536E+04	8.1233E-07	6.2812E-07	3.5399E-11	0.0000E+00	0.0000E+00	0.0000E+00	0.0000E+00	0.0000E+00
2.2036E+04	8.1342E-07	6.4532E-07	4.7028E-11	0.0000E+00	0.0000E+00	0.0000E+00	0.0000E+00	0.0000E+00
2.2536E+04	8.1451E-07	6.6132E-07	6.1756E-11	0.0000E+00	0.0000E+00	0.0000E+00	0.0000E+00	0.0000E+00
2.3036E+04	8.1559E-07	6.7617E-07	8.0221E-11	0.0000E+00	0.0000E+00	0.0000E+00	0.0000E+00	0.0000E+00
2.3536E+04	8.1666E-07	6.8989E-07	1.0315E-10	0.0000E+00	0.0000E+00	0.0000E+00	0.0000E+00	0.0000E+00
2.4036E+04	8.1773E-07	7.0253E-07	1.3137E-10	0.0000E+00	0.0000E+00	0.0000E+00	0.0000E+00	0.0000E+00
2.4536E+04	8.1880E-07	7.1415E-07	1.6581E-10	0.0000E+00	0.0000E+00	0.0000E+00	0.0000E+00	0.0000E+00
2.5036E+04	8.1986E-07	7.2478E-07	2.0751E-10	0.0000E+00	0.0000E+00	0.0000E+00	0.0000E+00	0.0000E+00
2.5536E+04	8.2091E-07	7.3449E-07	2.5765E-10	0.0000E+00	0.0000E+00	0.0000E+00	0.0000E+00	0.0000E+00
2.6036E+04	8.2196E-07	7.4332E-07	3.1751E-10	0.0000E+00	0.0000E+00	0.0000E+00	0.0000E+00	0.0000E+00
2.6536E+04	8.2300E-07	7.5135E-07	3.8850E-10	1.9121E-16	0.0000E+00	0.0000E+00	0.0000E+00	0.0000E+00
2.7036E+04	8.2404E-07	7.5862E-07	4.7218E-10	5.1090E-16	0.0000E+00	0.0000E+00	0.0000E+00	0.0000E+00
2.7536E+04	8.2507E-07	7.6521E-07	5.7025E-10	9.7503E-16	0.0000E+00	0.0000E+00	0.0000E+00	0.0000E+00
2.8036E+04	8.2610E-07	7.7115E-07	6.8455E-10	1.5910E-15	0.0000E+00	0.0000E+00	0.0000E+00	0.0000E+00
2.8536E+04	8.2712E-07	7.7652E-07	8.1707E-10	2.5541E-15	0.0000E+00	0.0000E+00	0.0000E+00	0.0000E+00
2.9036E+04	8.2814E-07	7.8136E-07	9.6996E-10	3.9215E-15	0.0000E+00	0.0000E+00	0.0000E+00	0.0000E+00
2.9536E+04	8.2915E-07	7.8573E-07	1.1455E-09	5.7416E-15	0.0000E+00	0.0000E+00	0.0000E+00	0.0000E+00
3.0036E+04	8.3016E-07	7.8968E-07	1.3461E-09	8.1795E-15	0.0000E+00	0.0000E+00	0.0000E+00	0.0000E+00
3.0536E+04	8.3116E-07	7.9325E-07	1.5745E-09	1.1351E-14	0.0000E+00	0.0000E+00	0.0000E+00	0.0000E+00
3.1036E+04	8.3216E-07	7.9648E-07	1.8333E-09	1.5733E-14	0.0000E+00	0.0000E+00	0.0000E+00	0.0000E+00
3.1536E+04	8.3315E-07	7.9942E-07	2.1255E-09	2.1429E-14	0.0000E+00	0.0000E+00	0.0000E+00	0.0000E+00
3.2036E+04	8.3414E-07	8.0210E-07	2.4540E-09	2.8875E-14	0.0000E+00	0.0000E+00	0.0000E+00	0.0000E+00
3.2536E+04	8.3512E-07	8.0455E-07	2.8222E-09	3.8664E-14	0.0000E+00	0.0000E+00	0.0000E+00	0.0000E+00
3.3036E+04	8.3610E-07	8.0680E-07	3.2333E-09	5.1093E-14	0.0000E+00	0.0000E+00	0.0000E+00	0.0000E+00
3.3536E+04	8.3707E-07	8.0888E-07	3.6908E-09	6.7480E-14	0.0000E+00	0.0000E+00	0.0000E+00	0.0000E+00
3.4036E+04	8.3803E-07	8.1080E-07	4.1983E-09	8.8084E-14	0.0000E+00	0.0000E+00	0.0000E+00	0.0000E+00
3.4536E+04	8.3899E-07	8.1260E-07	4.7593E-09	1.1435E-13	0.0000E+00	0.0000E+00	0.0000E+00	0.0000E+00
3.5036E+04	8.3995E-07	8.1428E-07	5.3778E-09	1.4738E-13	0.0000E+00	0.0000E+00	0.0000E+00	0.0000E+00
3.5536E+04	8.4090E-07	8.1587E-07	6.0576E-09	1.8861E-13	0.0000E+00	0.0000E+00	0.0000E+00	0.0000E+00
3.6036E+04	8.4185E-07	8.1737E-07	6.8039E-09	2.4003E-13	0.0000E+00	0.0000E+00	0.0000E+00	0.0000E+00
3.6536E+04	8.4279E-07	8.1879E-07	7.6209E-09	3.0360E-13	0.0000E+00	0.0000E+00	0.0000E+00	0.0000E+00
3.7036E+04	8.4372E-07	8.2016E-07	8.5117E-09	3.8150E-13	0.0000E+00	0.0000E+00	0.0000E+00	0.0000E+00
3.7536E+04	8.4465E-07	8.2146E-07	9.4806E-09	4.7691E-13	0.0000E+00	0.0000E+00	0.0000E+00	0.0000E+00
3.8036E+04	8.4558E-07	8.2273E-07	1.0532E-08	5.9291E-13	0.0000E+00	0.0000E+00	0.0000E+00	0.0000E+00

3.8536E+04	8.4650E-07	8.2395E-07	1.1669E-08	7.3314E-13	0.0000E+00	0.0000E+00	0.0000E+00	0.0000E+00
3.9036E+04	8.4741E-07	8.2513E-07	1.2897E-08	9.0216E-13	0.0000E+00	0.0000E+00	0.0000E+00	0.0000E+00
3.9536E+04	8.4832E-07	8.2629E-07	1.4219E-08	1.1045E-12	0.0000E+00	0.0000E+00	0.0000E+00	0.0000E+00
4.0036E+04	8.4923E-07	8.2742E-07	1.5638E-08	1.3460E-12	0.0000E+00	0.0000E+00	0.0000E+00	0.0000E+00
4.0536E+04	8.5013E-07	8.2853E-07	1.7159E-08	1.6325E-12	0.0000E+00	0.0000E+00	0.0000E+00	0.0000E+00
4.1036E+04	8.5102E-07	8.2961E-07	1.8785E-08	1.9717E-12	0.0000E+00	0.0000E+00	0.0000E+00	0.0000E+00
4.1536E+04	8.5191E-07	8.3068E-07	2.0519E-08	2.3709E-12	0.0000E+00	0.0000E+00	0.0000E+00	0.0000E+00
4.2036E+04	8.5280E-07	8.3173E-07	2.2366E-08	2.8393E-12	0.0000E+00	0.0000E+00	0.0000E+00	0.0000E+00
4.2536E+04	8.5368E-07	8.3277E-07	2.4328E-08	3.3864E-12	0.0000E+00	0.0000E+00	0.0000E+00	0.0000E+00
4.3036E+04	8.5455E-07	8.3379E-07	2.6409E-08	4.0237E-12	0.0000E+00	0.0000E+00	0.0000E+00	0.0000E+00
4.3536E+04	8.5542E-07	8.3481E-07	2.8613E-08	4.7627E-12	0.0000E+00	0.0000E+00	0.0000E+00	0.0000E+00
4.4036E+04	8.5629E-07	8.3581E-07	3.0941E-08	5.6176E-12	0.0000E+00	0.0000E+00	0.0000E+00	0.0000E+00
4.4536E+04	8.5715E-07	8.3680E-07	3.3397E-08	6.6024E-12	0.0000E+00	0.0000E+00	0.0000E+00	0.0000E+00
4.5036E+04	8.5800E-07	8.3779E-07	3.5983E-08	7.7338E-12	0.0000E+00	0.0000E+00	0.0000E+00	0.0000E+00
4.5536E+04	8.5885E-07	8.3876E-07	3.8703E-08	9.0291E-12	0.0000E+00	0.0000E+00	0.0000E+00	0.0000E+00
4.6036E+04	8.5970E-07	8.3973E-07	4.1556E-08	1.0508E-11	0.0000E+00	0.0000E+00	0.0000E+00	0.0000E+00
4.6536E+04	8.6054E-07	8.4069E-07	4.4546E-08	1.2192E-11	0.0000E+00	0.0000E+00	0.0000E+00	0.0000E+00
4.7036E+04	8.6138E-07	8.4165E-07	4.7675E-08	1.4103E-11	0.0000E+00	0.0000E+00	0.0000E+00	0.0000E+00
4.7536E+04	8.6221E-07	8.4260E-07	5.0942E-08	1.6266E-11	0.0000E+00	0.0000E+00	0.0000E+00	0.0000E+00
4.8036E+04	8.6303E-07	8.4354E-07	5.4350E-08	1.8708E-11	0.0000E+00	0.0000E+00	0.0000E+00	0.0000E+00
4.8536E+04	8.6386E-07	8.4447E-07	5.7899E-08	2.1458E-11	0.0000E+00	0.0000E+00	0.0000E+00	0.0000E+00
4.9036E+04	8.6467E-07	8.4540E-07	6.1590E-08	2.4547E-11	0.0000E+00	0.0000E+00	0.0000E+00	0.0000E+00
4.9536E+04	8.6548E-07	8.4633E-07	6.5422E-08	2.8009E-11	0.0000E+00	0.0000E+00	0.0000E+00	0.0000E+00
5.0036E+04	8.6629E-07	8.4725E-07	6.9397E-08	3.1878E-11	0.0000E+00	0.0000E+00	0.0000E+00	0.0000E+00
5.0536E+04	8.6710E-07	8.4816E-07	7.3513E-08	3.6195E-11	0.0000E+00	0.0000E+00	0.0000E+00	0.0000E+00
5.1036E+04	8.6790E-07	8.4907E-07	7.7770E-08	4.0998E-11	0.0000E+00	0.0000E+00	0.0000E+00	0.0000E+00
5.1536E+04	8.6870E-07	8.4997E-07	8.2167E-08	4.6333E-11	0.0000E+00	0.0000E+00	0.0000E+00	0.0000E+00
5.2036E+04	8.6949E-07	8.5087E-07	8.6704E-08	5.2246E-11	0.0000E+00	0.0000E+00	0.0000E+00	0.0000E+00
5.2536E+04	8.7027E-07	8.5176E-07	9.1378E-08	5.8785E-11	0.0000E+00	0.0000E+00	0.0000E+00	0.0000E+00
5.3036E+04	8.7105E-07	8.5264E-07	9.6189E-08	6.6004E-11	0.0000E+00	0.0000E+00	0.0000E+00	0.0000E+00
5.3536E+04	8.7182E-07	8.5352E-07	1.0113E-07	7.3957E-11	0.0000E+00	0.0000E+00	0.0000E+00	0.0000E+00
5.4036E+04	8.7259E-07	8.5440E-07	1.0621E-07	8.2704E-11	0.0000E+00	0.0000E+00	0.0000E+00	0.0000E+00
5.4536E+04	8.7336E-07	8.5527E-07	1.1142E-07	9.2305E-11	0.0000E+00	0.0000E+00	0.0000E+00	0.0000E+00
5.5036E+04	8.7412E-07	8.5614E-07	1.1676E-07	1.0283E-10	0.0000E+00	0.0000E+00	0.0000E+00	0.0000E+00
5.5536E+04	8.7487E-07	8.5700E-07	1.2222E-07	1.1434E-10	0.0000E+00	0.0000E+00	0.0000E+00	0.0000E+00
5.6036E+04	8.7562E-07	8.5785E-07	1.2780E-07	1.2691E-10	0.0000E+00	0.0000E+00	0.0000E+00	0.0000E+00
5.6536E+04	8.7637E-07	8.5871E-07	1.3350E-07	1.4062E-10	0.0000E+00	0.0000E+00	0.0000E+00	0.0000E+00
5.7036E+04	8.7711E-07	8.5955E-07	1.3932E-07	1.5555E-10	0.0000E+00	0.0000E+00	0.0000E+00	0.0000E+00
5.7536E+04	8.7784E-07	8.6039E-07	1.4525E-07	1.7177E-10	0.0000E+00	0.0000E+00	0.0000E+00	0.0000E+00
5.8036E+04	8.7857E-07	8.6123E-07	1.5129E-07	1.8939E-10	0.0000E+00	0.0000E+00	0.0000E+00	0.0000E+00
5.8536E+04	8.7930E-07	8.6206E-07	1.5744E-07	2.0848E-10	0.0000E+00	0.0000E+00	0.0000E+00	0.0000E+00
5.9036E+04	8.8002E-07	8.6289E-07	1.6368E-07	2.2915E-10	0.0000E+00	0.0000E+00	0.0000E+00	0.0000E+00
5.9536E+04	8.8074E-07	8.6371E-07	1.7003E-07	2.5149E-10	0.0000E+00	0.0000E+00	0.0000E+00	0.0000E+00
6.0036E+04	8.8145E-07	8.6453E-07	1.7647E-07	2.7561E-10	0.0000E+00	0.0000E+00	0.0000E+00	0.0000E+00
6.0536E+04	8.8216E-07	8.6534E-07	1.8300E-07	3.0162E-10	0.0000E+00	0.0000E+00	0.0000E+00	0.0000E+00
6.1036E+04	8.8288E-07	8.6615E-07	1.8961E-07	3.2962E-10	0.0000E+00	0.0000E+00	0.0000E+00	0.0000E+00
6.1536E+04	8.8358E-07	8.6696E-07	1.9630E-07	3.5974E-10	0.0000E+00	0.0000E+00	0.0000E+00	0.0000E+00
6.2036E+04	8.8428E-07	8.6775E-07	2.0308E-07	3.9209E-10	0.0000E+00	0.0000E+00	0.0000E+00	0.0000E+00
6.2536E+04	8.8497E-07	8.6855E-07	2.0992E-07	4.2680E-10	0.0000E+00	0.0000E+00	0.0000E+00	0.0000E+00
6.3036E+04	8.8566E-07	8.6934E-07	2.1683E-07	4.6401E-10	0.0000E+00	0.0000E+00	0.0000E+00	0.0000E+00
6.3536E+04	8.8634E-07	8.7012E-07	2.2381E-07	5.0384E-10	0.0000E+00	0.0000E+00	0.0000E+00	0.0000E+00
6.4036E+04	8.8702E-07	8.7090E-07	2.3085E-07	5.4644E-10	0.0000E+00	0.0000E+00	0.0000E+00	0.0000E+00
6.4536E+04	8.8769E-07	8.7167E-07	2.3794E-07	5.9194E-10	0.0000E+00	0.0000E+00	0.0000E+00	0.0000E+00
6.5036E+04	8.8836E-07	8.7244E-07	2.4508E-07	6.4051E-10	0.0000E+00	0.0000E+00	0.0000E+00	0.0000E+00
6.5536E+04	8.8902E-07	8.7321E-07	2.5227E-07	6.9229E-10	0.0000E+00	0.0000E+00	0.0000E+00	0.0000E+00
6.6036E+04	8.8968E-07	8.7397E-07	2.5949E-07	7.4744E-10	0.0000E+00	0.0000E+00	0.0000E+00	0.0000E+00
6.6536E+04	8.9034E-07	8.7473E-07	2.6676E-07	8.0612E-10	0.0000E+00	0.0000E+00	0.0000E+00	0.0000E+00
6.7036E+04	8.9099E-07	8.7548E-07	2.7406E-07	8.6851E-10	0.0000E+00	0.0000E+00	0.0000E+00	0.0000E+00
6.7536E+04	8.9164E-07	8.7622E-07	2.8139E-07	9.3478E-10	0.0000E+00	0.0000E+00	0.0000E+00	0.0000E+00
6.8036E+04	8.9228E-07	8.7697E-07	2.8874E-07	1.0051E-09	0.0000E+00	0.0000E+00	0.0000E+00	0.0000E+00
6.8536E+04	8.9291E-07	8.7770E-07	2.9611E-07	1.0796E-09	0.0000E+00	0.0000E+00	0.0000E+00	0.0000E+00
6.9036E+04	8.9355E-07	8.7844E-07	3.0350E-07	1.1586E-09	0.0000E+00	0.0000E+00	0.0000E+00	0.0000E+00
6.9536E+04	8.9417E-07	8.7916E-07	3.1090E-07	1.2422E-09	0.0000E+00	0.0000E+00	0.0000E+00	0.0000E+00
7.0036E+04	8.9480E-07	8.7989E-07	3.1831E-07	1.3306E-09	0.0000E+00	0.0000E+00	0.0000E+00	0.0000E+00
7.0536E+04	8.9541E-07	8.8061E-07	3.2573E-07	1.4241E-09	0.0000E+00	0.0000E+00	0.0000E+00	0.0000E+00
7.1036E+04	8.9603E-07	8.8132E-07	3.3314E-07	1.5227E-09	0.0000E+00	0.0000E+00	0.0000E+00	0.0000E+00
7.1536E+04	8.9664E-07	8.8203E-07	3.4055E-07	1.6268E-09	0.0000E+00	0.0000E+00	0.0000E+00	0.0000E+00
7.2036E+04	8.9725E-07	8.8274E-07	3.4796E-07	1.7366E-09	0.0000E+00	0.0000E+00	0.0000E+00	0.0000E+00
7.2536E+04	8.9785E-07	8.8344E-07	3.5535E-07	1.8522E-09	0.0000E+00	0.0000E+00	0.0000E+00	0.0000E+00
7.3036E+04	8.9845E-07	8.8414E-07	3.6273E-07	1.9739E-09	0.0000E+00	0.0000E+00	0.0000E+00	0.0000E+00
7.3536E+04	8.9904E-07	8.8483E-07	3.7009E-07	2.1020E-09	0.0000E+00	0.0000E+00	0.0000E+00	0.0000E+00
7.4036E+04	8.9963E-07	8.8552E-07	3.7743E-07	2.2366E-09	0.0000E+00	0.0000E+00	0.0000E+00	0.0000E+00
7.4536E+04	9.0021E-07	8.8620E-07	3.8475E-07	2.3780E-09	0.0000E+00	0.0000E+00	0.0000E+00	0.0000E+00
7.5036E+04	9.0079E-07	8.8688E-07	3.9204E-07	2.5265E-09	0.0000E+00	0.0000E+00	0.0000E+00	0.0000E+00
7.5536E+04	9.0137E-07	8.8755E-07	3.9931E-07	2.6823E-09	0.0000E+00	0.0000E+00	0.0000E+00	0.0000E+00
7.6036E+04	9.0194E-07	8.8822E-07	4.0654E-07	2.8456E-09	0.0000E+00	0.0000E+00	0.0000E+00	0.0000E+00
7.6536E+04	9.0250E-07	8.8888E-07	4.1373E-07	3.0168E-09	0.0000E+00	0.0000E+00	0.0000E+00	0.0000E+00
7.7036E+04	9.0307E-07	8.8954E-07	4.2089E-07	3.1960E-09	0.0000E+00	0.0000E+00	0.0000E+00	0.0000E+00
7.7536E+04	9.0363E-07	8.9020E-07	4.2800E-07	3.3836E-09	0.0000E+00	0.0000E+00	0.0000E+00	0.0000E+00
7.8036E+04	9.0418E-07	8.9085E-07	4.3508E-07	3.5797E-09	0.0000E+00	0.0000E+00	0.0000E+00	0.0000E+00
7.8536E+04	9.0473E-07	8.9149E-07	4.4211E-07	3.7848E-09	0.0000E+00	0.0000E+00	0.0000E+00	0.0000E+00

7.9036E+04	9.0528E-07	8.9214E-07	4.4909E-07	3.9990E-09	0.0000E+00	0.0000E+00	0.0000E+00	0.0000E+00
7.9536E+04	9.0582E-07	8.9277E-07	4.5602E-07	4.2226E-09	0.0000E+00	0.0000E+00	0.0000E+00	0.0000E+00
8.0036E+04	9.0636E-07	8.9341E-07	4.6290E-07	4.4559E-09	0.0000E+00	0.0000E+00	0.0000E+00	0.0000E+00
8.0536E+04	9.0690E-07	8.9403E-07	4.6973E-07	4.6993E-09	0.0000E+00	0.0000E+00	0.0000E+00	0.0000E+00
8.1036E+04	9.0743E-07	8.9466E-07	4.7651E-07	4.9529E-09	0.0000E+00	0.0000E+00	0.0000E+00	0.0000E+00
8.1536E+04	9.0795E-07	8.9528E-07	4.8322E-07	5.2172E-09	0.0000E+00	0.0000E+00	0.0000E+00	0.0000E+00
8.2036E+04	9.0847E-07	8.9589E-07	4.8988E-07	5.4923E-09	0.0000E+00	0.0000E+00	0.0000E+00	0.0000E+00
8.2536E+04	9.0899E-07	8.9650E-07	4.9648E-07	5.7785E-09	0.0000E+00	0.0000E+00	0.0000E+00	0.0000E+00
8.3036E+04	9.0950E-07	8.9711E-07	5.0302E-07	6.0763E-09	0.0000E+00	0.0000E+00	0.0000E+00	0.0000E+00
8.3536E+04	9.1001E-07	8.9771E-07	5.0950E-07	6.3858E-09	0.0000E+00	0.0000E+00	0.0000E+00	0.0000E+00
8.4036E+04	9.1052E-07	8.9831E-07	5.1591E-07	6.7074E-09	0.0000E+00	0.0000E+00	0.0000E+00	0.0000E+00
8.4536E+04	9.1102E-07	8.9890E-07	5.2227E-07	7.0414E-09	0.0000E+00	0.0000E+00	0.0000E+00	0.0000E+00
8.5036E+04	9.1152E-07	8.9949E-07	5.2855E-07	7.3881E-09	0.0000E+00	0.0000E+00	0.0000E+00	0.0000E+00
8.5536E+04	9.1201E-07	9.0008E-07	5.3477E-07	7.7477E-09	0.0000E+00	0.0000E+00	0.0000E+00	0.0000E+00
8.6036E+04	9.1250E-07	9.0066E-07	5.4092E-07	8.1207E-09	0.0000E+00	0.0000E+00	0.0000E+00	0.0000E+00
8.6536E+04	9.1298E-07	9.0123E-07	5.4700E-07	8.5072E-09	0.0000E+00	0.0000E+00	0.0000E+00	0.0000E+00
8.7036E+04	9.1346E-07	9.0181E-07	5.5302E-07	8.9077E-09	0.0000E+00	0.0000E+00	0.0000E+00	0.0000E+00
8.7536E+04	9.1394E-07	9.0237E-07	5.5896E-07	9.3224E-09	0.0000E+00	0.0000E+00	0.0000E+00	0.0000E+00
8.8036E+04	9.1441E-07	9.0294E-07	5.6484E-07	9.7517E-09	0.0000E+00	0.0000E+00	0.0000E+00	0.0000E+00
8.8536E+04	9.1488E-07	9.0350E-07	5.7065E-07	1.0196E-08	0.0000E+00	0.0000E+00	0.0000E+00	0.0000E+00
8.9036E+04	9.1535E-07	9.0405E-07	5.7638E-07	1.0655E-08	0.0000E+00	0.0000E+00	0.0000E+00	0.0000E+00
8.9536E+04	9.1581E-07	9.0460E-07	5.8205E-07	1.1130E-08	0.0000E+00	0.0000E+00	0.0000E+00	0.0000E+00
9.0036E+04	9.1627E-07	9.0515E-07	5.8764E-07	1.1620E-08	0.0000E+00	0.0000E+00	0.0000E+00	0.0000E+00
9.0536E+04	9.1672E-07	9.0569E-07	5.9316E-07	1.2127E-08	0.0000E+00	0.0000E+00	0.0000E+00	0.0000E+00
9.1036E+04	9.1716E-07	9.0623E-07	5.9862E-07	1.2650E-08	0.0000E+00	0.0000E+00	0.0000E+00	0.0000E+00
9.1536E+04	9.1761E-07	9.0677E-07	6.0400E-07	1.3190E-08	0.0000E+00	0.0000E+00	0.0000E+00	0.0000E+00
9.2036E+04	9.1805E-07	9.0730E-07	6.0931E-07	1.3746E-08	0.0000E+00	0.0000E+00	0.0000E+00	0.0000E+00
9.2536E+04	9.1849E-07	9.0782E-07	6.1454E-07	1.4320E-08	0.0000E+00	0.0000E+00	0.0000E+00	0.0000E+00
9.3036E+04	9.1892E-07	9.0834E-07	6.1971E-07	1.4912E-08	0.0000E+00	0.0000E+00	0.0000E+00	0.0000E+00
9.3536E+04	9.1935E-07	9.0886E-07	6.2480E-07	1.5521E-08	0.0000E+00	0.0000E+00	0.0000E+00	0.0000E+00
9.4036E+04	9.1978E-07	9.0937E-07	6.2983E-07	1.6149E-08	0.0000E+00	0.0000E+00	0.0000E+00	0.0000E+00
9.4536E+04	9.2020E-07	9.0988E-07	6.3478E-07	1.6795E-08	0.0000E+00	0.0000E+00	0.0000E+00	0.0000E+00
9.5036E+04	9.2062E-07	9.1039E-07	6.3966E-07	1.7460E-08	0.0000E+00	0.0000E+00	0.0000E+00	0.0000E+00
9.5536E+04	9.2103E-07	9.1089E-07	6.4448E-07	1.8144E-08	0.0000E+00	0.0000E+00	0.0000E+00	0.0000E+00
9.6036E+04	9.2144E-07	9.1139E-07	6.4922E-07	1.8847E-08	0.0000E+00	0.0000E+00	0.0000E+00	0.0000E+00
9.6536E+04	9.2184E-07	9.1188E-07	6.5389E-07	1.9570E-08	0.0000E+00	0.0000E+00	0.0000E+00	0.0000E+00
9.7036E+04	9.2225E-07	9.1237E-07	6.5849E-07	2.0313E-08	0.0000E+00	0.0000E+00	0.0000E+00	0.0000E+00
9.7536E+04	9.2265E-07	9.1285E-07	6.6303E-07	2.1075E-08	0.0000E+00	0.0000E+00	0.0000E+00	0.0000E+00
9.8036E+04	9.2304E-07	9.1334E-07	6.6750E-07	2.1859E-08	0.0000E+00	0.0000E+00	0.0000E+00	0.0000E+00
9.8536E+04	9.2343E-07	9.1381E-07	6.7190E-07	2.2663E-08	0.0000E+00	0.0000E+00	0.0000E+00	0.0000E+00
9.9036E+04	9.2382E-07	9.1429E-07	6.7623E-07	2.3488E-08	0.0000E+00	0.0000E+00	0.0000E+00	0.0000E+00
9.9536E+04	9.2420E-07	9.1475E-07	6.8050E-07	2.4334E-08	0.0000E+00	0.0000E+00	0.0000E+00	0.0000E+00
1.0004E+05	9.2458E-07	9.1522E-07	6.8470E-07	2.5201E-08	0.0000E+00	0.0000E+00	0.0000E+00	0.0000E+00
Total	8.1101E-02	7.0971E-02	1.9671E-02	2.8859E-04	0.0000E+00	0.0000E+00	0.0000E+00	0.0000E+00

Botflux source code listing:

```
      program botflux

      parameter (maxnstime=20000, maxntime=6000, maxnkd=8)

      integer i,istep,ioresult,nnodes,nx,ny,nstep(maxnkd),maxstep
      real time,x(200),y,z,conc(200),flow(500),fdat(maxnstime,maxnkd)
      real stime(maxnstime),dumtime(maxntime,maxnkd)
      real ztime(maxnkd),ftotdat(maxnkd),dumdat(maxntime,maxnkd)
      character filename*80,line*80,line2*80,line3*80,message*80

      message="Botflux 1.0: flux out the bottom of a VAM transport run"

      open(20,file="botflux.out")
      open(22,file="botflux.dat")


      write(*,*)'Enter Fluid Flux Filename: '
      read(*,*)filename
      open(12,file=filename,status="old",readonly)


      read(12,*)
      read(12,'(a80)',iostat=ioresult)line

      write(*,*)
      write(*,'(a80)')message
      write(*,*)
      write(*,*)'Flow Run: '
      write(*,'(a80)')line

      write(20,*)
      write(20,'(a80)')message
      write(20,*)
      write(20,*)'Flow Run: '
      write(20,'(a80)')line


c     get fluid flux data from flow run

      read(12,*,iostat=ioresult)n,nbnd
      nline=ceiling(float(nbnd)/20.0)

      do i=1,nline
        read(12,*)
      enddo

      nline=ceiling(float(nbnd)/8.0)

c     assume that bottom boundary nodes are listed first
      do while (ioresult.eq.0)
        read(12,'(a80)',iostat=ioresult)line
        if(ioresult.eq.0)then
          line3=line
          do i=1,nline
            iptr=(i-1)*8+1
            iptr2=min(iptr+7,nbnd)
            read(12,'(a80)')line2
            read(line2,'(8e10.3)')(flow(j),j=iptr,iptr2)
          enddo
        endif
```

```
      enddo

       close(12)

      write(*,'(a80)')line3

c     get solute data
      write(*,*)
       write(*,*)'Enter Number of Nodes in X and Y Axes'
       read(*,*)nx,ny
       nnodes=nx*ny
       write(20,*)
       write(20,*)'nodes: ',nx,ny,nnodes
       write(*,*)
       write(*,*)'Enter Assumed Inventory for Normalization',
     &    ' (value to divide results by): '
       read(*,*)rinv
       write(20,*)'Inventory: ',rinv
      write(*,*)
       write(*,*)'Enter a 1 to Normalize Integral to 1.0'
       read(*,*)normflag
       write(20,*)'Normalization Flag: ',normflag
      write(*,*)
       write(*,*)'Enter Delay (in years) Before Initiation of Release: '
       read(*,*)delay
       write(20,*)'Delay Time (yrs): ',delay
       write(*,*)
      write(*,*)'Enter Number of Transport Cases to Read (Max=8): '
       read(*,*)nfiles
       write(20,*)'Number of Transport Cases: ',nfiles
       write(20,*)

      nfiles=min(nfiles,maxnkd)
       maxstep=0

       do ifile=1,nfiles
         write(*,*)'Enter Filename for Transport Run #',ifile,' : '
         read(*,*)filename
         open(10,file=filename,status="old",readonly)
         read(10,*)
         read(10,*)
         read(10,'(a80)')line

         write(*,*)
        write(*,*)'Transport Run: '
         write(*,'(a80)')line

         write(22,*)
        write(22,*)'Transport Run: '
         write(22,'(a80)')line
         write(22,*)

         write(20,*)
        write(20,*)'Transport Run: '
         write(20,'(a80)')line
         write(20,*)

        read(10,*)n1,n2,n3

         istep=-1
         ioresult=0
         pflux=0
         fluxtot=0
```

```
         nstep(ifile)=0

c       assume that bottom boundary nodes are listed first
         do while (ioresult.eq.0)
           read(10,'(a80)',iostat=ioresult)line
           if(ioresult.eq.0)then
             nstep(ifile)=nstep(ifile)+1
             line2=line
             if(istep.lt.0)then
               istep=0
               time=0.
               ptime=0.
             else
               read(line,'(11x,i6,7x,e11.0)')istep,time
             endif
                  do i=1,nx
                    read(10,*,iostat=ioresult),x(i),y,z,conc(i)
                  enddo
                  do i=1,nnodes-nx
                    read(10,'(a80)')
                  enddo
             flux=0
             do i=1,nx
               flux=flux+conc(i)*flow(i)*-1.
             enddo
             flux=flux/rinv
             fluxtot=fluxtot+0.5*(flux+pflux)*(time-ptime)
             pflux=flux
             ptime=time
             dumtime(nstep(ifile),ifile)=time
             dumdat(nstep(ifile),ifile)=flux
             ftotdat(ifile)=fluxtot

             write(22,*)time,flux

           endif
         enddo

         write(22,*)
         write(22,*)'Total flux =     ',fluxtot


        write(*,*)line2
         write(*,*)
         write(*,*)'Number of recorded time steps = ',nstep(ifile)-1
        write(*,*)'Last time step =  ',istep,time,flux
         write(*,*)'Total flux =     ',fluxtot
        if(normflag.eq.1)then
           write(*,*)'Integral Normalized to 1.0'
         endif

        close(10)

      enddo

c     establish time array
c     initialize array
      do j=1,nfiles
         do i=1,maxnstime
           fdat(i,j)=-1
         enddo
       enddo
```

```
c     insert first data array into final array
      do i=1,nstep(1)
         stime(i)=dumtime(i,1)
         fdat(i,1)=dumdat(i,1)
       enddo
      is1=nstep(1)

c     insert remaining arrays
       do j=2,nfiles
         i2=1
         do i1=1,nstep(j)
           do while(i2.le.is1 .and. dumtime(i1,j).gt.stime(i2))
            i2=i2+1
           enddo
           if(dumtime(i1,j).eq.stime(i2))then
             fdat(i2,j)=dumdat(i1,j)
           elseif(i2.gt.1)then
c            insert new time into array and shift array down
            if (i2.le.is1)then
               is1=is1+1
               if(is1.gt.maxnstime)then
                 write(*,*)'Too many time steps - aborting!'
                 stop
               endif
               do i=is1,i2+1,-1
                 stime(i)=stime(i-1)
                 do j1=1,j-1
                   fdat(i,j1)=fdat(i-1,j1)
                 enddo
               enddo
               stime(i2)=dumtime(i1,j)
               do j1=1,nfiles
                 fdat(i2,j1)=-1.
               enddo
               fdat(i2,j)=dumdat(i1,j)
             endif
           endif
         enddo
       enddo


c     interpolate data
      do i=1,is1
         do j=1,nfiles
           if(fdat(i,j).lt.0.)then
             i2=nstep(j)
             if(stime(i).le.dumtime(1,j))then
               fdat(i,j)=((stime(i)-dumtime(1,j))/(dumtime(2,j)-
     &           dumtime(1,j)))*(dumdat(2,j)-dumdat(1,j))+dumdat(1,j)
            else if(stime(i).ge.dumtime(i2,j))then
               fdat(i,j)=((stime(i)-dumtime(i2,j))/(dumtime(i2,j)-
     &           dumtime(i2-1,j)))*(dumdat(i2,j)-dumdat(i2-1,j))+
     &           dumdat(i2,j)
             else
c              find first time greater than stime(i)
               i2=1
               do while(i2.lt.nstep(j) .and. dumtime(i2,j).le.stime(i))
                 i2=i2+1
               enddo
c              interpolate
               fdat(i,j)=((stime(i)-dumtime(i2-1,j))/(dumtime(i2,j)-
     &           dumtime(i2-1,j)))*(dumdat(i2,j)-dumdat(i2-1,j))+
     &           dumdat(i2-1,j)
```

```
            endif
            fdat(i,j)=max(fdat(i,j),0.0)
          endif
        enddo
      enddo

c     normalize data to integral of 1.0
      if(normflag.eq.1)then
        do i=1,is1
          do j=1,nfiles
            if(ftotdat(j).gt.0.0)then
              fdat(i,j)=fdat(i,j)/ftotdat(j)
            endif
          enddo
        enddo
      endif

c     add delay to time so that decay calculations will be correct
      do i=1,is1
       write(20,'(1p,e10.4,8(e12.4))')stime(i)+delay,
     &    (fdat(i,j),j=1,maxnkd)
       enddo

       write(20,'("Total     ",1p,8(e12.4))')(ftotdat(j),j=1,maxnkd)

       end
```

APPENDIX F. PEER REVIEW

Practice 134 290 1112
Publication Date 22Nov99
Attachment 02 - Sheet 1 of 1

FLUOR DANIEL NORTHWEST

TECHNICAL PEER REVIEWS

CHECKLIST FOR TECHNICAL PEER REVIEW

Document Reviewed:
Title: RPP-7463 Rev 0 Calcs for the ILAW PA-2001
Author: Fastrock, Freeman, Khakeel, Puigh
Date: 1-5-2001
Scope of Review: INTEG + Bathtub dose calcs

Yes	No*	NA	
[X]	[ ]	[ ]**	Previous reviews complete and cover analysis, up to scope of this review, with no gaps.
[X]	[ ]	[ ]	Problem completely defined.
[X]	[ ]	[ ]	Accident scenarios developed in a clear and logical manner.
[X]	[ ]	[ ]	Necessary assumptions explicitly stated and supported.
[X]	[ ]	[ ]	Computer codes and data files documented.
[X]	[ ]	[ ]	Data used in calculations explicitly stated in document.
[X]	[ ]	[ ]	Data checked for consistency with original source information as applicable.
[X]	[ ]	[ ]	Mathematical derivations checked including dimensional consistency of results.
[X]	[ ]	[ ]	Models appropriate and used within range of validity or use outside range of established validity justified.
[X]	[ ]	[ ]	Hand calculations checked for errors. Spreadsheet results should be treated exactly the same as hand calculations.
[X]	[ ]	[ ]	Software input correct and consistent with document reviewed.
[X]	[ ]	[ ]	Software output consistent with input and with results reported in document reviewed.
[X]	[ ]	[ ]	Limits/criteria/guidelines applied to analysis results are appropriate and referenced. Limits/criteria/guidelines checked against references.
[X]	[ ]	[ ]	Safety margins consistent with good engineering practices.
[X]	[ ]	[ ]	Conclusions consistent with analytical results and applicable limits.
[X]	[ ]	[ ]	Results and conclusions address all points required in the problem statement.
[X]	[ ]	[ ]	Format consistent with applicable guides or other standards.
[ ]		[X]**	Review calculations, comments, and/or notes are attached.
[X]	[ ]	[ ]	Document approved (i.e., the reviewer affirms the technical accuracy of the document).

Paul Rittmann Paul Rittmann — Jan 5, 2001
Reviewer: (Printed and Signed) — Date

* All "NO" responses must be explained below or on an additional page.

** Any calculations, comments, or notes generated as part of this review should be signed, dated and attached to this checklist. Such material should be labeled and recorded in such a manner as to be intelligible to a technically qualified third party.

NUCLEAR ENGINEERING

Practice 134 290 1112
Publication Date 22Nov99
Attachment 02 - Sheet 1 of 1

FLUOR DANIEL NORTHWEST

TECHNICAL PEER REVIEWS

CHECKLIST FOR TECHNICAL PEER REVIEW

Document Reviewed: Title: "Near Field, Far Field, & Estimated Impact Calculations for the Hanford Immobilized Low-Activity Waste Performance Assessment: 2001 Version"
Author: S. H. Finfrock, et al.
Date:
Scope of Review: "I/O" Data Files for VAM3DF calculations in Near Field & Far Field Regions. Details for Base Case & Differences for other cases Verified against expectations for model geometries, boundary conditions, & convergence.

Yes	No*	NA	
[ ]	[ ]	[X]**	Previous reviews complete and cover analysis, up to scope of this review, with no gaps.
[X]	[ ]	[ ]	Problem completely defined.
[ ]	[ ]	[X]	Accident scenarios developed in a clear and logical manner.
[ ]	[ ]	[X]	Necessary assumptions explicitly stated and supported.
[ ]	[ ]	[X]	Computer codes and data files documented.
[X]	[ ]	[ ]	Data used in calculations explicitly stated in document.
[X]	[ ]	[ ]	Data checked for consistency with original source information as applicable.
[ ]	[ ]	[X]	Mathematical derivations checked including dimensional consistency of results.
[ ]	[ ]	[X]	Models appropriate and used within range of validity or use outside range of established validity justified.
[ ]	[ ]	[X]	Hand calculations checked for errors. Spreadsheet results should be treated exactly the same as hand calculations.
[X]	[ ]	[ ]	Software input correct and consistent with document reviewed.
[X]	[ ]	[ ]	Software output consistent with input and with results reported in document reviewed.
[ ]	[ ]	[X]	Limits/criteria/guidelines applied to analysis results are appropriate and referenced. Limits/criteria/guidelines checked against references.
[ ]	[ ]	[X]	Safety margins consistent with good engineering practices.
[ ]	[ ]	[X]	Conclusions consistent with analytical results and applicable limits.
[ ]	[ ]	[X]	Results and conclusions address all points required in the problem statement.
[ ]	[ ]	[X]	Format consistent with applicable guides or other standards.
[ ]		[X]**	Review calculations, comments, and/or notes are attached.
[X]	[ ]	[ ]	Document approved (i.e., the reviewer affirms the technical accuracy of the document).

Edward R. Siciliano / ERSiciliano
Reviewer: (Printed and Signed) Date 01/04/01

* All "NO" responses must be explained below or on an additional page.

** Any calculations, comments, or notes generated as part of this review should be signed, dated and attached to this checklist. Such material should be labeled and recorded in such a manner as to be intelligible to a technically qualified third party.

~~NUCLEAR ENGINEERING~~

Practice 134 290 1112
Publication Date 22Nov99
Attachment 02 - Sheet 1 of 1

FLUOR DANIEL NORTHWEST

TECHNICAL PEER REVIEWS

CHECKLIST FOR TECHNICAL PEER REVIEW

Document Reviewed:
Title: Near Field, Far Field, & Estimated Impact Calculations for the Hanford Immobilized Low-Activity Waste Performance Assessment: 2001 Version
Author: S.H. Finfrock, et al.
Date:
Scope of Review: "Bath Tub" Effect: Release Model Output Data & Subsequent Impact from Instantaneous Vadose Zone Travel.

Yes	No*	NA	
[ ]	[ ]	[X]**	Previous reviews complete and cover analysis, up to scope of this review, with no gaps.
[X]	[ ]	[ ]	Problem completely defined.
[X]	[ ]	[ ]	Accident scenarios developed in a clear and logical manner.
[X]	[ ]	[ ]	Necessary assumptions explicitly stated and supported.
[ ]		[X]	Computer codes and data files documented.
[X]	[ ]	[ ]	Data used in calculations explicitly stated in document.
[X]	[ ]	[ ]	Data checked for consistency with original source information as applicable.
[X]	[ ]	[ ]	Mathematical derivations checked including dimensional consistency of results.
[ ]	[ ]	[X]	Models appropriate and used within range of validity or use outside range of established validity justified.
[X]	[ ]	[ ]	Hand calculations checked for errors. Spreadsheet results should be treated exactly the same as hand calculations.
[ ]	[ ]	[X]	Software input correct and consistent with document reviewed.
[ ]	[ ]	[X]	Software output consistent with input and with results reported in document reviewed.
[ ]	[ ]	[X]	Limits/criteria/guidelines applied to analysis results are appropriate and referenced. Limits/criteria/guidelines checked against references.
[ ]	[ ]	[X]	Safety margins consistent with good engineering practices.
[X]	[ ]	[ ]	Conclusions consistent with analytical results and applicable limits.
[X]	[ ]	[ ]	Results and conclusions address all points required in the problem statement.
[ ]	[ ]	[X]	Format consistent with applicable guides or other standards.
[ ]		[X]**	Review calculations, comments, and/or notes are attached.
[X]	[ ]	[ ]	Document approved (i.e., the reviewer affirms the technical accuracy of the document).

Edward R. Siciliano E.R. Siciliano
Reviewer: (Printed and Signed)

Date 01/04/01

* All "NO" responses must be explained below or on an additional page.

** Any calculations, comments, or notes generated as part of this review should be signed, dated and attached to this checklist. Such material should be labeled and recorded in such a manner as to be intelligible to a technically qualified third party.

~~NUCLEAR ENGINEERING~~

APPENDIX B

APPENDIX B

Waste Form Release Calculations for the 2001 Immobilized Low-Activity Waste Performance Assessment

D. H. Bacon
B. P. McGrail

February 2001

Prepared for the U.S. Department of Energy
under Contract DE-AC06-76RL01830

DISCLAIMER

This report was prepared as an account of work sponsored by an agency of the United States Government. Neither the United States Government nor any agency thereof, nor Battelle Memorial Institute, nor any of their employees, makes **any warranty, express or implied, or assumes any legal liability or responsibility for the accuracy, completeness, or usefulness of any information, apparatus, product, or process disclosed, or represents that its use would not infringe privately owned rights**. Reference herein to any specific commercial product, process, or service by trade name, trademark, manufacturer, or otherwise does not necessarily constitute or imply its endorsement, recommendation, or favoring by the United States Government or any agency thereof, or Battelle Memorial Institute. The views and opinions of authors expressed herein do not necessarily state or reflect those of the United States Government or any agency thereof.

PACIFIC NORTHWEST NATIONAL LABORATORY
operated by
BATTELLE
for the
UNITED STATES DEPARTMENT OF ENERGY
under Contract DE-AC06-76RL01830

Printed in the United States of America

Available to DOE and DOE contractors from the
Office of Scientific and Technical Information,
P.O. Box 62, Oak Ridge, TN 37831-0062;
ph: (865) 576-8401
fax: (865) 576-5728
email: reports@adonis.osti.gov

Available to the public from the National Technical Information Service,
U.S. Department of Commerce, 5285 Port Royal Rd., Springfield, VA 22161
ph: (800) 553-6847
fax: (703) 605-6900
email: orders@ntis.fedworld.gov
online ordering: http://www.ntis.gov/ordering.htm

This document was printed on recycled paper.
(2/01)

PNNL-13369

Waste Form Release Calculations for the 2001 Immobilized Low-Activity Waste Performance Assessment

D. H. Bacon
B. P. McGrail

February 2001

Prepared for
the U.S. Department of Energy
under Contract DE-AC06-76RL01830

Pacific Northwest National Laboratory
Richland, Washington 99352

Summary

A set of reactive chemical transport calculations was conducted with the Subsurface Transport Over Reactive Multiphases (STORM) code to evaluate the long-term performance of a representative low-activity waste glass in a shallow subsurface disposal system located on the Hanford Site. One-dimensional simulations were conducted out to times in excess of 20,000 yr. A two-dimensional simulation was run to 2,000 yr. The maximum normalized Tc release rate from a trench-type conceptual design under a constant recharge rate of 4.2 mm/yr is 0.93 ppm/yr. Factors that were found to significantly impact the predicted release rate were water recharge rate, chemical affinity control of glass dissolution rate, diffusion coefficient, and disposal system design (trench versus a concrete-lined vault). In contrast, corrosion of the steel pour canister surrounding the glass waste and incorporation of a chemical conditioning layer of silica sand at the top of the trench had little impact on Tc release rate. However, because of large inventory of Cr associated with the 304L steel containers and assumed short release time (1000 yr) relative to the glass, a four orders of magnitude higher release rate of Cr(VI) was predicted relative to the ILAW glass alone.

Contents

Summary B-4

Introduction B-11

Approach and Rationale B-11

Computer Model Selection B-12

Methods B-13

Model Setup and Parameterization B-13

Unsaturated Flow and Transport Input B-13

Lithographic Units B-13

Computational Grid B-15

Material Hydraulic Properties B-15

Hydraulic Initial Conditions B-15

Hydraulic Boundary Conditions B-16

Solute Transport Coefficients B-17

Chemistry Input B-17

Aqueous Species B-17

Gas Species B-18

Solid Species B-19

Equilibrium Reactions B-19

Kinetic Reactions B-21

Initial and Boundary Conditions B-24

Model Output B-26

Results B-29

Base Case B-29

Other Radionuclide Release Rates B-33

Recharge Rates B-34

Glass Dissolution Model B-34

Surrounding Materials B-35

Preconditioning Layer B-35

Effect of Steel Container B-37

Aqueous Diffusion Coefficient B-39

Two-Dimensional Simulation B-40

Vault Scenario B-44

Extend Base Case to Water Table B-44

Bathtub Effect B-46

Higher Waste Loading and Alternate Glass Formulation B-46

Conclusion B-53

References B-55

Figures

1 Lithographic Units for Remote-Handled (RH) Trench Waste Form Release Simulations.....B-14

2 Lithographic Units for New ILAW Vault Waste Form Release Simulations B-14

3 Tc Flux to the Vadose Zone, Corrected for Radioactive Decay, Normalized to the Amount of Tc Originally in LAWABP1 Waste Glass, for Base Case Trench Simulation B-30

4 TcO_4^- Concentrations for RH Trench Simulation with Recharge Rate of 4.2 mm/yr (Horizontal Dotted Lines Represent Boundaries Between Material Zones and Material Names Are Shown Along Right Axis).....B-31

5 Glass Dissolution Rate for LAWABP1 in RH Trench Simulation with Recharge Rate of 4.2 mm/yr (horizontal dotted lines represent boundaries between material zones and material names are shown along right axis).....B-31

6 Solution pH for RH Trench Simulation with Recharge Rate of 4.2 mm/yr (horizontal dotted lines represent boundaries between material zonesand material names are shown along right axis) B-32

7 SiO_2(aq) Concentrations for RH Trench Simulation with Recharge Rate of 4.2 mm/yr (horizontal dotted lines represent boundaries between material zones and material names are shown along right axis) B-32

8 Secondary Mineral Relative Volumes at 20,000 yr for RH Trench Simulation with Recharge Rate of 4.2 mm/yr (horizontal dotted lines represent boundaries between material zones and material names are shown along right axis).....B-33

9 Comparison of Pu and Tc Flux to the Vadose Zone for Base Case Trench Simulation B-34

10 Flux of ^{99}Tc to the Vadose Zone, Relative to the Amount of Tc Originally in LAWABP1 Waste Glass, for Recharge Rates Ranging from 0.1 to 50 mm/yr.....B-35

11 Water Content vs. Depth for Selected Recharge Rates for the RH Trench B-36

12 Tc Flux to the Vadose Zone, Relative to the Amount of Tc Originally in LAWABP1 Waste Glass, for Different Glass Dissolution Models B-36

13 Tc Flux to the Vadose Zone, Relative to the Amount of Tc Originally in LAWABP1 Waste Glass, Assuming Different Surrounding Materials B-37

14 Tc Flux to the Vadose Zone, Relative to the Amount of Tc Originally in LAWABP1 Waste Glass, Including Stainless Steel Waste Packages.....B-38

15 Tc Flux to the Vadose Zone, Relative to the Amount of Tc Originally in LAWABP1 Waste Glass, Including Stainless Steel Waste Packages.....B-39

16 Tc Flux to the Vadose Zone, Relative to the Amount of Tc Originally in LAWABP1 Waste Glass, Assuming Different Aqueous Diffusion Coefficients B-40

17 Tc Flux to the Vadose Zone, Relative to the Amount of Tc Originally in LAWABP1 Waste Glass, Comparing 1-D and 2-D Simulations B-41

18 Volumetric Water Content for 2-D Trench Simulation B-41

19 Total Aqueous Tc Concentration (μmol/kg) for 2-D Trench Simulation at 2,000 yr B-42

20 Glass Dissolution Rate (mol s^{-1}) for LAWABP1 in 2-D Trench Simulation at 2,000 yr B-42

21 Solution pH for 2-D Trench Simulation B-43

22 SiO_2(aq) Concentrations (mol/kg) for 2-D Trench Simulation B-43

23 Tc Flux to the Vadose Zone, Relative to the Amount of Tc Originally in LAWABP1 Waste Glass, Comparison of Vault Simulations at Different Recharge Rates to Trench Base Case B-44

24 Water Contents for Selected Recharge Rates for Vault Simulations B-45

25 Effect of Concrete on pH for Vault Simulations B-46

26 Solution pH Profile for RH Trench Simulation Extended to Water Table (See Figure 7 for location of boundaries between material zones and material names) B-47

27 Concentration Profile of TcO_4^- for RH Trench Simulation Extended to Water Table (See Figure 4 for location of boundaries between material zones and material names) B-48

28 TcO_4^- for Fully-Saturated RH Trench Simulation with no Flow ("bathtub effect") B-49

29 Total Water Mass per Node (each node has a volume of 0.05 m^3) for Fully-Saturated RH Trench Simulation with no Flow ("bathtub effect") B-50

30 VHT Corrosion Rate as a Function of Waste Loading (Vienna et al. 2000) B-51

31 Dependence of HLP-31 Glass Dissolution Rate on Concentration of SiO_2(aq) B-51

32 Tc Flux to the Vadose Zone, Relative to the Amount of Tc Originally in LAWABP1 Waste Glass, Comparison of Trench Base Case Simulation with LAWABP1 Glass Replaced by HLP-31 Waste Glass B-52

Tables

1 Relative Volume of Solid Species in Material Zones B-14

2 Particle Radius (m) of Solid Species in Material Zones B-15

3 Material Hydraulic Properties Used In Simulations B-16

4 Key Aqueous Species Produced by the Dissolution of Calcite and LAWABP1 Glass Containing Trace Amounts of I, Tc, Se, U, and Pu in Deionized Water B-18

5 Composition (Mole Fraction) of ILAW Glasses Used in Simulations B-20

6 Composition of Native and Other Surrounding Materials Used in Simulations B-20

7 Composition of Secondary Minerals Used in Simulations B-21

8 Equilibrium Reactions From Dissolution of LAWABP1 Glass at 15°C B-21

9 Summary of Kinetic Rate Parameters Used for Glasses B-24

10 Secondary Phase Reaction Network for LAWABP1 Glass B-25

11 Initial Aqueous Concentrations Used in Simulations B-26

12 List of Waste Form Sensitivity Cases B-29

13 Summary of Waste Form Sensitivity Calculations B-54

This page intentionally left blank.

Introduction

The Hanford Site in southeastern Washington State has been used extensively to produce nuclear materials for the U.S. strategic defense arsenal by the U.S. Department of Energy (DOE). A large inventory of radioactive and mixed waste has accumulated in 177 buried single- and double-shell tanks. Liquid waste recovered from the tanks will be pretreated to separate the low-activity fraction from the high-level and transuranic wastes. The low-activity waste (LAW) will be immobilized in glass and placed in a near-surface disposal system on the Hanford Site. Vitrifying the LAW will generate over 160,000 m^3 of glass. The immobilized low-activity waste (ILAW) at Hanford is among the largest volumes of waste within the DOE complex and is one of the largest inventories of long-lived radionuclides planned for disposal in a low-level waste facility (approximately 2.4 million curies total activity). Before the ILAW can be disposed, DOE must approve a performance assessment (PA), which is a document that describes the long-term impacts of the disposal facility on public health and environmental resources. A sound scientific basis for determining the long-term release rates of radionuclides from LAW glasses must be developed if the PA is to be accepted by regulatory agencies, stakeholders, Native Americans, and the public.

Approach and Rationale

The 1998 version of the ILAW PA (Mann et al. 1998) showed that one of the key variables in the analysis is the waste form release rate, which must be calculated over thousands of years. To conduct this calculation, we used a methodology where the waste form release rate is evaluated by modeling the basic physical and chemical processes that are known to control dissolution behavior instead of using empirical extrapolations from laboratory “leaching” experiments commonly used in other performance assessments. We adopted this methodology for the following reasons:

- The dissolution rate, and hence radionuclide release rate from silicate glasses is not a static variable, i.e., a constant that can be derived independent of other variables in the system. Glass dissolution rate is a function of three variables (neglecting glass composition itself): temperature, pH, and composition of the fluid contacting the glass (McGrail et al. 2001). The temperature of the ILAW disposal system is a known constant. However, both pH and composition of the fluid contacting the glass are variables that are affected by flow rate, reactions with other engineered materials, gas-water equilibria, secondary phase precipitation, alkali ion exchange, and by dissolution of the glass itself (a classic feedback mechanism). Consequently, glass dissolution rates will vary both in time and as a function of position in the disposal system. There is no physical constant such as a “leach rate” or radionuclide release rate parameter that can be assigned to a glass waste form in such a dynamic system.

- One of the principal purposes of the ILAW PA is to provide feedback to engineers regarding the impacts of design options on disposal system performance. A model based on empirical release behavior of the waste form could not provide this information. For example, we have found little effect on waste form performance regardless of whether stainless or cast steel is used for the waste form pour canister. However, significant impacts have been observed when large amounts of concrete are used in constructing vaults for ILAW. The concrete raises the pH of the pore water entering the waste packages and so increases glass corrosion.

Unfortunately, the robust methodology we used does not come without additional requirements. First, detailed information is needed regarding the reaction mechanisms controlling the dissolution behavior of the waste form. Significantly more laboratory experiments are required to obtain the rate law parameters needed for the models used for our simulations. Second, the model now being used (described in the next section) is markedly more complex because of its ability to simulate reactive transport coupled with heterogeneous, unsaturated flow. Execution times with today's fastest workstations can take weeks for one-dimensional (1-D) and two-dimensional (2-D) simulations, and three-dimensional (3-D) simulations can be attempted only on today's most sophisticated massively parallel computers. Still, we believe the benefits, particularly with regards to the technical defensibility of the methodology and results, far outweigh the penalties.

Computer Model Selection

The code selection criteria and selection process used is documented in *Selection of a Computer Code for Hanford Low-Level Waste Engineered-System Performance Assessment* (McGrail and Bacon 1998). The needed capabilities were identified from an analysis of the important physical and chemical processes expected to affect LAW glass corrosion and the mobility of radionuclides. The available computer codes with suitable capabilities were ranked in terms of the feature sets implemented in the code that match a set of physical, chemical, numerical, and functional capabilities needed to assess release rates from the engineered system. The highest ranked computer code was found to be the STORM code developed at Pacific Northwest National Laboratory (PNNL) for DOE for evaluation of arid land disposal sites. The verification studies for STORM are documented in *Subsurface Transport Over Reactive Multiphases (STORM): A General, Coupled Nonisothermal Multiphase Flow, Reactive Transport, and Porous Medium Alteration Simulator, Version 2, User's Guide* (Bacon et al. 2000).

Methods

Model Setup and Parameterization

This section details the data used in the STORM code input data file (Bacon et al. 2000). Input data to STORM can be conveniently divided into two parts: 1) unsaturated flow and transport, and 2) chemistry. Entries for unsaturated flow and transport include: 1) lithographic units, 2) hydraulic properties, 3) hydraulic initial conditions, and 3) hydraulic boundary conditions. These data were principally defined from facility design documents (Puigh 1999), the near-field hydraulic properties data package (Meyer and Serne 1999), or the far-field hydraulic properties data package (Khaleel 1999). STORM was used to compute the flow-field in the near-field region based upon hydraulic properties for the materials, and specified initial and boundary conditions. Chemistry input to STORM consists of entries for 1) aqueous species, 2) gas species, 3) solid species, 4) equilibrium reactions, 5) kinetic reactions, and 6) geochemical initial and boundary conditions. Each of these inputs is described below.

Unsaturated Flow and Transport Input

Lithographic Units

To establish a consistent framework for overlaying a computational grid on the spatial domain of interest, a set of material zones or lithographic units are established with similar hydrogeological and geochemical properties. These zones are usually related to disposal design components, geologic formations, or geologic facies determined from borehole analyses. However, because there are practical limits to the resolution of the model grid, material zones may also include combinations of materials that are assigned uniform hydraulic and/or chemical properties. Classification of these materials into appropriate zones was performed as a part of the near-field hydraulics data package (Meyer and Serne 1999).

The remote-handled (RH) trench simulations encompass a 1-D vertical profile near the center of a single trench (Figure 1). It is assumed that the material representing the waste packages is 85% glass and 15% filler by volume. For the new ILAW vault simulations, waste packages with 85% glass and 15% filler by volume (Figure 2) were also assumed. The principal differences between the cases involve the incorporation of degraded concrete layers at the top and bottom of the ILAW vault and thinner layers of filler between waste package layers.

For each lithographic unit, a list of the solid species that comprise the unit is required. For each solid, the following data is needed:

- Relative volume
- Particle radius

Figure 1. Lithographic Units for Remote-Handled (RH) Trench Waste Form Release Simulations

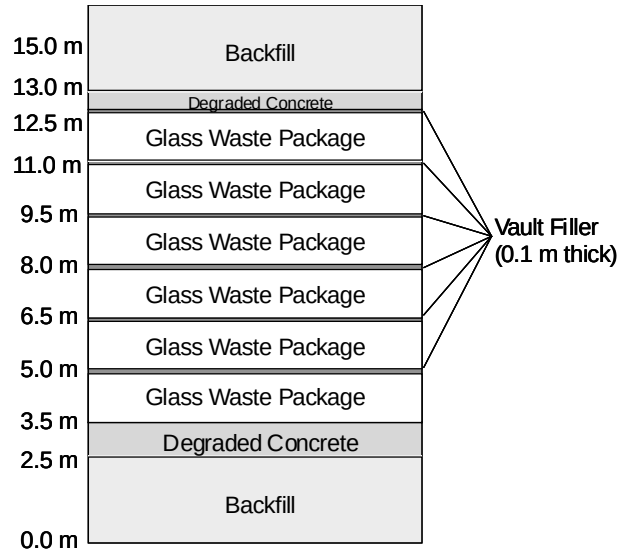

Figure 2. Lithographic Units for New ILAW Vault Waste Form Release Simulations

Values for these variables for each lithographic unit are listed in Table 1 and Table 2. The waste package is assumed to consist of 304L stainless steel container filled with LAWABP1 waste glass. For Hanford sands, backfill soil, petrologic, and particle size data was obtained from the near-field hydrology data package (Meyer and Serne 1999). For the vault simulations, the filler material between waste packages is assumed to be quartz sand. The vault concrete is assumed to consist of back-filled soil mixed with 15% Portland cement. Other materials in the simulations include vault concrete, backfill, Hanford Sand, vault filler, and additional solid phases. For the RH trench simulations, the backfill material is assumed to consist of 40% albite, 40% quartz, 10% K-feldspar, and 10% illite (Mann et al. 1998). Degraded vault concrete is assumed to consist of backfill with 15% Portlandite added. The vault filler and Hanford Sand were assumed to have the same mineral composition as the backfill material.

Table 1. Relative Volume of Solid Species in Material Zones

	ILAW Glass	304L ss	Quartz	Albite	K-Feldspar	Illite	Portlandite
Waste Package	0.99	0.01	0	0	0	0	0
Filler	0	0	1	0	0	0	0
Vault Concrete	0	0	0.34	0.34	0.085	0.085	0.15
Back-filled Soil	0	0	0.4	0.4	0.100	0.100	0
Hanford Sands	0	0	0.4	0.4	0.100	0.100	0

The assumed particle radius values for Hanford sediments and backfill soil are consistent with petrologic and particle size data obtained from laboratory-measured values (Kaplan and Serne 1999). The particle size of the filler material between waste packages is assumed to be the same as that for the backfill soil. For the Portland cement, we have simply assumed that the material is heavily degraded into

Table 2. Particle Radius (m) of Solid Species in Material Zones

	ILAW Glass	304L ss	Quartz	Albite	K-Feldspar	Illite	Portlandite
Waste Package	5.00E-02	5.00E-02		0	0	0	0
Filler	0	0	1.00E-0	0	0	0	0
Vault Concrete	0	0	1.00E-0	1.00E-04	1.00E-04	5.00E-0	1.00E-04
Back-filled Soil	0	0	1.00E-0	1.00E-04	1.00E-04	5.00E-0	0
Hanford Sands	0	0	1.00E-0	1.00E-04	1.00E-04	5.00E-0	0

rubble (Krupka and Serne 1998) with consistency similar to surrounding soil. Comparatively, the glass is assumed to have an average 500 times larger radius. This is consistent with the expected sparse degree of glass fracturing in the waste package based on prior experience with high-level waste glasses (Farnsworth et al. 1985; Peters and Slate 1981). Fracturing is expected to increase the glass surface area a maximum of 10X over its geometric surface area.

Computational Grid

The computational grid was set at 5 cm in vertical resolution; this is slightly larger than the 3.66 cm grid spacing used in the 1998 ILAW PA. The time step used in the calculations was calculated automatically by the code given a convergence criterion of $1x10^{-6}$. This ensures that predicted values of aqueous species concentrations and mineral volumes are accurate between iterations for a given time step. If this cannot be achieved within a certain number of iterations, the time step is automatically reduced. Numerous simulations were conducted to ensure that the grid spacing and convergence criteria chosen for the simulations were small enough to ensure accuracy, yet large enough to allow the simulations to finish in a reasonable amount of time. For comparison, the base case remote-handled trench simulation was rerun with a grid spacing of 2.5 cm, and with a convergence criterion of $5x10^{-7}$. Results from these simulations were not significantly different from the results reported herein.

Material Hydraulic Properties

The hydraulic properties for each lithographic unit in the simulation were defined as a part of the near-field hydraulics data package (Meyer and Serne 1999), or the far-field hydraulic properties data package (Khaleel 1999) but are provide in Table 3 for convenience.

Hydraulic Initial Conditions

Initial hydraulic conditions for each lithographic unit include the following parameters:

- Water content
- Water flux
- Dissolved gas content of aqueous phase
- Gas pressure

- Relative humidity of gas phase
- Temperature

Table 3. Material Hydraulic Properties Used In Simulations

Material	Particle Density (g/cm^3)	Bulk Density (g/cm^3)	Saturated Water Content	Residual Water Content	van Genuchten α (cm^{-1})	van Genuchten *n*	Saturated Hydraulic Conductivity (cm/s)
Vault Concrete	2.63	2.46	0.067	0.00	3.87×10-5	1.29	1.33×10^{-9}
Vault Filler	2.63	1.59	0.397	0.005	0.106	4.26	3.79×10^{-2}
Glass Waste	2.68	2.63	0.020	0.00	0.200	3.00	0.01
Backfill	2.76	1.89	0.316	0.049	0.035	1.72	1.91×10^{-3}
Conditioning Layer	2.63	1.59	0.397	0.005	0.106	4.26	3.79×10^{-2}
Degraded Concrete	2.76	1.89	0.313	0.00	2.43	1.41	1.34×10^{-3}
Hanford Sand	2.74	1.71	0.375	0.041	0.055	1.77	2.88×10^{-3}

The initial conditions were calculated by assuming a steady state water flux at the upper boundary, which results in a steady state water content distribution consistent with the hydraulic properties defined for each material. A wide spectrum of water flux rates, ranging from 0.1 mm/y to 50 mm/y were used for different sensitivity cases. A constant subsurface temperature, equal to the average ambient temperature of 15°C was assumed. The dissolved gas content of the aqueous phase was assumed to be negligible with respect to flow. The relative humidity of the gas phase was assumed to be 100%.

Hydraulic Boundary Conditions

The following data is needed as a function of time and space along each boundary:

- Water flux
- Dissolved gas content of aqueous phase
- Gas pressure
- Relative humidity of gas phase
- Temperature

The upper boundary is located just beneath the engineered barrier system (EBS) and was assigned a specified flux. A wide spectrum of water flux rates, ranging from 0.1 mm/y to 50 mm/y were used for different sensitivity cases. The ambient recharge rates, 0.9 or 4.2 mm/y, were determined as a part of the recharge data package (Fayer et al. 1999). The lowest recharge rate of 0.1 mm/y represents a perfectly working EBS. The highest recharge rate (50 mm/y) represents the highest probable flux running off the edge of the EBS.

The location of the lower boundary was selected so that vertical gradients are small. For the trench simulations, the lower boundary is a free drainage boundary 4.5 m below the lowest layer of backfill. For the vault simulations, the lower boundary is a free drainage boundary 2.5 m below the lowest layer of concrete. For hydraulic boundary conditions at this lower boundary, free drainage under gravity will be assumed. For two-dimensional simulations, the side boundaries are placed at axes of symmetry so that they can be assumed to be no-flow boundaries.

A constant subsurface temperature, equal to the average ambient temperature of 15°C was assumed. The dissolved gas content of the aqueous phase was assumed to be negligible with respect to flow. The relative humidity of the gas phase was assumed to be 100%.

Solute Transport Coefficients

For each gaseous and aqueous species, the following data is needed:

- Aqueous diffusion coefficient ($m^2\ s^{-1}$)
- Gas diffusion coefficient ($m^2\ s^{-1}$) or an assumption that the gas partial pressure is fixed

The aqueous diffusion coefficients were assumed to be $5x10^{-9}$ m^2/s for all aqueous species (Mann et al. 1998). The gas partial pressure for CO_2 and O_2 were fixed at atmospheric values of $3x10^{-4}$ and $2.1x10^{-1}$ atm, respectively.

Chemistry Input

Aqueous Species

Aqueous species are the cations, anions, or neutral complexes present in the aqueous phase. For each aqueous species, the following data is needed:

- Molecular Weight
- Charge
- Hard core diameter
- Number of elements in aqueous species
- Stoichiometric coefficient of each element

The aqueous species listed in Table 4 were identified by simulating the dissolution of LAWABP1 glass (along with a trace amount of calcite) in deionized water at 15°C with the EQ3/6 code package (Wolery and Daveler 1992). All data were obtained from the EQ3/6 data0.com.R8 database (Daveler and Wolery 1992). These simulations were not intended to be representative of disposal system conditions. The intent was only to make use of the EQ3/6 software to extract a subset of aqueous (and solid) species from the large thermodynamic database that were relevant for ILAW simulations. Since LAWABP1 glass contains all of the elements that are currently expected to be part of the final ILAW

Table 4. Key Aqueous Species Produced by the Dissolution of Calcite and LAWABP1 Glass Containing Trace Amounts of I, Tc, Se, U, and Pu in Deionized Water

Species	Mol.Wt.	Hard Core Diameter
AlO_2^-	58.98	4.0
$B(OH)_3(aq)$	61.83	3.0
Ca^{2+}	40.08	6.0
$CO_2(aq)$	44.01	3.0
CO_3^{2-}	60.01	5.0
CrO_4^{2-}	115.99	4.0
$Fe(OH)_3(aq)$	106.87	3.0
H_2O	18.01	-4.0
H^+	1.01	9.0
HCO_3^-	61.02	4.0
$HCrO_4^-$	117.00	4.0
$HSiO_3^-$	77.09	4.0
IO_3^-	126.90	3.0
K^+	39.10	3.0
La^{3+}	138.91	9.0
Mg^{2+}	24.31	8.0
Na^+	22.99	4.0
Ni++	58.69	4.5
$O_2(aq)$	32.00	3.0
OH^-	17.01	3.0
$PuO_2(CO_3)_3^{4-}$	456.03	4.0
SeO_4^{2-}	142.96	4.0
$SiO_2(aq)$	60.08	3.0
TcO_4^-	162.00	4.0
$Ti(OH)_4(aq)$	115.91	3.0
$UO_2(CO_3)_2^{2-}$	390.05	4.0
$UO_2(CO_3)_3^{4-}$	450.06	4.0
$UO_2(OH)_2(aq)$	304.04	3.0
Zn^{2+}	65.39	6.0
$Zr(OH)_4(aq)$	159.25	3.0

product to be produced by the private contractor, and adding calcite caused the software to load Ca species that might be important in a disposal system with a concrete vault, the list of aqueous species given in Table 4 is expected to be reasonably complete. However, for conducting actual disposal system simulations, a number of these species were excluded from the simulations because their concentration will be extremely small over the range of chemical conditions anticipated for the ILAW disposal system.

Gas Species

Gas species are compounds such as CO_2 and O_2 that make up the air phase in STORM simulations. For each gas species, the following data is needed:

- Molecular Weight
- Number of elements in gaseous species
- Stoichiometric coefficient of each element

Only CO_2 and O_2 are expected to significantly influence the chemical environment in the near and far field.

Solid Species

For each solid species, the following data is needed:

- Mass Density (g cm^{-3})
- Stoichiometric coefficient of each element

The simulation results presented in the following sections will reference two different ILAW glass compositions, which are provided in Table 5 for reference.

The mass density of both glasses was assumed to be 2.68 g cm^{-3}. The compositions of the materials making up the backfill, filler, Hanford soil, and degraded concrete used in the simulations are listed in Table 6. The mass density is obtained by dividing the molecular weight by the molar volume of the compound.

Secondary phases are solids that precipitate from a supersaturated aqueous solution. A list of potential secondary phases that form from long-term weathering experiments with LAWABP1 glass and from modeling the solution chemistry observed in experiments with the EQ3/6 code is provided by (McGrail et al. 2001). McGrail et al. (2001), eliminated a large number of phases from consideration because: 1) formation of the phase is kinetically prohibited at the disposal system temperature of 15°C, 2) selection of the phase would violate the Gibbs phase rule, 3) simulations show that allowing the phase to form is inconsistent with a large body of laboratory test data with borosilicate glasses, or 4) the phase is unstable over the range of chemical environments expected for the ILAW disposal system. The final phase assemblage used in STORM simulations (see Table 7) was further constrained because preliminary runs showed that the phase never formed or formed in such small amounts that the effects were insignificant. The composition of the secondary minerals used in the simulations is listed in Table 7. The mass density is obtained by dividing the molecular weight by the molar volume of the solid.

Equilibrium Reactions

For each equilibrium reaction, the following data is needed:

- Stoichiometric coefficient of each aqueous species in each reaction
- Equilibrium constant at a temperature of 15°C.

Table 5. Composition (Mole Fraction) of ILAW Glasses Used in Simulations

Element	LAWABP1	HLP-31
Al	1.36×10^{-1}	5.06×10^{-2}
B	1.84×10^{-1}	2.22×10^{-1}
Ca		1.15×10^{-4}
Cl	1.13×10^{-2}	5.82×10^{-3}
Cr	1.82×10^{-4}	7.64×10^{-4}
F	1.46×10^{-3}	3.39×10^{-4}
Fe	2.16×10^{-2}	2.71×10^{-2}
I	1.54×10^{-7}	1.66×10^{-7}
K	3.23×10^{-2}	6.44×10^{-3}
La	8.48×10^{-3}	
Mg	1.71×10^{-2}	1.47×10^{-2}
Na	4.46×10^{-1}	4.79×10^{-1}
O	1.87	1.87
P	7.79×10^{-4}	5.45×10^{-4}
Pu	3.52×10^{-8}	3.78×10^{-8}
Tc	6.59×10^{-7}	7.58×10^{-7}
S	8.63×10^{-4}	6.44×10^{-4}
Se	1.77×10^{-8}	1.90×10^{-8}
Si	4.82×10^{-1}	5.58×10^{-1}
Ti	2.15×10^{-2}	1.48×10^{-2}
U	9.81×10^{-5}	1.05×10^{-4}
Zn	2.20×10^{-2}	7.29×10^{-3}
Zr	2.94×10^{-2}	4.82×10^{-3}

Table 6. Composition of Native and Other Surrounding Materials Used in Simulations

Species	Formula	Mol.Wt.	Molar Volume
Albite	$NaAlSi_3O_8$	262.2	100.4
Illite	$K_{0.6}Mg_{0.25}Al_{1.8}Al_{0.5}Si_{3.5}O_{10}(OH)_2$	383.9	500.0
K-Feldspar	$KAlSi_3O_8$	278.3	108.8
Portlandite	$Ca(OH)_2$	74.0	500.0
Quartz	SiO_2	60.0	22.6

Table 7. Composition of Secondary Minerals Used in Simulations

Species	Formula	Mol.Wt.	Molar Volume
Amorphous silica	SiO_2	60.0	29.0
Analcime	$Na_{0.96}Al_{0.96}Si_{2.04}O_6$	201.2	89.1
Anatase	TiO_2	79.8	18.8
Baddeleyite	ZrO_2	123.2	21.9
Gibbsite	$Al(OH)_3$	78.0	31.9
Goethite	FeOOH	88.8	20.8
Herschelite	$Na_{1.62}K_{0.5}Al_{2.26}Si_4O_{12.45}\cdot 6H_2O$	537.4	29.9
La(OH)3	$La(OH)_3$	189.9	54.5
Nontronite-Na	$Na_{0.33}Fe_2Al_{0.33}Si_{3.67}O_{11}\cdot H_2O$	425.2	184.8
PuO2	PuO_2	276.0	23.8
Sepiolite	$Mg_4Si_6O_{15}(OH)_2{:}6H_2O$	647.8	285.6
Soddyite	$(UO_2)2(SiO_4){:}2H_2O$	668.1	131.2
Theophrasite(1)	$Ni(OH)_2$	92.7	22.3
Weeksite	$K_2(UO_2)_2Si_6O_{15}\cdot 4H_2O$	1098.8	500.0
Zn(OH)2	$Zn(OH)_2$	99.4	500.0

(1) Used in sensitivity case with steel container. See Section entitled "Surrounding Materials, Effect of Steel Container."

The equilibrium reactions in Table 8 were identified by simulating the dissolution of LAWABP1 glass in deionized water at 15°C with the EQ3/6 code package (Wolery and Daveler 1992) and the data0.com.R8 database (Daveler and Wolery 1992; Wolery and Daveler 1992). It was possible to exclude a significant number of secondary aqueous species from the simulations because their concentration was extremely small over the range of chemical conditions anticipated for the ILAW disposal system.

Table 8. Equilibrium Reactions From Dissolution of LAWABP1 Glass at 15°C

Reaction	Log K	Source
$CO_2(aq) + H_2O \rightleftharpoons H^+ + HCO_3^-$	-6.417	(Shock et al. 1989)
$CO_3^{2-} + H^+ \rightleftharpoons HCO_3^-$	10.429	(Shock and Helgeson 1988)
$HCrO_4^- \rightleftharpoons CrO_4^{2-} + H^+$	-6.491	(Shock and Helgeson 1988)
$HSiO_3^- + H^+ \rightleftharpoons SiO_2(aq) + H_2O$	10.101	(Sverjensky and Sahai 1996)
$OH^- + H^+ \rightleftharpoons H_2O$	14.344	(Shock and Helgeson 1988)
$UO_2(CO_3)_3^{4-} + 2H_2O + H^+ \rightleftharpoons 3HCO_3^- + UO_2(OH)2(aq)$	-0.970	(Grenthe et al. 1992)
$UO_2(CO_3)_2^{2-} + 2H_2O \rightleftharpoons 2HCO_3^- + UO_2(OH)2(aq)$	-6.520	(Grenthe et al. 1992)

Kinetic Reactions

For each kinetic reaction, the following data is needed:

- Mass action law type: {full = 1} {reduced = -1} {glass = 0}
- Stoichiometric coefficient of aqueous species in each reaction

- Equilibrium constant at a temperature of 15°C.
- Rate constant of reaction

A full mass action law type will be used for each solid phase except the waste glass. A special mass action law type implemented in the STORM code will be used for the glass, and will be discussed in the following section.

Compilations of kinetic rate constants, equivalent to thermodynamic databases for important mineral phases, are not available. Also, the available mineral dissolution/precipitation kinetics data are much more limited as compared with thermodynamic data. Consequently, sufficiently large rate constants will be used to approximate equilibrium conditions, i.e. ensure that the phase will precipitate rapidly if the local chemical environment at a grid node is saturated with respect to the particular phase. This has an additional advantage in that uncertainty in the exact value of a particular rate constant will have little impact on the calculations.

Glass Rate Law

The corrosion reaction for LAWABP1 glass used in the waste form release calculations is:

$$\begin{aligned}
\text{LAWABP1} + 4.42\times10^{-1}\ H^+ + 1.89\times10^{-1}\ H_2O \rightarrow 1.36\times10^{-1}\ AlO_2^- \\
+1.84\times10^{-1}\ B(OH)_3(aq) + 1.13\times10^{-2}\ Cl^- + 1.82\times10^{-4}\ CrO_4^{2-} \\
+1.46\times10^{-3}\ F^- + 2.16\times10^{-2}\ Fe(OH)_3(aq) + 1.54\times10^{-7}\ IO_3^- \\
+3.23\times10^{-2}\ K^+ + 8.48\times10^{-3}\ La^{3+} + 1.71\times10^{-2}\ Mg^{2+} + 4.46\times10^{-1}\ Na^+ \\
+7.79\times10^{-4}\ HPO_4^{2-} + 3.52\times10^{-8}\ PuO_2(CO_3)_3^{4-} + 8.63\times10^{-4}\ SO_4^{2-} \\
+1.77\times10^{-8}\ SeO_4^{2-} + 4.82\times10^{-1}\ SiO_2(aq) + 6.59\times10^{-7}\ TcO_4^- \\
+2.15\times10^{-2}\ Ti(OH)_4(aq) + 9.81\times10^{-7}\ UO_2(OH)_2(aq) \\
+2.20\times10^{-2}\ Zn^{2+} + 2.94\times10^{-2}\ Zr(OH)_4(aq)
\end{aligned} \tag{1}$$

Similarly, the corrosion reaction for HLP-31 glass is

$$\begin{aligned}
\text{HLP-31} \rightarrow 6.84\times10^{-1}\ OH^- + 5.06\times10^{-2}\ Al^{3+} + 2.22\times10^{-1}\ B(OH)_3(aq) \\
+1.15\times10^{-4}\ Ca^{2+} + 7.64\times10^{-4}\ CrO_4^{2-} + 2.72\times10^{-2}\ Fe(OH)_3(aq) \\
+1.66\times10^{-7}\ IO_3^- + 6.44\times10^{-3}\ K^+ + 1.47\times10^{-2}\ Mg^{2+} + 4.78\times10^{-1}\ Na^+ \\
+3.78\times10^{-8}\ PuO_2(CO_3)_3^{4-} + 1.90\times10^{-8}\ SeO_4^{2-} + 5.58\times10^{-1}\ SiO_2(aq) \\
+7.58\times10^{-7}\ TcO_4^- + 1.48\times10^{-2}\ Ti(OH)_4(aq) + 1.05\times10^{-4}\ UO_2(OH)_2(aq) \\
+7.29\times10^{-3}\ Zn^{2+} + 4.82\times10^{-3}\ Zr(OH)_4(aq)
\end{aligned} \tag{2}$$

The stoichiometric coefficients for the radionuclides I, Pu, Se, and Tc are based on the average package concentration from the *Immobilized Low Activity Tank Waste Inventory Data Package* (Wootan 1999). For a dissolution reaction involving glass, parameters associated with the following kinetic rate law are needed

$$r_g = \vec{k} a_{\mathrm{H}^+}^{-\eta} e^{\frac{-E_a}{\mathrm{RT}}} \left[1 - \left(\frac{Q}{K_g} \right)^{\sigma} \right] \tag{3}$$

where r_g = dissolution rate, g m^{-2} d^{-1}
$\vec{k}$ = intrinsic rate constant, g m^{-2} d^{-1}
a_{H^+} = hydrogen ion activity (variable to be calculated by STORM)
E_a = activation energy, kJ/mol
R = gas constant, kJ/(mol·K)
T = temperature, K (assumed constant at 15°C)
Q = ion activity product Glass(variable to be calculated by STORM)
K_g = pseudoequilibrium constant
η = pH power law coefficient
σ = Temkin coefficient (σ = 1 assumed).

Equation (3) is an approximation for glass because glass is metastable, and the reaction proceeds one way (i.e., glass dissolves). The unknown parameters in Equation (1) ($\vec{k}$, E_a, K_g, and η) have been determined for LAWABP1 and HLP-31 (McGrail et al. 2001) glasses and these values are given in Table 9. The values given by McGrail et al. (2001) for LAWABP1 glass differ slightly with respect to the values given in Table 9, which were based on an earlier revision of the Waste Form Release Data Package (McGrail et al. 2000). Additional data were developed between the time the STORM calculations were performed and when the data package was updated that changed the parameters slightly.

Test results with HLP-31 glass showed that unlike most silicate glasses, the dissolution rate did not diminish with increasing concentration of Si in solution. Consequently, no pseudoequilibrium phase or K_g was assigned to this glass. In addition, test results with LAWABP1 glass (and most other ILAW glasses) show that it is susceptible to a secondary reaction mechanism, alkali ion exchange. This reaction results in the selective extraction of Na via a reaction

$$\text{LAWABP1-Na} + \mathrm{H}^+ \rightarrow \text{LAWABP1-H} + \mathrm{Na}^+ \tag{4}$$

where LAWABP1-Na represents the unreacted glass containing Na and LAWABP1-H represents a hydrated glass where the Na has been replaced with an equimolar amount of hydrogen. The rate of this reaction has been determined from single-pass flow-through experiments by (McGrail et al. 2001) and the rate constant is 2.5 x 10^6 g m^{-2} s^{-1} (again, slightly different from the value given in Table 9). STORM keeps track of the amount of hydrated glass formed via Reaction (4) and then allows it to dissolve

according to the same kinetic rate law (3) as the parent glass. The ion-exchange rate for HLP-31 glass was set at zero, consistent with the results reported by (McGrail et al. 2001).

Secondary Phase Equilibrium Constants

McGrail et al. (2001) describe the methods used to develop a solubility product for the key secondary phases identified from laboratory testing and from simulations with the EQ3/6 code. For convenience, the log K they derived for each secondary phase given in Table 7 is reproduced in Table 10. For the secondary phases where a log K was not available or could not be estimated, the reaction was not included in the STORM simulations.

Table 9. Summary of Kinetic Rate Parameters Used for Glasses

Parameter	Meaning	LAWABP1	HLP-31	Comment
$\vec{k}$	Intrinsic rate constant	3.5×10^{5} g m^{-2} d^{-1}	3 x 10^{6} g m^{-2} d^{-1}	HLP-31 assumed roughly 10 times faster than LAWABP1
K_g	Apparent equilibrium constant for glass based on activity of SiO_2(aq)	$10^{-2.9}$	N/A	HLP-31 glass dissolution rate did not change as a function of SiO_2(aq)
η	pH power law coefficient	0.5	0.5	HLP-31 value assumed same as LAWABP1
E_a	Activation energy of glass dissolution reaction	75 kJ/mol	75 kJ/mol	HLP-31 value assumed same as LAWABP1
σ	Temkin coefficient	1	1	Assigned constant
r_x	Na ion-exchange rate	3.5×10^{-6} mol m^{-2} d^{-1}	0	No detectable ion exchange for HLP-31

Initial and Boundary Conditions

For each specified gas species concentration, the following data are needed:

- Partial pressure of gaseous species

The gas partial pressure for CO_2 and O_2 were fixed at atmospheric values of $3\text{x}10^{-4}$ and $2.1\text{x}10^{-1}$ atm, respectively.

Table 10. Secondary Phase Reaction Network for LAWABP1 Glass

Reaction	Log K (15°C)
$Al(OH)_3(am) \rightleftharpoons AlO_2^- + H^+ + H_2O$	-13.10
$Analcime \rightleftharpoons 0.96AlO_2^- + 0.96Na^+ + 2.04SiO_2(aq)$	-9.86
$Anatase + 2H_2O \rightleftharpoons Ti(OH)_4(aq)$	-6.64
$Baddeleyite + 2H_2O \rightleftharpoons Zr(OH)_4(aq)$	-9.29
$Goethite + H_2O \rightleftharpoons Fe(OH)_3(aq)$	-11.09
$Herschelite \rightleftharpoons 1.62Na^+ (aq) + 0.50K^+ (aq) + 2.26AlO_2^- + 4SiO_2(aq) + 0.14H^+ + 5.93H_2O$	-40.94
$La(OH)_3(am) + 3H^+ \rightleftharpoons 3H_2O + La^{3+}$	22.55
$Nontronite\text{-}Na + 2H_2O \rightleftharpoons 0.330AlO_2^- + 2Fe(OH)_3(aq) + 0.330Na^+ + 3.67SiO_2(aq)$	-43.33
$PuO_2 + HCO_3^- + 0.5O_2(aq) \rightleftharpoons PuO_2(CO_3)_3^{4-} + H_2O + H^+$	-15.92
$Sepiolite + 8H^+ \rightleftharpoons 4Mg^{2+} + 6SiO_2(aq) + 11H_2O$	31.29
$SiO_2(am) \rightleftharpoons SiO_2(aq)$	-2.85
$Weeksite + 2H^+ \rightleftharpoons 2K^+ + 2\ UO_2(OH)_2(aq) + 6SiO_2(aq) + 3H_2O$	-5.25
$Soddyite \rightleftharpoons 2UO_2(OH)_2(aq) + SiO_2(aq)$	-20.24
$Theophrasite + 2H^+ \rightleftharpoons 2H_2O + Ni^{2+}$	13.33
$Zn(OH)_2(am) + 2H^+ \rightleftharpoons 2H_2O + Zn^{2+}$	14.44

For each specified aqueous species, the following data are needed:

- Specified total concentration
- Stoichiometric coefficient of each aqueous species.

Aqueous species concentrations at the upper boundary, and for initial conditions, were specified as a part of the near-field geochemistry data package (Kaplan and Serne 1999) and are given in Table 11.

For water flow the following boundary conditions were used: constant specified flux at the upper boundary and free drainage at the lower boundary. The reactive transport simulations used the following boundary conditions: specified aqueous species concentrations at the upper boundary and no diffusion across the lower boundary. The contaminant flux across the lower boundary is therefore limited to advection

$$f = c\rho_w v \tag{5}$$

where c = concentration (mol kg^{-1})
ρ_w = density of water (kg m^{-3})
v = specific discharge (m s^{-1})

Table 11. Initial Aqueous Concentrations Used in Simulations

Species	Initial Concentration (mol kg-1)
AlO_2^-	10^{-6}
$B(OH)_3(aq)$	10^{-10}
Ca^{2+}	10^{-7}
Cr (total)	10^{-10}
$Fe(OH)_3(aq)$	10^{-10}
H_2O	1
H^+	10^{-7}
IO_3^-	10^{-10}
K^+	10^{-6}
La^{3+}	10^{-10}
Mg^{2+}	10^{-10}
Na^+	10^{-6}
Ni^{2+}	10^{-10}
$PuO_2(CO_3)_3^{4-}$	10^{-10}
SeO_4^{2-}	10^{-10}
Si (total)	10^{-5}
TcO_4^-	10^{-10}
$Ti(OH)_4(aq)$	10^{-10}
U (total)	10^{-10}
Zn^{2+}	10^{-10}
$Zr(OH)_4(aq)$	10^{-10}

Model Output

The normalized flux to the vadose zone is calculated by summing the flux at each node across the bottom boundary of the model, and normalizing the total flux according to the amount of each radionuclide in all the waste packages at the start of the simulation. The normalized flux across the lower boundary, *F*, in units of ppm/yr, was calculated using

$$F = \frac{\sum_{i=1}^{N} f_i \Delta x_i \Delta y_i}{I_j} (3.1558 \times 10^7 \text{ s yr}^{-1})(1 \times 10^6 \text{ ppm}) \tag{6}$$

where f_i = flux across the bottom of an individual grid block (μmole m^{-2} s^{-1})

$\Delta x_i \Delta y_i$ = cross-sectional area of an individual grid block (m^2)

I_j = inventory of *j*th radionuclide in the waste packages (μmol), where

$$I_j = V_{wp}(1 - \theta_T) V_G \rho_G \gamma_j \tag{7}$$

where V_{wp} = volume of the waste packages (m^3)

θ_T = total porosity of the material representing the waste packages (0.02)

V_G = fraction of glass in each waste package (0.85)

ρ_G = molar density of LAWABP1 glass (38776.1450 moles m^{-3})

γ_j = mole fraction of *j*th radionuclide in LAWABP1 glass (i.e., 6.59×10^{-1} μmoles Tc $mole^{-1}$ glass)

The volume of the waste packages, V_{wp}, was 5.6 m^3 for the RH Trench simulations and 8.4 m^3 for the new ILAW concrete vault simulations. For 1-D simulations, the cross-sectional area of the grid block was 1 m^2.

Results

A total of 22 simulations were run to test the sensitivity of model calculations to various assumptions (Table 12). Discussion of the results of each simulation is contained in the following sections.

Table 12. List of Waste Form Sensitivity Cases

Case	Description	Basic Model
WFA	4.2 mm/yr infiltration	Trench
WFB	Forward rate, 4.2 mm/yr infiltration	Trench
WFC	4.2 mm/yr infiltration	Vault
WFD	0.1 mm/yr infiltration	Trench
WF1	Assume no Ion Exchange	Trench
WF2	Assume no Secondary Phase Formation	Trench
WF4	0.9 mm/yr infiltration rate	Trench
WF6	50 mm/yr infiltration rate	Trench
WF7	0.5 mm/yr infiltration rate	Trench
WF8	10 mm/yr infiltration rate	Trench
WF9	Extend WFA to groundwater	Trench
WF10	Add conditioning layer at top	Trench
WF11	Change filler material in trench to sand	Trench
WF14	Increase diffusion for all aqueous species by a factor of 10	Trench
WF16	Replace concrete everywhere with backfill material	Vault
WF19	0.9 mm/yr infiltration rate	Vault
WF21	0.1 mm/yr infiltration	Vault
WF25	Include steel in waste packages	Trench
WF26	Replace Tc w/U	Trench
WF27	Full 2-D simulation	Trench
WF28/WFx	Increase Waste Loading / Alternate Glass Formulation (HLP-31)	Trench
WF30	Increase ion exchange rate by 5 times for WFB	Trench

Base Case

The maximum flux of Tc to the vadose zone for the RH Trench base case simulation is 0.93 ppm/yr at 100,000 yr as shown in Figure 3. The Tc flux to the vadose zone is proportional to the TcO_4^- concentration at the lower boundary and the water flux rate. At early times, the TcO_4^- concentrations (Figure 4) increase sharply in the glass layers. Glass dissolution, and low water contents in the glass layers, coupled with a low water flux rate, causes TcO_4^- concentrations to increase rapidly in the glass layers. In contrast, mass transport from the glass layers is required to build up Tc concentrations in the backfill layers. Therefore, concentrations in the backfill layers increase slowly as products of glass dissolution diffuse from the glass layers into the backfill layers, where dilution also occurs because of the

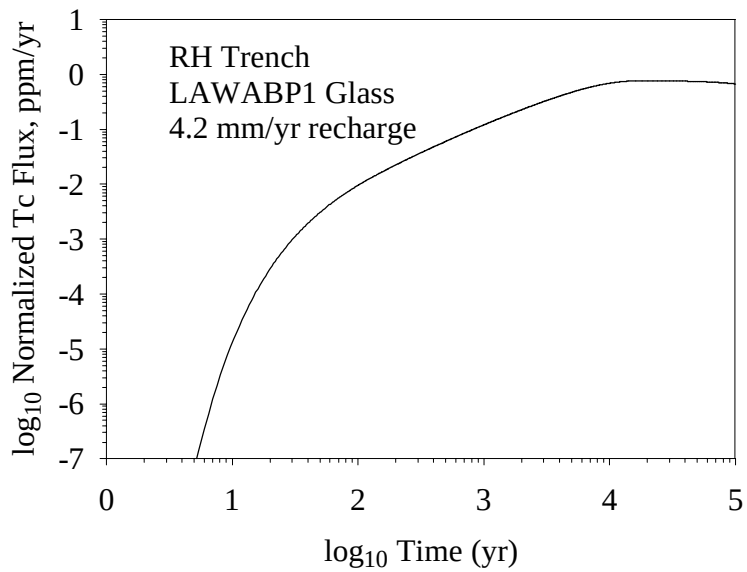

Figure 3. Tc Flux to the Vadose Zone, Corrected for Radioactive Decay, Normalized to the Amount of Tc Originally in LAWABP1 Waste Glass, for Base Case Trench Simulation

much higher water content in the backfill layers compared with the glass layers. Predicted glass dissolution rates (Figure 5) increase with time in each of the glass layers, but are relatively similar for each layer. The pH and TcO_4^- concentrations increase more rapidly in the glass layers early in the simulation, although by 20,000 yr, concentrations throughout the profile are relatively similar. This indicates that at early times, the TcO_4^- flux across the lower boundary is limited by the diffusion rate of TcO_4^- out of the glass layers.

The glass dissolution rate for these simulations is highest on the edges of the glass layers. This is where the pH of the pore water is highest (Figure 6) and the SiO_2(aq) concentrations are lowest (Figure 7). Concentration of SiO_2(aq) is lower in the backfill due to precipitation of quartz, one of the primary minerals that make up the backfill. As was mentioned in the Methods Section, dissolution/precipitation rate constants for each mineral were set to relative high values to approximate equilibrium conditions in the simulations. However, quartz precipitation is extremely slow at the disposal system temperature (15°C) and would not be expected to precipitate in significant amounts. Future simulations will correct this, but by enforcing equilibrium with quartz, the present calculations are conservative as the effect is to increase the calculated glass dissolution rates at the glass/backfill interface.

Because the glass dissolution rate is relatively low, the surface area of the glass does not decrease noticeably by 20,000 yr. Similarly, the volume of secondary minerals precipitated is also low (Figure 8).

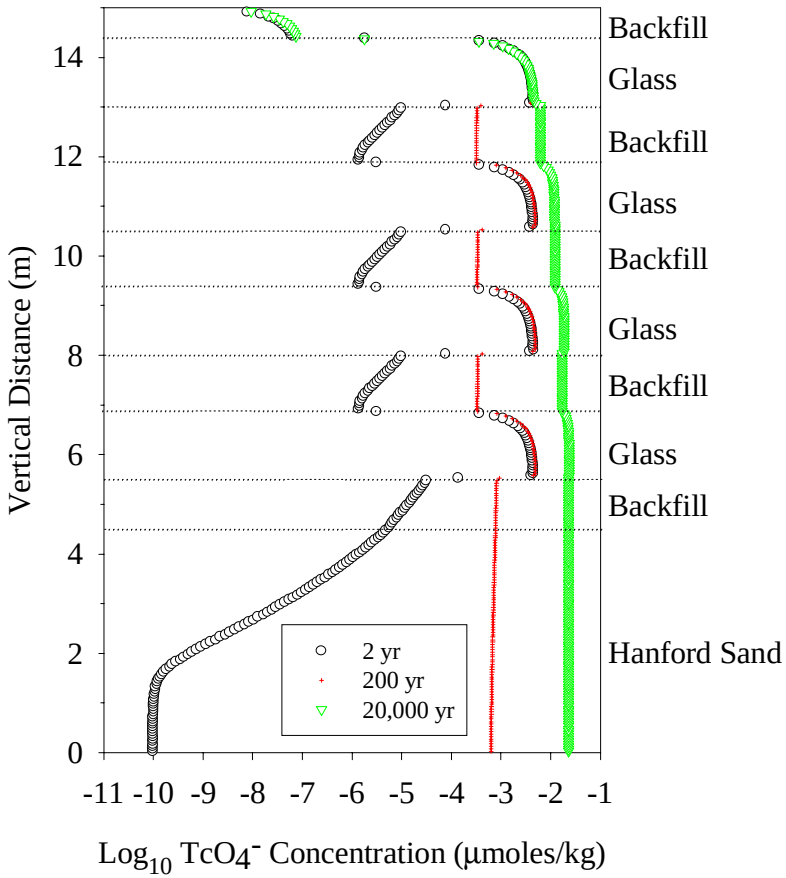

Figure 4. TcO_4^- Concentrations for RH Trench Simulation with Recharge Rate of 4.2 mm/yr (Horizontal Dotted Lines Represent Boundaries Between Material Zones and Material Names Are Shown Along Right Axis)

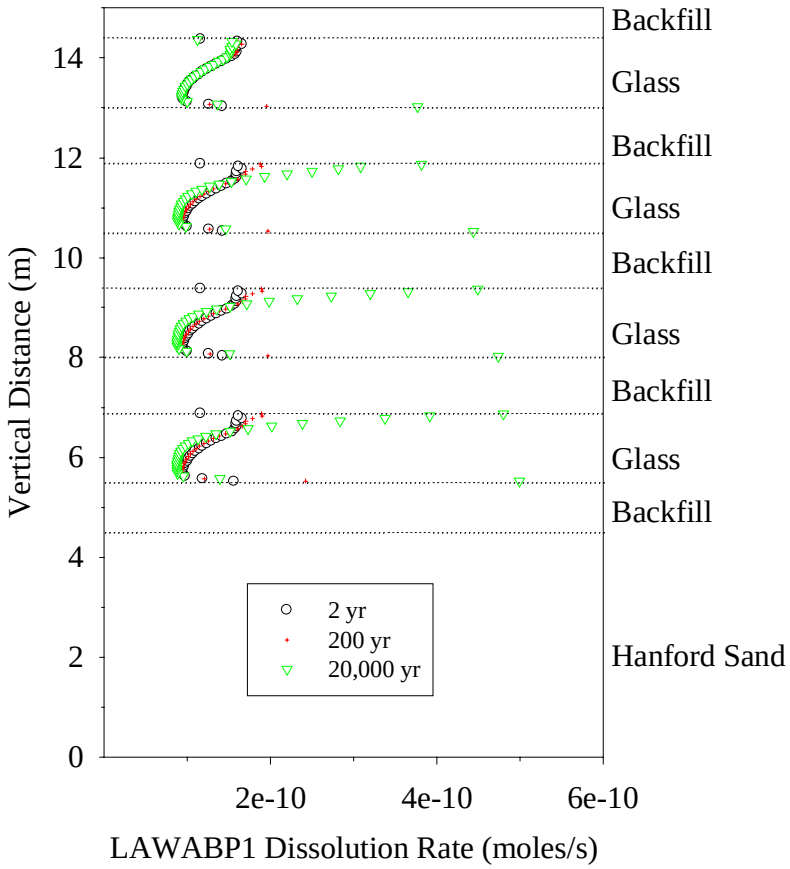

Figure 5. Glass Dissolution Rate for LAWABP1 in RH Trench Simulation with Recharge Rate of 4.2 mm/yr (horizontal dotted lines represent boundaries between material zones and material names are shown along right axis)

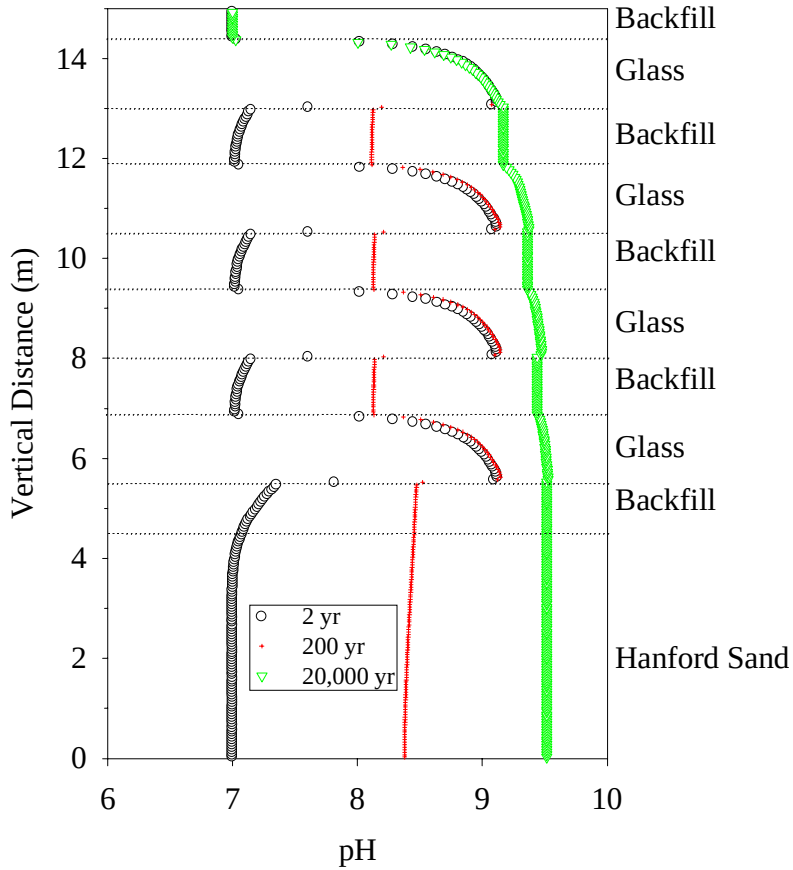

Figure 6. Solution pH for RH Trench Simulation with Recharge Rate of 4.2 mm/yr (horizontal dotted lines represent boundaries between material zonesand material names are shown along right axis)

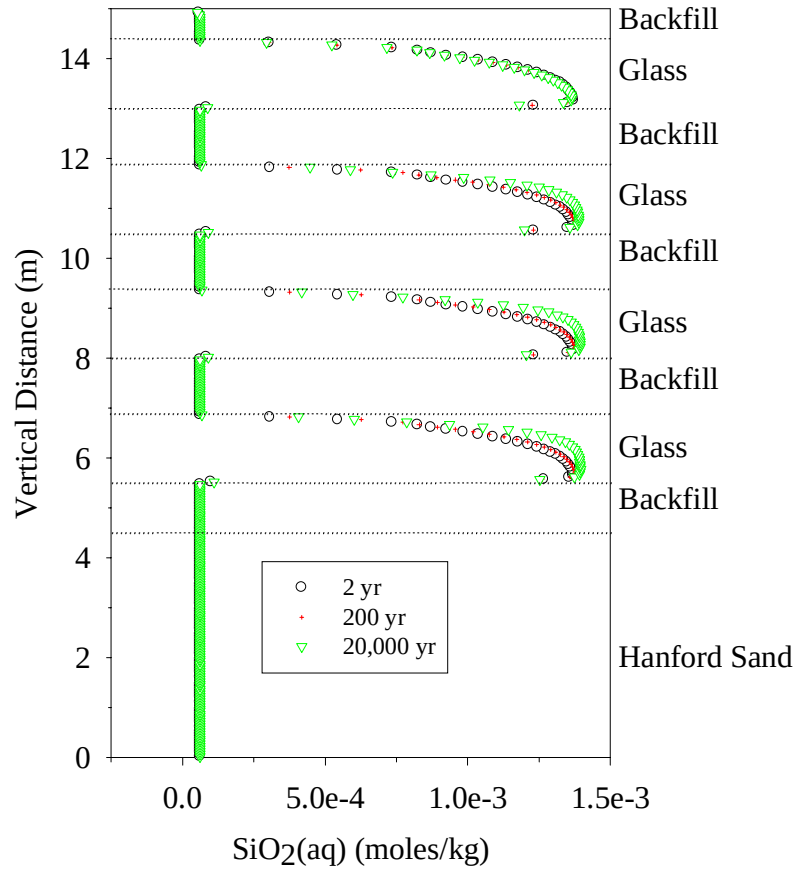

Figure 7. SiO_2(aq) Concentrations for RH Trench Simulation with Recharge Rate of 4.2 mm/yr (horizontal dotted lines represent boundaries between material zones and material names are shown along right axis)

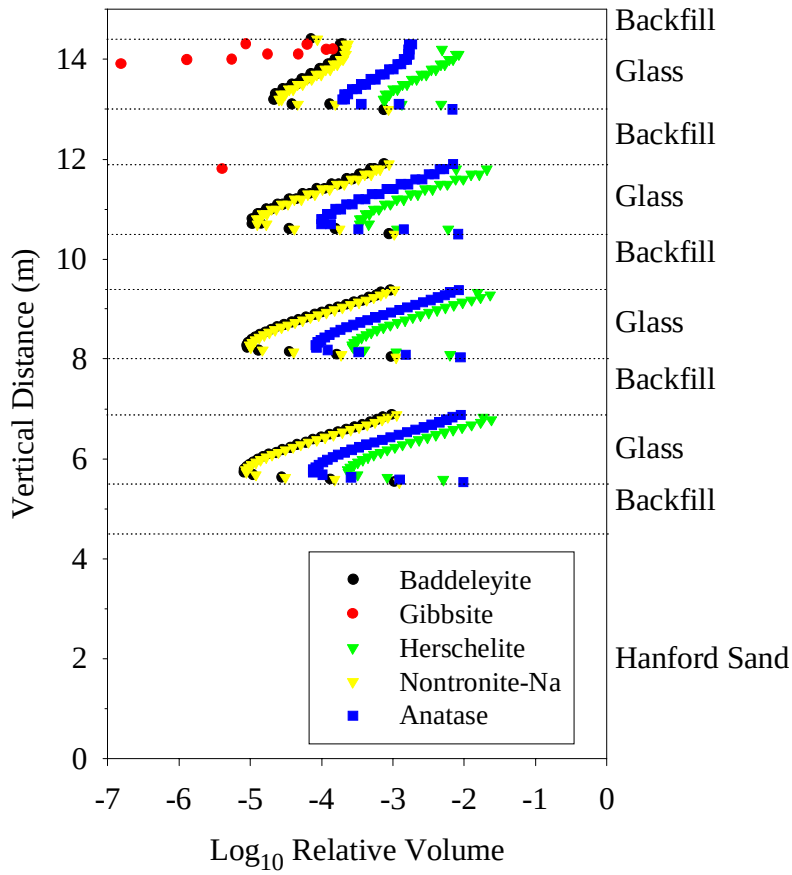

Figure 8. Secondary Mineral Relative Volumes at 20,000 yr for RH Trench Simulation with Recharge Rate of 4.2 mm/yr (horizontal dotted lines represent boundaries between material zones and material names are shown along right axis)

Other Radionuclide Release Rates

The base case simulation was modified to consider the release of uranium species from the waste glass. Three aqueous uranium species were considered: $UO_2(CO_3)_2^{2-}$, $UO_2(CO_3)_3^{4-}$, and $UO_2(OH)_2(aq)$. Two secondary minerals were considered: Weeksite, $K_2(UO_2)_2Si_6O_{15}\cdot 4H_2O$, and soddyite, $(UO_2)_2(SiO_4)\cdot 2H_2O$. Only soddyite precipitated, in miniscule amounts, and for a very short period. Because of the slow release rate from the glass, steady rate of mass transport through the system, and strong carbonate complexes associated with U(VI), the pore fluid remained undersaturated with respect to weeksite and soddyite and the uranium remained dissolved in the aqueous phase. Hence, the normalized fluxes for total U release are identical to those predicted for Tc.

Because no solid phases were identified that could limit Se and I solubility, their release rates were determined by the rate of glass dissolution, normalized by their inventory. Hence, the normalized fluxes for Se and I are also identical to those predicted for Tc. In contrast, Pu release is controlled by the solubility of PuO_2 (Table 10) with the major aqueous species being $PuO_2(CO_3)_3^{4-}$. Therefore, the normalized flux for Pu is several orders of magnitude lower than that for Tc as shown in Figure 9.

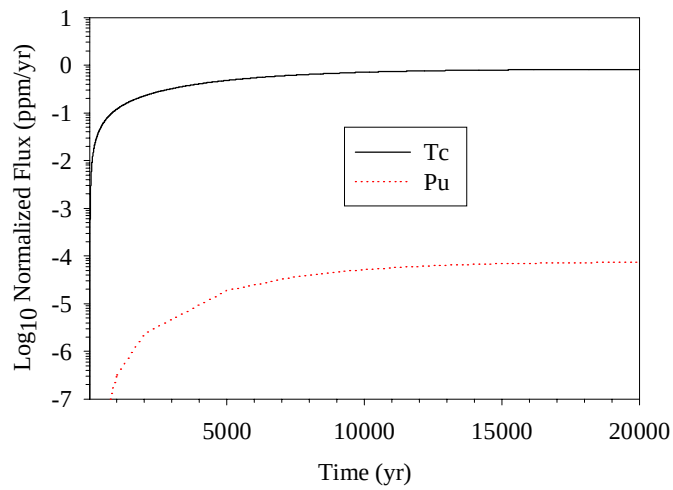

Figure 9. Comparison of Pu and Tc Flux to the Vadose Zone for Base Case Trench Simulation

Recharge Rates

Assuming steady-state flow with a constant recharge rate results in a constant water flux, equal to the recharge rate, throughout the entire depth of the profile. Water content, however, will vary with depth in the profile. Water content is a dimensionless variable defined as the volume of water per volume of porous or fractured media. The unique relationship between water flux and water content for each material is defined by the hydraulic parameters (Meyer and Serne 1999).

The flux of ^{99}Tc increases with increasing recharge rate (Figure 10). Higher recharge rates flush dilute water through the system, increasing water contents in the glass layers (Figure 11), lowering the $SiO_2(aq)$ concentration, thus increasing the glass dissolution rate. However, the diluting effect of higher recharge also limits increases in pH, thereby limiting increases in the glass dissolution rate.

Glass Dissolution Model

The effect of the assumptions inherent in the glass dissolution model was also considered. A comparison of the base case with a simulation at the forward rate of reaction is shown in Figure 12. At the forward rate of reaction, buildup in the activities of species caused by glass dissolution, such as AlO_2^- and $SiO_2(aq)$, is not considered to decrease the glass dissolution rate. In this case, Equation (3) simplifies to

$$r_g = \vec{k} a_{H^+}^{-\eta} e \frac{-E_a}{RT} \tag{8}$$

so that only solution pH affects the dissolution rate (temperature is constant at 15°C). Allowing the glass dissolution rate to decrease as the concentration of SiO_2(aq) increases lowers the relative flux of Tc to the vadose zone by a factor of 8 as compared with the case with glass dissolving at the forward rate, as shown in Figure 12.

If no ion exchange is assumed, the glass dissolution rate decreases slightly from the lower pH. If no secondary mineral precipitation is allowed, the amount of SiO_2(aq) in solution is greater, thus lowering the dissolution rate further relative to the forward rate. If, for the forward rte simulation, the ion exchange rate is increased by a factor of five, the overall glass dissolution rate increases only slightly. The strong buffering effect of dissolution of CO_2(g) to produce carbonic acid prevents the increased ion-exchange rate from affecting the pH significantly.

Surrounding Materials

Preconditioning Layer

Placing a 1-m thick layer of silica sand on the top of the trench lowers the glass dissolution rate very slightly by increasing the amount of silica in solution (Figure 13). The effect is small because the high solid to liquid ratio associated with the glass dominates the solution chemistry after only a short

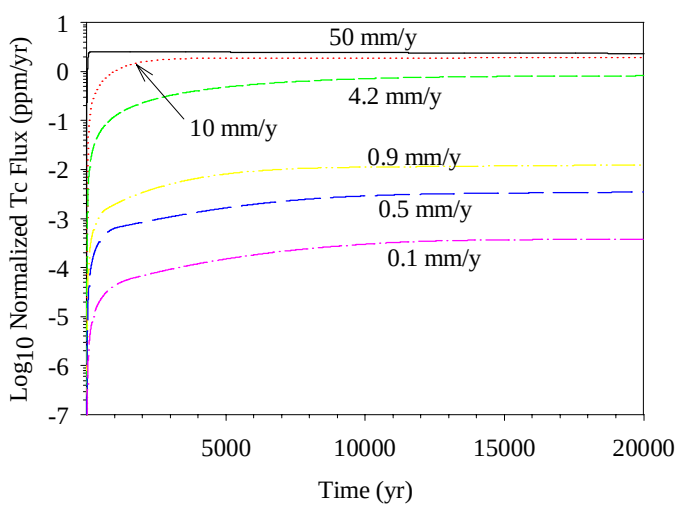

Figure 10. Flux of ^{99}Tc to the Vadose Zone, Relative to the Amount of Tc Originally in LAWABP1 Waste Glass, for Recharge Rates Ranging from 0.1 to 50 mm/yr

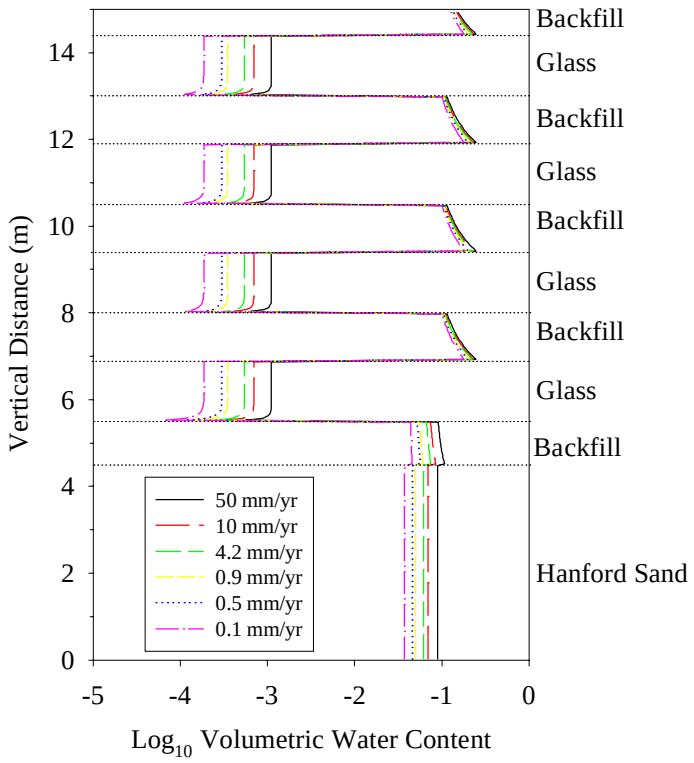

Figure 11. Water Content vs. Depth for Selected Recharge Rates for the RH Trench

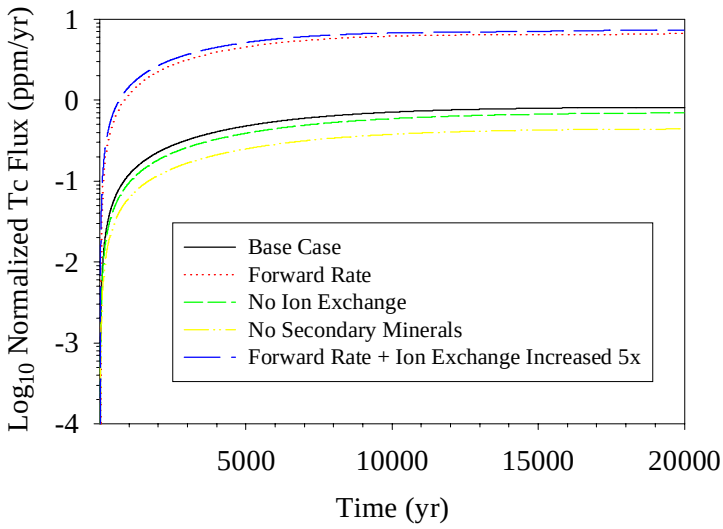

Figure 12. Tc Flux to the Vadose Zone, Relative to the Amount of Tc Originally in LAWABP1 Waste Glass, for Different Glass Dissolution Models

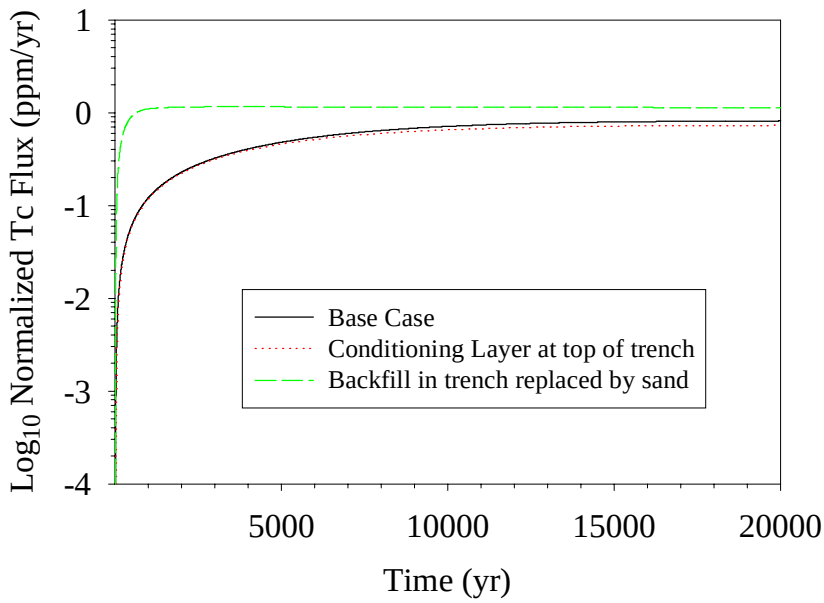

Figure 13. Tc Flux to the Vadose Zone, Relative to the Amount of Tc Originally in LAWABP1 Waste Glass, Assuming Different Surrounding Materials

penetration depth into the first layer of waste packages. Hence, the silica-sand layer only affects a small volume of glass right at the silica-sand/glass interface. Replacing the backfill material in the trench with sand (hydraulic properties only were changed to those of the Vault Filler material) causes an increase in the release rate. The sand has lower moisture content and thus, a higher linear pore velocity than the backfill at a recharge of 4.2 mm/y. This allows more rapid transport of Tc to the bottom of the facility.

Effect of Steel Container

Two sensitivity cases considered the effect of including the 304L stainless steel containers in which the molten LAW is poured. The corrosion reaction for 304 stainless steel is (Cloke et al. 1997):

$$\begin{aligned}\text{Steel} + 2.9262\times10^{-2}\ H^+ + 1.7618\ H_2O + 3.4169\times10^{-1}\ O_2(aq) \rightarrow \\ 3.4667\times10^{-3}\ HCO_3^- + 3.4701\times10^{-1}\ CrO_4^{2-} + 1.1828\ Fe(OH)_3(aq) \\ + 3.5167\times10^{-2}\ Mn^{2+} + 9.9093\times10^{-3}\ NO_3^- + 1.8583\times10^{-1}\ Ni^{2+} \\ + 8.8004\times10^{-4}\ HPO_4^{2-} + 5.2008\times10^{-4}\ SO_4^{2-} + 1.7325\times10^{-2}\ SiO_2(aq)\end{aligned} \tag{9}$$

The 304L stainless steel corrosion rate was assumed to be a constant $6.87\text{x}10^{-14}$ mol cm^{-2} s^{-1} (Cloke et al. 1997). Thus, the steel corrosion rate is not affected by changes in pH or water chemistry. By assuming this rate, the stainless steel corrodes away entirely within 1,000 yr. For the first sensitivity case, stainless steel was included in the upper and lower nodes of each glass waste package layer.

Including the stainless steel waste containers increases the pH slightly, because the corrosion reaction consumes H^+, but the effect on the glass dissolution rate is negligible (Figure 15). However, 304L contains approximately 20% Cr and 10% Ni. The estimated inventory of chromium in the 304L is approximately 9.3×10^6 kg. In contrast, the ILAW glass contains only about 7×10^4 kg of Cr. As mentioned previously, using the assumed steel corrosion rate establishes a release time of approximately 1000 y. The short release time combined with the larger inventory of Cr in the steel combine to produce a much higher calculated release rate of Cr from the disposal system (Figure 14).

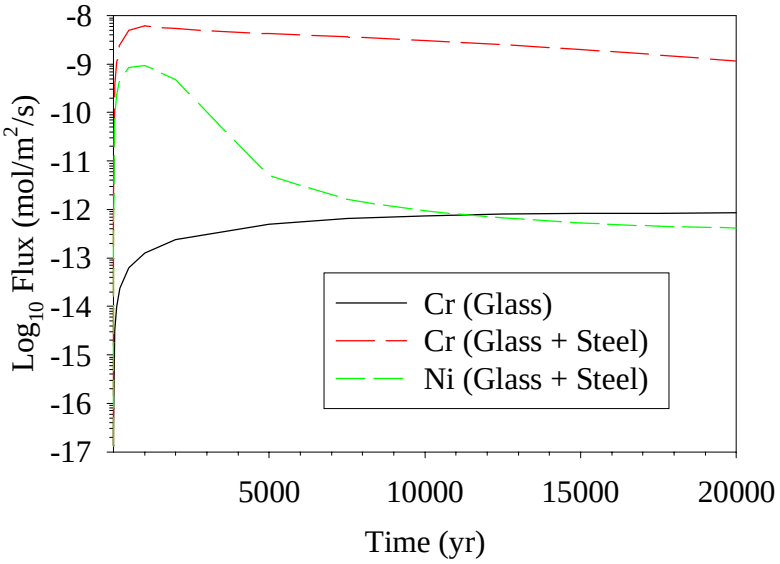

Figure 14. Tc Flux to the Vadose Zone, Relative to the Amount of Tc Originally in LAWABP1 Waste Glass, Including Stainless Steel Waste Packages

Because we have assumed global equilibrium with the atmosphere at all times, the Cr is released as soluble and mobile CrO_4^{2-}. The simulations do not account for the likely slow kinetics associated with oxidation of Cr(III) to Cr(VI) and thus represent the most conservative release case. The EQ3/6 database we have used has only a few solid alkali chromates, all of which are very soluble. A solubility product for $MgCrO_4$ and $CaCrO_4$ is available in the MINTEQA2 database. However, independent calculations using the listed log Ks and the composition of fluids exiting the LAW disposal show that these phases are several orders of magnitude undersaturated. So, no solid phase precipitated in our simulations that would limit the Cr release from the disposal system.

In contrast, the release rate of Ni is many times lower than that for Cr (Figure 14). Nickel release rate is constrained by precipitation of theophrasite, $Ni(OH)_2$. Because the solubility of theophrastite decreases with the square of the OH^- activity, the calculated release rate decreases markedly at later times as the pH increases throughout the disposal system.

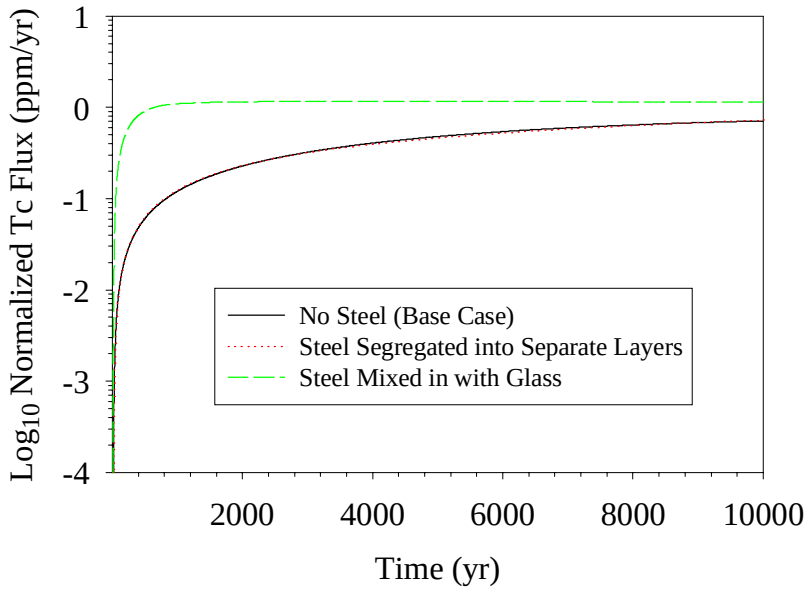

Figure 15. Tc Flux to the Vadose Zone, Relative to the Amount of Tc Originally in LAWABP1 Waste Glass, Including Stainless Steel Waste Packages

In a separate sensitivity case, the stainless steel was mixed uniformly throughout the entire glass layer. In this case, the steel corrosion reaction causes enhanced precipitation of nontronite, which lowers the activity of SiO_2(aq), and gives a 10-fold increase in the glass dissolution rate during the first few thousand years (the steel is completely dissolved after 1,000 yr so the effect is transient). This sensitivity case approximates batch (closed-system) laboratory experiments where glass and steel have been reacted together (Jantzen 1984; McGrail 1986). In these experiments, the presence of iron was found to significantly enhance glass dissolution rates because the steel corrosion products adsorbed Si or caused precipitation of ferrous silicate clay that acted as a sink for Si. Although these experimental findings are incontrovertible, assuming direct translation of the effects to an open disposal system is not correct. As the STORM simulations show, segregation of the stainless steel into layers, which is the more realistic case, had essentially no impact on glass performance. This is because Fe(III) is extremely insoluble and so the mass transported into the glass layers in very small. Consequently, the steel layers affect only a very small volume of glass near the steel/glass interface. In contrast, the homogeneous mixing of the steel with the glass impacts the entire volume within each glass layer. The large difference in results between these two scenarios emphasizes the importance of modeling the disposal system as realistically as possible and suggests caution when generalizing experimental results (particularly from batch experiments) to an open system.

Aqueous Diffusion Coefficient

Increasing the aqueous diffusion coefficient for all species to $5x10^{-8}$ m^2/s from a base case value of $5x10^{-9}$ m^2/s lowers the Tc flux to the vadose zone. The increased diffusion coefficient significantly

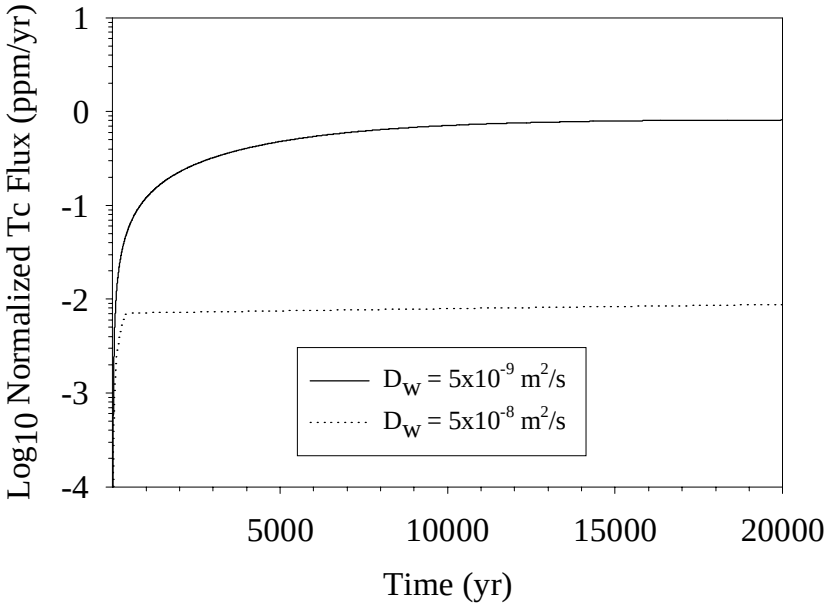

Figure 16. Tc Flux to the Vadose Zone, Relative to the Amount of Tc Originally in LAWABP1 Waste Glass, Assuming Different Aqueous Diffusion Coefficients

increases mixing of the aqueous products of glass dissolution into the backfill layers, the minerals in which act as a pH buffer. This results in a significantly lower pH in the glass layers, and hence a much lower glass dissolution rate (Figure 16).

Two-Dimensional Simulation

A full 2-D simulation of the trench scenario was developed for comparison to the 1-D simulation used as the base case. The 2-D simulation reaches steady state earlier and shows a lower normalized Tc release rate than the 1-D simulation (Figure 17). In the 2-D simulations, water flows around the glass waste packages. This lowers the water content (Figure 18) in, and water flux through, the waste packages, and increases the Tc concentrations (Figure 19) in the waste packages. The glass dissolution rate (Figure 20) for these simulations is highest on the edges of the glass layers. This is where the pH of the pore water is highest (Figure 21) and the SiO_2(aq) concentrations are lowest (Figure 22). Again, this is a consequence of quartz precipitation in the backfill.

This 2-D simulation required over a month to reach a simulation time of 2,000 yr, whereas the 1-D simulation required only 5.3 days to reach a simulation time of 100,000 yr. The results of this comparison show that the 1-D simulations are conservative with respect to the results from the 2-D simulations.

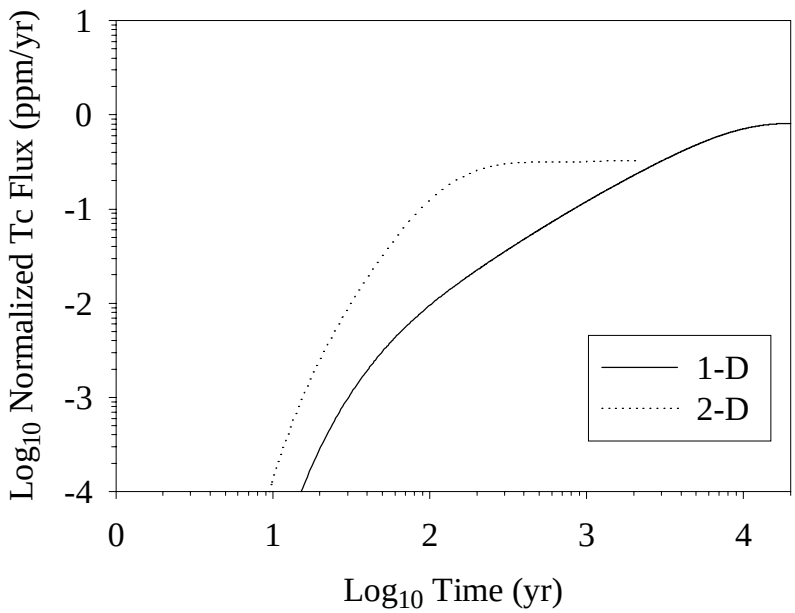

Figure 17. Tc Flux to the Vadose Zone, Relative to the Amount of Tc Originally in LAWABP1 Waste Glass, Comparing 1-D and 2-D Simulations

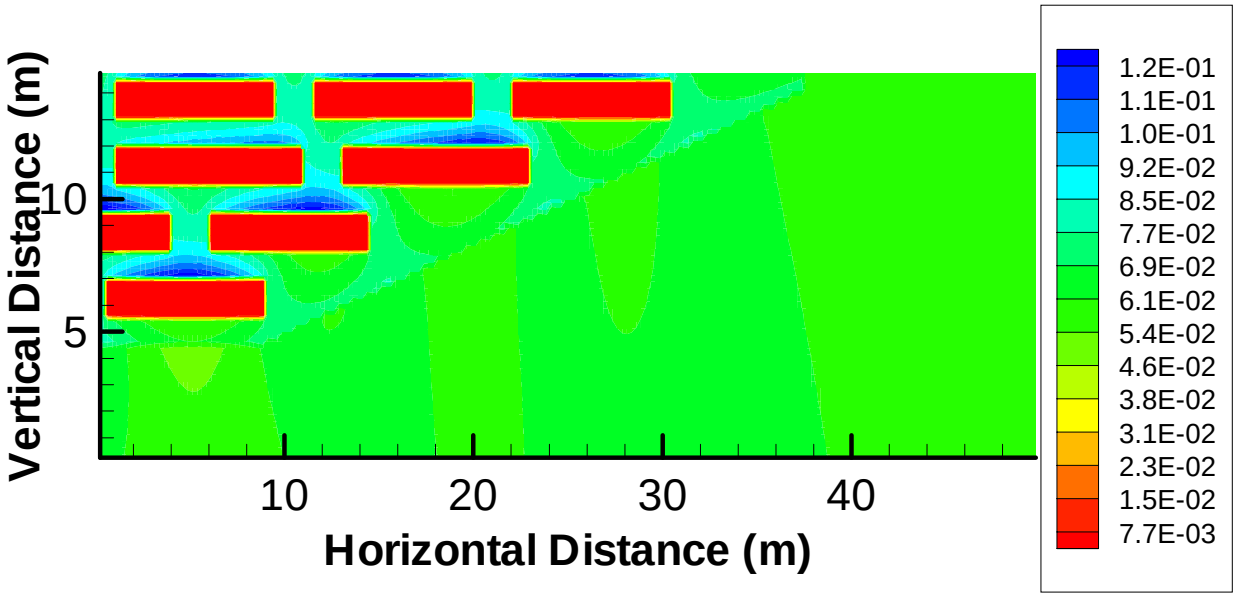

Figure 18. Volumetric Water Content for 2-D Trench Simulation

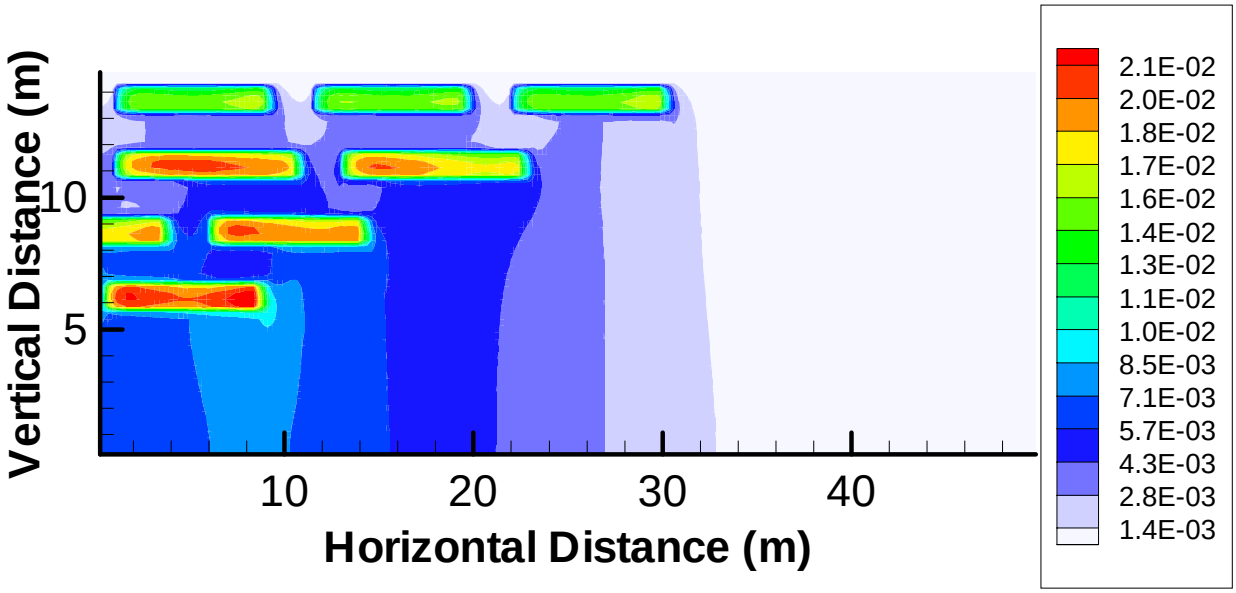

Figure 19. Total Aqueous Tc Concentration (μmol/kg) for 2-D Trench Simulation at 2,000 yr

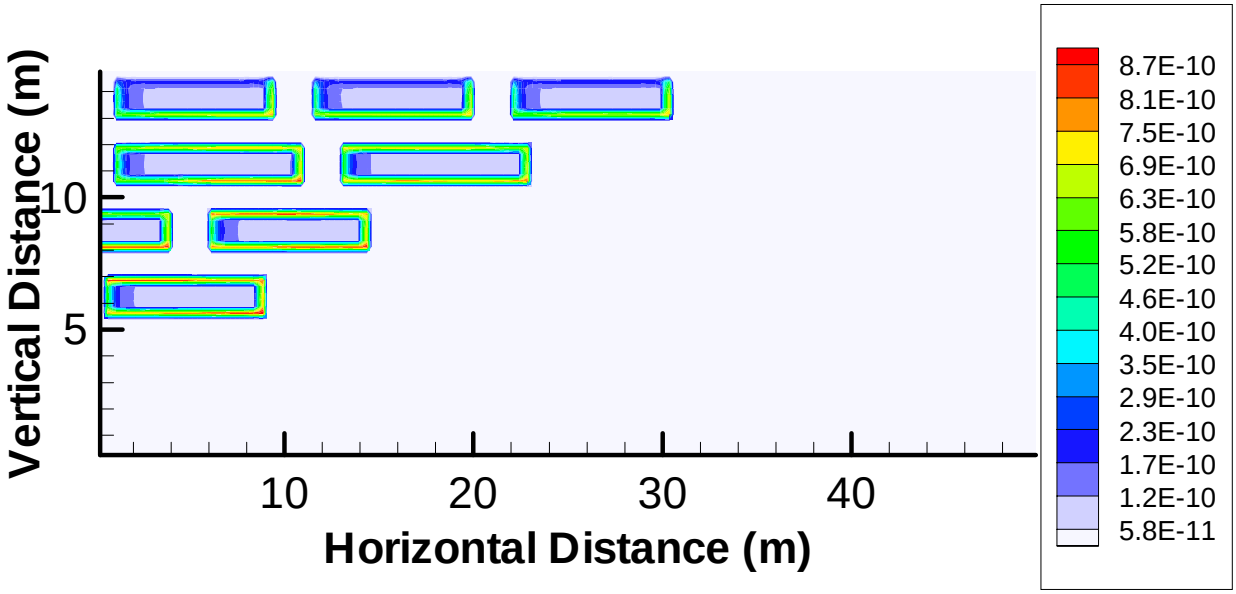

Figure 20. Glass Dissolution Rate (mol s^{-1}) for LAWABP1 in 2-D Trench Simulation at 2,000 yr

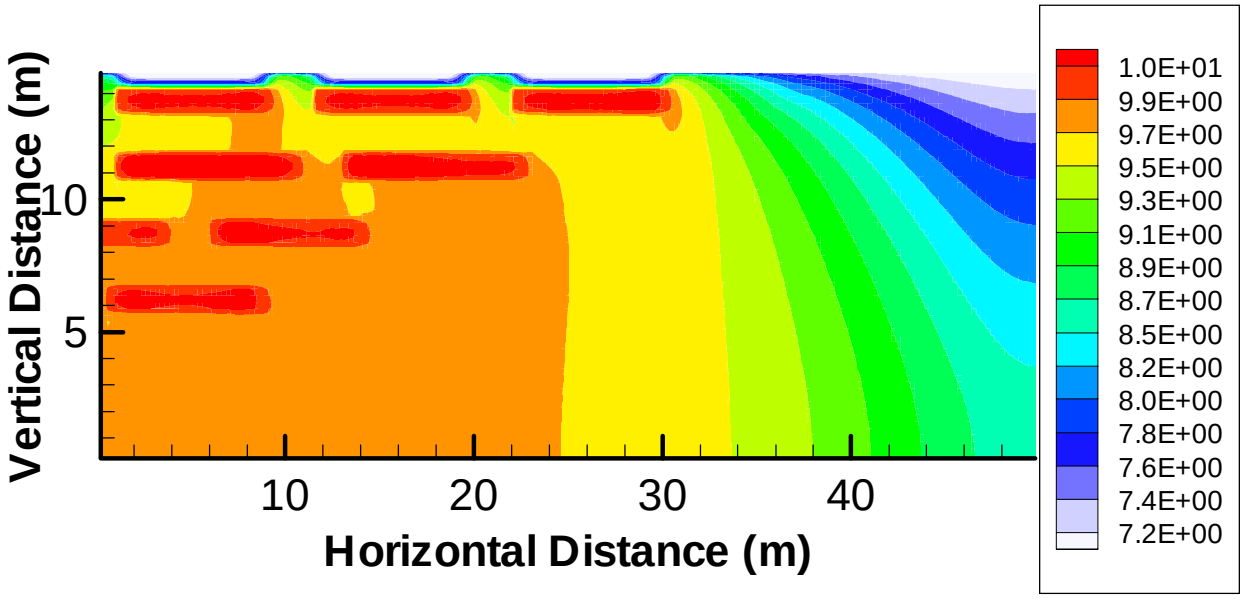

Figure 21. Solution pH for 2-D Trench Simulation

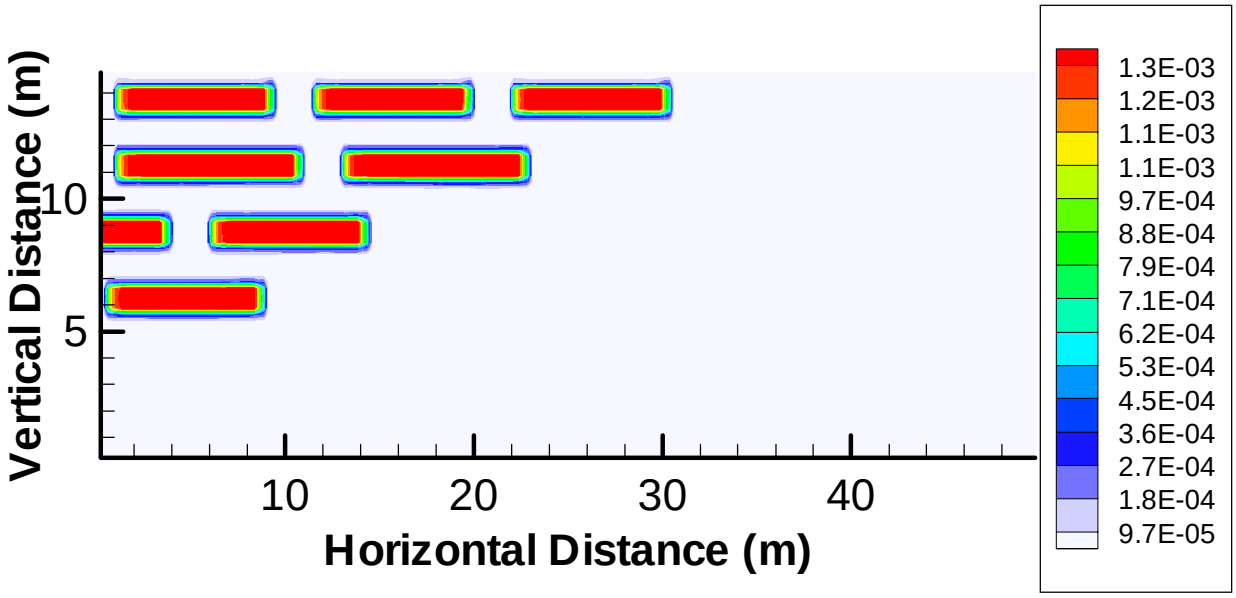

Figure 22. SiO_2(aq) Concentrations (mol/kg) for 2-D Trench Simulation

Vault Scenario

The normalized Tc flux to the vadose zone is 20% higher for the vault simulations than for the trench simulation at a recharge rate of 4.2 mm/yr (Figure 23). The glass packages are more closely packed in this simulation than in the trench simulation. This raises the pH inside the vault relative to the RH Trench simulation because there is less dilution available from the higher water contents in the intervening backfill layers (Figure 24). Substituting backfill for the degraded concrete has a negligible effect on the glass dissolution rate. Although the concrete layer causes an increase in pH as recharging waters enter (Figure 25), the glass layers cause a greater increase. As in the trench simulations, assuming lower recharge rates results in significantly smaller Tc flux to the vadose zone. The 0.1-mm/yr-recharge rate simulation was unable to progress past 1,800 yr because of high concentrations in the pore water percolating through the vault that caused convergence problems.

Extend Base Case to Water Table

This simulation is identical to the base case, except that the Hanford Sand layer was assumed to extend 88 m to the water table. Thus, the total depth of the model was 103 m for the extended grid, as opposed to 15 m for the base case simulation. Simulated pH (Figure 26) and TcO_4^- (Figure 27) concentrations for the upper 15 m of the extended simulation are very similar to those of the base case

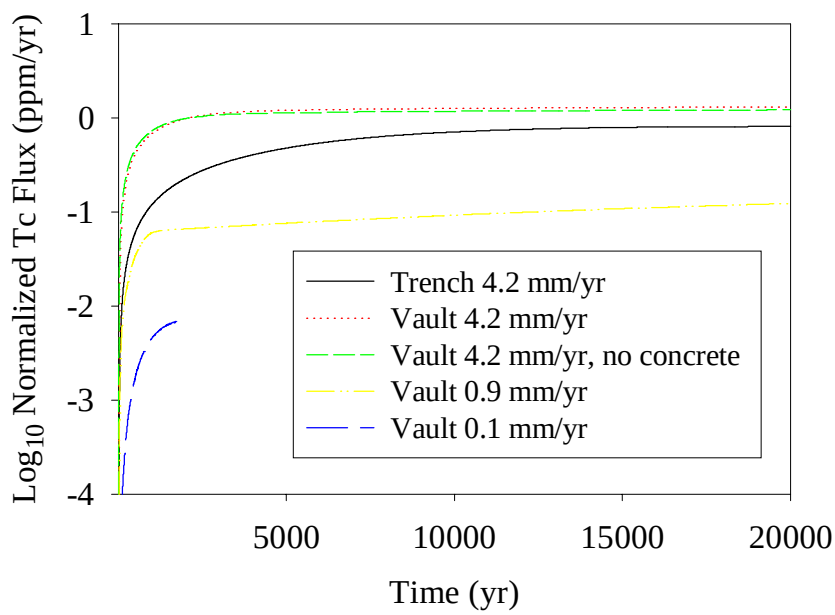

Figure 23. Tc Flux to the Vadose Zone, Relative to the Amount of Tc Originally in LAWABP1 Waste Glass, Comparison of Vault Simulations at Different Recharge Rates to Trench Base Case

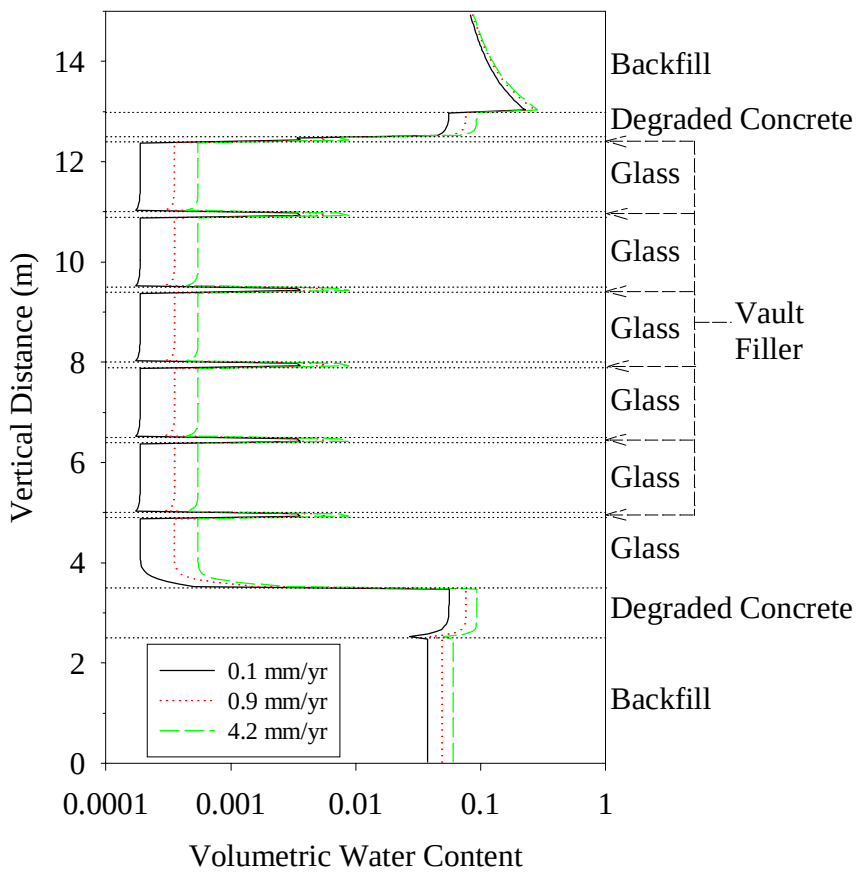

Figure 24. Water Contents for Selected Recharge Rates for Vault Simulations

until after 10,000 years, when the effect of the lower water table boundary begins to propagate up the profile. Even so, the Tc release rate is very similar for the base case and the extended simulation, the flux from the extended simulation being 7% lower at 1,000 years and 9% higher at 10,000 years than the base case. Longitudinal diffusion causes a decrease in the concentrations of aqueous species across the depth of the Hanford Sand. Solution pH decreases slightly from the top of the Hanford Sand to the water table (Figure 26). Aqueous TcO_4^- decreases from the top of the Hanford Sand to the water table by a factor of 3 at 2,000 yr. By 20,000 yr, the profile is closer to steady state, and the decrease in Tc from the top of the Hanford Sand to the water table is only 9%.

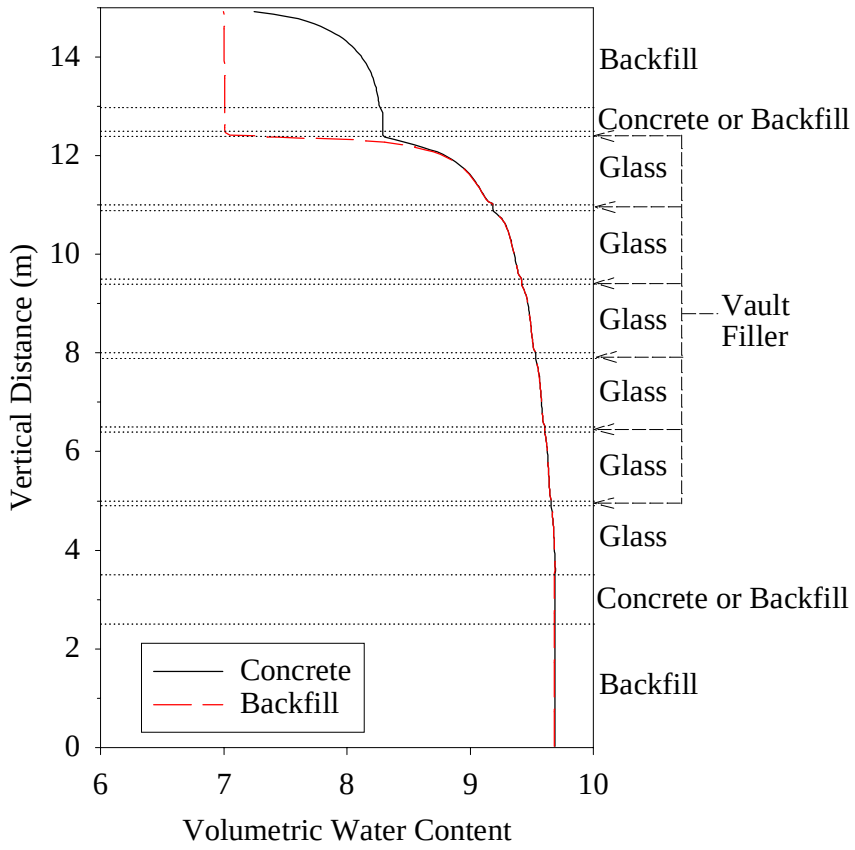

Figure 25. Effect of Concrete on pH for Vault Simulations

Bathtub Effect

This simulation considers the consequences of the trench liner being impermeable to flow, thus causing the trench to become saturated with water. The trench was initially considered to be saturated with water, with no flow across the bottom boundary. Simulated pH (Figure 28) and TcO_4^- concentrations are similar to those predicted by the base case. However, because the total amount of water in the profile is so much higher than for the base case, the total amount of Tc released is much higher.

Higher Waste Loading and Alternate Glass Formulation

The base analysis case uses a Na_2O waste loading of 20 weight percent. Increasing the Na_2O loading in LAW glasses has several impacts that can affect the long-term dissolution rate of the product. First, sodium is a glass "network breaker." Adding sodium to silicate glasses depolymerizes the glass, making its structure less interconnected and, so, generally less durable when contacted by water. Second, increased sodium content may make the glass more susceptible to alkali ion exchange reactions.

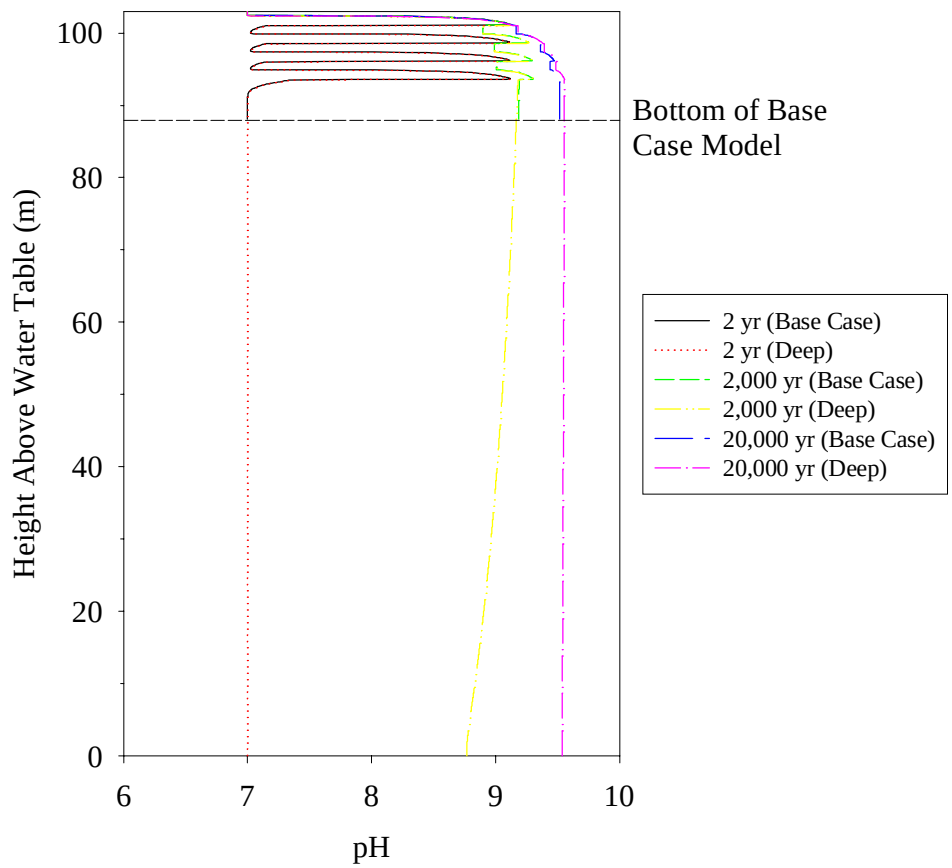

Figure 26. Solution pH Profile for RH Trench Simulation Extended to Water Table (See Figure 7 for location of boundaries between material zones and material names)

The net affect of ion exchange is to raise the pH of water percolating through the disposal system, thereby increasing the glass dissolution rate. Lastly, increasing the Na_2O content tends to expand the stability field and rate of zeolitic alteration phase formation as the glass reacts with water. Zeolite formation can cause dissolution rate excursions, sometimes all the way back to the forward rate of reaction. Thus, higher sodium loading will likely shrink the composition region from which acceptable LAW glasses can be formulated.

There is only a limited experimental base for LAW glasses at other than 20 weight percent Na_2O loading. From the limited data in Figure 30, a simple linear regression gives a slope of $10^{0.2x}$, where x is the mass percent Na_2O. Consequently, a 5 percent increase in Na_2O loading would increase the glass corrosion rate by approximately ten times. However, to conduct a more detailed analysis, laboratory experiments with HLP-31 glass (Vienna et al. 2000), which has a Na_2O loading of 23 weight percent, were performed to establish the necessary input parameters for STORM simulations. The results (see Figure 31) show a very unusual glass corrosion behavior in that the dissolution rate is apparently unaffected by an increasing concentration of silicon in the aqueous phase, up to near saturation with respect to amorphous silica. Also, the congruent release of Na and B indicates that little or no Na ion

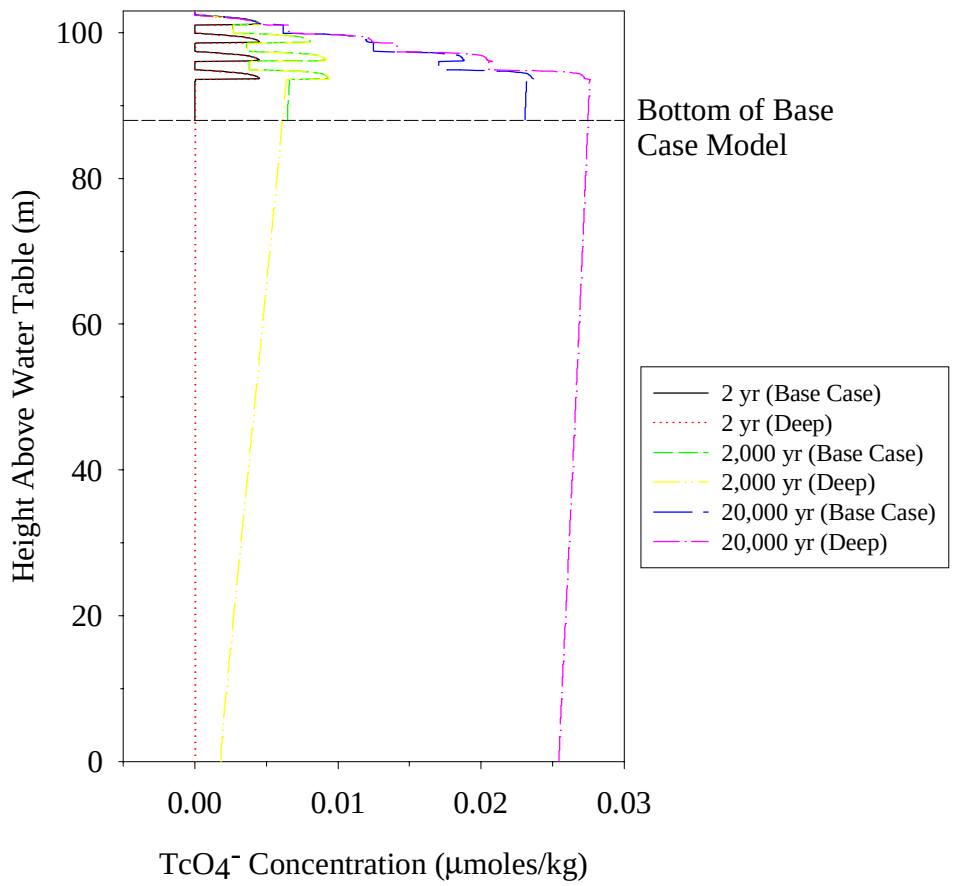

Figure 27. Concentration Profile of TcO_4^- for RH Trench Simulation Extended to Water Table (See Figure 4 for location of boundaries between material zones and material names)

exchange is occurring, despite the higher waste loading. Finally, the forward rate of reaction for this glass is about ten times larger than for LAWABP1 glass at the same temperature and pH. The reasons for this unusual behavior may be related to microscale phase separation as a result of the heat treatment used to simulate canister cooling (McGrail et al. 2001). In any event, to model the performance of this glass in the disposal system, the glass dissolution rate was not allowed to decrease as the Si concentration in the disposal system pore water increased. No experimental data was available on the pH-dependence of the dissolution rate so it was assumed that the reaction rate increased according to $10^{0.5*pH}$, identical to the power law determined for LAWABP1 glass.

The calculated normalized contaminant flux to the vadose zone for HLP-31 glass is 75 to 164 times larger (Table 13) than that for the base case simulation with LAWABP1 glass, as shown in Figure 32. The higher forward reaction rate of HLP-31 glass generates a higher calculated pH in the glass layers as compared with LAWABP1 glass. The combined effect of these factors, and the fact that the rate does not diminish with increasing Si concentration, increases the total release rate much more than the

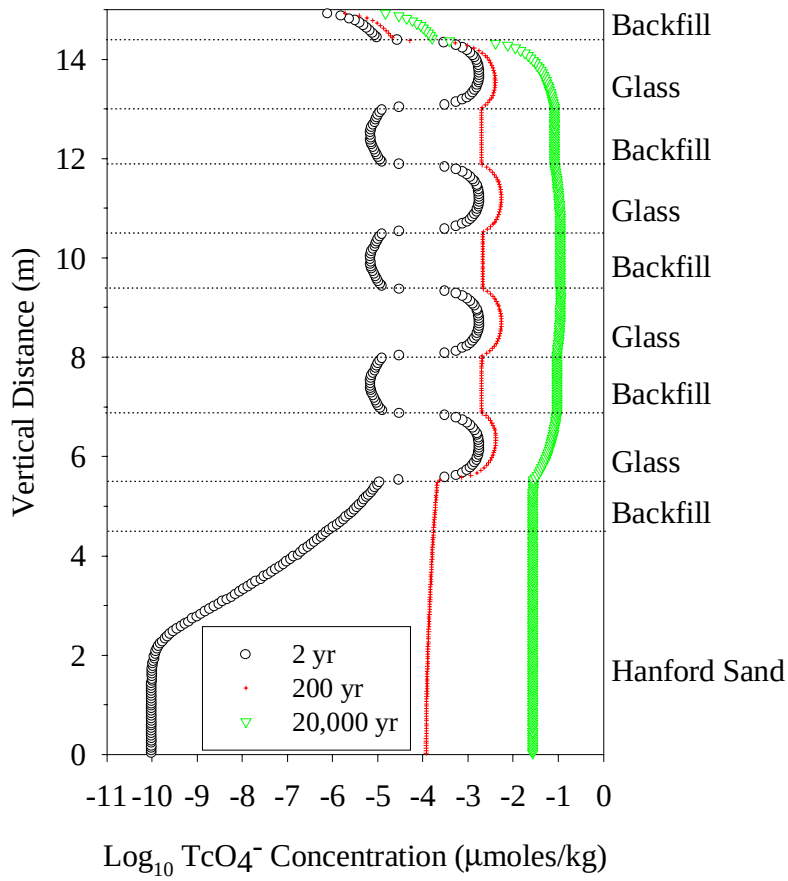

Figure 28. TcO_4^- for Fully-Saturated RH Trench Simulation with no Flow ("bathtub effect")

forward rate difference between the glasses alone would indicate. The decline in release rate after 5,000 years occurs because of the decreasing surface area of HLP-31 glass, which changed very little for the slower dissolving LAWABP1 glass over the same period.

The STORM simulations show the strong sensitivity of release rates to the durability of the glass. Available testing data indicate that Na_2O loadings of 20 to 25 weight percent might be achieved and still produce glasses that will have acceptable long-term performance. VHT testing shows several glasses at 23 weight percent Na_2O loading with a corrosion rate that is nearly as good as LAWABP1 glass (Vienna et al. 2000). Only very limited data at waste loadings above 25 weight percent Na_2O is available. Although it may be possible to formulate acceptable glasses at this waste loading, the acceptable glass composition region will be much smaller than is observed at waste loadings of 20 weight percent Na_2O and lower. Additional studies are needed if waste loadings approaching 25 weight percent Na_2O are desired. Major increases in waste loading on the order of 50 to 100 percent (30 to 40 weight percent Na_2O) are probably not possible with silicate-based glasses. A different glass-forming system, such as

the phosphate system, would need to be considered. However, changing to a different glass forming system would also require a different melter design, flow sheet, etc. Also, non-silicate waste glasses have received almost no attention since the early 1980's. Consequently, a significant research and development effort would be required to evaluate long-term performance issues with these glasses.

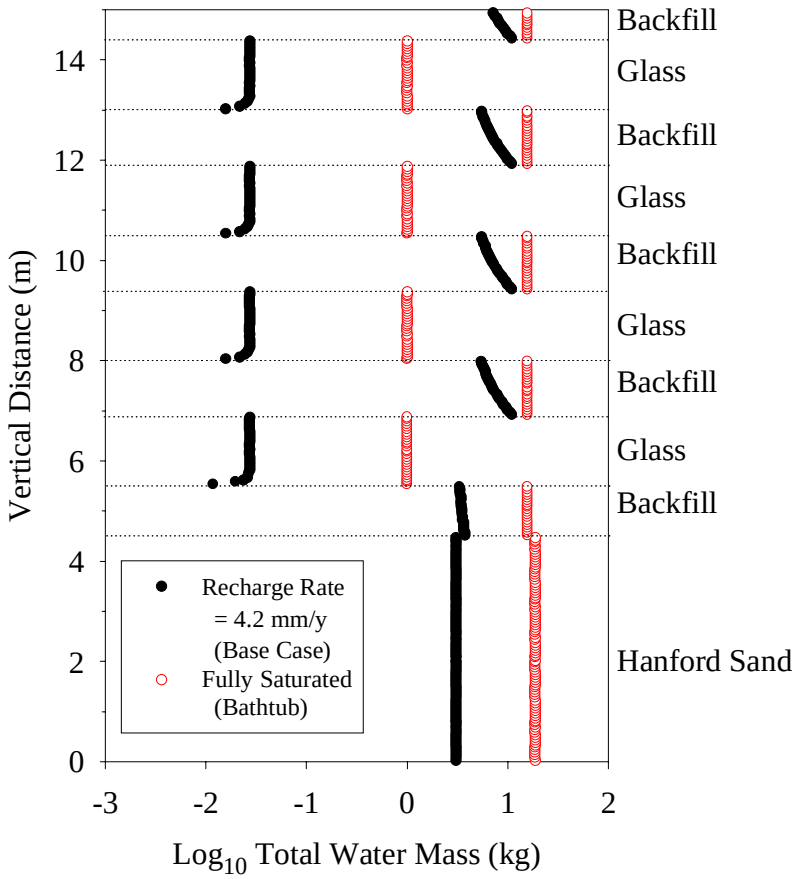

Figure 29. Total Water Mass per Node (each node has a volume of 0.05 m^3) for Fully-Saturated RH Trench Simulation with no Flow ("bathtub effect")

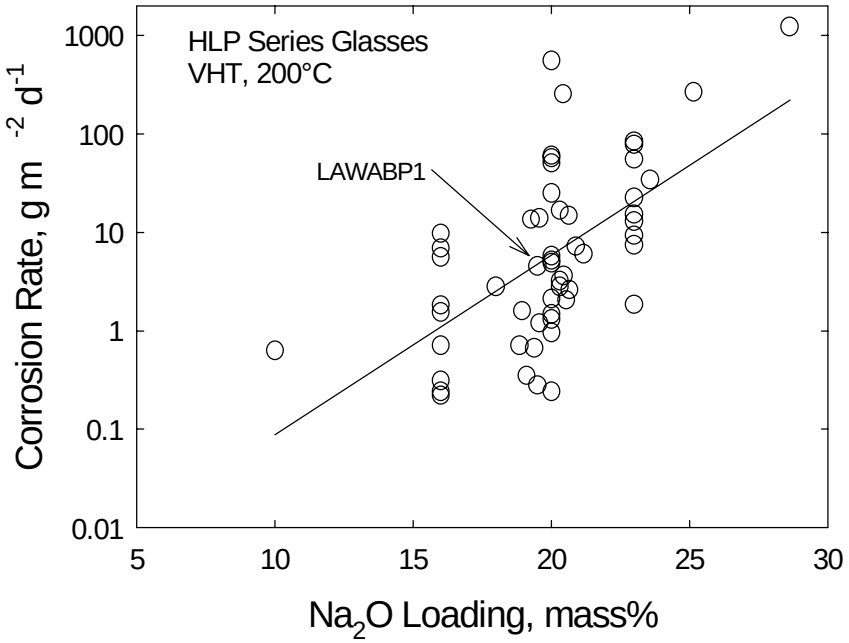

Figure 30. VHT Corrosion Rate as a Function of Waste Loading (Vienna et al. 2000)

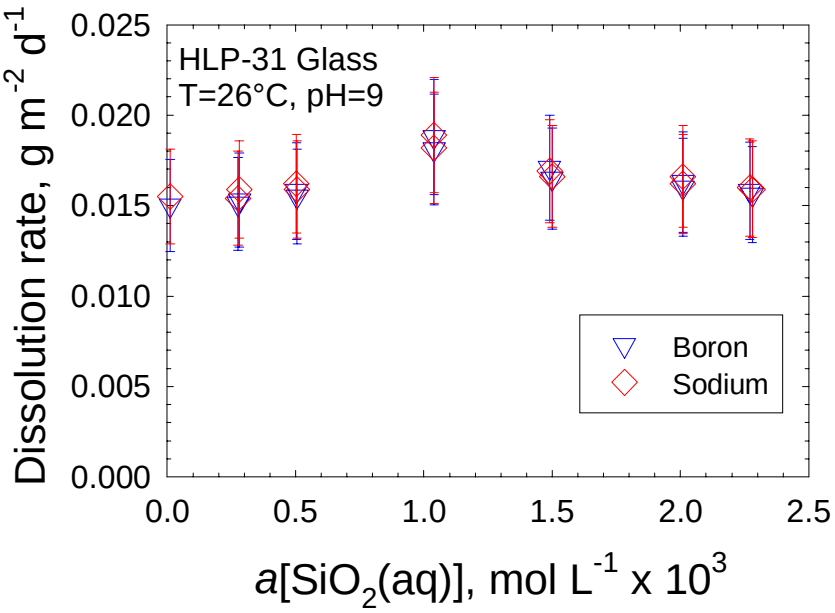

Figure 31. Dependence of HLP-31 Glass Dissolution Rate on Concentration of SiO_2(aq)

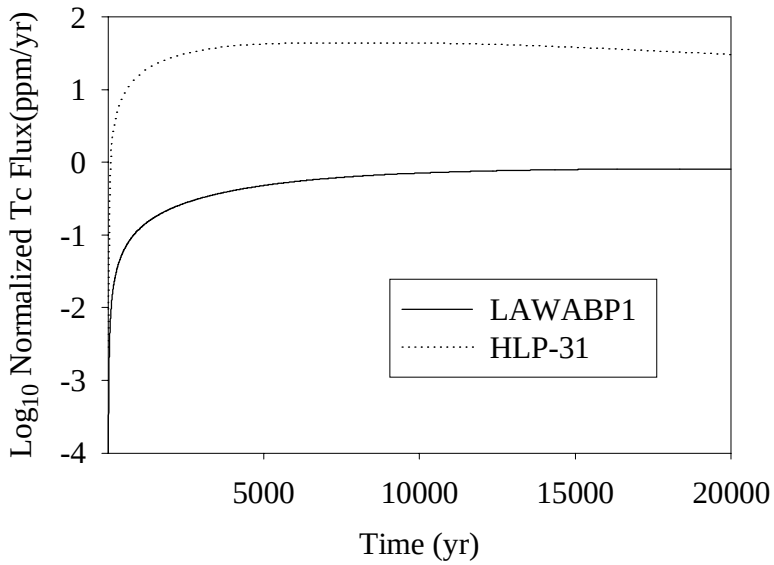

Figure 32. Tc Flux to the Vadose Zone, Relative to the Amount of Tc Originally in LAWABP1 Waste Glass, Comparison of Trench Base Case Simulation with LAWABP1 Glass Replaced by HLP-31 Waste Glass

Conclusion

The maximum normalized Tc release rate from the trench under a recharge rate of 4.2 mm/yr is 0.93 ppm/yr at 100,000 yr. The relevant performance objective of the disposal system for protecting groundwater resources is a beta-photon drinking water dose of no more than 4 mrem/yr (40 CFR 141 1975). Based on estimated transport to a well 100 m down gradient of the disposal facility (Mann et al. 2000), at a recharge rate of 4.2 mm/yr, the maximum allowable Tc release rate is 166 ppm/yr. The Tc release rate predicted by the base case simulation is 200 times less than the maximum allowable Tc release rate. Even the forward rate simulation, which has the highest predicted Tc release rates, is 25 times lower than the maximum allowable Tc release rate.

The sensitivity cases that have significantly higher normalized Tc release rates than the base case are the cases that consider: higher recharge rates, glass dissolution at forward rate of reaction, backfill replaced with sand, stainless steel mixed with glass, and the vault scenarios (Table 13). The sensitivity cases that have significantly lower normalized Tc release rates than the base case are the cases that consider: lower recharge rates, increased diffusion coefficient for all species, and the 2-D simulations. The sensitivity cases that are not significantly different than the base case are the cases that consider: no ion exchange, no secondary mineral formation, added conditioning layer at the top of the trench, stainless steel added at edges of glass layers, and U release. However, simulations including the stainless steel showed four orders of magnitude higher release rates of Cr(VI) due to the short release time relative to the glass and 100X higher inventory of Cr in the steel. In contrast, precipitation of theophrastite, $Ni(OH)_2$, limited Ni release rates to 1 to 3 orders of magnitude lower than those for Cr.

The results of these simulations display the complex interactions between the waste glass, native materials, and secondary minerals. The importance of having accurate rate constant data is shown by the difference between the base case and forward rate simulations. The need to accurately characterize the hydraulic properties of the materials in the disposal facility is shown by the significant effect of replacing the trench backfill material with sand. The importance of considering the proper spatial relationships between the different materials is highlighted by the 10X difference in Tc release between the two simulations where the stainless steel containers are treated as thin layers versus homogeneous mixing with the glass.

The exceedingly long time (months) required to conduct full 2-D simulations needs to be addressed if STORM is to be used for more extensive modeling studies. Improvements in execution speed can be obtained by implementing faster and more robust numerical algorithms to speed the rate of convergence and by substituting parallel algorithms for the principal time-consuming numerical routines in the code. This would allow execution of STORM on today's fastest massively parallel computers.

Table 13. Summary of Waste Form Sensitivity Calculations

Case	Description	Basic Model	Note	Radionuclide Flux Ratio @ 1,000 yr	Radionuclide Flux Ratio @ 10,000 yr	Reason Radionuclide Flux Ratio is Higher or Lower Than Base Case
WFA	4.2 mm/yr infiltration	Trench		1	1	This is the base case
WFB	Forward rate, 4.2 mm/yr infiltration	Trench		9.9	8.7	Forward rate
WFC	4.2 mm/yr infiltration	Vault		8.5	2.7	Vault, glass packed closer, higher pH
WFD	0.1 mm/yr infiltration	Trench		0.0004	0.0004	Lower recharge
WF1	Assume no Ion Exchange	Trench		0.8	0.8	Lower pH
WF2	Assume no Secondary Phase Formation	Trench		0.51	0.53	Higher Si concentration
WF4	0.9 mm/yr infiltration rate	Trench		0.016	0.016	Lower recharge
WF6	50 mm/yr infiltration rate	Trench		20.9	3.4	Higher recharge
WF7	0.5 mm/yr infiltration rate	Trench		0.005	0.004	Lower recharge
WF8	10 mm/yr infiltration rate	Trench		8.4	2.6	Higher recharge
WF9	Extend WFA to groundwater	Trench		0.93	1.09	Deeper lower boundary
WF10	Add conditioning layer at top	Trench		0.99	0.92	Higher Si concentration
WF11	Change filler material in trench to sand	Trench		9.1	1.6	Water content/diffusion higher in sand
WF14	Increase diffusion for all aqueous species by a factor of 10	Trench		0.06	0.01	Lower pH
WF16	Replace concrete everywhere with backfill material	Vault		9.1	2.5	Vault, glass packed closer, higher pH
WF19	0.9 mm/yr infiltration rate	Vault		0.75	0.20	Vault, lower recharge
WF21	0.1 mm/yr infiltration	Vault	Could not converge after 1,800 yr	0.055	-	Vault, lower recharge
WF25	Include steel in waste packages	Trench		1.03 (49,000	1.02 (4,100)	Steel corrosion increases pH, note: values in parentheses are Cr flux ratios relative to base case
WF26	Replace Tc w/U	Trench		1.03	0.99	Soddyite precipitation
WF27	Full 2-D simulation	Trench	Could not converge after 2,000 yr	2.65	0.46	Lower water flux through glass
WF28/ WFx	Increase Waste Loading / Alternate Glass Formulation (HLP-31)	Trench	Could not converge after 5,500 yr	164	76	Higher release rate, no dependence on Si
WF30	Increase ion exchange rate by 5 times for WFB	Trench		12.17	9.51	Forward rate, higher pH

References

40 CFR 141. 1975. U.S. Environmental Protection Agency, "National Primary Drinking Water Regulations." *US Code of Federal Regulations*.

Bacon DH, MD White, and BP McGrail. 2000. *Subsurface Transport Over Reactive Multiphases (STORM): A General, Coupled, Nonisothermal Multiphase Flow, Reactive Transport, and Porous Medium Alteration Simulator, Version 2, User's Guide*. PNNL-13108, Pacific Northwest National Laboratory, Richland, Washington.

Cloke PL, DM Jolley, and DH Lester. 1997. *Waste Package Development Design Analysis*. BBA000000-01717-0200-0050 Rev. 00, CRWMS/M&O, Las Vegas, Nevada.

Daveler SA, and TJ Wolery. 1992. *EQPT, A Data File Preprocessor for the EQ3/6 Software Package: User's Guide and Related Documentation (Version 7.0)*. UCRL-MA-110662 PT II, Lawrence Livermore National Laboratory, Livermore, California.

Farnsworth RK, MKW Chan, and SC Slate. 1985. "The Effect of Radial Temperature Gradients on Glass Fracture in Simulated High-Level Waste Canisters." *Mat. Res. Soc. Symp. Proc.*, 44:831-838.

Fayer MJ, EM Murphy, JL Downs, FO Khan, CW Lindenmeier, and BN Bjornstad. 1999. *Recharge Data Package for the Immobilized Low-Activity Waste 2001 Performance Assessment*. PNNL-13033, Pacific Northwest National Laboratory, Richland, Washington.

Grenthe I, J Fuger, RJM Konings, RJ Lemire, AB Muller, C Nguyen-Trung, and H Wanner. 1992. *Chemical Thermodynamics, Volume 1: Chemical Thermodynamics of Uranium*. North-Holland, Amsterdam.

Jantzen C. 1984. "Methods of simulating low redox potential (Eh) for a basalt repository." *Mat. Res. Soc. Symp. Proc.*, 26:613-621.

Kaplan DI, and RJ Serne. 1999. *Geochemical Data Package for the Hanford Immobilized Low-Activity Tank Waste Performance Assessment (ILAW-PA)*. PNNL-13037, Pacific Northwest National Laboratory, Richland, Washington.

Khaleel R. 1999. *Far-Field Hydrology Data Package For Immobilized Low-Activity Tank Waste Performance Assessment*. HNF-4769, Rev. 1, Fluor Daniel Northwest, Inc., Richland, Washington.

Krupka KM, and RJ Serne. 1998. *Effects on Radionuclide Concentrations by Cement/Ground-Water Interactions in Support of Performance Assessment of Low-Level Radioactive Wate Disposal Facilities*. PNNL-11408, NUREG/CR-6377, Pacific Northwest National Laboratory, Richland, Washington.

Mann FM, SH Finfrock, EJ Freeman, RJ Puigh, II, DH Bacon, MP Bergeron, BP McGrail, and SK Wurstner. 2000. *White Paper Updating Conclusions of 1998 ILAW Performance Assessment*. DOE/ORP-2000-07 Rev. 0, Department of Energy, Office of River Protection, Richland, Washington.

Mann FM, RJ Puigh, II, CR Eiholzer, Y Chen, NW Kline, AH Lu, BP McGrail, PD Rittmann, GF Williamson, NR Brown, and PE LaMont. 1998. *Hanford Immobilized Low Activity Tank Waste Performance Assessment*. DOE/RL-97-69 Rev. B, Project Hanford Management Contractor, Richland, Washington.

McGrail B. 1986. "Waste package component interactions with Savannah River defense waste glass in a low-magnesium salt brine." *Nuc. Tech.*, 75(2):168-186.

McGrail BP, and DH Bacon. 1998. *Selection of a Computer Code for Hanford Low-Level Waste Engineered-System Performance Assessment*. PNNL-10830 Rev. 1, Pacific Northwest National Laboratory, Richland, Washington.

McGrail BP, DH Bacon, JP Icenhower, WL Ebert, PF Martin, HT Schaef, and EA Rodriguez. 2000. *Waste Form Release Data Package for the 2001 Immobilized Low-Activity Waste Performance Assessment*. PNNL-13043, Rev. 1, Richland, Washington.

McGrail BP, DH Bacon, JP Icenhower, WL Ebert, PF Martin, HT Schaef, and EA Rodriguez. 2001. *Waste Form Release Data Package for the 2001 Immobilized Low-Activity Waste Performance Assessment*. PNNL-13043, Rev. 2, Richland, Washington.

Meyer PD, and RJ Serne. 1999. *Near Field Hydrology Data Package for the Immobilized Low-Activity Waste 2001 Performance Assessment*. PNNL-13035, Richland, Washington.

Peters RD, and SC Slate. 1981. "Fracturing of Simulated High-Level Waste Canisters." *Nuc. Eng. Design*, 67:425-445.

Puigh R. 1999. *Disposal Facility Data for the Hanford Immobilized Low-Activity Tank Waste*. HNF 4950 Rev. 0, Washington, Richland.

Shock EL, and HC Helgeson. 1988. "Calculation of the thermodynamic and transport properties of aqueous species at high pressures and temperatures: Correlation algorithms for ionic species and equation of state predictions to 5kb and 1000°C." *Geochim. Cosmochim. Acta*, 52:2009-2036.

Shock EL, HC Helgeson, and DA Sverjensky. 1989. "Calculation of the thermo-dynamic and transport properties of aqueous species at high pressures and temperatures: Standard partial molal properties of inorganic neutral species." *Geochim. Cosmochim. Acta*, 53:2157-2183.

Sverjensky D, and N Sahai. 1996. "Theoretical prediction of single-site surface-protonation equilibrium constants for oxides and silicates in water." *Geochim. Cosmochim. Acta*, 60:3773-3797.

Vienna JD, A Jiricka, BP McGrail, BM Jorgensen, DE Smith, BR Allen, JC Marra, DK Peeler, KG Brown, IA Reamer, and WL Ebert. 2000. *Hanford Immobilized LAW Product Acceptance Testing: Initial Data Package*. PNNL-13101, Pacific Northwest National Laboratory, Richland, Washington.

Wolery TJ, and SA Daveler. 1992. *EQ6, A Computer Program for Reaction Path Modeling of Aqueous Geochemical Systems: Theoretical Manual, User's Guide, and Related Documentation (Version 7.0)*. UCRL-MA-110662 PT IV, Lawrence Livermore National Laboratory, Livermore, California.

Wootan DW. 1999. *Immobilized Low-activity Tank Waste Inventory Data Package*. HNF-4921, Rev. 0, Fluor Daniel Northwest, Inc., Richland, Washington.

APPENDIX C

PNNL-13400

APPENDIX C

Groundwater Flow and Transport Calculations Supporting the Immobilized Low-Activity Waste Disposal Facility Performance Assessment

M. P. Bergeron
S. K. Wurstner

December 2000

Prepared for
the U.S. Department of Energy
under Contract DE-AC06-76RLO 1830

Pacific Northwest National Laboratory
Richland, Washington 99352

DISCLAIMER

This report was prepared as an account of work sponsored by an agency of the United States Government. Neither the United States Government nor any agency thereof, nor Battelle Memorial Institute, nor any of their employees, makes **any warranty, expressed or implied, or assumes any legal liability or responsibility for the accuracy, completeness, or usefulness of any information, apparatus, product, or process disclosed, or represents that its use would not infringe privately owned rights.** Reference herein to any specific commercial product, process, or service by trade name, trademark, manufacturer, or otherwise does not necessarily constitute or imply its endorsement, recommendation, or favoring by the United States Government or any agency thereof, or Battelle Memorial Institute. The views and opinions of authors expressed herein do not necessarily state or reflect those of the United States Government or any agency thereof.

PACIFIC NORTHWEST NATIONAL LABORATORY
operated by
BATTELLE MEMORIAL INSTITUTE
for the
UNITED STATES DEPARTMENT OF ENERGY
under Contract DE-AC06-76RLO 1830

Printed in the United States of America

**Available to DOE and DOE contractors from the
Office of Scientific and Technical Information, P.O. Box 62, Oak Ridge, TN 37831;
prices available from (865) 576-8401.**

**Available to the public from the National Technical Information Service,
U.S. Department of Commerce, 5285 Port Royal Rd., Springfield, VA 22161**

Summary

This report summarizes the Hanford Site-Wide Groundwater Model and its application to the Immobilized Low-Activity Waste (ILAW) Disposal Facility Performance Assessment (PA). The site-wide model and supporting local-scale models are used to evaluate impacts from the transport of contaminants at a hypothetical well 100 m downgradient of the disposal facilities and to evaluate regional flow conditions and transport from the ILAW disposal facilities to the Columbia River. These models were used to well-intercept factors (WIFs) or dilution factors from a given areal flux of a hypothetical contaminant released to the unconfined aquifer from the ILAW disposal facilities for two waste-disposal options: 1) a remote-handled trench concept and 2) a concrete-vault concept. The WIF is defined as the ratio of the concentration at a well location in the aquifer to the concentration of infiltrating water entering the aquifer. These WIFs are being used in conjunction with calculations of released contaminant fluxes through the vadose zone to estimate potential impacts from radiological and hazardous chemical contaminants within the ILAW disposal facility at compliance points.

Transport model calculations for a basecase considered a six trench configuration representing a remote-handled-trench concept and were based on local-scale flow conditions postulated after site-closure. These conditions were developed based on boundary conditions provided by the steady-state simulation of Post-Hanford flow conditions performed with the site-wide model.

Regional and local-scale flow results for the base case show that groundwater beneath the ILAW site moves in a southeasterly direction and then an easterly direction over about 15 km before reaching the Columbia River. For the six remote-handled trench configuration examined in the base case, predicted concentration profiles reach steady state within about 10 yr after the start of source release at the water table.

Concentration levels, based on an assumed infiltration rate of 4.2 mm/yr and input concentration of 1 Ci/m^3 at the source release area, reach a maximum value of 1.1×10^{-3} Ci/m^3 at a hypothetical 100-m well downgradient of the site and 7.8×10^{-4} Ci/m^3 at a 1-km well. For this assumed recharge rate (4.2 mm/yr), the calculated WIFs would be 1.1×10^{-3} at the 100-m well and 7.8×10^{-4} at the 1-km well.

Calculations of the WIFs in this analysis in general yielded different levels of dilution than those developed in previous calculations of an ILAW disposal-facility performed by Lu (1996). The differences in the calculated WIFs can be attributed to a number of factors.

The Lu (1996) analysis estimated the water table beneath the facility to be at about the same level considered in this analysis, but assumed that the water table would be situated in the Ringold Formation. The current model predicted that the water table would largely be along the edge of a

buried channel containing very permeable Hanford Formation. The difference in the distribution and hydraulic properties between the two conceptual models has led to higher levels of dilution using the current model. Additional work with the current model will be needed to evaluate the predictability of the WIF as a function of the hydraulic properties of the major hydrogeologic units beneath the facility.

Differences in the conceptual model of the unconfined aquifer used in the current analysis resulted in differences in the simulated direction of flow. The analysis by Lu (1996) predicted an easterly flow direction. The current local-scale model predicts a southeasterly flow direction. This difference in flow direction may be primarily attributable to including the highly permeable ancestral channel of the Columbia River, which contains the Hanford Formation in this analysis. The differences may also be a function of including natural recharge in the current regional-scale and local-scale analysis. Further work with the local-scale model will be needed to evaluate the predictability of the WIF as a function of the direction of flow.

Key factors affecting the current calculations appear to be related to the use of higher estimated hydraulic conductivities and groundwater velocities beneath the facility by the current model. The hydraulic conductivities used by the current model and the previous model used by Lu (1996) for the Ringold Formation are on the same order of magnitude (between 40 and 300 m/day in the current model; between 70 and 245 m/day in the model used by Lu [1996]). However, the current model contains areas of the Hanford formation beneath the facility and as a result has areas of very high permeability (between 2,200 and 30,000 m/day) in the area of the source release.

Uncertainties in the following key factors affecting calculated WIFs were investigated with sensitivity analyses:

- the source-release area at the water table
- the vertical position of the post-closure water table and the associated direction of groundwater flow
- the lateral position of the Hanford-Ringold Formation contact
- the hydraulic properties of Hanford and Ringold sediments.

Results of these analyses suggested that calculated WIFs are linearly related to the source-release area over the range of assumed surface areas of release. Calculated WIFs are also affected by the long-term predicted position of the water table and the resulting estimated distribution of hydraulic properties underlying the ILAW disposal facilities. The new facility is located in an area of the Hanford Site where it is underlain by an ancestral channel of the Columbia River that consists of highly permeable sediments of the Hanford Formation. For the predicted water table position used in this analysis, the current interpretation places the contact between the Hanford Formation and the

underlying less-permeable Ringold Formation along the south edge of the new ILAW disposal facility area.

Assumptions made about long-term regional natural recharge rates and boundary conditions are uncertain and can also change the predicted position of the water table and the position of the contact between the Hanford and Ringold sediments. Higher assumed rates of recharge can increase the water-table elevation and the level of saturation in the Hanford-formation sediments, leading to lower calculated WIFs (i.e., higher levels of dilution) from releases from the ILAW facilities.

Estimates of the hydraulic properties used in this assessment are based on past calibration of the site-wide model that provides a reasonable approximation of the regional observations and trends. Estimates of these properties on the local-scale model used in this analysis are uncertain and can affect calculated WIFs. Reducing the estimated hydraulic conductivities of the Hanford formation underlying the disposal facilities to those estimated for the Ringold Formation resulted in an order of magnitude increase in the WIFs (i.e., less dilution) from releases from the ILAW disposal facilities.

Reference

A. H. Lu. 1996. *Contaminant Transport in the Unconfined Aquifer, Input to the Low Level Tank Waste Interim PA*, WHC-SD-WM-RPT-241, Westinghouse Hanford Company, Richland, Washington.

Acronyms

CFEST	Coupled Fluid, Energy, and Solute Transport
Dl	longitudinal dispersivity
DOE	U.S. Department of Energy
DOE-RL	DOE-Richland Operations
Dt	transverse dispersivity
HPDE	high density polyethylene
ILAW	Immobilized Low-Activity Waste
LLW	low-level waste
PA	Performance Assessment
PUREX	Plutonium-Uranium Extraction
RCRA	Resource Conservation and Recovery Act
RI/FS	Remedial Investigation/Feasibility Study
RL	Richland Operations Office
WIF	Well Intercept Factor

Contents

Summary C-3

Acronyms C-6

1.0 Introduction C-15

2.0 Disposal Facility and Site Information C-16

2.1 Geography of the Hanford Site C-16
2.2 Disposal Facility Design C-16
2.2.1 New ILAW Disposal Area C-19
2.2.2 Existing Disposal Area C-22

3.0 Relation of Groundwater Modeling to LAW Disposal Facility Assessment C-24

3.1 Overall Strategy for Disposal Facility Assessment C-24
3.2 Integration of Individual Model Component Results C-28

4.0 Conceptual and Numerical Model Framework C-30

4.1 Hydrogeologic Framework C-30
4.2 Recharge and Aquifer Boundaries C-32
4.3 Flow and Transport Properties C-33

5.0 Groundwater Flow and Contaminant Transport Calculations C-36

5.1 Site-Wide Flow and Transport Simulations C-36
5.1.1 Site-Wide Steady-State Flow Conditions C-36
5.1.2 Contaminant Transport Between Disposal Facilities and Columbia River C-39

5.2 Local-Scale Model Development and Description C-40
5.2.1 Grid Designs C-40
5.2.2 Hydraulic Properties C-45
5.2.3 Transport Properties C-46

6.0 Results of the Groundwater Transport Analysis C-59

6.1 New Disposal Facility C-59
6.1.1 Remote-Handled Trench Concept C-59
6.1.2 Concrete Vault Concept C-61

6.2 Existing Disposal Facility C-63
6.2.1 Concrete Vault Concept C-64

7.0 Results of Sensitivity Analysis C-83

7.1 Disposal Site Location (Case 1) C-83
7.2 Disposal Site Orientation (Case 2) C-84
7.3 Pumping at 100-m (328-ft) Well (Case 3) C-85
7.4 Reduction in Hydraulic Properties of Hydrogeologic Unit at Water Table (Case 4) .. C-85
7.5 Increasing Surface Area of Release (Case 5 and 6) C-87
7.6 Changes in the Position of the Water Table C-88
7.6.1 Increase in Regional Areal Recharge (Case 7) C-89
7.6.2 Decrease in Regional Areal Recharge (Case 8) C-89
7.6.3 Decrease in Regional Upgradient Boundary Fluxes (Case 9) C-91

8.0 Summary and Conclusions C-112

9.0 References C-114

Figures

2.1 Map of the Hanford Site and Its Location Within Washington C-17

2.2 Location of the ILAW Disposal Site in the 200 East Area C-18

2.3 Remote-Handled Trench Pre-Conceptual Layout at the ILAW Disposal Site..... C-20

2.4 Remote-Handled Trench Pre-Conceptual Design C-21

3.1 Eight Sequential Steps for the Groundwater Pathway C-25

3.2 Modeling Strategy for Assessing ILAW Disposal System C-27

4.1 Comparison of Generalized Geology and Hydrostratigraphic Columns C-31

4.2 Hydraulic Conductivity Distribution Obtained from Inverse Calibration for 1979 Conditions..... C-34

5.1 Predicted Water Table for Post-Hanford Conditions for Assumed Steady-State Conditions C-38

5.2 Predicted Water Table for Post-Hanford Conditions for Assumed Steady-State Conditions between ILAW Disposal Facility and Columbia River C-39

5.3 Finite Element Grid Used in Local-Scale Model at the New ILAW Disposal Facility Area..... C-42

5.4 Finite Element Grid Used in the Local-Scale Model at the Existing ILAW Disposal Facility Area..... C-43

5.5 Three-Dimensional Distribution of Major Hydrogeologic Units in the New Local-Scale Model C-44

5.6 Three-Dimensional Distribution of Major Hydrogeologic Units in the Existing Local Scale Model..... C-45

5.7 Distribution of Hydraulic Conductivities Used in the Local-Scale Model of the New ILAW Disposal Facility..... C-47

5.8 Distribution of Hydraulic Conductivities used in the Local Scale Model of the Existing ILAW Disposal Facility Area C-53

6.1 Distribution of Hydraulic Head in Unconfined Aquifer in Local-Scale Model – New Disposal Facility Area C-67

6.2 Areal Distribution of Contaminant Plume Resulting the Remote-Handled Trench Concept, New Disposal Facility Area C-68

6.3 Vertical Distribution of a Contaminant Plume Resulting the Remote-Handled Trench Concept (Along the Approximate Centerline of the Plume) – New Disposal Facility Area C-69

6.4 Concentration History at 100-m (328-ft) and 1000-m (3281-ft) Wells, Local Scale Model – New Disposal Facility Area C-70

6.5 Areal Distribution of Contaminant Plume between ILAW New Facility and Columbia River, Remote Trench Concept – New Disposal Facility Area C-71

6.6 Concentration History at Selected Well Locations, Site-Wide Model, – New Disposal Facility Area C-72

6.7 Areal Distribution of Contaminant Plume Resulting from the Concrete Vault Concept – New Disposal Facility Area C-73

6.8 Vertical Distribution of a Contaminant Plume Resulting from the Simulation of the Concrete Vault Concept (Along the Approximate Centerline of the Plume) – New Disposal Facility Area C-74

6.9 Concentration History at 100-m (328-ft) and 1000-m (3281-ft) Wells, Local Scale Model, Concrete Vault Concept – New Disposal Facility Area C-75

6.10 Areal Distribution of Contaminant Plume Between ILAW New Facility and Columbia River, Concrete Vault Concept – New Disposal Facility Area C-76

6.11 Concentration History at Selected Well Locations, Site-Wide Model – Concrete Vault Concept – New Disposal Facility Area C-77

6.12 Areal Distribution of a Contaminant Plume Resulting from the Simulation of the Concrete Vault Concept – Existing Disposal Facility Area C-78

6.13 Vertical Distribution of a Contaminant Plume Resulting from the Concrete Vault Concept (Along the Approximate Centerline of the Plume) – Existing Disposal Facility Area C-79

6.14 Concentration History at 100-m (328-ft) and 1000-m (3281-ft) Wells, Local Scale Model – Existing Disposal Facility Area C-80

6.15 Areal Distribution of Contaminant Plume Between ILAW New Facility and Columbia River, Concrete Vault Concept – Existing Disposal Facility C-81

6.16 Concentration History at Selected Well Locations, Site-Wide Model – Existing Disposal Facility Area C-82

7.1 Areal Distribution of Contaminant Plume Resulting from the Remote-Handled Trench Concept – Sensitivity to Placing Disposal Trenches at South End of Disposal Facility Area C-92

7.2 Areal Distribution of Contaminant Plume Resulting from the Remote-Handled Trench Concept – Sensitivity to Rotation of Remote Handled Trenched by 90 degrees C-93

7.3 Local-Scale Model Head Distribution Resulting from the Remote-Handled Trench Concept – Sensitivity to Increased Pumping at 100-m (328-ft) Well: A) 30 l/Day, B) 100 l/Day, C) 300 l/Day, and D) 1000 l/Day C-94

7.4 Distribution of Hydraulic Conductivity Used in Decreased Hydraulic Conductivity Sensitivity Case C-98

7.5 Local-Scale Head Distribution Resulting from Decreased Hydraulic Conductivity of Hanford Formation C-99

7.6 Areal Distribution of Contaminant Plume Resulting from the Remote-Handled Trench Concept – Sensitivity to Decreased Hydraulic Conductivity of Hanford Formation C-100

7.7 Areal Distribution of Contaminant Plume Resulting from the Remote-Handled Trench Concept – Sensitivity to Increase in Source-Release Area (Case 5) C-101

7.8 Areal Distribution of Contaminant Plume Resulting from the Concrete Vault Concept – Sensitivity to Increase in Source-Release Area (Case 6) C-102

7.9 Regional-Scale Head Distribution Resulting from Increased (Factor of 3) Regional Natural Recharge C-103

7.10 Local-Scale Head Distribution Resulting from Increased (Factor of 3) Regional Natural Recharge C-104

7.11 Areal Distribution of Contaminant Plume Resulting from the Remote-Handled Trench Concept – Sensitivity to Increased (Factor of 3) Regional Natural Recharge C-105

7.12 Regional-Scale Head Distribution Resulting from Decreased (Factor of 3) Regional Natural Recharge C-106

7.13 Local-Scale Head Distribution Resulting from Decreased (Factor of 3) Regional Natural Recharge C-107

7.14 Areal Distribution of Contaminant Plume Resulting from the Remote-Handled Trench Concept – Sensitivity to Decreased (Factor of 3) Regional Natural Recharge..... C-108

7.15 Regional-Scale Head Distribution Resulting from Decreased (Factor of 3) Regional Natural Recharge C-109

7.16 Local-Scale Head Distribution Resulting from Decreased (Factor of 2) Regional Boundary Flux C-110

7.17 Areal Distribution of Contaminant Plume Resulting from the Remote-Handled Trench Concept – Sensitivity to Decreased (Factor of 2) Regional Boundary Flux..... C-111

Tables

6.1 Well Intercept Factors at the 100-m (328-ft) and 1000-m (3280-ft) Wells for the Remote-Handled-Trench Disposal Concept Using Different Infiltration Rates C-60

6.2 Well Intercept Factors at Several Downgradient Well Locations for the Remote-Handled-Trench Disposal Concept Using Different Infiltration Rates C-61

6.3 Well Intercept Factors at 100-m (328-ft) and 1000-m (3280-ft) Well Locations for the Concrete-Vault Disposal Concept Using Different Infiltration Rates C-62

6.4 Well Intercept Factors at Several Downgradient Well Locations for the Concrete-Vault Disposal Concept Using Different Infiltration Rates C-63

6.5 Well Intercept Factors at 100-m (328-ft) and 1000-m (3281-ft) Well Locations for the Concrete Vault Disposal Concept Using Different Infiltration Rates C-65

6.6 Well Intercept Factors at Several Downgradient Well Locations for the Concrete-Vault Disposal Concept Using Different Infiltration Rates C-66

7.1 Well Intercept Factors at 100-m (328-ft) and 1000-m (3281-ft) Wells for the Remote-Handled Trench Disposal Concept with all trenches Situated in the south end of the New Disposal Facility (Case 1)..... C-84

7.2 Well Intercept Factors at 100-m (328-ft) and 1000-m (3281-ft) Wells for the Remote-Handled Trench Disposal Concept with a 90 Degree Change in Trench Orientation (Case 2)..... C-84

7.3 Well Intercept Factors at the 100-m (328-ft) and 1000-m (3281-ft) Wells for the Remote-handled Trench Disposal Concept Using Increased Pumping Rates at the 100-m (328-ft) Downgradient Well (Case 3)..... C-86

7.4 Well Intercept Factors at 100-m (328-ft) and 1000-m (3281-ft) Wells for the Remote-Handled Trench Disposal Concept Using a Reduction in the Hydraulic Conductivity of the Hanford formation (Case 4) C-87

7.5 Well Intercept Factors at 100-m (328-ft) and 1000-m (3281-ft) Wells for the Remote-Handled Trench Disposal Concept Using an Increase in Source Area of Release (Case 5)..... C-88

7.6 Well Intercept Factors at 100-m (328-ft) and 1000-m (3281-ft) Wells for the Concrete-Vault Disposal Concept Using an Increase in Source Area of Release (Case 6) C-88

7.7 Well Intercept Factors at 100-m (328 ft) and 1000-m (3281-ft) Wells for the Remote-handled Trench Disposal Concept Using an Increase (Factor of 3) in Regional Natural Recharge Rates (Case 7) C-89

7.8 Well Intercept Factors at 100-m (328 ft) and 1000-m (3281-ft) Wells for the Remote-handled Trench Disposal Concept Using a Decrease (Factor of 3) in Regional Natural Recharge Rates (Case 8) C-90

7.9 Well Intercept Factors at 100-m (328-ft) and 1000-m (3281-ft) Wells for the Remote-Handled Trench Disposal Concept Using a Decrease (Factor of 2) in Regional Boundary Fluxes (Case 9) C-91

1.0 Introduction

This report summarizes methods and results of groundwater flow and transport analyses used to support the Immobilized Low Activity Waste (ILAW) disposal facility performance assessment (PA). The waste stored in the ILAW disposal facility will migrate downward through the vadose zone into the underlying unconfined aquifer system. Contaminants entering into the unconfined aquifer will migrate laterally within the aquifer until they are discharged into the Columbia River downgradient of the disposal facilities.

The flow and transport analysis applied to this assessment used site-wide and local-scale models. A regional scale site-wide groundwater model was used to evaluate regional flow conditions and transport from the ILAW disposal facility to the Columbia River. Local-scale models were used to evaluate impacts from the transport of contaminants at a hypothetical well 100 m downgradient of the disposal facility.

The development and calibration of the site-wide model that was used are described in detail in Wurstner et al. (1995) and Cole et al. (1997). The primary objectives in using the site-wide model to support the ILAW PA are to 1) develop a conceptual model describing the general flow regime for post-Hanford conditions following the cessation of past and current liquid-waste discharges to the vadose zone and groundwater systems at the Hanford Site, 2) ensure that hydraulic properties used for both the site-wide groundwater model and local-scale models are consistent and adequately simulate local-scale conditions, and 3) evaluate the regional distribution and concentration trends of contaminant plumes that could potentially develop beneath the ILAW disposal facility.

Section 2.0 of this report provides an overview of the Hanford Site and describes the disposal-facility design. Section 3.0 describes the relation of the groundwater modeling component of the ILAW disposal facility PA to other model components used in the analysis. Section 4.0 provides a brief history and chronology of the development of the site-wide conceptual and numerical model framework used in the analysis, and the data and methods used in performing the groundwater analysis within the overall ILAW PA methodology. Section 5.0 provides groundwater flow and transport calculations. Section 6.0 provides the results from applying the groundwater flow and transport analysis of well intercept factors (WIFs) calculated using both the local-scale and site-wide scale models. Section 7.0 provides results of a series of sensitivity analyses that were performed to evaluate the effect of several factors on modeling results, and conclusions are provided in Section 8.0.

2.0 Disposal Facility And Site Information

2.1 Geography of the Hanford Site

The Hanford Site is a 1450-km^2 (560-mi^2) area of semiarid land located in south-central Washington State (Figure 2.1). The Hanford Site is owned by the U.S. Government and restricted to uses approved by the U.S. Department of Energy (DOE). The major cities in the region are Seattle, Portland, and Spokane, which are more than 160 km (100 mi) away from the Hanford Site.

The major geographical features of the region are the nearby rivers and mountains. The Columbia River, which forms the eastern boundary of the Hanford Site, is an important source of water and hydroelectric power for the region. Other important rivers near the Hanford Site are the Yakima River to the southwest and the Snake River to the east. The Cascade Mountains, about 160 km (100 mi) to the west, have an important effect on the climate of the area.

Figure 2.2 shows the locations of two disposal sites that have been considered in the 1998 ILAW PA: the ILAW disposal site (located southwest of the Plutonium-Uranium Extraction [PUREX] Plant) and the existing vaults (located east of the PUREX plant and formerly known as the Grout Vaults). Both sites are located in the 200 East Area within the Hanford Site. The current plan is to use the ILAW disposal site as the primary site for disposal of ILAW waste.

2.2 Disposal Facility Design

According to Mann et al. (2000), the ILAW disposal plan is to use the existing disposal vaults from the grout program, suitably modified to receive ILAW packages, and build a new disposal facility of concrete vaults that is currently in the early design phase. In December 1999, DOE identified the remote-handled trench as the baseline concept for ILAW disposal at Hanford (Taylor 1999).

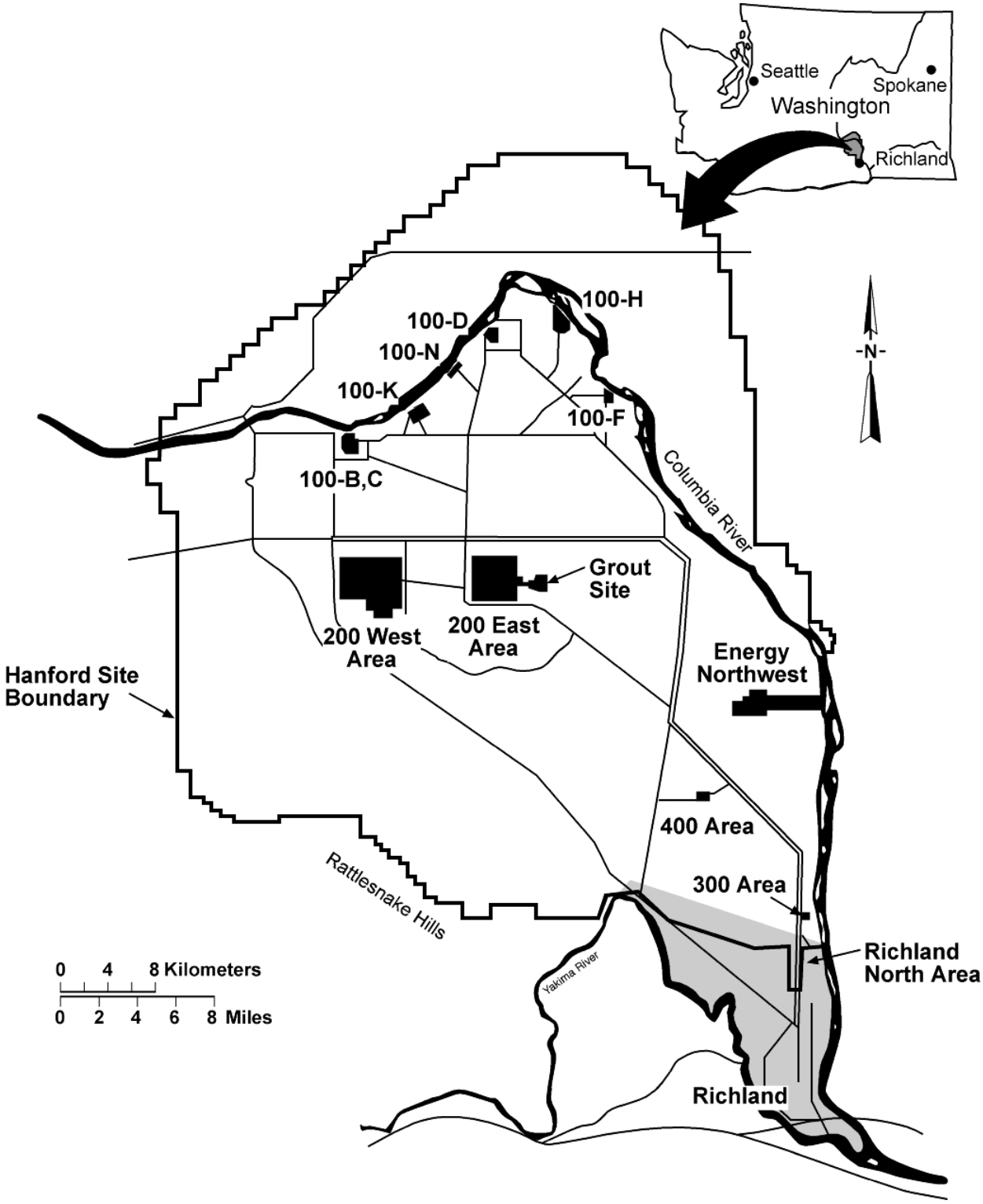

Figure 2.1. Map of the Hanford Site and Its Location Within Washington

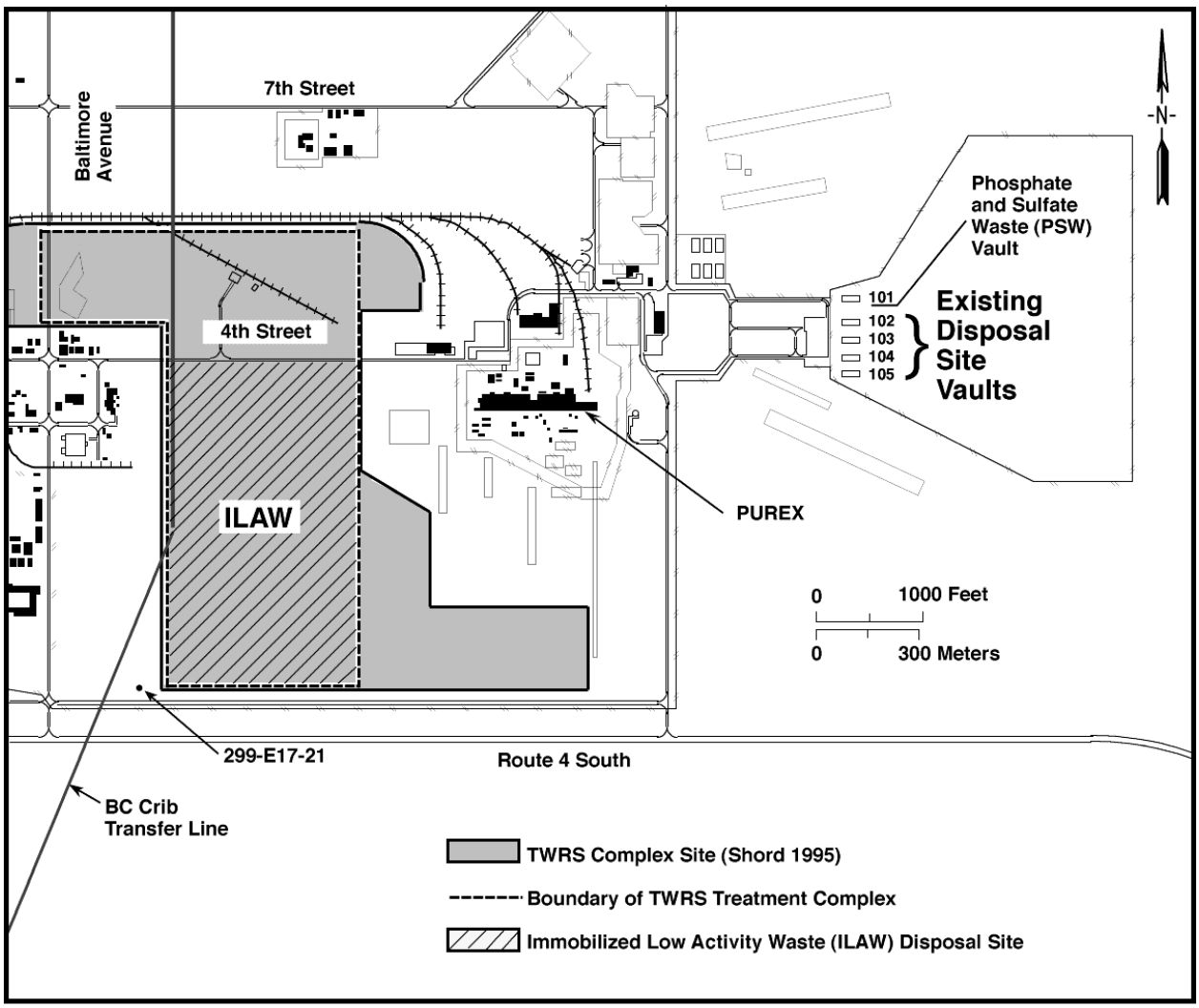

Figure 2.2. Location of the ILAW Disposal Site in the 200 East Area

2.2.1 New ILAW Disposal Area

2.2.1.1 Remote-Handled Trench Pre-Conceptual Design

The remote-handled trench concept has been chosen as the baseline for the ILAW Disposal Project (Taylor 1999). This trench concept is similar to the Radioactive Mixed Waste Burial Trench that was designed and constructed to accept solid waste at Hanford. Under the ILAW disposal plan described below, the disposal facility is a Resource Conservation and Recovery Act (RCRA)-compliant landfill (i.e., double-lined trench with leachate collection system). Many operational aspects and ancillary activities of the landfill (e.g., leachate collection and disposition, stormwater control, installation of surface barrier at closure, etc.) would be similar to those incorporated into the Radioactive Mixed Waste Burial Trench. However, operational activities for receiving ILAW packages and placing them in the trench would be modified to accommodate the different package sizes of remote-handled ILAW packages.

The conceptual-design layout of the six remote-handled trenches conceptualized for the ILAW disposal site is shown schematically in Figure 2.3. The trench side slopes are in a ratio of 3:1. The dimensions shown in Figure 2.3 represent the inner trench dimensions. Figure 2.4 shows the conceptual-design layout for the waste package loading into the remote-handled trench.

The design of the closure cover shown in Figure 2.4 is not yet complete. For this report, the closure cap (surface barrier) is assumed to have the same relative thickness, materials, and slope as the modified RCRA subtitle C closure cap defined in Puigh (2000, Section 4). A capillary break is assumed to consist of a 1-m-thick sand layer immediately below the surface barrier and gravel between the top of the trench and the sand layer. The sand and gravel layers together are 4 m over the center of the trench and have a 2% slope toward the long edge of each trench.

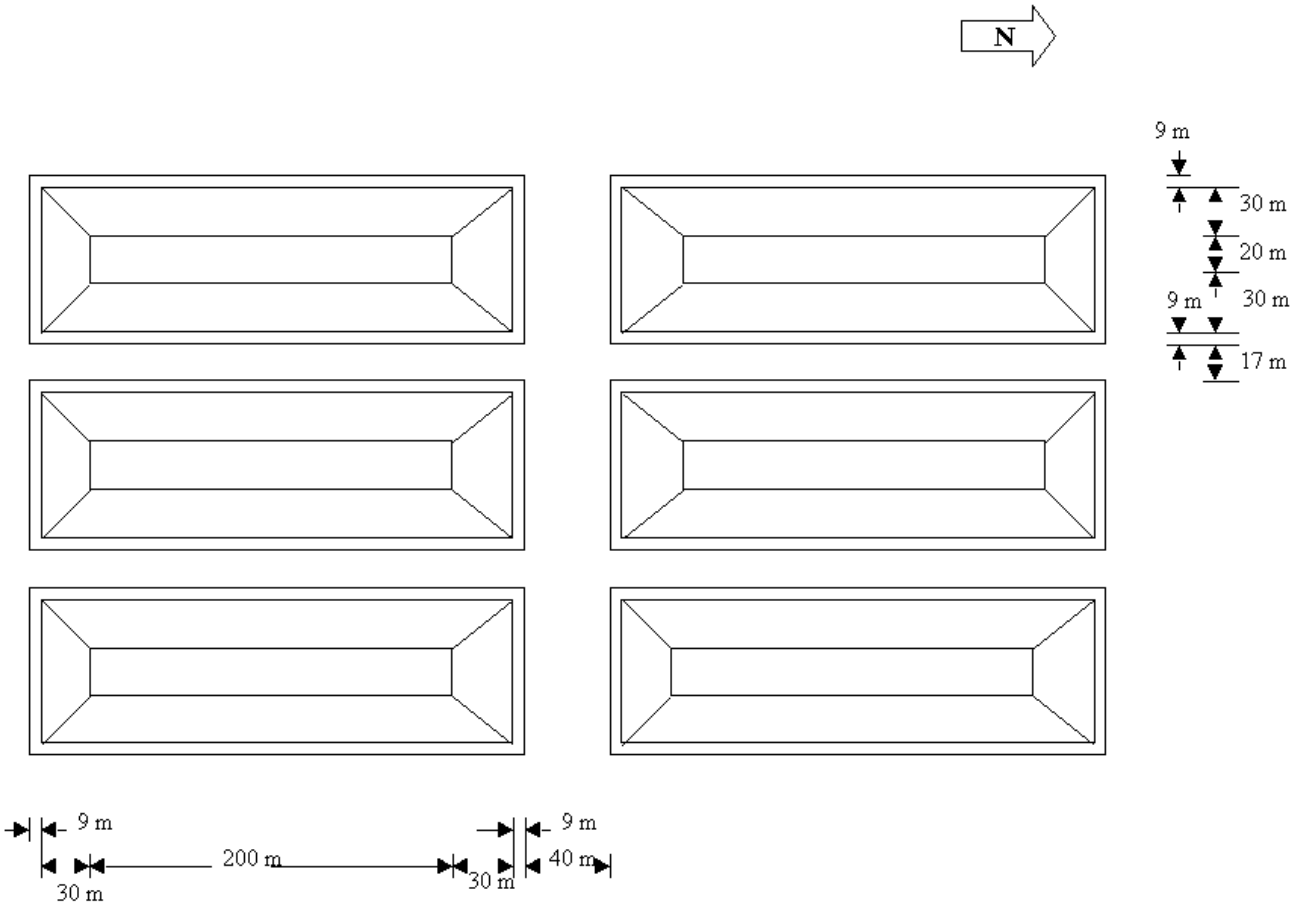

Figure 2.3. Remote-Handled Trench Pre-Conceptual Layout at the ILAW Disposal Site

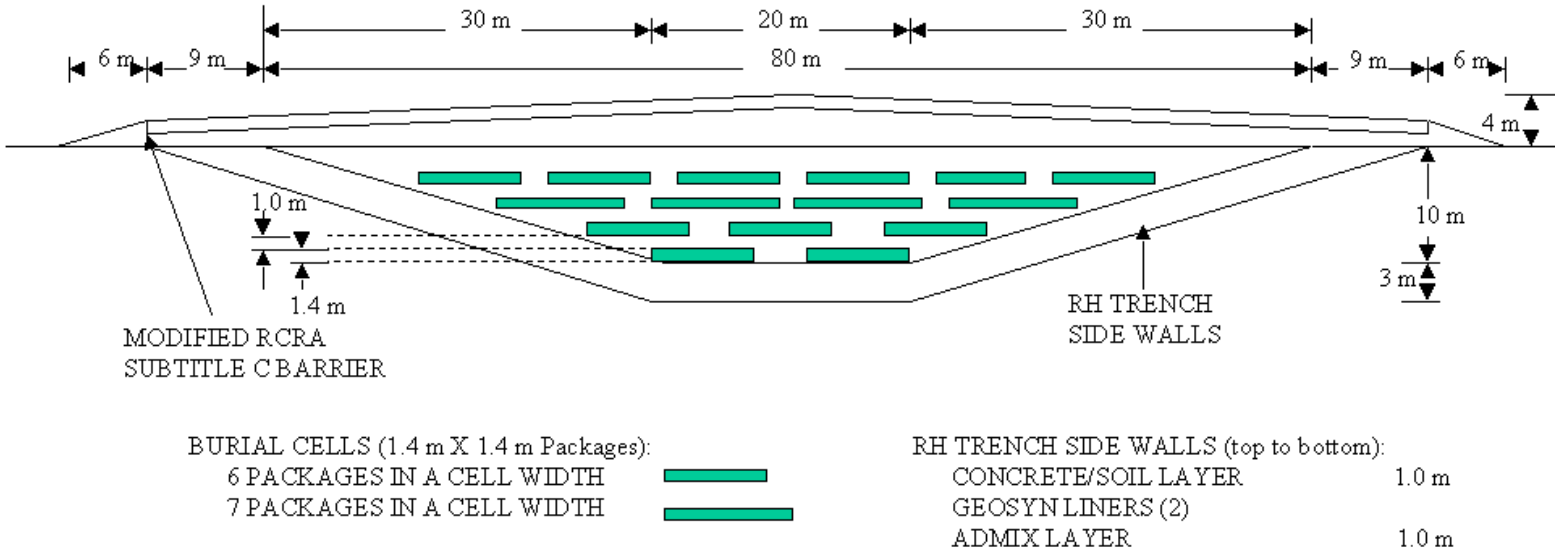

Figure 2.4. Remote-Handled Trench Pre-Conceptual Design

2.2.1.2 Concrete-Vault Conceptual Design

An alternate set of calculations for a concrete-vault design is based on an earlier conceptual design for the new ILAW disposal facility (Pickett 1998) that uses a long concrete-vault concept divided into cells. Each vault is an underground, open-topped, concrete vault approximately 23 m (76 ft) wide, 207.8 m (686 ft) long, and 11.0 m (26.7 ft) high. The top of the vault walls extends 1 m (3.3 ft) above grade. Each vault is divided into 11 cells, separated by concrete partition walls (0.45 m [1.5 ft] thick). Each vault can accommodate six layers of waste packages with 168 waste packages in each layer. Assuming that the waste package geometry is 1.4 m^3, the spacing between each waste package (including the walls) is 9.3 cm (3.7 in.) along the width, 11.5 cm (4.5 in.) along the length, and 10 cm (4 in.) between each layer of waste packages. Based on the Kirkbride (1999) estimate of approximately 70,000 packages needed for disposal of all planned ILAW waste, only seven new disposal vaults would be required to complete the disposal of all ILAW (assuming the existing vaults are not used).

Each vault is built above a RCRA-compliant leak detection and collection system. It consists of a cast-in-place reinforced concrete basin approximately 209.5 m (687.0 ft) long and 24.7 m (81 ft) wide with walls 1.07 m (3.5 ft) high. The basin floor is 0.6 m (2 ft) thick and contains steel reinforcing bars within. The catch basin is lined with two flexible membrane liners, and on top of these lies a layer of gravel with a perforated collection pipe routed to sumps, one at each end of a vault. Liquids entering the sump can be removed by using a portable pump lowered down a riser pipe.

Interim closure for each filled cell in the new disposal facility will consist of placing concrete shield covers (assumed to be 1.4 x 1.4 x 0.3 m [4.6 x 4.6 x 1 ft]) on the top layer of waste packages. The filler-material layer is assumed to have a depth of 0.3 m (1 ft) above the concrete shield covers. A “controlled density fill” consisting of a mixture of Portland cement, fly ash, aggregate, water, and admixtures is then placed on top of the filler-material layer. The depth of the “controlled density fill” is 0.45 m (1.5 ft). A waterproof membrane layer (assumed to be 60 mil, high-density polyethylene [HPDE]) is placed over the interim-closed vault. After all cells in the vault have been filled and interim-closed, a closure cap consisting of a capillary break followed by a modified RCRA subtitle C surface barrier will be placed over the entire vault (Puigh 2000). Again, it is assumed that the capillary break consists of a 1-m-thick sand layer immediately below the surface barrier and gravel between the top of the concrete vault and the sand layer. The sand and gravel layers together are assumed to be 4 m (13 ft) over the center of the trench and to have a 2% slope towards the long edge of each vault.

2.2.2 Existing Disposal Area

According to Puigh (1999), current disposal plans will use disposal vaults at the existing ILAW disposal facility (Figure 2.2), suitably modified to receive ILAW waste packages. The existing disposal vaults were originally constructed by a previous waste program in the late 1980s and early

1990s. They were designed to contain a liquid low-level waste (LLW) grout mixture during a curing and solidification period and to serve as a disposal structure for the resulting grouted waste monolith. Five vaults were originally constructed. One of the vaults was filled before the program was terminated, leaving four empty vaults available for use.

According to Puigh (1999), each vault is 37.6 m (123.5 ft) long and 15.4 m (50.5 ft) wide, with a roof clearance of 10.4 m (34.0 ft), providing 5,579 m^2 (6,236 ft^2) of floor space. The vaults are constructed of reinforced concrete and are designed and constructed in compliance with RCRA requirements for both hazardous waste surface impoundments and land disposal units. Each vault is built above a RCRA-compliant leak-detection and collection system. The leak-detection system consists of a sealed concrete slab sloped to a collection sump fitted with a riser pipe to the land surface and is capable of collecting, detecting, sampling, and removing any leachate that might escape from the primary structure.

A conceptual design activity has been performed to modify the existing disposal vaults to accept and serve as a disposal facility for the ILAW wastes (Pickett 1998). The modifications will consist of the following elements:

- Existing asphalt layer and concrete topping layer above the precast concrete roof slabs will be removed from all vaults.
- Side wall and wall extensions 1.8 m (6.0 ft) high will be added to the original top of the side and end walls in each vault.
- Rails for a gantry crane will be placed on the top of the side-wall extensions along the full length of the vaults to support the unloading of ILAW waste disposal packages from transportation vehicles.

3.0 Relation of Groundwater Modeling to Performance Assessment Modeling of ILAW Disposal System

This section of the report summarizes the relationship of groundwater modeling calculations described in this report to the overall performance assessment of the ILAW disposal facility. Topics covered include:

- Overall Strategy for Disposal Facility Assessment
- Integration of Results of Individual Model Components

3.1 Overall Strategy for Disposal Facility Assessment

In Mann et al. (2000), the overall strategy for looking at the long-term performance of the ILAW disposal facility involves a conceptual model that considers the following eight processes or steps as illustrated in Figure 3.1:

- The movement of infiltrating water as it leaves the very-near-surface soil region above the proposed disposal facility

- The movement and diversion of water as it migrates downward and interacts with an intact capillary barrier situated above the disposed wastes

- For water that is not diverted away by the capillary barrier, the chemical interaction of infiltrating water as it is modified by the local geochemical environment and waste form, accumulating contaminants.

- The movement of contaminant-laden water as it leaves the disposal facility, carrying contaminants with it. Some contaminants may interact with the material in the disposal facility, slowing the release of the contaminants to the surrounding natural environment.

- The movement of contaminated water as it moves through the undisturbed, unsaturated zone (vadose zone) below the disposal facility down to the unconfined aquifer. Some of the contaminants in the water undergo some geochemical sorption as they are transported through the vadose zone.

- The movement and mixing of contaminated water in the vadose zone with the water in the unconfined aquifer. Resultant contaminated groundwater migrates laterally to the point of water use where it is extracted from the aquifer by wells and brought to the surface, or until it reaches the Columbia River.

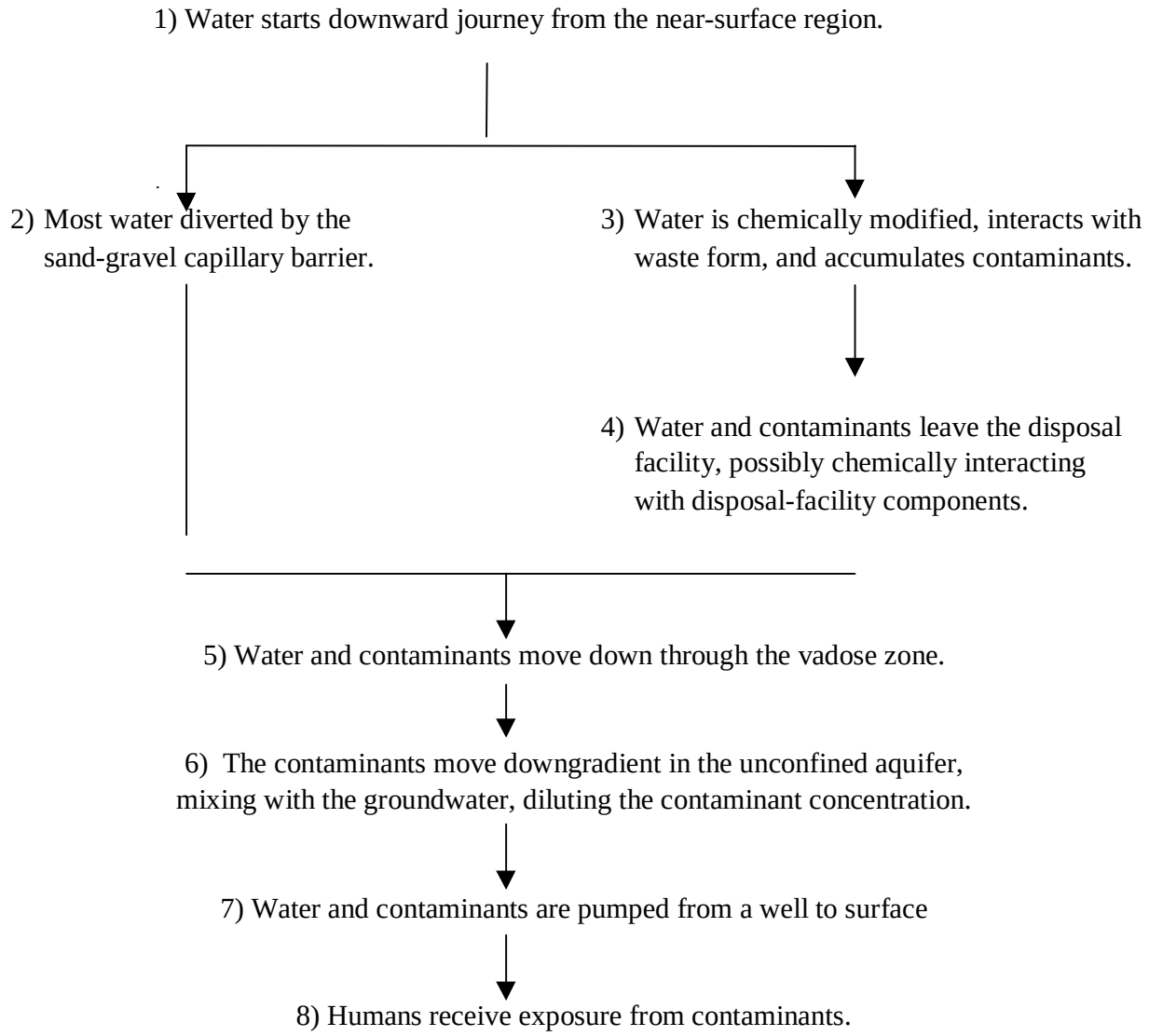

Figure 3.1. Eight Sequential Steps for the Groundwater Pathway

- The use of water containing radionuclides or other hazardous chemical contaminants then results in human exposure through a variety of pathways (ingestion, inhalation, and external radiation).

According to Mann et al. (2000), each component of the conceptual model of the ILAW disposal-facility PA was analyzed separated as illustrated in Figure 3.2 using a variety of component-specific computational models. A coupled, unsaturated flow, and reactive contaminant-transport model of the near field in the vicinity of the disposal facility was used to analyze the near-field interaction of infiltrating water with the ILAW disposal facilities and the proposed glass waste form. This model was based on the STORM code (Bacon et al. 1999). An unsaturated flow and transport model of the vadose zone above and below the disposal facility was used to estimate the moisture flow into the disposal facility and the moisture flow and contaminant transport from the disposal facility into groundwater. This model was based on the VAM3DF code (Huyakon et al. 1999)

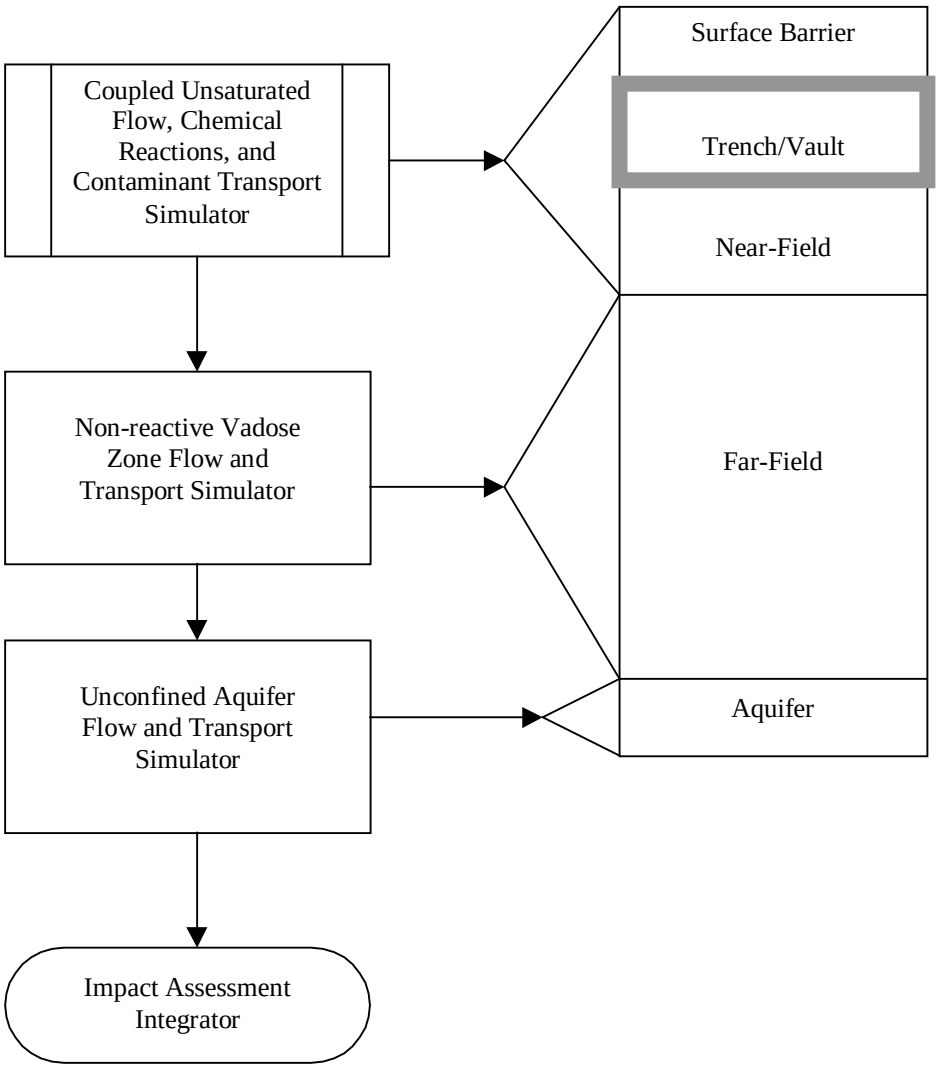

Figure 3.2. Modeling Strategy for Assessing ILAW Disposal System

A local-scale and regional-scale model of the unconfined aquifer (Wurstner et al. 1995; Cole et al. (1997) was used to evaluate the mixing of contaminated water from the vadose zone into the underlying aquifer and the subsequent lateral migration of contaminants to receptor points and/or points of groundwater discharge along the Columbia River. This model was based on the Coupled Fluid, Solute and Energy Transport (CFEST) code (Gupta et al.1987; Gupta 1996). - Mann et al. (2000) provided specific descriptions of the underlying assumptions and the implementation of the disposal facility and the vadose zone computational models and codes for the ILAW PA.

3.2 Integration of Results of Individual Model Components

According to Mann et al (2000), the computational code, INTEG (Mann 1996), calculates a specific impact (whether dose rate or concentration level) based on the inventory, vadose zone transport, aquifer transport, and dosimetry factors. The dose rate calculated depends on the type of dosimetry factor (i.e., all-pathways, drinking water). The program solves the following equation for each year under consideration.

$$\textit{Response} = \sum_I I_i(t)\, \Gamma_i(t)\, w_i\, D_i \,/\, (r\, A) \qquad (3.1)$$

where

I_i = the amount (or inventory) of radionuclide i (Ci). The time-dependent value is calculated by INTEG, based on the initial inventory and on decay and the ingrowth from other radionuclides.

Γ_i = the flux of contaminants at the bottom of the vadose zone normalized to a unit-source inventory for radionuclide i ([Ci/y]/Ci). The time-dependent value is calculated by VAM3DF.

w_i = the ratio of the concentration of radionuclide i at the well location relative to the contaminant concentration at the bottom of the vadose zone (dimensionless). This quantity was called the well intercept factor in earlier Hanford PAs. The peak value as calculated by CFEST is used.

D_i = the dose rate factor (mrem/y per Ci/m^3). The values are taken from the tables in Appendix B. D_i is unity when the response that is calculated is a concentration.

r = the recharge rate (m/y). The value at 10,000 years is used at all analysis times.

A = the area over which the contaminant flux enters the aquifer (m^2). The value used is the area of the disposal facility being modeled.

The program is modeled after GRTPA (Rittmann 1993), which served a similar function in earlier work (Rawlins et al. 1994; Mann et al. 1995). INTEG allows greater freedom in specifying data used in the integration. The code has been benchmarked against the results of GRTPA (Mann 1996). An auxiliary code was written to translate the output of VAM3DF into a readable format for INTEG.

4.0 Conceptual And Numerical Model Framework

The base-case groundwater flow and transport of contaminants from the ILAW facility was calculated with the current version of the Hanford site-wide groundwater model. This three-dimensional model, currently being used by the Hanford Groundwater Project and recommended as the proposed site-wide groundwater model in the Hanford Site groundwater model consolidation process, is based on the Coupled Fluid, Energy, and Solute Transport (CFEST-96) Code (Gupta et al. 1987; Gupta 1997). This model is fully described in Wurstner et al. (1995) and Cole et al. (1997) and was most recently used in the Hanford Site Composite Analysis (Cole et al. 1997; Kincaid et al. 1998), which is a companion analysis to the existing preliminary PA analyses of the ILAW disposal facility (Mann et al. 1997) and the solid waste burial grounds in the 200-East and 200-West areas (Wood et al. 1995, 1996). The Composite Analysis is also a companion document to the Remedial Investigation/Feasibility Study (RI/FS) (DOE 1994) that supports the Environmental Restoration Disposal Facility.

4.1 Hydrogeologic Framework

The conceptual model of the groundwater system is based on nine major hydrogeologic units identified in the left column presented in Figure 4.1. The basis for the identification of these major hydrogeologic units in the aquifer system is described in Thorne and Chamness (1992), Thorne and Newcomer (1992), and Thorne et al. (1993, 1994). Although nine hydrogeologic units were defined, only seven are found below the water table during post-Hanford conditions. Odd-numbered Ringold model units (5, 7, and 9) are predominantly coarse-grained sediments. Even-numbered Ringold model units (4, 6, and 8) are predominantly fine-grained sediments with low permeability. The Hanford formation combined with the pre-Missoula gravel deposits were designated Model Unit 1. Model units 2 and 3 correspond to the early Palouse soil and Plio-Pleistocene deposits, respectively. These units lie above the current water table. The predominantly mud facies of the upper Ringold unit identified by Lindsey (1995) was designated Model Unit 4. However, a difference in the definition of model units is that the lower, predominantly sand portion of the upper Ringold unit described in Lindsey (1995) was grouped with Model Unit 5, which also includes Ringold gravel/sand units E and C. This was done because the predominantly sand portion of the upper Ringold is expected to have hydraulic properties similar to units E and C. The lower mud unit identified by Lindsey (1995) was designated as Units 6 and 8. Where they exist, the gravel and sand units B and D, which are found within the lower Ringold, were designated as Model Unit 7. Gravels of Ringold Unit A were designated Unit 9 for the model, and the underlying basalt was designated Model Unit 10. However, the basalt was assigned a very low hydraulic conductivity and was essentially treated as an impermeable unit in the model.

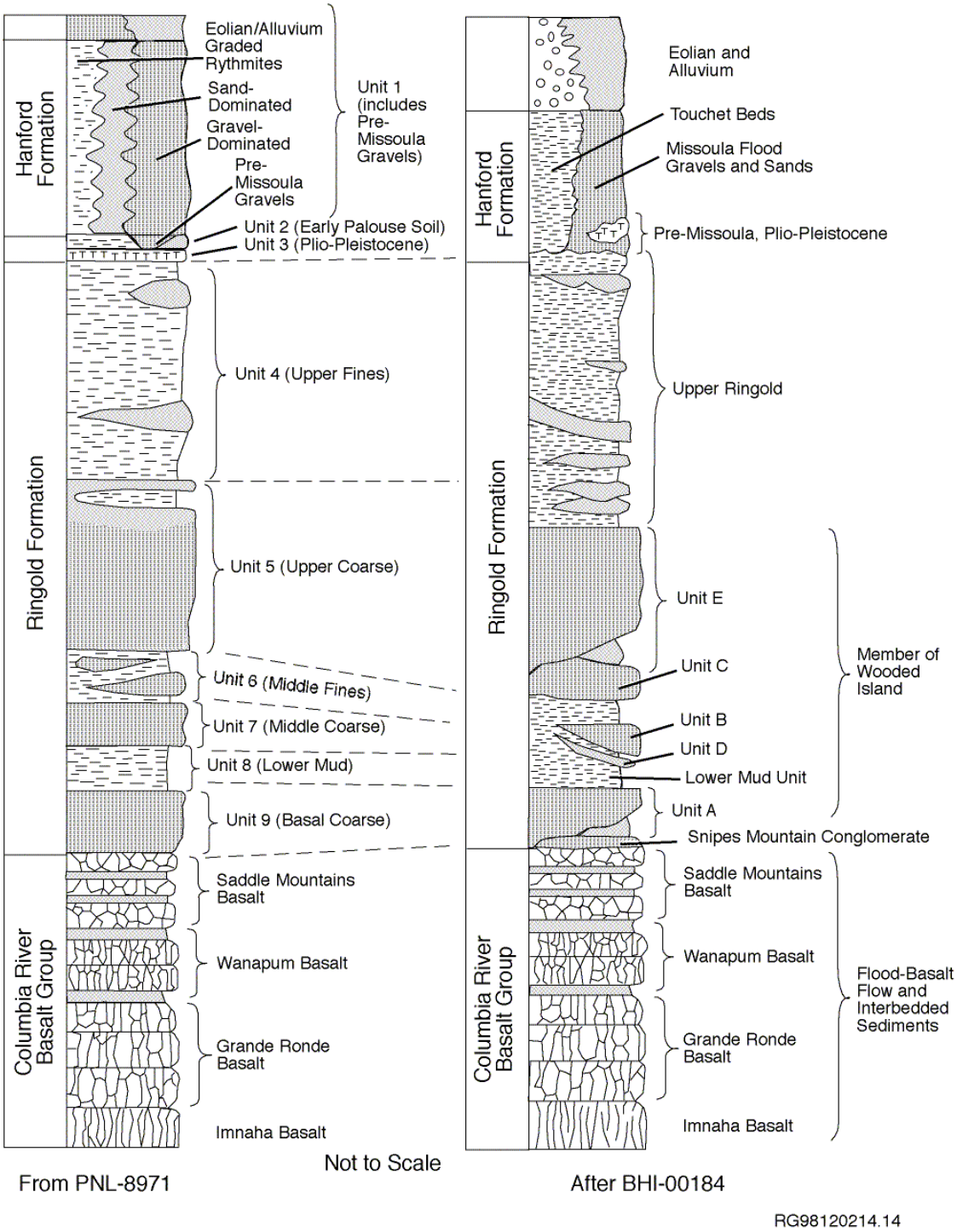

Figure 4.1. Comparison of Generalized Geology and Hydrostratigraphic Columns

The lateral extent and thickness distribution of each hydrogeologic unit were defined based on information from well drillers' logs, geophysical logs, and an understanding of the geologic environment. These interpreted areal distributions and thicknesses were then integrated into EarthVision (Dynamic Graphics, Inc., Alameda, California), a three-dimensional, visualization, software package used to construct a database of the three-dimensional hydrogeologic framework.

4.2 Recharge and Aquifer Boundaries

Both natural and artificial recharge to the aquifer were incorporated in the model. Natural recharge to the unconfined aquifer system occurs from infiltration of 1) runoff from elevated regions along the western boundary of the Hanford Site, 2) spring discharges originating from the basalt-confined aquifer system, also along the western boundary, and 3) precipitation falling across the site. Some recharge also occurs along the Yakima River in the southern portion of the site. Natural recharge from runoff and irrigation in the Cold Creek and Dry Creek Valleys up gradient of the site also provides a source of groundwater inflow. Areal recharge from precipitation on the site is highly variable, both spatially and temporally, and depends on local climate, soil type, and vegetation. A recharge distribution estimated for 1979 conditions in Cole et al. (1997) was applied in the model. The general methods used to develop these recharge estimates are described in detail in Fayer and Walters (1995).

The other source of recharge to the unconfined aquifer is wastewater disposal. Large volumes of artificial recharge from wastewater discharged to disposal facilities on the Hanford Site over the past 50 years has significantly impacted groundwater flow and contaminant transport in the unconfined aquifer system. However, the volume of artificial recharge will decrease significantly in the near future, and the water table is expected to return to more natural conditions after site closure.

The flow system is bounded by the Columbia River on the north and east and by the Yakima River and basalt ridges on the south and west. The Columbia River represents a point of regional discharge for the unconfined aquifer system. The amount of groundwater discharging to the river is a function of the local hydraulic gradient between the groundwater elevation adjacent to the river and the river-stage elevation. This hydraulic gradient is highly variable because the river stage is affected by releases from upstream dams. To approximate the long-term effect of the Columbia River on the unconfined aquifer system in the three-dimensional model, the CHARIMA river-simulation model (Walters et al. 1994) was used to generate the long-term, average river-stage elevations for the Columbia River. The river itself is represented as a constant-head boundary in the uppermost nodes of the model at the approximate locations of the river's left bank and channel midpoint. Nodes representing the thickness of the aquifer below the nodes representing mid-point of the river channel were treated as no-flow boundaries. This boundary condition is used to approximate the location of

the groundwater divide that exists beneath the Columbia River where groundwater from the Hanford Site and the other side of the river discharge into the Columbia. The Yakima River was also represented as a specified-head boundary at surface nodes approximating its location. Like the Columbia River, nodes representing the thickness of the aquifer below the Yakima River channel were treated as no-flow boundaries.

At Cold Creek and Dry Creek Valleys, the unconfined aquifer system extends westward beyond the boundary of the model. To approximate the groundwater flux entering the modeled area from these valleys, both constant-head and constant-flux boundary conditions were defined. A constant-head boundary condition was specified for Cold Creek Valley for the steady-state-model calibration runs. Once calibrated, the steady-state model was used to calculate the flux condition that was then used in the post-Hanford steady-state flow simulation. The constant-flux boundary was used because it better represents the response of the boundary to a declining water table than a constant-head boundary. Discharges from Dry Creek Valley in the model area, resulting from infiltration of precipitation and spring discharges, are approximated with a prescribed-flux boundary condition.

The basalt underlying the unconfined aquifer sediments represents a lower boundary to the unconfined aquifer system. The potential for interflow (recharge and discharge) between the basalt-confined aquifer system and the unconfined aquifer system is largely unquantified, but is postulated to be small relative to the other flow components estimated for the unconfined aquifer system. Therefore, interflow with underlying basalt units was not included in the current three-dimensional model. The basalt was defined in the model as an essentially impermeable unit underlying the sediments.

4.3 Flow and Transport Properties

To model groundwater flow, the distribution of hydraulic properties, including both horizontal and vertical hydraulic conductivity and porosity, were needed for each hydrogeologic unit defined in the model. In addition, to simulate movement of contaminant plumes, transport properties were needed, including contaminant-specific distribution coefficients, bulk density, effective porosity, and longitudinal and transverse dispersivities (D_l and D_t).

In the original model calibration procedure described in Wurstner et al. (1995), measured values of aquifer transmissivity were used in a two-dimensional model with an inverse model-calibration procedure to determine the transmissivity distribution. Hydraulic head conditions for 1979 were used in the inverse calibration because measured hydraulic heads were relatively stable at that time. Details concerning the updated calibration of the two-dimensional model are provided in Cole et al. (1997).

Hydraulic conductivities were assigned to the three-dimensional model units so that the total aquifer transmissivity from inverse calibration was preserved at every location. The vertical distribution of hydraulic conductivity at each spatial location was determined based on the transmissivity value and other information, including facies descriptions and hydraulic property values measured for similar facies. A complete description of the seven-step process used to vertically distribute the transmissivity among the model hydrogeologic units is described in Cole et al. (1997). The resulting hydraulic conductivity distribution resulting from this redistribution of aquifer transmissivity in the upper part of the aquifer is provided in Figure 4.2.

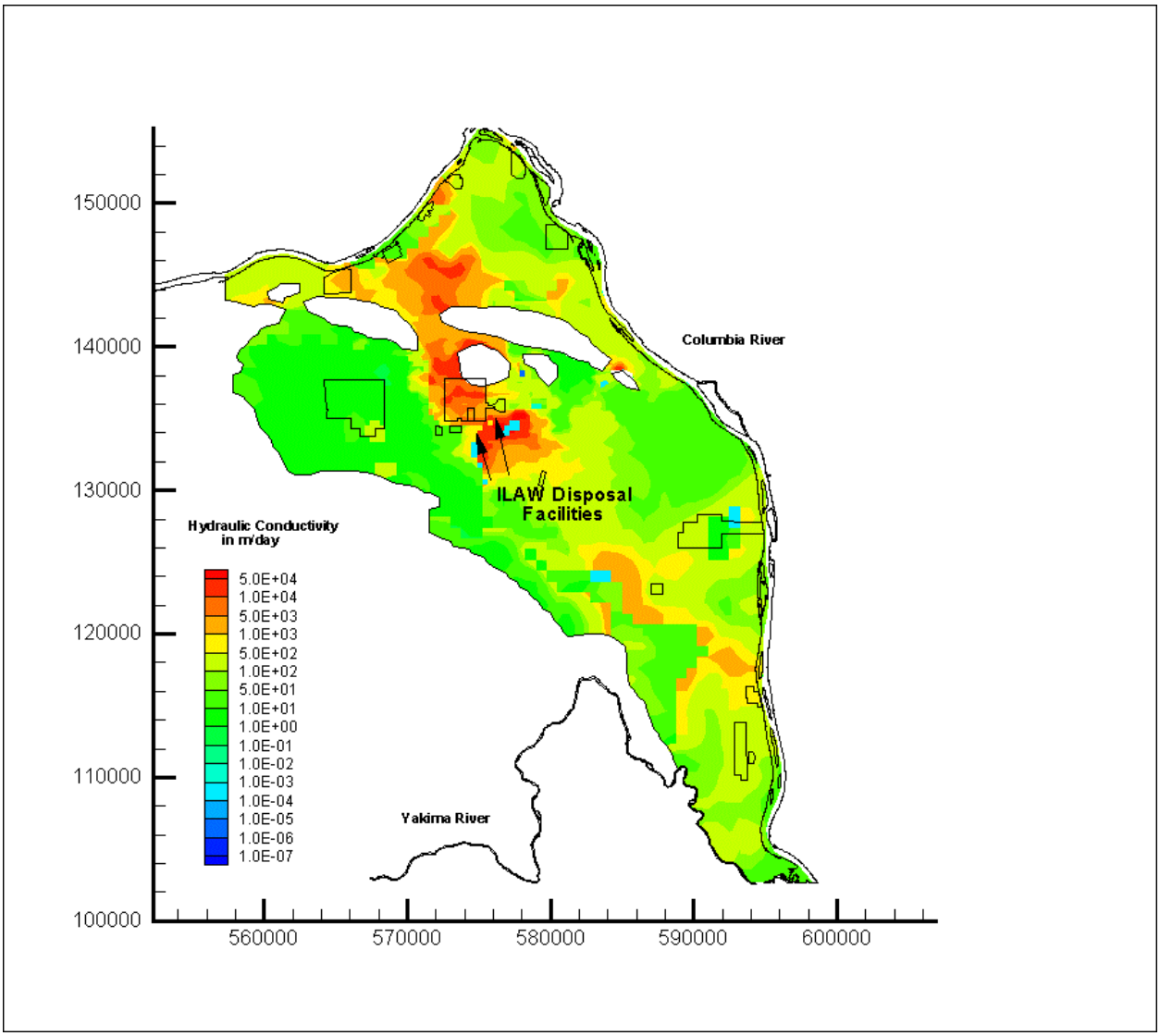

Figure 4.2. Hydraulic Conductivity Distribution Obtained from Inverse Calibration for 1979 Conditions

Information on transport properties used in past modeling studies at the Hanford Site is provided in Wurstner et al. (1995). Estimates of model parameters were developed to account for contaminant transport and dispersion in all transport simulations. Specific model parameters estimated included longtitudinal and transverse dispersivities (D_l and D_t) and aquifer porosity. This section briefly summarizes estimated transport properties.

For the regional scale analysis, a D_l of 95 m (311.7 ft) was selected to be within the range of recommended grid Peclet numbers (Pe < 4) for acceptable solutions. The 95-m (311.7 ft) estimate is about one-quarter of the grid spacing in the finest part of the model grid in the 200-Area plateau, where the smallest grid spacing is about 375 m (1230.3 ft) by 375 m (1230.3). The effective D_t was assumed to be 10 percent of the D_l. Therefore, 9.5 m (31 ft) was used in all simulations.

The effective porosity was estimated from limited measurements of porosity and specific yield obtained from multiple-well aquifer tests. These values range from 0.01 to 0.37. Laboratory measurements of porosity, which range from 0.19 to 0.41, were available for samples from a few Hanford Site wells and were also considered. The few tracer tests conducted indicate effective porosities ranging from 0.1 to 0.25. Based on the ranges of values considered, a best estimate of an effective porosity value for all simulations was assumed to be 0.25.

5.0 Groundwater Flow and Contaminant Transport Calculations

This section of the report describes the technical approach and use of the Hanford site-wide flow and transport model and the local-scale model developed in the vicinity of the existing and new ILAW disposal facility areas. These models were used to assess impacts from the transport of contaminants at hypothetical wells 100 m and 1 km down gradient of the disposal facilities and to evaluate regional flow conditions and transport from the ILAW disposal facilities to the Columbia River.

The first part of this section described the establishment of estimated Hanford post-closure flow conditions that provided the basis for all site-wide and local-scale flow and transport in the base-case calculations. The second of this section describes the development and implementation of local-scale models that were used to perform flow and transport simulations in the immediate vicinity of the disposal facility areas.

5.1 Site-Wide Flow and Transport Simulations

Site-wide flow-model simulations were used to establish future flow conditions that provided the basis for boundary conditions for local-scale models to evaluate impacts from the transport of contaminants immediately down gradient of the disposal facilities. These same flow conditions also provided the hydraulic basis for site-wide transport simulations used to evaluate concentration levels of contaminants released from the disposal facilities to the Columbia River. Following is a summary discussion of the establishment of post-Hanford steady-state flow conditions and the approach used in site-wide transport-model simulations of contaminant release from disposal facilities to the Columbia River.

5.1.1 Site-Wide Steady-State Flow Conditions

Past projections of post-Hanford water-table conditions have estimated the impact of Hanford operations ceasing and the resulting changes in artificial discharges that have been used extensively as a part of site waste-management practices. Simulated results of future transient behavior in the Hanford unconfined aquifer by Cole et al. (1997) showed an overall decline in the hydraulic head and hydraulic gradient across the entire water table over the entire Hanford Site. The results of these simulations indicate that the water table would reach steady state in 100–350 years in different areas over the Hanford Site.

Given the expected long delay of contaminants reaching the water from the low-level waste burial grounds, the hydrologic framework of all groundwater transport calculations was based on a postulated post-Hanford steady-state water table as estimated with the three-dimensional model. The

predicted water table for post-Hanford conditions for these assumed steady-state conditions across the site and in the area between the ILAW new disposal facility and the Columbia River are illustrated in Figures 5.1 and 5.2. The overall flow attributes of this water-table surface are consistent with the previously simulated flow patterns described in Wurstner et al. (1995), Cole et al. (1997), and Law et al. (1996). From the ILAW new disposal facility, groundwater moves southeasterly near the site and then in an easterly and northeasterly direction before discharging into the Columbia River north of the old Hanford town site.

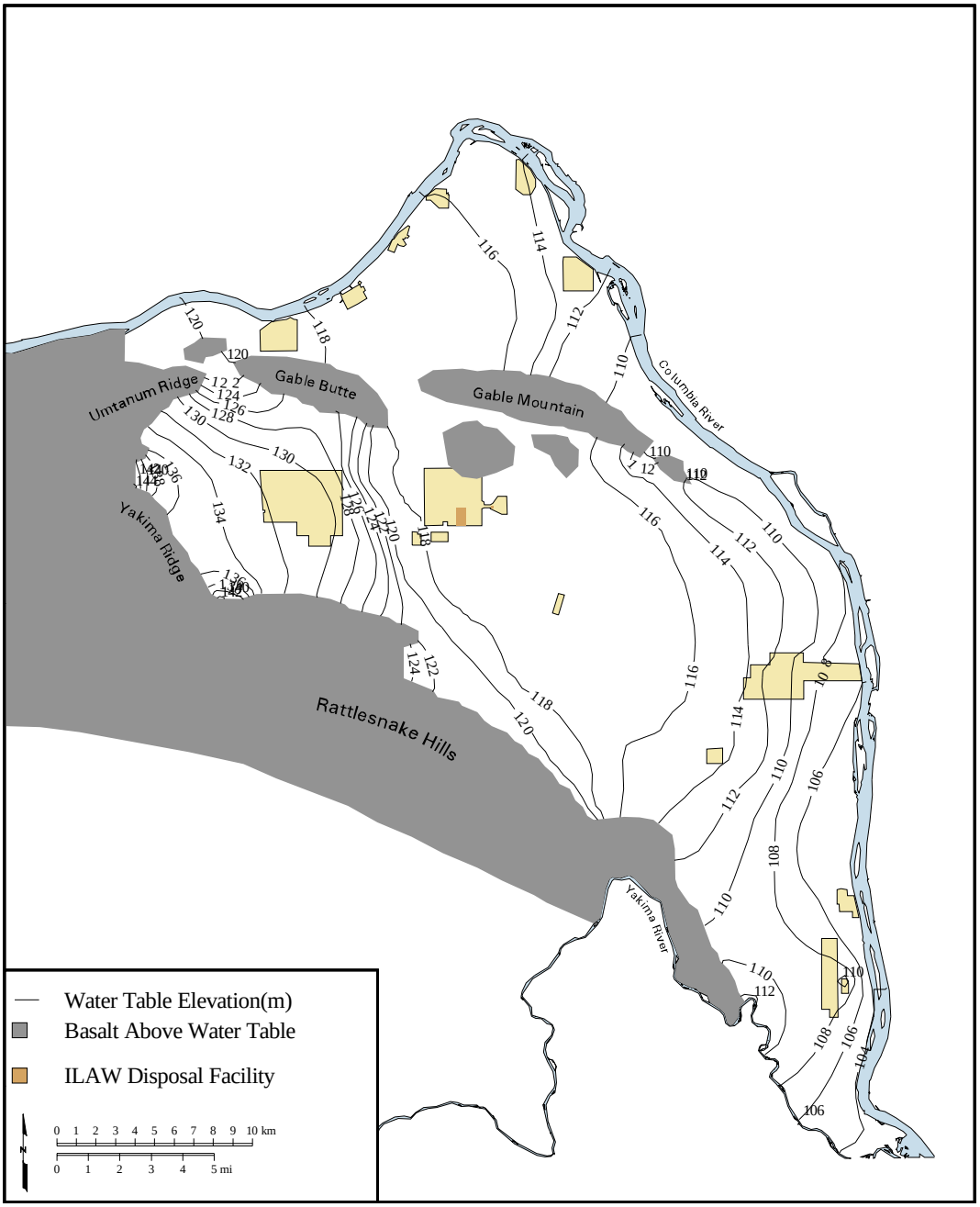

skw00068.eps December 28, 2000

Figure 5.1. Predicted Water Table for Post-Hanford Conditions for Assumed Steady-State Conditions

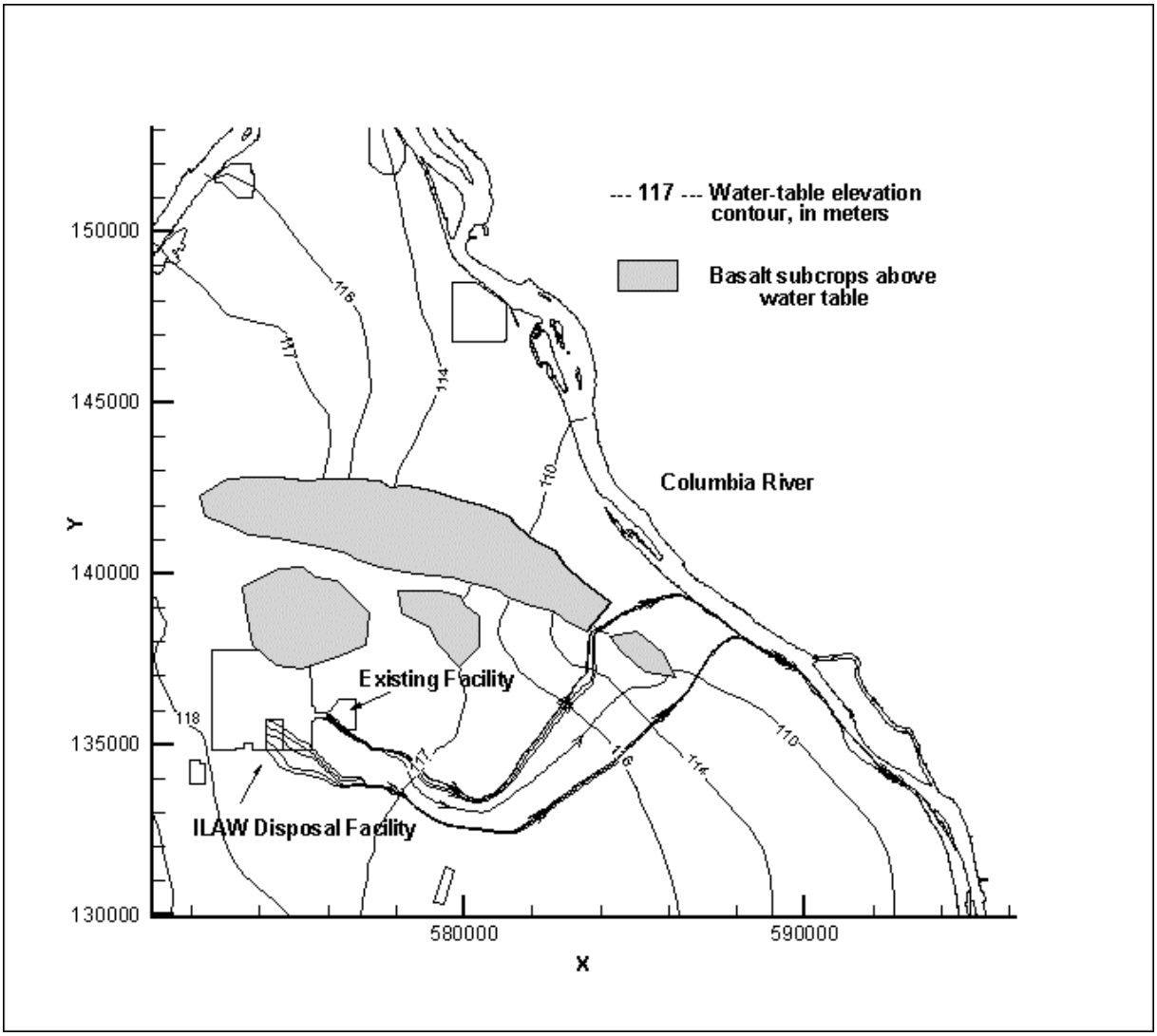

Figure 5.2. Predicted Water Table for Post-Hanford Conditions for Assumed Steady-State Conditions Between the ILAW Disposal Facility and Columbia River

5.1.2 Contaminant Transport Between Disposal Facilities and Columbia River

Flow conditions established with the site-wide model (Figures 5.1 and 5.2) provide the basis for the transport simulations of contaminants released from disposal facilities toward the Columbia River. Constant mass releases equivalent to those used in the local-scale model were introduced into the site-wide model at the approximate location of the ILAW disposal facilities. Concentration levels and WIFs were evaluated in groundwater in close proximity to the Columbia River as well as several

intermediate points between the disposal areas and the river. To establish consistency of the site-wide scale calculations with those made in the local scale models, concentrations levels were evaluated and compared at approximately 1 km down gradient of the source areas in both the local-scale and site-wide models. Predicted concentration levels at 1 km in the site-wide and local-scale models are expected to be somewhat consistent with each other, but will not be the same because of inherent differences in the grid resolution used in each model. Predicted concentration levels in the site-wide model close to the source areas will in general be expected to be somewhat lower than are predicted in the local-scale models.

5.2 Local-Scale Model Development and Description

The base-case analysis for the groundwater flow and transport calculations evaluated current disposal concepts at the new ILAW disposal facility to be located in the south-central 200 East area. The approach used in this analysis was to construct local-scale models based on flow conditions calculated in the site-wide model to adequately represent flow and transport conditions near these facilities to a hypothetical well 100 m downgradient.

5.2.1 Grid Designs

Two separate local-scale models were developed to evaluate the current design concepts. One model evaluated the remote-handled trench and concrete-vault concepts at the new ILAW disposal facility. Another local-scale model was used to evaluate the concrete-vault concept at the existing ILAW disposal facility.

The grid used in the local-scale model in both areas required refinement areally and vertically. The discretized grids for the local-scale models telescope in from the grid used in regional-scale calculations.

The grid used in the new ILAW disposal facility area extends over an area of about 4,100 m (2.5 mi) west to east and 4,100 m (2.5 mi) north to south (Figure 5.3). It varies in size progressively from the outmost subdivided coarse triangular grids (regional-scale 375 by 375 m [1230 by 1230 ft] grid spaces) to the finest grid spacing (20 m by 20 m [65.6 by 65.6 ft]) in the vicinity of the ILAW disposal area. The three-dimensional model, based on this surface grid, comprises a total of 31,604 elements (9,157 surface and 22,447 subsurface elements) and 32,618 nodes.

The grid used at the existing ILAW disposal-facility area extends over an area of about 2,600 m (1.5 mi) west to east and 2600 m (1.6 mi) north to south (Figure 5.4). It varies in size progressively from the outmost subdivided coarse triangular grids (regional-scale 375 by 375 m [1230 by 1230 ft] grid spaces) to the finest grid spacing (20 m by 20 m [65.6 by 65.6 ft]) in the vicinity of the existing

ILAW disposal area. This three-dimensional model comprises a total of 18,317 elements (9,157 surface and subsurface elements) and 18,914 nodes.

The vertical grid spacing for the transport (as well as the flow) model consisted of multiple transport layers that subdivided the major hydrostratigraphic units. The basic approach for this subdivision is the same approach used in Kincaid et al. (1998) to support groundwater transport calculations used in the Composite Analysis. The basic thickness of each transport layer was 8 m (26.2 ft). The transport layers were defined from the water-table surface to the basalt to account for the overall saturated thickness and to adequately represent contaminant concentrations in the three-dimensional model. At every model node, each of the major hydro-stratigraphic units below the water table was represented by at least one transport-model layer. Nonconductive (e.g., mud) units below the water table were always represented by at least two transport-model layers, regardless of their saturated thickness, to ensure that the vertical flow and transport through these units was appropriately represented.

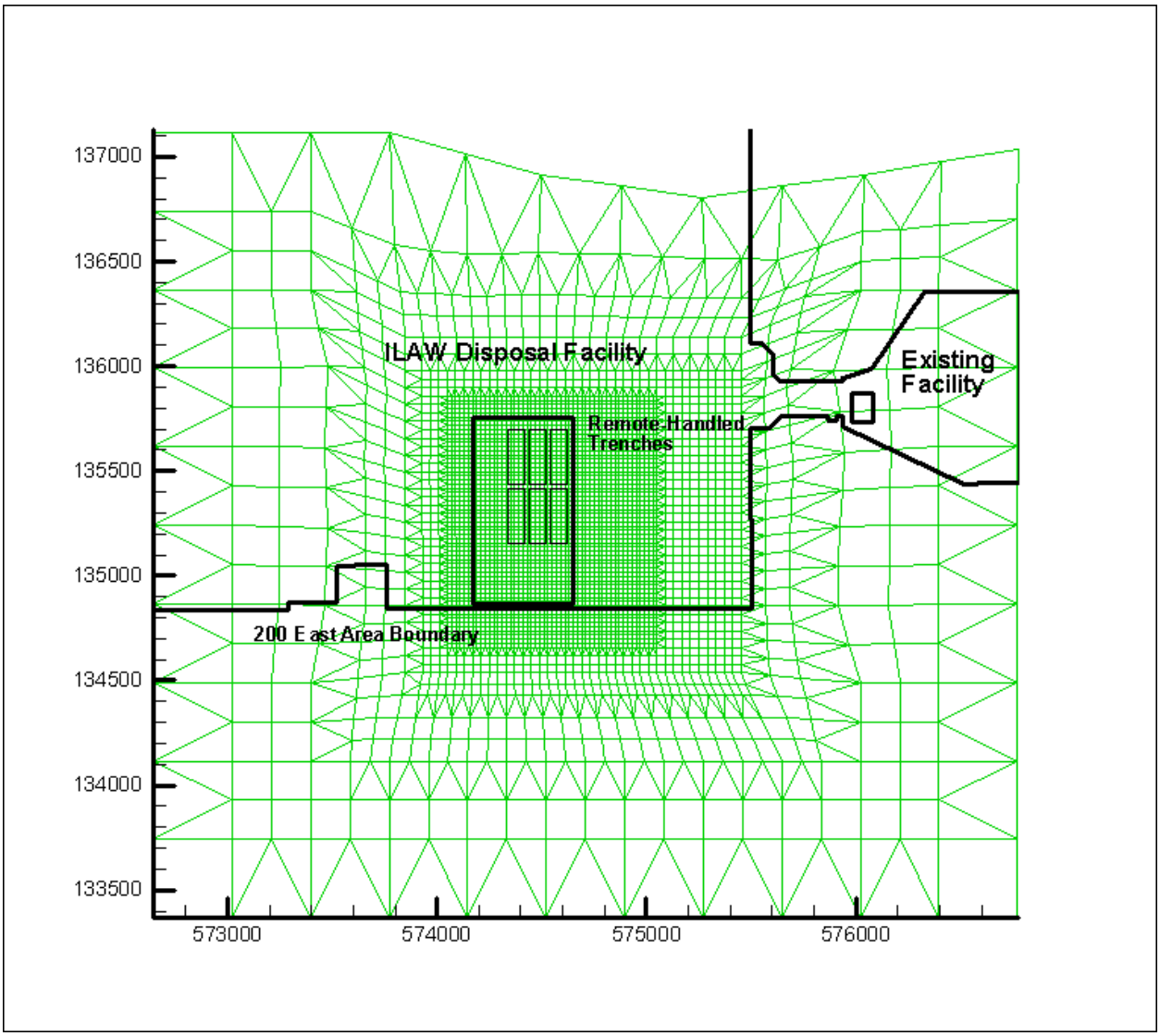

Figure 5.3. Finite Element Grid Used in the Local-Scale Model at the New ILAW Disposal Facility Area

For units with a saturated thickness <12 m (<39.4 ft), the layer thickness was set to the actual saturated thickness of the unit. Nonconductive and conductive units with saturated thickness >12 m (>39.4 ft) were divided into multiple transport-model layers in the same manner. For all units with thickness >12 m (>39.4 ft), the transport layering algorithm is as follows: create as many uniform 8-m (26.2-ft) transport layers as possible until the remaining unaccounted for saturated thickness is >12 m (>39.4 ft) but <16 m (<52.5 ft), and then create two additional transport layers set to half of the remaining saturated thickness of the hydrostratigraphic unit being layered.

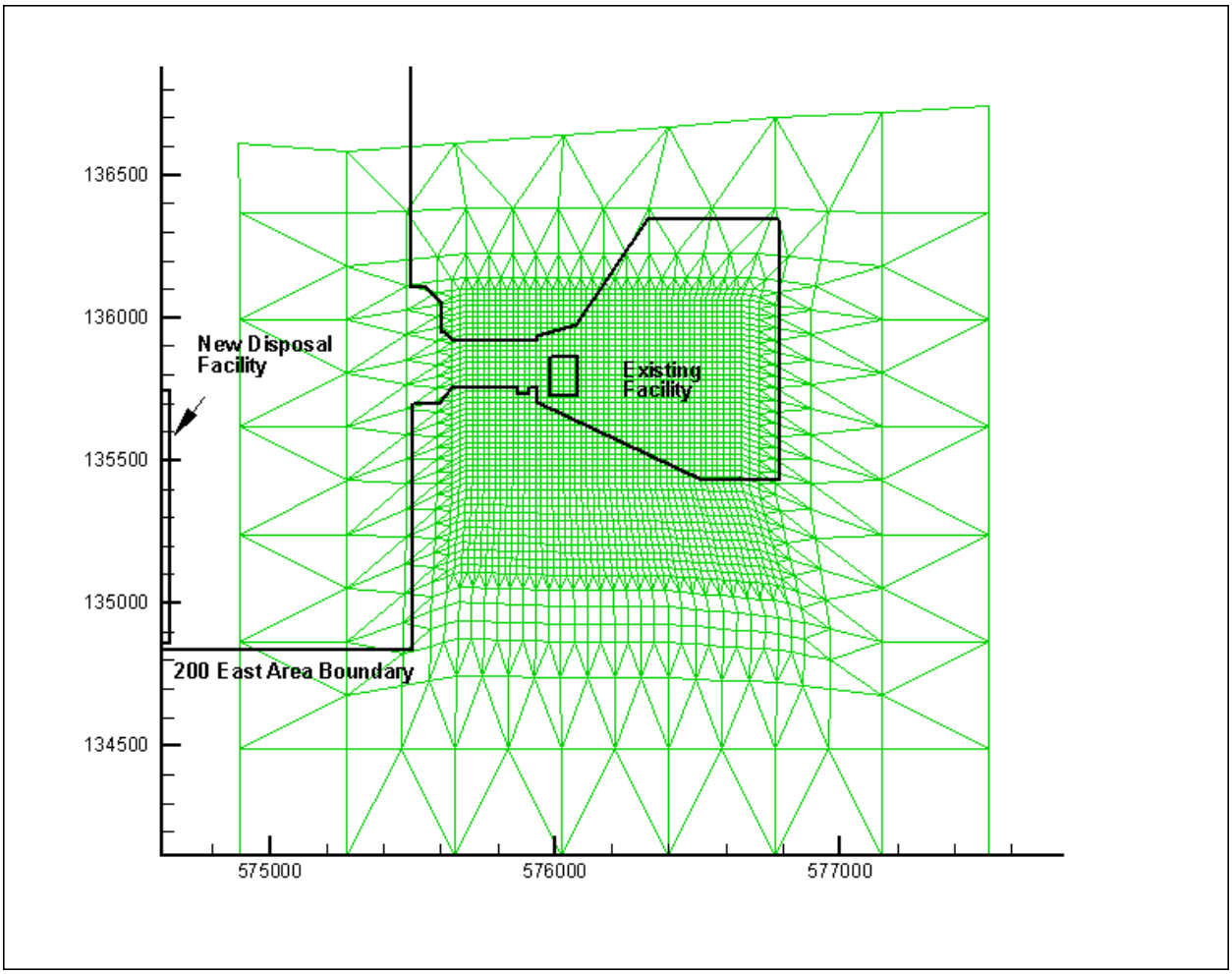

Figure 5.4. Finite Element Grid Used in the Local-Scale Model at the Existing ILAW Disposal Facility Area

At the local-scale, a total of six hydrogeologic units was found to be present, the Hanford formation (Unit 1) and several units belonging to the Ringold Formation (Units 5, 6, 7, 8, and 9). The three-dimensional distribution of these units in the local-scale model used in the new ILAW disposal area is depicted in Figure 5.5. The three-dimensional distribution of these units in the local-scale model used in the existing ILAW disposal area is depicted in Figure 5.6.

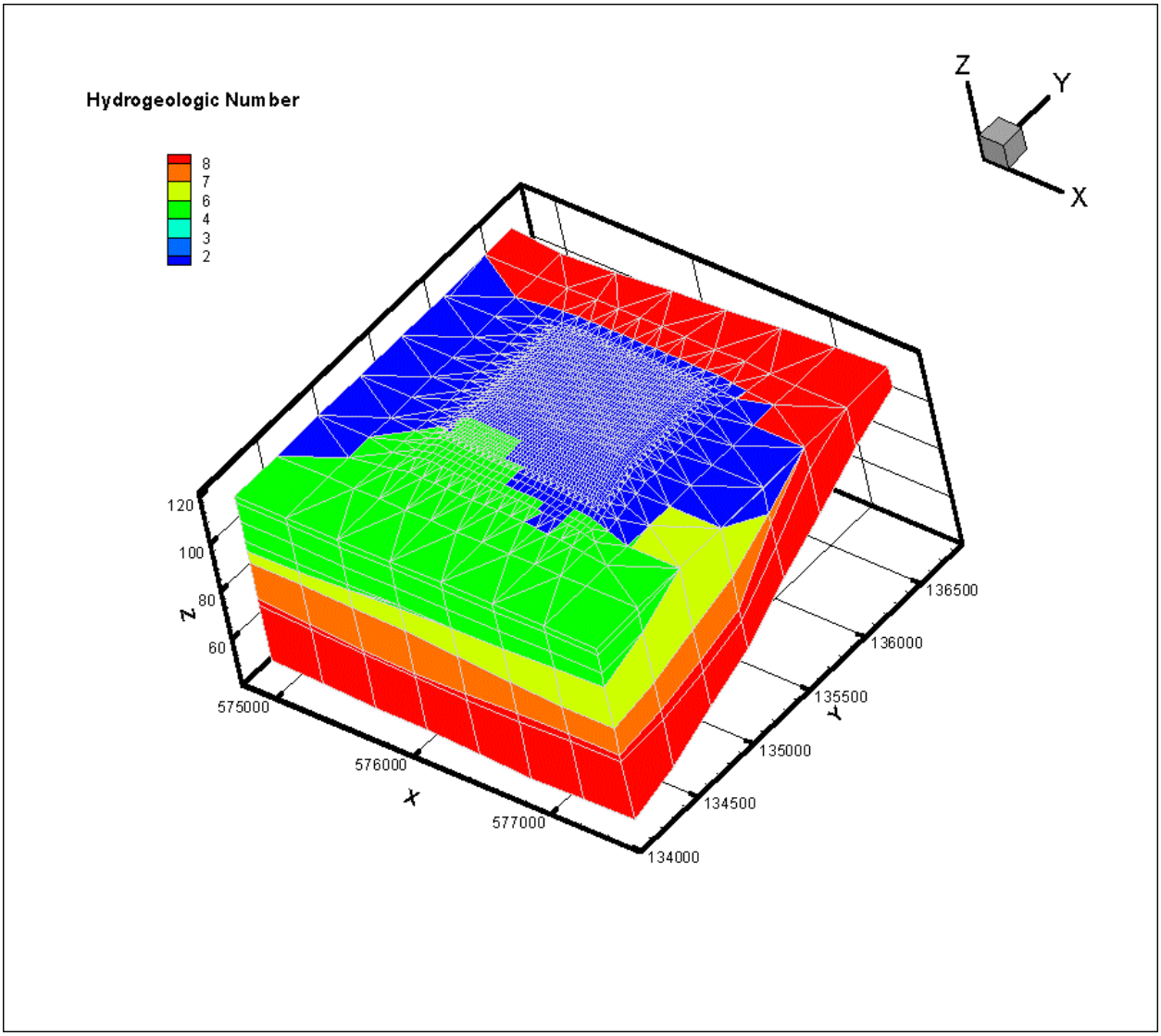

Figure 5.5. Three-Dimensional Distribution of Major Hydrogeologic Units in the New Local-Scale Model

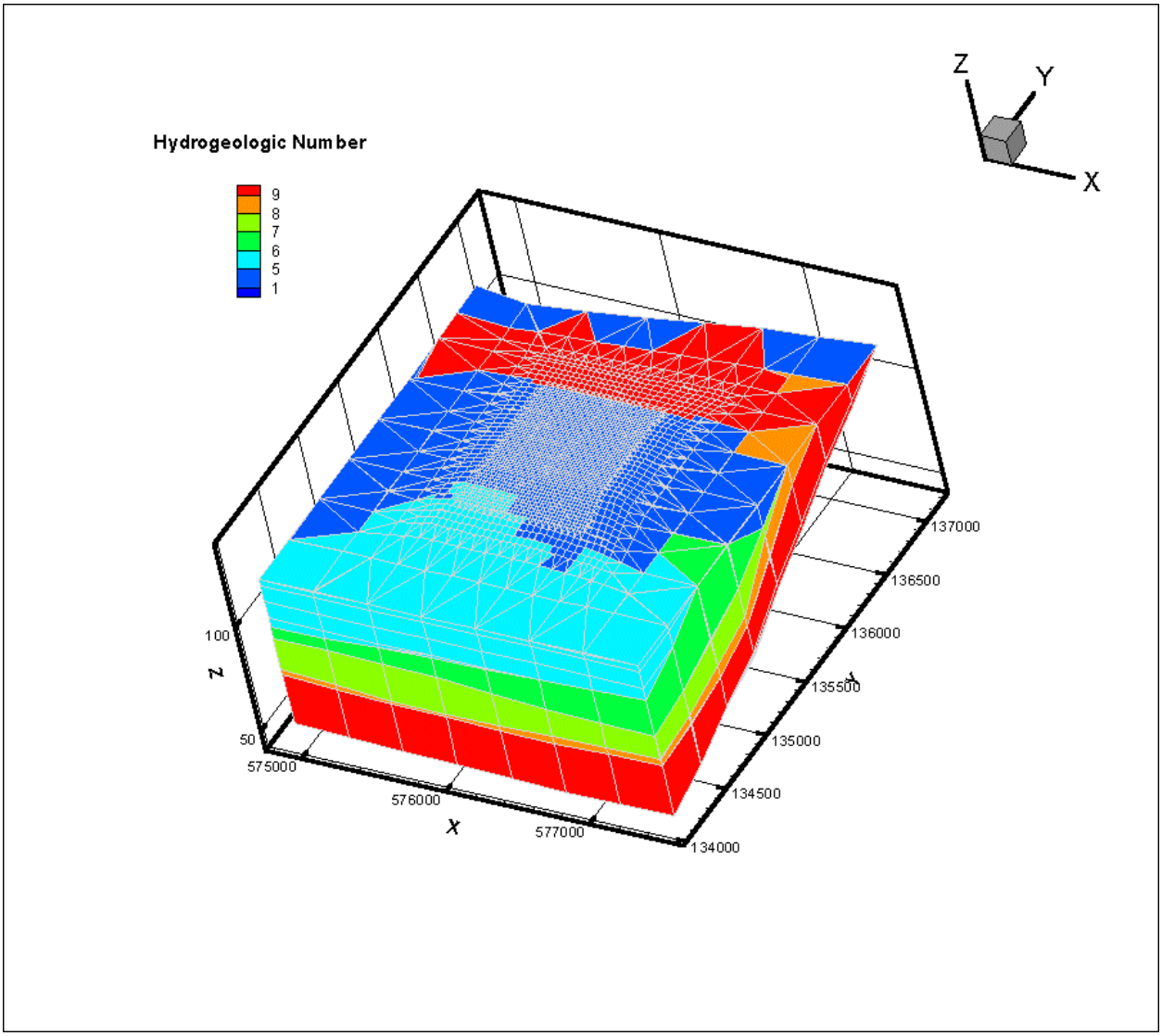

Figure 5.6. Three-Dimensional Distribution of Major Hydrogeologic Units in the Existing Local-Scale Model

5.2.2 Hydraulic Properties

The hydraulic conductivity and porosity estimates used in the local-scale model were developed based on the assumption that interpolating regional-scale estimates of hydraulic properties in the site-wide model using grid coordinates from the local-scale model can be used to represent local-scale properties in the vicinity of the ILAW disposal facility. The resulting three-dimensional distribution of these properties for the new ILAW Disposal Facility model is provided in Figure 5.7. The

resulting three-dimensional distribution of these properties for the existing ILAW Disposal Facility model is provided in Figure 5.8. The estimated values generally indicate the regional high trends in hydraulic properties found in the central part of the Hanford Site. This is where the ancestral Columbia River deposited very coarse alluvial deposits in a deep channel extending to the south of the ILAW site and to the north through Gable Butte and Gable Mountain. Estimated hydraulic conductivities directly below the disposal-facility region range from several thousand to tens of thousands of m/day in the Hanford formation and several hundred m/day in the permeable parts of the Ringold Formation (Units 5, 7, and 9). Relatively low hydraulic conductivities are estimated for low-permeability units within the Ringold Formation (Units 6 and 8).

5.2.3 Transport Properties

Estimates of model parameters were developed to account for contaminant dispersion in all transport simulations. Specific model parameters examined included longitudinal and transverse dispersion coefficients (D_l and D_t) as well as estimates of effective bulk density and porosity of the aquifer materials. This section briefly summarizes estimated transport properties.

For purposes of this analysis, no adsorption was accounted for in simulating releases from the new and existing disposal facilities. All simulations were based on the release and transport of a non-sorbed, long-lived radionuclide. Iodine-129 was used as the surrogate radionuclide in all calculations.

For purposes of these calculations, a bulk density of 1.9 g/cm^3 was used for all simulations. The effective porosity was estimated from specific yields obtained from multiple-well aquifer tests. These values range from 0.01 to 0.37. Laboratory measurements of porosity, which range from 0.19 to 0.41, were available for samples from a few Hanford Site wells and were also considered. The few tracer tests conducted indicate effective porosities ranging from 0.1 to 0.25. Based on the ranges of values considered, a best estimate of an effective porosity value for all simulations was assumed to be 0.25.

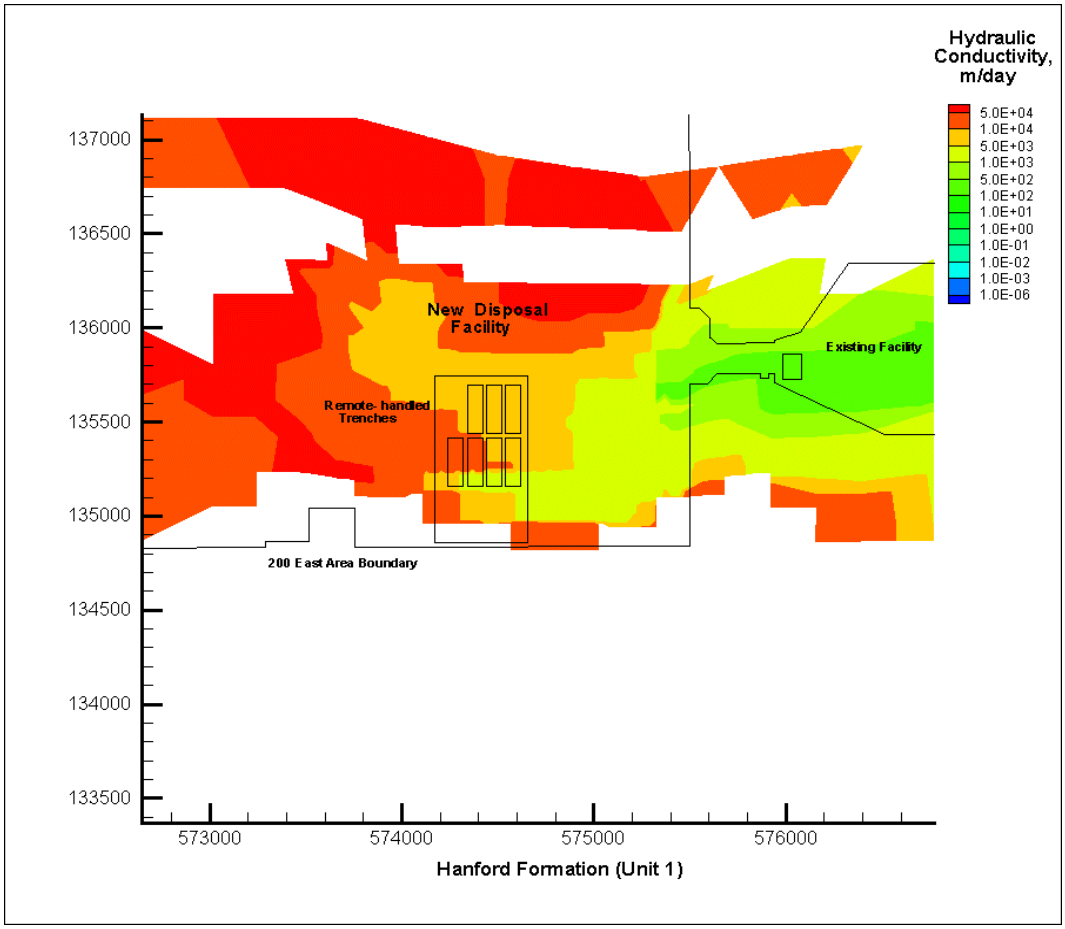

Figure 5.7. Distribution of Hydraulic Conductivities Used in the Local-Scale Model of the New ILAW Disposal Facility

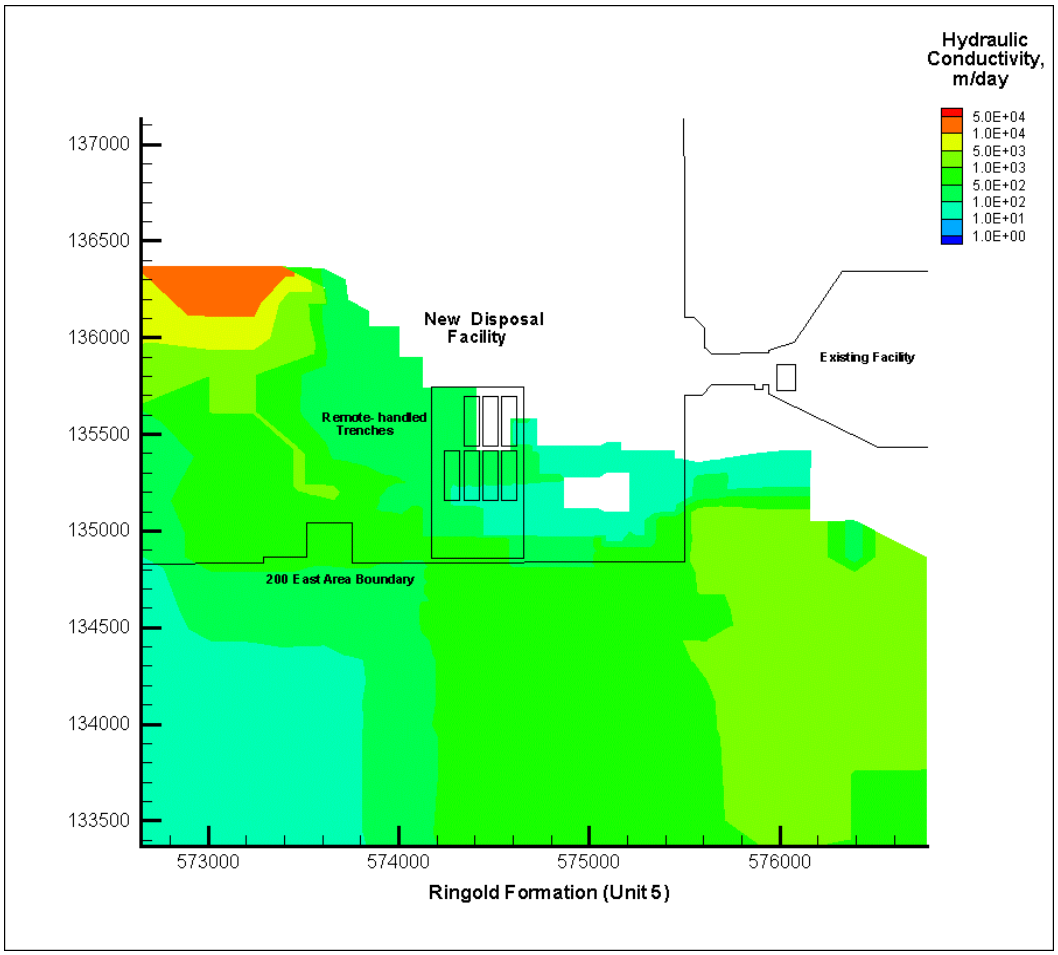

Figure 5.7 (Continued)

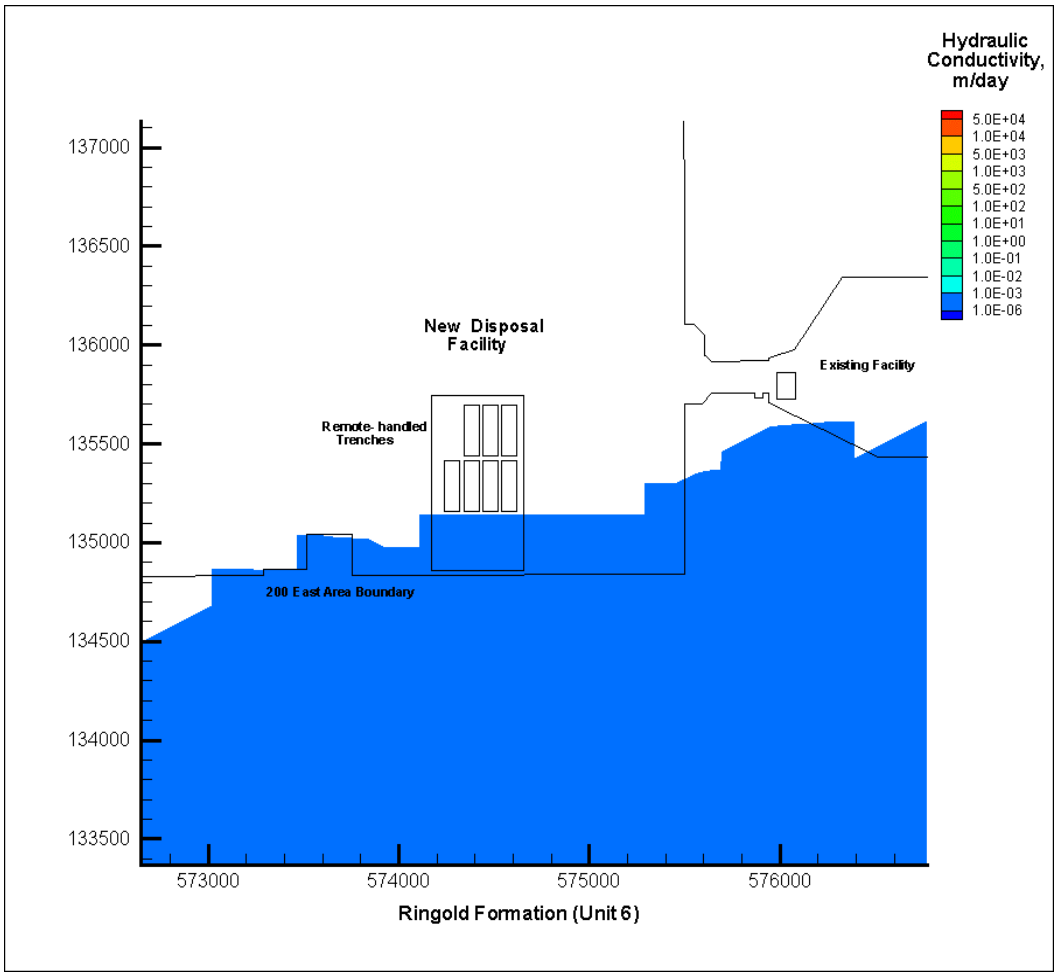

Figure 5.7 (Continued)

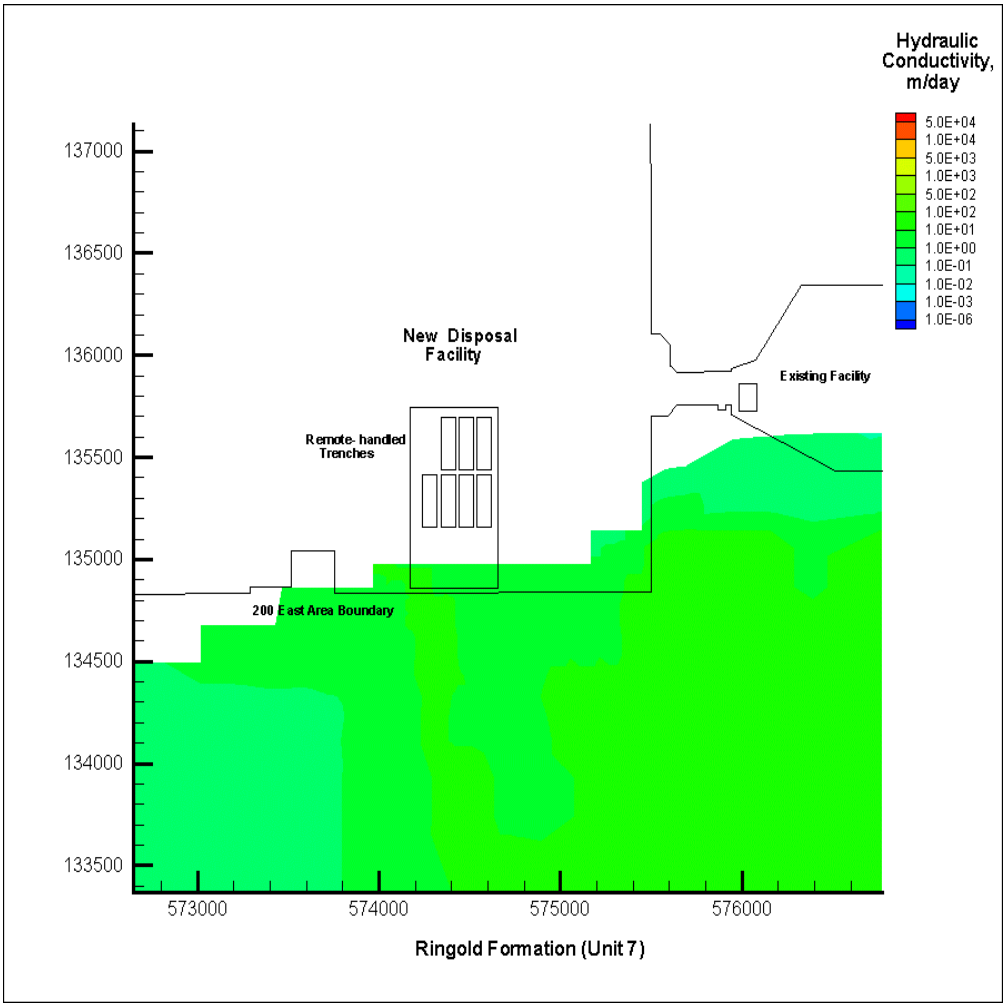

Figure 5.7 (Continued)

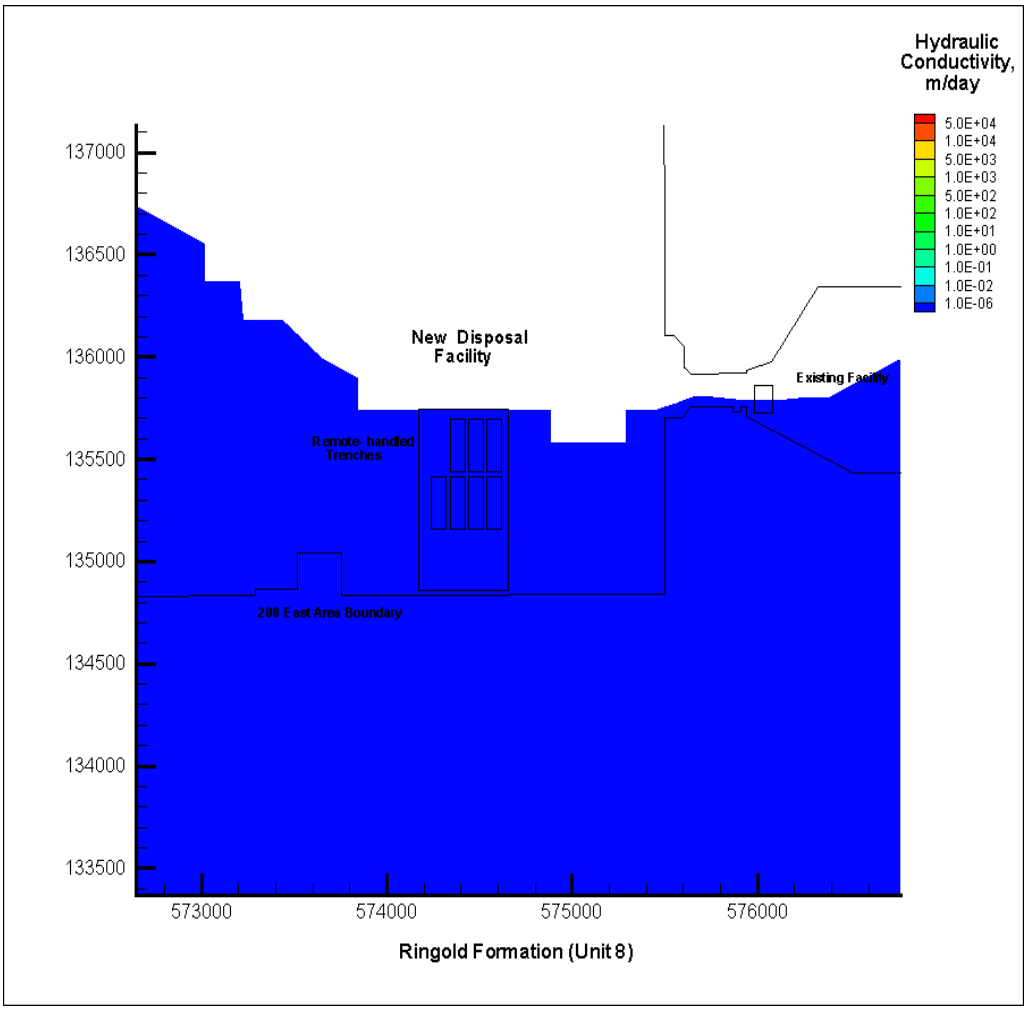

Figure 5.7 (Continued)

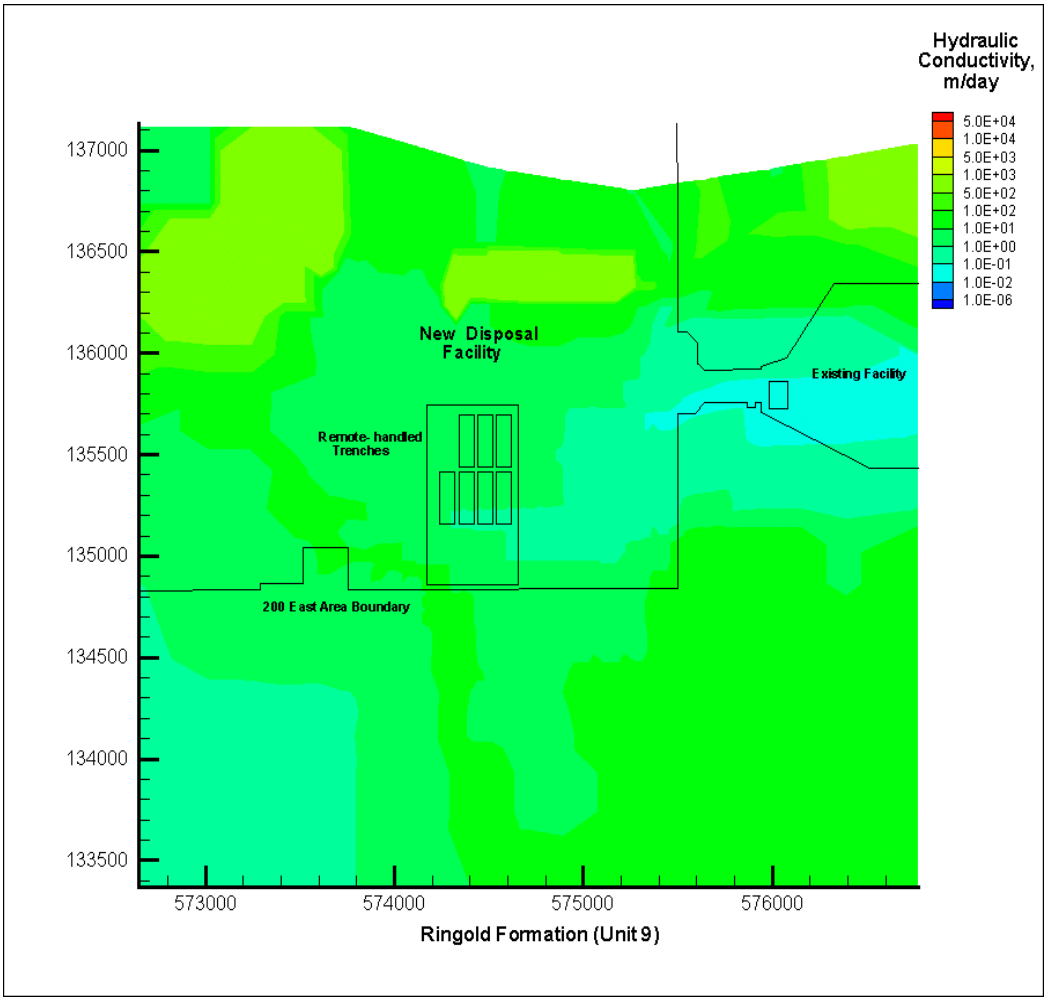

Figure 5.7 (Continued)

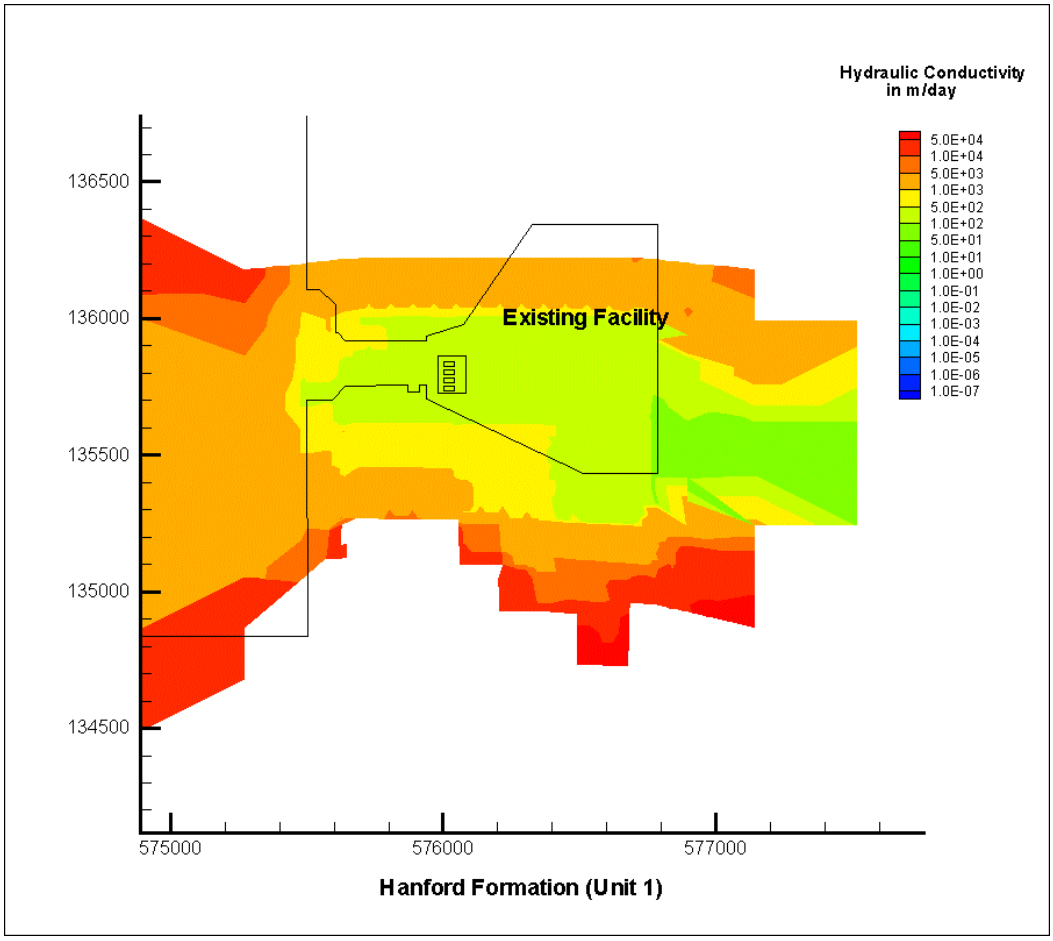

Figure 5.8. Distribution of Hydraulic Conductivities Used in the Local Scale Model of the Existing ILAW Disposal Facility Area

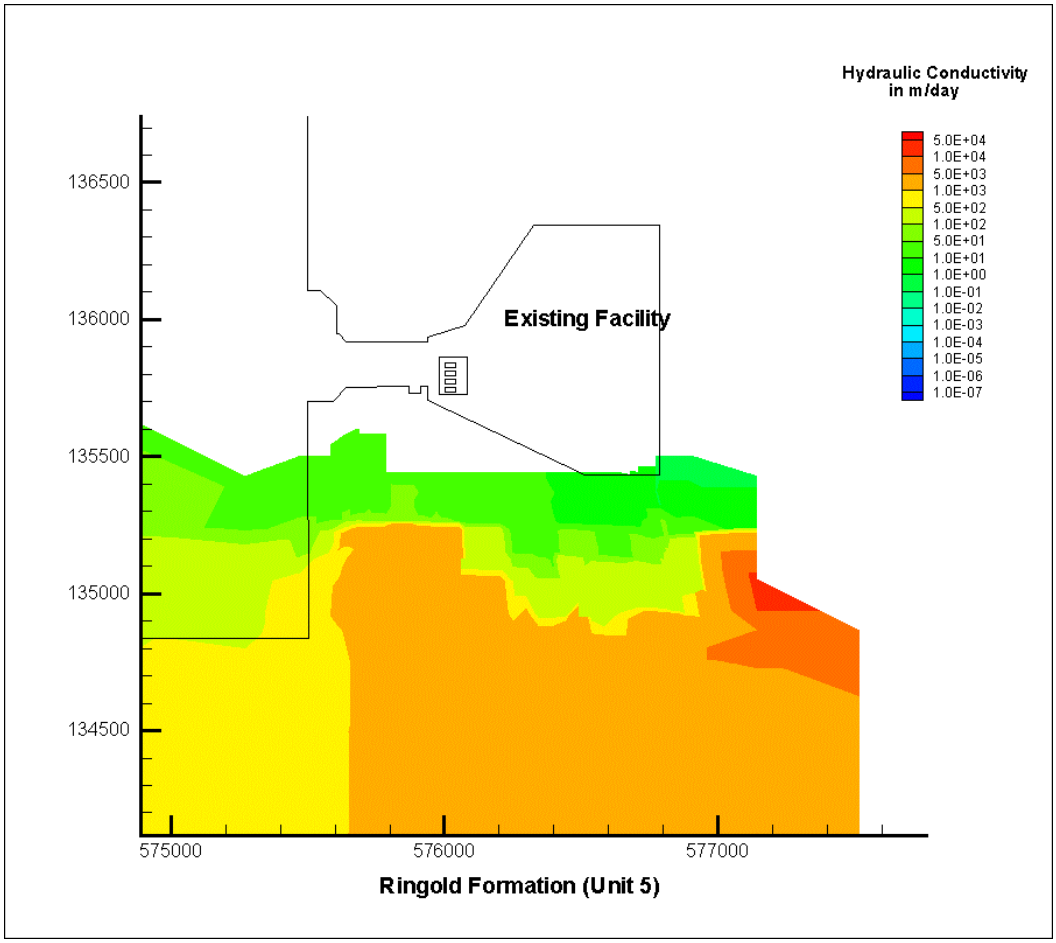

Figure 5.8 (Continued)

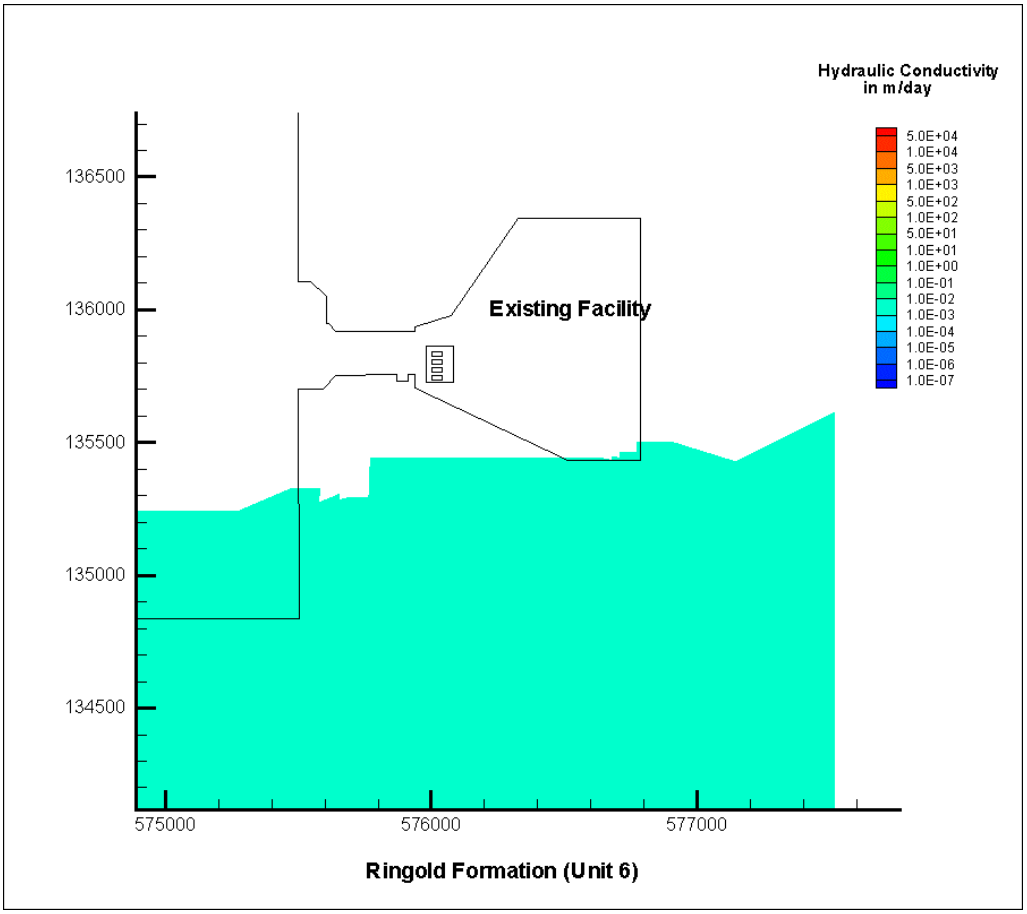

Figure 5.8 (Continued)

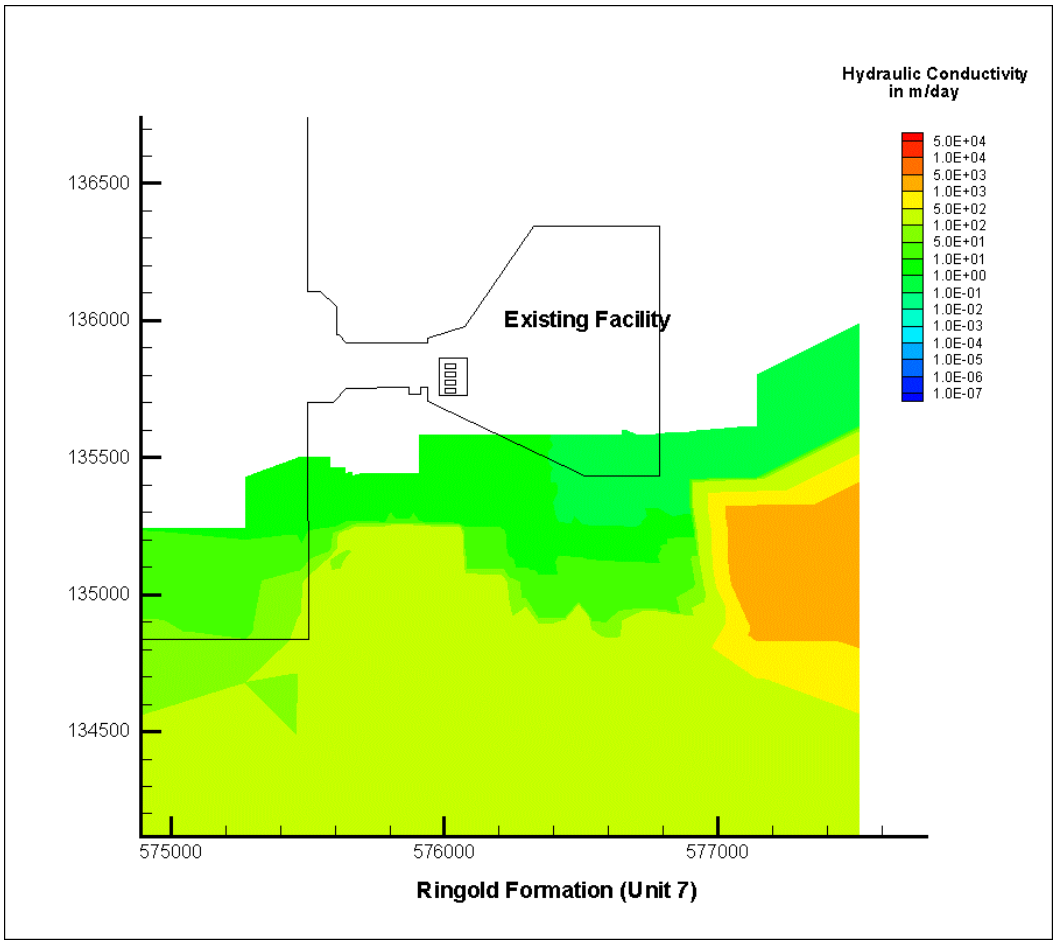

Figure 5.8 (Continued)

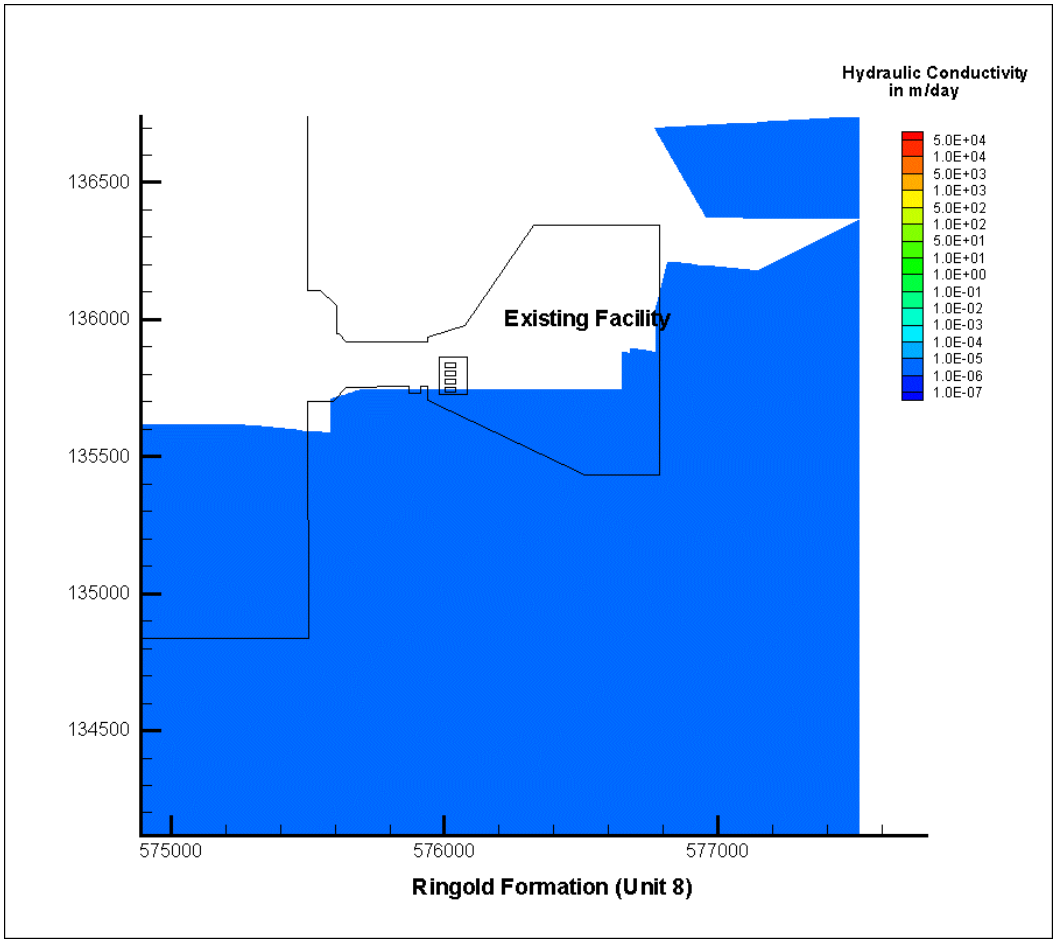

Figure 5.8 (Continued)

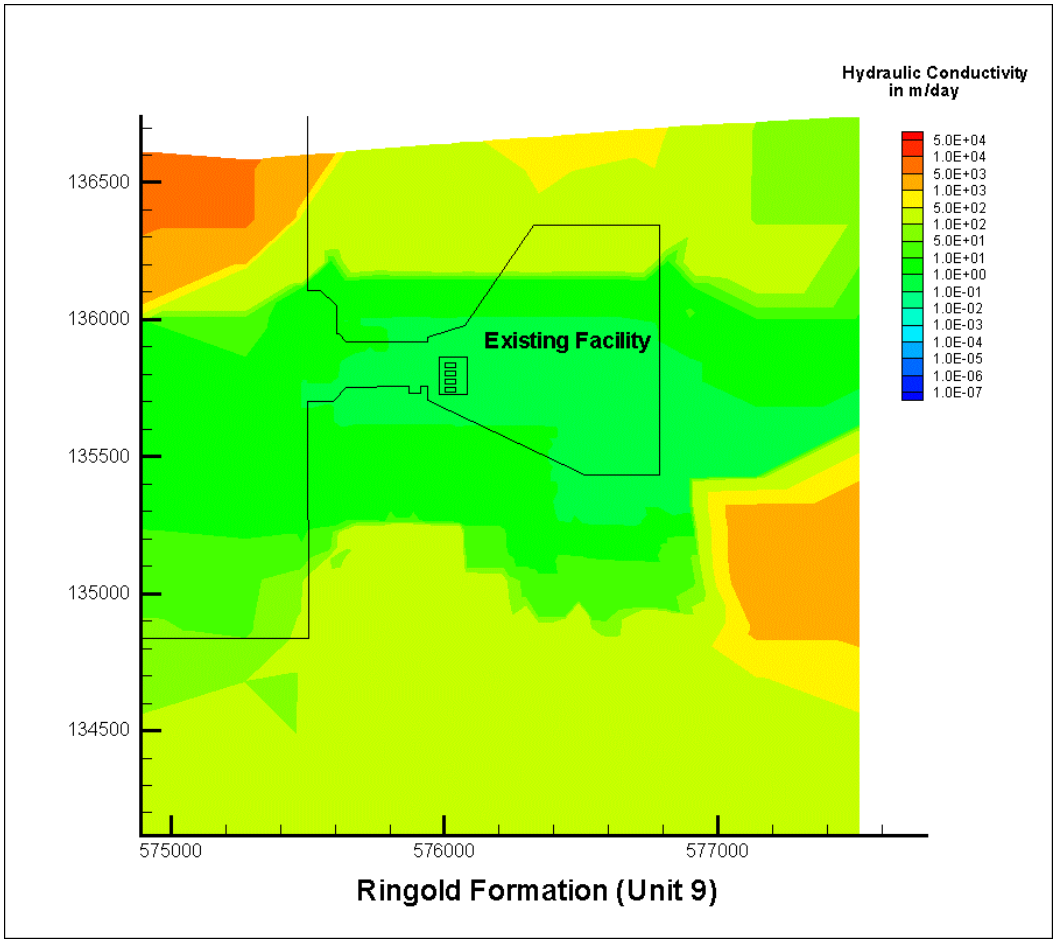

Figure 5.8 (Continued)

6.0 Results of the Groundwater Transport Analyses

This section presents the results of the groundwater transport analyses performed with the site-wide and local-scale models. The section in divided into two parts. One examines the impacts of the remote-handled-trench and concrete-vault concepts in the new ILAW disposal facility. The other evaluates the concrete-vault concept within the existing ILAW disposal facility.

6.1 New Disposal Facility

This subsection summarizes the impacts on calculated WIFs of the remote-handled trench and concrete-vault disposal concepts in the new ILAW disposal facility.

6.1.1 Remote-Handled Trench Concept

The remote-handled-trench disposal concept was evaluated in the base-case calculations. For this concept, the new ILAW disposal facility will consist of a set of six remote-handled waste trenches located in the northern part of the new ILAW disposal facility area. Each waste trench will be an underground, open-topped trench approximately 80 m (262.5 ft) wide, 260 m (853 ft) long, and 10 m (32.8 ft) deep with 3:1 side slopes. The release from these trenches in the model was approximated using the plan view area (80 m [62.5 ft] wide by 260 m [853 ft] long) of each individual trench.

The primary objective of the groundwater flow and transport calculations was to determine the WIF, defined as the ratio of the concentration at a well location in the aquifer to the concentration of infiltrating water entering the aquifer. For the purposes of these calculations, the concentration of source entering the aquifer was assumed to be 1 Ci/m^3. The rate of mass flux associated with this concentration is a function of the infiltration rate assumed for the disposal facility covered by the modified RCRA subpart C barrier. With a rate of 4.2 mm/yr assumed for the disposal facility, the resulting solute flux entering the aquifer from each of the disposal concepts is 4.2×10^{-3} $Ci/yr/m^2$. This is the product of the contaminant concentration in the infiltrating water and the infiltration rate.

Because of the uncertainty in expected infiltration rates, results developed for the 4.2 mm/yr rate for each of the cases presented were scaled to other infiltration rates that have been postulated from surface and soil conditions in the vicinity of the ILAW disposal facility by Fayer (1999). Other infiltration rates evaluated and summarized in each of the result tables included 0.1, 0.9, 1.0, and 50 mm/yr.

In all model simulations performed, the WIF was calculated at a hypothetical well located approximately 100 m (328 ft) downgradient from the boundary of the disposal along the centerline of the simulated plume. A pumping rate of 10 L (2.6 gal) per day was used at the hypothetical

downgradient well location. This pumping rate would provide sufficient drinking water for a family of five at an assumed intake of 2 L (0.5 gal) per person (per day).

6.1.1.1 Simulated Results at a 100-m (328-ft) Downgradient Well

Transport model results provided for the remote-handled-trench concept were based on local-scale flow conditions (Figure 6.1). These conditions were developed based on boundary conditions provided by the steady-state simulation of Post-Hanford flow conditions performed with the site-wide model. Groundwater moves across the ILAW site in a southeasterly direction before exiting the local-scale model in the southeast corner.

The results are expressed in WIFs, which relate the contaminant concentration in groundwater to the vadose zone contaminant flux. WIFs were calculated at a distance of 100 m (328 ft) downgradient from the facility and at an approximate distance of 1,000 m (3280 ft) downgradient of the disposal-facility boundaries. The WIFs for 4.2 mm/yr and other assumed infiltration rates at this location are summarized in Table 6.1.

Simulated concentration histories at 100 m (328 ft) downgradient of the disposal facilities containing six trenches are presented in Figures 6.2 through 6.4. Figure 6.2 shows the distribution of contaminant concentration in the uppermost element of the local-scale model. Figure 6.3 shows concentration profiles in a cross section from the source area through the 100-m (328 ft) well to the edge of the local-scale model region. Figure 6.4 shows concentration histories at the 100-m (328 ft) and 1000-m (3280 ft) wells for a period of 100 yr after the source is introduced into the aquifer. In this six-trench calculation, the concentration profile reaches steady state within about 10 yr with a maximum value of 1.1×10^{-3} Ci/m^3 at the 100-m well and 7.8×10^{-4} Ci/m^3 at the 1-km well. At an assumed recharge rate of 4.2 mm/yr, the calculated WIF would be 1.1×10^{-3} at the 100-m well and 7.8×10^{-4} at the 1-km well.

Table 6.1. Well Intercept Factors at the 100-m (328-ft) and 1000-m (3280-ft) Wells for the Remote-Handled-Trench Disposal Concept Using Different Infiltration Rates – New Disposal Facility

	Infiltration Rates (mm/yr)				
Well Locations	**0.1**	**0.9**	**1.0**	**4.2**	**50**
100 m	2.5E-05	2.3E-04	2.5E-04	1.1E-03	1.3E-02
1000 m	1.9E-05	1.7E-04	1.9E-04	7.8E-04	9.3E-03

6.1.1.2 Well-Intercept Factor at Distant Downgradient Wells

Steady-state flow conditions established with the site-wide model as presented in Section 5 (Figures 5.1 and 5.2) provide the basis for transport calculations of source releases from the remote-handled-trench concept between the disposal site area and the Columbia River. Simulated transport results at several locations downgradient of the disposal facilities containing multiple remote-handled trenches are presented in Figures 6.5 and 6.6. Figure 6.5 shows the distribution of contaminant concentration in the uppermost element of the site-wide scale model. Figure 6.6 shows concentration histories at the several well locations for a period of 400 yr after the source is introduced into the aquifer. In this six-trench calculation, the concentration profile reaches steady state within about 30 to 50 yr, with a maximum value of 5.4×10^{-4} Ci/m^3 at the 1000-m (3280-ft) well location. Steady state is reached within 400+ yr, with a maximum value of 9.8×10^{-5} Ci/m^3 at the well located near the Columbia River. As expected, the associated WIF at the 1000-m (3280-ft) well location is somewhat less than with those calculated at a similar distance in the local-scale model, but is generally consistent with local-scale concentration levels, given the large differences in model resolution. At an assumed recharge rate of 4.2 mm/yr, the calculated WIFs would range from 5.4×10^{-4} at 1000 m (3280 ft) downgradient to 9.8×10^{-5} at a hypothetical well near the Columbia River. The WIF factors for 4.2 mm/yr and other assumed infiltration rates at all locations examined are summarized in Table 6.2.

Table 6.2. Well Intercept Factors at Several Downgradient Well Locations for the Remote-Handled-Trench Disposal Concept Using Different Infiltration Rates – New Disposal Facility

	Infiltration Rates (mm/yr)				
Well Locations*	**0.1**	**0.9**	**1.0**	**4.2**	**50**
1.0 km	1.3E-05	1.2E-04	1.3E-04	5.4E-04	6.4E-03
3.1 km	9.0E-06	8.1E-05	9.0E-05	3.8E-04	4.5E-03
5.0 km	7.9E-06	7.1E-05	7.9E-05	3.3E-04	3.9E-03
7.6 km	6.7E-06	6.0E-05	6.7E-05	2.8E-04	3.3E-03
9.3 km	5.8E-06	5.2E-05	5.8E-05	2.4E-04	2.9E-03
11.1 km	4.5E-06	4.0E-05	4.5E-05	1.9E-04	2.2E-03
14.8 km (river well)	2.3E-06	2.1E-05	2.3E-05	9.8E-05	1.2E-03

* Well locations are shown in Figure 6.5.

6.1.2 Concrete Vault Concept

For this concrete-vault concept, the new ILAW disposal facility will consist of a set of seven concrete vaults located in the northern part of the ILAW disposal facility area. As described in Chapter 2, each vault is built above a RCRA-compliant leak detection and collection system. It

consists of a cast-in-place reinforced concrete basin approximately 209.5 m (687 ft) long and 24.7 m (81 ft) wide with walls 1.07 m (3.5 ft) high. The release from these vaults in the model was approximated using the plan view area (approximately 25 m [82 ft] wide by 210 m [689 ft] long) of each individual vault. The same assumption used for mass release and the hypothetical downgradient wells used for the remote-handled concept described in the previous section were used for the concrete-vault concept.

6.1.2.1 Simulated Results at the 100-m (328-ft) Downgradient Well

Local-scale flow conditions, illustrated in Figure 6.1, also provide the basis for transport-model results developed for the concrete-vault concept. This concept was based on releases from seven individual concrete vaults distributed in the new disposal-facility area. The WIFs were calculated at a distance of 100 m (328 ft) downgradient from the facility and at an approximate distance of 1,000 m (3280 ft) downgradient of the disposal-facility boundaries. The WIF factors for 4.2 mm/yr and other assumed infiltration rates at this location are summarized in Table 6.3.

Simulated concentration histories at 100 m (328 ft) downgradient of the disposal facilities containing seven vaults are presented in Figures 6.7 through 6.9. Figure 6.7 shows the distribution of contaminant concentration in the uppermost element of the local-scale model. Figure 6.8 shows concentration profiles in a cross section from the source area through the 100 m (328 ft) well to the edge of the local-scale model region. Figure 6.9 shows concentration histories at the 100 m (328 ft) well for a period of 100 yr after the source is introduced into the aquifer. In the concrete vault calculation, the concentration profile at the 100-m (328-ft) well reaches steady state within about 10 yr, with a maximum value of 2.8×10^{-4} Ci/m^3. At 1000 m (3280 ft), the concentration profile reaches a steady-state maximum value of 2.2×10^{-4} Ci/m^3. At an assumed recharge rate of 4.2 mm/yr, the calculated WIF at the 100 m (328 ft) well would be 2.8×10^{-4} Ci/m^3. The WIF factors for 4.2 mm/yr and other assumed infiltration rates at 100 and 1000 m (328 and 3280 ft), respectively, are summarized in Table 6.3

Table 6.3. Well Intercept Factors at the 100-m (328-ft) and 1000-m (3280-ft) Well Locations for the Concrete-Vault Disposal Concept Using Different Infiltration Rates

	Infiltration Rates (mm/yr)				
Well Locations	**0.1**	**0.9**	**1.0**	**4.2**	**50**
100 m	6.7E-06	6.1E-05	6.7E-05	2.8E-04	3.4E-03
1000 m	5.4E-06	4.8E-05	5.4E-05	2.2E-04	2.7E-03

Differences between the WIFs calculated for this case compared to the remote-handled-trench case are directly attributable to assumptions used for source-release areas in both cases. The remote-handled-trench calculations were based on an assumed release area of 124,800 m^2, reflecting the

footprint of the six-trench configuration. The concrete-vault calculations were based on the assumption of a 36,750 m^2 release area, reflecting the footprint of the seven-concrete-vault configuration. The ratio of the WIFs between the two cases at 100 m are on the order of 3.9, which is reflective, though slightly higher, than the ratio of the release areas (3.4).

6.1.2.2 Well-Intercept Factor at Distant Downgradient Wells

Simulated concentration histories at several locations downgradient of the disposal facilities containing the seven concrete vaults were also developed using the regional flow field described previously and illustrated in Figure 6.5. In this seven-concrete-vault calculation, the concentration profile reaches steady state at the 1000-m well location within about 30 to 50 yr, with a maximum value of 1.6 x 10^{-4} Ci/m^3, assuming a recharge of 4.2 mm/yr. Steady state is reached within 400+ yr at the well located near the Columbia River with a maximum value of 3.9 x 10^{-4} Ci/m^3. As expected, the associated WIF at the 1000-m well location is less but similar to those calculated at a similar distance in the local-scale model. At an assumed recharge rate of 4.2 mm/yr, the calculated WIFs would range from 2.1 x 10^{-4} at 1000 m downgradient and 4.1 x 10^{-5} at a hypothetical well near the Columbia River. The WIF factors for 4.2 mm/yr and other assumed infiltration rates at all locations examined are summarized in Table 6.4.

Table 6.4. Well Intercept Factors at Several Downgradient Well Locations for the Concrete-Vault Disposal Concept Using Different Infiltration Rates

	Infiltration Rates (mm/yr)				
Well Locations*	**0.1**	**0.9**	**1.0**	**4.2**	**50**
1.0 km	3.8E-06	3.5E-05	3.8E-05	1.6E-04	1.9E-03
3.1 km	2.7E-06	2.4E-05	2.7E-05	1.1E-04	1.4E-03
5.0 km	2.4E-06	2.1E-05	2.4E-05	1.0E-04	1.2E-03
7.6 km	2.1E-06	1.9E-05	2.1E-05	8.6E-05	1.0E-03
9.3 km	1.8E-06	1.6E-05	1.8E-05	7.6E-05	9.0E-04
11.1 km	1.5E-06	1.3E-05	1.5E-05	6.1E-05	7.3E-04
14.8 km (river well)	9.2E-07	8.3E-06	9.2E-06	3.9E-05	4.6E-04

* Well locations are shown in Figure 6.10.

6.2 Existing Disposal Facility

This subsection summarizes the impacts on calculated WIFs of the concrete-vault concept in the existing ILAW disposal facility.

6.2.1 Concrete-Vault Concept

For this concrete vault concept, the existing ILAW disposal facility will contain a set of four concrete vaults as described in Section 2.2.2. Each vault at the existing disposal facility would be built above a RCRA-compliant leak-detection and collection system and would consist of a cast-in-place reinforced concrete basin. Each vault would be approximately 37.6 m (687.0 ft) long and 15.4 m (81 ft) wide with a roof clearance of 10.4 m (3.5 ft) high. The release from these vaults in the model was approximated using the plan view area (approximately 16 m [52.5 ft] wide by 40 m [131 ft] long) of each individual vault. The same assumption used for mass release and the hypothetical downgradient wells used for the concrete vault concept described in the previous section were used for the concrete-vault concept considered here.

6.2.1.1 Simulated Results at the 100-m (328-ft) Downgradient Well

Local-scale flow conditions, illustrated in Figure 6.10, provide the basis for transport-model results developed for the concrete-vault concept at the existing disposal facility. As in the other cases, concentration levels and WIFs were calculated at a distance of 100 m (328 ft) downgradient from the facility and approximately 1,000 m (3281 ft) downgradient of the disposal-facility boundaries.

Simulated concentration histories at 100 m (328 ft) downgradient of the disposal facilities containing four vaults are presented in Figures 6.11 through 6.13. Figure 6.11 shows the distribution of contaminant concentration in the uppermost element of the local-scale model. Figure 6.12 shows concentration profiles in a cross section from the source area through the 100-m (328-ft) well to the edge of the local-scale model region. Figure 6.13 shows concentration histories at the 100-m (328-ft) well for a period of 100 yr after the source is introduced into the aquifer. In the concrete vault calculation, the concentration profile at the 100-m (328-ft) well reaches steady state within about 10 yr, with a maximum value of 4.6×10^{-4} Ci/m^3. At 1000 m (3281 ft), the concentration profile reaches a steady-state maximum value of 5.7×10^{-5} Ci/m^3. At an assumed recharge rate of 4.2 mm/yr, the calculated WIF at the 100-m (328-ft) well would be 4.6×10^{-4} Ci/m^3. The WIF factors for 4.2 mm/yr and other assumed infiltration rates at 100 and 1000 m (328 and 3281 ft) respectively, are summarized in Table 6.5

Table 6.5. Well Intercept Factors at the 100-m (328-ft) and 1000-m (3281-ft) Well Locations for the Concrete-Vault Disposal Concept Using Different Infiltration Rates – Existing Disposal

	Infiltration Rates (mm/yr)				
Well Locations	**0.1**	**0.9**	**1.0**	**4.2**	**50**
100 m	1.1E-05	9.7E-05	1.1E-04	4.5E-04	5.4E-03
1000 m	1.4E-06	1.2E-05	1.4E-05	5.7E-05	6.8E-04

The large differences between the WIFs calculated for this case compared to those calculated for the remote-handled-trench case are attributable to assumptions used for source release areas and the lower estimated values for hydraulic properties used for hydrogeologic units in the existing grout facility model. The remote-handled-trench calculations were based on an assumed release area of 124,800 m^2, reflecting the footprint of the assumed six-trench configuration. The concrete-vault calculations were based on the assumed 2,560 m^2 release area, reflecting the footprint of the smaller four-concrete-vault configuration. The ratio of the WIFs between the two cases at 100 m are on the order of 2.4, which is much lower than expected, given that the ratio of the release area is on the order of 50. The higher-than-expected WIF in this case is affected by the lower hydraulic conducitivities used in this lowcal scale model. Hydraulic conductivities used for the Hanford Formation beneath the existing grout facilities, which are on the order of 200 to 300 m/day, are about a factor of 25 to 50 times lower than those used beneath the new ILAW disposal-facility area, which vary from about 6,500 to 14,500 m/day). In general, the lower hydraulic conductivities used in the existing grout-facility model contribute to lower pore water velocities and lower horizontal flow beneath the existing grout facility; they create an overall increase in the calculated WIF. The general increase in the WIF for this case reflects differences in the release area and the estimated hydraulic properties.

6.2.1.2 Well-Intercept Factor at Distant Downgradient Wells

Simulated transport results at several locations downgradient of the existing disposal facility containing four concrete vaults were also developed using the regional flow field described previously and illustrated in Figure 5.2. In this four-concrete-vault calculation, the concentration profile reaches steady state at the 1000 m (3281 ft) well location within about 30 to 50 yr, with a maximum value of 3.0×10^{-5} Ci/m^3, assuming a recharge of 4.2 mm/yr. Steady state is reached within 400+ yr at the well located near the Columbia River, with a maximum value of 5.2×10^{-6} Ci/m^3. The associated WIF at the 1000-m (3281-ft) well location is similar to those calculated at a similar distance in the local-scale model. At an assumed recharge rate of 4.2 mm/yr, the calculated WIFs would range from 3.0×10^{-5} at 1000 m (3281 ft) downgradient and 5.2×10^{-6} at a hypothetical

well near the Columbia River. The WIF factors for 4.2 mm/yr and other assumed infiltration rates at all locations examined are summarized in Table 6.6.

Table 6.6. Well Intercept Factors at Several Downgradient Well Locations for the Concrete-Vault Disposal Concept Using Different Infiltration Rates – Existing Disposal Facility

	Infiltration Rates (mm/yr)				
Well Locations*	**0.1**	**0.9**	**1.0**	**4.2**	**50**
1.0 km	7.1E-07	6.4E-06	7.1E-06	3.0E-05	3.6E-04
3.1 km	3.5E-07	3.1E-06	3.5E-06	1.5E-05	1.7E-04
5.0 km	2.3E-07	2.0E-06	2.3E-06	9.5E-06	1.1E-04
7.6 km	2.0E-07	1.8E-06	2.0E-06	8.3E-06	9.9E-05
9.3 km	1.9E-07	1.7E-06	1.9E-06	7.8E-06	9.3E-05
11.1 km	1.5E-07	1.4E-06	1.5E-06	6.4E-06	7.6E-05
14.8 km (river well)	1.2E-07	1.1E-06	1.2E-06	5.2E-06	6.2E-05

* Well locations are shown in Figure 6.14

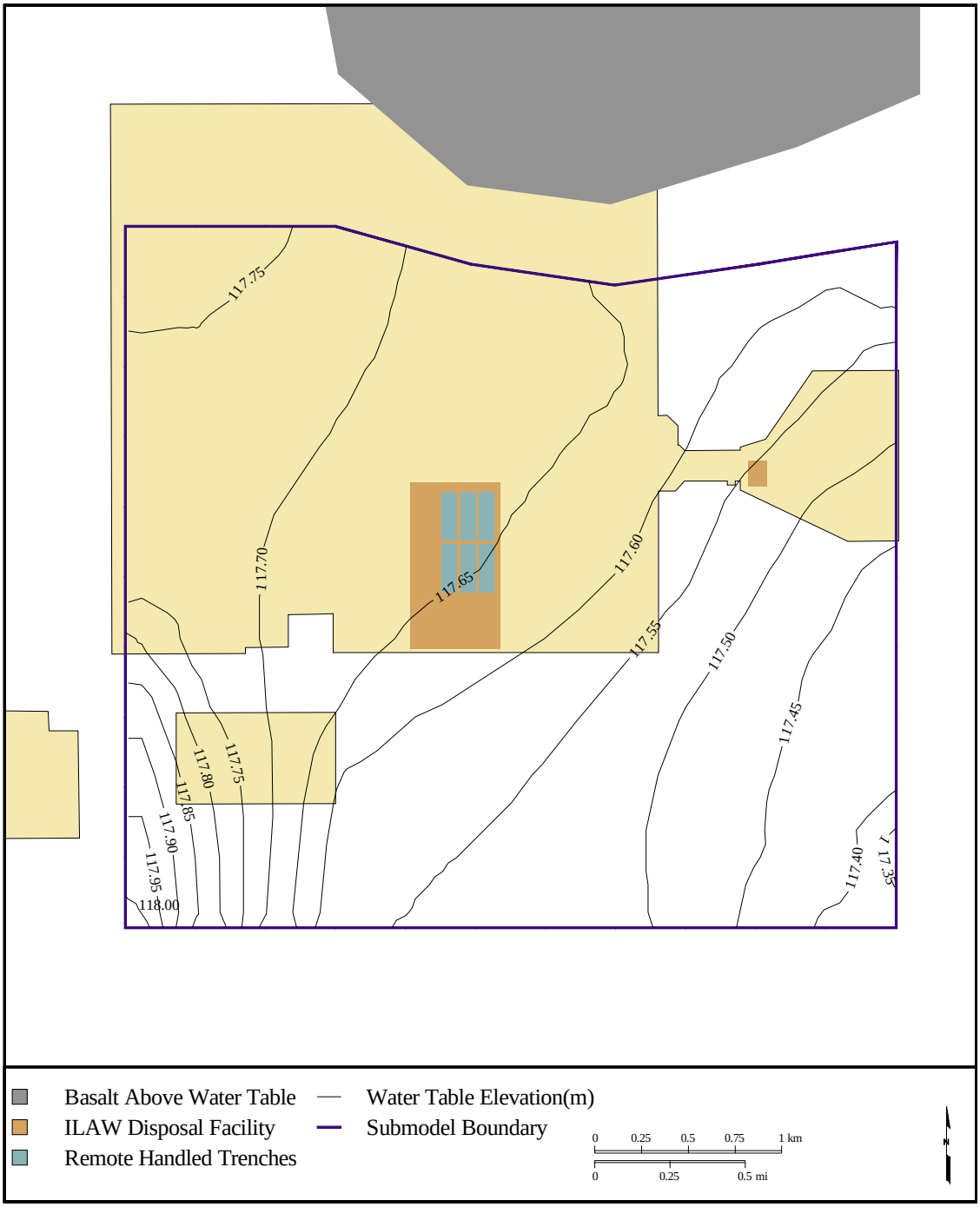

skw00072.eps December 28, 2000

Figure 6.1. Distribution of Hydraulic Head in Unconfined Aquifer in Local-Scale Model – New Disposal Facility Area

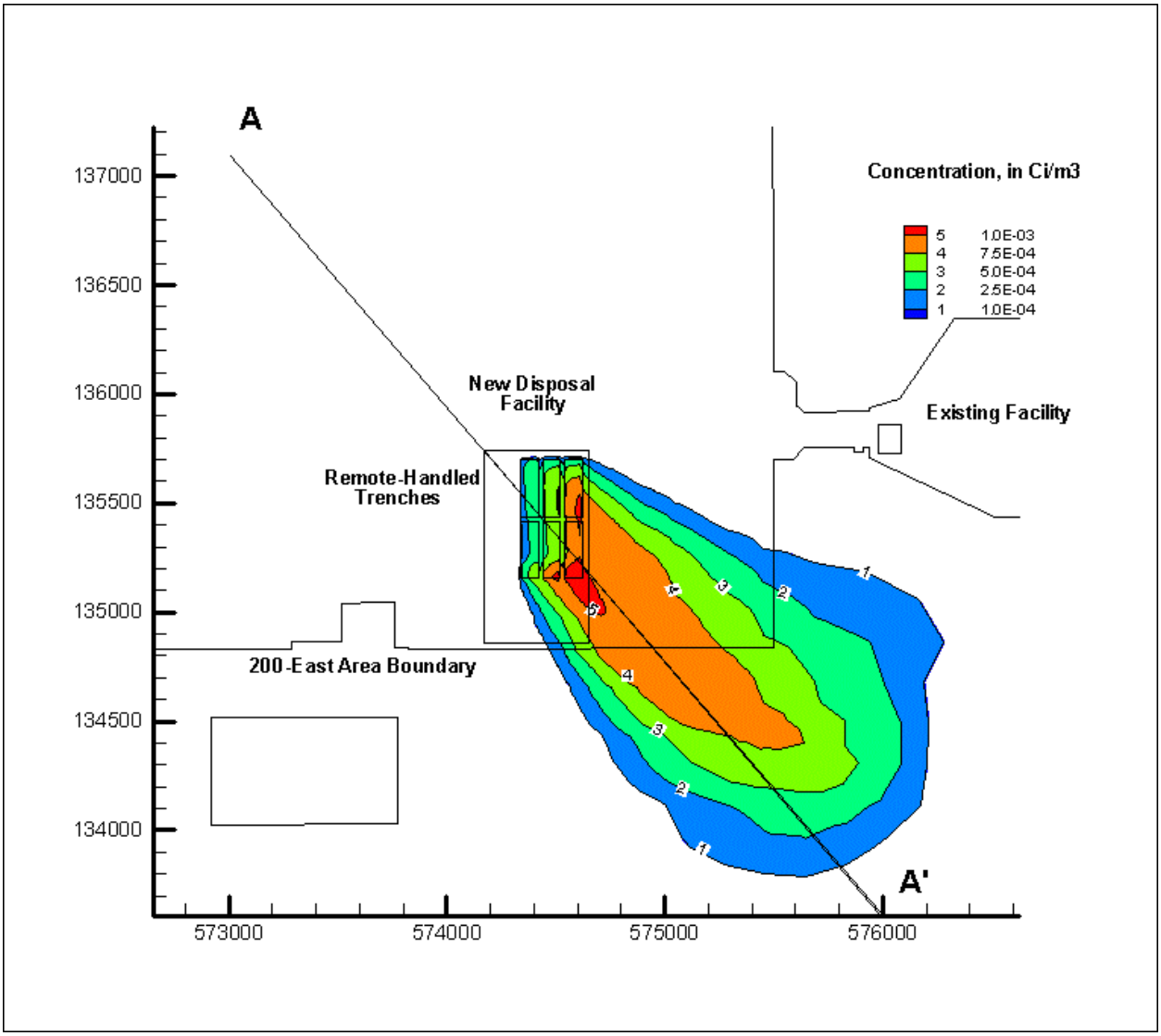

Figure 6.2. Areal Distribution of Contaminant Plume Resulting From Simulation of the Remote-Handled Trench Concept – New Disposal Facility Area

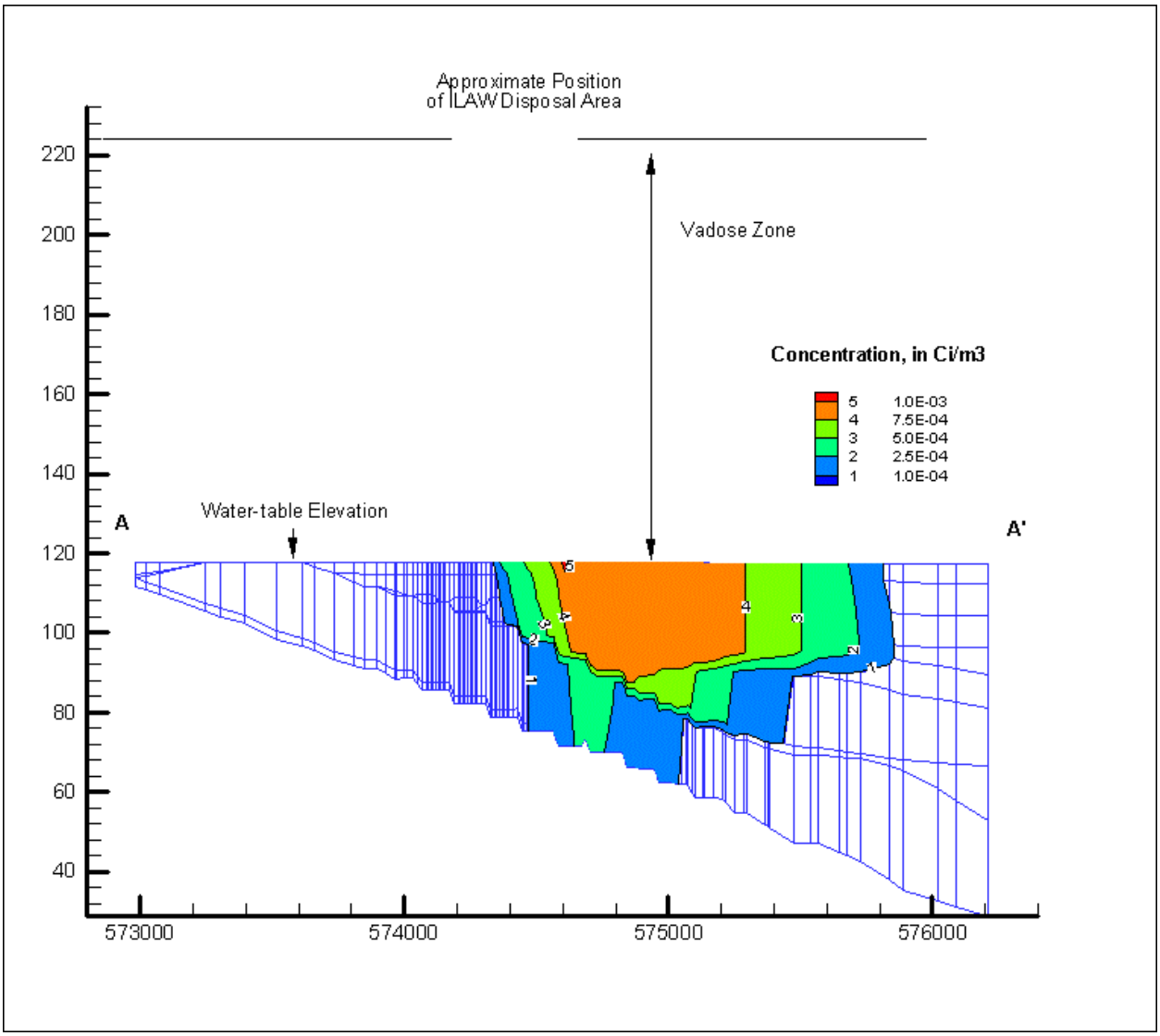

Figure 6.3. Vertical Distribution of a Contaminant Plume Resulting from Simulation of the Remote-Handled Trench Concept (Along the Approximate Centerline of the Plume) – New Disposal Facility Area

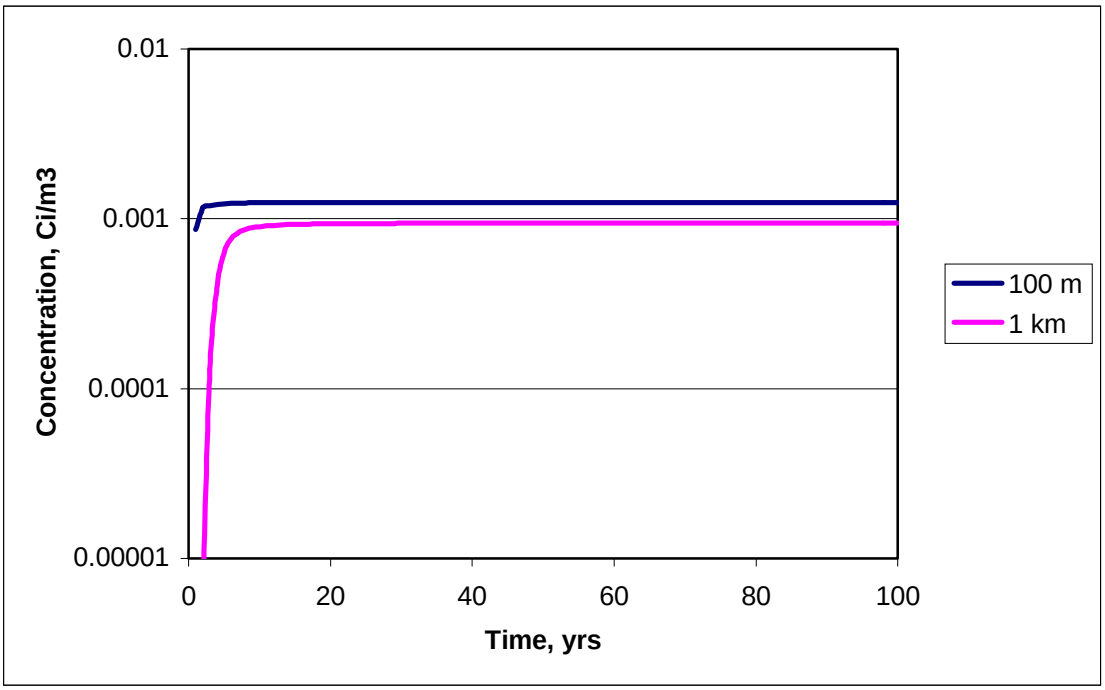

Figure 6.4. Concentration History at 100-m (328-ft) and 1000-m (328-ft) Wells, Local Scale Model – New Disposal Facility Area

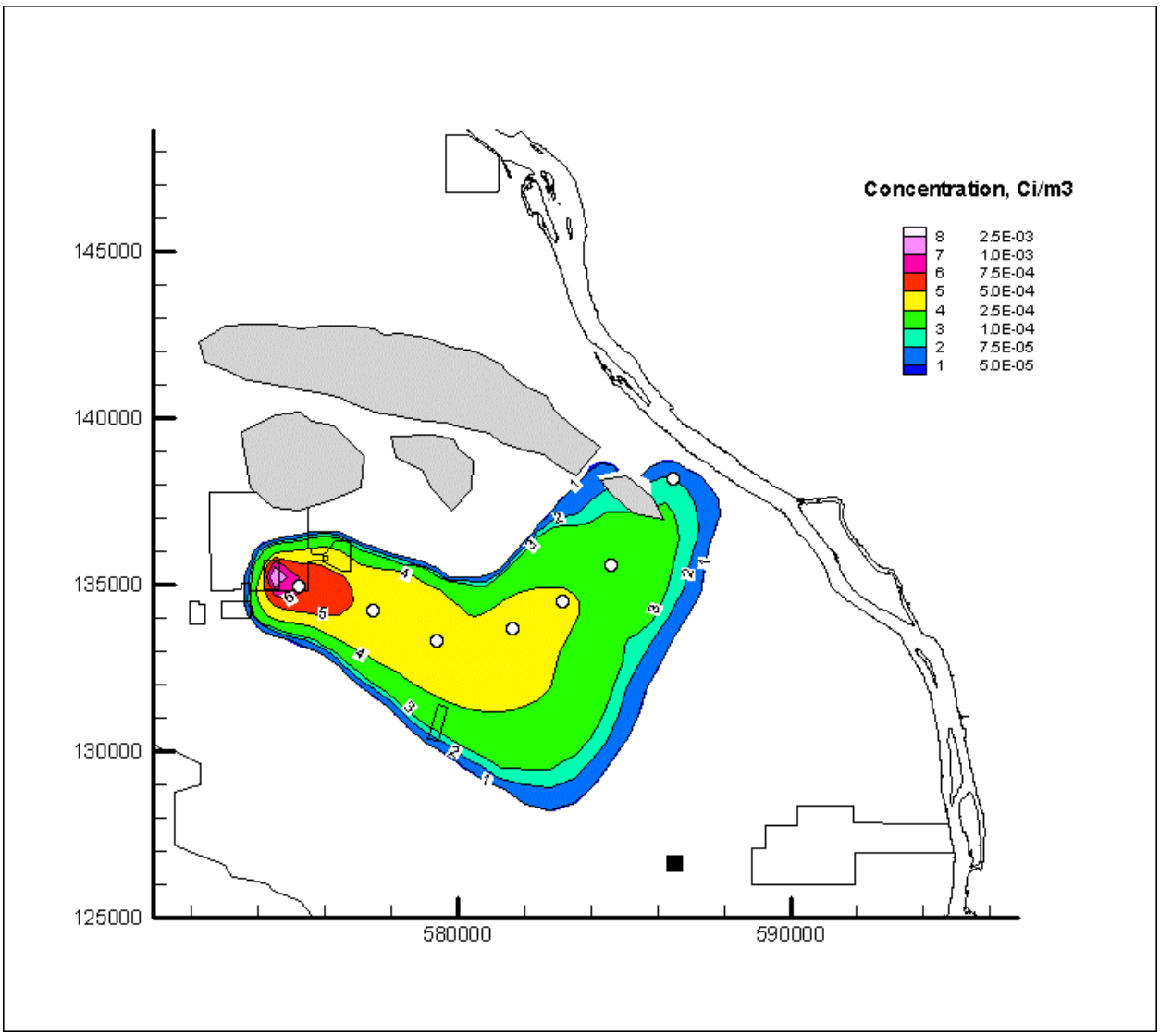

Figure 6.5. Areal Distribution of Contaminant Plume between the ILAW New Facility and the Columbia River, Remote Trench Concept – New Disposal Facility Area

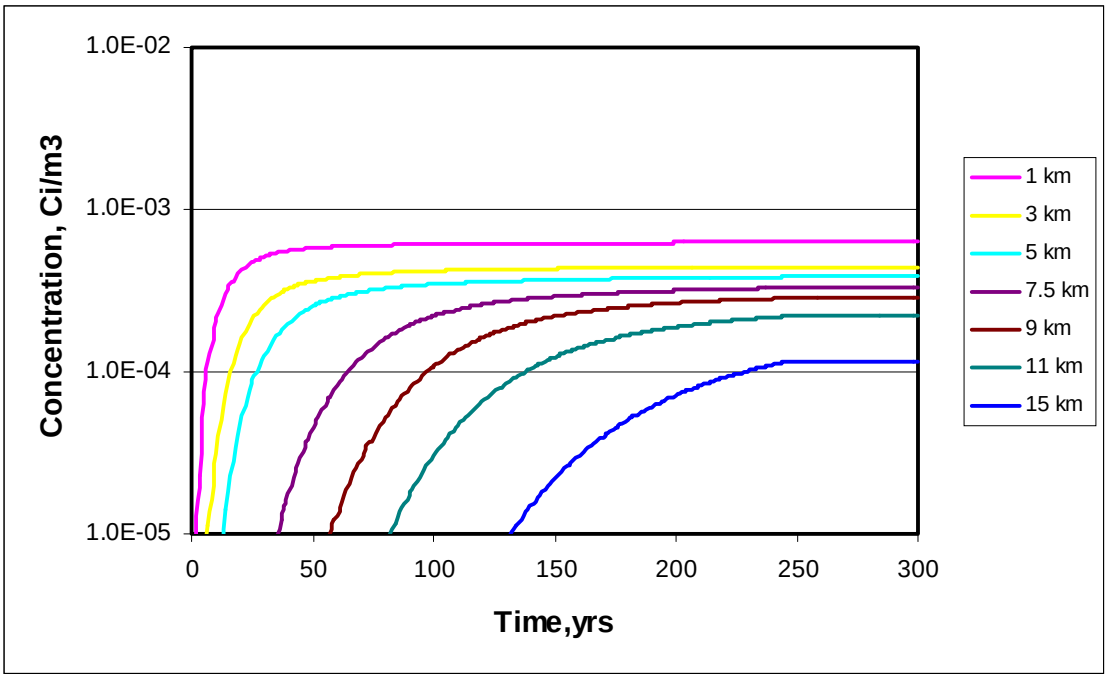

Figure 6.6. Concentration History at Selected Well Locations, Site-Wide Model – New Disposal Facility Area

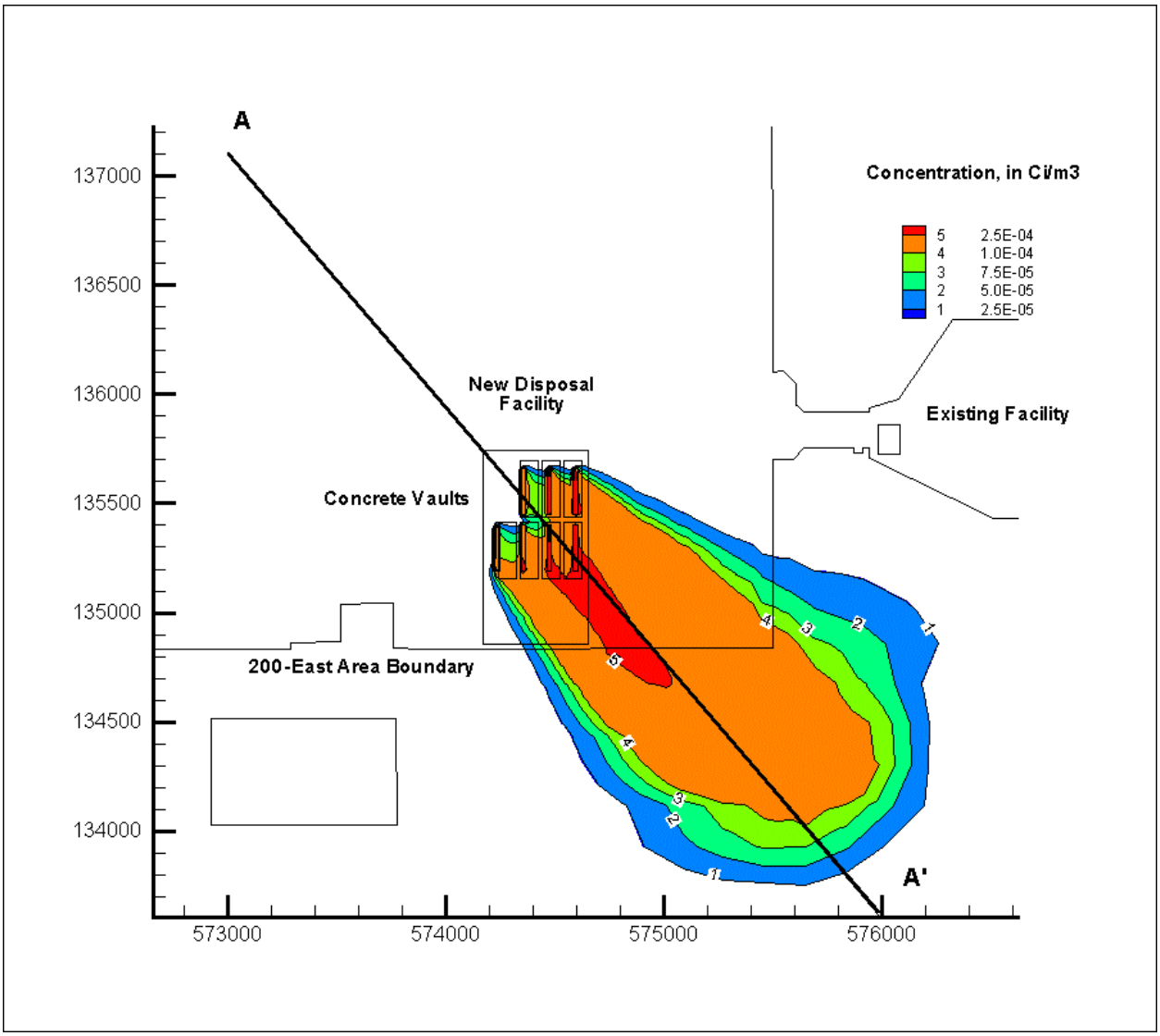

Figure 6.7. Areal Distribution of Contaminant Plume Resulting from Simulation of the Concrete Vault Concept – New Disposal Facility Area

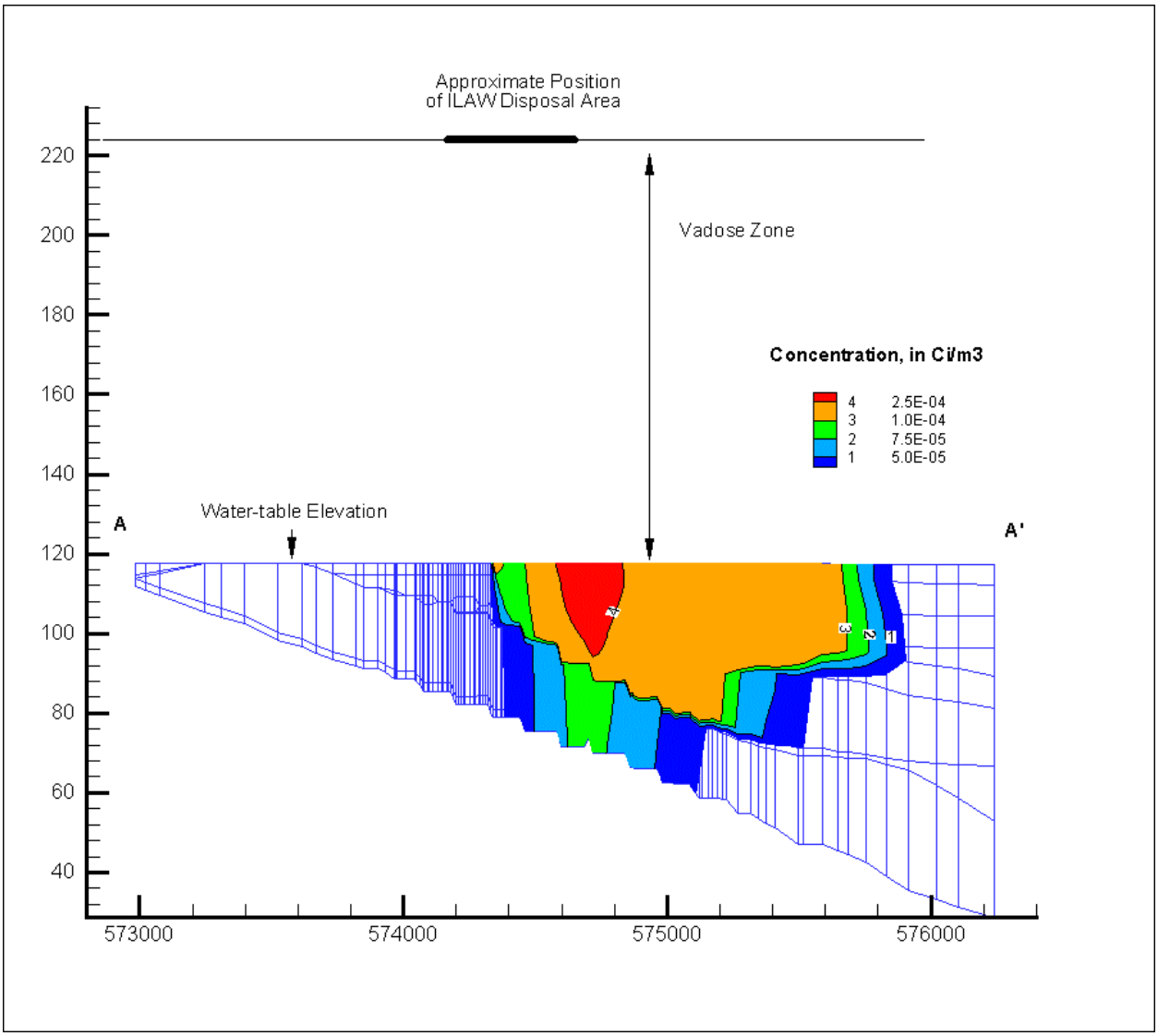

Figure 6.8. Vertical Distribution of a Contaminant Plume Resulting from Simulation of the Concrete Vault Concept (Along the Approximate Centerline of the Plume) – New Disposal Facility Area

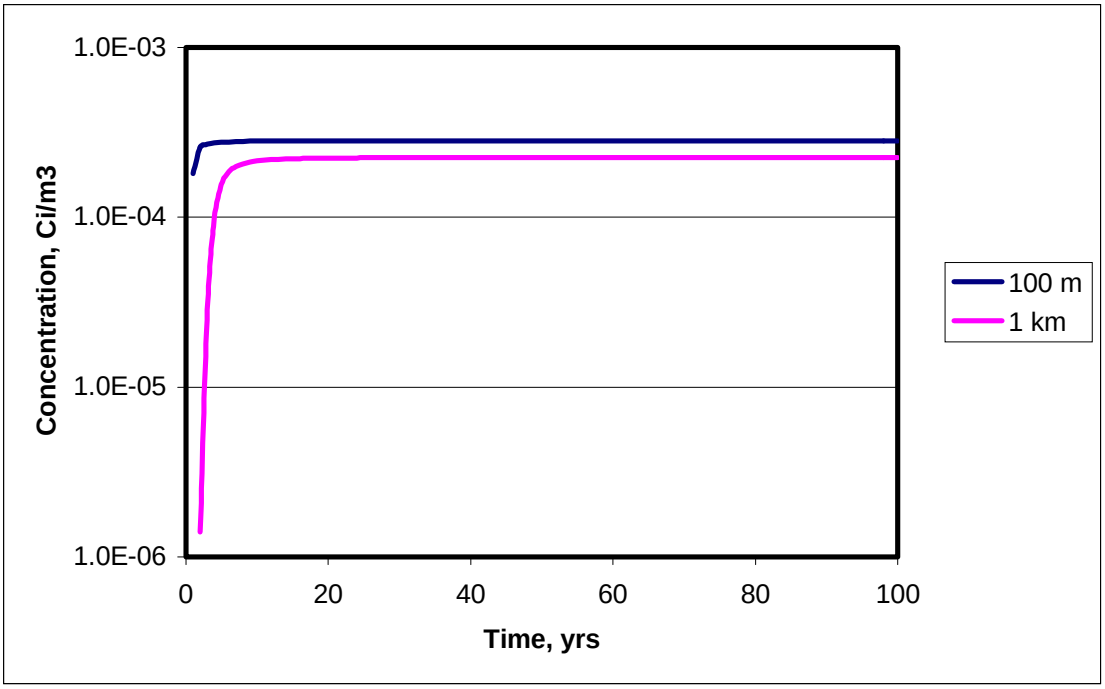

Figure 6.9. Concentration History at 100-m (328-ft) and 1000-m (3281-ft) Wells, Local Scale Model, Concrete Vault Concept – New Disposal Facility Area

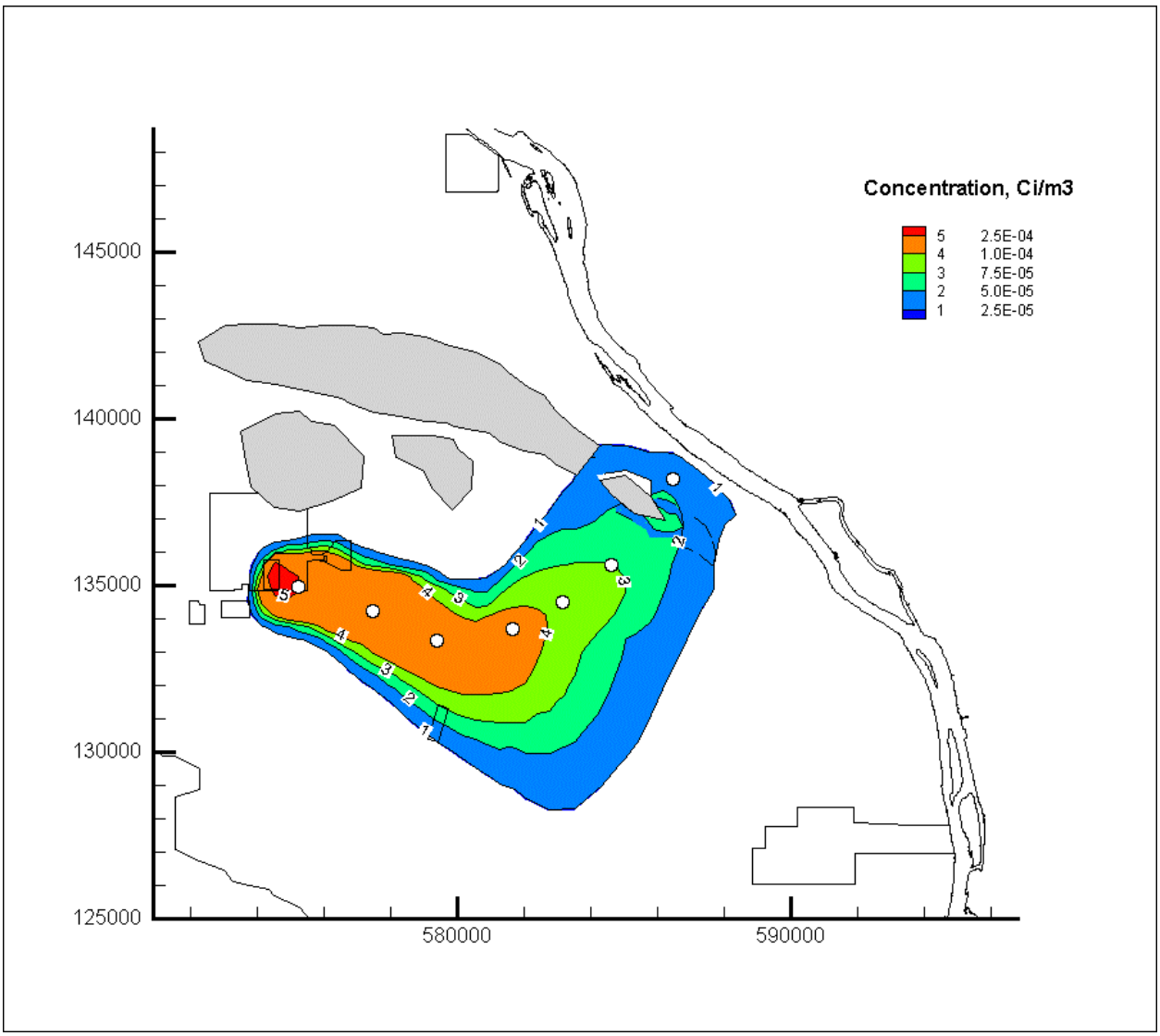

Figure 6.10. Areal Distribution of Contaminant Plume Between ILAW New Facility and Columbia River, Concrete Vault Concept – New Disposal Facility Area

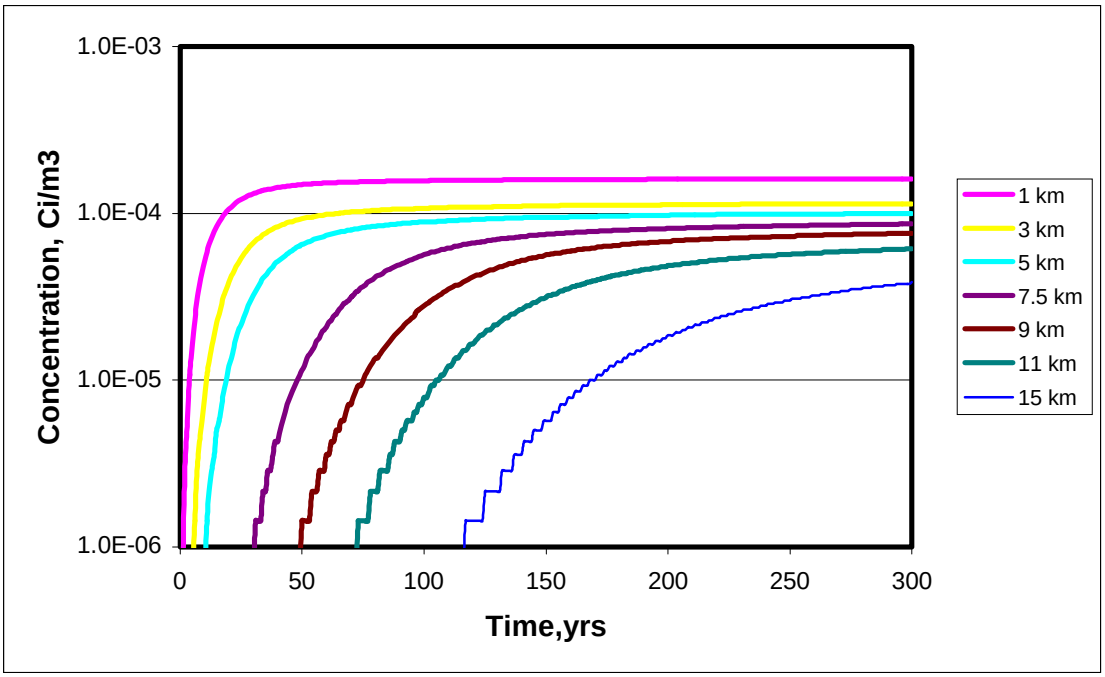

Figure 6.11. Concentration History at Selected Well Locations, Site-Wide Model, Concrete Vault Concept – New Disposal Facility Area

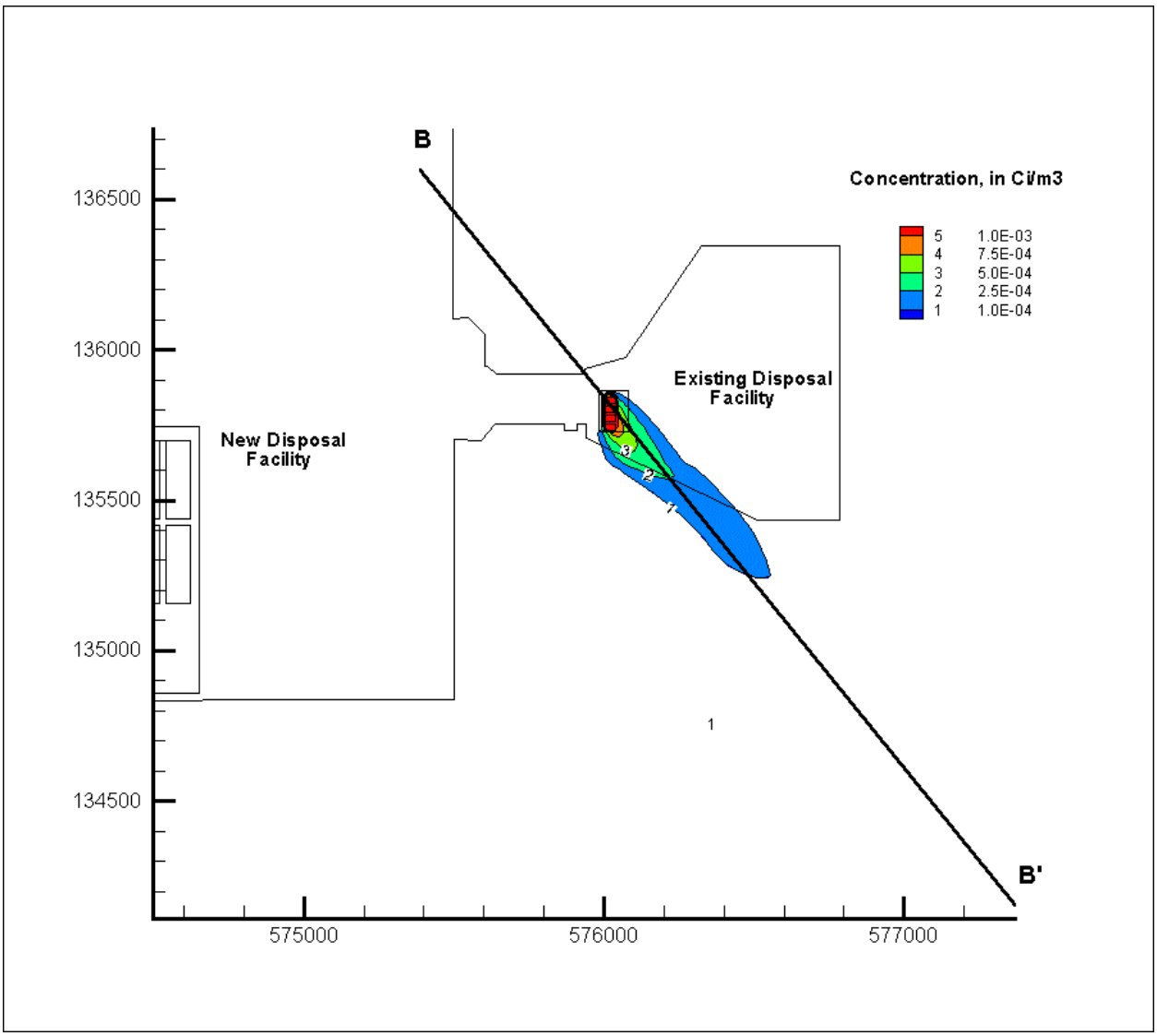

Figure 6.12. Areal Distribution of Contaminant Plume Resulting from Simulation of the Concrete Vault Concept – Existing Disposal Facility Area

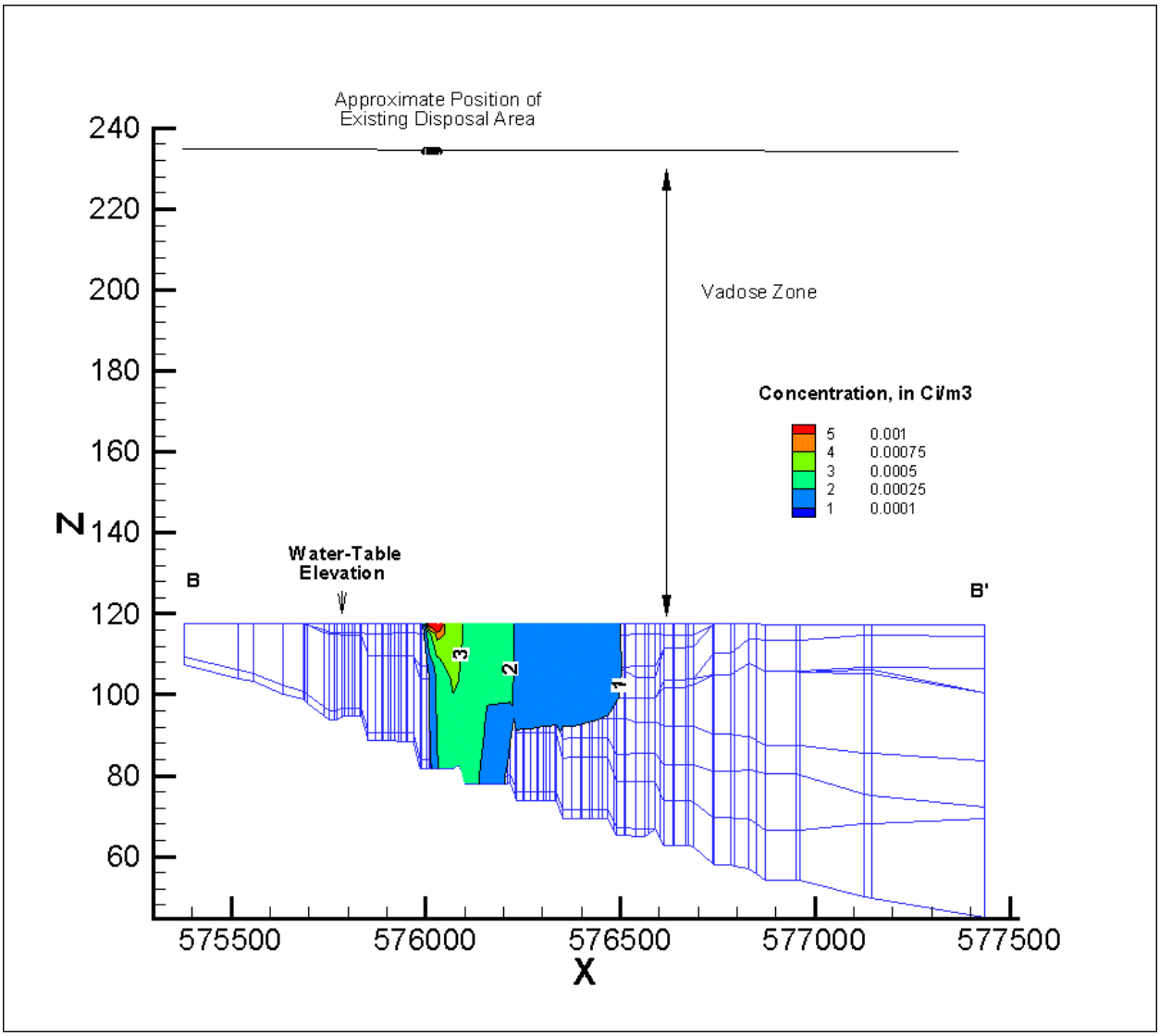

Figure 6.13. Vertical Distribution of a Contaminant Plume Resulting from Simulation of the Concrete-Vault Concept (Along the Approximate Centerline of the Plume) – Existing Disposal Facility Area

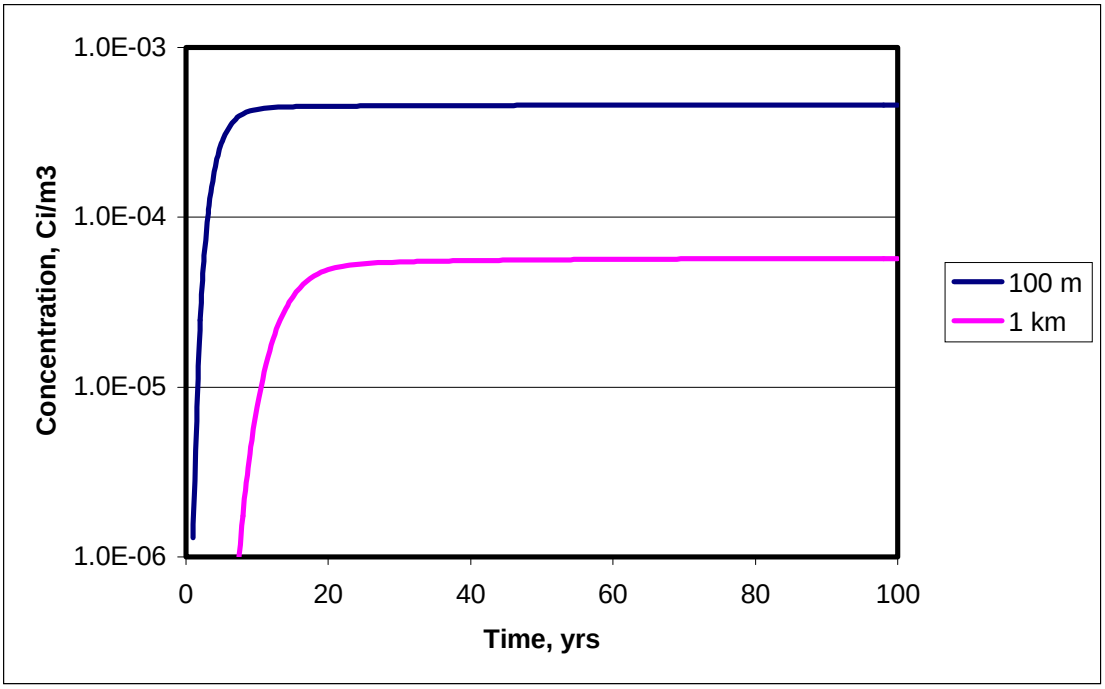

Figure 6.14. Concentration History at 100-m (328-ft) and 1000-m (3281-ft) Wells, Local Scale Model – Existing Disposal Facility Area

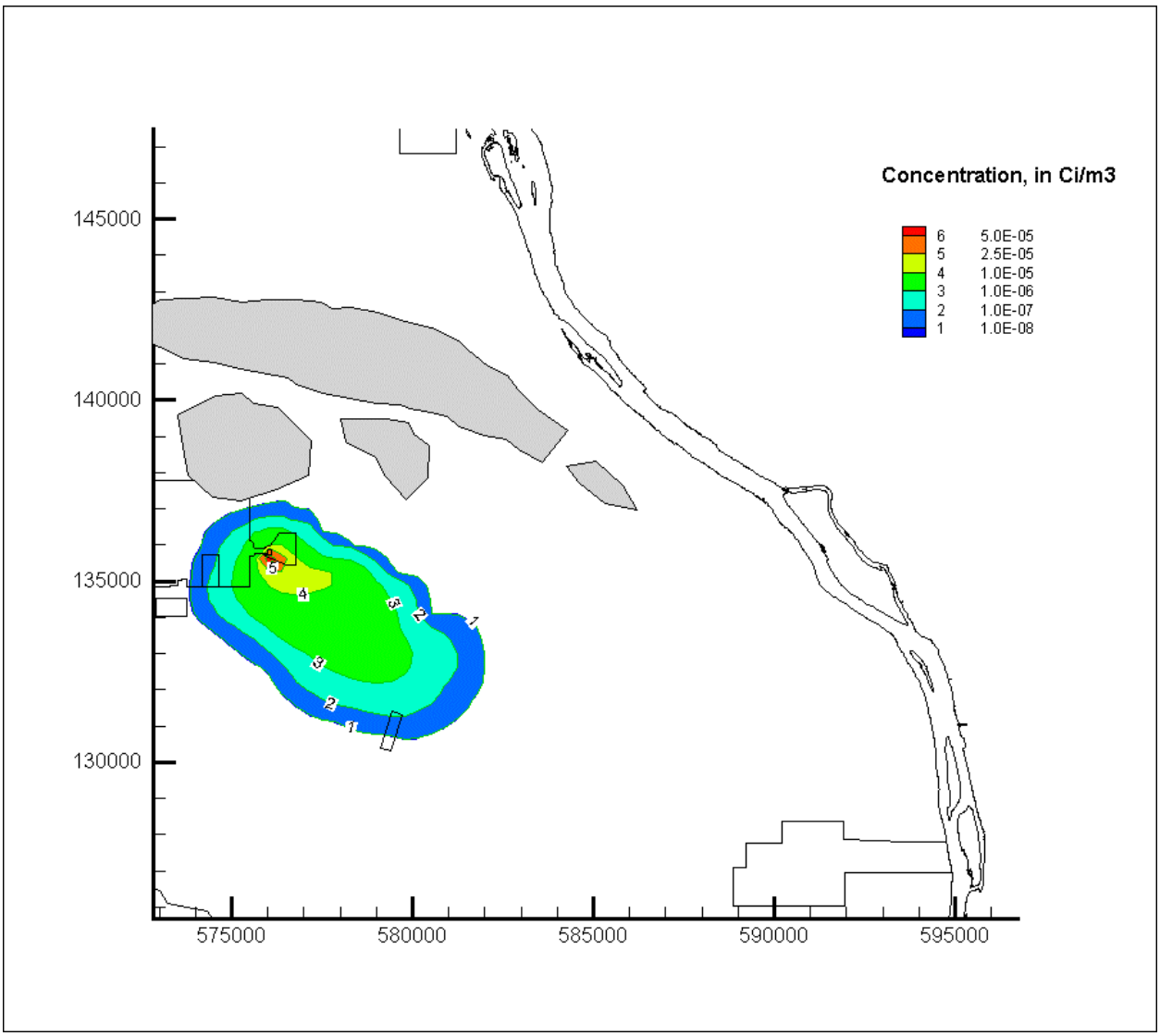

Figure 6.15. Areal Distribution of Contaminant Plume Between ILAW New Facility and Columbia River, Concrete Vault Concept - Existing Disposal Facility

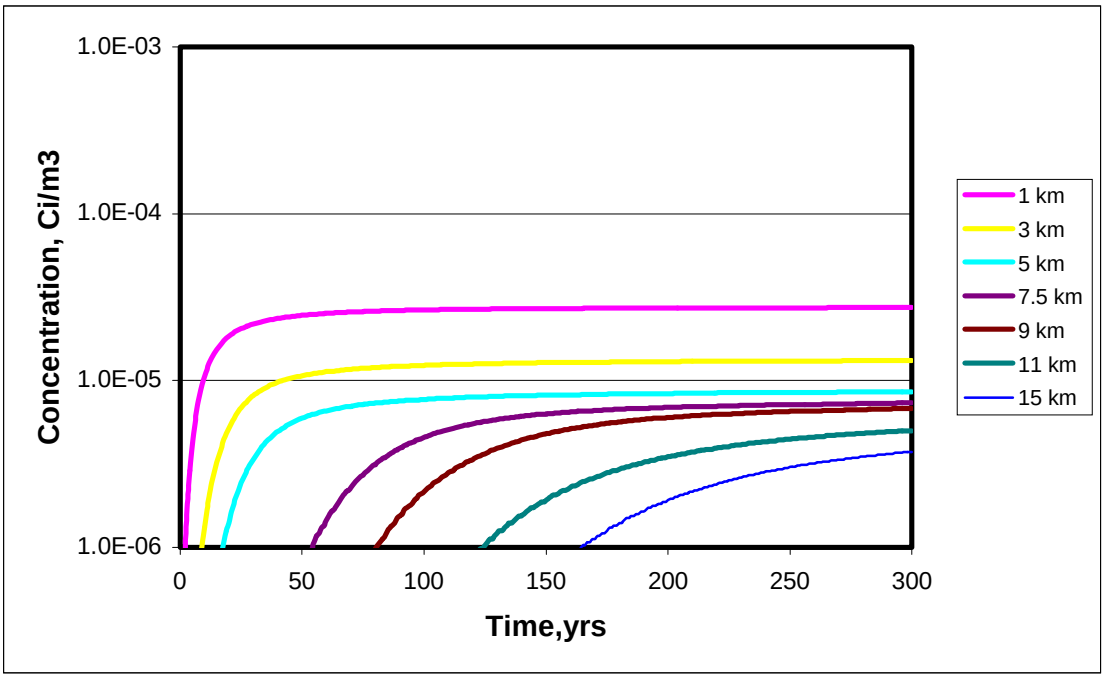

Figure 6.16. Concentration History at Selected Well Locations, Site-Wide Model – Existing Disposal Facility Area

7.0 Results of Sensitivity Analyses

This section of the report describes and presents results from several sensitivity analyses that were performed to evaluate the effect of key factors and assumptions used in the base-case analyses discussed in the previous section. The sensitivity cases evaluated the effect of the following changes:

- Disposal site location
- Disposal site orientation
- Increasing pumping rates at the hypothetical 100-m (328-ft) well downgradient of the facility
- Decreasing hydraulic conductivities in the hydrogeologic unit at the water table beneath the site
- Increasing the effective source-release area
- Raising and lowering the water-table position by:
  - increasing regional estimates of natural recharge
  - decreasing regional estimates of natural recharge
  - reducing in regional boundary fluxes upgradient of the disposal site

Following are results associated with each one of the sensitivity cases.

7.1 Disposal Site Location (Case 1)

This sensitivity study examined the effect of locating the seven disposal-facility remote-handled trenches evaluated in the base case at the southern end of the ILAW disposal-facility area. One of the key factors in the calculated WIF for base-case analysis was the assumed hydrogeologic unit and corresponding hydraulic conductivity found at the water table directly below the facility. With the disposal trenches located in the northern part of the ILAW disposal facility area, the disposal facility is largely underlain by relatively high-permeability sediments associated with the Hanford Formation. Moving the disposal trenches to the southern end of the facility area will position the disposal facility closer to the water-table contact between the Hanford Formation and the lower permeability sediments associated with the Ringold Formation. The change in postulated hydraulic properties at the water table will result in a different velocity distribution beneath the facility that could affect calculated WIFs.

Model-simulation results of the contaminant plume and the trench configuration used for this case are provided in Figure 7.1. Tabular results of the calculated WIFs at 100 m (328 ft) and 1 km (0.62 mi) downgradient of the source area are provided in Table 7.1. The direction of plume movement in this case is very similar to the base case, but calculated WIFs are a factor of 80 percent higher than in the base case. This result is consistent with the postulation that with a thinner distribution of Hanford formation sediments in the south end of the facility, the overall distribution of groundwater velocities would be lower and the resulting WIF would be higher than the base case.

Table 7.1. Well Intercept Factors at the 100-m (328-ft) and 1000-m (3281-ft) Wells for the Remote-Handled Trench Disposal Concept with All Trenches Situated in the South End of the New Disposal Facility (Case 1)

	Infiltration Rates (mm/yr)				
Well Locations	**0.1**	**0.9**	**1.0**	**4.2**	**50.0**
BaseCase					
100 m	2.5E-05	2.3E-04	2.5E-04	1.1E-03	1.3E-02
1000 m	1.9E-05	1.7E-04	1.9E-04	7.8E-04	9.3E-03
Case 1					
100 m	4.8E-05	4.3E-04	4.8E-04	2.0E-03	2.4E-02
1000 m	2.7E-05	2.4E-04	2.7E-04	1.1E-03	1.4E-02

7.2 Disposal Site Orientation (Case 2)

This sensitivity case examines the effect on the WIF of rotating the orientation of the seven remote-handled trenches evaluated in the base case by 90 degrees. Conceptually, flow across the facility is predominantly in a northwest to southeast direction. The change in orientation would put the longest dimension of the individual remote-handled trenches in an orientation closer to perpendicular to the dominant direction of flow. This would conceivably decrease the overall width of the disposal facility and increase the magnitude of the WIF.

Model simulation results of the contaminant plume and the trench configuration used for this case are provided in Figure 7.2. Tabular results of calculated WIFs at 100 m (328 ft) and 1 km (0.62 mi) downgradient of the source area are provided in Table 7.2. While changing the trench configuration did have some effect on the calculated WIFs, the resulting WIF at the 100-m (328-ft) well was only a factor of 15 percent higher than the 100-m (328-ft) well WIFs calculated for the base case. The calculated WIF at 1 km (0.62 mi) was increased by a factor of about 4 percent over the 1 km (0.62 mi) WIF in the basecase.

Table 7.2. Well Intercept Factors at 100-m (328-ft) and 1000-m (3281-ft) Wells for the Remote-Handled Trench Disposal Concept with a 90-Degree Change in Trench Orientation (Case 2)

	Infiltration Rates (mm/yr)				
Well Locations	**0.1**	**0.9**	**1.0**	**4.2**	**50. 0**
BaseCase					
100 m	2.5E-05	2.3E-04	2.5E-04	1.1E-03	1.3E-02
1000 m	1.9E-05	1.7E-04	1.9E-04	7.8E-04	9.3E-03
Case 2					
100 m	3.1E-05	2.8E-04	3.1E-04	1.3E-03	1.5E-02
1000 m	1.9E-05	1.7E-04	1.9E-04	8.1E-04	9.7E-03

7.3 Pumping at a 100-m (328-ft) Well (Case 3)

This sensitivity study examines the effect of varying the assumed pumping rate at the 100-m (328-ft) well downgradient of the facility on the calculated WIF and the behavior of the contaminant plume. Conceptually, increased pumping would reduce the calculated WIFs and contaminant levels at downstream wells as the capture zone caused by the increased pumping at the well reaches out beyond the contaminated water zone. This sensitivity case examined four pumping rates: 30 L (8 gal)/day, 100 L (26.4 gal)/day, 300 L (79 gal)/day, and 1000 L (264 gal)/day.

Results of these sensitivity cases showed that pumping in the ranges of rates investigated would have little effect on the calculated WIFs. The effect of these relatively low pumping rates is consistent with the fact that water pumped at the 100-m (328-ft) well location is largely derived from the Hanford Formation. Given the magnitude of the estimated permeabilities of the Hanford Formation at the location of the 100-m (328 ft) well (about 4,400 m/day), the hydraulic effect of the pumping would be minimal and would not significantly alter the local flow field and the overall plume movement (Figure 7.3). Calculated WIFs for these cases are virtually identical as those calculated at the 100-m (328 ft) well and 1 km (0.62 mi) in the base case (Table 7.3).

7.4 Reduction in Hydraulic Properties of the Hydrogeologic Unit at Water Table (Case 4)

The estimated hydraulic properties and interpretations of the distribution of major hydrogeologic units used in the site-wide model and local-scale models are based on interpretations of limited measurements and well log information. Uncertainties in estimates of hydraulic properties and boundaries of the major units are associated with these interpretations. In this sensitivity study, the effect of the position and the associated hydraulic-property differences between the Hanford formation and the underlying Ringold Formation (Unit 5) is investigated. Directly beneath the disposal-facility area, the estimated hydraulic properties of the Hanford formation are relatively higher compared to the Ringold Formation (Unit 5) where they range from 2500 to 30,000 m/day (27,340 to 32,808 yd/day). In contrast, the hydraulic conductivity of the Ringold Formation (Unit 5) ranges from 40 to 350 m/day (44 to 383 yd/day). For purposes of this sensitivity study, the permeability of the Hanford Formation where it exists beneath the disposal facility was lowered to hydraulic-conductivity levels of the underlying Ringold Formation. The resulting distribution of hydraulic conductivity for Unit 1 is provided in Figure 7.4. Conceptually, this change effectively reduces simulated velocities and flow rates in the hydrogeologic unit at the water table and would result in an increase in the calculated WIFs.

Table 7.3. Well Intercept Factors at the 100-m (328-ft) and 1000-m (3281-ft) Wells for the Remote-Handled Trench Disposal Concept Using Increased Pumping Rates at the 100-m (328-ft) Downgradient Well (Case 3)

	Infiltration Rates (mm/yr)				
Well Locations	**0.1**	**0.9**	**1.0**	**4.2**	**50. 0**
BaseCase					
100 m	2.5E-05	2.3E-04	2.5E-04	1.1E-03	1.3E-02
1000 m	1.9E-05	1.7E-04	1.9E-04	7.8E-04	9.3E-03
Case 3					
a) 30 lpd					
100 m	2.5E-05	2.3E-04	2.5E-04	1.1E-03	1.3E-02
1 km	1.9E-05	1.7E-04	1.9E-04	7.8E-04	9.3E-03
b) 100 lpd					
100 m	2.5E-05	2.3E-04	2.5E-04	1.1E-03	1.3E-02
1 km	1.9E-05	1.7E-04	1.9E-04	7.8E-04	9.3E-03
c) 300 lpd					
100 m	2.5E-05	2.3E-04	2.5E-04	1.1E-03	1.3E-02
1 km	1.9E-05	1.7E-04	1.9E-04	7.8E-04	9.3E-03
d) 1000 lpd					
100 m	2.5E-05	2.3E-04	2.5E-04	1.1E-03	1.3E-02
1 km	1.9E-05	1.7E-04	1.9E-04	7.8E-04	9.3E-03

The reduction in hydraulic properties changed the primary direction of groundwater beneath the facility to a more easterly direction as shown in Figure 7.5. Calculated WIFs for this case are calculated at the 100-m (328 ft) well and 1 km (0.62 mi) in the base case (Table 7.4). These results indicate that a reduction in the hydraulic conductivity of the underlying Hanford Formation to those in the Ringold Formation (Unit 5) below Hanford would increase calculated WIFs by about an order of magnitude at the 100-m (328-ft) well (1.25×10^{-2} versus 1.25×10^{-3} for the 4.2 mm/yr infiltration rate). The resulting WIF for the 4.2 infiltration rate at 1-km (0.62-mi) location (4.0×10^{-3}) was calculated to be a factor of 5 higher than at the same location in the base case (9.7×10^{-4}). The predicted distribution of contaminant concentrations from the seven trenches' release is provided in Figure 7.6.

Table 7.4. Well Intercept Factors at the 100-m (328-ft) and 1000-m (3281-ft) Wells for the Remote-Handled Trench Disposal Concept Using a Reduction in the Hydraulic Conductivity of the Hanford Formation (Case 4)

	Infiltration Rates (mm/yr)				
Well Locations	**0.1**	**0.9**	**1.0**	**4.2**	**50. 0**
BaseCase					
100 m	2.5E-05	2.3E-04	2.5E-04	1.1E-03	1.3E-02
1000 m	1.9E-05	1.7E-04	1.9E-04	7.8E-04	9.3E-03
Case 4					
100 m	3.0E-04	2.7E-03	3.0E-03	1.3E-02	1.5E-01
1000 m	9.6E-05	8.7E-04	9.6E-04	4.0E-03	4.8E-02

7.5 Increasing Surface Area of Release (Cases 5 and 6)

This sensitivity analysis examines the effect of increasing the effective surface area of release at the water table beyond the basic footprint of the either the remote-handled trenches or the concrete vault. After transport through the vadose zone, contaminants originating from the individual disposal trenches or vaults will disperse in a pattern that will be much larger than the original footprint of the individual trench configuration. In this sensitivity case, two subcases were evaluated. Case 5 evaluated a source-release area for the remote-handled trench concept reflective of not only the individual remote-handled trench areas but the intervening inter-trench areas. Case 6 evaluated a source-release area for the concrete-vault concept reflective of not only the individual remote-handled trench areas but the intervening inter-trench areas.

Model-simulation results of the contaminant plume and the trench configuration used for Case 5 are provided in Figure 7.5. Tabular results of the calculated WIFs at 100 m (328 ft) and 1 km (0.62 mi) downgradient of the source area are provided in Table 7.5. Calculations for this case showed that the assumed 21 percent increase in the source-release area resulted in about a 21 percent increase in the WIFs over the base-case values at both the 100-m and 1-km wells. This result is consistent with the additional contaminant mass introduced at the water-table for this case. This result combined with previous results for remote-handled trench basecase and the concrete vault releases suggest a linear relationship between source-release area and calculated WIFs over the range of assumed release area.

Model-simulation results of the contaminant plume and the trench configuration used for Case 6 are provided in Figure 7.6. Tabular results of the calculated WIFs at 100 m (328 ft) and 1 km (0.62 mi) downgradient of the source area are provided in Table 7.6. Calculations for this case also showed a result consistent with those for case 5. The assumed increase in the source-release area (580 percent) resulted in about a 580 percent increase in the WIFs over the base-case values at both

the 100-m and 1-km wells. This result is consistent with the previous conclusion of a linear relationship between source-release area and calculated WIFs over the range of assumed release areas.

Table 7.5. Well Intercept Factors at the 100-m (328-ft) and 1000-m (3281-ft) Wells for the Remote-Handled Trench Disposal Concept Using an Increase in Surface Area of Release (Case 5)

	Infiltration Rates (mm/yr)				
Well Locations	**0.1**	**0.9**	**1.0**	**4.2**	**50. 0**
Base Case					
100 m	2.5E-05	2.3E-04	2.5E-04	1.1E-03	1.3E-02
1000 m	1.9E-05	1.7E-04	1.9E-04	7.8E-04	9.3E-03
Case 5					
100 m	3.0E-05	2.7E-04	3.0E-04	1.3E-03	1.5E-02
1000 m	2.3E-05	2.1E-04	2.3E-04	9.8E-04	1.2E-02

Table 7.6. Well Intercept Factors at the 100-m (328-ft) and 1000-m (3281-ft) Wells for the Concrete-Vault Disposal Concept Using an Increase in Surface Area of Release (Case 6)

	Infiltration Rates (mm/yr)				
Well Locations	**0.1**	**0.9**	**1.0**	**4.2**	**50. 0**
BaseCase					
100 m	6.7E-06	6.1E-05	6.7E-05	2.8E-04	3.4E-03
1000 m	5.4E-06	4.8E-05	5.4E-05	2.2E-04	2.7E-03
Case 6					
100 m	3.9E-05	3.5E-04	3.9E-04	1.6E-03	1.9E-02
1000 m	3.0E-05	2.7E-04	3.0E-04	1.3E-03	1.5E-02

7.6 Changes in the Position of the Water Table

Results of previous work by Lu (1996) and the results of this study have shown that the characteristics of the hydrogeologic unit and the estimated water table are an important consideration and will have an influence on the calculated WIFs downgradient of the ILAW facility. The actual position of the water-table in the far future is indeed uncertain, and a series of sensitivity studies were done to examine the effect of factors that could affect the position of the water-table position beneath the ILAW facility. The two main factors that could have an influence include the estimated levels of regional natural recharge and inflow onto the Hanford Site from upgradient off-site sources. Following is a summary of these sensitivity studies that investigated these two factors.

7.6.1 Increase in Regional Areal Recharge (Case 7)

This sensitivity case examines the effect of increasing regional natural recharge on the regional and local water-table conditions. In this case, the recharge was increased by a factor of 3 in the site-wide model, and the resulting predicted water table was used to evaluate the effect of these changes in the local-scale flow and transport model.

The simulated change in natural recharge in the site-wide model (shown in Figure 7.9) raised the regional water table and significantly changed the overall predicted regional flow path for the ILAW facility from southeast and east toward the Columbia River to a predominant flow path north through the gap between Gable Butte and Gable Mountain to the Columbia River. The discharge area to the Columbia River for these conditions is eventually in the vicinity of 100-N Area.

Locally, water-table conditions were raised by about 3 m (50 ft) in the vicinity of the new disposal facility (Figure 7.10), resulting in an increased saturation of the Hanford Formation beneath the ILAW facility. Results for these conditions, summarized in Table 7.7, indicate about a 25 to 30 percent reduction in the calculated WIF over the base case WIF at the 100-m (328 ft) well location (9.8×10^{-4} versus 1.25×10^{-3}) for the 4.2 infiltration rate case. At the 1-km (0.62 mi) location, the resultant WIF (8×10^{-4}) 18 to 20 percent than the WIF at the same location in the base case (9.8×10^{-4}) for the same assumed infiltration rate. The predicted distribution of contaminant concentrations from the seven-trenches release is provided in Figure 7.11.

Table 7.7. Well Intercept Factors at the 100-m (328-ft) and 1000-m (3281-ft) Wells for the Remote-Handled Trench Disposal Concept Using an Increase (Factor of 3) in Regional Natural Recharge Rates (Case 7)

	Infiltration Rates (mm/yr)				
Well Locations	**0.1**	**0.9**	**1.0**	**4.2**	**50. 0**
BaseCase					
100 m	2.5E-05	2.3E-04	2.5E-04	1.1E-03	1.3E-02
1000 m	1.9E-05	1.7E-04	1.9E-04	7.8E-04	9.3E-03
Case 7					
100 m	2.3E-05	2.1E-04	2.3E-04	9.7E-04	1.2E-02
1000 m	8.0E-06	7.2E-05	8.0E-05	3.4E-04	4.0E-03

7.6.2 Decrease in Regional Areal Recharge (Case 8)

This sensitivity case examines the effect of reducing regional natural recharge on the regional and local water-table conditions. In this case, the recharge was reduced by a factor of 3.

Results of the simulated change in natural recharge in the site-wide model (shown in Figure 7.12) lowered the regional water table, but did not significantly change the overall predicted regional flow path for the ILAW facility from southeast and east toward the Columbia River. The discharge area into the Columbia River for these conditions is, as in the base case, in the vicinity of the old Hanford Town Site.

Locally, water-table conditions were changed slightly from the base-conditions and were lowered by about 1.2 m (4 ft) in the vicinity of the new disposal facility (Figure 7.13), resulting in a slight decrease in saturation of the Hanford Formation beneath the ILAW facility. Although the water table dropped for this case, the overall hydraulic gradient in the vicinity of the disposal facility is over a factor of 2.4 higher than was calculated using the basecase areal recharge (1.6e-4 m/m versus 6.6e-5 m/m). The resulting effect was an overall reduction in the calculated WIF and an increase in dilution for this case. Results for these simulated conditions, summarized in Table 7.8, indicate about a 50-percent reduction in the calculated WIF over the base case WIF at the 100-m (328 ft) well location (7.9 x 10-4 versus 1.25 x10^{-3}) for the 4.2 infiltration rate case. At the 1 km (0.62 mi) location, the resultant WIF (6 x 10^{-4}) was 55 percent lower than the WIF at the same location in the base case (9.8 x 10^{-4}) for the same assumed infiltration rate. The predicted distribution of contaminant concentrations from the seven-trenches release is provided in Figure 7.14.

Table 7.8. Well Intercept Factors at the 100-m (328-ft) and 1000-m (3281-ft) Wells for the Remote-Handled Trench Disposal Concept Using A Decrease (Factor of 3) in Regional Natural Recharge Rates (Case 8)

	Infiltration Rates (mm/yr)				
Well Locations	**0.1**	**0.9**	**1.0**	**4.2**	**50. 0**
BaseCase					
100 m	2.5E-05	2.3E-04	2.5E-04	1.1E-03	1.3E-02
1000 m	1.9E-05	1.7E-04	1.9E-04	7.8E-04	9.3E-03
Case 8					
100 m	1.7E-05	1.5E-04	1.7E-04	7.1E-04	8.5E-03
1000 m	1.3E-05	1.2E-04	1.3E-04	5.4E-04	6.4E-03

7.6.3 Decrease in Regional Upgradient Boundary Fluxes (Case 9)

This sensitivity case examines the effect of reducing regional boundary fluxes on the regional and local water table conditions at the Cold Creek and Dry Creek entrances to the Hanford Site as well as recharge to the unconfined aquifer from springs emanating along the base of Rattlesnake Hills. In this case, the simulated boundary fluxes were reduced by a factor of 2.

Results of the simulated change in natural recharge in the site-wide model (shown in Figure 7.15) lowered the regional water table, but did not significantly change the overall predicted regional flow path for the ILAW facility from southeast and east toward the Columbia River. The discharge area into the Columbia River for these conditions is, as in the base case, in the vicinity of the old Hanford Town Site.

Locally, water-table conditions were changed slightly from the base conditions and were lowered by about 0.5 m (1.6 ft) in the vicinity of the new disposal facility (Figure 7.16), resulting in a slight decrease in saturation of the Hanford Formation and slight changes to flow conditions beneath the ILAW facility. As in the previous case, although the water table dropped for this case, the overall hydraulic gradient in the vicinity of the disposal facility is over a factor of 2.4 higher than was calculated using the base case areal recharge (1.6e-4 m/m versus 6.6e-5 m/m). The resulting effect was a small increase in the calculated WIF and an increase in dilution for this case. Results for these simulated conditions, summarized in Table 7.9, indicate about a 50-percent reduction in the calculated WIF over the base case WIF at the 100-m (328 ft) well location (1.0×10^{-3} versus 1.25×10^{-3}) for the 4.2 infiltration rate case. At the 1 km (0.62 mi) location, the resultant WIF (7.8×10^{-4}) was 25 percent lower than the WIF at the same location in the base case (9.8×10^{-4}) for the same assumed infiltration rate. The distribution of predicted contaminant concentration, for this case is illustrated in Figure 7.17.

Table 7.9. Well Intercept Factors at the 100-m (328-ft) and 1000-m (3281-ft) Wells for the Remote-Handled Trench Disposal Concept Using a Decrease (Factor of 2) in Regional Boundary Fluxes (Case 9)

	Infiltration Rates (mm/yr)				
Well Locations	**0.1**	**0.9**	**1.0**	**4.2**	**50.0**
BaseCase					
100 m	2.5E-05	2.3E-04	2.5E-04	1.1E-03	1.3E-02
1000 m	1.9E-05	1.7E-04	1.9E-04	7.8E-04	9.3E-03
Case 9					
100 m	2.1E-05	1.9E-04	2.1E-04	8.8E-04	1.1E-02
1000 m	1.6E-05	1.5E-04	1.6E-04	6.8E-04	8.1E-03

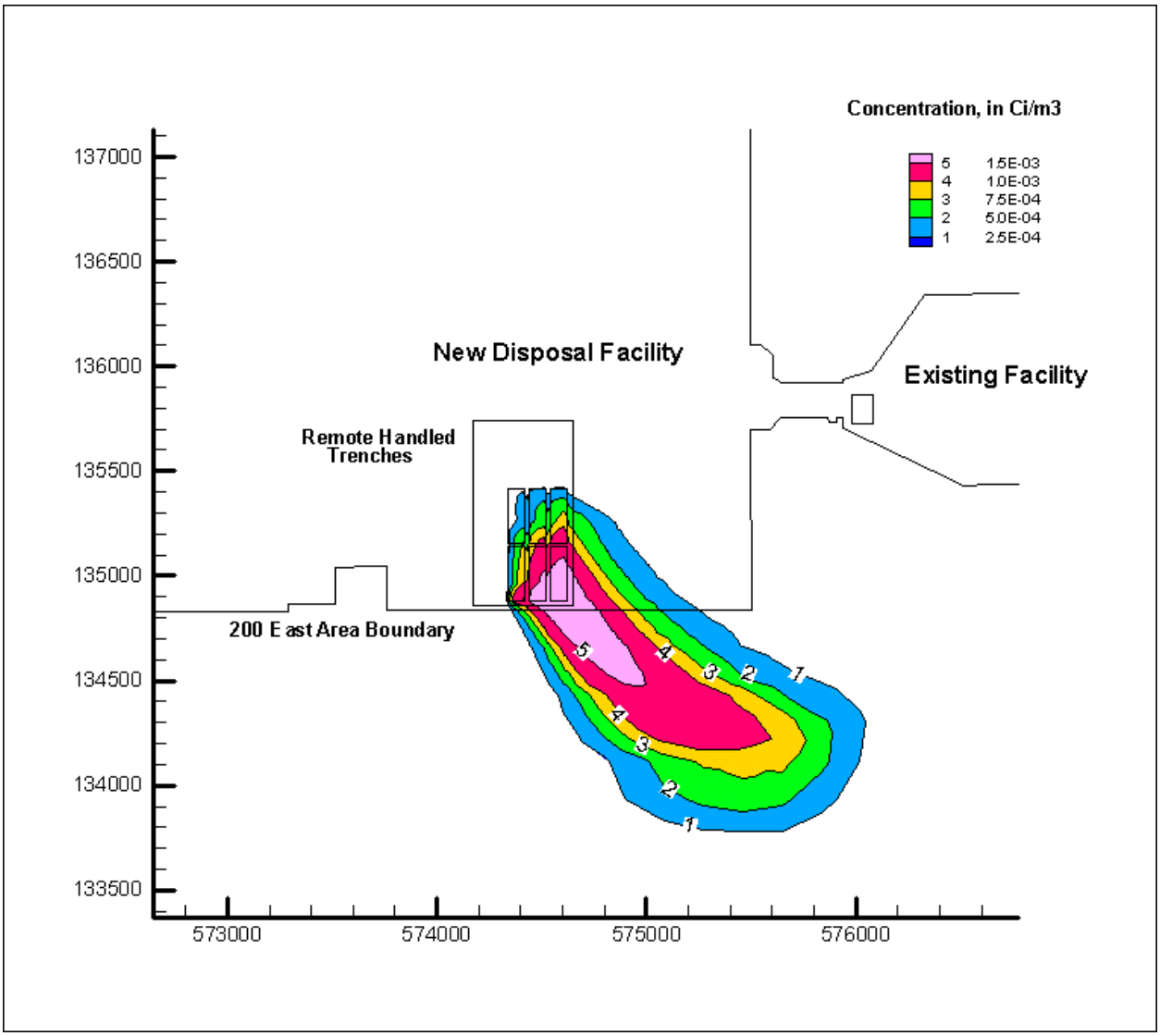

Figure 7.1. Areal Distribution of Contaminant Plume Resulting from the Remote-Handled Trench Concept – Sensitivity to Placing Disposal Trenches at South End of Disposal Facility Area

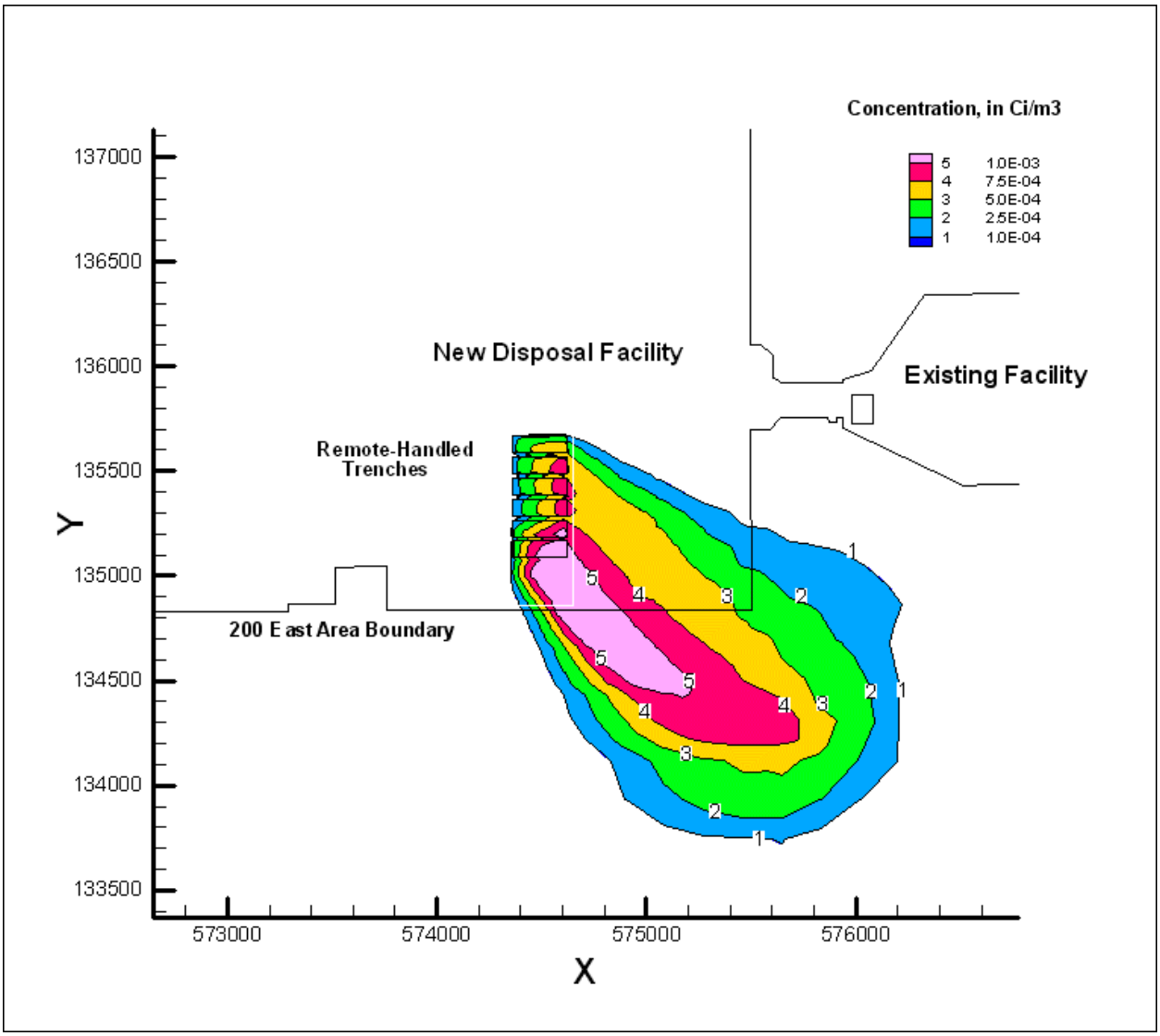

Figure 7.2. Areal Distribution of Contaminant Plume Resulting from the Remote-Handled Trench Concept – Sensitivity to Rotation of Remote Handled Trenched by 90 degrees

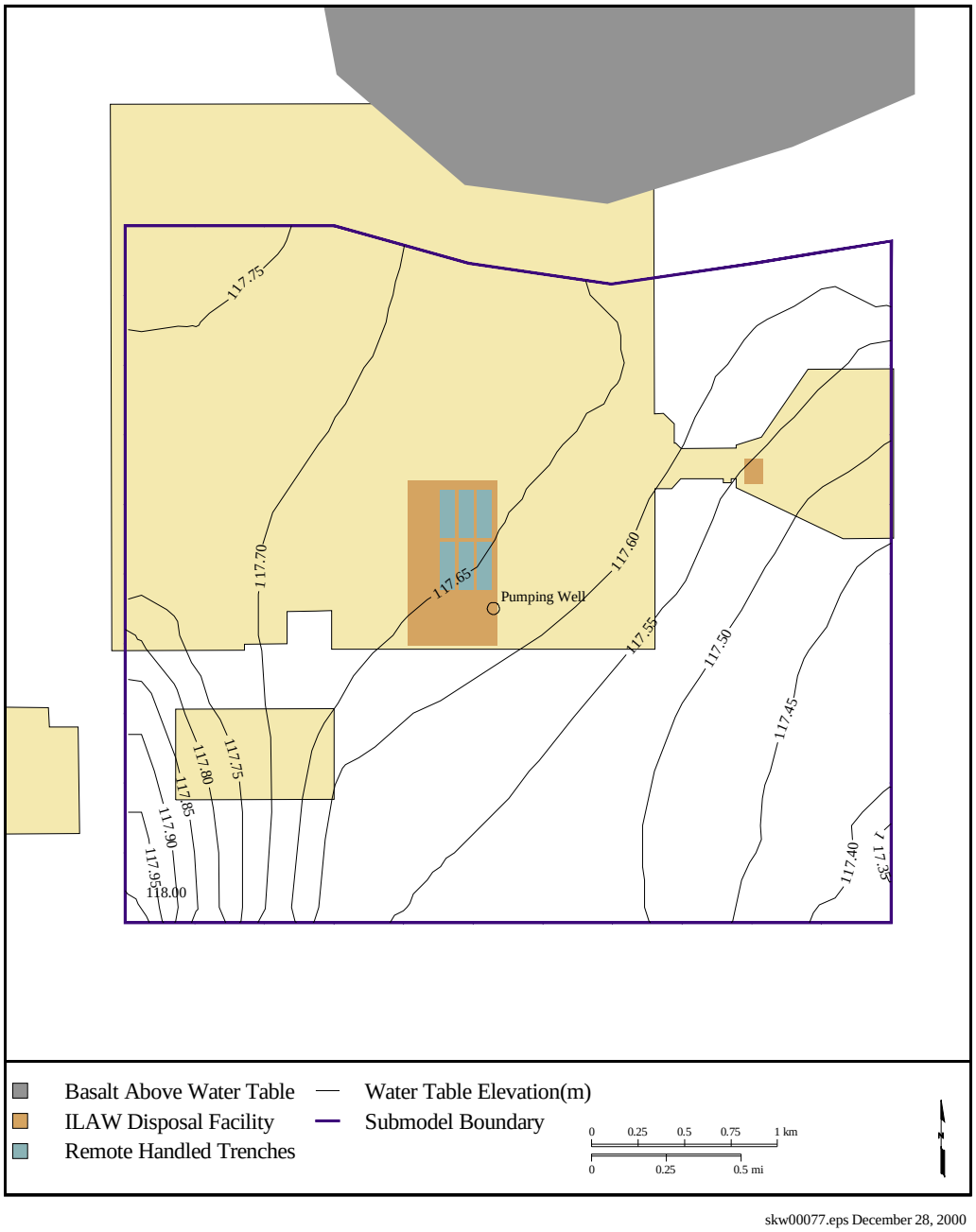

A) 30 1/Day

Figure 7.3. Local-Scale Model Head Distribution Resulting from the Remote-Handled Trench Concept – Sensitivity to Increased Pumping at 100-m (328-ft) Well: A) 30 l/Day, B) 100 l/Day, C) 300 l/Day, and D) 1000 l/Day

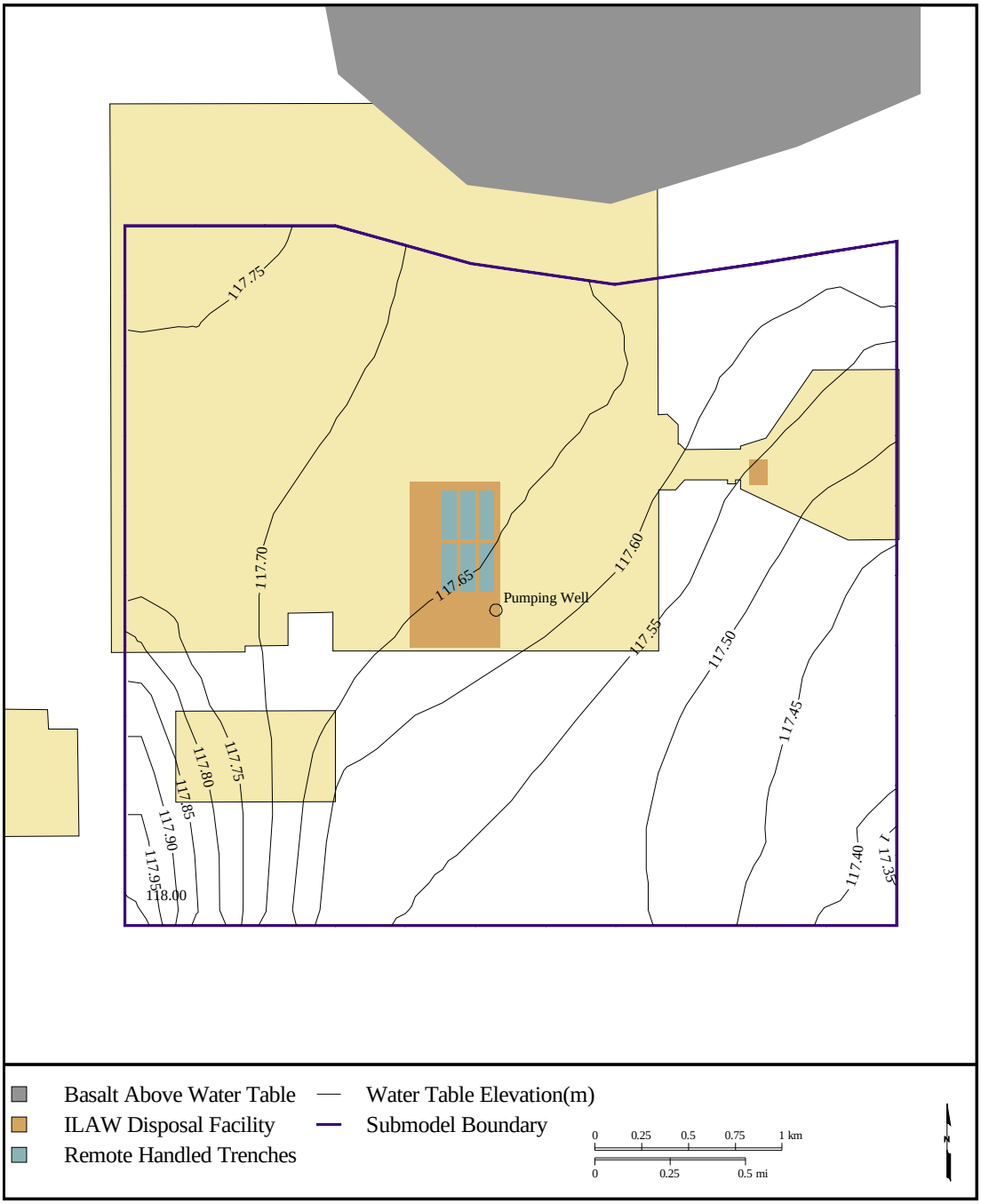

skw00077.eps December 28, 2000

B) 100 1/Day

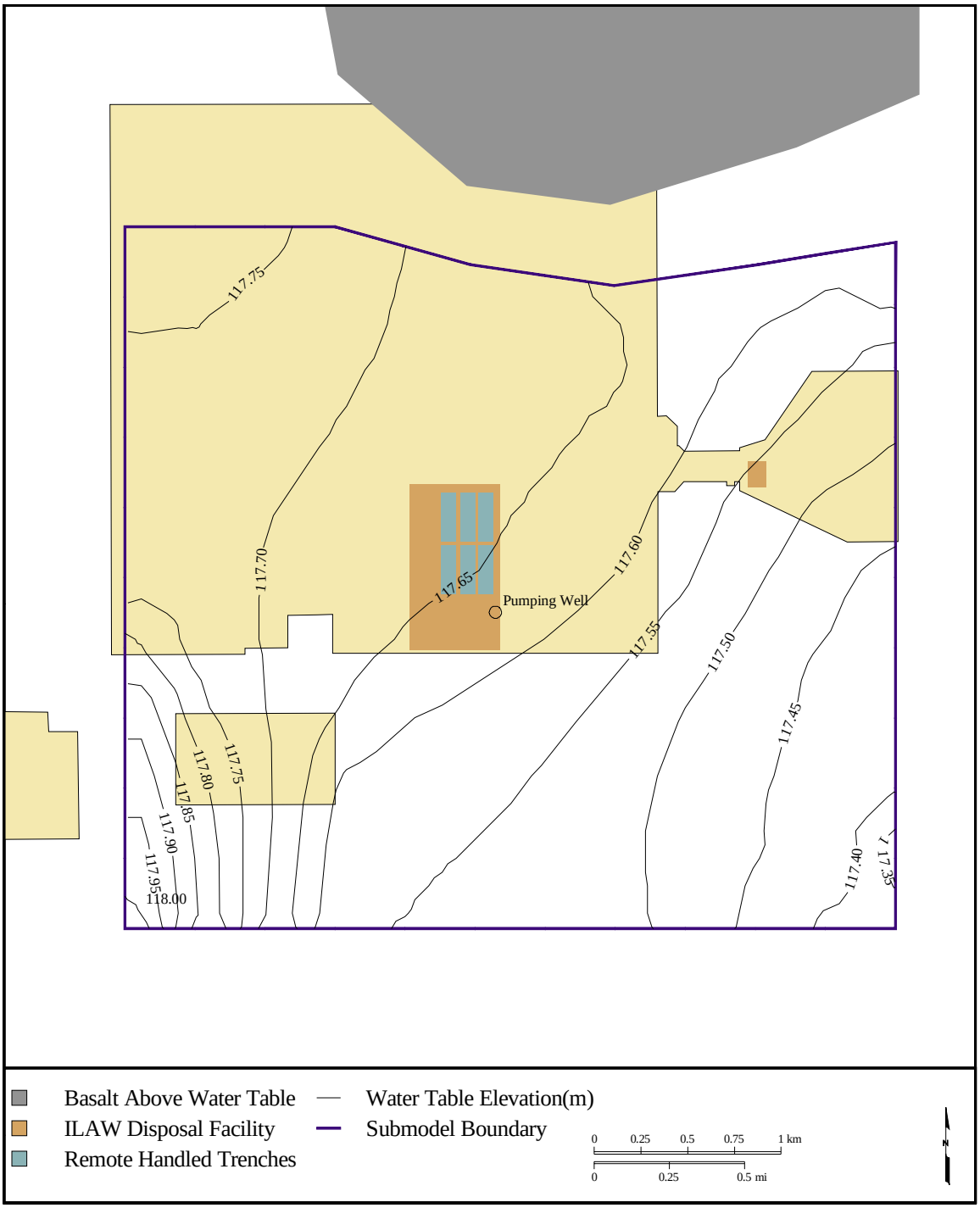

skw00077.eps December 28, 2000

C) 300 1/Day

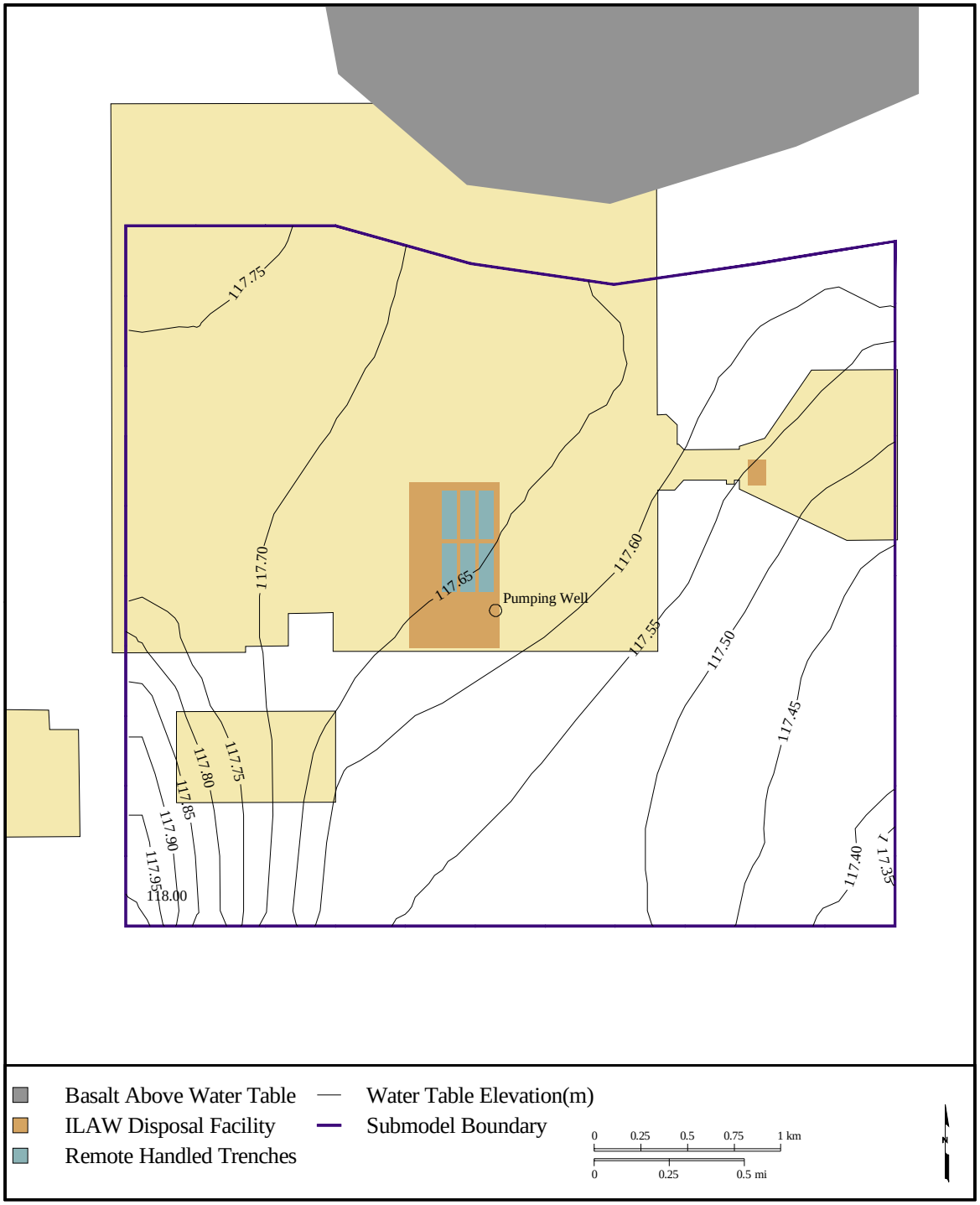

skw00077.eps December 28, 2000

D) 1000 l/Day

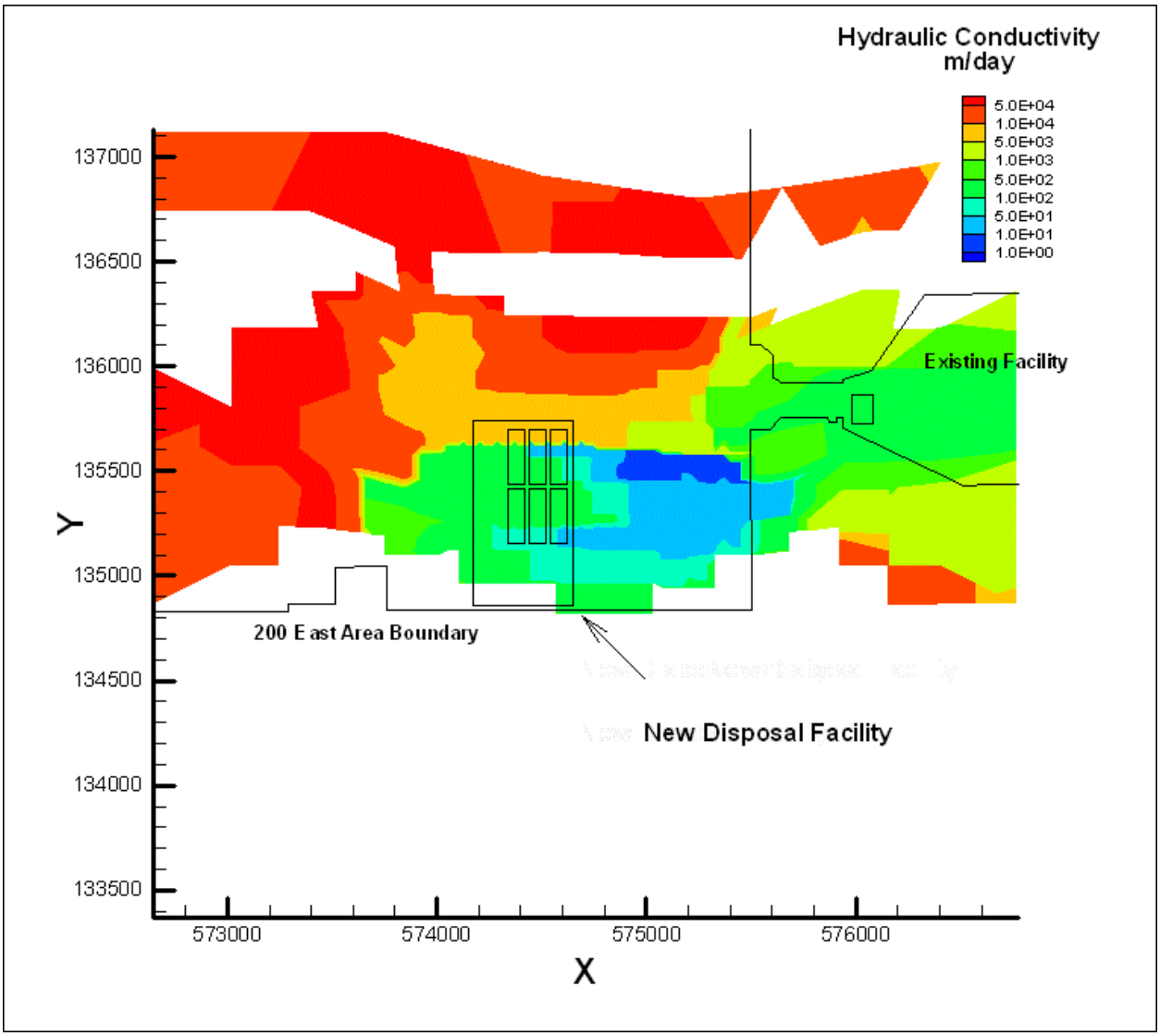

Figure 7.4. Distribution of Hydraulic Conductivity Used in Decreased Hydraulic Conductivity Sensitivity Case

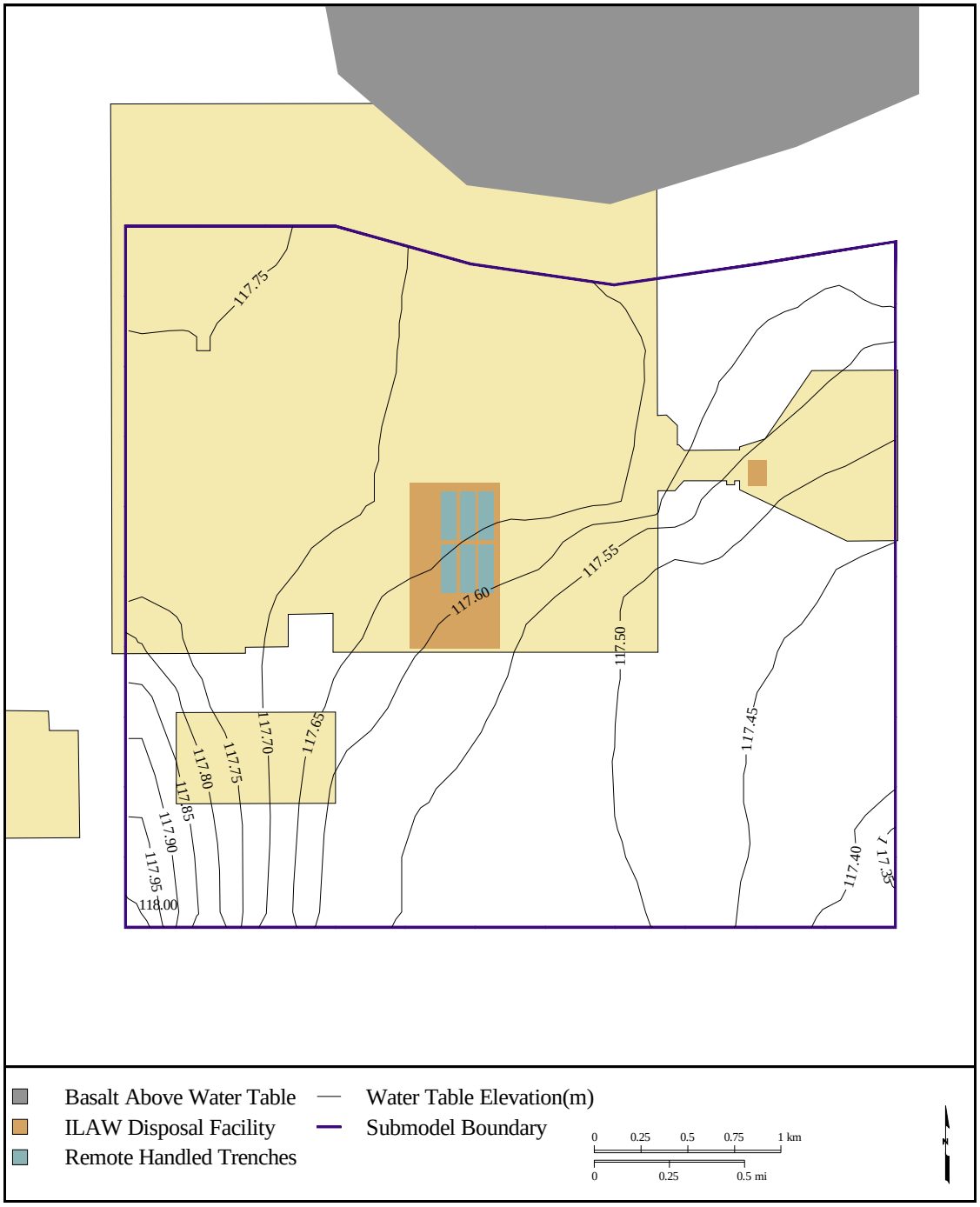

skw00076.eps December 28, 2000

Figure 7.5. Local-Scale Head Distribution Resulting from Decreased Hydraulic Conductivity of Hanford Formation

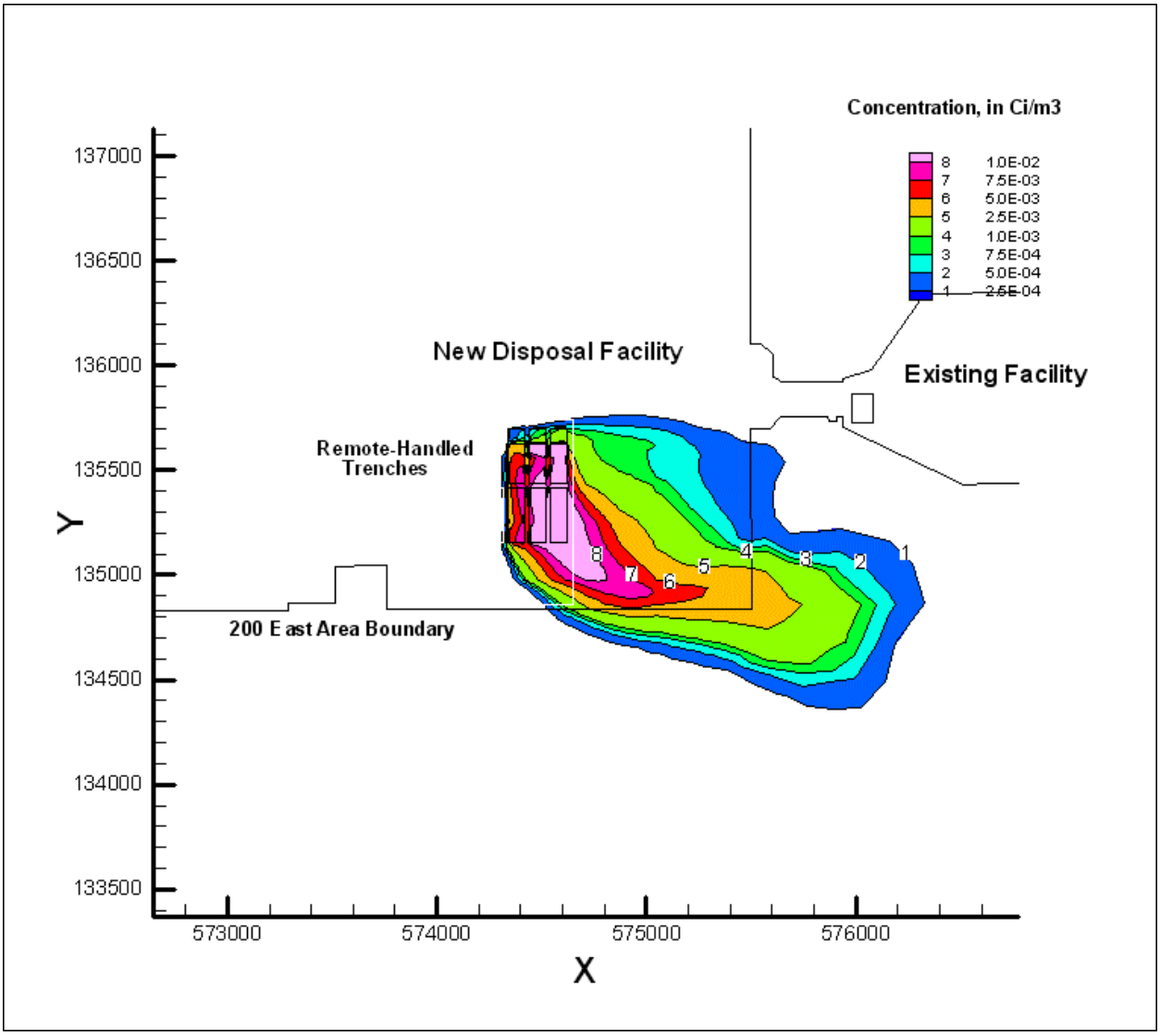

Figure 7.6. Areal Distribution of Contaminant Plume Resulting from the Remote-Handled Trench Concept – Sensitivity to Decreased Hydraulic Conductivity of Hanford Formation

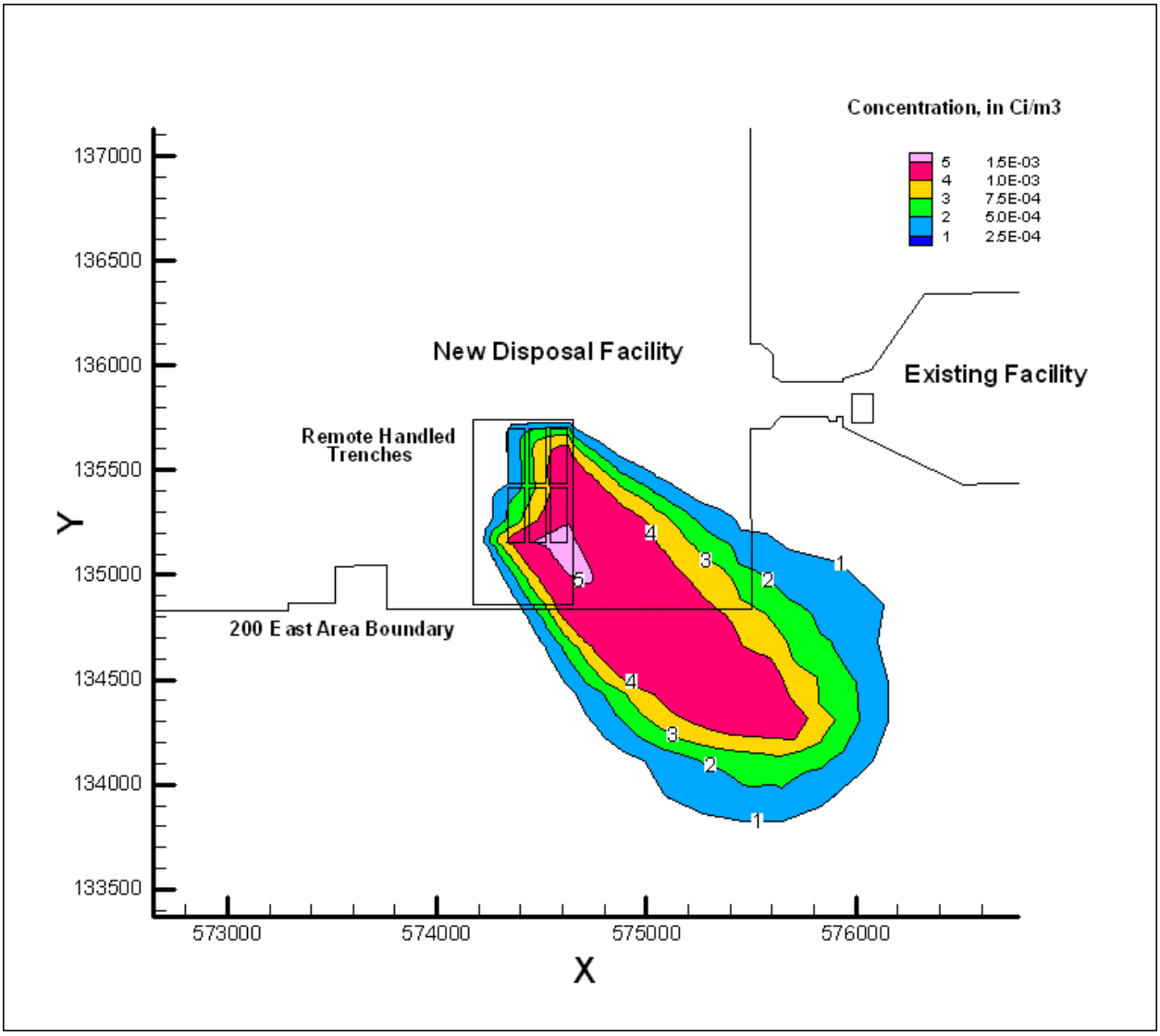

Figure 7.7. Areal Distribution of Contaminant Plume Resulting from the Remote-Handled Trench Concept – Sensitivity to Increase in Source-Release Area (Case 5)

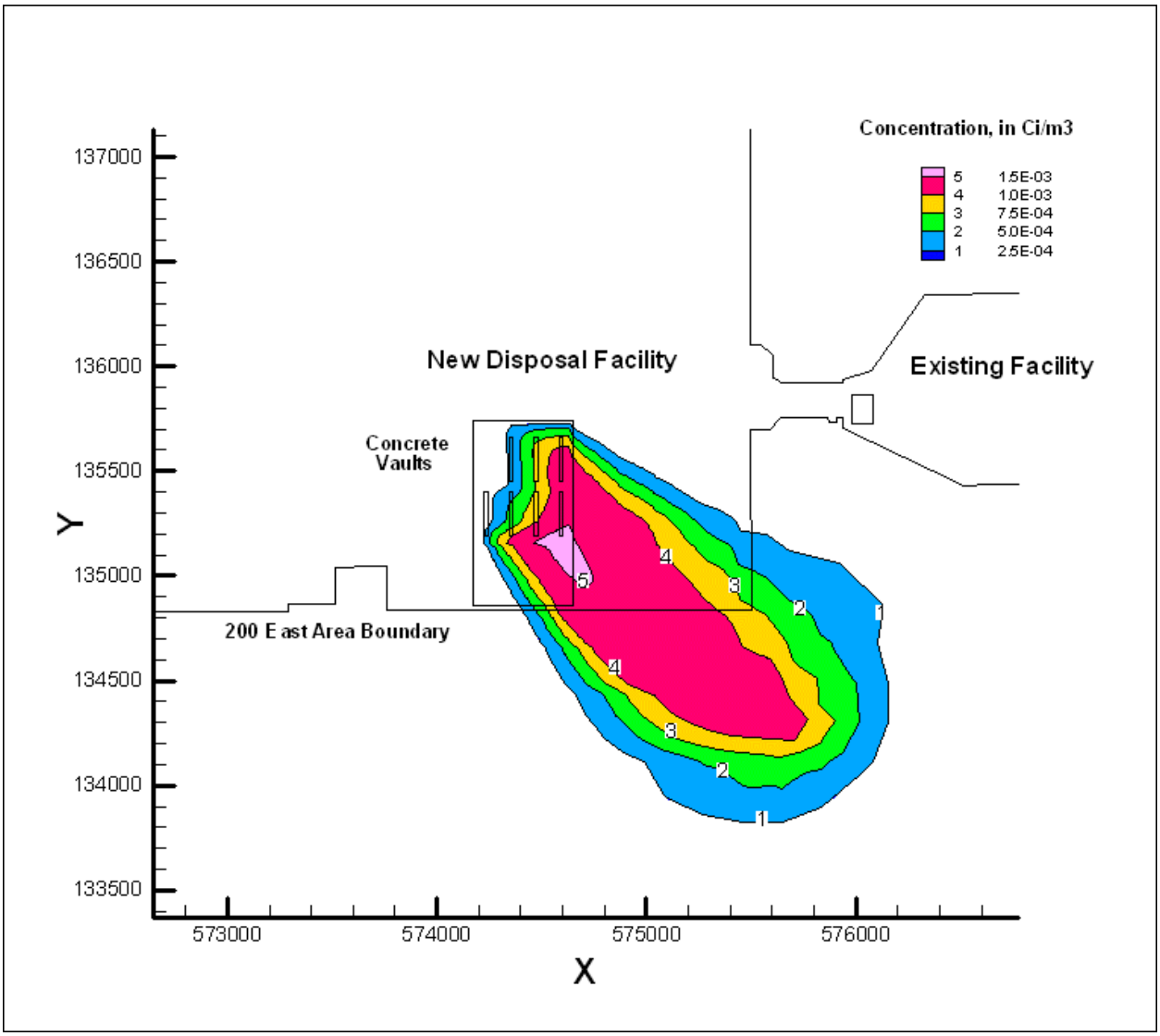

Figure 7.8. Areal Distribution of Contaminant Plume Resulting from the Concrete-Vault Concept – Sensitivity to Increase in Source-release Area (Case 6)

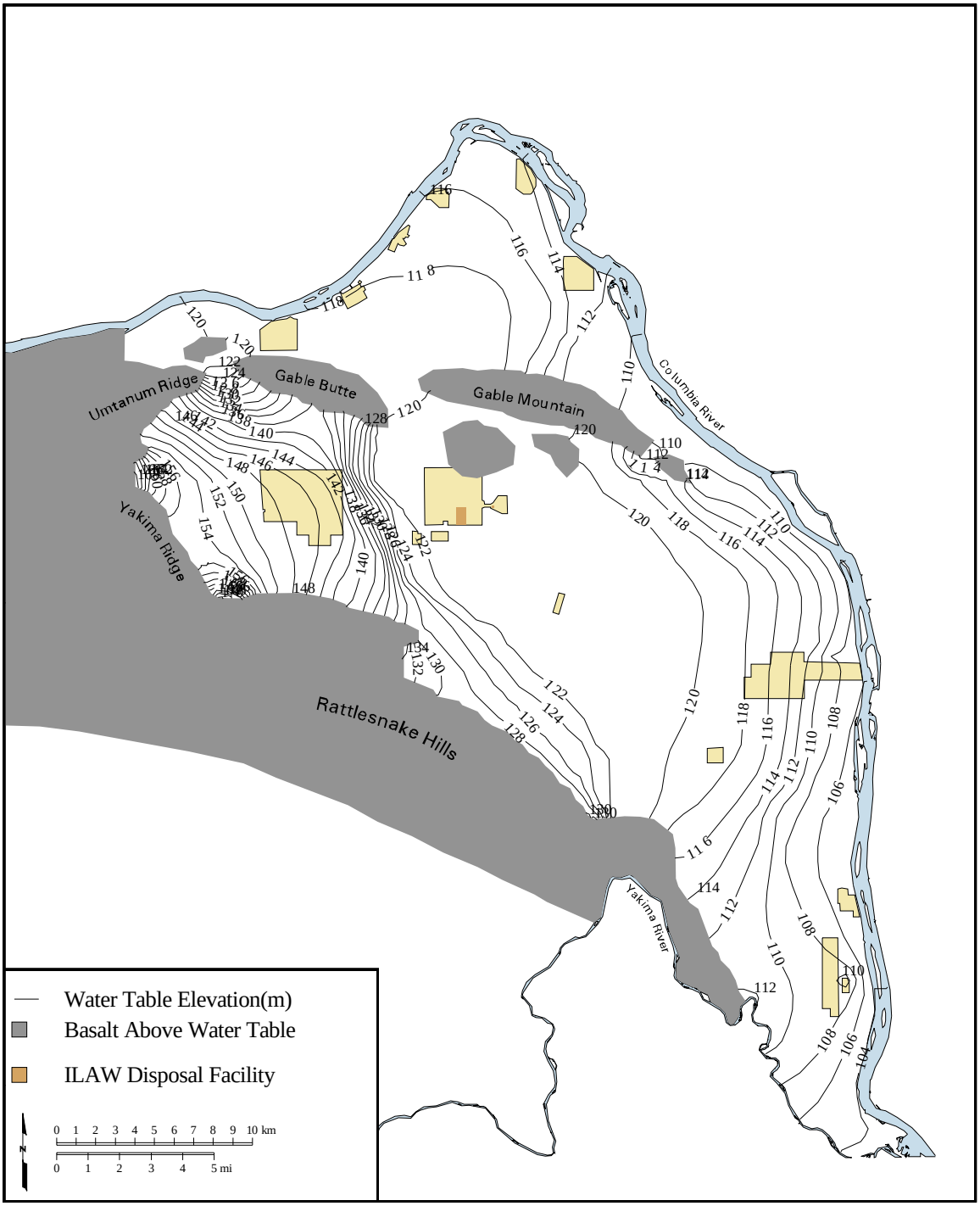

skw00069.eps December 28, 2000

Figure 7.9. Regional-Scale Head Distribution Resulting from Increased (Factor of 3) Regional Natural Recharge

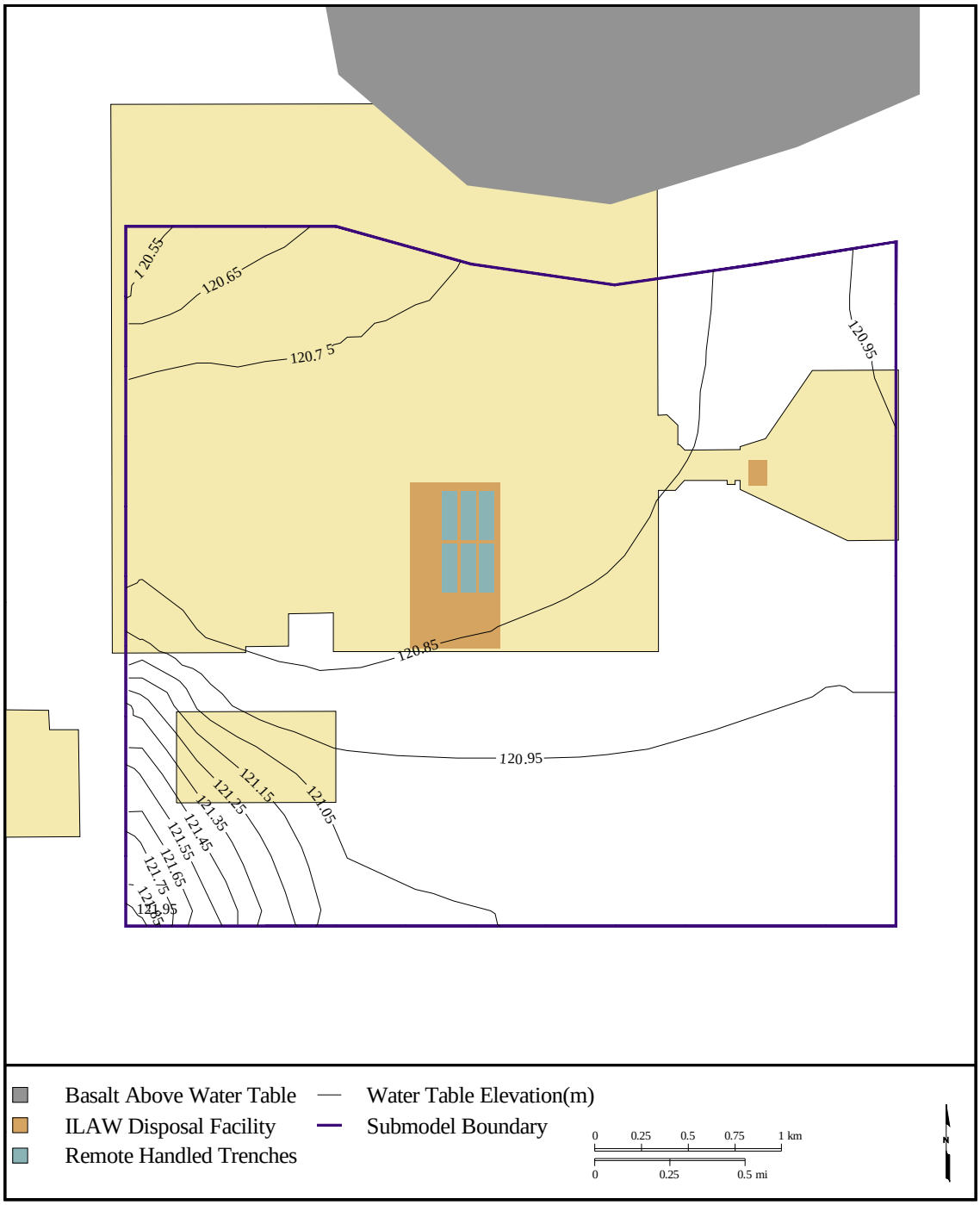

skw00073.eps December 28, 2000

Figure 7.10. Local-Scale Head Distribution Resulting from Increased (Factor of 3) Regional Natural Recharge

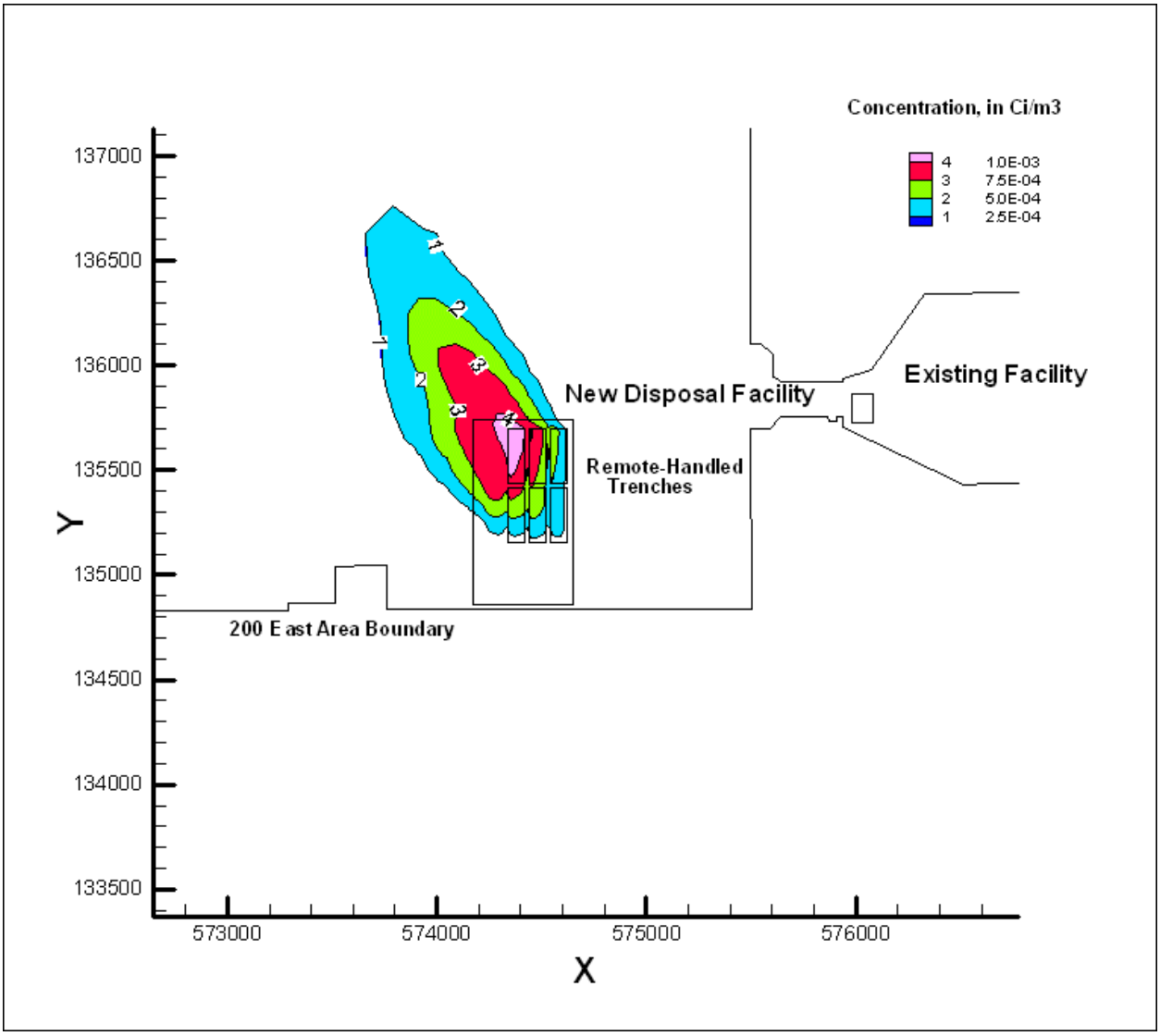

Figure 7.11. Areal Distribution of Contaminant Plume Resulting from the Remote-Handled Trench Concept – Sensitivity to Increased (Factor of 3) Regional Natural Recharge

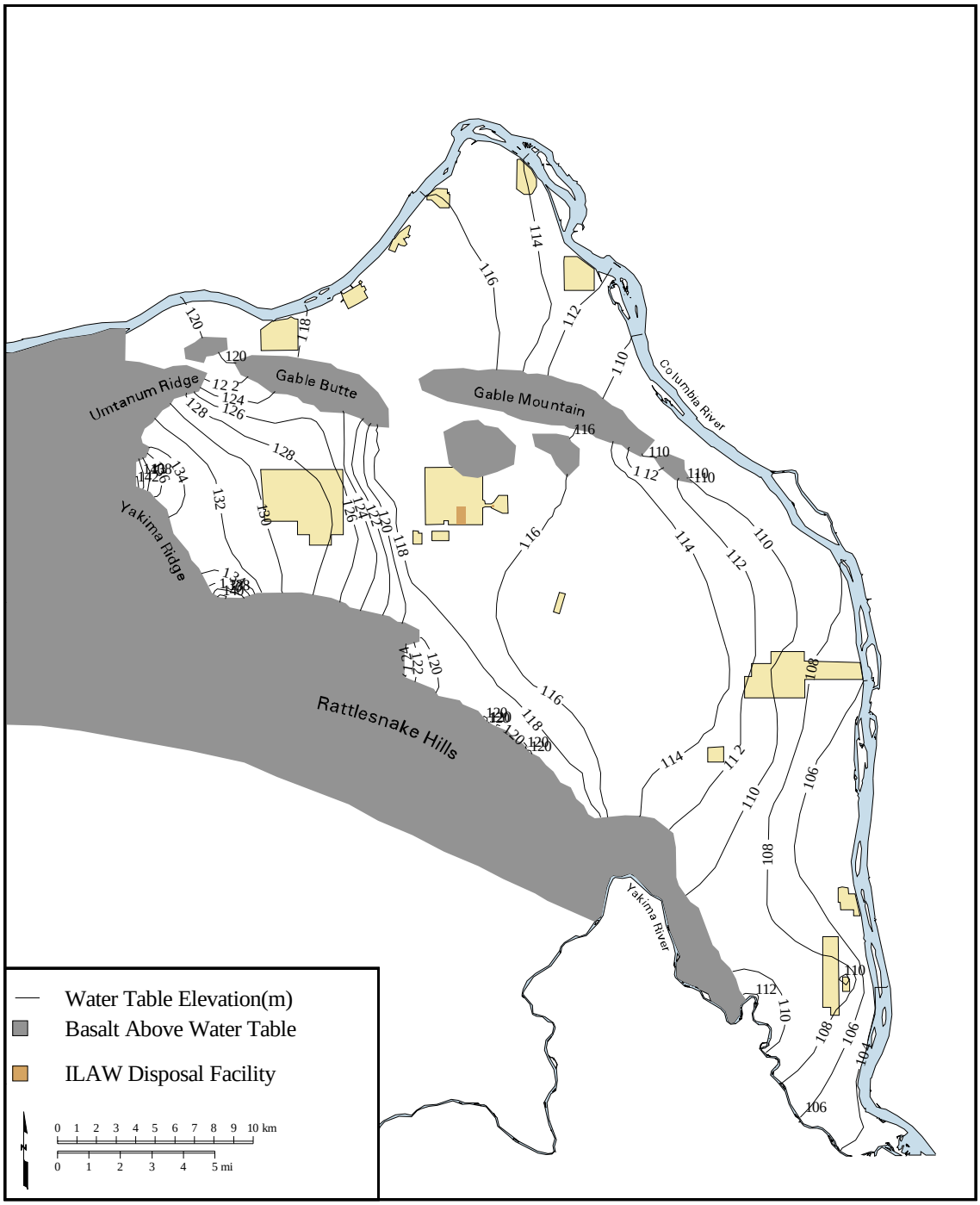

skw00070.eps December 28, 2000

Figure 7.12. Regional-Scale Head Distribution Resulting from Decreased (Factor of 3) Regional Natural Recharge

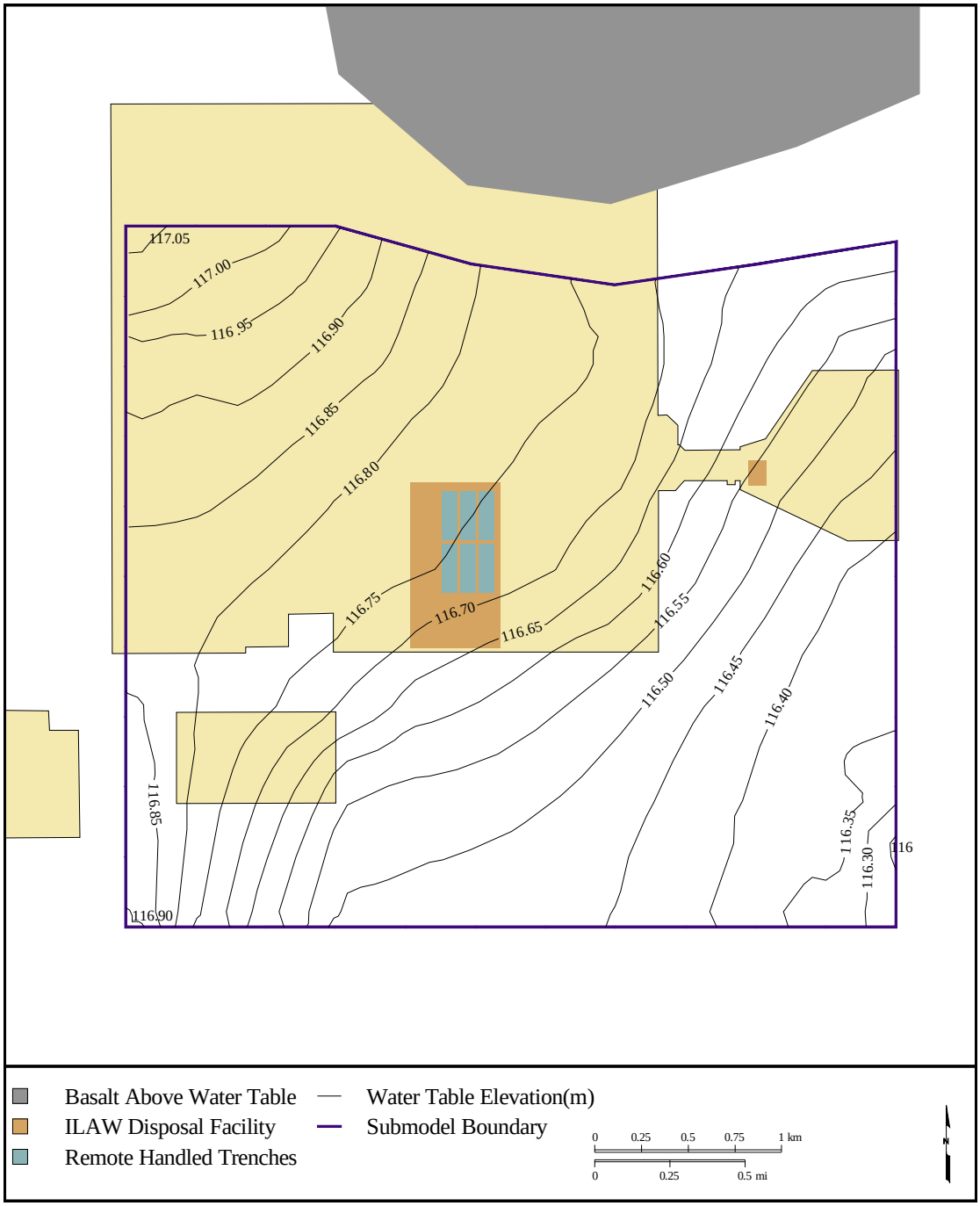

skw00074.eps December 28, 2000

Figure 7.13. Local-Scale Head Distribution Resulting from Decreased (Factor of 3) Regional Natural Recharge

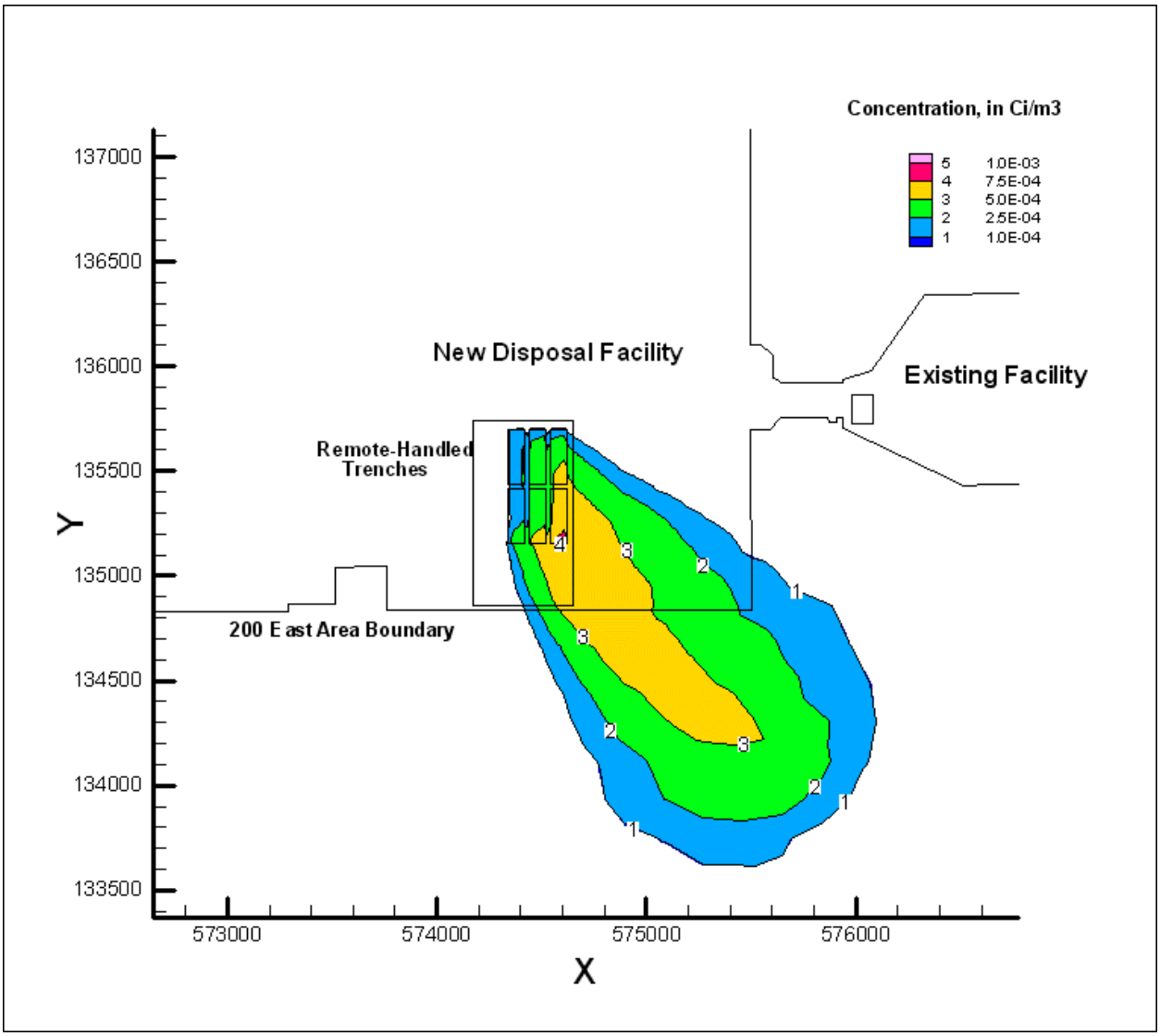

Figure 7.14. Areal Distribution of Contaminant Plume Resulting from the Remote-Handled Trench Concept – Sensitivity to Decreased (Factor of 3) Regional Natural Recharge

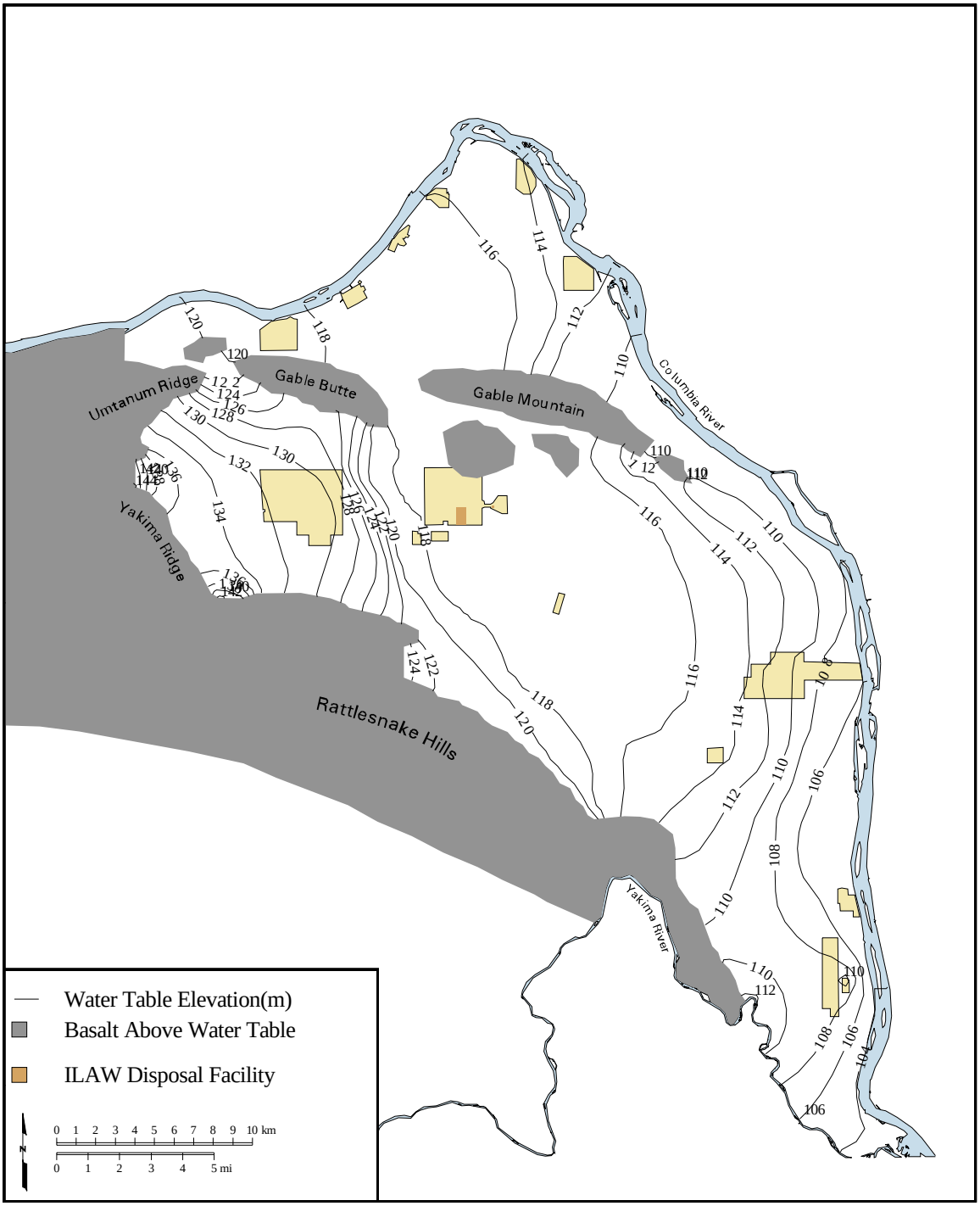

skw00071.eps December 28, 2000

Figure 7.15. Regional-Scale Head Distribution Resulting from Decreased (Factor of 3) Regional Natural Recharge

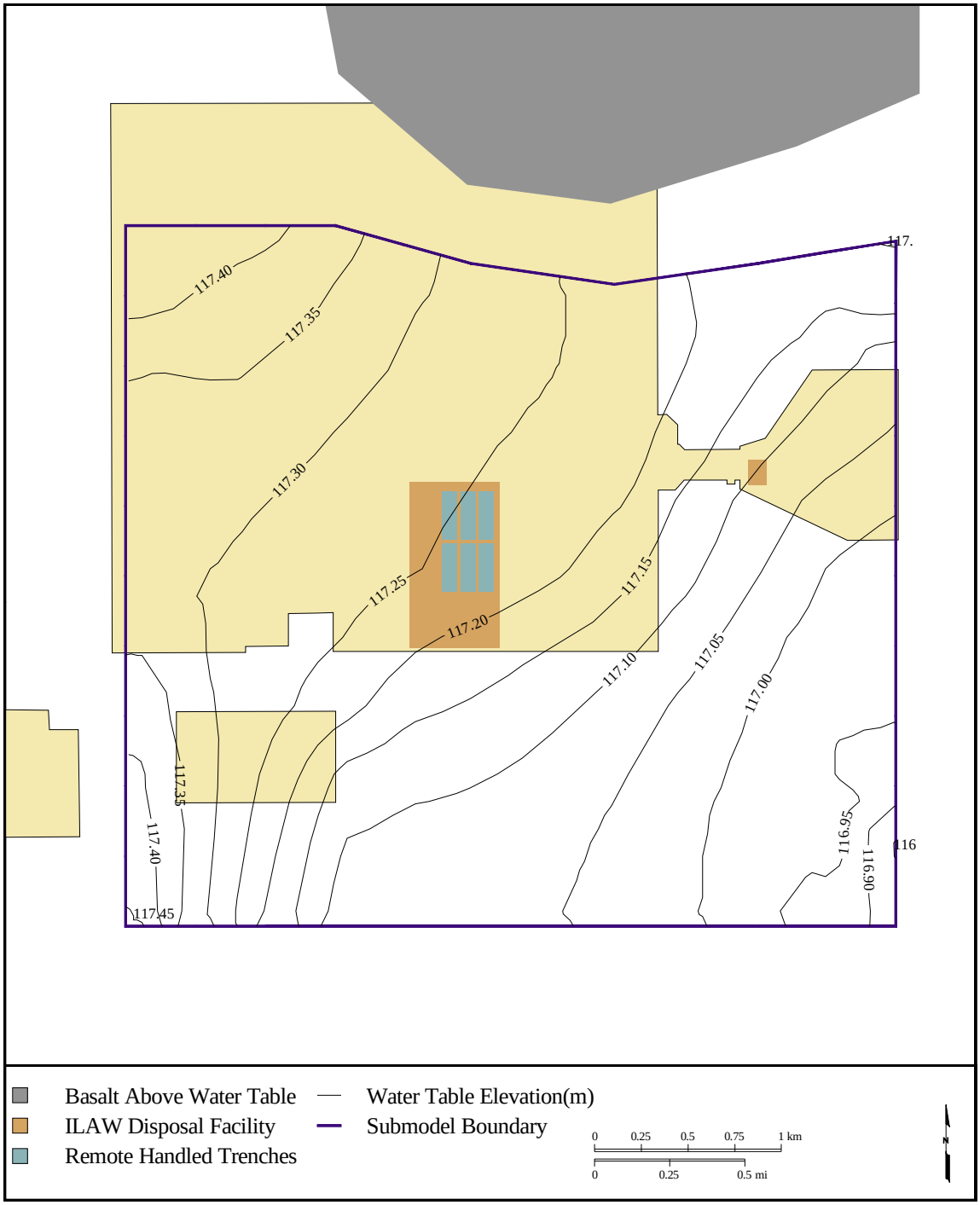

skw00075.eps December 28, 2000

Figure 7.16. Local-Scale Head Distribution Resulting from Decreased (Factor of 2) Regional Boundary Flux

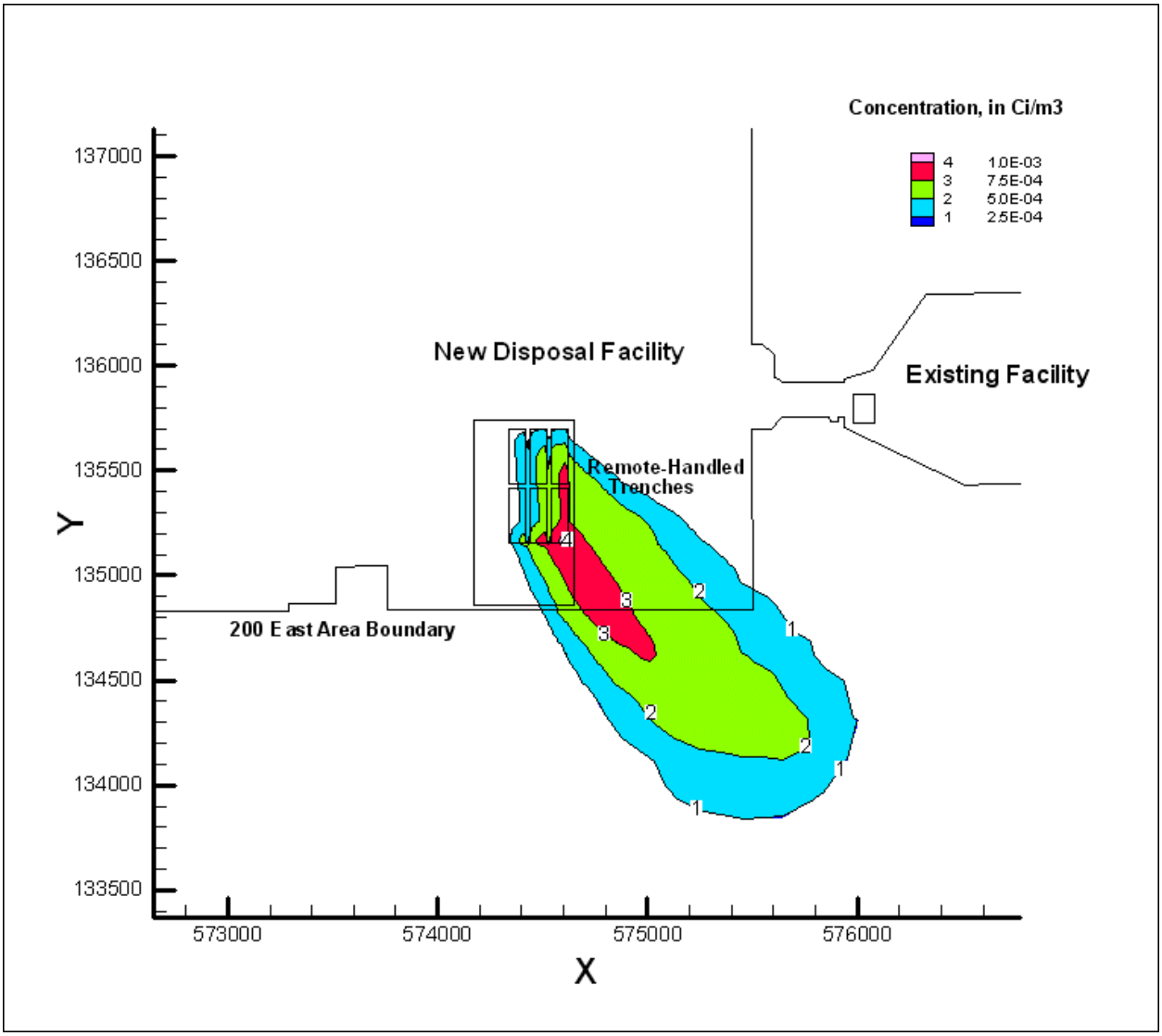

Figure 7.17. Areal Distribution of Contaminant Plume Resulting from the Remote-Handled Trench Concept – Sensitivity to Decreased (Factor of 2) Regional Boundary Flux

8.0 Summary and Conclusions

Calculations of the WIFs in this analysis in general yielded different levels of dilution than those developed in previous calculations of ILAW disposal facility performed by Lu (1996). The differences in the calculated WIFs can be attributed to a number of factors:

The Lu (1996) analysis estimated the water table beneath the facility to be at about the same level considered in this analysis, but assumed the water table would be situated in the Ringold Formation. The current model predicted that the water table would largely be along the edge of a buried channel containing very permeable Hanford formation. The difference in the distribution and hydraulic properties between the two conceptual models has led to higher levels of dilution using the current model. Additional work with the current model will be needed to evaluate the predictability of the WIF as a function of the hydraulic properties of the major hydrogeologic units beneath the facility.

Differences in the conceptual model of the unconfined aquifer used in the current analysis resulted in differences in the simulated direction of flow. The analysis by Lu (1996) predicted an easterly flow direction. The current local-scale model predicts a southeasterly flow direction. This difference in flow direction may be primarily attributable to including the highly permeable ancestral channel of the Columbia River, which contains the Hanford Formation in this analysis. The differences may also be a function of including natural recharge in the current regional-scale and local-scale analysis. Further work with the local-scale model will be needed to evaluate the predictability of the WIF as a function of the direction of flow.

Key factors affecting the current calculations appear to be related to the use of higher estimated hydraulic conductivities and groundwater velocities beneath the facility with the current model. The hydraulic conductivities used by the current model and the previous model used by Lu (1996) for the Ringold Formation are on the same order of magnitude (between 40 and 300 m/day in the current model; between 70 and 245 m/day in the model used by Lu [1996]). However, the current model contains areas of the Hanford formation beneath the facility and as a result has areas of very high permeability (between 2,200 and 30,000 m/day) in the area of the source release.

Uncertainties in the following key factors affecting calculated WIFs were investigated with sensitivity analyses:

- the assumed source-area of release
- the vertical position of the post-closure water table and the associated direction of groundwater flow
- the lateral position of the Hanford-Ringold Formation contact
- the hydraulic properties of Hanford and Ringold sediments.

Results of these analyses suggested that calculated WIFs are linearly related to the source-release area over the range of assumed surface areas of release. Calculated WIFs are also affected by the long-term predicted position of the water table and the resulting estimated distribution of hydraulic properties underlying the ILAW disposal facilities. The new facility is located in an area of the Hanford Site where it is underlain by an ancestral channel of the Columbia River that consists of highly permeable sediments of the Hanford Formation. For the predicted water-table position used in this analysis, the current interpretation places the contact between the Hanford Formation and the underlying less-permeable Ringold Formation along the south edge of the new ILAW disposal facility area.

Assumptions made about long-term regional natural recharge rates and boundary conditions are uncertain and can also change the predicted position of the water table and the position of the contact between the Hanford and Ringold sediments. Higher assumed rates of recharge can increase the water-table elevation and the level of saturation in the Hanford formation sediments leading to lower calculated WIFs (i.e., higher levels of dilution) from releases from the ILAW facilities.

Estimates of the hydraulic properties used in this assessment are based on past calibration of the site-wide model that provides a reasonable approximation of the regional observations and trends. Estimates of these properties on the local-scale model used in this analysis are uncertain and can affect calculated WIFs. Reducing the estimated hydraulic conductivities of the Hanford formation underlying the disposal facilities to those estimated for the Ringold Formation resulted in an order of magnitude increase in the WIFs (i.e., less dilution) from releases from the ILAW disposal facilities.

9.0 References

Bacon, D. H., M. D. White, and B. P. McGrail. 1999. *Subsurface Transport Over Reactive Multiphases (STORM): A General, Coupled, Non-isothermal Multiphase Flow, Reactive, Transport, and Porous Medium Alteration Simulator, Version 2; User's Guide*, PNNL-13108, Pacific Northwest National Laboratory, Richland, Washington

Cole, C. R., S. K. Wurstner, M. P. Bergeron, M. D. Williams, and P. D. Thorne. 1997. *Three-Dimensional Analysis of Future Groundwater Flow Conditions and Contaminant Plume Transport in the Hanford Site Unconfined Aquifer System: FY 1996 and 1997 Status Report*, PNNL-11801, Pacific Northwest National Laboratory, Richland, Washington.

Fayer, M. J., and T. B. Walters. 1995. *Estimated Recharge Rates at the Hanford Site*, PNL-10285, Pacific Northwest Laboratory, Richland, Washington.

Fayer, M. J. 1999. *Recharge Data Package for the Immobilized Low-Activity Waste 2001 Performance Assessment*, PNNL-13033, Pacific Northwest National Laboratory, Richland, Washington

Gupta, S. K., C. R. Cole, C. T. Kincaid, and A. M. Monti. 1987. *Coupled Fluid, Energy, and Solute Transport (CFEST) Model: Formulation and User's Manual*, Report BMI/ONWI-660, Battelle Memorial Institute, Columbus, Ohio.

Gupta, S. K. 1996. *Draft User's Manual, CFEST-96 Flow and Solute Transport, Constant/Variable Density, Computationally Efficient, and Low Disk PC/Unix Version*. Consultant for Environmental System Technologies, Irvine, California.

Huyakon, P. S., and S. Panday. 1999. *VAM3DF - Variably Saturated Analysis Model in Three Dimensions for the Data Fusion System: Documentation and User's Guide, Version 2.0*, HydroGeoLogic, Inc., Herndon, Virginia.

Kincaid, C. T., M. P. Bergeron, C. R. Cole, M. D. Freshley, N. L. Hassig, V. G. Johnson, D. I. Kaplan, R. J. Serne, G. P. Streile, D. L. Strenge, P. D. Thorne, L. W. Vail, G. A. Whyatt, and S. K. Wurstner. 1998. *Composite Analysis for Low-Level Waste Disposal in the 200-Area Plateau of the Hanford Site*, PNNL-11800, Pacific Northwest National Laboratory, Richland, Washington.

Kirkbride, R. A. 1999. *Tank Waste Remediation System Operational Utilization Plan*, HNF-SD-WM-SP-012, Rev. 1, Volume I and II, Numatec Hanford Company, Richland, Washington.

Law, A., S. Panday, C. Denslow, K. Fetch, and A. Knepp. 1996. *Hanford Sitewide Groundwater Flow and Transport Model Calibration Report*, BHI-00608, Rev. 0, Bechtel Hanford Inc., Richland, Washington.

Lindsey, K. A. 1995. *Miocene- to Pliocene-Aged Suprabasalt Sediments of the Hanford Site, South Central Washington*, BHI-00184, Bechtel Hanford, Inc., Richland, Washington.

Lu, A.H. 1996. *Contaminant Transport in the Unconfined Aquifer, Input to the Low Level Tank Waste Interim PA*, WHC-SD-WM-RPT-241, Westinghouse Hanford Company, Richland, Washington.

Mann, F. M., C. R. Eiholzer, R. Khaleel, N. W. Kline, A. H. Lu, B. P. McGrail, P. D. Rittmann, and F. Schmittroth. 1995. *Definition of the Base Analysis Case of the Interim Performance Assessment*, WHC-SD-WM-RPT-200, Revision 0, Westinghouse Hanford Company, Richland, Washington, December 1995

Mann, F. M. 1996. I*NTEG: A Program to Calculate Groundwater Contamination and Human Doses*, WHC-SD-WM-RPT-219, Westinghouse Hanford Company, Richland, Washington,

Mann, F. M., R. J. Puigh II, P. D. Rittmann, N. W. Kline, J. A. Voogd, Y. Chen, C. R., Eiholzer, C. T. Kincaid, B. P. McGrail, A.H. Lu, G. F. Williamson, N. R. Brown, and P. E. LaMont. 1998. *Hanford Immobilized Low-Activity Tank Waste Performance Assessment*, DOE/RL-97-69, Rev. 0, U.S. Department of Energy-Richland Operations Office, Richland, Washington.

Mann F. M., S. H. Finfock, E. J. Freeman, R. J. Puigh III, D. H. Bacon, M. P. Bergeron, B. P. McGrail, and S. K. Wurstner. 2000. White Paper: *Updating Conclusions of 1998 ILAW Performance Assessment*, DOE/ORP-2000-07, Revision 0, U. S. Department of Energy, Office of River Protection, Richland, Washington.

Pickett, W. W. 1998. *Immobilized Low-Activity Waste Interim Storage Facility, Project W-520 Conceptual Design Report [DRAFT]*, HNF-3013, Rev. B, Fluor Daniel Northwest Company, Richland, Washington

Puigh II, R. J. 1999. *Disposal Facility Data for the Hanford Immobilized Low-Activity Tank Waste*, HNF-4950, Rev. 1, Fluor Federal Services, Richland, Washington, December 1999.

Rawlins, J. A., R. A. Karnesky, R. Khaleel, A. H. Lu, F. M. Mann, B. P. McGrail, W. J. McMahon, M. G. Piepho, P. D. Rittmann, and F. Schmittroth. 1994. *Impacts of Disposal System Design Options on Low-Level Glass Waste Disposal System Performance*, WHC-EP-0810, Revision 0, Westinghouse Hanford Company, Richland, Washington

Rittmann, P. D. 1993. *GRTPA - A Program to Calculate Human Dose from PORFLOW Output*, WHC-SD-WM-UM-018, Westinghouse Hanford Company, Richland, Washington.

Taylor, W.J. 1999. *Contract No. DE-AC06-99RL14047 – Decision to Change the Immobilized Low-Activity Waste (ILAW) Disposal Baseline to Proceed with the Remote-Handled Trench Alternative*, letter 99-DPD-066 (correspondence control number 9958849), Department of Energy, Richland, Washington.

Thorne, P. D., and M. A. Chamness. 1992. *Status Report on the Development of a Three-Dimensional Conceptual Model for the Hanford Site Unconfined Aquifer System*, PNL-8332, Pacific Northwest Laboratory, Richland, Washington.

Thorne, P. D., and D. R. Newcomer. 1992. *Summary and Evaluation of Available Hydraulic Property Data for the Hanford Site Unconfined Aquifer System*, PNL-8337, Pacific Northwest Laboratory, Richland, Washington.

Thorne, P. D., M. A. Chamness., F. A. Spane Jr., V. R. Vermeul, and W. D. Webber. 1993. *Three-Dimensional Conceptual Model of the Hanford Site Unconfined Aquifer System, FY 93 Status Report*, PNL-8971, Pacific Northwest Laboratory, Richland, Washington.

Thorne, P. D., M. A. Chamness., V. R. Vermeul, Q. C. MacDonald, and S. E. Schubert. 1994. *Three-Dimensional Conceptual Model for the Hanford Site Unconfined Aquifer System, FY 1994 Status Report*, PNL-10195, Pacific Northwest Laboratory, Richland, Washington.

U.S. Department of Energy (DOE). 1994. *Remedial Investigation and Feasibility Study Report for the Environmental Restoration Disposal Facility*, DOE/RL-93-99, Rev. 1, Richland, Washington.

Walters, W. H., M. C. Richmond, and B. G. Gilmore. 1994. *Reconstruction of Radionuclide Concentrations in the Columbia River from Hanford, Washington to Portland, Oregon, January 1950 - January 1971*, BNWD-2225 HEDR, Battelle Pacific Northwest Division, Richland, Washington.

Wood, M. I., R. Khaleel, P. D. Rittmann, A. H. Lu, S. H. Finfrock, R. J. Serne, K. J. Cantrell, and T. H. DeLorenzo. 1995. *Performance Assessment for the Disposal of Low-Level Waste in the 200 West Area Burial Grounds*, WHC-ED-0645, Westinghouse Hanford Company, Richland, Washington.

Wood, M. I., R. Khaleel, P. D. Rittmann, S. H. Finfrock, T. H. DeLorenzo, and D. Y. Garbrick. 1996. *Performance Assessment for the Disposal of Low-Level Waste in the 200-East Area Burial Grounds*, WHC-SD-WM-TI-730, Rev. 0, Westinghouse Hanford Company, Richland, Washington.

Wurstner, S. K., P. D. Thorne, M. A. Chamness, M. D. Freshley, and M. D. Williams. 1995. *Development of a Three-Dimensional Groundwater Model of the Hanford Site Unconfined Aquifer System: FY 1995 Status Report*, PNL-10886, Pacific Northwest Laboratory, Richland, Washington.

This page intentionally left blank.

APPENDIX D

APPENDIX D

This appendix describes the information associated with the simulations that have been placed onto a compact disk (CD). This information consists predominantly of input files and selected output files that document the details of the simulation calculations performed for the 2001 ILAW performance assessment. The structure of the information placed on the CD is partitioned into three major folders: ILAW VAM/INTEG, ILAW Waste Form; and ILAW Groundwater. A detailed description of the information and file structure for each folder is provided below.

D.1 Near Field, Far Field, and Estimated Impacts Data Files (ILAW VAM/INTEG)

The input and selected process and output files associated with the calculations provided in *Near Field, Far Field, And Estimated Impact Calculations For The Hanford Immobilized Low-Activity Tank Waste Performance Assessment: 2001 Version,* RPP-7463, Revision 0, have been archived on a compact disk (CD). For a complete description of the sensitivity cases see the report (RPP-7463). The near field and far field calculations were conducted with the VAM3DF code. The estimated impact calculations were performed with the INTEG code. This section describes the directory structure of the archive on the CD.

The output files for each sensitivity case have been copied onto a CD that is available on request. Table D-1 provides a cross-reference between the sensitivity case descriptions and the summary output files for the waste form, vadose zone, and estimated impact results.
All files on the CD are stored under a directory structure that defines the type of files and case names. The top directory is named 'ILAW VAM/INTEG;' beneath it are four directories named 'Near Field', 'Far Field', 'Waste Form' and 'Integration.' The 'Near Field' directory contains subdirectories corresponding to different near field VAM3DF calculations, which in turn contain the input and output files associated with that case. The 'Far field' directory contains similar information for the VAM3DF far field calculations. The 'Waste Form' directory contains subdirectories corresponding to different waste form cases, which in turn contain the data files used in the calculations. The 'Integration' directory contains subdirectories corresponding to the INTEG cases, which in turn contain the input and output files for each INTEG calculation.
The near field case subdirectory names correspond to the near field cases identified in Table D-1. Each subdirectory contains four files: 'casename.inp', 'casename.out', 'casename.fpl', (where 'casename' is replaced with the case name), and 'bcflow.out'. The '.inp' file is the standard VAM3DF input file that specifies the calculation parameters. The 'casename.out' file is the VAM3DF standard output file, and the '.fpl' file contains the fluid flux data that is used by the Bcflow code to create the boundary condition inputs for the far field calculations. The 'bcflow.out' file is the result of the Bcflow calculation.

The far field case subdirectory names correspond to the far field cases identified in Table D-1. The cases are divided into two categories: flow (indicated by a '-f' suffix) and transport (indicated by a '-t-#' suffix, where the '#' indicates the K_d value used in that case). Each flow case subdirectory contains four files: 'casename.inp', 'casename.out', 'casename.fpl', and 'casename.vel' (where 'casename' is replaced with the case name). The '.inp' file is the standard VAM3DF input file that specifies the calculation parameters. The '.out' file is the VAM3DF standard output file, and the '.fpl' file contains the fluid flux data that is used by the Botflux code to calculate the flux across the bottom boundary. The '.vel' file contains the velocity field used in the transport calculation. Each transport case subdirectory contains five files: 'casename.inp',

‘casename.out’, ‘casename.ppl’ (where ‘casename’ is replaced with the case name), ‘bf.inp’, and ‘botflux.out’. The ‘.inp’ file is the standard VAM3DF input file that specifies the calculation parameters. The ‘.out’ file is the VAM3DF standard output file, and the ‘.ppl’ file (which is ‘zipped’) contains the contaminant concentration data that is used by the Botflux code to calculate the flux across the bottom boundary. The ‘bf.inp’ file contains the input parameters for Botflux, and the ‘botflux.out’ file contains the results of the Botflux calculation (which are used as input to the INTEG calculations).

The waste form case subdirectory names begin with the name of the STORM case (e.g., case WFA is in directory WFA-base-42) identified in Table D-1. Each subdirectory contains two files: ‘storm2vam.out’ and ‘storm2vam.g17.’ Some subdirectories may contain multiple versions of each file, with a suffix indicating which near field flow calculation they are associated with. The ‘.out’ files contain excerpted data from the STORM output data. These data are in three columns, corresponding to time (year), release rate (micromols/m^2/secomd), and release rate (Ci/m^2/year). The ‘.g17’ files contain the release rate data (converted to Ci/year for each node) in the format required for input to the far field transport calculations.

The integration subdirectory names correspond to the INTEG cases identified in Table D-1. Each subdirectory contains four files named: ‘run.bat,’ ‘vad casename.bac,’ ‘casename.out,’ and ‘casename.dat’ (where ‘casename’ is replaced with the case name). The ‘run.bat’ file contains some of the input parameters required for the INTEG run, including the well intercept factor (WIF), recharge rate, and the names of the data files used in the INTEG calculation (all the data files are in the ‘lib’ subdirectory under the integration directory). The ‘vad-casename.bac’ file contains the data from the corresponding far field transport calculations. These data are the release rate (in Ci/year) from the vadose zone into the groundwater with the first column being time (in years) and the subsequent columns each corresponding to a different K_d (typically only the first two K_d columns are used, with the remainder being filled with 0s). The ‘casename.out’ file contains the general results of the INTEG calculation and the ‘casename.dat’ file contains the detailed results for each nuclide.

Table D-1. ILAW Cases

Case	Description	Waste Form Case	Near Field Case	Far Field Flow Case	Far Field Transport Case	INTEG Case
1	Base Case:					
1-1	Base Analysis Case	wfa	nf42	42base-f	42base-t	42base
2	Scenario Cases:					
2-1	Well at 1000m	Hand calculated by multiplying base case by ratio of WIF's.				
2-2	Well at Col. River	Hand calculated by multiplying base case by ratio of WIF's.				
2-3	30 L/d pumping	Hand calculated by multiplying base case by ratio of WIF's.				
2-4	100 L/d pumping	Hand calculated by multiplying base case by ratio of WIF's.				
2-5	300 L/d pumping	Hand calculated by multiplying base case by ratio of WIF's.				
2-6	1000 L/d pumping	Hand calculated by multiplying base case by ratio of WIF's.				
2-7	Reduced Hydraulic Conductivity (3x) in Groundwater	Hand calculated by multiplying base case by ratio of WIF's.				
2-8	Regional Recharge Increase (3x)	Hand calculated by multiplying base case by ratio of WIF's.				
2-9	Regional Recharge Decrease (3x)	Hand calculated by multiplying base case by ratio of WIF's.				
2-10	Decrease Regional Upgradient Boundaries (2x)	Hand calculated by multiplying base case by ratio of WIF's.				
2-11	Industrial	wfa	nf42	42base-f	42base-t	ind-100m
2-12	Residential	wfa	nf42	42base-f	42base-t	res-100m
2-13	Agricultural	wfa	nf42	42base-f	42base-t	agr-100m
2-14	Native American	wfa	nf42	42base-f	42base-t	nat-cr
2-15	Columbia River Population	wfa	nf42	42base-f	42base-t	crpop-cr
2-16	DOE Dose Factors	wfa	nf42	42base-f	42base-t	doe-100m
3	Inventory Cases:					
3-1	Upper Bound Inventory.	wfa	nf42	42base-f	42base-t	42ub
3-2	Maximum Tc99.	wfa	nf42	42base-f	42base-t	42maxtc
3-3	No Tc	wfa	nf42	42base-f	42base-t	42notc
3-4	Double I	wfa	nf42	42base-f	42base-t	42-2I
3-5	Double U	wfa	nf42	42base-f	42base-t	42-2u
3-6	Upper bound + max Tc	wfa	nf42	42base-f	42base-t	42ubmaxtc

Case	Description	Waste Form Case	Near Field Case	Far Field Flow Case	Far Field Transport Case	INTEG Case
4	Recharge Cases:					
4-1	Rupert Sand.	wf4	nf09	09-f	09-t	09
4-2	High Recharge.	wf6	nf50	50-f	50-t	50
4-3	Low Recharge.	wfd	nf01	01-f	01-t	01
5	Geology Cases:					
5-1	Hanford Formation Sandy.	wfa	nf42	42sand-f	42sand-t	42sand
5-2	Hanford Formation Gravelly.	wfa	nf42	42grav-f	42grav-t	42grav
5-3	Clastic Dikes.	wfa	nf42	42dike-f	42dike-t	42dike
5-4	Deep Water Table.	wfa	nf42	42deep-f	42deep-t	42deep
6	Facility Cases:					
6-1	Capillary Break (Best Estimate Case).	wfd	nf42-break	42break-f	42break-t	42break
6-2	No Side Slope	wfa	nf42-all	42all-f	42all-t	42all
6-3	Vertical Capillary Break.	wfd	nf42-vert	42vert-f	42vert-t	42vert
6-4	Short Break.	wfd	nf42-shortbreak	42short-f	42short-t	42short
6-5	Capillary Break with High Recharge	wfd	nf50-break	50break-f	50break-t	50break
6-6	Sand Backfill.	wf11	nf42-sand	42sandfill-f	42sandfill-t	42sandfill
6-7	Alternate Facility Design (Vault).	wf16	nf42-vault	42vault-f	42vault-t	42vault
6-8	Trench Located at South End of Site	Hand calculated by multiplying base case by ratio of WIF's.(1)				
6-9	Trench Rotated 90°	Hand calculated by multiplying base case by ratio of WIF's.(1)				
6-10	Smaller Layout	Hand calculated by multiplying base case by ratio of WIF's.(1)				
6-11	Larger Layout	Hand calculated by multiplying base case by ratio of WIF's.(1)				
6-12	Existing Vault Site	Hand calculated by multiplying new vault case by ratio of WIF's.(1)				
7	Degradation Cases:					
7-1	Surface Barrier.	no barrier = base case; barrier ~ cap break				
7-2	Degraded Capillary Break (Subsidence).	wfa	nf42-subsidence	42sub-f	42sub-t	42sub
7-3	Bath Tub Effect.	See Section 5.5.1				
8	Hydrologic Parameter Cases:					
8-1	Isotropic	wfa	nf42	42iso-f	42iso-t	42iso

Case	Description	Waste Form Case	Near Field Case	Far Field Flow Case	Far Field Transport Case	INTEG Case
	Conductivity.					
8-2	Sand Backfill.	Same as 6-5				
8-3	Hanford Formation Sandy	Same as 5-1				
8-4	Hanford Formation Gravelly	Same as 5-2				
8-5	Instantaneous Transport	wfa	N/A	N/A	N/A	42instant
8-6	High Diffusion	wfa	nf42	42base-f	42diff-t	42diff
8-7	High Dispersion	wfa	nf42	42base-f	42disp-t	42disp
9	Waste Form Cases:					
9-1	Forward Rate.	wfb	nf42	42base-f	42for-t	42for
9-2	Simplified Full Reaction Network (no ion exchange).	wf1	nf42	42base-f	42noion-t	42noion
9-3	Infiltration Rate. Same as recharge cases above.	Same as 4-1 – 4-3				
9-4	Sand Backfill.	Same as 6-5				
9-5	Steel Containers.	wf25	nf42	42base-f	42steel-t	42steel
9-6	Chemical Conditioning Layer.	wf10	nf42	42base-f	42cond-t	42condlayr
9-7	Alternate Facility (Vault)	Same as 6-6				
9-8	Alternate Glass.	wf28	nf42	42base-f	42altglass-t	42altglass
9-9	Diffusion Parameter.	wf14	nf42	42base-f	42diff-t	42diff
9-10	No secondary reactions.	wf2	nf42	42base-f	42nosec-t	42nosec
9-11	High Ion Exchange.	wf30	nf42	42base-f	42highion-t	42highion
9-12	Pulse.	N/A	nf42	42base-f	pulse-t	pulse42
10	Geochemical Cases:					
10-1	Uranium Trapping.	wfa	nf42	42base-f	42base-t, 42conc-t	42conc
10-2	Uranium K_d = 0.0 mL/g.	wfa	nf42	42base-f	42base-t	42ukd0
10-3	All K_d = 0.0 mL/g.	wfa	nf42	42base-f	42base-t	42kd0

(1) WIF's for these cases are provided in Bergeron 2000.

D.2 Waste Form Data Files (ILAW Waste Form)

This directory contains input and output files for the waste form release calculations. Each folder contains the files for a single sensitivity case. Table D-2 contains descriptions of each case.

Table D-2. Waste Form Case Descriptions

CASE	Description	BASIC MODEL
WFA	4.2 mm/y infiltration	Trench
WFB	Forward rate, 4.2 mm/y infiltration	Trench
WFC	4.2 mm/y infiltration	Vault
WFD	0.1 mm/y infiltration	Trench
WF1	Assume no Ion Exchange	Trench
WF2	Assume no Secondary Phase Formation	Trench
WF4	0.9 mm/y infiltration rate	Trench
WF6	50 mm/y infiltration rate	Trench
WF7	0.5 mm/y infiltration rate	Trench
WF8	10 mm/y infiltration rate	Trench
WF9	Extend WFA to groundwater	Trench
WF10	Add conditioning layer at top	Trench
WF11	Change filler material in trench to sand	Trench
WF14	Increase diffusion for all aqueous species by a factor of 10	Trench
WF16	Replace concrete everywhere with backfill material	Vault
WF19	0.9 mm/y infiltration rate	Vault
WF21	0.1 mm/y infiltration	Vault
WF25	Include steel in waste packages	Trench
WF26	Replace Tc w/U	Trench
WF27	Full 2-D simulation	Trench
WF28	Increase Waste Loading / Alternate Glass Formulation (HLP-31)	Trench
WF30	Increase ion exchange rate by 5 times for WFB	Trench
WF31	Bathtub effect: Fully water saturated, no flow	Trench

Each directory contains similar files. Table D-3 contains a description of each file.

Table D-3. Description of Files Associated with Each Waste Form Case

File Name	Description
d_flux1d.f	program to read in fluxes file for one-dimensional cases and output normalized fluxes
d_flux2d.f	program to read in fluxes file for two-dimensional cases and output normalized fluxes
input	STORM input data file
fluxes	Tc or U fluxes across bottom boundary of model, either in moles/m^2/s or μmoles/m^2/s.

File Name	Description
normflux.f	FORTRAN program to calculate normalized U fluxes across bottom boundary of model
uflux.f	FORTRAN program to calculate total U flux across bottom boundary from refnod file
*.dat	text file containing all output variables at a specific time for input into Tecplot
*Crtotalmoles.csv	Total Cr concentration at bottom boundary vs time
*LAWABP1Ratem.csv	Glass dissolution rate vs time
*normtcflx.csv	normalized Tc fluxes across lower boundary vs time, ppm/y
*ph.csv	pH vs time
*SiO2aqmolesk.csv	SiO2(aq) concentration vs time, moles/kg
*TcO4moleskg.csv	TcO_4^- concentration vs time, μmoles/kg (moles/kg for WF21 and WF28 only)

D.3 Groundwater Data Files (ILAW Groundwater)

This directory contains input and output files for the groundwater transport calculations for local-scale and regional-scale calculations. Each folder contains folders of both base case and sensitivity case simulations files. Table D-4 contains descriptions of each case contained within the base case and sensitivity case folders within the Local-scale Calculations Directory.

Table D-4. Description of Groundwater Cases – Local-scale

CASE	Description	DISPOSAL OPTION
Base Case subdirectory		
GWLSBCa	Local-scale Basecase – New Facility	R. Trench
GWLSBCb	Local-scale Basecase – New Facility	C. Vault
GWLSBCc	Local-scale Basecase – Existing Grout Facility	C. Vault
Sensitivity Cases subdirectory		
GWLSSC1	Local-scale Sensitivity Case 1 – Trench Placement at South End of New Disposal Facility Area	R. Trench
GWLSSC2	Local-scale Sensitivity Case 2 – Trenches Rotated by 90 degrees from Basecase	R. Trench
GWLSSC3a	Local-scale Sensitivity Case 3a - Pumping rate (100 m well) 30 liters per day	R. Trench
GWLSSC3b	Local-scale Sensitivity Case 3b - Pumping rate (100 m well) 100 liters per day	R. Trench
GWLSSC3c	Local-scale Sensitivity Case 3c - Pumping rate (100 m well) 300 liters per day	R. Trench
GWLSSC3d	Local-scale Sensitivity Case 3d - Pumping rate (100 m well) 1000 liters per day	R. Trench
GWLSSC4	Local-scale Sensitivity Case 4 - Hydraulic Conductivity of Hanford	R. Trench

CASE	Description	DISPOSAL OPTION
	formation (Unit 1) reduced to hydraulic conductivity of underlying Ringold Formation (Unit 5)	
GWLSSC5	Local-scale Sensitivity Case 5 - Increased Surface Source Area	R. Trench
GWLSSC6	Local-scale Sensitivity Case 6 - Increased Surface Source Area	C. Vault
GWLSSC7	Local-scale Sensitivity Case 7 – Increased Natural Recharge (factor of 3 times basecase values)	R. Trench
GWLSSC8	Local-scale Sensitivity Case 8 – Reduced Natural Recharge (factor of 0.33 times basecase values)	R. Trench
GWLSSC9	Local-scale Sensitivity Case 9 – Reduced Upgradient Boundary fluxes (factor of 0.5 times basecase values)	R. Trench

Table D-5 contains descriptions of each case contained within the base case and sensitivity case folders within the Regional-scale Calculations Directory.

Table D-5. Description of Groundwater Cases – Regional-scale

CASE	Description	DISPOSAL OPTION
Base Case subdirectory		
GWRSBCa	Regional-scale Basecase – New Facility	R. Trench
GWRSBCb	Regional-scale Basecase – New Facility	C. Vault
GWRSBCc	Regional-scale Basecase – Existing Grout Facility	C. Vault
Sensitivity Cases subdirectory		
GWRSSC7	Regional-scale Sensitivity Case 7 - Natural Recharge x 3	Flow only
GWRSSC8	Regional-scale Sensitivity Case 8 - Natural Recharge x 0.33	Flow only
GWRSSC9	Regional-scale Sensitivity Case 9 - Boundary flux x 0.5	Flow only

Each individual simulation level consists of similar input and output folders that contain the basic input and output files. Table D-6 contains a description of each of these files. The actual input files in each case were based on a source concentration of 1 Ci/m^3 entering the aquifer at an assumed local scale infiltration rate of 0.9 mm/y. The resultant solute flux entering the aquifer through the trench or vault area for this infiltration is 9.0 x 10^{-4} Ci/y/m^2. Each of these calculations used I-129 as the surrogate long-lived contaminant. The specific activity used for iodine-129 in these calculations was 5.56521 kg/Ci. The well intercept factor (WIF) results reported in the main body of this report and in Mann et al. (2000) are results based on scaling the results from the 0.9 mm/y calculations to an assumed infiltration rate of 4.2 mm/y. The file, “well_wif_sum.txt”, provided in the Selected Output Files subdirectories for each case, presents the range of WIFs at specified locations for different assumed local-scale infiltration rates.

Table D-6. Description of Files Associated with Each Groundwater Case

File Name	Description
Input Files subdirectory	
readme.doc	Description of simulation
cfest.ctl	Control for running CFEST_96 code
input.lp1	CFEST_96 input file containing node and element descriptions, constant-head boundary descriptions, and hydraulic properties
input.l3i	CFEST_96 input file containing flow and transport options, specified natural recharge, source input information, and other specific boundary flux information
run.bat	Batch file to run CFEST-96
Selected Output Files subdirectory	
tec_allhc.zip	Zipped-up ascii file of model outputs of head and concentrations suitable for graphical processing using TECPLOT
well_wif_summ.txt	Summary of well intercept factors (WIF) at specific downgradient locations scaled for various specified infiltration rates. These files are only specified for transport simulations.

This page intentionally left blank.